marine reSEArch@CNR.it

Coastal and Marine Spatial Planning

National Research Council of Italy

Coastal and Marine Spatial Planning

Current Measurements in the Bonifacio Mouths and La Maddalena Archipelago: First Analyses

A. Ribotti[1], M. Borghini[2], K. Schroeder[2], A. Satta[1], B. Sorgente[1], R. Gerin[3], A. Cucco[1], A. Olita[1], L. Fazioli[1], R. Giovannini[4], R. Sorgente[1]
1, Institute for Coastal Marine Environment, CNR, Oristano, Italy
2, Institute of Marine Sciences, CNR, Pozzuolo di Lerici (SP), Italy
3, National Institute of Oceanography and Experimental Geophysics, Trieste, Italy
4, RAM del Corpo delle Capitanerie di Porto, Italian Ministry for the Environment, Land and Sea, Roma, Italy
alberto.ribotti@cnr.it

Abstract

At the end of August 2009 an ADCP Workhorse Sentinel 600 kHz was mounted on a 10.4 metres long unsinkable fibreglass unit patrol boat model Class 500 of the Italian Coast Guard. The aim was the acquisition of current data in the very shallow waters of the La Maddalena Archipelago, northeast of Sardinia (Italy), in order to validate a high resolution forecasting numerical system for the management of oil-spill emergencies in an area of very high environmental value. Three transects perpendicular to the coast closing the narrowest passages in the Archipelago were realised. Other currentmeter data have been acquired inside the Bonifacio Mouths from an ADCP mounted on the R/V Urania along transects in the main east-west trough crossing the Mouths. Finally three experiments with a drifter floating on the surface have also been organised in the period April-June 2009 to acquire data on the surface circulation in the area of the Bonifacio Mouths and La Maddalena Archipelago. Here preliminary results on the circulation in the area are given, followed by final indications on the feasibility of the ADCP configuration on Italian Coast Guard patrol boats.

1 Introduction

The Bonifacio Mouths (or Strait) is between Sardinia (Cape Testa and Punta Falcone) and Corsica (Cape Pertusato) with high environmental value for the outstanding importance to the landscape and the wide variety of habitats and the presence of protected areas (Habitat Directive, 1992 [1]; D.L. 10/94; D.P.R. 17.05.1996; Décret du 23 09 1999 "Création de la Réserve Naturelle des Bouches de Bonifacio"; D.L. 11.05.2001, n.391; [2]). For the legal status of International Strait, every year it is crossed by thousands of ships particularly carrying dangerous or polluting materials [3, 4, 5, 6] and, during summer months, by thousands of small boats as well as large yachts.

In order to manage environmental emergencies caused by spills of hydrocarbons (oil spill) into the sea, the implementation of an innovative system of forecasting and monitoring of marine circulation at coastal scale started in 2009 in the framework of the SOS-BONIFACIO project (www.sos-

bocchedibonifacio.eu).
The system is composed by nested numerical models with different spatial scales and by in-situ measurements for the characterization of the current and the meteorological field in the area. The measurement of currents was realised through several experiments with Lagrangian CODE drifters and hydrodynamic measurements by vessel mounted acoustic currentmeters (Acoustic Doppler Current Profiler, ADCP). The acquired data have been used both to characterize the hydrodynamics in the area and verify the numerical coastal model outputs inside the Bonifacio Mouths as in the La Maddalena Archipelago.
In this paper the first results from the analyses of some experiments are shown with short technical aspects particularly regarding one experiment with the ADCP mounted on a patrol boat of the Italian local Coast Guard, a new approach to this kind of measurements. This configuration of the ADCP permits the characterization of the full water profile interesting reconstructions along tracks, apart the first meters from the surface. This instrument has been widely used since several years [7, 8, 9, 10] but with different modes of acquisitions than in our experiments that is quite innovative. In order to evaluate the circulation also at the surface, Lagrangian CODE drifters have been used to measure the hydrodynamics with some differences in the instruments configurations than what realised in the past by several authors in other Mediterranean coastal areas [11, 12, 13].
In the following paragraphs the area, the bibliographic data and then the methods used to acquire and elaborate the current data will be described. The analyses of the current data will follow then concluding with a final discussion.

1.1 The area

In the western Mediterranean, the Bonifacio Mouths are a 11 kilometres-wide strait between Sardinia and Corsica, and dividing the Algero-Provencal basin (west) from the Tyrrhenian sea (east) through a threshold with a maximum depth of about 100 m. La Maddalena Archipelago is composed by several small islands, rocks, banks and covers the eastern part of the Mouths with a maximum depth of about 50-60 meters. High current fields cross the area particularly during strong Mistral (north-western) or Greco (north-eastern) wind events. The wind speed is amplified due to the Venturi effect, causing high waves decreasing safety at sea, also during summer when touristic presence increases a lot. For all these reasons several accidents have occurred during the years involving both large vessels and small yachts, with a consequence increase in danger for the marine environment (Sorgente B., personal communication).

1.2 Historical data

After the establishment in 1972 of the NATO military base on the island of Santo Stefano, in the second half of the ‘70s studies have been conducted on the circulation in the La Maddalena Archipelago [15, 16, 17, 18, 19, 20, 21, 22] and, particularly, in the Bucinara Channel (Figure 1). This is 8 km long and northwest-southeast oriented, 2 km at its longest width and with a maximum depth of 40 m, placed between Sardinia and the Archipelago. Its orientation and shallow depth permits Mistral winds to sensibly act on the water transport influencing the circulation in the whole Archipelago with water coming from the Mouths.

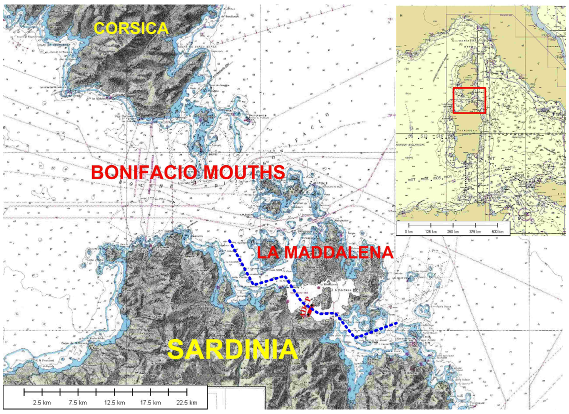

Figure 1: Map of the area of study. Blue dots indicate the Bucinara Channel, while red line the ADCP track mounted on the Coast Guard patrol boat.

Comparisons of current and meteorological data coming from the station of Guardia Vecchia show a direct correspondence between wind and current both in direction and intensity with short periods of transition between the reversal of wind and current. High coherence at low frequencies is also verified by [19] between the east-west component of the wind stress and currents along-coast and that 50-60% of the variance of sea currents is related to the stress of the prevailing winds. Also in the studies from CNR-CNEN [15] it is possible to note that, with westerly winds, the "current speed progressively increases along the length of the Channel so to register at Cape d'Orso around twice the speed measured as the beginning of same Channel", as also reported by [22]. [22] measured seasonal differences with a uniform behaviour of the water mass in winter while a two layer system in summer with one more superficial layer, often 15-30 m, which follows the wind and sometimes reverses.

[23] finally establishes that the morphology of the Archipelago may enhance the effect of the wind so that it can form large-scale internal waves that lead to sudden large changes in sea temperature, up to 20 m depth in summer and throughout the column in the winter, and with a delay of up to 6 hours compared to the passage of weather fronts over the area.

About the reconstruction of the surface circulation in the Mouths, Canò and Stocchino [14] (Figures 2 and Figure 3), identify two main north-westward strands along the western Corsican coast, but also south-eastward to the Gulf of Porto Torres, while with westerly winds (Figure 3) the main stream enters the Mouths dividing into two branches and creating strong currents in the Mouths and also in the Bucinara Channel. At the eastern exit of the Bucinara Channel the current moves southward along the eastern coast of Sardinia following the general circulation, while that leaving east of the island of Lavezzi meets the cyclonic vortex in the Tyrrhenian Sea [23]. During the summer, surface longshore currents opposite to the wind are also observed, especially near the island of

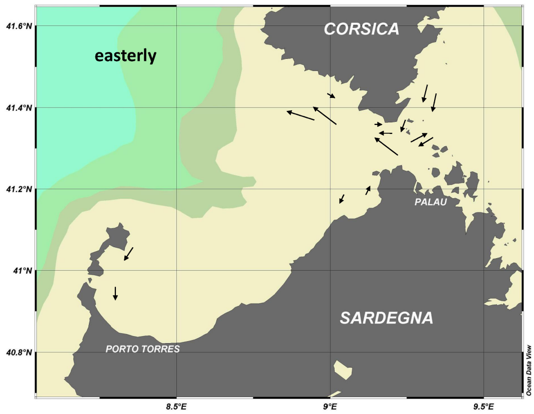

Figure 2: The surface circulation in the Bonifacio Mouths as by Canò and Stocchino (1966, [14]) with easterly winds.

Lavezzi [23].

2 Methods

The acquisition of current data from patrol boats and Lagrangian drifters has been done in strict collaboration with the local Coast Guard of La Maddalena that is in charge for the control of the marine area and to which the realising oil-spill forecasting system is addressed. Current data have been correlated to meteorological ones acquired at the local meteorological station of Guardia Vecchia, on the La Maddalena island. It is important to notice the location of the station of Guardia Vecchia in the extreme south-east of the Mouths, lightly covered by northern and southern winds for the presence of Corsica and Sardinia and where Mistral and Libeccio winds are measured as westerly, due to the Venturi effect crossing the Mouths.

2.1 ADCP acquisitions

Two different approaches have been used to characterise the hydrodynamics in the area by ADCP. Where depth was over 50-60 m as in the Bonifacio Mouths, the acoustic RDI Workhorse 300 kHz, mounted on the R/V Urania of CNR, was used, while in shallower waters, as in the Bucinara Channel, a RDI Workhorse Sentinel 600 kHz mounted on a local Coast Guard patrol boat.

The experiment in the shallow Bucinara Channel was realised on August 28th using a patrol boat unsinkable fibreglass unit model Class 500 with a length overall of 10.4 m, a width of 3.75 m and a draught of 0.65 m. Here the ADCP 600 kHz by Teledyne RD Instruments (CA, USA) was mounted and used in Broadband mode. The external structure holding the ADCP was a 3 meters aluminium pile fixed horizontally by aluminium bars to stanchions of the patrol boat (Figure 4). The ADCP was fixed at the lowest extremity of the pile through flanges, downward oriented with

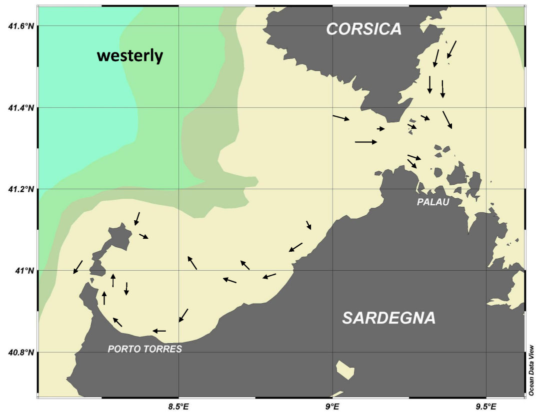

Figure 3: The surface circulation in the Bonifacio Mouths as by Canò and Stocchino (1966, [10]) with westerly winds.

the beam 3 at 45 degrees to starboard of the vessel stem. The ADCP measured currents in a depth range from 2 meters to 52 meters. Inside the patrol boat a PC acquired current data from the ADCP through the RD Instruments VMDAS software linked in real-time with a Global Positioning System (GPS) for the position. Outside the patrol, the GPS by C-map acquired boat position with a frequency of 3 seconds. The acquisition was along one transect perpendicular to the coast from Punta Fico to Cape D'Orso, a narrow passage in the Bucinara Channel, with a boat speed of 4-4.5 knots (Figure 1). Finally data have been elaborated using the CODAS3 programme, interfaced with MATLAB for the graphic. The ACDP on the R/V Urania of CNR acquired current data along the water column, like the previous one mounted on the patrol boat, in 4 m-wide cells with an interval of 1 second then averaged at 5 minutes by the Data Acquisition System (VMDAS). Data have been processed with CODAS3 software as above. One-day acquisition along three transects along the Mouths were realised in November 2008 during the MedCO08 cruise organised by IAMC CNR Oristano and ISMAR CNR La Spezia.

2.2 Drifter experiments

Measurements of the current field at surface were obtained with floating buoys (coastal drifters with GPS and satellite telemetry). The drifter used in all experiments is the CODE drifter, from US Technocean, and consists of a white cylinder 110 cm high and with a diameter of 15 cm and four arms perpendicular to the hull then supporting four blue sails, for a total area of 2 m^2. The frequency of acquisition was hourly during the first experiment and every 20-minutes in the followings. It mounted an ARGOS satellite transmitter, a GPS and a temperature sensor. The position of the buoy was measured either by satellite triangulation and GPS. Three experiments have been carried out using the drifters with a variable duration between 2 and 36 days until the stranding of the drifters: LEONIDA (22/04-27/05/2009);

Figure 4: The ADCP mounted on the left side of the Coast Guard patrol boat is visible in the water in the red circle.

BOCCHE0609 (01-05/06/2009); PROSPERO (30/06-02/07/2009). During the months of July and August the experiments were interrupted because of the intense boat traffic in the study area.
Data from the experiments have been downloaded from the French ArgosWeb-CLS website in ASCII format for the first experiment and in binary format for the following three experiments. Data have been cleaned making a median for each interval of one hour (in the first experiment) or 20 minutes (the following two experiments) then eliminating data out of a range set by the mean + / - three times their standard deviations.

3 Analyses

3.1 Lagrangian data

In the first experiment called LEONIDA, drifter speed ranged between 0-0.5 $m{\cdot}s^{-1}$ with peaks up to about 1 $m{\cdot}s^{-1}$. The highest speeds have been during westerly winds, usually quite strong Mistral events several days long while the lowest during easterly ones. In the following Figures 5, 6, 7 the different winds have been divided into four directional classes:

- northern wind ($\alpha < 45°$ and $\alpha > 315°$) in blue;
- eastern winds ($45° < \alpha < 135°$) in red;
- southern winds ($135° < \alpha < 225°$) in cyan;
- western winds ($225° < \alpha < 315°$) in green.

What Figure 5 shows is that Mistral events coincide with a sudden and strong increase of the drifter speed but not always wind and drifter directions. In fact at the beginning and at the end of the experiment drifter moved differently, opposite in the first case due to local currents inside the island of La Maddalena archipelago and north-westerly in the second due to a strong alongshore current generated or increased by the Mis-

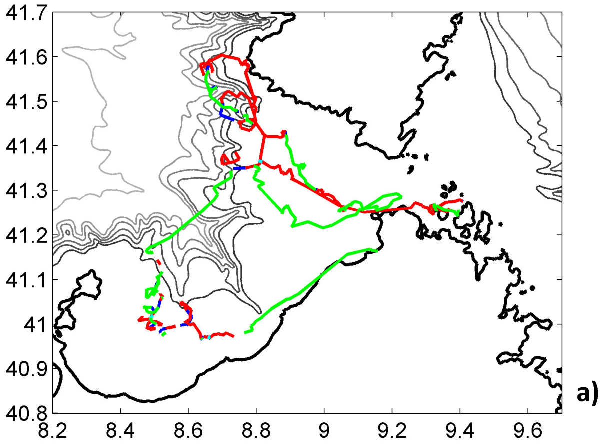

Figure 5: Drifter tracks with different wind conditions during the experiment LEONIDA.

tral.
This experiment, the longest of the three played with over 35 days of measurements, clearly shows the main forcing of surface currents in the Strait of Bonifacio, i.e. in order of importance, wind and tides. Without the wind forcing or during eastern low winds, tidal shows its presence by forcing the buoy to draw circles or ellipses with a period of 17-18 hours.
The buoy in the second experiment called BOCCHE0609 (Figure 6) shows very low speeds and generally less than 0.3 m·s^{-1} (over 89%). Some data (9%) show the rate of about 0.6 m·s^{-1}, with peaks up to 0.9 m·s^{-1}, probably due to a strong southwestern wind with about 20 m·s^{-1} which has also triggered a sharp drop in the surface temperature. Finally, despite its short duration of only 2 days, the experiment PROSPERO (Figure 7) was affected by a wind of moderate intensity (maximum of 9-10 m·s^{-1}) determining speed of the buoy generally less than 0.3 m·s^{-1} (66% data) with peaks of 0.7-0.8 m·s^{-1}.
Looking at the Figures 6 and 7 of the last two experiments, unfortunately really short in time, the drifter moved following the wind before beaching.

3.2 ADCP data

In Figure 8 the maps of horizontal current speed of the measured by ADCP mounted on the Urania vessel, the MedCO08 cruise during which a very low quite constant Mistral blew all the time of the acquisition, are represented with two depths (23 m and 43 m) at three levels of magnification. The two depths does not greatly differ and the water column moves barotropically (i.e. there are no vertical variations of horizontal velocity in the considered depth range). The whole region (maps on the left) shows a cyclonic circulation (clockwise) in the upper Tyrrhenian Sea. From the following zooms is clear that the water flow at the Mouths is directed from west to east, mainly driven by the wind that blows

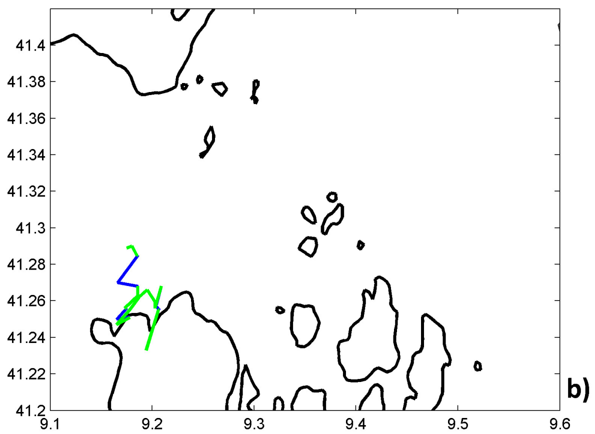

Figure 6: Drifter tracks with different wind conditions during the experiment BOCCHE0609.

mainly in the same direction.
The ADCP data collected in the Bucinara Channel on the section between Punta Fico and Cape d'Orso, performed in a day of constant north-eastern mean wind, show a relatively high speed (Figure 9) along the section with an increase on the Cape d'Orso (west side) and near the bottom while lower speeds at the center of that section. This is also visible with the current direction (Figure 10), constant throughout the water column, but passing gradually from about 180° in the vicinity of Punta Fico to about 140° near Cape d'Orso.

4 Conclusions

The work done in the Bonifacio Mouths and the Archipelago of La Maddalena has yielded interesting information on two aspects, one scientific and related to the study of the circulation in the area, also in view of the validation of a local numerical circulation model, and a second aspect mainly technical with the verification of the validity of using Coast Guard patrol boats to take measurements of current meters in coastal areas, generally not reachable by large vessels with hull mounted ADCP.
The circulation inside the Bonifacio Mouths and the La Maddalena Archipelago has substantially verified what described by several authors in years between '60s and early '80s [14, 15, 18, 19, 22, 23, 21]. Inside the Mouths the water column moves barotropically with a stream of water at the Mouths mainly driven by the wind. When the wind misses, the main forcing is the tide. In its upper layer, however, current arising within the Archipelago led to the current direction opposite to those of the wind sometimes, as happened early in the first experiment LEONIDAS with the Lagrangian buoy between the islands of the La Maddalena Archipelago. Inside the Bucinara Channel the flow is continuous throughout the described section and

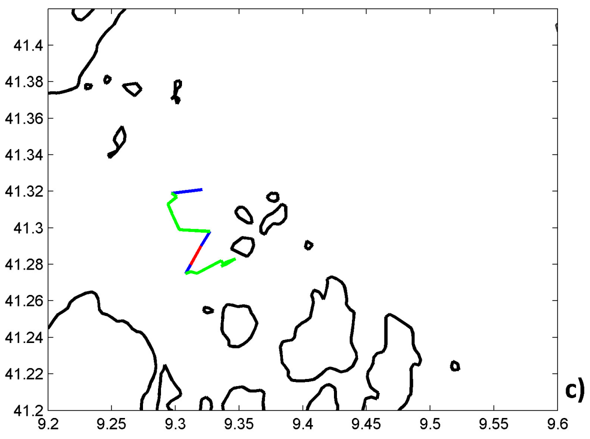

Figure 7: Drifter tracks with different wind conditions during the experiment PROSPERO.

enforced mainly by the wind, as also observed by [19].
Further analysis, data and experiments and the support of the numerical model will allow to obtain important information and details on the circulation in a so environmentally and touristic important area like that of the Bonifacio Mouths and La Maddalena Archipelago.
Finally, about the technical aspect, the use of Coast Guard patrol boats permits a frequent repetition of the experiments in different weather conditions and in very shallow waters with a reduction in time and costs to assembly and disassembly the external support apparatus and other logistic costs. Limits are due to the sudden stops for emergency and reduced times of operations (usually possible during light hours).

5 Acknowledgements

A special thank to the La Maddalena Coast Guard for its strong support to the project activities. Thanks also to Captain Vincenzo Lubrano Lavadera of the R/V Urania vessel and its crew and technicians onboard. This work is part of the project SOS-BONIFACIO (contract DEC/DPN 2291 of 19/12/2008) funded by the Directorate General for Nature Protection of the Italian Ministry for Environment, Land and Sea.

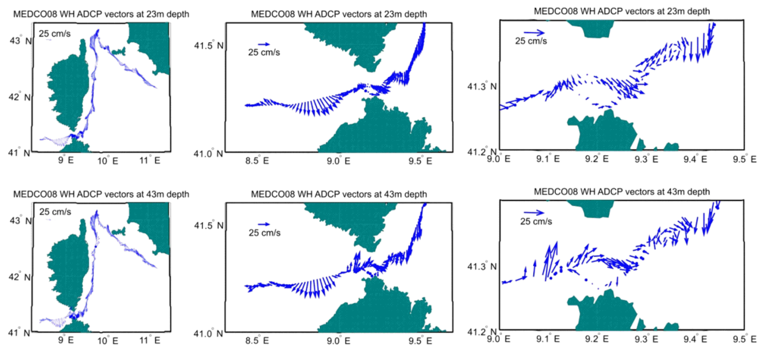

Figure 8: Circulation maps at 23 m and at 43 m of depth, at three zoom levels.

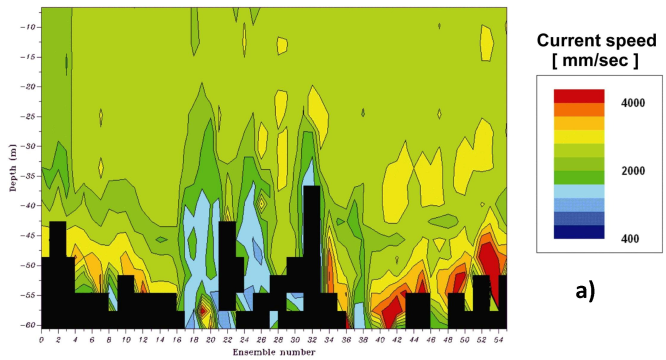

Figure 9: Current speed measured in the Bucinara Channel with the ADCP.

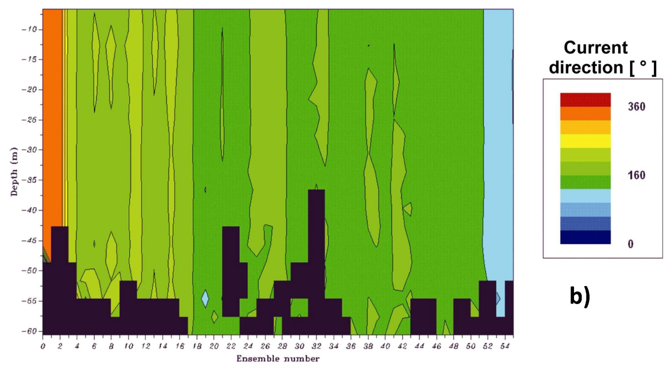

Figure 10: Current direction measured in the Bucinara Channel with the ADCP.

References

[1] European Commission. Habitat Directive 92/43/CEE del 21 maggio 1992 relativa alla conservazione degli habitat naturali e seminaturali e della flora e della fauna selvatiche. 1992.

[2] A. Cossu, V. Gazale, M.R. Martinelli, I. Milella, C. Morucci, A. Pais, A. Porcheddu, S. Saba, P.L. Solinas, and G. Virdis. L'Arcipelago di La Maddalena: Aspetti naturalistici e prospettive per la costituzione di un Parco Internazionale. *Atti del I convegno Internazionale S.Teodoro*, 1989.

[3] AP. Arrete' Prefectoral n. 84/94 du 03.11.1998 de la Prefecture Maritime de Toulon - Reglementant la navigation dans le Bouches de Bonifacio en vue de prevenir les pollution marines accidentelles. 1998.

[4] D.M. Decreto Ministero dei Trasporti e della Navigazione 27 novembre 1998 - "Disposizioni relative all'organizzazione del traffico nelle Bocche di Bonifacio". *Gazzetta Ufficiale*, 1998.

[5] European Commission. Regulation (EC) No 417/2002. *OJ L 64 of 7.3.2002*, 2002.

[6] IMO. Risoluzione dell'IMO A.766(18) "Navigazione nello Stretto di Bonifacio" del 4 novembre 1993. *Ships' Routeing, eigthth editing 2003*, 2004.

[7] Y. Leredde, C. Denamiel, E. Brambilla, C. Lauer-Leredde, F. Bouchette, and P. Marsaleix. Hydrodynamics in the Gulf of Aigues-Mortes, NW Mediterranean Sea: In situ and modelling data. *Continental Shelf Research*, 27(18):2389–2406, 2007.

[8] A. Rubio, P. A. Arnau, M. Espino, M.M. Flexas, G. Jordà, J. Salat, J. Puigdefabregas, and S.-A. Arcilla. A field study of the behaviour of an anticyclonic eddy on the Catalan continental shelf (NW Mediterranean). *Progress in Oceanography*, 66:142–156, 2005.

[9] E. Garcia-Gorriz, J. Candela, and J. Font. Near-inertial and tidal currents detected with a vessel-mounted acoustic Doppler current profiler in the western Mediterranean Sea. *Journal of Geophysical Research*, 108(C5):1–21, 2003.

[10] G.P. Gasparini, M. Abbate, A. Bordone, G Cerrati, C. Galli, L. Lazzoni, and A. Negri. Circulation and biomass distribution during warm season in the Gulf of La Spezia(north-western Mediterranean). *Journal of Marine Systems*, 78(Suppl.):S48–S62, 2009.

[11] P.M. Poulain. Drifter observations of surface circulation in the Adriatic Sea, between December 1994 and March 1996. *J. Mar. Syst.*, 20:231–253, 1999.

[12] P.M. Poulain and E. Zambianchi. Surface circulation in the central Mediterranean Sea as deduced from Lagrangian drifters in the 1990s. *Continental Shelf Research*, 27(7):981–1001, 2007.

[13] A. Molcard, P.M. Poulain, P. Forget, A. Griffa, Y. Barbin, J. Gaggelli, J.C. De Maistre, and M. Rixen. Comparison between VHF radar observations and data from drifter clusters in the Gulf of La Spezia (Mediterranean Sea). *J. Mar. Syst.*, 78:S63–S78, 2009.

[14] M. Canò and C. Stocchino. Sulle correnti nel Golfo dell'Asinara e nelle Bocche di Bonifacio. *Atti Convegno dell'Associazione Geofisica Italiana*, pages 31–36, 1966.

[15] CNR, S. Terenzo and CNEN, Fiascherino. Data report: current and temperature measurements in the Archipelago of La Maddalena. *CNEN, RT/FI (78)*, 14:1–311, 1978.

[16] CNR, S. Terenzo and CNEN, Fiascherino. Risultati degli esperimenti con traccianti svolti nell'Arcipelago della Maddalena per la determinazione del coefficiente di diffusione turbolenta locale. *CNEN, RT/FI (78)*, 13(1):1–131, 1978.

[17] CNR, S. Terenzo and CNEN, Fiascherino. Misure di temperatura e salinità con sonda automatica nell'Arcipelago della Maddalena. *CNEN, RT/FI (79)*, 3:1–16, 1979.

[18] A. Bruschi, G. Buffoni, A.J. Elliot, A. Esposito, and G.M.R. Manzella. A numerical investigation of the wind-driven circulation in the Archipelago of La Maddalena. *CNEN, RT/FI (80)*, 14:1–33, 1980.

[19] A. Bruschi, G. Buffoni, A.J. Elliott, and G.M.R. Manzella. A numerical investigation of the circulation in the Archipelago of La Maddalena. *Oceanologica Acta*, 4(3):289–295, 1981.

[20] M. Astraldi, G.M.R. Manzella, and C. Stocchino. Circolazione delle correnti nell'arcipelago di La Maddalena. *CNEN, RT/FI (80)*, 8:1–48, 1980.

[21] A. Esposito, G.P. Gasparini, R. Meloni, and C. Stocchino. Circolazione nei Canali dell'Arcipelago della Maddalena. *Atti del 4° Congresso AIOL*, 1983.

[22] M. Astraldi, G. Buffoni, A. Bruschi, A. Esposito, G.P. Gasparini, G.M.R. Manzella, and R. Meloni. Sviluppo di modelli idrodinamici dell'arcipelago della Maddalena. *Atti del 4° Congresso AIOL*, 1983.

[23] G.M.R. Manzella, E. Bohm, and E. Salusti. Evidence of internal waves in the Archipelago of La Maddlena. *Il Nuovo Cimento*, 6C(4):381–400, 1983.

Long Term Ecological Research (LTER) in the marine coastal environment: basic concepts and keystones from the plankton communities

A. Pugnetti[1], M. Bastianin[1], F. Bernardi Aubry[1], E. Camatti[1], A. Conversi[2], G. Socal[1], M. Ravaioli[3]
1, Institute of Marine Sciences, CNR, Venezia, Italy
2, Institute of Marine Sciences, CNR, Pozzuolo di Lerici (SP), Italy
3, Institute of Marine Sciences, CNR, Bologna, Italy
alessandra.pugnetti@ismar.cnr.it

Abstract

Long-Term Ecological Research (LTER), which focuses on multidecadal observations, provides the correct approach and temporal context needed to avoid misjudgements in our attempts to understand and predict changes in marine ecosystems and to manage them. The LTER approach is particularly important when trend detection is a central issue, as in global change, and it is also critical for testing ecological theories on community dynamics, variability and resilience, enhancing our capacity of forecasting and of managing resources. Coastal marine ecosystems is among the most ecologically and socio-economically vital ecosystems in the planet; they are intrinsically highly variable, as a consequence of their connectivity to both land and open sea. Within these systems plankton is a primary driver of chemical and biological dynamics, directly affecting water quality, biogeochemical cycling and food supply to consumers. In marine costal ecosystems many regulatory processes fluctuate over multiple time scales and human disturbance is intense, making it a challenge the individuation of plankton "patterns". The study of coastal plankton communities, with a LTER perspective and with an across-system comparisons, appears crucial, in order to identify common patterns of variability and how they change with scales. In this paper we review the contribution to these issues coming from the Italian marine LTER sites, with emphasis on the researches carried out in the Northern Adriatic Sea.

1 Introduction

A typical psychological human trait is the so-called "change blindness" [1] that deals with the difficulties observers have in noticing large environmental changes, when they are not framed in the appropriate long-term recordings context. At the time scale of decades (or even less) human beings are inclined to perceive the world as static, typically underestimating the degree of change that does occur [2, 1]. From this inability to perceive slow changes and to interpret their cause-effect relationships, it stems that processes acting over years (namely: decades) are hidden and reside in what has been defined by Magnuson [3] as the "invisible present". The human knowledge of the natural world is strongly shaped and guided by the frequency, duration and geographic magnitude of our observations. The so called "Long-Term Ecological Research" (LTER), which is based on the analysis of multi-decadal observations, supplies the appropriate approach and temporal context that are needed to avoid misjudgements in our efforts to understand and predict changes in the world around us and to manage our environment. LTER may have different meanings, according to the resource being considered and to the phenomenon under investigation: it should, anyhow, be based on the time scale that enables signals of environmental change to be distinguished from background noise. LTER indeed should allow the recognition of the range of natural variability of ecological systems, providing baselines against which determining if a system has significantly changed. Therefore, ecological time series can be regarded as essential tools to detect meaningful shifts and assess whether changes are attributable to human or natural causes, thus enhancing our capacity of forecasting and of managing resources. Furthermore, LTER is a crucial tool to challenge paradigms and scientific dogmas of ecology, being critical for testing ecological theories on the way ecosystems or biological communities are organized and on community dynamics, variability and resilience. LTER is, indeed, intrinsically involved in what can be defined the "fundamental problem of ecology", that is: the attempts to discover and define patterns, their causes and consequences, within and across ecosystems [4]. In this paper we aim to highlight the role and contribution of the LTER networks to the multifaceted and composite nature of marine LTER, considering the Italian marine LTER sites, with emphasis on the plankton communities and on the researches carried out in the Northern Adriatic Sea.

2 The LTER sites network

Although time-series observations are recognized to represent a critical element of ecology, they are also, paradoxically, among the easiest victims of funding shortage. The predominant picture of LTER research and monitoring shows that it frequently leans on the personal effort and dedication of individual scientists, with a frequent imbalance between the energy invested and the scientific result yield [5]. In the last decades, however, some programmes initiated a new era in time-series investigations [6]. The International LTER network (I-LTER) began in 1993, fostered by the United States LTER (US-LTER), and it was fuelled by the exigency of cooperation at local, regional and national levels through sharing and integrating data and findings, creating synergies on global projects and delivering scientifically-sound research to decision makers and public [7]. LTER sites consist of various reference ecosystems, research and monitoring facilities that set a network across the world. At the European level the LTER networking process started in 2004, in the framework of the network of excellence "AlterNet" and in compliance with the European strategy to overcome fragmentation in the field of environmental research and monitoring. LTER-Europe (E-LTER, [8]) could not rely on a steady long-term support from a central funding body and stakeholder, comparable to National Science Foundation for US-LTER, and it was essentially built on existing facilities with a strong LTER connotation. Thus, E-LTER developed into a complicated prospect of European environmental monitoring schemes, data bases,

Marine Environment	Transitional Environments	Lacustrine Environment	Terrestrial Environment
Northern Adriatic Sea	Po River Delta	Subalpine lakes	High altitude Apennines
Gulf of Naples	Lagoon of Venice	Lentic ecosystems of the Apennines	Forests of the Alps
Marine Ecosystems of Sardinia		Lacustrine Ecosystems of Sardinia	Forests of the Apennines
Marine Protected Area of Portofino		Himalayan Lakes (*)	Mediterranean Forests
Antarctica Research Stations (*)			Lowland Forests
			Mediterranean Island (Pianosa)
			Castelporziano Natural Park
			Western Alps
			Coastal dunes of central Italy

(*) Extra-territorial sites

Table 1: List of the twenty LTER-Italy Sites (updated at January 2011)

and institutions. In March 2010 E-LTER comprised 18 formal national LTER member networks [8]: Austria, Czech Republic, Finland, France, Germany, Hungary, Israel, Italy, Latvia, Lithuania, Poland, Portugal, Romania, Slovenia, Slovakia, Spain, Switzerland, and the United Kingdom. Each country established a national network according to national peculiarities, as it concerns funding of research projects, institutions and infrastructures. However, a process of design, integration and harmonisation of the LTER research activities and facilities is successfully ongoing and comparable overviews are defined [8]. Although a number of similar organizations exists, LTER is the only one that has the whole set of the following attributes: i) it generates field data at different scales, in a wide array of ecosystems, with a marked trans-ecodomain and across ecosystems approach, ii) it dedicates itself to the provisioning, documentation and continuous use of long-term information and data on ecosystems with a time horizon of decades to centuries, iii) it contributes to better understanding the complexity of natural ecosystems and coupled socio-ecological systems, iv) it aims to the integration of LTER and Long-Term Ecological Monitoring (LTEM). Italy entered the ILTER network in 2006, at the end of a scientific and organizing process that started during the 1990s [9]. At the moment (2010), LTER-Italy consists of a group of 20 sites belonging to terrestrial, freshwater and marine ecosystems (Table 1).

3 LTER and plankton in marine coastal ecosystems

Marine coastal ecosystems are among the most ecologically and socio-economically vital sites on Earth. Given their global importance in terms of ecological diversity and economical value, and the potential impacts of men's activities (primarily: over-harvesting, pollution, and direct or indirect effects of climate change), their health is a matter of major concern, both for scientists and resource managers. The synergistic effects among climate change and other anthropogenic impacts, from one side, and among abiotic and biotic responses, from the other, require improvements to our definition of natural variability and to existing predictive framework [10]. Also the restoration of human impacted marine costal systems calls for LTER, as a tool supporting the formulation of clear and biologically sound hypotheses. The fundamental interdisciplinary nature of LTER, claiming for the actual share of methodologies, experiments, ecological data and findings, generates an intellectual and experimental partnership among disciplines and researchers that represents an essential requirement for knowledge driven environmental policy too. Coastal systems represent a hard challenge when facing the task of determining status and trends in water quality and ecological conditions. These systems are, by their very nature, highly variable, at different spatial and temporal scales, due to some unique attributes, e.g.: the shallowness, the strict benthic-pelagic coupling and the connectivity to both land and sea [11]. Indeed, human and natural perturbations often interact in these systems, over multiple time and space scales. The plankton communities are the bases of the food webs in marine systems and, therefore, the pathways and efficiencies of transfer of carbon and energy to upper trophic levels depend on the quantity and composition of the plankton community. Recent evidences suggest that plankton is a more sensitive indicator of environmental change than the abiotic variables themselves: the non linear response of biological communities may, indeed, amplify the environmental perturbations [12, 13]. Environmental perturbations may interfere with life histories and with the synchrony between trophic levels, leading to a trophic mismatch, with severe implications for energy flow to higher trophic level [14]. The definition of recurrent patterns and trends of plankton represents a standing task for the study of marine coastal environments. Indeed, the presence of many regulatory processes fluctuating over multiple timescales and the intense human disturbance in the nearshore coastal ecosystems across the world, makes uncertain even the existence of canonical plankton patterns [15]. Moreover, when interpreting the impacts of long-term changes on plankton communities, we must be aware that almost all plankton time series, across the world, are shorter than 50 years in duration [12], frequently spanning only the last 2-3 decades. The dynamics of phytoplankton, the dominant primary producers in most aquatic systems, have been recently reviewed by Cloern and Jassby

[11], showing that variability of coastal phytoplankton cannot be identified with a small set of common patterns. Whereas much of phytoplankton variability in the open oceans is generated by the annual cycles of solar radiation and atmospheric inputs, phytoplankton variability in coastal waters is related to many additional processes (e.g.: interactions with land, sea, atmosphere, sediments), with the main controlling processes varying both regionally and temporally. The intrinsically high variability of this community must be taken into account, also for environmental management purpose: actually, the phytoplankton is, at present, the only planktonic element included among the water quality indicator in the European Water Framework Directive (EC 2000). In this viewpoint, any effective use of the phytoplankton community as a biological quality element poses several constraints and implies a strong necessity of individuation and definition of adequate baselines against which evaluate local vs. large scale changes, as well as trends [16, 17, 18]. Multidecadal studies are fundamental also for the definition of patterns and trends of the zooplankton communities. Zooplankton are critical for the functioning of aquatic food webs, being the major grazers and, therefore, providing the principal pathway for energy transfer from primary producers to consumers at higher trophic levels. Copepods, the most prominent zooplankton taxon, are the most abundant multicellular animals on the planet [19]; however, zooplankton communities are actually highly diverse, performing, therefore, a variety of ecosystem functions. The relations between climate change and other anthropogenic stressors with zooplankton [20], analyzed through a long-term perspective, show manifest changes in the distribution and phenology of zooplankton, in the timing of important life-cycle events, in the abundance and community structure.

4 The marine component of the lter-italy network

The institution of LTER-Italy, leaded by a Steering Committee, had a strong bottom-up nature and it can rely only on the different institutions' responsibilities and funding, and on the researchers' personal efforts and willingness. As for its governance structure (laid down by the LTER-Italy bylaws), LTER - Italy is made up by the responsibles of each LTER site, which constitutes the "National Site Representative Conference" and by a Coordinating Committee, whose members are elected by the site responsibles and are representative of the main institutions involved in LTER research.

In accordance with I-LTER and E-LTER, the driving aims of LTER-Italy are, first of all, to foster collaboration and coordination among LTER ecosystems, researchers and institution; then, to improve comparability and exchange of LTER data and findings; finally, to deliver information to policymakers and the public. LTER-Italy has a strong interdisciplinary nature, being made up by terrestrial, marine and freshwater ecosystems (Table 1). The links and feedbacks among terrestrial and aquatic ecosystems, when addressing global scale issues, such as climate change, are readily acknowledged but poorly investigated. The comparison across eco-domains is rarely achieved in ecological studies and conceptual and practical barriers among scientists working in the different domains have profound implication for addressing critical

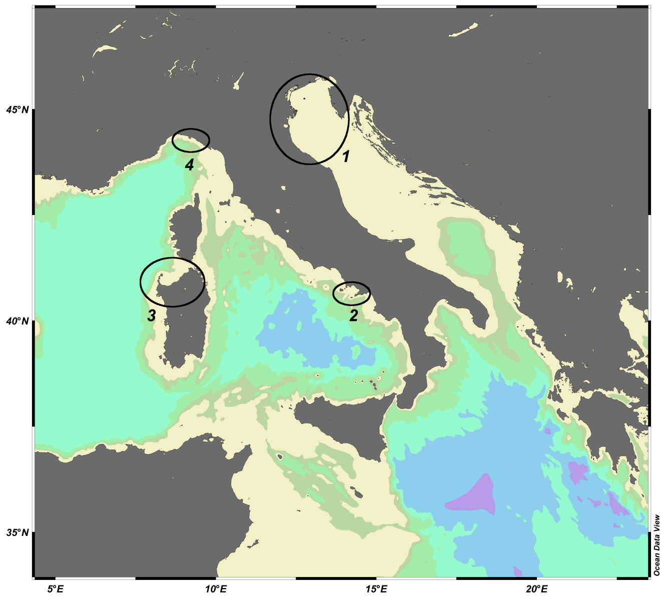

Figure 1: Location of the LTER-Italy marine sites and institutions responsible of each site: 1) Northern Adriatic sea - CNR ISMAR and OGS 2) Gulf of Naples – SZN A. Dohrn 3) NW Sardinia coast Univ. Sassari 4) Marine protected area of Portofino – Univ. Genova

ecological issues (e.g. biodiversity, climate change, invasive species), that are of basic importance also for conservation and management policies. Beside their obvious differences, marine and terrestrial systems may be seen to represent end-points of a continuum: the cross-sector collaboration among marine and terrestrial expertise, which is one of the most peculiar features of LTER-Italy, should represent a unique chance for approaching this insight.

Four out of the 20 LTER-Italy sites are coastal marine sites (the others being terrestrial and freshwater): the Northern Adriatic Sea, the Gulf of Naples, the Sardinia costal waters and the Portofino marine Protected Area (Fiure 1). These sites are under the responsibility of different institutions (Fiure 1). Despite the differences characterizing their history, these institutions share similar LTER philosophy, objectives and plans. The study of the plankton communities represents the main subject of common activities. The truly integration of the LTER observations on marine plankton at the national level, through the comparison of the plankton time series in each site, the individuation of shared hypotheses, the definition of common experimental protocols and activities, represents a difficult challenge, but also a vital necessity for a meaningful and fruitful evo-

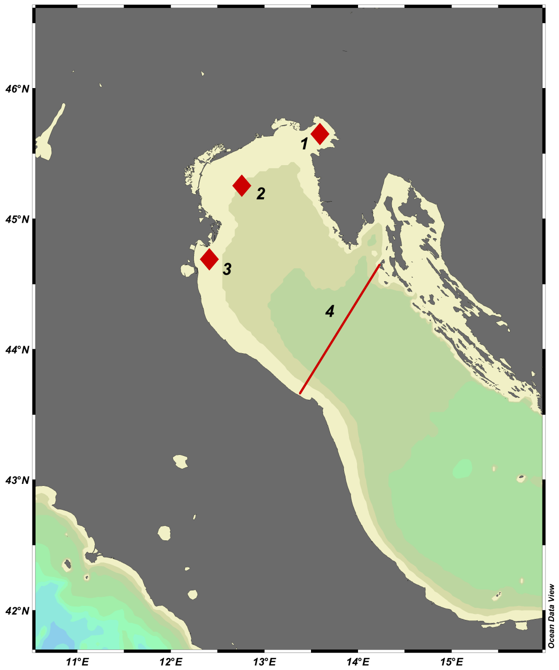

Figure 2: Stations of the Northern Adriatic LTER site and institutions responsible of each station 1) Gulf of Trieste, OGS Trieste-ISMAR Trieste 2) Gulf of Venice ISMAR Venezia 3)Po river Delta S1 ISMAR Bologna 4) Senigaglia-Susak transect, ISMAR Ancona

lution of LTER activities. The research focuses mainly on plankton patterns and scales of variability, on the identification of drivers and processes, and on the importance of species-specific attributes. A close collaboration with environmental monitoring programs and oceanographic observation networks is also fostered, with the goal of contributing to coastal resource management too, making the best use of the available information.

Some key issues represent the core of the research on plankton in the LTER-Italy marine sites: i) individuation the dominant scales of variability in plankton biomass and species composition, ii) identification of regime shifts or common trends and of the coherence of their occurrence in space and time, iii) recognition of evidence for external forcing (e.g.: basin scale oscillation, nutrient inputs, alien species, climate change) of variability and the differentiation between long-term signals from interannual noise, iv) search for consistent patterns among ecosystems in terms of relationships between environmental pa-

rameters, plankton biomass and changes in species composition.
The Northern Adriatic Sea (NAS) is one of the 4 LTER-Italy marine sites (Table 1). Three institutions (Figure 2), which hold a long tradition of ecological studies in this ecosystem, are jointly responsible for the 4 LTER research stations in the NAS. The NAS is the northernmost basin of the Mediterranean Sea and is one of the most productive Mediterranean areas. It is characterized by a shallow depth and by a dominant cyclonic circulation. The oceanographic and meteorological parameters show a marked seasonal and interannual variability. The remarkable river inputs (along the Italian coast), the istrodalmatian current (bringing high salinity and oligotrophic waters from the southern basin), and the notable sea-level range (relatively to the Mediterranean area), represent major forcings of the system.
Of ecological relevance are also the urban and industrial inputs and the hydrodynamic exchange between the NAS and the lagoons, located along the Italian coast. The NAS is subjected to a marked anthropic impact (e.g.: nutrient inputs, coastal urbanization, fishing activity, tourism, maritime trade). In the past the basin has undergone eutrophication, and, more recently, has been subject to frequent episodes of large mucilage aggregates [21]. Many ecological researches have been carried out in the NAS, since the second half of the last century, by national and international institutions, most of them focusing on the ecology of plankton communities, also in relation to the main environmental emergencies (e.g.: eutrophication, mucilage aggregates, toxic algae). A huge amount of data and information are available for the NAS and its plankton communities, and in this chapter we synthesize some critical issues about these communities, within the national and international LTER context and principles.
First of all, the LTER activity on plankton has allowed identifying the main seasonal patterns of both phytoplankton [22, 23] and zooplankton taxa [24, 25]. Notwithstanding the elevated spatial and temporal variability, at different scales, of climatic and oceanographic factors that characterize the basins, a seasonal pattern does exist and a sort of "calendar of plankton" is known, at least for the areas that have been sampled with the highest consistency: it represents a baseline against which evaluate possible specific changes and future trends. In particular, as it regards phytoplankton communities, event though species group together in different ways over the year, the taxonomic composition of the dominant associations seems to be highly dependant on season, while environmental conditions can explain mainly the variability of total abundances and biomass [23, 26]. As a consequence, seasonal patterns in biological structure persist in spite of the large variations over time in environmental conditions.
Secondly, pluriannual trends have been identified in plankton communities in the NAS. An analysis of the chlorophyll variations in the years 1970 - 2007 at basin scale [27], demonstrates a tendency towards chlorophyll a reduction, which is particularly strong in the last decade and is mostly located in the eutrophic area under the influence of the Po River. This trend could not be related to temperature variations, but rather to a reduction in the Po nutrient inputs, which induced a general oligotrophication of the system. Also the analysis of the mesozooplankton series in the Gulf of Trieste (where is located the longest time series in Italy) for the pe-

riod 1970-2005 shows extensive changes in the copepod community around the end of the '80s. These include: i) a shift toward smaller species, ii) the appearance of a new species (*Diaixis pigmoea*), iii) the northward spreading of southern species and a general reduction of cold species, and iv) the changes in the phenology of most species. The main hypotheses for these variations include a large scale and abrupt change in the Mediterranean circulation at the end of the 1980s, and the 1°C warming in summer and fall that occurred over the 36 years sampled ([28], see also [29]).
Finally, we wish to stress that the patterns identified for the plankton variability and trends in the NAS, are partially shaped by the annual climatology at the basin scale, but also strongly guided by the area-specific relative importance of disturbance and nutrient enrichment. To this respect, the NAS can be seen as a paradigm of the difficulties that are retained in the LTER series: the choice of the appropriate data set, within the time series itself, and of study area, within the whole basin, are crucial for any descriptive and interpretative goals. The comparison among LTER series, within the NAS basin itself and across the other LTER sites, represents hence the step necessary to avoid misjudgments due to local drivers, and it is crucial for identifying the dominant processes and forcing factors, thus formulating clear and biologically-sound cause-effect hypotheses.

References

[1] D.J. Simons and R.A. Rensink. Change blindness: past, present, and future. *Trends in Cognitive Sciences*, 9(1):16–20, 2005.

[2] J. E. Hobbie. Scientific accomplishments of the long term ecological research program: An introduction. *Bioscience*, 53(1):17–20, 2003.

[3] J. J. Magnuson. Long-term ecological research and the invisible present - uncovering the processes hidden because they occur slowly or because effects lag years behind causes. *Bioscience*, 40(7):495–501, 1990.

[4] S. A. Levin. The problem of pattern and scale in Ecology. *Ecology*, 73(6):1943–1967, 1992.

[5] C. M. Duarte, J. Cebrian, and N. Marba. Uncertainty of detecting sea change. *Nature*, 356, 1992.

[6] H. W. Ducklow, S. C. Doney, and D. K. Steinberg. Contributions of Long-Term Research and Time-Series Observations to Marine Ecology and Biogeochemistry. *Annual Review of Marine Science*, 1:279–302, 2009.

[7] M. Bredemeier, P. Tennis, N. Sauberer, B. Petriccione, K. Torok, C. Cocciufa, G. Morabito, and A. Pugnetti. Biodiversity assessment and change: the challenge of appropriate methods. In R.E. Hester and R.M. Harrison, editors, *Biodiversity under threat*, pages 217–251. RCS Publ., Cambridge UK, 2007.

[8] M. Mirtl. *LTER-Europe design and implementation report – Enabling "nect generation ecological science": report on the design and implementation phase of LTER-Europe under Alter-Net & management plan 2009/2010*. Umweltbundesamt (Federal Environment Agency Austria), Vienna, 2009.

[9] G. Matteucci, F. Bianchi, R. Bertoni, A. Pugnetti, and M. Ravaioli. Ricerche ecologiche e cambiamenti climatici: il ruolo del CNR. In B. Carli, G. Cavarretta, M. Colacino, and S. Fuzzi, editors, *Clima e cambiamenti climatici: le attività di ricerca del CNR*, pages 417–420. Consiglio Nazionale delle Ricerche, Rome, 2007.

[10] C. D. G. Harley, A. R. Hughes, K. M. Hultgren, B. G. Miner, C. J. B. Sorte, C. S. Thornber, L. F. Rodriguez, L. Tomanek, and S. L. Williams. The impacts of climate change in coastal marine systems (vol 9, pg 228, 2006). *Ecology Letters*, 9(4):500–500, 2006.

[11] J. Cloern and A. Jassby. Patterns and Scales of Phytoplankton Variability in Estuarine–Coastal Ecosystems. *Estuaries and Coasts*, 33:230–241, 2009.

[12] G.C. Hays, A.J. Richardson, and C. Robinson. Climate change and marine plankton. *Trends in Ecology and Evolution*, 20:337–344, 2005.

[13] H. W. Paerl, Valdes L. M., B. L. Peierls, J. E. Adolf, and L.W. Jr. Harding. Anthropogenic and climatic influences on the eutrophication of large estuarine ecosystems. *Limnology and Oceanography*, 51:448–462, 2006.

[14] N.C. Stenseth and A. Mysterud. Climate, changing phenology, and other life history traits: Nonlinearity and match-mismatch to the environment. *PNAS*, 99(21):13379–13381, 2002.

[15] C. Duarte, D. Conley, J. Carstensen, and M. Sánchez-Camacho. Return to Neverland: Shifting Baselines Affect Eutrophication Restoration Targets. *Estuaries and Coasts*, 32(1):29–36, 2009.

[16] S. Loureiro, A. Newton, and J. Icely. Boundary conditions for the European water framework directive in the ria Formosa lagoon, Portugal (physico-chemical and phytoplankton quality elements). *Estuarine Coastal and Shelf Science*, 67(3):382–398, 2006.

[17] H. G. Marshall, R. V. Lacouture, C. Buchanan, and J. M. Johnson. Phytoplankton assemblages associated with water quality and salinity regions in Chesapeake Bay, USA. *Estuarine Coastal and Shelf Science*, 69(1-2):10–18, 2006.

[18] R. B. Domingues, A. Barbosa, and H. Galvao. Constraints on the use of phytoplankton as a biological quality element within the Water Framework Directive in Portuguese waters. *Marine Pollution Bulletin*, 56(8):1389–1395, 2008.

[19] H.K. Schminke. Entomology for the copepodologist. *Journal of Plankton Research*, 29(suppl_1):149–162, 2007.

[20] A. J. Richardson. In hot water: zooplankton and climate change. *ICES Journal of Marine Science*, 65(3):279–295, 2008.

[21] M. Giani, A. Rinaldi, and D. Degobbis, editors. *Mucilages in the Adriatic and Tyrrhenian Sea*, volume 353 of *Science of the Total Environment, The*. Elsevier Science, 2005.

[22] F. Bernardi Aubry, A. Berton, M. Bastianini, G. Socal, and F. Acri. Phytoplankton succession in a coastal area of the NW Adriatic, over a 10-year sampling period (1990–1999). *Continental Shelf Research*, 24:97–115, 2004.

[23] F. Bernardi Aubry, F. Acri, M. Bastianini, F. Bianchi, D. Cassin, A. Pugnetti, and G. Socal. Seasonal and interannual variations of phytoplankton in the Gulf of Venice (Northern Adriatic Sea). *Chemistry and Ecology*, 22:71–91, 2006.

[24] B. Cataletto, E. Feoli, S. Fonda Umani, and S. Cheng-Yong. Eleven years of time-series analysis on the net zooplankton community in the Gulf of Trieste. *ICES J. Mar. Sci.*, 52:669–678, 1995.

[25] E. Camatti, A. Comaschi, A. de Olazabal, and S. F. Umani. Annual dynamics of the mesozooplankton communities in a highly variable ecosystem (North Adriatic Sea, Italy). *Marine Ecology-an Evolutionary Perspective*, 29(3):387–398, 2008.

[26] G. Socal, F. Acri, V. Bandelj, M. Bastianini, A.M. Bazzoni, F. Bernardi Aubry, F. Bianchi, G. Cossarini, A. Pugnetti, and C Solidoro. Condizioni ambientali, ciclo vitale ed orologio endogeno nella dinamica del fitoplancton. Evidenze da osservazioni sperimentali nell'Adriatico Nord Occidentale. *Biol. Mar. Mediterr.*, 15(1):396–397, 2008.

[27] P. Mozetič, C. Solidoro, G. Cossarini, G. Socal, R. Precali, J. Francé, F. Bianchi, C. De Vittor, N. Smodlaka, and S. FondaUmani. Recent Trends Towards Oligotrophication of the Northern Adriatic: Evidence from Chlorophyll a Time Series. *Estuaries and Coasts*, 33(2):362–375, 2010.

[28] A. Conversi, T. Peluso, and S. Fonda-Umani. Gulf of Trieste: A changing ecosystem. *Journal of Geophysical Research-Oceans*, 114:10, 2009.

[29] L. Kamburska and S. Fonda-Umani. Long-term copepod dynamics in the Gulf of Trieste (Northern Adriatic Sea): recent changes and trends. *Climate Research*, 31(2-3):195–203, 2006.

Hydrological and Sedimentological Patterns in the Cabras Lagoon (Sardinia, Italy)

A. Perilli[1], A. Cucco[1], G. De Falco[1], P. Magni[1,2], S. Simeone[3], S. Como[3]
1, Institute for Coastal Marine Environment, CNR, Oristano, Italy
2, Institute of Marine Sciences, CNR, Venezia, Italy
3, International Marine Centre, Oristano, Italy
angelo.perilli@cnr.it

Abstract

In order to detect the main factors influencing the sediment transport processes in the Cabras Lagoon (Sardinia Sea, in Western Mediterranean Sea), the results of a 2D finite element hydrodynamical model (SHYFEM) have been compared with the observed bottom sediment distributions. This model has been used to simulate water circulation and residence time. The bottom sediment distribution has been obtained from the statistical analysis (mean diameter, sorting, skewness) of the in situ data. Analysis of the model results and observed sediment distribution indicates that there is a relation between the distribution of water current and the distribution of fine cohesive sediments (<8 micron). The sediment transport directions within the lagoon seem to be related with the gradient of water current velocity, suggesting that water circulation is responsible for the accumulation of fine cohesive sediments at the centre of the basin, where the velocity of current is low. In conclusion, these results illustrate the capability and usefulness of numerical modelling as a tool for understanding the role of hydrodynamics in the distribution and transport of sediments in lagoon environments.

1 Introduction

Coastal lagoons are typical environments of low-lying coasts, characterised by shallow water, presence of sediment barrier and connection with the open sea restricted to one or several inlets. The evaluation of sediment transport is a relevant issue in lagoon management. Sediment transport and erosion affect the lagoon geomorphology (e.g. development of barriers and inlets) and can have ecological relevance influencing the distribution of sedimentary organic matter, generally associated to fine sediments, and consequently to the features of the benthic ecosystems [1, 2]. According to the classification proposed by Hayes [3], Mediterranean lagoons can be classified as microtidal. However, most of the Mediterranean lagoons are subjected to a tidal range lower than 0.5 m (with the exception of the northern Adriatic sector) and can therefore be classified as non-tidal, as suggested by McLusky and Elliot [4]. The tidal range determines the morphology and textural distribution of sediments. In microtidal lagoons, water depth decreases moving inward from the inlets, whereas in non-tidal lagoons, the deepest areas tend to occur in the centre of the basin. Tidal action sorts the sediments: in microtidal lagoons, finest particles are distributed in the inner shallower areas, whereas in non-tidal lagoons silty-clayly sediments are found mostly in the deepest part. Sedimentary processes in coastal lagoons are strictly related to hydrodynamic ones, which are influenced by morphology, tides and wind. Morphological factors include the lagoon inlet dimension, controlling the exchange of water with the open sea, the bottom topography and the mean depth. Lagoons are typically shallow, with a large horizontal to vertical scale ratio, favouring vertical homogeneity in the water column and the absence of vertical density gradients. The horizontal components of the current velocity can therefore be representative of the water circulation. Furthermore, in shallow lagoons, bottom friction can extend its influence to the surface, damping the current velocity once the forcing ceases. In these environments, intense energy exchange characterizes the relationships between air, water and bottom compartments [5]. The water column can be often considered as a continuous boundary layer transferring energy generated by the wind from the surface to the bottom layers. The circulation in a coastal lagoon can be subdivided into tidal and non-tidal components [6]. The non-tidal circulation comprises the wind driven component and horizontal density gradients component associated with fresh water entering the lagoon. In shallow lagoons wind driven circulation dominates the one induced by the baroclinic non-tidal component. The tidal induced water transport [7] is a quasi-steady and predictable component of the circulation of a lagoon basin, but, often, tidal transport can be dominated and modified by normal wind forcing [7]. This is the case of micro lagoons, where tidal range is less than 1 meter and the induced tidal forcing is very weak. Many hydrological variables, such as sea surface elevation, tidal amplification and delay, residual currents, have to be considered in order to describe the spatial variability in lagoon water circulation. In particular, the Root Mean Square current Velocity (RMSV) and the water transport time scales (REST) were correlated to sediment grain size distribution [8]. The analysis of grain size characteristics provides information on the processes determining sediment distribution. Lagoon sediments are generally gravely free fine grained and the sand:silt:clay ratio is related to the relative energy of the environment. In the last decades, sedimentologists provided methods to evaluate the sediment transport direction from the variability of statistical moments, mean diameter (Mz), sorting (SO) and skewness (Sk) on the grain size distribution curve. Despite grain size trend analysis is becoming popular between sedimentologist, with the improvement of methods and applications, little work has been done on the relationship between grain size trend and hydrological variables and on cohesive sediments, particularly in Mediterranean non-tidal lagoons. The aim of this paper is to analyse the grain size trend in the Cabras lagoon, a non-tidal lagoon located in the Western Mediterranean, and establish the relationships between sediment texture and transport directions and the spatial variability of hydrological variables. The hydrological features of this lagoon were computed by finite element numerical modelling. In particular, as suggested by Molinaroli et al.[8], the Root Mean Square current Velocity (RMSV) and water transport time scales (REST) were calculated in order to relate the variability of the lagoon hydrodynamic in relation to sediment grain size.

2 The studied area

Cabras lagoon is a shallow water environment (mean depth 1.7 m), located on the west coast of Sardinia, western Mediterranean sea (39° 57'N, 008° 29'E; Figure 1), and is one of the largest brackish water basins in the Mediterranean region with a surface of 22 $km^{2\cdot}$ Cabras lagoon stretches perpendicular to the shoreline, in contrast to other Mediterranean lagoons generally parallel to the shoreline, and can be classified as chocked [9]. The lagoon is connected in the north to a small river, the Rio Mannu, which represents the major source of freshwater, an in the south to a smaller river, the Rio Mare Foghe. River discharge is rather limited due to a low rainfall regime in the region (ca. 10-100 mm for July-December, respectively) and the increasing water demand for land use, especially agriculture. Although salinity is a generally increasing, due to a progressive reduction of freshwater input, it may drop to 10 PSU during intense rainfall periods and raise up to 30 PSU, especially in summer. The tidal amplitude is less then 40 cm and water exchange between the lagoon and the coastal systems is very limited. A previous study analysed the distribution of sediment [1] and organic matter [10] in the Cabras Lagoon, reporting a sediment composition mainly silty-clayly, with a major percentage of finer in the inner central sector. The Total Organic Carbon (TOC) concentration was correlated to the percentage of <8 μm fraction. This grain size was considered the boundary between non-sortable and sortable particles [11].

3 Materials and methods

3.1 Hydrological parameters

The hydrology of the Cabras lagoon was investigated by means of a 2D hydrodynamic model. The model is based on the finite element method and resolves the vertically integrated shallow water equations in their formulations with water levels and transports. Details of formulations and numerical treatment are given in Cucco and Umgiesser [12] and in [13]. The model has been applied with success in other studies in order to reproduce the water circulation of lagoons and coastal basins [12]. In a previous study [14], it was used for investigating the hydrodynamics of the Cabras lagoon. Results obtained by Ferrarin and Umgiesser[14] showed that the model was well suited to reproduce the wind and tide induced water circulation and the water temperature and salinity distribution in this lagoon. In the present study, a simulation in which the model is forced by the tide, the Mistral wind and the rivers discharges has been carried out. In the present study, a simulation in which the model is forced by the tide, the Mistral wind and the rivers discharges has been carried out. We have considered the Mistral wind which is the main meteorological forcing influencing the water circulation in the basin. Over the 45% of the winds events are due to the Mistral, with peaks over 15kn during the winter . The southwest Libeccio wind represents only the15%, with typical intensity of 10 kn while the southeast Sirocco wind represents 25%, with typical intensity of 12 kn [14]. Therefore, neither Sirocco nor Libeccio wind were analysed as forcing scenario. The same model settings, boundary conditions and numerical grid used in Ferrarin and Umgiesser [14] has been adopted. In particular, the numerical computation has been carried out on a spatial domain that represents the Cabras lagoon, the main inlet and the net of small channels connecting the main inlet to the lagoon, through a finite element grid. The grid contains 10,948 nodes and 20,013 triangular elements (Figure 1b). The model has been initialized with no surface elevations and without any motion. A spin up time of 2 days has been used in order to damp out all the noise that was introduced through the initial conditions. The duration of the simulation is 56 days corresponding to about two full lunar cycles. The tidal forcing prescribed at the open boundary has been calculated by means of harmonic series. The amplitude and phase of the main constituents used to reproduce the tidal signal has been found in Ferrarin and Umgiesser [14]. The maximum water level displacement imposed at the inlet is about $\pm$ 0.12. A Mistral wind, homogeneous in space and with a daily varying intensity between 4 and 18 kn has been prescribed as upper boundary condition. This scenario represents the typical winter condition as reported by Ferrarin and Umgiesser [14]. Neither Sirocco nor Libeccio wind were considered as forcing scenario, being Mistral wind the main meteorological forcing condition influencing the water circulation in the basin. The discharges of the 2 main rivers have been considered in the simulation. A fresh water outflow of 10 $m^3 \cdot s^{-1}$ has been imposed for the Rio Mare Foghe river and 2 $m^3 \cdot s^{-1}$ for the Rio Tanui as suggested by Ferrarin and Umgiesser [14]. From simulation results, RMSV and REST have been computed for each element of the numerical grid. In particular, the RMSV has been computed through the formula:

$$RMSV(x, y) = \sqrt{(mean(vel(x, y)^2)},$$

where vel(x,y) is the horizontal velocity at point (x,y) and the bar means a suitable average. The RMSV (x, y) has been computed over the whole simulation (30 days) and for each element of the grid domain in order to capture the variability of the water circulation. It gives a good estimate of the hydrodynamic activity in the lagoon. The REST has been computed through an Eulerian approach. In particular, it has been defined as the time required for each element of the domain to replace most of the mass of a conservative tracer, originally released, with new water. To compute it we refer to the mathematical expression given by Takeoka [15, 16] known as the remnant function. A detailed description of the method adopted to compute it may be found in Umgiesser et al. [13] and in Cucco and Umgiesser [17].

3.2 Comparison between hydrological parameters and sedimentological data

Grain size composition was investigated by De Falco et al. [1] and Magni et al. [2]. Sediment samples were collected in 2001 in 30 stations covering the whole Cabras lagoon. We refer to these previous studies for a detailed description of the data collection and grain size analyses [1, 2]. Factor analysis was used to assess the relationships between hydrodynamic features and grain size composition. The hydrodynamic variables, RMSV and REST, were estimated by the model for each element of the numerical grid corresponding to each of the sediment sampling station. The sedimentological variables were obtained by sediment data collected in the sampling campaign of 2001. In particular, the grain size parameters (MZ, SO, SK), and grain size fractionations of silt-clay fraction (sortable non-sortable ratio [SR] and silt: clay ratio [SC]) were considered. Spatial variability of the grain size parameters is known to be related to sediment transport directions [18], whereas the grain size fractionations of siliciclastic sediments is known to be related to the physical environment and has often been used to characterize the depositional conditions [19]. In this analysis, silt:clay ratio was considered, as it is commonly related to the energy condition [20]. Sortable : non-sortable ratio was considered as the non-sortable particles represents the grain size fraction associated with the organic matter deposition in the lagoon of Cabras [1]. Hydrological and sedimentological variables were ranked before the analysis and factors normalized by orthogonal rotation according to the Varimax procedure.

3.3 Grain size trend analysis

The sedimentological parameters, Mean [MZ], Sorting [SO], Skewness [SK], resulting from the sampling grid of the lagoon, have been interpolated by using kriging procedure in order to obtain a regular interpolated grid for each parameter [21]. The grain size trend vectors have been computed on the interpolated grid, using the method proposed by Le Roux et al. [22] for grain size trend analysis. The TRANSVEC spreadsheet [22] has been applied. The distribution of the resultant vectorial data was analysed using the Watson nonparametric test, to determine whether it is preferential or uniform [22].

4 Results

4.1 Water circulation

The basin general circulation generated by the tide, Mistral wind and rivers output has been described in details by Ferrarin and Umgiesser [14]. In this work, the residual currents have been computed (Figure 2) in order to better understand the water circulation pattern induced by the meteo-marine forcing,. The circulation patterns were characterised by the presence of cyclonic and anticyclonic vortices. In particular, a big cyclonic vortex dominated the circulation in the central and northern part of the lagoon, whereas, in the southern part, two smaller vortices characterised the residual circulation of the area. The values of RMSV varied over the lagoon modulated by the residual circulation pattern (Figure 2). In particular, higher RMSV values were detected along the edge of the vortices and along the lagoon borders, whereas lower values were detected in the inner part of the lagoon and in the core of the vortices. The maximum RMSV value, about 0.35 $m \cdot s^{-1}$, was detected in the central part of the basin along the western lagoon border. An intensification of the RMSV was also detected in the southern part of the basin along the eastern border with a maximum value of about 0.29 $m \cdot s^{-1}$. REST varied between about 32 days in the central part of the lagoon and a few hours in the proximity of the river mouth and channels connecting the basin with the main inlet (Figure 3). As for the RMSV, the spatial distribution of the REST, was strongly influenced by the residual circulation pattern. In particular, higher REST values were found in the core of the circulation cells and lower values along the edges of the vortices and the basin borders. The ob-

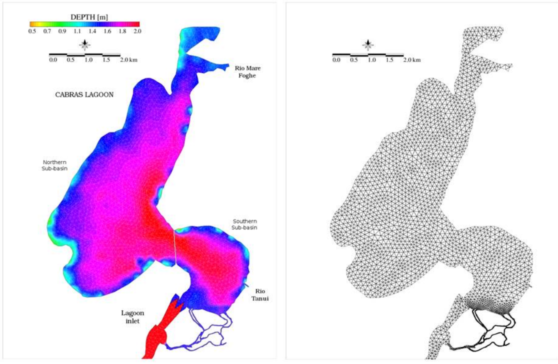

Figure 1: Bathymetry and finite element grid of the Cabras lagoon.

tained results revealed that, from a qualitative standpoint, the basin can be subdivided into two sub-basins characterised by different hydrodynamic regimes (Figure 1a): a northern sub-basin, characterised by higher values of RMSV and REST and anticlockwise circulation, and a southern sub-basin dominated by a pair of vortex system moving in opposite direction and characterised by lower values of RMSV and REST. The presence of a transitional area where water is exchanged between the two sub-basins can be deteceted.

4.2 Hydrodynamics VS sediment distribution and trasport

The spatial variability of sedimentological parameters in the Cabras lagoon is shown in Figure 4 (from [1] and [2]). In the northern sub-basin mean grain size (Mz) increased and sorting decreased toward the inner sector of the lagoon where sediments were finer and better sorted. Sediments were negatively skewed in the inner sector and in proximity of the river inlet, at north. In the southern sector sediments became finer and better sorted toward the south west direction (Figure 4). Results obtained by Factor Analysis are reported in Table 1. Collectively, Factor 1 and Factor 2 explained the 52.5% of the total variance (Table 1). Factor 1, explaining 28.6%, was significantly correlated to the hydrodynamic variable REST and the grain size parameters MZ, SO and SK. In particular, Factor 1 was positively correlated to REST, and grain size parameters MZ and SK. On the contrary, a negative correlation was found with SO (Table 1). Factor 2, which explained 23.9% of the total variance, was significantly correlated to the hydrodynamic variable RMSV, and to the sedimentological variables SC and SR (Table 1). In particular, a positive correlation was found with RMSV, SR and SC. Transport directions resulting from the vector analysis are shown in Figure 5. Particularly, there is a tendency of transport from the shores to the inner sector of the lagoons in the western main basin, and towards south-east in the eastern basin. In the north, in proximity of the river mouth, transport was toward the south-west direction.

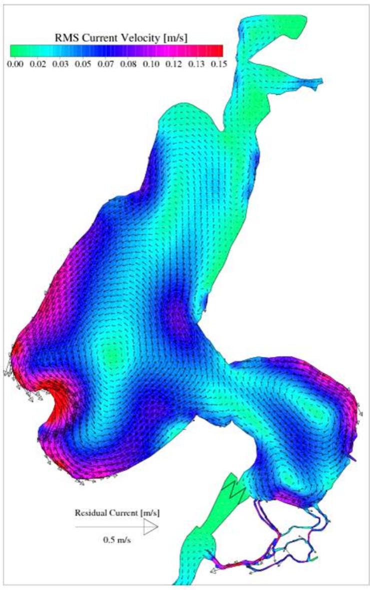

Figure 2: Residual currents (arrows) and RMSV distribution (colors) within the Cabras lagoon.

5 Discussion

The comparison of grain size data and hydrological variables, RMSV and REST, revealed the existence of two statistically relevant trends. RMSV was related to the grain size fractionations of silt-clay and sortable, non-sortable fraction. In particular, in areas where water circulation was more intense (high values of RMSV), such as the lagoon borders, sediments comprised an higher content of both sortable and silt fractions. On the contrary, in the deeper central areas of the basin, where water circulation is less intense (low values of RMSV), sediments were characterized by a higher percentage of clay and non-sortable fractions. The obtained results reflect the considerations proposed by Flemming [20], who argued that hydrodynamic vivacity is the factor which controls silt : clay ratio of inter-tidal sediments. REST was correlated to the grain size parameters. In particular, in areas characterised by low renewal efficiency (high values of REST), such as the central part of the basin, sediments were finer, better sorted and positively skewed whereas, in areas characterized by high renewal efficiency (low values of REST), such as the lagoon borders and the river mouths, sediments were coarser, lower sorted and more positively skewed. This pattern can be related to a depositional process occurring in the central areas where water residence times are higher (more than 20 days) and sediments are finer. The relationship between higher values of REST and the deposition of fine particles has been already reported in marine environments. Results obtained in this study revealed that the re-

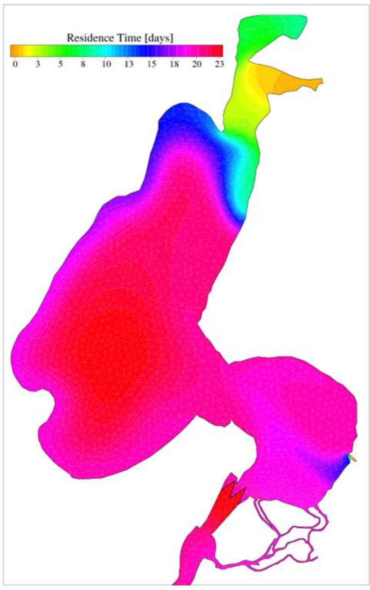

Figure 3: Distribution of REST within the Cabras lagoon.

lationship between water residence times and depositional process of finer sediments apply also to micro-tidal lagoon environments. In particular, the spatial variability of the water residence times, which is correlated to the grain size parameters, can be compared with the results obtained by the grain size trend analysis, which takes into accounts the grain size parameters themselves. Comparing the results obtained by TRANSVEC with the RESTs of the basin, a strong similarity was found between the sediment transport directions and the negative gradients of the REST spatial distribution. Results indicate that sediment transport (Figure 5) occurs from areas with low residence times to areas with high residence times (Figure 3). This is particularly evident in the northern sub-basin, where the results of the TRANSVECT are more accurate. In such sub-basin, REST distribution was able to detect both the transport direction from the lagoon borders toward the central areas and the influence of the Rio Mare Foghe river, which tend to reduce the REST values (Figure 3) and to force the transport direction southward (Figure 5). In the southern sub-basin, the complexity of the hydrological patterns, which was accurately computed by the model, is reflected over the bottom sediment distribution, whose real features were not investigated by the adopted sedimentological sampling strategy. The computed transport directions in such area should therefore be considered affected by a low degree of accuracy and not properly comparable with the REST spatial distribution.

	Factor 1	Factor 2
Current Velocity [RMS]	0.31	**0.73**
Residence Times [TR]	**0.68**	-0.01
Mean [Mz]	**0.88**	-0.35
Sorting [σi]	**-0.95**	0.02
Skewness [Sk]	**0.72**	0.49
Silt Clay ratio [SC]	-0.10	**0.87**
Sortable:Non-Sortable ratio [SR]	-0.31	**0.86**
Explained Variance (%)	28.6	23.9
Cumulative Variance (%)		52.49

Table 1: Results of Factor Analysis of hydrodynamic (Current Velocity [RMS] and Residence Times [TR]) and sedimentological variables (Mean [MZ], Sorting [SO], Skewness [SK], Sortable Non-sortable ratio and Silt Clay ratio). Eigenvectors are indicated. Significant correlation ($p<0.01$) between Factor and response variables are in bold.

6 Conclusions

The use of hydrodynamic models for investigating the water circulation and hydrological features is widely. In this work, we applied a hydrodynamic numerical model to a semi-enclosed basin, typical of a micro-tidal lagoon, and compared the simulated circulation to the characteristics of the bottom sediments distribution. Results showed that the distribution of water current velocity (RMSV) can be used preliminary to assess areas within the basin subjected to erosion processes. Sediment transport in a micro-tidal lagoon was successfully simulated by calculation of the hydrodynamic parameters. In particular, RMSV was used for indicating areas potentially subjected to erosion processes. However, it could not provide information about the sediment transport process itself. On the other hand, the REST was a good estimator of the relevant sediment transport process. Analysis of results showed that the distribution of the REST was correlated to the process of the sediment transport. Assessment of the relationship between water circulation and sediment transport if not accurately performed could be misleading, as in this particular case, sediment transport does not follow the direction of the current, instead occurs perpendicular, following the REST negative gradients. Transport processes were mainly governed by the diffusive components of the transport equation, which tends to move suspended particles from higher velocity areas (higher diffusion coefficient) to lower velocity areas (lower diffusion coefficient), which was taken into account in the computation of the REST. Finally these results show that, just by simulating the residence times of a basin, it is possible to predict the potential pattern of the transport process without using complicated sediment transport models.

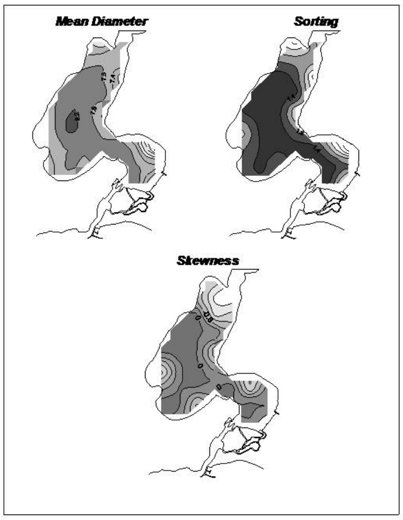

Figure 4: Distribution of the sedimentological parameters within the Cabras lagoon.

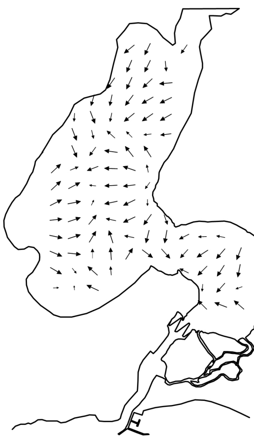

Figure 5: Sediment transport directions inferred by grain size trend using TRANSVEC application.

References

[1] G. De Falco, P. Magni, L. Terasvuori, and G. Matteucci. Sediment grain size and organic carbon distribution in the Cabras lagoon (Sardinia, Western Mediterranean). *Chemistry in ecology*, 20(SUP1):S367–S377, 2004.

[2] P. Magni, S. Micheletti, D. Casu, A. Floris, G. De Falco, and A. Castelli. Macrofaunal community structure and distribution in a muddy coastal lagoon. *Chemistry and Ecology*, 20(S1):S397–S407, 2004.

[3] M.O. Hayes. Barrier island morphology as a function of wave and tide regime. 1979.

[4] D.S. McLusky and M. Elliott. Transitional waters: A new approach, semantics or just muddying the waters? *Estuarine, Coastal and Shelf Science*, 71(3-4):359–363, 2007.

[5] N.P. Smith. Energy balance in a shallow, coastal lagoon: winter conditions. *Limnology Oceanography*, 26:482–491, 1981.

[6] J.L. Hedgepeth. Brackish waters, estuaries, and lagoons vol.5. 1983.

[7] N. Smith. Computer simulation of tide-induced residual transport in a coastal lagoon. *Journal of Geophysical Research*, 95:18205–1821, 1990.

[8] E. Molinaroli, S. Guerzoni, A. Sarretta, A. Cucco, and G. Umgiesser. Links between hydrology and sedimentology in the Lagoon of Venice, Italy. *Journal of Marine Systems*, 68(3-4):303–317, 2007.

[9] B. Kjerfve and K.E. Magill. Geographic and hydrodynamic characteristics of shallow coastal lagoons. *Marine Geology*, 88:187–199, 1989.

[10] P. Magni, S. Como, A. Cucco, G. De Falco, P. Domenici, M. Ghezzo, C. Lefrançois, S. Simeone, and A. Perilli. A multidisciplinary and ecosystemic approach in the Oristano Lagoon-Gulf system (Sardinia, Italy) as a tool in management plans. *Transitional Water Bulletin. Available on line: http://siba2.unile.it/ese/issues/55/724/twb_08v02n02p41a.pdf*, 2(2):41–62, 2008b.

[11] I.N. McCave. Grain-size trends and transport along beaches: an example from eastern England. *Marine Geology*, 28:M43–M51, 1995.

[12] A. Cucco and G. Umgiesser. Modeling water exchanges between the Venice Lagoon and the Adriatic Sea. 2005.

[13] G. Umgiesser, D.M. Canu, A. Cucco, and C. Solidoro. A finite element model for the Venice Lagoon. Development, set up, calibration and validation. *Journal of Marine Systems*, 51(1-4):123–145, 2004.

[14] C. Ferrarin and G. Umgiesser. Hydrodynamic modeling of a coastal lagoon: The Cabras lagoon in Sardinia, Italy. *Ecological Modeling*, 188:340–357, 2005.

[15] H. Takeoka. Fundamental concepts of exchange and transport time scales in a coastal sea. *Continental Shelf Research*, 3(3):311–326, 1984b.

[16] H. Takeoka. Exchange and transport time scales in the Seto Inland Sea. *Continental Shelf Research*, 3(4):327–341, 1984a.

[17] A. Cucco and G. Umgiesser. Modeling the Venice Lagoon Water Residence Time. *Ecological Modelling*, 193:34–51, 2006.

[18] P. McLaren. An interpretation of trends in grain size measures. *Journal of Sedimentary Petrology*, 51(2):611–624, 1981.

[19] K. Kranck and T.G. Milligan. Grain size in oceanography. In: SYVITSKY, J.P.M. (ed.). *Principles, Methods and Application of Particle Size Analysis, New York: Cambridge University Press*, 88:332–345, 1991.

[20] B.W. Flemming. A revised textural classification of gravel-free muddy sediments on the basis of ternary diagrams. *Continental Shelf Research*, 20:1125–1137, 2000.

[21] P.S. Lucio, E.C. Bodevan, H.S. Dupont, and L.V. Ribeiro. Directional kriging: a proposal to determine sediment transport. *Journal of Coastal Research*, 22(6):1340–1348, 2006.

[22] J.P Le Roux, R.D. O' Brian, F. Rios, and M. Cisterna. Analysis of sediment transport paths using grain-size parameters. *Computers and Geosciences*, 28:717–721, 2002.

Sustainable Management of the Coastal Environments in the Framework of the SPICOSA Project: the Study Case of the Mar Piccolo in Taranto (Ionian, Mediterranean Sea)

C. Caroppo[1], L. Giordano[2], F. Rubino[1], N. Palmieri[2], G. Bellio[1], A.P. Bisci[1], A. Petrocelli[1], P. Sclafani[2], T.S. Hopkins[2], E. Marsella[2]
1, Institute for Coastal Marine Environment, CNR, Taranto, Italy
2, Institute for Coastal Marine Environment, CNR, Napoli, Italy
carmela.caroppo@iamc.cnr.it

Abstract

The Institute of Coastal Marine Environment (IAMC) of the CNR shares the coordination of a four-year EU Integrated Project SPICOSA (Science and Policy Integration for COastal Zone Assessment). SPICOSA is developing and testing an operational research approach framework for the assessment of policy options in the context of Integrated Coastal Zone Management (ICZM). The integration of the economic, social and environmental components of the coastal zone is essential to supporting sustainable environmental policies. The SPICOSA methodology, System Approach Framework (SAF), is being implemented and tested simultaneously in eighteen European Study Sites. We are three-quarters through the exercise with the Mar Piccolo, and we are now analyzing the results of our simulation analyses. In 2010, the results will be translated into various formats for deliberation and distribution to Policy makers, Stakeholders, and Public to provide them with means to understand the effects of their policies and to promote a sustainable use of the Mar Piccolo resources. The results of the SPICOSA Study Site will be available on a user-based website for SAF support and archive of scientific reports and models.

1 Introduction

1.1 The SPICOSA FP6 Project

The coastal problems encountered today worldwide are primarily the result of unsustainable use and lack of appropriate directives. As an Integrated Project, SPICOSA is assisting Coastal sustainable development through the use of integrated, multidisciplinary of system-based models. These models are designed to provide higher-level information and decision-support tools for policy makers dealing with problematic issues in coastal zones.
The IAMC is sharing the science coordination of SPICOSA with the IFREMER - Institut Francais de Recherche pour l'Exploitation de la Mer. The two primary goals of SPICOSA are to develop a methodology for simulating coastal systems and to improve the science-policy interface of communicating research results to policy makers. The System Approach

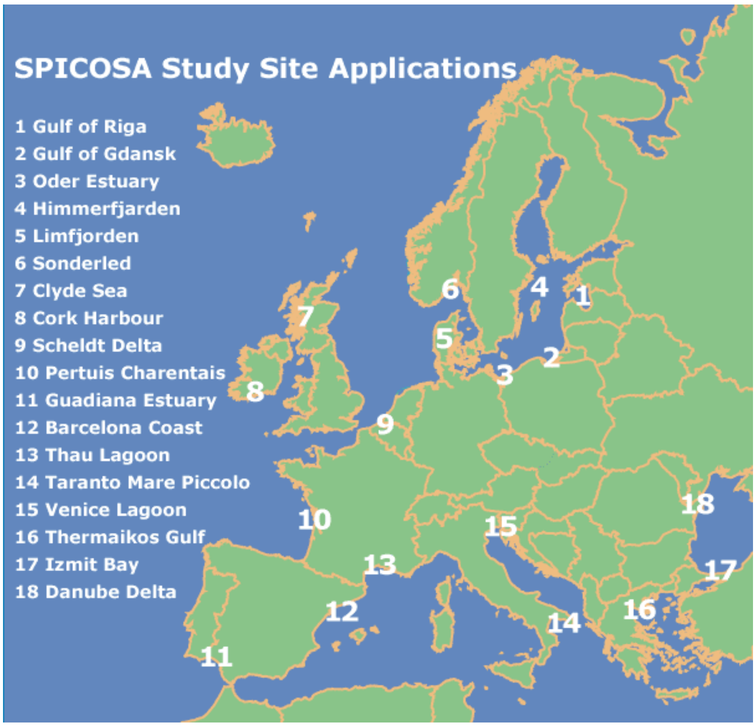

Figure 1: Map of the eighteen SPICOSA Study Sites.

Framework (SAF) is a holistic management strategy for coastal zones that allows to focus on specific problems and provides options for their resolution. The SAF is currently being tested and implemented in eighteen different Study Site Applications (SSAs) throughout Europe (Figure 1). The resulting data, models, and information are contributing to web-based center to support the continued use and evolution of the methodology dedicated to Integrated Coastal Zone Management (ICZM).

The IAMC SSA team is working on an ecological, social, and economic simulation to investigate the environmental and socio-economic factors relevant to the decline of mussel farming in the Mar Piccolo. In this paper, we discuss and illustrate our preliminary results on relevant policy options concerning this decline in the context of sustainable policy scenarios for the Mar Piccolo.

2 The System Approach Framework (SAF) for the Coastal Zone

The Systems Theory [1], states that complex, non-linear systems function differently *in vivo* than that sometimes indicated by a separate scrutiny of their components. The goal of the Systems Approach is to devise strategies to extract in-

formation on the functioning of complex systems that could not have been garnered from a sequence of subsystem-scale studies. This requires the best-possible understanding of the processes and dynamics of a system. The theory of Biocomplexity [2] implies that self-organization is a function of the diversity and interaction of its components, i.e. many diverse components constructively interacting can evolve to a more complex organization that better optimizes its available resources. This suggests that systems issues concerning resilience and recovery need to devise system indicators of the strength and number of interactions [3]. An essential characteristic of quasi-stable systems is their capacity to self-regulate in response to external inputs through adjustments in its internal interactions. These external inputs often exceed, in substance or intensity, those occurring naturally. Because natural systems re-organize slowly in response to changes in energy or mass inputs, but can degrade significantly in response to large changes as now occurring due to major human interventions that lead to a spiral of degradation.
In the SAF, Policy is regarded as a significant control mechanism that can influence change throughout a Coastal Zone (CZ) system in response to information from its constituent components. Therefore, if policy is going to be effective in assisting sustainability in the system, it must understand how its components interact and institute policies that will promote resilience and productivity in the system.
Thus, Science must be accountable for providing better quality information through its deliberations with Policy. For this reason, the SAF requires a participatory relationship and must include the concerns of local stakeholders, institutional structures, and public end-users that play a strongly determinant role in policymaking. Simply put, a broader participation is needed so research results can be objectively and effectively presented to all involved sectors. The SAF methodology is being written and revised during its implementation in all of the SSAs. The SAF is organized in a sequence of four different steps, e.g.:

- Design (problem definition and scope);
- Formulation (key interactions and analyses);
- Appraisal (simulations and assessments);
- Output (results, reformatting, deliberations).

Currently, we are working on the Appraisal Step and therefore the results reported here should be considered as preliminary.

3 The Spicosa Study Site: Mar Piccolo in Taranto

3.1 The Policy Issue

Since the year 2000, two important policy changes influenced the carrying capacity of the Mar Piccolo system. These involved the reduction and relocation of sewer discharges and the areal extension of mussel farming. The observed decline in the Taranto mussel production is apparently correlated with these policy changes in terms of quality (Figure 4). In accordance with the SAF procedure, we conducted initial meetings with policy makers to negotiate a ‘Policy Issue’ for our simulation exercise, which ultimately nominated this decline in mussel production.

3.2 Ecosystem Description

Mar Piccolo (Mediterranean Sea, Southern Italy) is a shallow, nearly enclosed estuary

Figure 2: Map of the Gulf of Taranto (Northern Ionian Sea).

of 21 km^2 consisting of two basins separated by an intruding promontory (Figure 2). The basins are referred to as Seno I and Seno II and have maximum depths of 13 and 10 m, respectively. The exchange with the larger semi-enclosed bay of Mar Grande occurs through a primary artificial navigation channel (12 m) and a small natural inlet. Mar Grande opens into the Gulf of Taranto and the Northern Ionian Sea.

The estuarine circulation in Mar Piccolo is driven by a positive water balance of $\sim$23 mil$\cdot \mathrm{m}^3 \cdot \mathrm{yr}^{-1}$. The exchange with Mar Grande is moderate and varies seasonally depending on the inter-basin pressure gradient. The exchange results in flushing times of 2-3 mos. During the summer, a sufficient stratification develops that can induce hypoxia in the lower layer that damages mussel growth. Wind mixing is low due to the limited fetch and tidal-mixing is low due to the limited tidal range of $\sim$30-40 cm.

In Mar Piccolo salinity is influenced by the input of freshwater deriving from small tributary rivers, runoff from the surrounding agricultural soils and from freshwater springs (locally called "Citri"). These Citri are situated in Mar Piccolo, to the N of the Seno I and to NE of the Seno II. The total number of Citri is 34 (20 at the Seno I and 14 at the Seno II), and the average quantity of freshwater which contributes is about 1,6 mil$\cdot \mathrm{m}^3 \cdot \mathrm{d}^{-1}$ [4].

The exchange with Mar Grande was modified in 1985 by the installation of a water-scooping machine (0.15 mil$\cdot \mathrm{m}^3 \cdot \mathrm{d}^{-1}$) which provides cooling water for the iron & steel industry. A more important disturbance has been the presence of discharge from 14 sewage pipes (5 at Seno I and 9 at the Seno II) coming from the Northern area of Taranto and from eight nearby towns (Figure 3). These wastes were equivalent

Figure 3: Map of the Mar Piccolo in Taranto and location of the main human activities.

to about 18,272 $\mathrm{m}^3 \cdot \mathrm{d}^{-1}$ (of which 85% at the Seno II), with organic matter equal to 6,767 kg·d^{-1} of BOD5, whereas N_{tot} andP_{tot} were of 17.2 and 0.3 $\mathrm{t} \cdot \mathrm{d}^{-1}$, respectively [5]. Since 2000 the number of sewage pipes has been progressively reduced to the actual 5 (1 at the Seno I and 4 at the Seno II) and are all subjected to depuration. These wastes have a capacity of about 3,000 $\mathrm{m}^3 \cdot \mathrm{d}^{-1}$ and the levels of nitrogen and phosphorus have been reduced to 8.0 and 0.12 $\mathrm{t} \cdot \mathrm{d}^{-1}$, respectively [6]. The combined effect of these changes appears to have influenced the phytoplankton communities. In the past these were dominated by diatoms, which have since been largely substituted by nanoflagellates (Caroppo, pers. com.). Taking into account that in shallow coastal environments phytoplankton represent the main component of the mussels diet [7], structural changes of this important food source have likely changed the quality of the mussels in Mar Piccolo.

3.3 Human activities

Mar Piccolo is strongly utilized by an intensive mussel commercial fishery at ∼30,000 tons per year (ISMEA-MIPAF data). Other important human activities exert additional stress on the system. Seno I is utilized for mooring the local fishing fleet and activities of the largest Italian naval base. The industrial site located to the West (Figure 3) indirectly influences the environmental quality of air, water, and sediments. The drainage of agricultural soils and the sewage inputs are also important factors that influence the water and sediment quality. As a result Mar Piccolo has been designated as a Site of National Interest for highly polluted areas. Large increases in these activities have character-

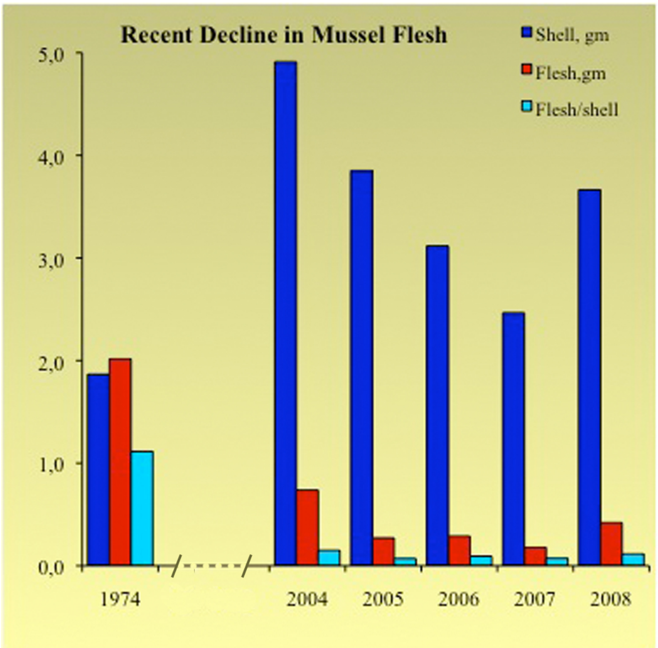

Figure 4: Changes in Taranto mussels quality expressed by flesh/shell ratio.

ized the city of Taranto in the last decades and induce changes in the socio-economic sectors as well as in the use of natural resources. For example, the heavy industry was established in Taranto in the 1950s and completely changed the economy of the city and Province, which had been based on agriculture, aquaculture, and naval port space.

During this period, the population of Taranto has doubled resulting in severe social problems, such as unemployment, in addition to ecological problems, such as increased substance loading in the Mar Piccolo. The aforementioned policy changes reflect an attempt to better manage the Mar Piccolo ecosystem.

4 Methods: Issue Definition, System Design and Formulation

4.1 Policy-stakeholders involvement

During the Design step the team began a negotiation and familiarization process with the Participant Group (PG) in regards to the objectives of SPICOSA. Of priority to the PG was their concern about the Impacts related to the decline in quantity and quality of mussel aquaculture. In subsequent meetings, the Policy Issue has been refined to define a set of specific scenarios for our SAF simulation analysis. The Policy Issue that resulted was: “How to include mussel culture in a management plan

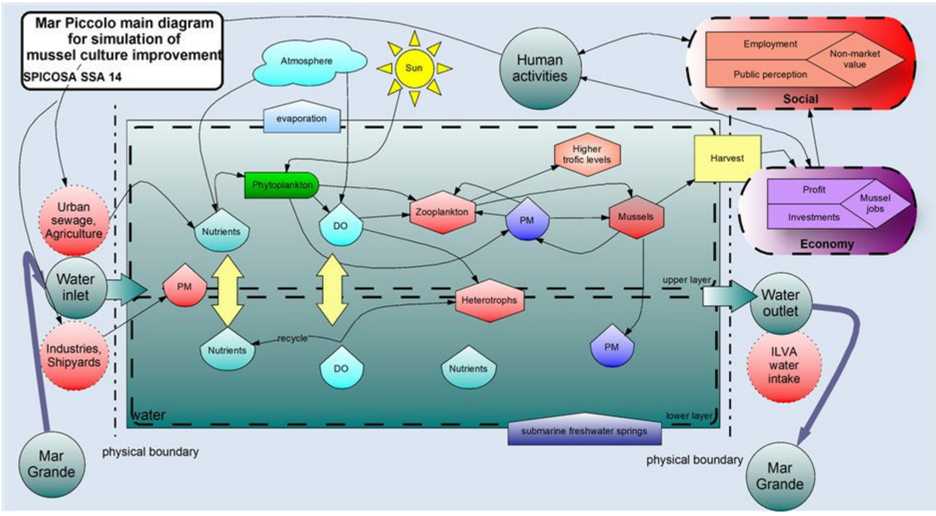

Figure 5: The diagram represents the VS functionality of the ecosystem with regard to the Impact.

for the sustainable use of the Mar Piccolo resources?".
Implicit in this Policy Issue is the question of whether it might be possible to compromise between economic, social, and ecological costs and benefits, which is an excellent objective for the SAF. The plot showed in Figure 4 illustrates changes in the size of mussel flesh and its shell in grams together with the flesh-to-shell ratio, which is taken as an indicator of mussel quality. The reduction of mussels flesh/shell ratio led to a consequent loss of market value for the Taranto mussels that in the past had a high reputation due to their little shell full of delicious meat. Recent trends in the quality decline coincide with the policy changes concerning waste discharge and mussel farming practices (see Sec. 3.1).

4.2 Virtual System Design

The Systems Approach requires an ability to focus on a specific functionality of a system and analyze how it responds to change. In the SAF, we try to represent the functionality that traces an Impact (problem) within the natural CZ system to a causal Human Activity and response in the social and economic sectors. This is done by defining a Virtual System (VS) that is an extraction from the real CZ system of the primary functionality causal and reacting to the Impact to be simulated. It is "virtual" in the sense that its boundaries are determined by relevance and are not necessarily coherent spatially. Moreover, conceptual models are a schematic way to obtain a downscaled configuration of the system and represent only those first-order inputs, interactions, and processes that govern the flows of information (mass, energy, money, employment) relevant to the cause & effect

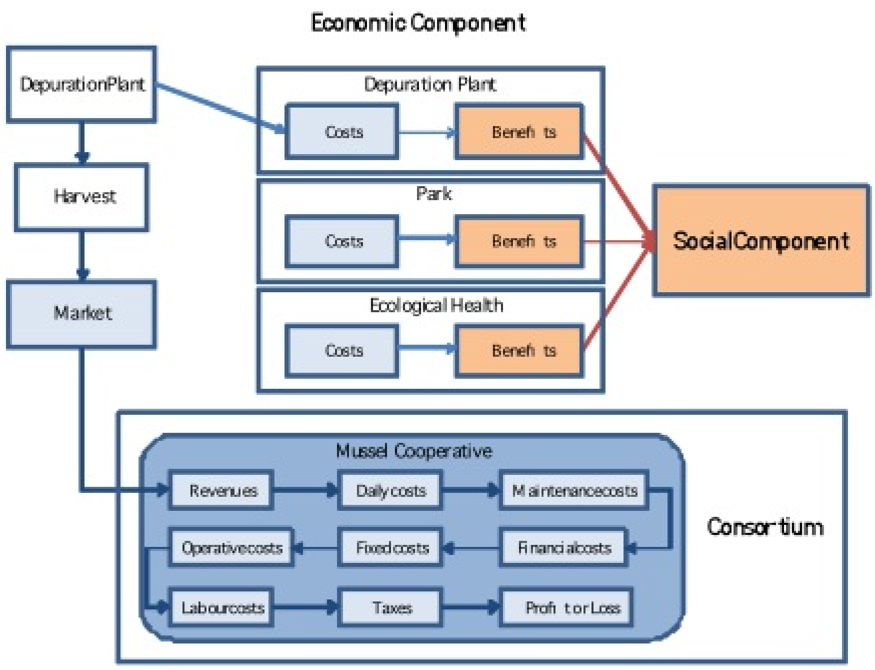

Figure 6: The conceptual diagram reports a blow-up of the socio-economic component.

chain.

The conceptual diagrams (Figures 5, 6) allow us to visualize the function of the primary components of the ecosystem and its connection with human activities through links to socio-economic components.

4.3 Formulation

In the SAF, a scenario is a specific policy question that concerns the Policy Issue. It is expressed as a question one would ask of the simulation analysis, to obtain quantitative information for decision making. For the Mar Piccolo SSA, three categories of scenarios were defined:

- What are the environmental conditions that control or are causing the mussel decline?
- What would be the costs and benefits derived by enacting the measures needed for sustainable mussel growth?
- What are the effects on human and ecological health resulting from the exposure to hazardous contaminants and organic wastes?

The aim of the CZ System Formulation Step is to represent the functioning of the system, in both quantitative and qualitative terms. This requires that processes and interactions, including the controls and constraints of the socio-economic components, be formulated into functional modeling blocks that are individually validated.

5 Research tools: the Ecological-Socio-Economic (ESE) simulation model

Historical studies of Mar Piccolo ecosystem are mostly limited only to circulation models [8, 9, 10, 11] and to statistical studies on hydrology and chemical-physical features [12]). The SPICOSA simulation effort represents the first comprehensive quantification of the marine ecosystem linked to relevant socio-economical components. The multidisciplinary modeling of Mar Piccolo utilized the simulation software EXTEND™-Sim (http://www.extendsim.com/) .

The purpose of the Simulation Model is to represent the productive capacity of the system in response to the specified scenarios. It was constructed to determine the potential Mussel harvest in units of Carbon based on the photosynthetic capacity, which in turn is driven by the nutrient discharges and controlled by the light availability and circulation. The mussel harvest is the main link with the economic component. The ecosystem health is a direct connection to the social component through public perception and to the economic component through harvest.

In the following section, a brief description of the components of the Ecological and Socio-Economic (ESE) model is given in order to provide the overview of the model functionality.

5.1 Ecological Model: physical and bio-chemical components overview

Geo-morphologically, the Mar Piccolo has two interacting basins with a double-layer stratification in which the following processes are simulated:

- Freshwater balance: The freshwater balance represents the sum of the rain on the estuarine surface, the land runoff, and the evaporation from the surface.
- Circulation exchange: An approximation of the Thermohaline Exchange Method (TEM) [13] is used to derive the circulation formulation.
- Salt budget: The total salt in the surface and bottom layers are calculated by simply considering that salt is a conservative parameter with a vertical diffusive exchange.
- Vertical diffusion: The magnitude of diffusion is inversely related to the salinity gradient and directly related to the KE available.
- Nitrogen budget: Nitrogen is a non-conservative property, with several processes that act as in-situ sources (e.g. external inputs, regeneration from POM, entrainment, advection) and sinks (e.g. uptake, sediment burial, sinking).
- Phosphate and Silicate Budgets: The purpose of modeling the P and Si concentrations is to retain information concerning any threshold limits with respect to the N concentrations. Main sources considered are regeneration and uptake strictly dependent on “F-ratio”.
- Oxygen Budget: The oxygen is modeled because hypoxia is a concern with respect to mussel growth, and it is a key indicator of several essential processes, several sources (e.g. photosynthetic production and the atmospheric input, and advectively entrained bottom water) and sinks (e.g. respiration of phytoplankton, mussels, and other heterotrophs, oxidation of organic matter in lower and sediment layers).

- Carbon Regeneration: The total bottom layer respiration of Carbon is taken as a delayed constant proportional to O_2:C ratio and calibrated with the bottom oxygen observations. Sediment respiration rates were based on literature values from studies of similar coastal waters.
- Irradiance simulation: The light input is used as a direct input but it is corrected with an attenuation parameter proportional to POM concentration.
- Primary Production: Growth equation for three phytoplankton groups [14] was considered in order to simulate seasonal variations in the food supply and, to a limited extent, its quality.
- Zooplankton: Zooplankton grazing is considered as forcing factor on phytoplankton growth and it is parameterized following a modified Ivlev equation proposed by Franks et al. [15].
- Particulate Organic Matter: The POM values combine the phytoplankton with an additive component estimated from the BOD values in the discharges.
- Mussel Growth: The growth equation for Mussel follows a bioenergetics model of Van Haren & Kooijman [16], based on the assumption that mussel food is POM mainly constituted by Phytoplankton and Detritus. The entire life cycle, for two generations, was simulated using parameters fitted on historical Mar Piccolo mussels biometric data-sets ([17, 18], Portacci, unpub. data).

5.2 Social and Economic Components

The Social and Economic Components analyze the response of the system to the Output (Impact variables) of the Ecological Model. They do this both through directly linked simulation modeling and through conventional analyses in order to satisfy the information needs of the specified scenarios. The main socio-economics components considered are:

- Mussels Farming and Harvest: The real mussel farming area was based on sea surface areas licensed to farmers (Harbour Office data). The volume is calculated considering that nets are disposed on lines and fixed as to be suspended under the sea level for 4-5 meters.
- Mussel Farm Profit: The market of Taranto is made up solely of mussel cooperatives, therefore we have analyzed all costs incurred and revenue obtained from a representative cooperative. The annual profit is the difference between total revenues and costs for the year. We considered the difference between two management structures: an individual cooperative and a consortium of cooperatives ([19], [20]). The objective is to investigate the variability of profit of these two structures from the harvest, which is simulated in accordance with the different scenarios.
- Cost-Benefit Analysis (CBA): The first CBA analysis [21] compares a limited set of costs and benefits for both a traditional-treatment plant and a natural-treatment plant [22]. The second CBA compares the construction costs against the market and non-market benefits of a shoreline public park, contingent on the scenario of pollution reduction in Mar Piccolo.

5.3 Simulation Scenarios on Mar Piccolo of Taranto

The simulation analysis will be focused on three main scenarios: 1) environmen-

tal conditions change; 2) sustainable mussel culture and 3) ecosystem-health benefits. For each one separate simulation runs will be performed. The first scenario is related to the improvement of environmental conditions (e.g. food quality, contaminants level, mussels stock, and farming techniques) that control or cause a decline in mussel growth, which influences the carrying capacity of the system. Consequently, the most important aspect concerns the optimal environmental conditions needed to reduce the costs of mussel culture through a different management strategy and an increase of socio-economic benefits.
The second considered scenario is directed to the quantification of costs and benefits derived from the enactment of measures needed for sustainable mussel growth, and better environmental conditions for mussel culture. This scenario is directly linked to the comparison of technological options or policy strategies that are available to mitigate damaging effects (e.g. Cost and Benefits of a Depuration Plant and the socio-economic consequences of these options or strategies). The third but not less important scenario concerns the potential benefits derived from a healthier ecosystem achieved through an improved waste management plan and cleaner shores, and more public facilities connected to the Mar Piccolo (e.g. health and exposure to pollution, Shoreline Park with accommodations).

6 Preliminary Results and Discussion

The results discussed are based on preliminary calibrations of the simulation model components of Mar Piccolo (Seno II) based on existing observational data of the external inputs. These were collected by the Institute, from literature, and from local Authorities. We calibrated our model of Seno II (Figures 7-10) first and are presently connecting it to Seno I for final calibrations. This procedure will reduce the margin of uncertainness allowing us to test the sensitivity of the two basins to variations in forcing. The environmental conditions are well reproduced, such as the fresh-water runoff, the water circulation, and the nitrogen. The model allowed us to obtain a simulation for water flux for each year considered e.g., Figure 7 shows the inflow, outflow, and freshwater input for 2003. Note that the exchange decreases exponentially with a cessation of freshwater input but increases linearly with pulses of freshwater. The circulation is calibrated by tuning the resistance of the opening (to Mar Grande) and the vertical diffusion coefficient until a best fit is achieved with the observed salinities.
Pulses in freshwater inputs induce a direct increase in nutrient concentration due to runoff, advection and diffusion. The Nitrogen concentration is primarily controlled both by runoff variability and by primary production (Figure 8).
The phytoplankton growth is driven by light and nutrient conditions, modified by circulation and diffusion. Its representation is complicated due to the feedback with nutrient regeneration and predation by zooplankton and mussels. Three phytoplankton groups are simulated because the diet of mussels is likely based on a food preference factor as suggested by Navarro et al. [23].
A typical cycle for mussels production (18 months) was simulated starting from a first generation of larvae and using biometrics data-sets of Mar Piccolo ([17], [18], Portacci unpub. data) and the reproductive cy-

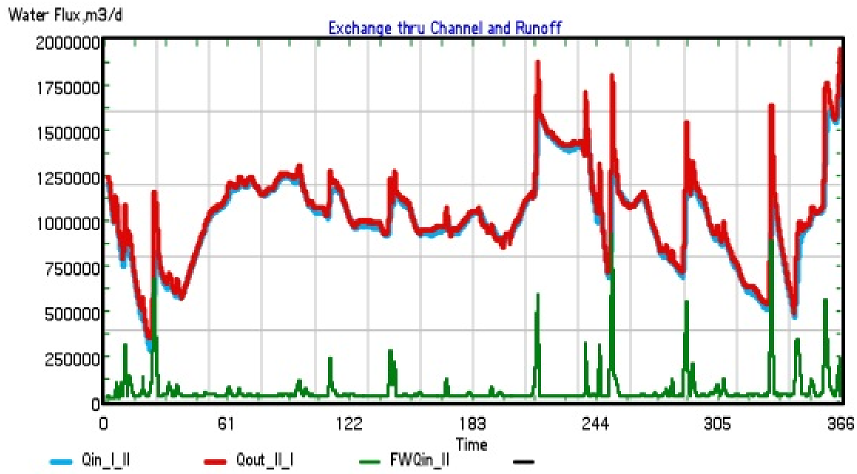

Figure 7: The inflow (blue), outflow (red), freshwater inflow (green) transport for the test year of 2003.

cles given by Matarrese et al. [24] (Figure 9). The simulation of growth was performed considering the mussels life-cycle and including a "mother" generation sown in January and a second "daughter" generation (the resulting spawn: e.g. 25 % of the total amount of the first generation) of the previous autumn of the first year of simulation. Some refinements, such as phytoplankton groups, mussels life-cycle and mussels food preference, were added to improve the balance between approximation and accuracy required on the outputs.

The harvest "pressure" is simulated on the mother generation starting in May and ending in September as suggested by the information obtained directly from the mussel farmers of Mar Piccolo.

The mussel biomass harvested from the system during the production cycle is the link between the biological and socio-economic model. According to available data, the mussels harvest of Mar Piccolo is about 24,000 tons (Portacci, pers. com.). Each mussel culture plan takes up areas comprised between 3,000 and 15,000 m^2, with a total extension of about 10 km^2. Mar Piccolo supports 31 mussel farms of which 25 are Cooperatives and 6 are small companies (Taranto Harbour Office) with ∼213 legal employees (Chamber of Commerce). The simulation model allows us to evaluate the costs and revenue for the two types of farm management (Figure 10). Preliminary analysis of costs and revenue lead to slightly higher profits for cooperatives belonging to a consortium than for individual cooperatives. The difference is due to the consortium capacity to fix the market price, support employment in the mussel sector and promote their product, covering costs that the individual cooperatives would otherwise not be able to support.

The simulation that includes the option of

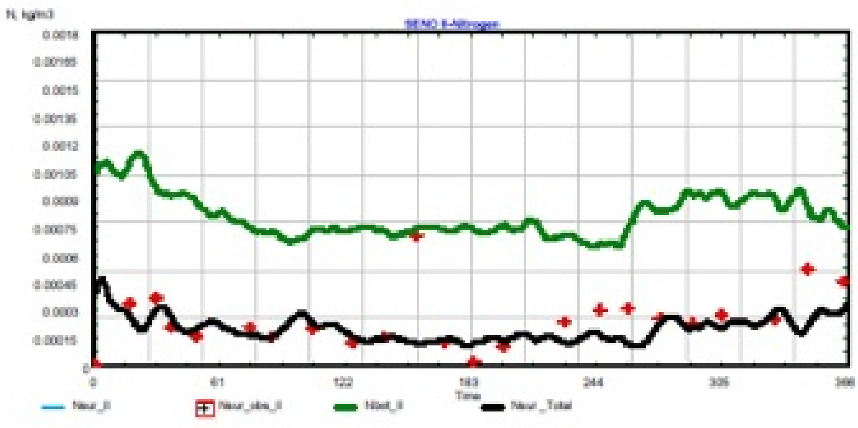

Figure 8: The simulated Nitrogen concentration in the top layer (black), in the bottom layer (green) and the observed values during the year 2003 (red stars).

mussels quality by means of a sewage management plan, (traditional or natural depuration plant) is now in progress of evaluation, to calculate in both cases the costs and benefits of different hypothetical scenarios. The other scenarios, discussed previously but not yet simulated, aim to demonstrate how mussel growth depends on its environmental conditions, how these conditions relate to sewerage management, how the ecological health of the Mar Piccolo might be improved. In the last case, we hope to demonstrate that the added socio-economic benefits of a public park for the city of Taranto.

7 Conclusions

The most obvious benefit of the Spicosa SAF application is certainly a modelling tool that allows us to perform a tuning of the whole system so as to embark on the complex understanding of the factors controlling mussel quality and Mar Piccolo carrying capacity. We also expect that our results will help integrate the socio-economic needs and promote a more integrated plan for sustainable development in the Taranto Region. In addition to the cited scenarios, we are planning some sensitivity analyses to consider some “extreme-disturbance” scenarios i.e. anoxia events, drought or exceptional storms so as to analyze not only the ecosystem resilience but also the economic response in the mussels farming. Despite some deficiencies in the input data (runoff and substance concentration), we have achieved a good level of accuracy for the simulation of the environmental conditions. Equally important has been our participatory exposure and dialogue with city officials, regional environmental agencies, and stakeholders which as proven to be a mutually rewarding experience. On a larger scale, the SAF “exercise” taught us how to manage a new approach to integrated multidisciplinary research and the ability to create a much wider, more ac-

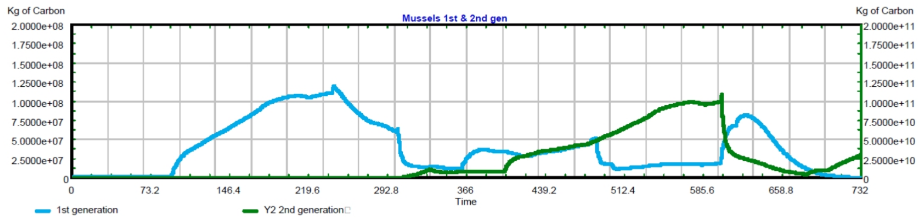

Figure 9: The mussel biomass of two age classes (2003 -2004). One harvest event is shown in June after which little growth occurred due to the declining phytoplankton production associated with decreases in runoff and new nitrogen, and a second one in late October allowing the younger class to profit from the increased availability of phytoplankton.

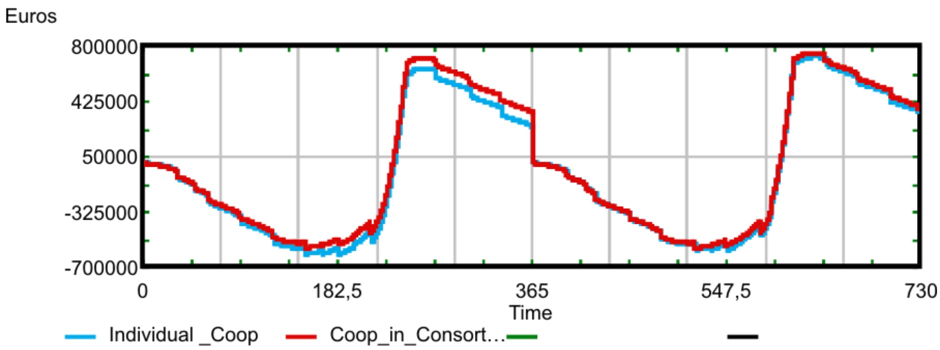

Figure 10: Cost and Revenue of an individual Cooperative (blue) and Cooperative in Consortium (red) simulated on a 730 days period.

curate tool with important benefits both for Science and Policy in the framework of environmental sustainability.

References

[1] L. Von Bertalanffy. General Systems Theory. 1968.

[2] S.A. Kauffman. At Home in the Universe. 1995.

[3] J. Patricio, R. Ulanowicz, M. A. Parda, and J. C. Marques. Ascendency as an ecological indicator: a case study of estuarine pulse eutrophication. *Estuarine Coastal and Shelf Science*, 60:23–35, 2004.

[4] A. Cerruti. Ricerche oceanografiche nel Mar Piccolo, nel Mar Grande e nel Golfo

di Taranto durante il triennio 1932-'34. *Proceedings of Royal Academy Science F. M., Naples*, 1:1–171, 1938.

[5] C. Caroppo and N. Cardellicchio. Phytoplankton of Mar Piccolo of Taranto (Jonian Sea). *Oebalia*, 21:61–76, 1995.

[6] C. Annichiarico, F. Bottiglia, N. Cardellicchio, A. Di Leo, S. Giandomenico, L. Lopez, and L. Spada. Caratterizzazione chimico-fisica delle acque del Mar Piccolo di Taranto (Campagna 2008). 2009.

[7] B. A. MacDonald and J. E. Ward. Variation in food quality and particle selectivity in the sea scallop *Placopecten magellanicus* (Mollusca: Bivalvia). *Marine Ecology Progress Series*, 108:251–264, 1994.

[8] A. Adduci, M. Bens, and M. Demarte. Modello di previsione delle correnti nel Mar Piccolo di Taranto. 2004.

[9] F. De Serio, D. Malcangio, and M. Mossa. Circulation in a Southern Italy coastal basin: Modelling and field measurements. *Continental Shelf Research*, 27:779–797, 2007.

[10] D. Malcangio and M. Mossa. Tidal current computation in the Mar Piccolo. 2004.

[11] G. Umgiesser, I. Scroccaro, and G. Alabiso. Mass exchange mechanisms in the Taranto Sea. *Transitional Waters Bulletin*, 2:59–71, 2007.

[12] G. Alabiso, M. Cannalire, D. Ghionda, M. Milillo, G. Leone, and O. Caciorgna. Particulate matter and chemical-physical conditions of an inner sea: the Mar Piccolo in Taranto. A new statistical approach. *Marine Chemistry*, 58:373–338, 1997.

[13] T.S. Hopkins. The thermohaline forcing of the Gibraltar exchange. *Journal of Marine Systems*, 20:1–4, 1999.

[14] A.G. Murray and J.S. Parslow. The analysis of alternative formulations in a simple model of a coastal ecosystem. *Ecological Modelling*, 119:149–166, 1999.

[15] P.J. Franks, S.J.S. Wroblewski, and G.R. Flierl. Behaviour of a simple plankton model with food-level acclimation by herbivores. *Marine Biology*, 91(1):121–129, 1986.

[16] R.J.F. Van Haren and S.A.L.M. Kooijman. Application of a Dynamic Energy Budget Model to *Mytilus edulis* (L.). *Netherlands Journal of Sea Research*, 31(2):119–133, 1993.

[17] M. Pastore, P. Panetta, C. Andreoli, and B. Dell'Angelo. Accrescimento di *Mytilus galloprovincialis* (Lam.) nei mari di Taranto. *Oebalia*, 2:20–61, 1976.

[18] G. Corriero, G. Lembo, C. Longo, C. Nonnis Marzano, G. Portacci, and M.T. Spedicato. Valutazione comparativa dell'accrescimento e della gestione di *Mytilus galloprovincialis* Lam. in differenti condizioni ambientali di allevamento. *Biologia Marina Mediterranea*, 8(1):574–576, 2001.

[19] B. Frizzera, C. Delladio, and M. Jannaccone. Guida alle Società Cooperative" Il Sole 24 Ore. 2008.

[20] A. Propersi and G. Rossi. I Consorzi: Aspetti legali, contabili e fiscali in tema di consorzi, società consortili, raggruppamenti temporanei di imprese, GEIE - Il Sole 24 Ore. 2008.

[21] G. Pennis and P.L. Scannizzo. Valutare l'incertezza: L'analisi costi benefici nel XXI secolo. 2003.

[22] S. Maglia and A. Tredanari. La quantificazione economica del danno ambientale alla luce del DL.VO 152/06: un caso di sversamento di liquami zootecnici in acque superficiali. 2008.

[23] E. Navarro, J.I.P. Iglesias, A. Perez Camacho, and U. Labarta. The effect of diets of phytoplankton and suspended bottom material on feeding and absorption of raft mussels (*Mytilus galloprovincialis* Lmk). *J Exp Mar Biol Ecol*, 198:175–189, 1996.

[24] A. Matarrese, A. Tursi, G. Costantino, and R. Pollicoro. The reproductive cycle of *Mytilus galloprovincialis* Lamarck in the Mar Piccolo and in the Mar Grande of Taranto (Ionian sea). *Oebalia*, 19:1–11, 1993.

Importance of Marine Allochthonous Inputs for Terrestrial Macroinvertebrates Inhabiting Sandy Beaches: Challenges for Disentangling Strategies of Zonal Recovery and Food Webs

I. Colombini, M. Fallaci, L. Chelazzi
Institute for Ecosystem Study, CNR, Sesto Fiorentino (FI), Italy
i.colombini@ise.cnr.it

Abstract

The role of marine allochthonous inputs (seagrasses and macroalgae) to sandy beach ecosystems is poorly known. Most studies have focused attention on their importance as nutrient sinks for nearshore communities or as key habitats for benthic and fish communities of coastal environments. Instead little work has been accomplished to understand their function when stranded on the beach. In the past thirty years beach ecology studies have evolved from baseline studies with a multidisciplinary approach to gain information on the diversity of terrestrial macroinvertebrates to studies on population dynamics in space and time. Recently, the potential transference of organic matter from the marine subtidal to the supralittoral zones was assessed using isotopic analysis to study its importance in the food web of terrestrial macroinvertebrates. It was also analysed to understand to what extent major guilds of the most abundant terrestrial arthropods derive energy from marine inputs in the form of stranded wrack along a gradient from shore to inland. The main results indicate that marine beach wracks represent an important but quite transient resource for food and shelter for resident macroinvertebrates that inhabit areas with low and /or absent primary production. Furthermore, marine stranded wracks are of fundamental importance for the maintenance of a high macrofaunal diversity in terrestrial coastal environments. Information on the role of beach wrack is extremely useful for local authorities for a sustainable management of sandy beach coastal environments.

1 State of Art

Marine allochthonous inputs are of primary importance for beaches which lack of autochthonous primary production. Coastal ecosystems receive substantial carbon and nitrogen inputs from the sea in the form of wrack debris from various origins. The importance of beach casts, their colonisation by macroinvertebrate species and subsequent successional patterns was reviewed by Colombini and Chelazzi [1]. Macroalgae and seagrasses have an important role in controlling coastal sedimentary processes, in operating as important nutrient sinks for nearshore communities, in influencing the geomorphology of sandy shores by attenuating waves and protecting from erosion, in acting as refuges and in supporting prey resources that are the basic element of food webs for vertebrate predators [2]. Recently, some studies has

Figure 1: Example of an experimental wrack placed into the sand at the site of Burano (Grosseto, Italy).

been carried out to determine the quantities and functions of beach-cast material and much attention has been focused on seagrass meadows of
textitPosidonia oceanica, an endemic and dominant species of the Mediterranean. However, most studies were conducted at sea and little information existed on the spatial and temporal variability of macrofauna associated with the stranded wrack. Furthermore, assessing the potential transference of energy and matter from marine subtidal to supralittoral zones becomes important as it represents the basis for sustaining the high biomass and diversity observed in sandy beach ecosystems. In coastal environments there has been the tendency to analyse and to highlight biodiversity of worldwide marine or intertidal ecosystems whereas for terrestrial sandy beaches studies have been more rare and occasional. Interest for terrestrial macrofauna of littoral environments was first expressed in pioneer studies of Italian researchers (L. Pardi and collaborators) that focused their attention not only on the ecology but also on the behavioural strategies in space and time of beach species.

2 Research Activities

In the past thirty years there has been a growing interest on behalf of CNR researchers to study terrestrial coastal environments of tropical (Somalia and Kenya) and temperate (Mediterranean and Atlantic coasts) areas. Baseline studies were carried out with a multidisciplinary approach (Bilateral projects CNR-CSIC Spain, CNR-CNRST Morocco and EU projects MECO, MEDCORE and WADI) to gain information on the ecology of beach ecosystems and to produce a data base on the diversity of terrestrial macroinvertebrates [3, 4, 5, 6, 1]. Contemporaneously, Colombini et al. [7] focused their attention on

Figure 2: Bird eye view of the study site at the Maremma Regional Park. The eulitoral the dune and the dune slack are clearly visible.

the role of marine allochthonous material stranded on the beach and showed that shore macroinvertebrates used wracks in space and in time in a dynamic way.
To test the role of *P. oceanica* wrack as provision of shelter for terrestrial macroinvertebrates a research was conducted at Burano (42°23 '50 "N, 11°22 '40 "E; Grosseto, Italy) in semi-natural conditions. Field experiments consisted in evaluating the successional colonisation of artificial beach wracks patches placed at different distances from the sea. These consisted in one hundred cylinders made in plastic net with one half buried into the sand and the other filled with a constant sample unit of textitP. oceanica leaf litter (Figure 1). To determine species succession after the deposition of the material, samples for each distance were collected at 1, 2, 3, 4, 5, 8, 13, 19, 26 and 33 day intervals from the onset of the experiment.
Contemporaneously during the experiments the macroinvertebrate population was sampled with standard methods (pitfall traps) to assess species quantitatively and qualitatively.
The experiments showed that macroinvertebrate density was higher in wracks compared to bare sand and that experimental wracks were promptly invaded by early colonisers with a high number of crustaceans in wracks closer to the sea. In particular, *Talitrus saltator* and *Tylos europaeus* colonised wracks differently both in space and in time (Figure 3, Table 1). However, in this study crustaceans abandoned the wracks after the first days, whereas in the controls they were present throughout the entire study period. The presence of the dipteran species on the more landward wracks already after day 2 confirms the findings on other beach dipterans. The latter exploited *Posidonia oceanica* leaves as nesting sites and made wracks attractive to predators (staphylinids

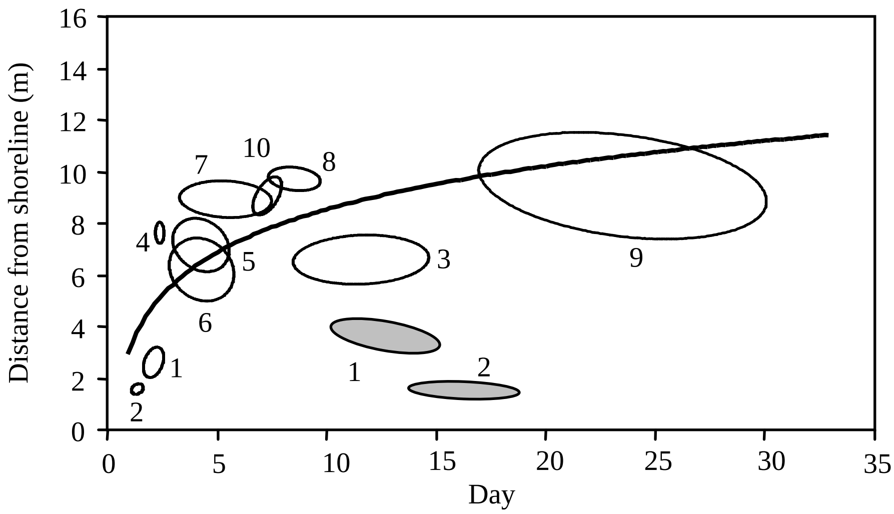

Figure 3: Hotelling's confidence ellipse (95%) of mean day of appearance and across-shore mean zonation of the different beach macroinvertebrates in the cylinders (empty ellipses) and controls (shaded ellipses). 1 *Tylos europaeus*, 2 *Talitrus saltator*, 3 Aranei, 4 Diptera, 5 Staphylinidae, 6 *Brachygluta globulicollis*, 7 *Phaleria bimaculata*, 8 *Phaleria* spp. larvae, 9 *Trachyscelis aphodioides*, 10 Formicidae.

and pselaphids) that successively invaded the wracks to feed on their eggs and larvae. Tenebrionids *(Phaleria bimaculata)* were mid-invaders and preferentially occupied experimental wracks higher up on the eulittoral. The differences found in the sex ratio in the experimental wracks compared to the active population (pitfall traps) indicated that females were attracted to the experimental cylinders before males suggesting that wracks, or sand beneath the wracks, might be used as sites for ovideposition or as a nursery ground. The tenebrionid *Trachyscelis aphodioides* was definitively a late invader appearing on wracks only in the last period of the experiment.
Interspecific facilitation is a process that probably occurs with late species benefiting from the presence of the earlier arrival of primary colonists. The presence of early arrivals modifies the resource qualitatively and makes it more suitable for later invaders.
To study the potential transference of energy and matter from the marine subtidal to the supralittoral zones and to assess the its importance in the food web of terrestrial macrofauna another study was carried out at the Maremma Regional Park (42° 37' 52.8" N, 11° 4' 42.3" E; Grosseto, Italy). At the site a transect (150 m) of pitfall traps was set perpendicularly to the shoreline and proceeded landwards to the dune slack (Figure 3). To assess the vegetation qualitatively and quantitatively in the different seasons quadrats of surface

	Hotelling's test	One-factor ANOVA	
		Time	Space
Experimental cylinders			
T. europaeus vs. *T. saltator*	26.775 ***	14.355 ***	49.063 ***
Staphylinidae vs. *B. globulicollis*	0.922 NS	0.002 NS	1.807 NS
Staphylinidae vs *P. bimaculata*	5.780**	1.115 NS	9.513 NS
P. bimaculata vs. *Phaleria* spp. larvae	9.546 ***	11.131 ***	4.899 *
P. bimaculata female vs. male	12.265 ***	24.010 ***	1.325 NS
Controls			
T. europaeus vs. *T. saltator*	29.119 ***	6.218 *	58.101 ***
Experimental cylinders vs. controls			
T. europaeus	71.870 ***	98.162 ***	7.244 **
T. saltator	764.933 ***	1529.664 ***	0.232 NS

Table 1: Hotelling's two-sample tests and one-factor ANOVA of spatial and temporal distributions of macroinvertebrates. * = $p<0.05$, ** = $p<0.01$, *** = $p<0.001$, NS = not significant.

vegetation were sampled and mean plant biomass was calculated. In this stretch of coast beach cast material was mainly composed of the marine angiosperm *Cymodocea nodosa* due to the presence of a conspicuous seagrass meadow in front of the study area. To determine seagrass deposits monthly samples were taken from the sealine limits to the first pioneer plants. Terrestrial macroinvertebrates collected from pitfall traps were used for stable isotope determination. Three intertidal species and seston, collected superficially in the surf zone, were selected to assess the possibility of marine items entering the terrestrial food web. Samples of the most abundant plants were selected to determine the terrestrial-derived component that entered the trophic web. Surface sediment samples were collected to assess sediment organic matter (SOM). Faeces of occasional visitors such as cattle, fallow deer and sea gulls were also sampled to assess other sources of allochthonous organic matter.

In the laboratory international standard methods were used to prepare and determine isotopic signature of plants, macrofauna and allochthonous material. The elimination of carbonates by acidification prior to isotopic analysis was considered for marine derived macrophytes and animals, intertidal crustacean species and SOM [8].

At the Maremma Regional Park *Cymodocea nodosa* was the main marine subsidy deposited on the eulittoral (Figure 4, Table 2) The marine biomass that irregularly reached the beach during the year was twice the size of the autochthonous plant biomass present in the area. This was mainly due to the presence of a conspicuous seagrass bed in the shallow waters in front of the study site but also to the particular instability of this section of the coast.

The analysis of the isotopic signatures of marine allochthonous inputs of algae, seston, diatoms and marine organisms (Figure 5) showed that seagrasses were definitively more enriched in carbon as in other C4 plants whereas seagull faeces had the highest nitrogen values. Carbon values of SOM were more depleted compared to items of marine origins and did not differ

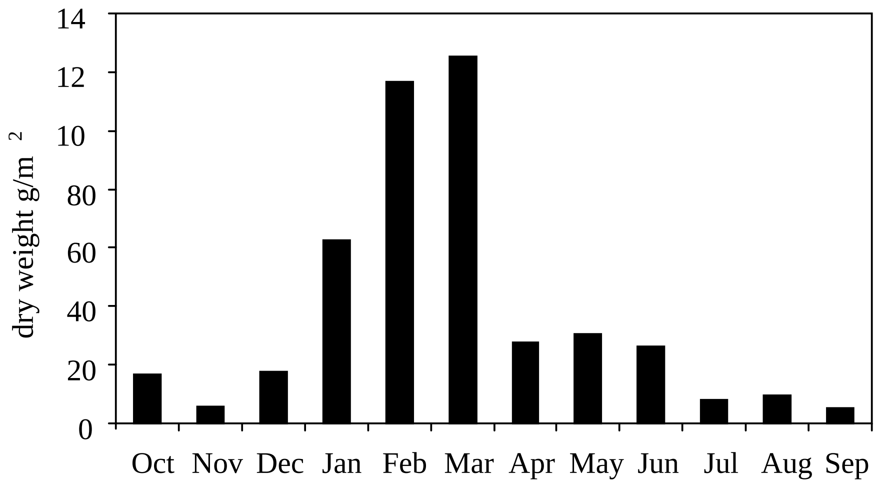

Figure 4: Monthly stranding of *Cymodocea nodosa* wracks (October 2006 – September 2007) at the Maremma Regional Park.

from the overall mean value of the plants. On the other hand nitrogen values of SOM was significantly different from that of the plants indicating a marine organic input. Faeces of fallow deer and cattle differed significantly for carbon values but not for those of nitrogen.

The analysis of stable isotopic signatures of the plant species (Figure 6, Table 2) showed a significant difference in the isotopic signatures of plants with C3 and C4 photosynthetic pathways. C4 plants (P1 group and seagrasses) were more enriched in δ13C compared to the C3 plants (P2 and P3 groups) providing them with an important adaptive mechanism in hot environments.

Analysing the spatial distribution (along the sea-land axis) of the macroinvertebrates of the four groups obtained with cluster analysis (Figure 6, Table 3), it appears clear that these groups include eu- and supralittoral species (A1 and A2 groups) on the one hand and extralittoral species (A3 and A4 groups) on the other. Furthermore, the A1 group derived carbon from marine sources as it had a stable isotope ratio more enriched in δ13C compared to the other groups (Table 4). Instead, A2 group derives carbon from both marine and terrestrial sources in an equal way or prevalently from terrestrial food items (Table 4). The species belonging to the A1 group were mainly primary and secondary consumers, the latter foraging on preys found within the stranded wracks. A2 group was more heterogeneous and exhibited species belonging to different trophic guilds. Primary consumers (herbivores feeding on vascular plants of marine and terrestrial habitats), scavengers, predators and top predators mainly belonged to the beach and to the foredune. However, other more mobile species (fliers or spi-

species	P	mean zonation	species	mean zonation
Plants		m	Others	m
Juniperus oxycedrus	3	102	Bacillariophyceae gen. sp.	s
Pancratium maritimum	3	70	Phaeophyceae gen. sp.	s
Ammophila arenaria	2	63	*Ulva lactuca*	s
Elymus farctus	3	64	Rhodophyta gen. sp.	s
Erianthus ravennae	1	137	*Cymodocea nodosa*	s
Sporobolus pungens	1	45	*Posidonia oceanica*	s
Sporobolus pungens	1	123	*Donax trunculus*	i
Schoenus nigricans	2	122	*Ophelia radiata*	i
Juncus acutus (stem)	2	122	*Eurydice* sp.	s
Juncus acutus (leaf)	3	122	*Larus cachinnans* faeces	nl
Salicornia fruticosa	2	123	*Dama dama* faeces	nl
Salsola kali	1	55	*Bos taurus* faeces	nl
Silene colorata	3	78	Seston	sz
Limonium etruscum	2	106	Wood debris	s
Euphorbia paralias	3	57	Stranded wood (a)	s
Euphorbia peplis	1	60	SOM	10
Medicago litoralis	3	85	SOM	30
Ononis variegata	3	75	SOM	50
Cakile maritima	2	40	SOM	70
Erica multiflora	3	145	SOM	90
Blackstonia perfoliata	3	107	SOM	110
Plantago coronopus	3	123	SOM	130
Echinophora spinosa	3	50	SOM	150
Pseudorlaya pumila	2	72		
Anthemis maritima	3	68		
Dittrichia viscosa	2	125		
Helichrysum stoechas	3	85		
Inula crithmoides	2	50		
Inula crithmoides	3	125		
Xanthium italicum	2	62		

Table 2: Mean zonation of plants and allochthonous inputs. Groups (P) found with cluster analysis are also reported m = meters from the shore line, a = associated to *M. remyi*, s = stranded, i = intertidal, sz = surf zone, nl = not localised.

ders) occupied the landward face of the dune. A3 group pooled species inhabiting the backdune which included a variety of species belonging to different trophic guilds (primary consumers, scavengers and predators). The A4 group included species feeding on pollen and others soil arthropods (collembolans, amphipods and mud snails) which fed on items such as monocellular algae, bacteria and fungi, for which isotopic signatures were not evaluated.
There was a decrease in the stable isotopic signatures of the macroinvertebrate population when proceeding towards land (Figure 7). This decrease in δ13C values indicated that the influence of marine subsides in the food web decrease at increasing distance from the sea. This was also confirmed by the results obtained with the mixing model based on five food sources (Table 4). A similar result was obtained by Paetzold et al. [9] that showed the relatively low contribution of marine-derived resources to the diet of terrestrial arthro-

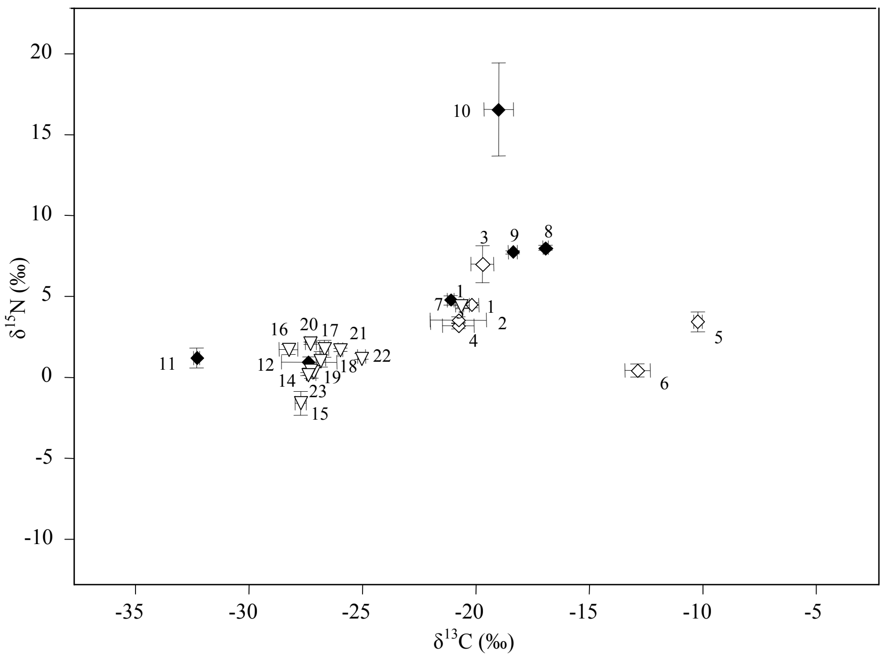

Figure 5: Stable isotopes of δ13C and δ15N (with standard errors) of allochthonous material obtained with cluster analysis. 1) Bacillariophyceae gen. sp., 2) Phaeophyceae gen. sp., 3) *U. lactuca*, 4) Rhodophyta gen. sp., 5) *C. nodosa*, 6) *P. oceanica*, 7) *D. trunculus*, 8) *O. radiate*, 9) *Eurydice sp.*, 10) *L. cachinnans* faeces, 11) *D. dama* faeces, 12) *B. taurus* faeces, 13) Seston, 14) Wood debris, 15) Stranded wood, 16) SOM 10 m, 17) SOM 30 m, 18) SOM 50 m, 19) SOM 70 m, 20) SOM 90 m, 21) SOM 110 m, 22) SOM 130 m, 23) SOM 150 m.

pod consumers of a productive temperate island.

3 Relevant results and Conclusions

In general, the presence of a specific fauna in the wrack is thus the result of a combination of factors such as species adaptation to specific microclimatic conditions of the wracks. As a matter of fact departure by crustaceans from the wracks was related to the microclimatic conditions of the wracks that changed through time. Also the tendency of tenebrionids to occupy wracks higher up on the eulittoral was in relation to their preference for lower moisture contents in the sand. However, the presence of macrofauna associated to the wrack was linked to the need of finding an adequate food source. Thus prey species could benefit by the presence of other species (both bacteria and inverte-

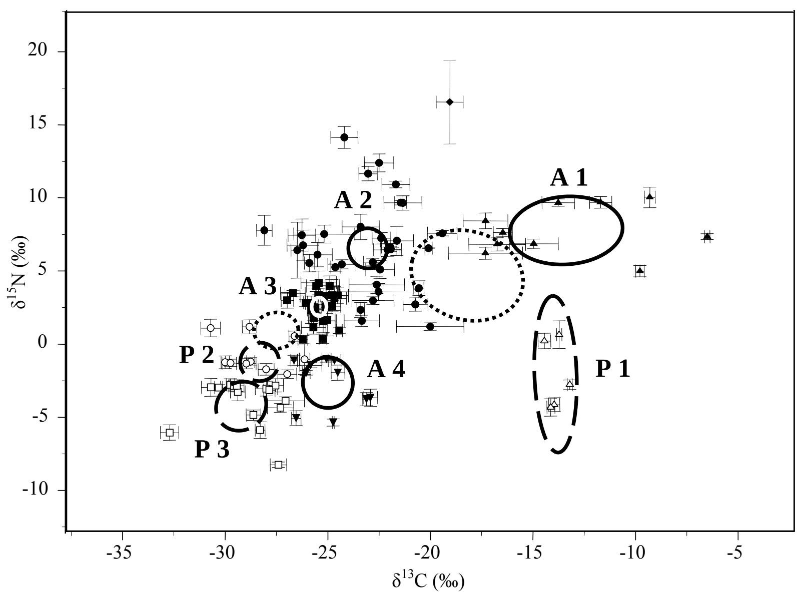

Figure 6: Stable isotopes of δ13C and δ15N (with standard errors) relative to terrestrial plant and macroinvertebrate species analysed with hierarchical cluster analysis. For plant species three groups are indicated (P1 empty triangles, P2 empty circles, P3 empty squares), for macroinvertebrates four groups are shown (A1 full triangles, A2 full circles, A3 full squares, A4 inverted full triangles). Hotelling's confidence ellipses at a 95% level of probability (Batschelet 1981) are also shown for plants (dashed line ellipses), macroinvertebrates (continuous line ellipses) and for allochthonous material (dotted line).

brates) inhabiting wrack of different age. Changes in the microclimatic conditions of the wrack suggests that beach deposits might represent an important but quite transient resource for food and shelter for resident macroinvertebrates as was shown for stranded wracks of tropical and temperate beaches.

In conclusion these studies show that marine allochthonous subsidises are extremely important to beaches as they represent a fundamental habitat in which beach macroinvertebrates find refuge against extreme environmental conditions on the one hand and trophic sources on the other. Stranded wracks are extremely variable habitats continuously undergoing changes due to sun, tides, wave and wind action, aging etc. Thus species, exploiting wracks, colonise the habitat only in species specific conditions that occur according to variations in time (days after deposition) and in space (along the sea-land axis). However, the study also showed that allochthonous marine material mainly subsidised macroinvertebrates species inhabiting the eulittoral and contributed very little to the food chains of more terrestrial

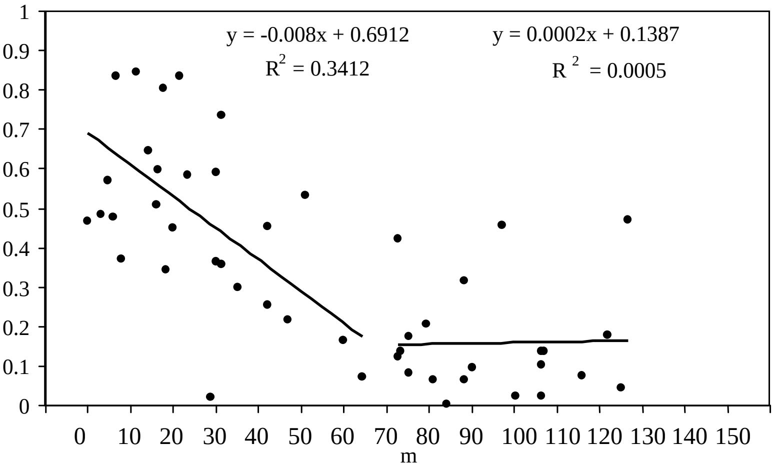

Figure 7: Proportion of marine food sources present in the diet of different macroinvertebrate species calculated with the multi-source mixing model) and plotted against their mean zonation (in metres). Regression equations and probability levels (P) are also shown for the two areas.

species. The complexity of the area backing up the beach and the presence of a dune slack rich in plant species probably were sufficient to provide subsistence to macroinvertebrates. Thus the presence of beach wrack is of fundamental importance for the maintenance of a high macrofaunal diversity in the terrestrial coastal environment. Its importance is further magnified by the fact that it can represent the basal source for resident and non-resident opportunistic vertebrate species.

4 Future Research

With an increase in the knowledge of ecosystem functioning there might be a chance that in the future managers and decision makers will enhance their awareness for a sustainable management of beach ecosystems. In fact sandy beach ecosystems are extremely vulnerable to anthropogenetic uses and to climatic changes through sea level rise and need adequate conservation strategies. Information on the role of beach wrack is useful for action plans in order to take correct decisions in managing coastal recreational activities. Understanding of the biological cycles of beach macroinvertabrates associated to beach wracks, their variation in space and time, the colonisation processes and its role in the trophic web is of fundamental importance for beach management. However future work needs to be done on key species, also on other beach types (different exposure, slope, width etc) to further understand how these can exploit different kinds of marine items throughout a larger time frame.

species	A	mean zonation	species	A	mean zonation
Hygromiidae		m	Staphylinidae		m
Trochoidea trochoides (a)	3	106	*Quedius* sp.	3	122
Trochoidea trochoides (b)	4	122	*Mycetoporus* sp.	2	20
Helicidae			*Tachyporus* sp.	2	20
Eobania vermiculata	3	25	*Phytosus nigriventris*	1	11
Phalangiidae			*Phytosus nigriventris* l.	1	11
Phalangium opilio	3	116	*Atheta* sp. 1	1	23
Pseudoscorpionida gen. sp.	2	73	*Atheta* sp. 2	2	12
Lycosidae			*Atheta* sp. 3	2	25
Arctosa cinerea	2	51	Geotrupidae		
Arctosa perita	2	88	*Thorectes intermedius*	3	88
Thomisidae			Cetonidae gen. sp. l.	3	40
Thomisus onustus	2	122	Elateridae		
Tylidae			*Isidus moreli*	2	31
Tylos europaeus ad.	2	14	*Isidus moreli* l.	1	32
Tylos europaeus juv.	2	6	Buprestidae		
Porcellionidae			*Acmaeodera quadrifasciata*	4	75
Agabiformius obtusus	2	79	Coccinellidae		
Talitridae			*Adalia decempunctata*	2	122
Macarorchestia remyi	2	30	Oedemeridae		
Orchestia gammarellus ad.	4	124	*Oedemera flavipes*	4	75
Orchestia gammarellus juv.	4	123	*Stenostoma rostratum*	2	75
Talitrus saltator ad.	2	8	Anthicidae		
Talitrus saltator juv.	2	3	*Cyclodinus constrictus*	2	122
Geophilidae			Tenebrionidae		
Geophilus sp.	2	42	*Tentyria grossa*	3	84
Collembola gen. sp.	4	113	*Stenosis brenthoides*	3	81
Machilidae gen. sp.	4	106	*Pimelia bipunctata*	2	64
Blattellidae			*Pimelia bipunctata* l.	3	60
Loboptera decipiens	4	92	*Gonocephalum pusillum*	3	97
Rhinotermitidae			*Trachyscelis aphodioides*	1	24
Reticulitermes lucifugus	3	60	*Phaleria provincialis*	1	18
Acrididae			*Phaleria provincialis* l.	1	21
Oedipoda caerulescens	2	45	*Halammobia pellucida*	2	47
Aiolopus strepens	3	90	*Xanthomus pellucidus*	2	42
Labiduridae			Bruchidae gen. sp.	4	27
Labidura riparia	3	107	Curculionidae		
Miridae			*Mesites pallidipennis*	3	25
Lygus pratensis	2	73	Myrmeleontidae		
Lygaeidae			*Acanthaclisis baetica* l.	2	56
Beosus maritimus	3	106	Ascalaphidae		
Carabidae			*Libelloides coccajus*	3	125
Cicindela campestris	3	127	Sepsidae gen. sp.	3	99
Cylindera trisignata	2	0	Heleomyzidae gen. sp.	2	18
Calomera littoralis	3	100	Drosophilidae gen. sp.	2	40
Eurynebria complanata	2	23	Diptera gen. sp. l.	1	20
Eurynebria complanata l.	2	16	Braconidae		
Scarites buparius	2	35	*Apanteles* sp.	3	29
Parallelomorphus laevigatus	2	5	Scoliidae		
P. laevigatus l.	1	7	*Scolia sexmaculata*	3	106
Licinus sp.	4	123	Mutillidae		
Histeridae			*Smicromyrme viduata*	3	73
Hypocaccus dimidiatus	1	2	Formicidae gen. sp.	3	75
			Pompilidae		
			Pompilus cinereus	2	30

Table 3: Mean zonation of terrestrial macroinvertebrates. Groups (A) found with cluster analysis are reported. m = metres from the shoreline, a = on *L. etruscum*, b = on *S. nigricans*.

beach dune species	land	sea	dune slack species	land	sea
A1			A3		
I. moreli l.	0.27	0.73	*T. grossa*	1.00	0.00
P. provincialis l.	0.16	0.84	*T. trochoides*	0.98	0.02
P. provincialis ad.	0.20	0.80	*C. campestris*	0.53	0.47
P. nigriventris	0.15	0.85	*Apanteles* sp.	0.98	0.02
P. laevigatus l.	0.16	0.84	*L. coccajus*	0.96	0.04
H. dimidiatus	0	1	*E. vermiculata*	0.92	0.08
A2			*P. opilio*	0.93	0.07
S. rostratum	0.83	0.17	*G. pusillum*	0.55	0.45
M. remyi	0.64	0.36	*T. intermedius*	0.94	0.06
A. obtusus	0.80	0.20	*S. brenthoides*	0.94	0.06
X. pellucidus	0.74	0.26	*A. strepens*	0.91	0.09
Pseudoscorpida gen. sp.	0.58	0.42	*B. maritimus*	0.90	0.10
S. buparius	0.70	0.30	*C. littoralis*	0.98	0.02
A. perita	0.69	0.31	*S. sexmaculata*	0.87	0.13
P. bipunctata	0.93	0.07	*S. viduata*	0.87	0.13
T. onustus	0.82	0.18	*L. riparia*	0.87	0.13
I. moreli	0.64	0.36	*P. bipunctata*	0.84	0.16
H. pellucida	0.78	0.22			
L. pratensis	0.88	0.12			
T. saltator ad.	0.63	0.37			
E. complanata l.	0.40	0.60			
C. trisignata	0.53	0.47			
T. europaeus juv.	0.52	0.48			
T. saltator juv.	0.52	0.48			
A. cinerea	0.47	0.53			
T. europaeus ad.	0.35	0.65			
Geophilus sp	0.55	0.45			
Heleomyzidae gen. sp.	0.66	0.34			
P. cinereus	0.41	0.59			
E. complanata	0.41	0.59			
P. laevigatus	0.43	0.57			
Mycetoporus	0.55	0.45			
Atheta sp. 1.	0.49	0.37			

Table 4: Proportion of terrestrial vs. marine food items entering the trophic web of macroinvertebrates (marine sources = seagull faeces, marine seagrasses and marine organisms; terrestrial sources = terrestrial plants and sediment organic matter). a = on *L. etruscum*.

5 Acknowledgements

These studies were partially supported by funds of the Italian National Council of Research (CNR) and by the MEDCORE and WADI Projects. We also would like to thank the WWF Burano Oasis, the Maremma Regional Park and the Azienda Regionale Agricola di Alberese.

References

[1] I. Colombini, M. Fallaci, F. Milanesi, F. Scapini, and L. Chelazzi. Comparative diversity analysis in sandy littoral ecosystems of the Western Mediterranean. *Estuarine, Coastal and Shelf Science*, 58S:93–104, 2003.

[2] A. Mc Lachlan and A. Brown. The Ecology of Sandy Shores. Second ed. *Academic Press*, page 362, 2006.

[3] M. Fallaci, I. Colombini, and L. Chelazzi. An analysis of the Coleoptera living along a Tyrrheian beach-dune system: population dynamics, zonation and ecological indices. *Vie et Milieu*, 44:243–256, 1994.

[4] I. Colombini, A. Aloia, M. Fallaci, and L. Chelazzi. Spatial and temporal strategies in the surface activity of some sandy beach arthropods living along the French Atlantic coast. *Marine Biology*, 127:247–257, 1996.

[5] I. Colombini, A. Aloia, M. Fallaci, G. Pezzoli, and L. Chelazzi. Spatial use of an equatorial coastal system (East Africa) by an arthropod community in relation to periodically varying environmental conditions. *Estuarine, Coastal and Shelf Science*, 47:633–647, 1998.

[6] I. Colombini, A. Aloia, M. F. Bouslama, M. El Gtari, M. Fallaci, L. Ronconi, F. Scapini, and L. Chelazzi. Small-scale spatial and seasonal differences in the distribution of beach arthropods on the northern Tunisian coast. Are species evenly distributed along the shore? *Marine Biology*, 140:1001–1012, 2002.

[7] I. Colombini, A. Aloia, M. Fallaci, G. Pezzoli, and L. Chelazzi. Temporal and spatial use of stranded wrack by the macrofauna of a tropical sandy beach. *Marine Biology*, 136:531–541, 2000.

[8] I. Colombini, M.A. Mateo, O. Serrano, M. Fallaci, E. Gagnarli, L. Serrano, and L. Chelazzi. On the role of Posidonia oceanica beach wrack for macroinvertebrates of a Tyrrhenian sandy shore. *Acta Oecologica*, 35:32–44, 2009.

[9] A. Paetzold, M. Lee, and D.M. Post. Marine resource flows to terrestrial arthropod predators on a temperate island: the role of subsidies between systems of similar productivity. *Oecologia*, 157:653–659, 2008.

The Use of Maps of Geo-Environmental Compatibility in Coastal Management: the Case of the Cilento Coast (Southern Italy)

M.M. Calandrelli[1], C. Cirillo[1], G. Acampora[1], L. Scarpa[2]
1, Institute of Agro-Envinronmental and Forest Biology, CNR, Napoli, Italy
2, University of Napoli "Federico II", Napoli, Italy
clelia.cirillo@ibaf.cnr.it

Abstract

Most of the land surface is affected by anthropic intervention with high environmental impacts; the rapid changes produced by man are opposed to the slowness of the biological time necessary for the adaptive natural counterstrategies of the living organisms to evolve. This leads to an environmental emergency which will increase over time. To protect ecosystems from anthropic pressures it is necessary that the behaviour of the human species evolves in line with the biological balance of the ecosystems. The application of environmental models to the processes of planning and management of coastal zones makes it possible to identify lines of sustainable actions to be taken to avoid, solve or mitigate environmental problems that affect these areas. In order to sustainably manage coastal development a methodology was experimented for the analysis of natural and anthropic contexts which led to the realization of the map of geo-environmental compatibility aiming at highlighting parts of the territory in which the anthropic interventions are at a high environmental impact. The use of GIS methodology was effective as allowed to manage the data using a relational database, structured according to data from graphs and alphanumeric data being logically connected. The study area covered the coastal area of the National Park of Cilento and Vallo di Diano, characterized by heavily populated areas but with a strong naturalistic and environmental value.

1 Introduction

The study area includes the Cilento coast. The Cilento is a short and wide, rectangular headland intervening between the Salerno Gulf and the Policastro Gulf. It corresponds on a morpho-structural high that merges landward into the main relief of the Apennines [1]. The area of the park is delimeted in the North by the Sele Plain, in the NE By Tanagro Valleys, in the South by Policastro Gulf and in the West by the Tirrenian sea. In this area a geological heritage characterized by a high degree of diversity is preserved; coastal and mountain areas made up both by carbonate and terrigenous successions give rise to a landscape alternating between steep mountainous districts and hilly areas [2].

The morphology of the coastal system is constantly changing due to erosion caused by the negative impact of anthropic activities and by the global climate change. These areas are affected by many environmental problems such as eutrophication and salinization caused by the scarcely eco-friendly use of water resources in farming practices. In order to stand up to the morphological imbalance and coastal pollution, an integrated decision-making process was developed at European level, aimed at managing the coasts taking into account all the associated aspects. Nevertheless, the implementation of the Integrated Management of Coastal Zone is hampered by the regulatory constraints of the Member States. In Italy, for example, coast planning is still characterized by an overlap of a number of national legal norms belonging to different competences of the State, Regions and Municipalities. Hence to achieve the integrated management of the coast it is necessary to establish principles and guidelines able to build innovative logics concerned with the integrity of environmental resources to support the sustainability of coastal areas at all territorial levels. In this respect the research may help to improve the territorial and environmental quality of the coasts through multidisciplinary scientific methodologies aiming at realizing methodologies of analysis to support decision makers. In order to stand up to the anthropogenic pressures, it is important to model the interactions between anthropic uses and natural resources and analyze the processes that characterize functioning and interaction. The environmental models represent valuable tools that can give reliable results by studying the internal dynamics of an ecosystem. The DPSIR models (Driving Pressure State Impact Replies) adopted in Europe under the European Water Directive (WFD EC 60/2000), establishes the relationship between the causes (Drivers, Pressures), effects (States, Impacts) and the possible responses (Responses)[3]. In this study, the parametric model was adopted [4] used for the first time to assess the vulnerability of aquifers to pollution, which is based on the selection of parameters. The research has been addressed using a similar approach, as parameters, identifying elements of land and man-made structures. With the help of the modern GIS technologies (Geographic Information System), which allow the processing of data and information and their return in the form of thematic maps [5], the synthetic map on the geo-environmental compatibility of the anthropic uses was realized with respect to the natural and historical-artistic values of the Cilento Coast.

The objective of this study was to highlight, through the analysis of the geo-environmental compatibility map, the situations of the impact of human activities in order to provide guidance for developing action of ecological recovery and environmental rehabilitation of degraded areas of the coastal areas at a high environmental value.

2 Maps of geo-environmental compatibility

To deal with environmental pollution of anthropogenic origin, it is important to be able to represent the interactions that are produced by environmental impacts; in order to organize environmental information in a way that highlight the causal sequence between anthropic activities (pressures), the effects on environmental conditions (state) and the responses of the society to mitigate the impacts (response) it is important to build models correlating the environmental data in a matrix form. To support territorial and environmental plan-

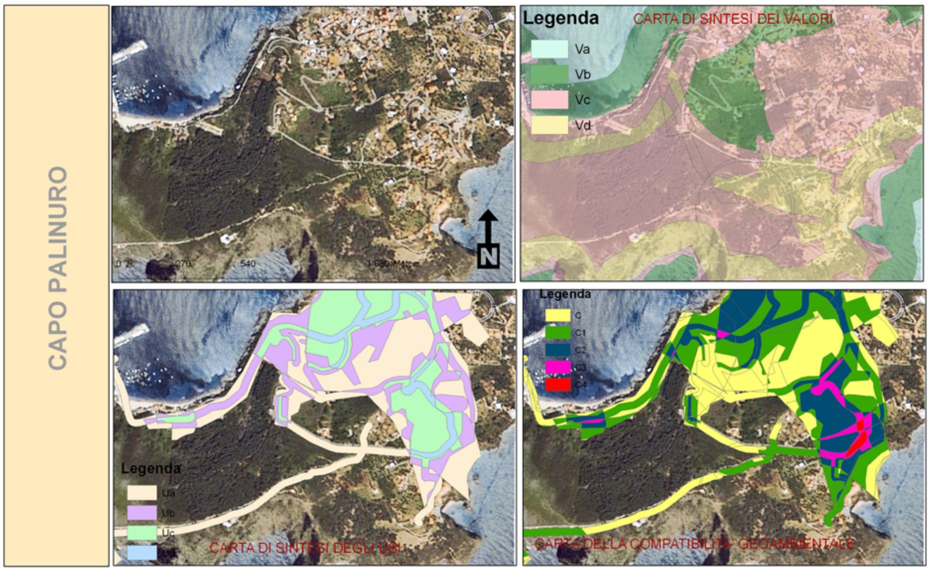

Figure 1: Synthesis map of values of the Cilento coastal area.

ning, these matrices must rely on geo-referenced databases so that they can report thematic and cartographic data from different sources as well as qualitative and quantitative information. GIS methodologies, with their flexibility in storing, sorting, processing and return of explicit spatial information of geographic areas of different extension and resolution [6], represent an effective tool for the integrated management of coastal areas. To make the environmental re-qualification of seacoasts with regard to the sustainability of the resources, the lines and strategies of territorial and environmental planning instruments should be articulated into inter-related sector plans, in production systems, transport systems, administrative systems, organizational systems in general paying special attention to the systems of cultural and natural asset.

The description of the environment through components, although involving simplifications, remains the starting point for the construction of a Geographic Information System able to represent all territorial and environmental phenomena. The analyses should be carried out aiming at a scientific evaluation, assigning to each component parameters able to measure and represent the selected environmental and/or territorial phenomenon. The identification of environmental components susceptible to anthropic pressures, is one of the main objectives to consider for environmental studies. This objective can be achieved by building a system of indicators and parameters able to analyze the quality and the degree of the environment vulnerability over time. The assessment of land vulnerability in this environmental model consists in the quantitative estimate, expressed as score, of the

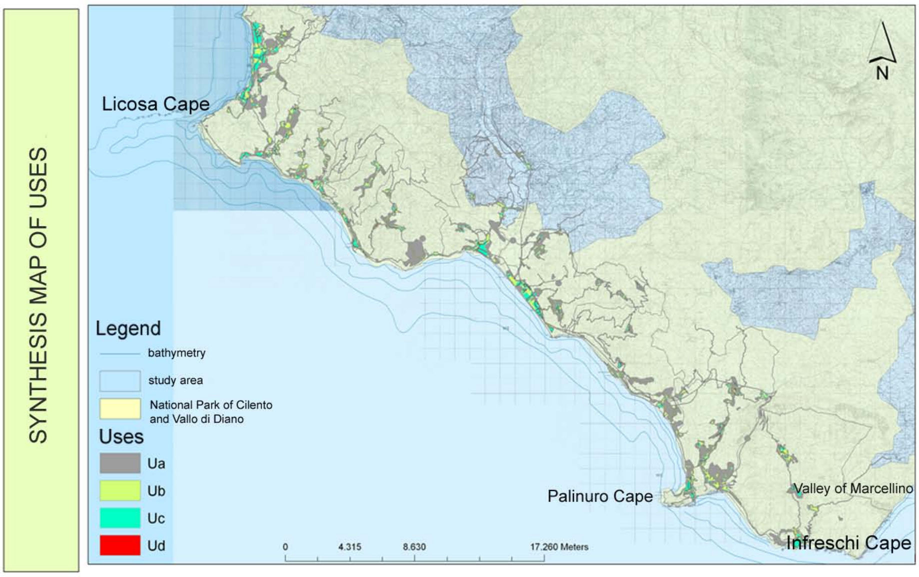

Figure 2: Comparison between charter of values, charter of uses and charter of geo-environmental compatibility for the area of Ogliastro Marina (Cilento, Southern Italy)

antropic impact, associated to the selected parameters. For the Cilento coastal area we selected the following parameters:

- protected areas (National Park of Cilento, SIC, ZPS, areas protected under the Legislative Decree no. 490/1999 and Legislative Decree no. 42/2004);
- naturalistic values (geosites);
- forests (coniferous and broadleaf);
- traditional crops (olive groves and vineyards);
- historical assets (emerging historical assets, archaeological sites, historical centers);
- urban areas;
- urban centres;
- road network (roads, railways);
- other man-made works (dams, quarries).

Each parameter was expressed by a thematic map in ArcGIS environment. The selected parameters were divided by selected ranges and / or declared types, and a growing score was assigned in light of the importance it plays in the final overall assessment. The scores obtained for each parameter can be added together (RS = Rating System) or crossed in a matrix (MS = Matrix System) or multiplied by strings of weights describing the hydrogeological and / or impact situation, emphasizing the varying action and importance of the various parameters (PCSM = Point Court System Model). The SINTACS method [4] belongs to the latter type with the acronym derived from the names of the seven parameters considered (each with scores ranging from 1 to 10) [7]. The assignment of scores is determined on the basis of the absolute value taken from it depending on the chosen scenario characterizing the context

of study. Given that the research aims at defining the degree of geo-environmental compatibility of Cilento area, higher scores were assigned to the parameters that express the degree of protection and naturalness of the area and lower scores to the parameters that, in contrast, are elements of impact [8].
After establishing the scores, the spatial analysis was carried out using the overlay function, which operates on different layers of information, it integrates the information and generates a new layer of information, where each component inherits all features from the previous ones. Thus, the scores of the previously defined nine parameters (Natural park, Special Protection Area, Site of Community Importance, Legislative Decree no. 490/1999, Legislative Decree no. 42/2004, naturalistic values, forests, traditional crops, historical assets) identifying the peculiarities of the study area were added together. The resulting new layer information called synthesis map of values summarizes the values referring to all natural, landscape and cultural resourcesin the Cilento coastal area (Figure 1). In it we identify four levels of increasing values: Va- low-valorization, Vb- medium valorization, Vc- high valorization, Vd- extreme valorization. Likewise, the map of the uses (Figure 2) was obtained by merging six information layers (National park uses, urban areas, urban centres, roads, railways, others man-made works) referred to the anthropic use, which shows the degree of anthropogenic land utilization. Even for this map we have four increasing levels of use: Ua, Ub, Uc and Ud, which respectively express a low, medium, high and extreme use. The resulting index value and the index of use are respectively correlated with the degree of exploitation as well as with the degree of utilization (ranging from low to extreme). This approach results in the quantification of the vulnerability of a natural system by evaluating a number of parameters; the purpose is to build maps of medium-large scale denominator (1:100.000-1:25.000); cartographic representations containing the infrastructures and the human activities are then overlaid to these maps of the intrinsic vulnerability of the territory. The result is a map of the territory being colored according to the importance of the human impact. Thanks to the structure into parameters it is possible to distinguish different situations of impact of a site thus allowing comparisons between very different and distant situations, so as to provide easily interpretable information to the institutions being responsible for the land management.

3 Results and discussion

The applied parametric model shows that the study area presents a medium degree of enhancement (Figure 1; Vb-colour green) distributed almost uniformly throughout the country. Outstanding features of high environmental value (Figure 1; Vc-colour violet) correspond to the areas where more elements of natural and historical interest are concentrated and areas at high biodiversity. Some examples are the marine terrace of Punta Licosa, the whole system of cliffs of Capo Palinuro and the Infreschi coast up to the deep Valley of Marcellino, considered a site of considerable geomorphological interest [9]. As far as the anthropic uses are concerned, a low-usage (Figure 2; Ua-colour gray) was registered in the areas adjacent to the inland built-up areas, and in the coastal areas next to small built-up areas that form the link between a small town and another. It reaches a high level

(Figure 2; Uc-colour blue) in the coastal urban centers, which are the most endangered and threatened by anthropic activities. The adopted method of analysis allows us to outline a broad cognitive framework of the environmental dynamics acting on a certain territory; it can be refined and strengthened according to the level of examination and knowledge to be achieved by defining each time the different scenarios, and calibrating the weights of the selected parameters. It is possible to match data on the degrees of use and value in a matrix thus defining the compatibility level between the uses and values of the land, where:

- C4 expresses the lack of compatibility between anthropic uses and environmental values
- C3 expresses scarce compatibility
- C2 expresses low compatibility
- C1 expresses medium compatibility
- C shows that uses are compatible with values

These indexes can be displayed in the map of geo-environmental compatibility (Figure 3), achieved by performing an overlay function between the two synthesis maps, which defines the degree of impact of the anthropic activities over the study area. The maps of geo-environmental compatibility, allowed us to quickly highlight the most critical situations for which restoration and re-qualification interventions should be provided. In the study area mitigation actions should be implemented just on the coast, where built-up areas, often abusive, and the occurrence of an invasive road network, invalidate land areas with a great landscape value.

4 Conclusions

From the general analysis of the results obtained, it may be concluded that the study area, despite the widespread anthropic activity occurred in the last twenty years, continues to present itself as a territory of great value which requires a careful protection. Based on the maps of geo-environmental compatibility the anthropic pressure still remains, on the whole on acceptable values. The statistical analysis of the data shows that the exploited areas cover 89.6% of the examined territory, corresponding to 427.30 sq km (including protected marine areas) and only 10.4% is affected by anthropic activities.
The ability to point out the functional relationships between the anthropic activities and the different environmental components is of a particular importance for management plans. The efforts of present and future managers will require to continue to combine the protection of the area with an advanced model of economic and social development that involves the use of this rich natural and cultural heritage. One of the most interesting aspects of the National Park of Cilento and Vallo di Diano is the high heterogeneity related to a number of environmental factors hardly occurring in other areas of the Italian Peninsula.

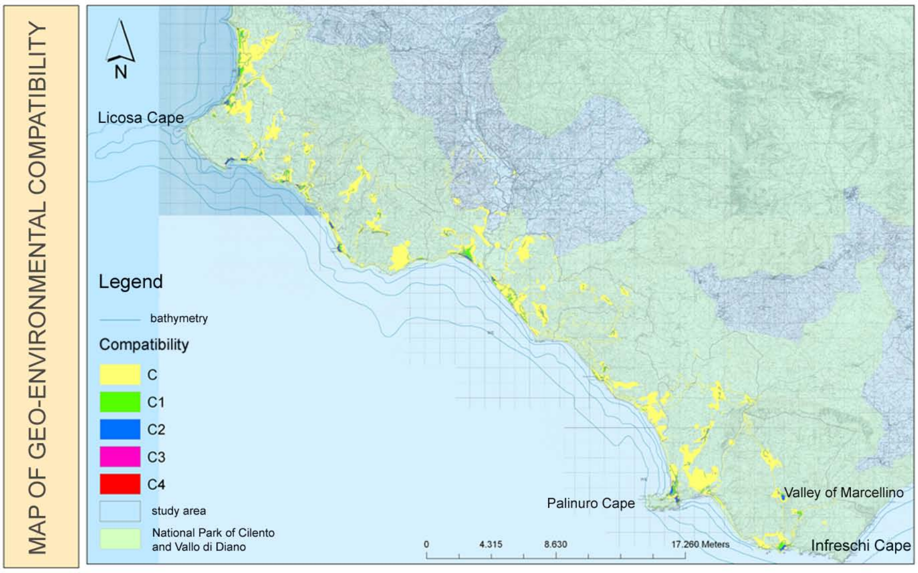

Figure 3: Map of geo-environmental compatibility.

References

[1] F. Antonioli, A. Ascione, A. Cinque, L. Ferranti, and P. Romano. Coastal and underwater geomorphology of Capo palinuro area. Guidebook to the field-sea trip. In: Convegno Internazionele di Geologia subacquea GEOSUB 1994 Guide to the excursion a cura di F. Antonioli, C. Donadio, L. Ferranti, De Frede Napoli. 1995.

[2] N. Santangelo, A. Santo, D. Guida, R. Lanzara, and V. Siervo. The geosites of the Cilento-Vallo di Diano National park (Campania region, Southern Italy). *Il Quaternario Italian Journal of Quaternary Sciences*, 18(1):103–114, 2005.

[3] S. Marsili Libelli. Ecological Modelling, in Computer Methods and software for simulating environmental pollution and its adverse effects (P. Zanetti ed.) Computational Mechanics Press. 1993.

[4] M. Civita and M. De Maio. SINTACS. Un sistema parametrico per la valutazione della cartografia della vulnerabilità degli acquiferi all'inquinamento. Metodologia ed automazione. *Quaderni di tecniche di protezione ambientale. Pitagora Editrice Bologna*, page 191, 1997.

[5] P.A. Burrough. Principles of Geographical Information Systems for Land Resources Assessment. Oxford University Press, New York. 1998.

[6] F.G. Hall, D.B. Botkin, D.E Strebel, K.D. Woods, and S.J. Goetz. Large-scale patterns of forest succession as determined by remote sensing. *Ecology*, 72:628–640, 1991.

[7] P. Barazzuoli, F. Capacci, J. Migliorini, B. Mocenni, R. Rigati, and M. Salleolini. La vulnerabilità degli acquiferi all'inquinamento nell'ambito dello schema metropolitano dell'area senese. *Giorn. di Geologia Applicata*, 2:151–155, 2005.

[8] M.M. Calandrelli. I valori paesaggistici e le instabilità geomorfologiche della fascia costiera cilentana in rapporto alla pianificazione territoriale e ambientale. Tesi di Dottorato in Scienze della Terra, Università degli studi di Napoli Federico II. page 181, 2008.

[9] C. Blasi, M. Milone, D. Guida, G. De Filippo, A. Di Gennaro, V. La Valva, and D. Nicoletti. Ecologia del paesaggio e qualità ambientale del Parco Nazionale del Cilento e Vallo di Diano. *Documenti del Territorio*, pages 20–30, 2000.

Modelling Environmental Fate and Transport of POPs and Metals using the Fugacity/Aquivalence approach: Two Aquatic Environments as a Case Study

C. Mugnai, S. Giuliani, L.G. Bellucci, S. Romano, M. Frignani
Institute of Marine Sciences, CNR, Bologna, Italy
cristian.mugnai@bo.ismar.cnr.it

Abstract

Multimedia environmental modelling is an useful tool to integrate the information necessary for the understanding of the mechanisms that drive the functioning of a complex system and to simulate its response to both natural and anthropogenic changes. The fundamental concept is that any chemical introduced into the environment is distributed between the components of the ecosystem according to its chemical-physical properties and those of each compartment. Fugacity (for the organics) and aquivalence (for non volatile chemicals) are used as equilibrium criteria. In this paper examples of multimedia modelling in two aquatic environments are shown. In the first case a pre-assembled level III fugacity model was used to screen the fate of PCB-118 in Lake Maggiore, using literature data. In the second example, the model was adapted to the Venice Lagoon accounting for spatial differences and water circulation. Modelled chemicals were octachlorodibenzodioxin/furan (OCDD and OCDF), PCB-180, Pb and Cu. The results described fairly well the fate of these chemicals in term of dominant processes, source apportionment and losses from the system. However, the available dataset for the Venice Lagoon is still not enough for a complete validation of the model. Consequently, the collection of field data on the key processes that drive contaminant variability is fundamental in order to extend its use as a decision supporting tool.

1 Introduction

Persistent organic pollutants and metals in aquatic environments are chemicals of concern due to their potential to negatively impact aquatic organisms and then humans. Over the past century industrial activities have contaminated many valuable coastal ecosystems. Moreover, due to the growth of the population, cities are becoming bigger and bigger, progressively incorporating the surrounding rural areas. These megacities require and use enormous amounts of energy and materials, metabolizing them and generating large quantities of waste products and pollutants, thus resulting in unsustainable conditions that adversely affect ecological integrity and diversity, human health and well-being.

In order to manage contaminants in the environment, it is important to identify and quantify their sources, transport mechanisms and fate. This can be achieved through the integration of measurements and the use of models. The advantage of models is that they assemble a wide array of information into a common framework. Furthermore, models allow determining process rates that are difficult to measure and permit the simulation of future scenarios for the assessment of the environmental response to natural or anthropogenic influences, such as new or reduced contaminant inputs, and climate changes. In this way, models will assist decision-makers in system management. They will also be useful tools for the orientation of further research and the results will be fundamental for the design of monitoring programmes that can provide the highest number of essential information with the minimum cost.

At present, Multimedia Models represent the most used instruments, thanks to their applicability to every type of environment and the capability to integrate and quantitatively describe different processes within and between compartments. The fundamental concept of multimedia modelling is that any chemical introduced into the environment is distributed between the various components of the ecosystem (e.g., air, water, soil, sediments, biota, etc.) according to its chemical-physical properties and those of each compartment.

Mackay et al. [1] introduced a family of multimedia, mass balance models that use fugacity as an equilibrium criterion. Fugacity, which accounts for the escaping tendency, has units of pressure (Pa) and can be viewed as the partial pressure that a chemical exerts as it attempts to escape from one phase to another. When equilibrium is achieved, the chemical will have the same fugacity in all phases. At environmental (low) concentrations, fugacity is linearly related to chemical concentration through the "fugacity capacity" Z, which expresses the capacity of a phase, or environmental medium, to hold a chemical. The largest is Z, the largest is the quantity of chemical that can be stored in a phase. The fugacity approach is suitable for not highly reactive organic compounds with a measurable vapour pressure.

The integrated models developed so far are unique for their applicability to many contaminants and their linkage of chemical loadings to potential health effects to human and ecosystem receptors. The current state of model development is summarized below.

1. Fate Model. The fate model component is based on the QWASI (Quantitative Water Air Sediment Interaction) model [1]. Over the years the models were extensively adapted, as described below:

   i. to take into consideration both volatile (hydrophobic organics) and non-volatile (metals) chemicals, [2] introduced the "aquivalence" formulation. Aquivalence (i.e. equivalent aqueous concentration, set as 1.00 for water) is analogous to fugacity as an equilibrium criterion, and Z values can be derived;

   ii. to model metals that exist as multiple, interconverting species, [3, 4] expanded the aquivalence formulation to assess the fraction of chemical species in each phase.

   iii. the multispecies model has been loosely coupled with a speciation/complexation model to create a connected TRANsport-SPECiation model [5]. This model (TRANSPEC) allows estimation of metal speciation in the aqueous phase (including binding to DOC in the colloidal phase) and complexation to solids that is governed by binding with Fe oxyhydroxides. In this way, [5] coupled MINEQL+ [6] with the multi-species aquivalence fate model to estimate the fate of Zn in a contaminated lake. The coupled model has also been applied to estimate the fate of Hg in a reservoir [7].

2. Food Web Model. The models of [8, 9] use the fugacity approach to estimate the uptake and transfer of hydrophobic organic contaminants in aquatic food webs. The food web model was applied in Lake Ontario [10], Lake Winnipeg [11] and Lake Ellasjoen (Bear Island, Norway, [12]).
3. Risk Assessment. A general risk assessment framework, applicable to ecosystem and human receptors, was developed [13, 14]. The approach is suitable for chronic exposure to low contaminant levels over the life-time. For ecological risk assessment, the method considers a first tier assessment that compares modelled contaminant concentrations in water and/or sediment with toxicological benchmarks for these media (e.g., [15, 16]. The second tier considers specific organisms and their intake rates of contaminants. The total daily intake (TDI), set for people, is then compared to suitable toxicological benchmark doses to obtain a hazard quotient.
4. Multimedia Urban Model (MUM). It was implemented by [17, 18] to describe the transport and fate of chemicals in urban areas. In addition to air, water, sediment, soil and vegetation compartments, the MUM takes into consideration the organic film that covers impervious surfaces (building walls, windows, streets, etc.) and enhance the mobility of chemicals through the wash off processes.

Despite its many advantages, an extensive modelling may be expensive because it requires a suitable amount of input data and a high degree of expertise, especially in the calibration and validation steps. Else, the uncertainty associated to complex models may be particularly high, and in most cases the simplest approach (identification of source-to-sink pathways) is commonly used. In this paper examples of application of fugacity multimedia models are presented for two aquatic environments that have both experienced strong anthropogenic pressures in the last decades. In the first case the level III QWASI model of [1] was applied as screening tool for the fate of PCB-118 in Lake Maggiore, whereas in the second one a more extended approach was adapted to the Venice Lagoon to assess the fate of various chemicals.

2 Methodological approach

The Level III Quantitative Water Air Sediment Interaction or QWASI model of [1], as modified by [19], which represents an aquatic environment with three well-mixed homogeneous bulk compartments (water, upper sediment layer and lower sediment layer, Figure 1), was used. Dissolved and particulate phases (e.g. suspended sediment and sediment pore water) are in equilibrium within each bulk compartment. The atmosphere is considered as an infinite source to the system with a constant con-

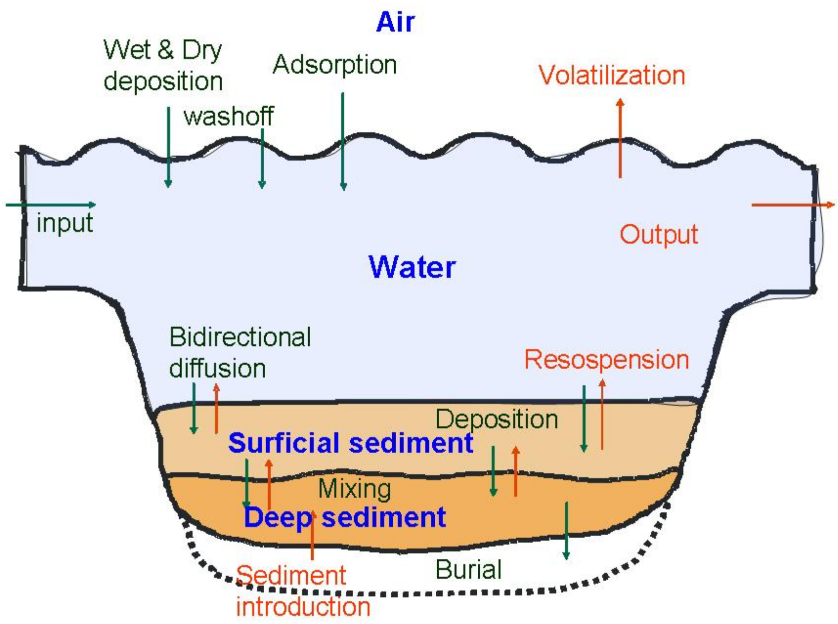

Figure 1: Diagram showing compartment and processes considered in the QWASI model. Input to the system are shown in green, whereas outputs are reported in red.

centration. Figure 1 summarizes all the inter media transport processes (both diffusive and advective) taken into account for the model formulation.

The model consists of a set of equations (Table 1) that define the Z values for each compartment of Figure 1, including both dissolved and particulate phases.

All transport processes are expressed in common mathematical terms as D values (mol $Pa^{-1}h^{-1}$), defined as:

$$\mathrm{D = GZ = kAZ}$$

where G (m^3h^{-1}) is the flow rate of a medium (e.g., air, water, suspended particles), k(m h^{-1}) is a mass transfer coefficient, and A($m^{2)}$ is the area across which the chemical mass transfer is occurring. The rate of inter-media transport (molh^{-1}) is thus:

$$\mathrm{N = Df = GC}$$

A mass balance equation is written for each compartment to represent the change in chemical mass with time. All input and removal pathways are assumed to occur simultaneously and instantaneously once a contaminant enters the system. The general mass balance equation for compartment b and chemical j is:

$$\mathrm{V_b Z_b \frac{df_{bj}}{dt} = E_{bj} + \sum (D_{abj} f_{aj}) - f_{bj} \sum D_{bj}}, \tag{1}$$

where V_b (m^3) is the volume of compartment b, f_{aj} is the fugacity (Pa) of chem-

ical j in compartment a, Z is the fugacity capacity for organics ($molm^{-3}Pa^{-1}$), E_{bj} ($molm^{-3}$) is the direct emission, Dabj ($molPa^{-1} \cdot m^{-3}$) is the transport rate moving chemical j from compartment a to b, and Dbj is the transport rate removing chemical j from compartment b. For metals, fugacity is replaced with aquivalence [2] in Equation 1.
In order to account for metal chemistry in each phase, the speciation-complexation model TRANSPEC [5] calculates two system- and species-specific values of distribution coefficients K_ds: K_{dCD} (colloidal-to-dissolved phases) and K_{dPD} (particulate-to-dissolved phases) for both total metal and its species, based on ambient aqueous phase chemistry. K_ds are used to calculate constituent species' Z values required for the weighted averaged bulk Z used in the fate and transport model [3].

3 Model Application to Lake Maggiore

The original QWASI model [1, 20] was applied under steady-state conditions as a simple exercise to describe the fate of 2,3',4,4',5-Pentachlorobiphenyl (PCB-118 according to IUPAC nomenclature), a "dioxin like" congener included also in the seven PCB indicator set (EFSA, 2005). The model software is freely available at the Canadian Environmental Modelling Centre website (CEMC, 2007).
The lake was considered as a whole and its environmental characteristics were taken from [21] and references therein. They were: lake proprieties (lake dimension, concentration and density of solids in the environmental compartments, organic carbon fractions of solids), water and sediment flows, atmospheric deposition parameters and mass transfer coefficients for diffusive transports. The physical-chemical proprieties of PCB-118 (water solubility, vapour pressure, melting point, log K_{ow}) were determined through the EPISUITE tool developed by the US Environmental Protection Agency's office for Pollution Prevention and Toxic and Syracuse Research Corporation (USEPA 2009). An emission of 2 $kg \cdot y^{-1}$ is assumed to be supplied to the lake, whereas the concentration in inflow water was considered as low as 4 pg L^{-1}. A bulk atmospheric PCB-118 concentration of 6.83 x $10^{-3}ngm^{-3}$, determined by Castro Jìmenez et al. [22] as averaged sum of measured gaseous and aerosol bound concentrations in the Ispra area of Lake Maggiore, was considered as model input. Any removal through degradation was assumed negligible.
Model output includes: chemical inputs to the system, Z and D values, fugacities, concentrations and amounts of chemical in each compartment, mass balances and residence times and details of process rates in a summary diagram. In particular, Figure 2 summarizes the transport processes and the resulting environmental fate of PCB-118 in the compartments of the lake.
The modelled surficial sediment concentration (3.44 ngg^{-1}) is close to the average PCB-118 surficial value in the Ispra Bay, determined by [22].
The residence time of PCB -118 in the system resulted 2.66 years.
This example shows the ability of a simple multimedia fate model to represent the fate and main processes of a chemical in an aquatic system, when its proprieties are well known and processes are properly parameterized. This allows to estimate the ranges of concentration in media (i.e. water

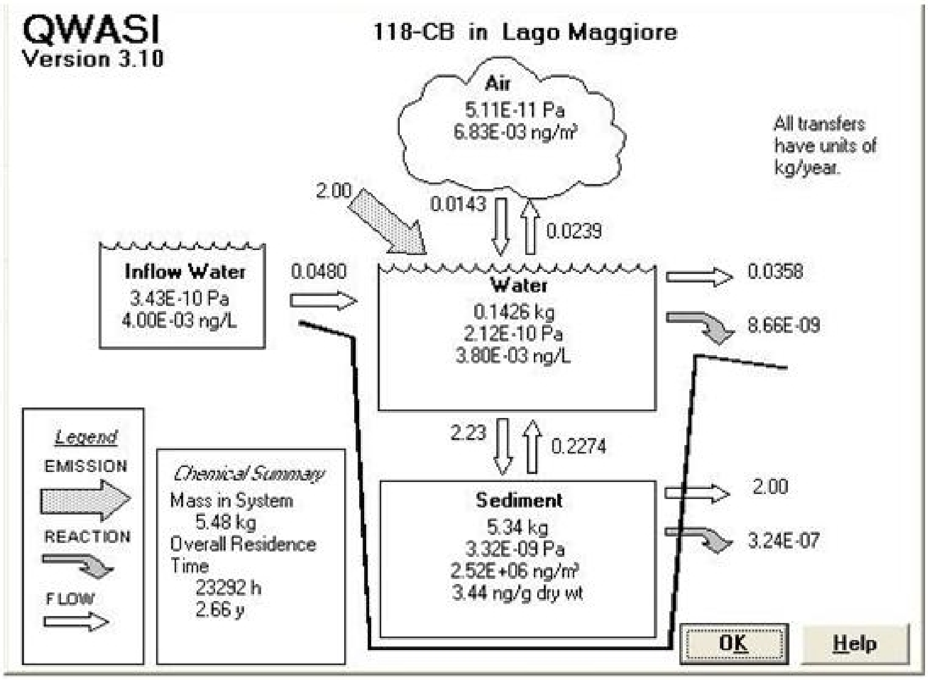

Figure 2: Diagram showing concentration of PCB-118 in air, water and sediment compartments in Lake Maggiore and resulting transport processes: water inflow, wet and dry deposition, rain dissolution, adsorption, volatilization, sediment deposition, resupension, diffusion, burial, emission to water, water outflow. Reaction rates in water and sediment are assumed as negligible.

and sediment) varying the direct emission and the water inflow, and thus to formulate previsions on the response of the system in terms of changing loadings.

4 Model Application to the Venice Lagoon

After a first attempt by [23] a multi media model of the Venice Lagoon has been implemented, while the parametric uncertainty was assessed through a Monte Carlo analysis. Here a summary of model formulation and achieved results is reported, whereas further details are available in [24, 25].

The model was applied to octachlorodibenzodioxin/furan (OCDD and OCDF), 2,2',3,4,4',5,5'-Heptachlorobiphenyl (PCB-180 according to IUPAC nomenclature), Pb and Cu to evaluate their behaviour and fate.

The lagoon was segmented into 10 areas (Figure **??**) according to the analysis of [26] who used a 2-dimensional finite element hydrodynamic model based on the

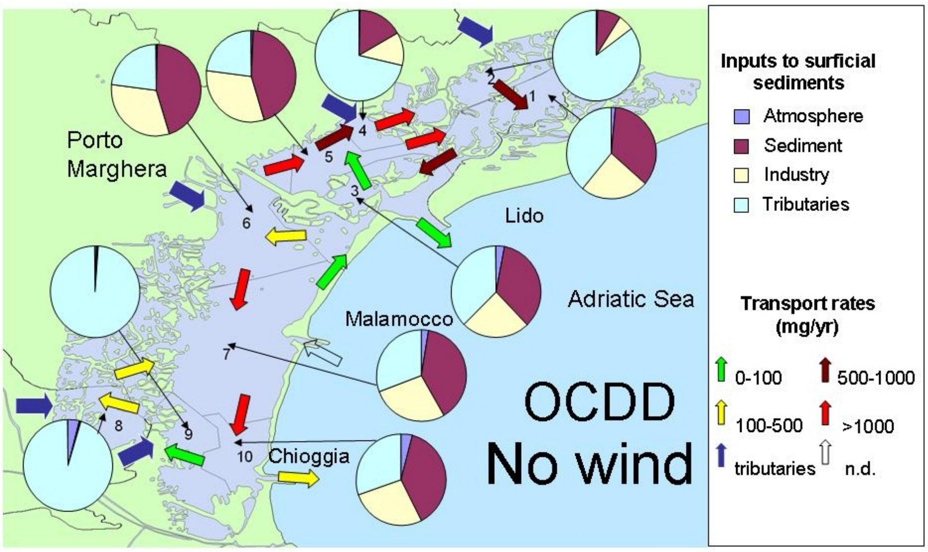

Figure 3: Output of the model showing the ten basins of the Venice lagoon, the direction of the net water movement and the magnitude of OCDD transport rates. The relative importance of OCDD loadings to surficial sediment is also shown.

spatial distribution of physical properties (salinity and water residence time) and other water quality parameters. The circulation patterns and net flow estimates from the reference scenario of "no wind", which reflects steady-state hydrologic conditions in the system, were first chosen, assuming mean annual tributary flows and an idealized sinusoidal M2 tide levels at inlets that force water circulation. To account for sediment loss in the central basin of the Lagoon, two additional transport pathways were included in the QWASI model (Figure 1): i) a sediment introduction term defined as the addition of sediment from the lowest sediment compartment into the subsurficial layer and ii) an upward transfer term that moves sediment from the lower to the upper sediment layer.

Compartment specific versions of Equation 1 are solved assuming steady-state or pseudo-steady state. The first approximation is used to represent average long term conditions. The pseudo-steady-state approach, in which the fugacity/aquivalence of the lower sediment layer was specified, is used for in-place pollution where sediment concentrations are not at steady state with respect to current loadings [27].

Our model considers inputs to the lagoon from tributaries, discharges from the industrial area of Porto Marghera, contributions from historically contaminated sediments and atmospheric deposition. Tributary inputs of dissolved and particulate phases of Pb, Cu and PCB-180 were obtained from [28]. Industrial loadings were calculated as the difference between contents in water entering and exiting a facility annually. As far as the contribution of in-place pollution is concerned, fugacity/aquivalence of the lower sediment (3-20 cm) was calculated from the geometric mean of the measured concentrations from three sediment cores [29, 30]. Bulk atmospheric deposition of PCBs and PCDD/Fs were modelled using direct gas-phase measurements [31]. Metal deposition was calculated from measured PM10 concentration. Atmospheric stack emissions were not explicitly taken into account in the model. The model was written in Visual Basic and runs on a PC in a Windows© environment.

4.1 Model evaluation

We evaluated the model by comparing measured and modelled concentrations for soluble (dissolved and colloidal phases) Pb and Cu in the water column and Pb, Cu, OCDD/F and PCB-180 concentrations in the upper sediment.
Measured and modelled concentrations of all contaminants in water and sediment were within an order-of-magnitude of each other. Among all contributions, industrial loadings of PCB-180 and other contaminants are probably most uncertain. To evaluate the reliability of PCB-180 inputs, several industrial loading scenarios were analyzed. The fraction of industrial emissions retained by the sediment of the industrial canals was estimated by running the model with export fractions varying from 0 to 1, while keeping all other loadings constant. The best fit with measured values corresponded to 10-20% industrial emissions suggesting that the transfer of PCB-180 as well as other contaminants from the canals to the lagoon might be overestimated in the model.

4.2 Source apportionment and contaminant fate

The source apportionment analysis reflected the location of loading sources and the dominant hydrologic circulation pattern of the Lagoon. 50% to 94% of total OCDD/F, PCB-180, Cu and Pb loadings enter the Lagoon in the central basin from industry and in-place pollution, followed by a significant contribution from tributaries. These loads circulate to the northern lagoon, with limited transport to the far southern lagoon. For example, 60 % of total OCDD loadings to basin 1 in the northern lagoon were from in-place pollution and present industrial sources originating from segment 6, whereas nearly 100 % of loadings in basin 9 in the southern lagoon were from tributaries (Figure 3).
Despite $\sim$75 % of Pb and Cu being in the soluble form (dissolved + colloidal phases), their fate, similar to that of OCDD/F and PCB-180, was mediated by particle dynamics (i.e., sediment deposition and resuspension). Moreover, contaminants were lost through lower sediment burial in non-erosive segments.
Water circulation is the dominant contaminant removal pathway from the northern and central basins (22-79% for OCDD/F and PCB-180 56-98% for Cu and Pb). In contrast, removal from the southern basin was dominated by burial (12-70% for all contaminants) further limiting transfer from the central to the far southern lagoon and to the Adriatic Sea (Figure 3). Despite the dominance of export as a sediment removal pathway within the northern and central lagoon, total export of contaminants to the Adriatic Sea through the Lido, Malamocco and Chioggia inlets was minimal under the “no wind” scenario. Less than 19% of total Pb and Cu loadings

and less than 2% of total PCB-180 and OCDD/F loadings were exported from the Venice Lagoon to the Adriatic Sea (Figure 3).

Our estimates of annual export rates to the Adriatic Sea, however, likely underestimated actual losses because episodic flooding events in the lagoon were not included in our model parameterization. Ultimately, we found that although substantial sediment-water exchange occurs, net contaminant loss from the Venice Lagoon was through burial, resulting in a high persistence of contaminants in the system.

As a further exercise, the model has been improved considering the two recurring winds in the area: 1) scirocco, a warm wind from SE, blowing year-round, responsible of flooding ("acqua alta") events in Venice (esp. in fall-winter); 2) bora, a strong (up to 30 m s^{-1}), cold NE wind blowing up to 40 day y^{-1} (esp. in winter). The model has been parameterized in the same way as the "no wind" scenario but changing the water circulation according to [26, 32].

Preliminary results shows that, under scirocco wind, deposition/resuspension processes are the main responsible of the spreading of the lagoon contaminants from the industrial area and burial is an important removal mechanism. Bora, in turn, may act as a "cleaning mechanism" for the lagoon by increasing export to the Adriatic sea. In fact the residence time of all the modelled contaminants resulted to be the lowest in this scenario.

4.3 Uncertainty examination

The more complex they are, models are indeed simplifications of reality and as such are inherently uncertain. Model uncertainty derives from both structural and parametric uncertainty. The former not only reflects the inability to capture all the essential components of the real system, but also the difficulty to express them in an unequivocal manner. On the other hand, parametric uncertainty stems from the analytical errors, the imprecision of measurements as well as spatio-temporal parameter variability. This latter source of uncertainty is of particular importance in fate and transport modelling in which the relative effects of individual parameters on model predictions are not well understood and can be contaminant-specific. In this regard, scientific knowledge, expert judgment, and observational data were used to formulate probability distributions and characterize the uncertainty of environmental parameters used in the model applied to the Venice Lagoon. Details of the procedure of uncertainty analysis are presented by [25].

Our analysis demonstrates that the range of model output distributions can vary up to an order of magnitude exhibiting both contaminant and site-specific variability. Generally, we found that the uncertainty of the contaminant concentrations in the Venice Lagoon is characterized by two modes of spatial variability (i.e., the northern and central parts of the Lagoon, and the more isolated southern basin) mainly driven by the local hydrodynamics.

Moreover we also found that the interplay among the in-place pollution in the central Lagoon and sediment burial rates drove the spatial heterogeneity of bulk water and upper sediment concentrations as well as total suspended solids (TSS) concentration.

5 Conclusions

In conclusion these models, developed in a user-friendly environment, are simple and useful tools for environmental studies of complex systems, where direct measurements of process velocity and concentrations in specific compartments are difficult or too expensive. Moreover, they can also be used in decision-making processes, like risk assessment and regulation. In these latter cases model validation becomes important. However, environmental models can not be validated in the same sense as models of highly reproducible closed systems. Credibility can be improved by using examples in which observed and predicted concentrations are compared, as single values or ranges with identification of dominant sources, fate processes, or partitioning characteristics. Consequently, the numerical output of these models is dependent on the amount of available data.

In case of the Venice Lagoon, despite the large number of studies, the dataset is still not enough for a complete validation of the model, thus the model output, in term of "numbers" should be used with care.

In particular, the uncertainty analysis distinguished between parametric and structural uncertainty. While the former is associated primarily to model parameters that drive the spatial variability of the lagoon, the latter resulted in systematic predictive bias.

Thus, the collection of field data about the key processes that drive contaminant variability in the system and the formulation of well-defined prior distributions for the corresponding parameters is a goal that will assist the calibration and validation of this model. This may be particular important for a proper management of the mobile gates (MOSE) in order to predict the environmental effects after repeated closures.

6 Acknowledgements

The authors are indebted with M. Diamond for having inspired this research, J. Sommerfreund and N. Gandhi for model coding. This is contribution No. 1702 from the Istituto di Scienze Marine, UOS of Bologna.

Compartment	Z value	Equation
Air	Z_Air	1/(R*Temp)
Aerosol	Z_Aerosol	Kqa*Z_Air
Interface	Z_Interface	Kia*Z_Air
Water	Z_Wat	1/HLC
Suspended Sediment	Z_SusSed	Z_Wat*Den_SusSed*Koc*OC_SusSed/Den_Wat
Upper Sediment	Z_USed	Z_Wat*Den_Sed*Koc*OC_USed/Den_Wat
Lower Sediment	Z_LSed	Z_Wat*Den_Sed*Koc*OC_LSed/Den_Wat
Bulk Air	Z_Bulk_Air	Z_Air + (Z_Aeroaol*Vol_Fr_Aerosol)
Bulk Water	Z_Bulk_Wat	Z_Wat* (1 - Vol_Fr_SS_Wat) + Z_SusSed*Vol_Fr_SS_Wat
Bulk Upper Sediment	Z_Bulk_USed	Z_Wat* (1 - Vol_Fr_Used_Solid) + Z_USed*Vol_Fr_Used_Solid
Bulk Lower Sediment	Z_Bulk_LSed	Z_Wat* (1 - Vol_Fr_Lsed_Solid) + Z_USed*Vol_Fr_Lsed_Solid

R = ideal gas constant = 8.314472 m^3 Pa K^{-1} mol^{-1}
Temp = Absolute temperature (K)
K is a partition coefficient
HLC = Henry's Law Constant (Pa m^3 mol^{-1})
Den is density, Wat is water, SS stand for suspended solid
Vol_Fr stands for volume fraction

Table 1: Definitions of Z values for organics (for metals Z is derived by aquivalence) for each environmental compartments.

References

[1] D. Mackay, S. Paterson, and M. Joy. A quantitative water, air, sediment interaction (QWASI) fugacity model for describing the fate of chemicals in water. *Chemosphere*, 12:1193–1208, 1983.

[2] D. Mackay and M.L. Diamond. Application of the QWASI (Quantitative Water Air Sediment Interaction) fugacity model to the dynamics of organic and inorganic chemicals in lakes. *Chemosphere*, 18:1343–1365, 1989.

[3] M.L. Diamond, D. Mackay, and P.M. Welbourn. Models of multi-media partitioning of multi-species chemicals: the fugacity/aquivalence approach. *Chemosphere*, 25:1907–1921, 1992.

[4] M.L. Diamond, M. Ganapathy, S. Peterson, and C. Mach. Mercury dynamics in the Lahontan Reservoir, Nevada: application of the QWASI fugacity/aquivalence multispecies model. *Water Air and Soil Pollution*, 117:133–156, 2000.

[5] S.P. Bhavsar, M.L Diamond, L.J. Evans, N. Gandhi, J. Nilsen, and P. Antunes. Development of a coupled metal speciation-fate model for surface aquatic systems. *Environmental Toxicology and Chemistry*, 23:1376–1385, 2004.

[6] W.D. Schecher and D.C. McAvoy. MINEQL+ A chemical equilibrium modelling system, Version 4.0 for windows, user's manual. 1998.

[7] N. Gandhi, S.P. Bhavsar, M.L. Diamond, J.S. Kuwabara, M.M. Di Pasquale, and D.P. Krabbenhoft. Development of a mercury speciation, fate, and biotic uptake (BIOTRANSPEC) model: application to Lahontan reservoir (Nevada, USA). *Environmental Toxicology and Chemistry*, 26(11):2260–2273, 2007.

[8] J. Campfens and D. Mackay. Fugacity-based model of PCB bioaccumulation in complex aquatic food webs. *Environmental Science and Technology*, 31(2):577–583, 1997.

[9] F.A.P. Gobas and H.A. Morrison. Bioconcentration and biomagnification in the aquatic environment. pages 189–231, 2000.

[10] F.A.P. Gobas, M.N. Z'Graggen, and X. Zhang. Time response of the Lake Ontario ecosystem to virtual elimination of PCBs. *Environmental Science and Technology*, 29:2038–2046, 1995.

[11] S.B. Gewurtz, N. Gandhi, G.A. Stern, W.G. Franzin, B. Rosenberg, and M.L. Diamond. Dynamics of PCBs in the Food Web of Lake Winnipeg. *Journal of Great Lakes Research*, 32(4):712–727, 2006.

[12] N. Gandhi, S.P. Bhavsar, S.B. Gewurtz, M.L. Diamond, A. Evenset, G.N. Christensen, and D. Gregor. Development of a Multichemical Food Web Model: Application to PBDEs in Lake Ellasjoen, Bear Island, Norway. *Environmental Science and Technology*, 40(15):4714–4721, 2006.

[13] J.A. Archbold. Development of a screening ecological risk assessment model and its coupling with the Multimedia Urban Model. *M.Sc. Thesis. Department of Geography, University of Toronto*, 2003.

[14] J.A. Archbold, H. Hull, and M.L. Diamond. Potential importance of inhalation exposures for wildlife using screening-level ecological risk assessment. *Human and Ecological Risk Assessment*, 13(4):870–883, 2007.

[15] D.S. Jones, G.W. Suter, and R.N Hull. Toxicological benchmarks for screening contaminants of potential concern for effects on sediment-associated biota: 1997 Revision. 1997.

[16] B.E. Sample, D.M. Opresko, and D.W. Suter. Toxicological benchmarks for wildlife: 1996 Revision. 1996.

[17] M.L. Diamond, D.A. Priemer, and N.L. Law. Developing a multimedia model of chemical dynamics in an urban area. *Chemosphere*, 47:1655–1667, 2001.

[18] D.A. Priemer and M.L. Diamond. Application of the Multimedia Urban Model To Compare the Fate of SOCs in an Urban and Forested Watershed. *Environmental Science and Technology*, 36:1004–1013, 2002.

[19] M.L. Diamond. Development of a fugacity/aquivalence model of mercury dynamics in lakes. *Water Air and Soil Pollution*, 111:337–357, 1999.

[20] D. Mackay. Multimedia environmental models: The fugacity approach. 2001.

[21] A. Di Guardo, C. Ferrari, and A. Infantino. Development of a Dynamic Aquatic Model (DynA Model): Estimating Temporal Emissions of DDT to Lake Maggiore (N. Italy). *Environmental Science and Pollution Research*, 13(1):50–58, 2006.

[22] J. Castro-Jimenez, G. Mariani, S.J.Eisenreich, E.H. Christoph, G. Hanke, E. Canuti, H. Skejo, and G. Umlauf. Atmospheric input of POPs into Lake Maggiore (Northern Italy): PCDD/F and dioxin-like PCB profiles and fluxes in the atmosphere and aquatic system. *Chemosphere*, 73:S122–S130, 2008.

[23] M. Dalla Valle, A. Marcomini, A. Sfriso, A.J. Sweetman, and K.C. Jones. Estimation of PCDD/F distribution and fluxes in the Venice Lagoon, Italy: Combining measurement and modelling approaches. *Chemosphere*, 51:603–616, 2003.

[24] J.K. Sommerfreund, N. Gandhi, M.L. Diamond, C. Mugnai, M. Frignani, G. Capodaglio, M. Gerino, L.G. Bellucci, and S. Giuliani. Contaminant fate and transport in the Venice Lagoon: Results from a multi-segment multimedia model. *Ecotoxicology and Environmental Safety*, 73:222–230, 2010.

[25] J.K. Sommerfreund, G.B. Arhonditsis, M.L. Diamond, M. Frignani, G. Capodaglio, M. Gerino, L.G. Bellucci, S. Giuliani, and C. Mugnai. Examination of the uncertainty in contaminant fate and transport modelling: A case study in the Venice Lagoon. *Ecotoxicology and Environmental Safety*, 73:231–239, 2010.

[26] C. Solidoro, D. Melaku Canu, A. Cucco, and G. Umgiesser. A partition of the Venice Lagoon based on physical properties and analysis of general circulation. *Journal of Marine System*, 51:147–160, 2004.

[27] M.L. Diamond. Application of a mass balance model to assess in-place arsenic pollution. *Environmental Science and Technology*, 28:29–42, 1995.

[28] F. Collavini, C. Bettiol, L. Zaggia, and R. Zonta. Pollutant loads from the drainage basin to the Venice Lagoon (Italy). *Environment International*, 31:939–947, 2005.

[29] M. Frignani, L.G. Bellucci, C. Carraro, and S. Raccanelli. Polychlorinated biphenyls in sediments of the Venice Lagoon. *Chemosphere*, 43:567–575, 2001.

[30] M. Frignani, L.G. Bellucci andC. Carraro, and M. Favotto. Accumulation of polychlorinated biphenyls in sediments of the Venice Lagoon and the industrial area of Porto Marghera. *Chemosphere*, 54:1563–1572, 2004.

[31] A. Gambaro, L. Manodori, I. Moret, G. Capodaglio, and P. Cescon. Determination of polychlorobiphenyls and polycyclic aromatic hydrocarbons in the atmospheric aerosol of the Venice Lagoon. *Analytical and Bioanalytical Chemistry*, 378:1806–1814, 2004.

[32] A. Cucco and G. Umgiesser. Modeling the Venice Lagoon residence time. *Ecological Modelling*, 193:34–51, 2006.

Flood Risk Estimation through Document Sources Analysis: the Case of the Amalfi Rocky Coast

E. Esposito[1], S. Porfido[1], C. Violante[1], F. Molisso[1], M. Sacchi[1], G. Santoro[1], E. Spiga[2]
1, Institute for Coastal Marine Environment, CNR, Napoli, Italy
2, Geologist, ES OR Campania n.85, Avellino, Italy

eliana.esposito@iamc.cnr.it

Abstract

In the last century the Amalfi Coast was affected by numerous severe floods in conjunction with exceptional rainfall that caused major damage in terms of lost lives and economic cost. Historical documentary sources are an important source of information for reconstructing exceptional flood events occurring prior to the instrumental era. Historical analysis also provides an opportunity to extend the time scale window for flood risk studies. To study historical floods we collected all the available information concerning the period between the 16th and the 20th centuries by analysing both published and unpublished sources. The great variety of historical sources made it necessary to formulate an ad hoc scientific procedure that takes into account not only the completeness and reliability of documents related to the period, but also the intrinsic quality of the material. Experience in historical data collection shows that not all documentary sources can provide useful information for flood characterization, but it is necessary to have a selective criteria in order to obtain the best information rather than the best dataset quality.

Analysis of the data in question allowed us to achieve a chronological reconstruction of more than 100 floods. In this task, the level of information was decisive to carry out space–time identification, estimate the affected area and define type of damage to public and private structures, and the geological effects induced.

1 Introduction

The Campania region is particularly subject to the hydrogeologic risk (landslides and flooding), which represents a threat to the natural environment and a persistent menace to urban areas, in terms of human lives and socio-economic costs. A reliable flood record frequency is the most available tool for flood risk assessment and it require long data series obtained mostly from our knowledge about historical events which occurred as far back in time as possible. The format and reliability of historic flood data are likely to be at least as varied as the sources from which they derive. If the collated information is to lead to an improvement in the flood frequency estimates based on relatively short formally gauged records alone, then a rigorous evaluation of the historical data should be undertaken. Without this review it is likely that much spurious information will be included, to the detriment of the estimates produced.

Nevertheless, the use of historical data in the estimation of flooding events have been tested and consolidated during the last decades, giving very important contribution to hazard prevention [1, 2, 3, 4, 5, 6, 7]. The physical landscape of the Amalfi coast, is characterized by steep rocky coast deeply dissected by ephemeral water courses with human activities mainly developed on the narrow stream banks located at the base of steep sided valley, or at the mouth of stream [8]. Such configuration expone this area to a high hydrogeological risk triggered by water events associated with heavy rain [9, 10]. In fact, since historical time, flooding and sliding phenomena have dramatically affected the Amalfi coast, suggesting rapid slope morphodynamics to ascribing to extensive displacement of volcanic (Somma-Vesuvius air-fall deposit) and sedimentary (talus breccia, alluvial and eluvial deposit) covers [11, 12, 13, 14]. These water events also induced severe overflowing of the main streams, resulting in significant damage to property, destruction of roads, bridges, aqueducts, railways and loss of livelihood.

2 Methodology

This study presents a historical reconstruction of the effects of a series of catastrophic floods that occurred along the southern flank of the Sorrento Peninsula (Amalfi coast). The research was based on critical reviews of about 4000 published and unpublished documents since XVI century including above all, technical and administrative documents and projects, memoirs, other public, private and ecclesial documents, contemporary maps and iconographic materials.

To evaluate the intrinsic value of such heterogeneous documents it has been necessary to define a selection criteria in order to obtain the best information versus the best quality of dataset. For this purpose a rigorous methodology of investigation consisting in: a) analysis of historic sources, throughout the completeness and the reliability of the document and b) source classification, based on published and unpublished papers, contemporary (or not) sources, official reports and general public information.

The main groups of sources found in Record Offices and Libraries consist of administrative records (Figure 1), financial reports, law acts, expert investigations, as well as maps, iconographies. and newspapers. This kind of sources provide three levels of information:

- scarce, poor information regarding the occurrence of flood in wide areas and, sometimes, the date of the flooding event;
- general, more accurate information on type, size (sometimes) and location of the event;
- detailed, precise information on location of the event, dimension of the flooded area, level of damages and description of flood-induced geological effects.

Subordinately parish archives, as well as local libraries, provide important contemporary (or not) documents consisting in memoirs, chronicles, diaries, books and other heterogeneous public, private and ecclesial documents, which often provide useful data to reconstruct the general dynamics of the event (Figure 2). They have been divided into two main groups:

- direct source, including text written by eyewitness, specific studies such as scientific literature and newspaper;
- indirect source, including texts written

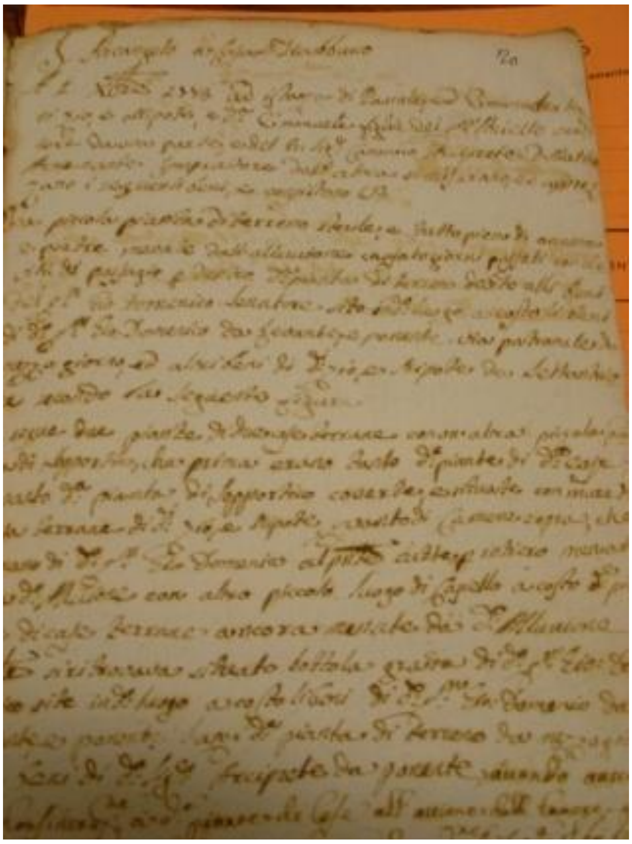

Figure 1: Documentary source related to the 1773 flooding event (Historical Archive, Cava de' Tirreni, Salerno).

after the event by local authors, scientific literature, chronicles and memoirs.

Another important type of sources is represented by photo, postcard, print, drawing and art reproduction available particularly for the XX century, where is often possible to visualize the effective impact of the disasters (Figure 3). Finally, law acts have not been overlooked, providing them too sometimes useful information on the damage distribution and size of destruction suffered by local communities.

3 Data analysing and chronology of flooding event

The reconstruction of the historical floods chronology comes from numerous and different sources with information of varying quality and completeness. To facilitate cross-referencing between the datasets provided by these different sources, the gathered information have been organized

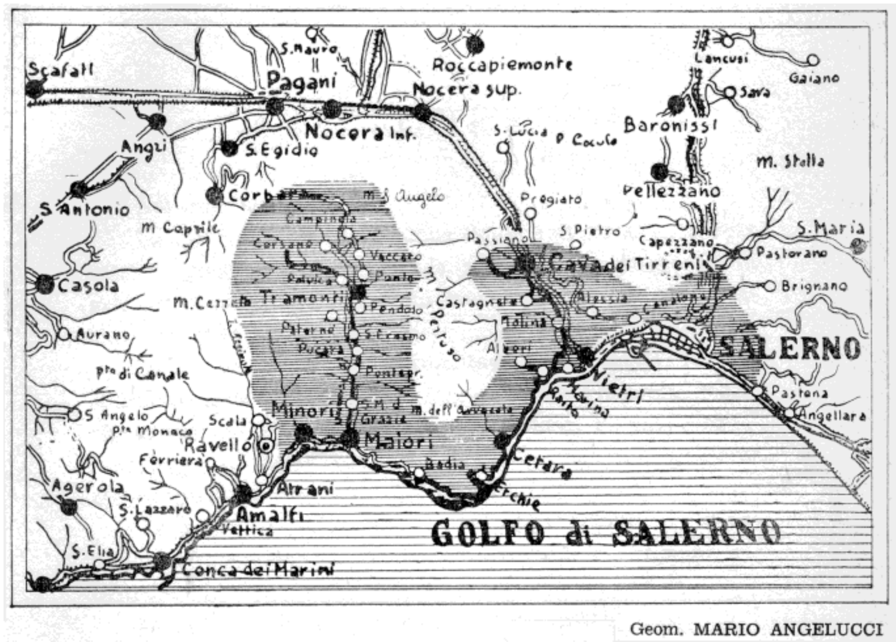

Figure 2: Bibliografic document: Map of 1954 flood event drown by Candido from Altavilla Silentina, 1955.

in a systematic way producing a specific spreadsheet that include all the available information to give greatest weight of the reliable source, the level of information, location and size of the flood, damage, victim as well as flood-induced geological effects [16]. In particular, data relating to each historic flood have been evaluated according to the completeness of the information and its authenticity. The authenticity weighting has been assessed on the base of such parameters:

1. document chronologically contemporary to the event, wrote by local or regional administrator, lower, historian, parish, journalist, scientist, academician and technician have been classified as highest quality of reference (HQR);
2. document or bibliographic sources, wrote from five until fifty years after the event, by local historian, parish, journalist, sometimes scientist and technician have been considered as medium-high quality of reference (MQR);
3. bibliographic sources, wrote over fifty years from the event by local literary man and journalist, have been classified as medium-scarce quality of reference (SQR).

A systematic investigation of historical sources was carried out on published and unpublished documents since 1500.

Results indicates that between 16th and 18th centuries have been analysed more than 1000 sources with HQR, consisting of archival sources (Protocolli Notarili 1581-

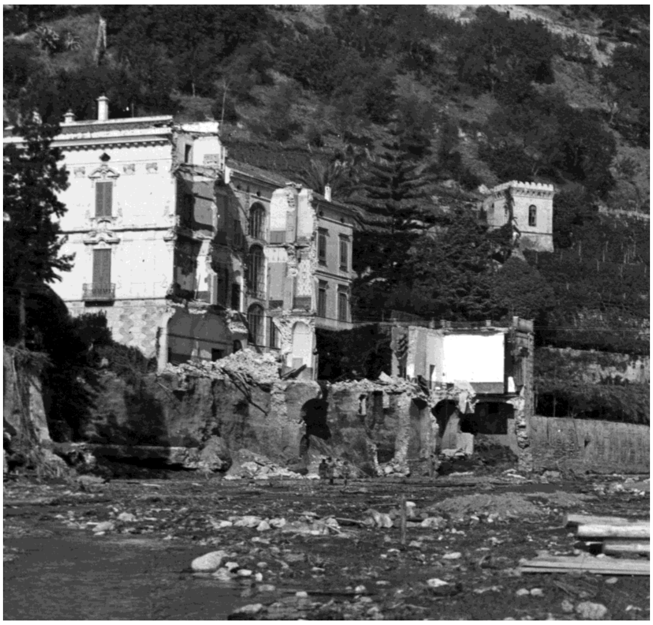

Figure 3: Photographic document: Marina di Vietri (SA) after the 1954 flooding event.

1798; Regia Udienza dei Principato Citra, 1620-1827; Genio Civile 1783-1901) as well as contemporary bibliographic documents, representing the 63% of the total sources; the MQR is represented by bibliographic sources for the 11% of the total, the last 26% includes bibliographic sources write over 50 years after the events. The highest quality of references (61% of the total) related to the 19th century is constituted by archival sources, (Genio Civile 1783-1901; Atti Demaniali, 1806-1961; Intendenza, 1815-1860; Società Economica, 1856-1960; Atti Prefettura, 1860-1932; Atti del Consiglio Provinciale di Salerno, 1899-1924; Bibliographical Sources, 1709-2004), contemporary national and local newspapers, scientific and tecnical reports for about 1500 sources. Of these only the 4% have been classified as MQR and 35% as SQR. As regards the 20th century most of the fonts (about 1300) have been classified as MQR coming from both archival and bibliographic sources as well as local and national news papers (starting from 1899 to 2000), represented by 55% of the total value, while HQR represented by a huge of documents from archival fonts to scientific and technical reports. Only the 8,5% of the founts have been classified into the third type of sources.

This pooling of data made it possible to determine some of the most relevant flood characteristics, such us magnitude, duration of the event, river location, extension of the basin area, damaged localities, deaths and induced geological effects. In particular the flood magnitude indicates the size of the past flood event based on degree of damage to both buildings and infrastruc-

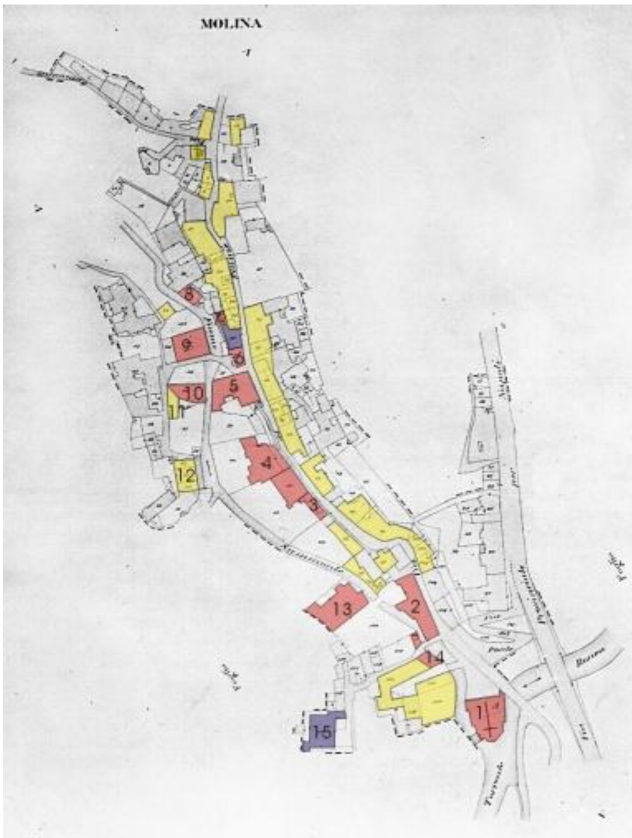

Figure 4: Detailed reconstruction of damage suffered after 1954 flooding event in locality Molina di Vietri (Esposito, 2004).

tures, extent of the flooded area, loss of lives and time recurrence.

According to Dartmouth Flood Observatory, three different level of severity class have been recognized:

- Class I – (small flood): restricted area of flooding, minor damage to buildings located adjacent to the river and no serious damage to the population. Overflows depend on the river bed obstruction and on the embankment conditions. Recurrence interval <20 years.
- Class II – (intermediate flood): large area of flooding, severe damage and partial destruction to buildings located adjacent to or along the river. Infrastructures are destroyed along several hundred metres. Other damage is caused by the overflow with its heavy sediment transport. Bankfull discharge is exceeded in several places. Recurrence interval <100 years.
- Class III – (catastrophic or large flood): large area of flooding, severe damage or complete destruction of infrastructures

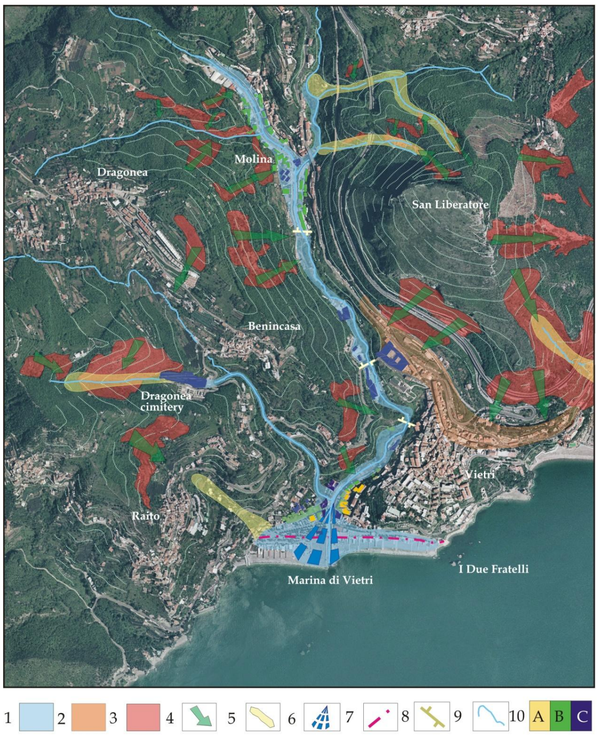

Figure 5: Geological effects and damage pattern induced by the 1954 flood event. (1) Overflowing area, (2) mud deposits, (3) evidence of past denudation, (4) landslide phenomena, (5) channelled debris flow, (6) alluvial fan, (7) shoreline before 1954 event, (8) temporary dam, (9) drainage network, (10) damage categories: (A) heavy, (B) medium, (C) light [15].

close to the river, and stretches of roadways may be swept away. Overflowing affects also zones far from the river bed. Large morphological changes with river bed changes are also possible. Recurrence interval >100 years.

The systematic search for historic sources has led to the identification and classification of 106 floods, which affected the whole province of Salerno, and specifically the Amalfi coast (Table 1and Table 2). The most intense events classified with a Magnitude III, occurred in 1581, 1773, 1899, 1954. A widespread pattern of destruction characterized these events: serious damage to buildings and to industries, together with destruction of roads, bridges, aqueducts, railways etc. The cultural heritage also suffered great damage. In addition, all these events caused a large number of victims. Also extensive environmental effects such as landslide, overflowing, change of coastline, characterized these events.

The large availability of data led us to re-

Date			TR	IL	Location	Magnitude
30	09	1581	1,3	a	Salerno, Cava T., Vietri M., Castiglione G., Giffoni C., Giffoni V. P.	III
31	08	1588	1,3	b	Atrani	II
03	11	1750	1	b	Vietri M., Salerno	II
19	01	1764	1,3	b	Naples and Salerno province	II
11	11	1773	1,2,3	a	Salerno, Coperchia, Cava T., Vietri M., Tramonti, Cetara, Nocera, Mercato S. S.	III
24	01	1823	1	a	Amalfi, Maiori, Cetara, Cava T., Nocera, Vietri M., Salerno, Bracigliano	II
7	10	1899	1,2,3	a	Castiglione G., Giffoni C., Giffoni V.P., Montecorvino R., Montecorvino P. Vietri M., Cava T., Salerno, Caposele, Calabritto, Quaglietta, Pontecagnano, Battipaglia	III
24	10	1910	1,2,3	a	Ravello, Tramonti, Furore, Amalfi, Scala, Cetara, Maiori, Minori, Vietri M., Salerno, Ischia	II
26	03	1924	1,2,3	a	Positano, Agerola, Vettica M., Praiano, Amalfi, Atrani, Furore, Minori, Maiori, Vietri M., Salerno	II
25	10	1954	1,2	a	Positano, Vettica M., Praiano, Amalfi, Atrani, Minori, Tramonti, Maiori, Vietri M., Cava T., Nocera, Salerno	III
26	10	1966	1,2	a	Giffoni, Salerno, Cava T., Baronissi,	II

References: (1) highest quality of reference; (2) medium-high quality of reference; (3) medium quality of reference; (IL) Information levels: (a) detailed level; (b) general level - (c) scarce level; Magnitude: Class II (intermediate flood); Class III (catastrophic or large flood).

Table 1: Major floods identified on the basis of the available sources occurred since XVI century along the Amalfi coast (Modified from [16]).

construct in detail the pattern of damage (Figure 4), as well as the geological induced effect (Figure 5) for some flooding events [17, 18, 14].

4 Conclusion

A systematic investigation of historical sources was carried out analysing both published and unpublished sources since XVI century. The great variety of historical sources made it necessary to formulate an ad hoc scientific procedure that would above all take into consideration the document's intrinsic quality in order to minimize spurious data.

In this task, the level of information was decisive: we were able to carry out space-time identification, estimate the area affected, the type of damage to public and private structures, and the geological effects induced. On the basis of the size of the areas hit by flooding, the type of effects induced on the urban and physical environment and the recurrence intervals, we estimated the magnitude of the events. The latter measure is undoubtedly fundamental for hydrogeological risk assessment and for estimating the return times of extreme events in the area.

Date			TR	IL	Location
20	12	1683	3	b	Maiori
15	10	1696	3	b	Minori
09	11	1735	1	b	Cetara, Cava T., Salerno, Vietri M.
25	01	1736	1	b	Vietri M.
26	09	1736	1	b	Vietri M.
	11	1738	1	b	Vietri M.
10	10	1751	1,2	b	Amalfi
01	09	1753	1,2	c	Amalfi
23	01	1757	1	a	Vietri M.
09	10	1757	1,2	a	Amalfi
25	05	1762	2	a	Cetara
	11	1770	1	b	Salerno
	02	1780	1	b	Atrani
25	12	1796	1	a	Cava T.,Vietri M., Salerno
12	11	1817	1	a	Cava T., Vietri M., Salerno
	12	1822	1	b	Salerno,Vietri M.
13	09	1834	1	b	Cetara
18	07	1835	1	b	Conca marina, Salerno, Cava T.
27	09	1837	1	b	Salerno,Vietri M.
01	01	1841	1	c	Salerno province
26	10	1843	3	b	Cetara, Maiori, Vietri M., Salerno
18	03	1845	3	b	Maiori, Vietri M.
05	01	1853	1	b	Vietri M.
11	10	1866	1	b	Vietri M.
	08	1866	3	a	Tramonti
11	11	1866	1	a	Vietri M.
16	03	1867	1	b	Vietri M., Salerno
12	11	1868	1	b	Salerno
01	04	1875	1	b	Conca M, Salerno
	12	1875	3	c	Salerno province
01	02	1878	1	a	Conca M.
	11	1881	3	c	Salerno province
15	09	1882	1	b	Salerno
05	02	1885	1	b	Amalfi
		1891	3	b	Tramonti
		1896	3	b	Conca M., Castiglione G., Baronissi, Bracigliano, Salerno
		1898	3	c	Salerno province
		1899	3	b	Conca M.
	02	1903	1	b	Vietri M.
07	10	1904	2	b	Ravello
23	06	1905	3	c	Salerno province
01	09	1905	3	c	Salerno province
11	12	1908	3	c	Salerno province
02	01	1911	1	a	Cetara, Vietri M., Salerno
21	09	1912	1	c	Salerno province
03	01	1915	2	a	Minori
06	11	1916	1	b	Vietri M.
13	11	1921	1	a	Furore, Salerno Salerno province
21	09	1929	2	b	Montecorvino R., Giffoni, Vietri sul M.
01	03	1935	2,3	b	Conca M., Minori, Tramonti, Ravello, Cava T.
18	11	1935	2	b	Salerno, Vietri M.
14	09	1939	1,2	b	Conca M., Amalfi, Maiori, Salerno, Pontecagnano
		1940	3	c	Salerno province
18	06	1944	2	b	Minori
09	12	1946	2	b	Minori
02	03	1947	2	b	Minori
25	10	1947	2	b	Minori
23	05	1948	2	b	Minori
05	09	1948	2	b	Minori
28	10	1948	2	b	Minori
01	10	1949	1,2	b	Praiano, Maiori, Vietri M., Salerno, Giffoni
21	01	1951	2	b	Minori
09	11	1951	1,2	b	Montecorvino R., Giffoni
11	09	1953	2,3	b	Agerola, Ravello, Salerno
11	09	1955	2	b	Tramonti, Agerola, Pellezzano
22	10	1957	2	b	Tramonti, Minori, Cava T.
	03	1960	2	c	Salerno province
16	02	1963	2	b	Tramonti, Cava T., Pellezzano
25	09	1963	2	b	Cetara, Minori, Cava T., Pellezzano
08	10	1963	1, 2	b	Amalfi, Cetara, Cava T., Salerno
16	12	1963	1,2	b	Tramonti, Pellezzano
09	01	1968	2	c	Salerno province
19	12	1968	1,2	b	Amalfi, Tramonti
15	03	1969	2	b	Agerola, Cava T.
02	10	1970	1,2	b	Salerno, Pellezzano, Baronissi, Giffoni
25	12	1970	1,2	b	Amalfi, Minori, Baronissi, Pellezzano
15	10	1971	1,2	b	Tramonti, Cava T.
23	11	1971	1,2	b	Amalfi, Minori
06	03	1972	1,2	b	Tramonti, Cava T.
21	10	1972	1,2	b	Tramonti, Cava T.
21	11	1972	1,2	b	Cava T., Baronissi, Pellezzano
02	01	1973	1,2	b	Amalfi,Tramonti, Minori, Maiori, Cava T.
28	06	1976	2	b	Salerno
09	04	1978	2	c	Salerno province
12	10	1980	1,2	b	Tramonti, Minori, Maiori, Cava T.
15	11	1980	2	b	Cava T.
17	11	1985	1,2	b	Tramonti, Maiori, Cava T., Salerno
13	03	1986	1,2	b	Cava T., Pellezzano, Pontecagnano
24	11	1986	1,2	b	Tramonti, Cava T.
16	10	1987	1,2	b	Baronissi, Pellezzano
10	11	1987	1,2	b	Positano,Ravello,Tramonti,Minori,Cava T.
15	09	1988	1,2	b	Tramonti, Pellezzano, Baronissi, Salerno
25	09	1992	1,2	b	Tramonti, Cava T., Salerno
04	10	1992	1,2	b	Cava T., Baronissi, Salerno
20	09	1996	1,2	b	Tramonti, Cava T., Salerno, Giffoni

References: (1) highest quality of reference; (2) medium-high quality of reference; (3) medium quality of reference;
(IL) Information levels: (a) detailed level; (b) general level
(c) scarce level.

Table 2: Minor floods identified on the basis of the available sources occurred since XVI century along the Amalfi coast. All the event have been classify as small flood, Magnitude I (Modified from [16]).

References

[1] AVI Project. http://avi.gndci.pg.cnr.it/welcome_en.htm. 1989.

[2] R. Brazdil, r R. Glase, C. Pfister, J. M. Antoine, M. Barriendos, et al. Flood events of selected rivers of Europe in the Sixteenth Century. *Climatic Change*, 43:239–285, 1999.

[3] T. Glade, P. Albini, and F. Francès. The use of historical data in natural hazard assessments. 2001.

[4] V.T. Thorndycraft, G. Benito, M. Barriendos, and M.C. Llasat. Palaeofloods, Historical data and climatic variability: Applications in flood risk assessment. *Proceedings of the PHEFRA International Workshop*, pages 1–378, 2003.

[5] F. Guzzetti and G. Tonelli. SICI: an information system on historical landslides and floods in Italy. *Natural Hazards and Earth System Sciences*, 4(2):213–232, 2004.

[6] IFFI Project. http://www.mais.sinanet.apat.it/cartanetiffi/default_nosso.asp. 2004.

[7] SICI Project. http://sici.irpi.cnr.it/index.htm. 2009.

[8] L. Brancaccio. Genesi e caratteri delle forme costiere nella Penisola Sorrentina. *Bollettino della Società dei Naturalisti in Napoli*, 77:247–274, 1968.

[9] P. Budetta, D. Calcaterra, and A. Santo. Engineering-geological zoning of potentially unstable rock slopes in Sorrentine Peninsula (Southern Italy). pages 2119–2126, 1994.

[10] C. Violante, C. Biscarini, E. Esposito, F. Molisso, et al. The consequences of hydrologic events on steep coastal watersheds: the Costa d'Amalfi, eastern Tyrrhenian sea. *IAHS*, 327:102–113, 2009.

[11] E. Esposito, S. Porfido, C. Violante, C. Biscarini, et al. Water events and historical flood recurrences in the Vietri sul Mare coastal area (Costiera Amalfitana, southern Italy). *Proceedings of the UNESCO/IAHS/IWHA Symposium on The Basis of Civilization - Water Science?*, 286:95–106, 2004.

[12] F. Molisso, E. Esposito, D. Insinga, C. Lubritto, et al. Facies analysis of flood dominated fan-deltas off Amalfi coast, Eastern Tyrrhenian Sea. *This volume*, 2010.

[13] C. Violante. Geohazard in rocky coastal areas. *Geological Society of London*, 322:1–210, 2009.

[14] C. Violante. Rocky coast: geological constraints for hazard assessment. *Geological Society of London*, 322:1–32, 2009.

[15] E. Esposito, S. Porfido, and C. Violante. Il nubifragio dell'ottobre 1954 a Vietri sul Mare-Costa di Amalfi Salerno. *CNR GNDCI*, (2870):1–381, 2004.

[16] S. Porfido, E. Esposito, F. Alaia, F. Molisso, and M. Sacchi. The use of documentary sources for reconstructing flood chronologies on the Amalfi Coast (southern Italy). *Geol. Soc. of London*, 322:173–187, 2009.

[17] E. Esposito, S. Porfido, C. Violante, and F. Alaia. Disaster induced by historical floods in a selected coastal area (Southern Italy). *Thorndycraft V.R., Palaeofloods, Historical data and climatic variability: Applications in flood risk assessment. Proceedings of the PHEFRA International Workshop*, pages 143–148, 2003.

[18] E. Esposito, S. Porfido, and C. Violante. Reconstruction and recurrence of flood-induced geological effects: the Vietri sul Mare case history (Amalfi coast, Southern Italy). *AGI Fast Slope Movements Prediction and Prevention for Risk Mitigation*, 1:169– 172, 2003.

Integrated Management of Coastal Hypoxia in the Northern Adriatic Sea: the Case Study of the Province of Rimini

A. Luchetta[1], F. Alvisi[2], S. Cozzi[1], C. Cantoni[1], A. Russo[3], P. Serratore[4] , O. Bajt[5], P. Focaccia[2], C.R. Ferrari[6], G. Catalano[1], M. Ravaioli[2]
1, Institute of Marine Sciences, CNR, Trieste, Italy
2, Institute of Marine Sciences, CNR, Bologna, Italy
3, Dipartimento di Scienze della Vita e dell'Ambiente, Università Politecnica delle Marche, Ancona, Italy
4, Department of Veterinary Medical Sciences, University of Bologna, Bologna, Italy
5, Marine Biology Station, National Institute of Biology, Piran, Slovenia
6, DAPHNE Oceanographic Structure, Environmental Agency of Emilia-Romagna, Cesenatico, Italy
a.luchetta@ts.ismar.cnr.it

Abstract

An integrated monitoring network aimed at the management and mitigation of environmental and socio-economic costs of hypoxia was developed for the coastal zone of Rimini (Emilia Romagna - Italy).
This area was chosen for the presence of high anthropogenic pressure (416,000 equivalent inhabitants and tourist summer peak of up to 973,110), industrial and agricultural activities, as well as maritime traffic and nutrient river discharges (about 600 $t \cdot y^{-1}$ of N and 300 $t \cdot y^{-1}$ of P in 2002).
EMMA monitoring network was planned by linking scientific knowledge on hypoxia phenomenon with in situ experimental investigations. Its integration with existing environmental monitoring, available facilities and data resources was considered in order to increase the cost effectiveness of the project.
The structure of EMMA monitoring network was based on four main components:

- an instrumental monitoring network of the coastal zone, by means of an automated remote station coupled by traditional sampling at fixed stations, to provide a set of high resolution environmental data;
- a 3-D numerical model (ROMS) implemented to perform hydrological simulations and forecast of hypoxia in the area of interest;
- a Local Information Centre (LIC) devoted to the acquisition and exchange of data and model results among network components;
- a Decision Supporting System to bring scientific aspects of hypoxia phenomena into management requirements of local institutions and socio-economic operators.

1 Introduction

Eutrophication often causes symptoms of marine ecosystem stress ranging from elevated growth of algal biomass to low dissolved oxygen concentrations, massive mortality of marine organisms, defaunation of benthic populations, low quality of bathing waters, or even more serious problems connected to the occurrence of toxic algal blooms. Among these aspects, hypoxia and anoxia crises are common consequences of eutrophication in coastal zones. Over the past few decades both coastal eutrophication and hypoxia have become such widespread phenomena as to be regarded on a global rather than on a local scale [1, 2].

The causes of hypoxia are generally associated to an excess of continental nutrient loads, although the response of each marine ecosystem to this anthropogenic pressure is strongly modulated by the timing of water stratification, mixing and circulation at regional and local scales. Even global scale factors, such as climate change, may alter local ecosystem productivity therefore further exacerbate the problems related to anoxia and hypoxia. Microbial communities also affect the biogeochemical cycles of C, N and P, since nitrogen is considered the major limiting nutrient for marine primary production. An estimation of the abundances of bacterial groups specifically involved in the nitrogen cycle then results essential to understand the mechanisms acting in eutrophic ecosystems [1, 2, 3, 4].

Bottom water oxygen deficiency influences the living species and affects the biogeochemical processes controlling nutrient concentrations in the water column too. The importance of the benthic-pelagic coupling increases with decreasing water depth and nutrient load. The knowledge of sea floor characteristics is therefore crucial to study hypo-anoxia, as they can determine conditions favourable to local development of such phenomena. In addition to this, the sedimentary records provide information on the evolution of organic matter degradation, nutrient cycling and hydrodynamics over different spatial and temporal scales [5]. Northen (N) Adriatic Sea is highly productive and characterized by a trophic gradient decreasing from West to East. Nevertheless, production processes in this basin are highly variable, as a result of the interactions between meteorology, river inputs, nutrient dynamics and water circulation. These different factors play a role in the occurrence of large offshore anoxia and hypoxia and mucilage appearance. Hypoxia and anoxia in N Adriatic mainly occur in the western area where they were reported since the beginning of the last century. However, the analysis of their evolution, triggering mechanisms and consequences was often episodic, since most of the historical oceanographic data were collected at few coastal stations. More recently, specific observations on mass mortality of marine organisms, temporary cyst formation, unusually high catches of fish and invertebrates stressed by low oxygen concentrations and disturbance of meiobenthic copepod communities were reported at different locations as a consequence of the intensification of hypoxia and anoxia [1, 6, 7, 8, 9]. At regional scale, the coastal zone of Emilia Romagna plays a considerable role in the demographic and socio-economic perspective at national and European levels. Tourism, industry, fishing and aquaculture provide important contributions to the economy of this region. Here, the scientific community, local authorities and socio-economic operators often debated problems related to eutrophication and hypoxia since the 1970s. As a consequence, regular marine monitoring programmes, supported by regional institutions, was implemented since 1977. For these reasons, EMMA research project (Environmental Management through Monitoring and Modelling of Anoxia LIFE04ENV/IT/0479) operated from 2004 to 2007, with the aim of building an integrated monitoring/forecasting network to manage and possibly reduce the impact of hypoxia on the coastal zone of Rimini. EMMA was the first attempt in Italy to create an integrated network specifically dedicated to hypoxia and anoxia, through the combined efforts of scientific institutions, monitoring EPA, local and regional authorities and socio-economic actors. The project was carried out in collaboration with the National Institute of Biology of Slovenia (NIB), which is also involved in the monitoring program of marine eutrophication and hypoxia events in Slovenia. The aim of this paper is to present scientific background, planning activity and experimental investigations performed in the area of interest to define the operational characteristics of the monitoring/forecasting network.

2 Experimental activities

2.1 Study site

Within the 150 km long coastal zone under Emilia Romagna Region jurisdiction, the province of Rimini was chosen to implement the EMMA project (Figure 1). Very shallow waters characterize this 40 km long area, lying between Cesenatico and Cattolica. The water column structure is strongly influenced by the inputs of Po River and of other regional streams, which induce a complex circulation mostly dominated by a southward flowing current (Western Adriatic Current). High levels of nutrients, dissolved organic matter and suspended particulate matter are supplied to the coastal zone in concomitance with the spreading of the coastal front, their dynamics being modulated both by continental inputs and by in situ production/assimilation processes. Primary production and chlorophyll-a concentrations are high, particularly in a narrow belt within few miles from the coast [1, 10, 9, 11]. Temporal variations in the extension of low-salinity coastal waters also exert a strong influence on the deposition and biogeochemistry of sediments. Despite lateral transport and periodic resuspension, a net sediment accumulation characterizes the benthic compartment along the Italian coast South of the Po delta [5].

2.2 Field activity, data acquisition and elaboration

The EMMA monitoring network was set up taking into account the available monitoring activity in the area carried out by the Regional Environmental Protection Agency (ARPA Daphne). In details, it was integrated by:

- one fixed automated station (buoy) with real time data transmission;
- a new monitoring network of microbial communities, including some species potentially harmful for human health;
- a bulletin reporting about unusual catches of fish and other benthic organisms.

Ongoing environmental monitoring activities carried out by the Municipality of Rimini were also used to provide infor-

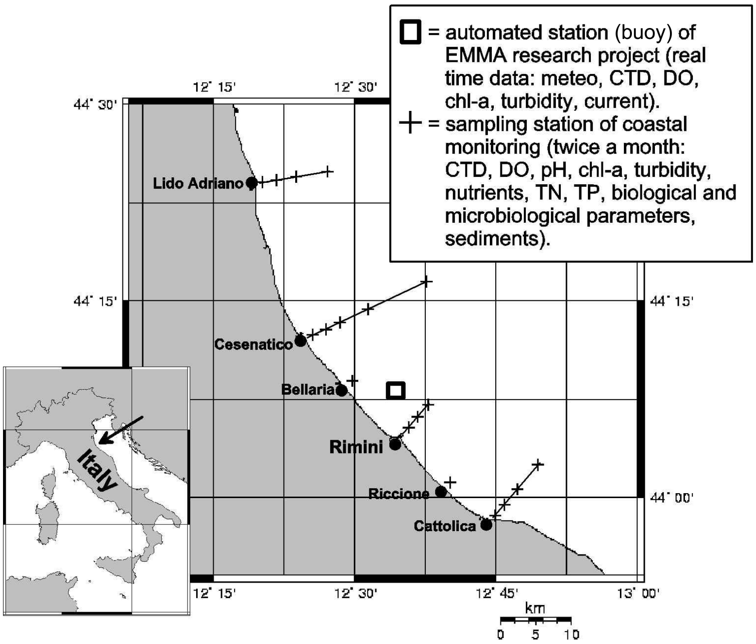

Figure 1: Study area: coastal zone of Rimini Province (NW Adriatic Sea), location of the automated station (buoy) of the EMMA research project and of the sampling stations of the regional environmental monitoring network.

mation on hypoxia events at very local scale. Meteorological data were obtained from the high resolution operational forecasts produced by COSMO-I7 model, operated by the Regional Servizio Idro-Meteorologico (ARPA Emilia-Romagna) in agreement with the Meteorological Office of the Italian Air Force. Flow rates of the Po River (mean daily discharge) and climatologic flow rates for the other local streams located along the coast were also used. Overall, the EMMA system was based on the activities described in the following.

2.3 Water quality investigations and pelagic/demersal resources

The automated station (Figure 2) was implemented for remote acquisition of meteorological data (wind direction and intensity, air temperature, air pressure, humidity, solar radiation) and CTD data (temperature, conductivity, dissolved oxygen, turbidity, Chl-a) at the water surface (0.5 m) and near the bottom (1 m above sea floor). A single-point Doppler Aanderaa DCS-4100 current meter measured current direction and speed in the deeper layer. The buoy was equipped with independent power supply and data transmission systems.

Environmental monitoring by ARPA

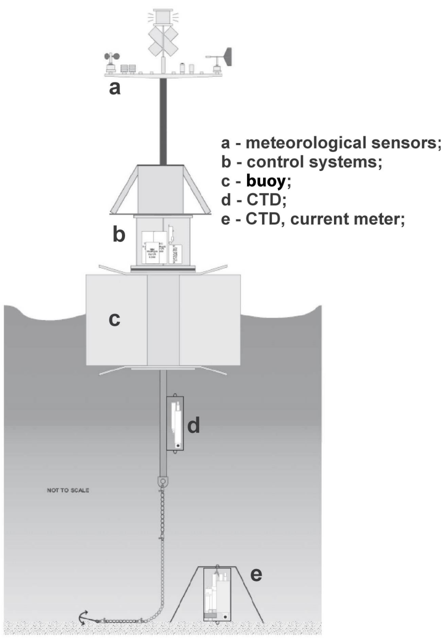

Figure 2: Schematic structure of the automated station of EMMA.

Daphne was periodically performed in the area by sampling 18 fixed stations located along 4 transects twice a month, whereas a higher frequency of sampling should be carried out in case of an early-warning for hypoxia. Profiles of temperature, salinity, dissolved oxygen, pH and chlorophyll-a are acquired by CTD downcasts. Bottle sampling is used for chemical (dissolved inorganic nutrients, ammonia, TN, TP) and biological (phyto and zooplankton) analyses, corer and box-corer for sediment sampling. ROV and photo camera for underwater environmental observation and record. Microbiological monitoring was carried out by collecting water samples north of the port of Rimini, with the aim of studying the microbial community involved in the nitrogen cycle [12], and those species that can be considered harmfull for human health under hypoxic conditions. *Nitrosomonas*, *Nitrobacter* and Total Denitrifying Bacteria (TDB) were determined by the MPN method. Total Heterotrophic Marine Bacteria (THMB), *Vibrio* spp., and *Pseudomonas* spp. were determined as CFU ml^{-1} using spread plate techniques. Presumptive *Vibrio vulnificus* strains were determined as previously reported [13]. Past monitoring, performed by the City of Rimini (2002-2004), has shown the occurrence of local events in canals and inland waters close to the coast. An analysis of physical, chemical and microbiological parameters of these brackish waters and sediments was performed to gain insight into the triggering factors and dynamics of these events. Since unusual catches of fish and demersal species may be the result of stressful conditions in the marine environment due to low oxygen concentration, these data were collected with the co-participation of local fisheries providing regular reports on catches including physical size and species abundances.

2.4 Sea floor characterization

Sea floor and sediment characterization of the area was carried out during a preliminary cruise in September 2005. Sediments were sampled by box coring at 14 stations located along three transects coinciding with the regional water quality monitoring (Cesenatico, Bellaria, Rimini). Sediment sections were photographed and their lithostratigraphy described. Sub-samples for pH, redox potential (Eh) and temperature were immediately measured after collection. Analyses of short-lived radioisotopes (^{210}Pb,^{137}Cs,^{7}Be,^{234}Th), organic carbon, $\delta^{13}C$, C/N ratio of the organic matter and mineralogical characterization were also performed at CNR-ISMAR laboratories.

2.5 Data collection and management

Meteorological forecasts, river discharges, in situ observations and hydrological and chemical data acquired by the automated station and by traditional sampling fed the Local Information Centre (LIC) and are organized on a database server with the utilization described in the following.

2.6 Modelling and processing

A 3-D numerical model, the Regional Ocean Modelling System [5], which includes a biogeochemical module, was used for short-term forecasting and early warning of hypoxia. ROMS model is a primitive equation, finite difference, hydrostatic, free surface model using generalised terrain following s-coordinates and a staggered Arakawa C grid on the horizontal, using a split-explicit, non-homogeneous predictor/corrector time stepping. The biogeochemical module is a relatively simple representation of nutrient cycling processes in the water column and organic matter remineralisation at the water-sediment interface that explicitly accounts for sediment denitrification. It incorporates only one phytoplankton class and one zooplankton class. The minimum set of equations is adapted from the Fasham plankton dynamics model [14]. Data provided by LIC was used for initialization and verification of the model. The model provides hindcasts and forecasts of circulation and dissolved oxygen content of the water in the area of interest every day for the following 3 days (limit imposed by the COSMO-I7 forecast) as daily averaged and 3 hour instantaneus fields. The Decision Supporting System implemented by EMMA assimilates all information and data provided by the forecasting model and by in situ observations. It is designed as a tool to help local authorities in the management of hypoxia crises.

3 Results and Discussion

3.1 Analysis of hypoxic/anoxic events in the coastal zone of Rimini

The coastal waters of the NW Adriatic are generally eutrophic, particularly along the coast of the Emilia Romagna and Marche down to Ancona. Here, high production events and stable meteorological conditions often lead to hypoxia or anoxia in deeper waters, which can extend over hundreds of square kilometres. Usually, the major events break out in proximity of the Po Delta then spreading southward, showing dynamics related to river discharge and water circulation. The analysis of the data provided by ARPA confirmed that wide hypoxia almost never originate in the area between Cesenatico and Cattolica, but are here advected from north. Concentrations of dissolved oxygen less than 3 $mg \cdot l^{-1}$ are here considered the limit for hypoxia since critical for marine benthonic organisms, which slow their metabolism below these values, suffer and are in danger of life [2]. In the North Adriatic, massive mortality of benthonic communities starts at values around 0.7 $mg \cdot l^{-1}$, while the mortality of more sensitive and weaker individuals was already observed at values less than 1.4 $mg \cdot l^{-1}$.

Historical data show that the frequency of hypoxia increased since the 1970s, progressively losing its characteristics of being a merely occasional phenomenon, and becoming chronic. Studies on local benthic foraminifera associations in Po delta sediments showed a steadily increase of eutrophication since 1900, with a more frequent occurrence of hypoxia/anoxia during summer since the 1960s [1]. On a local scale, the analysis of data gathered by the regional EPA monitoring showed that oxygen deficiencies occurred quite often in the period 1994-2004. Hypoxia affected waters extending from the beach to 6 km offshore. These events often occur in June - September and in October - November. Other events were reported on a very local scale, within the bathing belt (500 m from the coast) or in the inner brackish canals connected to the sea. They were caused by the degradation of huge algal biomasses, developed thanks to strong runoff and scarce circulation.

3.2 Socio-economic relevance of the region and inventory of anthropogenic loads

From a demographic and socio-economic perspective, the Emilia Romagna Region is important for the European Community as a whole. The population in this region increased markedly up to the 1970s, stabilizing to around 4 millions inhabitants (6.9% of national population). Population density is 180 inhab. km^{-2}, especially high in the plain and along the coast, with peaks of 871 inhab. km^{-2} in Rimini. Industry employs 1.5 million people, and tourism shows a constant increment of visitors (+15% over the decade 1992-2001). Fishing contributed to the regional economy in 2001 with 14,587 $t \cdot y^{-1}$ of fish, corresponding to a wholesale value of k€ 34,000, and with amounts ranging from 800 to 1,800 $t \cdot y^{-1}$ over the decade 1994-2004, whereas aquaculture ranged from 1,500 to 3,000 $t \cdot y^{-1}$ over the same period. From these data, it is clear that anthropogenic load in regional coastal waters is high. If estimated as equivalent inhabitants (eq. inhab. = resident population + tourism + industry), they peak at 6.7 millions in summer, corresponding to a 5.4 millions annual average, whereas sewage disposal plants operating in the area are able to treat loads corresponding to 6.2 millions eq. inhab. [7]. The Rimini Province increased its economic activities and population over the past few decades up to 416,000 eq. inhab., as its coastal area is able to attract 20% of visitors from the whole region. Fishing and aquaculture contribute to local and regional economies in a significant way (1,000 $t{\cdot}y^{-1}$, 1,400 $t{\cdot}y^{-1}$), while contributions from agriculture and industry cannot be neglected. The anthropogenic load into coastal waters is 1 million eq. inhab. in summer, and may not be completely treated by the available disposal plants corresponding to about 900,000 eq. inhab. The Municipality of Rimini and the regional authorities are aware of this environmental pressure, as it affects economic activities and the quality of life of their inhabitants. For these reasons, the area of Rimini may be considered as a case study exportable to other coastal zones affected by a similar combination of environmental problems.

3.3 Sediment characterization in the coastal zone of Rimini

Sediments play an important role as nutrient sink and/or source in the shallow pelagic environment, if the following four conditions are met:

- high input of fresh organic matter sinking to sea floor without undergoing a complete oxic degradation in the water column;
  - high input of fine inorganic particulate matter;
- scarce influence of (biological?, physical?) mixing processes on the sea floor;
- high sediment accumulation rates both on short and long timescales.

In the coastal area from Cesenatico to Cattolica, local rivers generally affect the onshore zone, whereas low salinity offshore waters are originated by Po River discharges. The circulation pattern determines a general land-to-sea gradient from sandy to silty-clay deposits. However, the present study evidenced a more complex grain size distribution of surface sediments, originated by small morphological irregularities of the sea floor which, in combination with those of the coastline, determine an inhomogeneous distribution of currents and an irregular transport and deposition of surface sediments. All stations showed increasing hydrated and oxidized surface-active layers from the coast to the open sea except for the centre of the study area. This indicated the accumulation of sediments in NE coastal area as probably due to Po River, whereas onshore sporadic transport from SW to NE is due to local rivers. The low content of ^{7}Be($<$17 $Bq{\cdot}kg^{-1}$) and the sporadic presence of ^{137}Cs in surface near-shore sediments indicated that hydrodynamic conditions in the area prevent a regular alongshore sedimentation of riverine particulate matter, or that they periodically cause the resuspension of the sediments recently settled. Since the amount and quality of the sedimentary organic matter have a great influence on benthic degradation rates, the abundant presence of fresh highly degradable organic matter in concomitance with high temperatures and low hydrodynamics can lead to the development of hypoxic conditions on the sea floor. On the whole, the sea floor characterization showed that the hydrodynamic circulation in the area follows a complex pattern, which is not only dominated by the West Adriatic Current as previously thought. Locally derived sediments seem to be transported onshore and from South to North, whereas extra-local sediments (from the Po plain and northern Adriatic) offshore 6-10 km are mostly transported in a SE direction. Around 3-6 km from the coast, a clockwise gyre carries part of the offshore sediments toward the studied coastal zone. Moreover, several artificial infrastructures located more or less permanently in this shelf area cause changes in water circulation and sea floor morphology on a very local scale.

3.4 Microbiological monitoring

Hypoxia occurs when production processes and respiration are uncoupled. Under these conditions, monitoring of the "physiological groups" of bacteria involved in the nutrient cycles and of those considered hazardous for human health may be important to understand the quality of coastal waters.

Nitrifying bacteria (*Nitrosomonas* and *Nitrobacter*) and TDB were considered as predictive factors for the development of eutrophic conditions. In fact, nitrifying bacteria oxidize ammonia compounds to nitrite and nitrate, whereas denitrifying bacteria reduce nitrate to nitrite or N_2. Ammonifying bacteria decompose organic nitrogen and produce NH_4+. Since inorganic nitrogen is regarded as the main factor responsible for eutrophication, nitrifying bacteria substantially act as promoters of algal blooms, while denitrifying bacteria act as competitors of algae. Moreover, given that autochthonous bacteria such as *V. vulnificus*, and some *Pseudomonas* spp., are well known to be human pathogens through contact [15], their monitoring was carried out together with THMB. The risks of exposure to waterborne pathogenic and opportunistic microorganisms for swimmers and fishermen include wound infections, otitis, conjunctivitis, sinusitis, gastroenteritis and respiratory diseases.

Two events of hypoxia were observed in the area of interest in September and November 2005. The abundance of *Nitrosomonas* and *Nitrobacter* did not show correlation with these events, whereas TDB showed a considerable increase. This observation suggested that terrestrial inputs of nitrate, which are reduced by denitrifying bacteria, were an important N source for bacterial community with respect to the decomposition of organic compounds. The abundance of THMB and *Vibrio* spp. were strictly correlated, *Vibrio* spp. representing the largest fraction of the total population of marine heterotrophs. During hypoxia events, *Vibrio* spp. and presumptive *V. vulnificus* increase their abundance, given that they are facultative anaerobes, whereas *Pseudomonas* spp., are strictly aerobes and thus not favoured under low oxygen conditions. These data showed that strong nutrient inputs and variable oxygenation of coastal waters affect the abundance and composition of the bacterial community.

3.5 Forecasting model

The forecasting system has to predict hypoxia events their spatial extension and duration. A low resolution ROMS model was implemented on the whole Adriatic Sea at 2 km horizontal resolution. Heat, water and momentum fluxes through the sea surface were computed interactively from the COSMO-I7 3-hourly outputs. In our application, shortwave radiation was taken from COSMO-I7, while the other fluxes were calculated interactively with ROMS using its own sea surface temperature and COSMO-I7 atmospheric data. Forty-eight rivers and springs were included as sources of mass and momentum using available daily discharges (Po, Pescara, Biferno rivers) and monthly climatological values otherwise. Biogeochemical input is defined for every river on the basis of published data. Further details and results are described in [16].

The hydrodynamic model was able to simulate the circulation and the dissolved oxygen dynamics in the North Adriatic Sea with good agreement with data for up to a few days. To reach an optimum resolution in the coastal zone, multiple nesting was afterward implemented. An intermediate model was defined in the Northern Adriatic with 0.5 km horizontal resolution. In the vertical, there are 20 s-levels, which in the shallow western coastal area correspond to a vertical resolution of less than 1 m.

3.6 Decision Supporting System (DSS)

The development of a DSS to manage hypoxia and anoxia crises was one of the most important tasks of the project. It was designed to provide a practical and easy-to-use tool for local authorities and socio-economic partners in order to reduce environmental and socio-economic costs of these events. DSS acquires and integrates a series of indicators derived from scientific community, monitoring activities and past knowledge, outputs of the forecasting models and other additional information in order to evaluate effectiveness and environmental and socio-economic impacts of different intervention strategies. It represents a sort of "manual" to drive public authorities toward a correct management of the coastal zone with regard to dystrophic phenomena.

DSS was planned to approach hypoxia/anoxia phenomena on two different spatial-temporal scales. In the short-term and for local events, it provides practical instructions and guidance to local authorities for the immediate management of the emergency. Over the long-term and in the case of basin-wide extended events, it contributes to the identification of major risks and concurrence of factors that may worsen the evolutionary trend of hypoxic events.

Since the aim of DSS was though as a tool user-friendly for decision makers and local authorities, it was planned to act at three levels:

- a scientific level: to produce and update knowledge for corrective actions of prevention, mitigation and recovery. These actions were evaluated on the basis of a cost/benefit analysis;
- a management level: to choose the best management options among various alternative proposals, on the basis of cost/benefit analyses as well as social acceptability. Such actions could represent a proposal to develop legislative and administrative measures;
- a communication level: to raise awareness through educational and informative actions on best management practices and derived decisions and measures, especially addressed to local and regional policy makers, public authorities and citizens.

3.7 Structure of EMMA monitoring network

The structure of the monitoring/forecasting network of EMMA is shown in Figure 3. Available resources and facilities are integrated into a network specifically designed to manage hypoxia and anoxia. EMMA network has four main components:

1. the Local Information Centre operates as a centre for collection and exchange of data and model results among the different parts of the network;
2. the coastal monitoring system provides the high-resolution environmental data, which are needed to define hypoxia scenarios and to implement the early-warning system. These data are col-

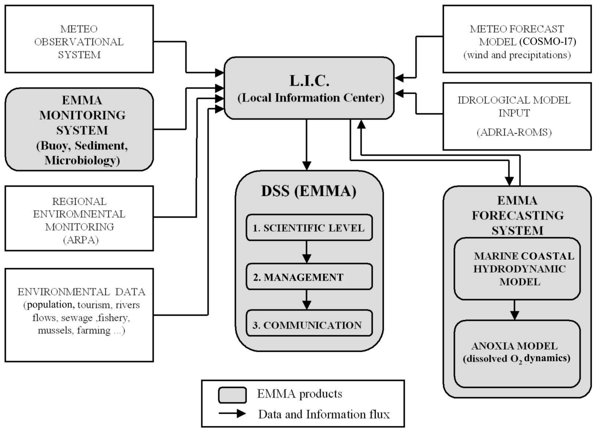

Figure 3: Components of the monitoring network of the EMMA research project (grey) and available environmental data, monitoring activities and model processing used by the project.

lected by means of an automated remote station (buoy) and by traditional monitoring activity in fixed sampling stations;

3. the forecasting model provides hydrological simulations and oxygen budgets in the area of interest with high temporal and spatial resolutions;
4. the Decision Supporting System acts as an interface between the scientific knowledge of the hypoxia phenomenon and the operative needs of local institutions and socio-economic operators.

4 Conclusions

The coastal zone of Rimini was chosen among others to study hypoxia in the coastal marine environment because of several scientific, socio-economic and logistic reasons:

- previous studies and time series of environmental data showed the presence of various and complex mechanisms at the basis of hypoxia phenomenon;
- the Province of Rimini provides an important contribution to the economy of the region based on marine resources;
- the environmental impact of hypoxia on the economy of this area is considerable;
- the integration with existing monitoring activities, meteorological forecasting systems and available facilities may improve the cost effectiveness of the network.

The application of the monitoring network of EMMA is expected to be a "case study", which could be used in other national and European coastal zones with similar characteristics.

5 Acknowledgements

A special thanks to the LIFE Financing Programme of the European Commission, to the Rimini Municipality, to the captain and crew of the R/V Urania and to the Voluntaries for the Marine Assistance of Rimini.

References

[1] R. A. Vollenweider, R. Marchetti, and R. Viviani. *Marine Coastal Eutrophication, in: Vollenweider, R.A., R. Marchetti and R. Viviani (eds)*. Elsevier, 1992.

[2] R.S.S. Wu. Hypoxia: from molecular responses to ecosystem responses. *Marine Pollution Bulletin*, 45:35–45, 2002.

[3] IPCC. The regional impacts of climate change: an assessment of vulnerability. Summary for policymakers. (Watson R.T., Zinyowera M.C., Moss R.H., Dokken D.J. Eds.) A special report of Intergovernmental Panel on Climate Change, Working Group II. OMM, WMO, PNUE, UNEP. page 27, 1997.

[4] F. Azam and B.C. Cho. *Bacterial utilization of organic matter in the sea, in: Fletcher, M. (eds.), Ecology of Microbial Communities*. Cambridge University Press, 1987.

[5] M. Frignani, L. Langone, M. Ravaioli, D. Sorgente, F. Alvisi, and S. Albertazzi. Fine sediment mass balance in the western Adriatic continental shelf over a century time scale. *Marine Geology*, pages 222–223: 113–133, 2005.

[6] S. Cozzi, I. Ivančić, G. Catalano, T. Djakovac, and D. Degobbis. Dynamics of the oceanographic properties during mucilage appearance in the northern Adriatic Sea: analysis of the 1997 event in comparison to earlier events. *Journal of Marine Systems*, 50:223–241, 2004.

[7] M. Giani, D. Degobbis, and A. Rinaldi. *Mucilages in the Adriatic and Tyrrhenian Seas. In: (Giani M., Degobbis D., Rinaldi A. eds.). Science of The Total Environment*, volume 353. 2005.

[8] T. Legovic, D. Petricioli, and V. Zutic. Hypoxia in a pristine stratified estuary (Krka, Adriatic Sea). *Marine Chemistry*, 32:347–359, 1991.

[9] M. Pettine, L. Patrolecco, M. Camuso, and S. Crescenzio. Transport of carbon and nitrogen to the Northern Adriatic Sea by the Po River. *Estuarine, Coastal and Shelf Science*, 46:127–142, 1998.

[10] S. Cozzi, G. Bortoluzzi, A. Di Maio, and M. Marcelli. 3-D structure of the marine coastal front and quantitative estimation of nutrient budgets in a seawater volume of the NW Adriatic Sea. *P.S.Z.N. Marine Ecology*, 23 (Suppl. 2002):111–121, 2002(a).

[11] A. Zoppini, M. Pettine, C. Totti, A. Puddu, A. Artegiani, and R. Pagnotta. Nutrients, standing crop and primary production in the Western coastal waters of the Adriatic Sea. *Estuarine, Coastal & Shelf Science*, 41:493–513, 1995.

[12] S.W. Naqvi, D.A. Jayakumar, P.V. Narvekar, H. Naik, et al. Increased marine production of N_2O due to intensifying anoxia on the Indian continental shelf. *Nature*, 408(6810):346–349, 2000.

[13] P. Serratore, G.C. Tortura, E. Rinaldini, S. Milandri, and D. Presepi. Phenotypic characterization of some bacterial populations belonging to the genus *Vibrio*. *Annali di Microbiologia ed Enzimologia*, 49:79–88, 1999.

[14] M. Fasham, H.W. Ducklow, and S.M. McKelvie. A nitrogen-based model of plankton dynamics in the oceanic mixed layer. *Journal of Marine Research*, 48:591–639, 1990.

[15] L. Elko, K. Rosenbach, and J. Sinnott. Cutaneous Manifestations of Waterborne Infections. *Current Infectious Disease Reports*, 5:398–406, 2003.

[16] A. Russo, A. Coluccelli, I. Iermano, F. Falcieri, M. Ravaioli, et al. An operational system for forecasting hypoxic events in the northern Adriatic Sea. *Geofizika*, 26:191–213, 2009.

Thermal Fluid Discharges from Submarine Springs at the Formiche di Grosseto Islets (Tyrrhenian Sea, Tuscany, Italy) and their Relation with Regional Anti-Apennine Tectonic Lineaments

G. Fasano[1], G. Gabbani[2], F. Tassi[2], O. Vaselli[2]
1, Institute for Biometeorology, CNR, Sassari, Italy
2, Department of Earth Sciences, University of Firenze, Firenze, Italy
g.fasano@ibimet.cnr.it

Abstract

The Formiche di Grosseto (southern Tuscany, Italy) islets are a reef system of about 1,500 m^2, 9 nautical miles offshore the outfall of the Ombrone river and are constituted by Liassic carbonate rocks of the Tuscan Series (Calcare Massiccio, and are part of the Giannutri-Formiche di Grosseto (GFR) ridge separating Neogene basins of the Tuscan Shelf.
In 2005, during a monitoring survey several thermal springs discharging from the sea bottom close to Formiche islets were noticed. Thermal fluids discharge from several points mainly located along the N-NE scarp bordering the main reef at depths varying from 6 to 32 m. and an outlet temperature of about 41 °C was measured. Accordingly, continental Tuscany is characterized by a large amount of Ca-SO_4 thermal water discharges, such as Bagni Osa and Roselle located inland in the proximity of the Formiche di Grosseto area, whose chemistry is to be related to mixing of fluids from different sources, i.e. hydrothermal and seawater (Bagni Osa) and/or hydrothermal and meteoric (Roselle). For these considerations, the occurrence of CO_2-rich submarine thermal discharges at Formiche di Grosseto may conveniently be related to the regional anti-Apennine tectonic lineaments.

1 Introduction

The Formiche di Grosseto (southern Tuscany, Italy) islets are a reef system of about 1,500 m^2, 9 nautical miles offshore the outfall of the Ombrone river. They are constituted by Liassic carbonate rocks of the Tuscan Series (Calcare Massiccio, [2, 3]) and are part of the Giannutri-Formiche di Grosseto (GFR) ridge separating Neogene basins of the Tuscan Shelf [4].

In 2005, during a monitoring campaign aimed to investigate the effects of polluted sea water on local submarine vegetation several thermal springs discharging from the sea bottom close to the Formiche di Grosseto were noticed . Thermal fluids discharge from several points mainly located along the N-NE scarp bordering the main reef (Figure 1) at depths varying from 6 to 32 m.

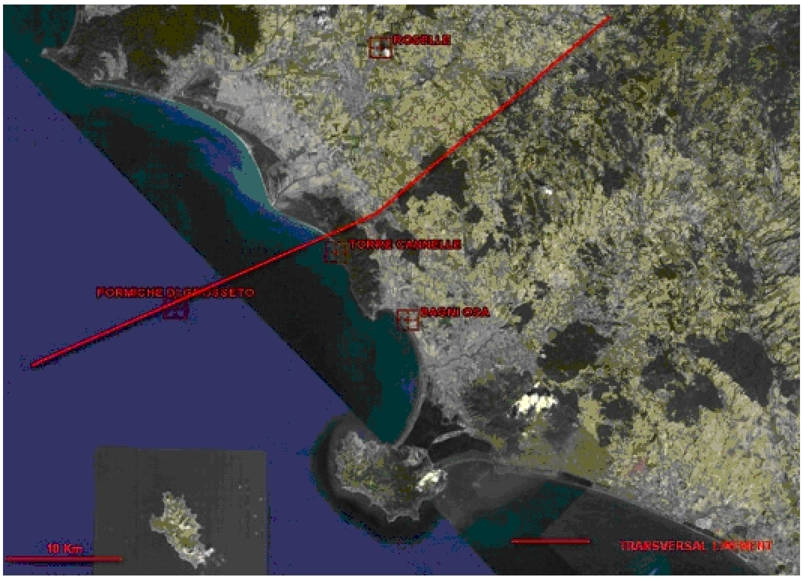

Figure 1: Map of southern Tuscany and Formiche di Grosseto with the location of the sampling sites and the anti-Apennine lineations.

2 Methodology and data analysis

During the first recognition an outlet temperature of about 41 °C was measured. In 2007, a second scuba expedition was organized to collect water and dissolved gas samples for chemical analysis. The main aim of the present work is to assess the origin of discharged fluids and their relation with local and regional tectonics.

The results show that the chemical compositions of the water samples are quite similar to that of seawater, although marked by significant enrichments of SO_4, Ca and B and Mg depletion (Table 1).

These compositional characteristics are likely to be ascribed to the mixing of seawater with hydrothermal fluids, the latter reaching the sea bottom through a long hydrological pattern.

Actually, in the Mg vs. SO_4 binary diagram (Figure 2) Formiche di Grosseto samples plot close to an hypothetical mixing line between seawater and a SO_4-rich hydrothermal end-member, which is typically depleted in Mg [5] due to water-rock interaction at relatively high temperature [6].

Accordingly, continental Tuscany is characterized by a large amount of Ca-SO_4 thermal water discharges, such as Bagni Osa and Roselle (Table 1) located inland in the proximity of the Formiche di Grosseto area (Figure 1), whose chemistry is to be related to mixing of fluids from different sources, i.e. hydrothermal and seawater (Bagni Osa) and/or hydrothermal and meteoric (Roselle) (Figure 2).

The chemical features of the hydrothermal end-member are derived by rock-water interactions processes involving carbonate-anhydrite rocks, such as those of the quite

sample	North	East	T°C	pH	HCO_3	Cl	SO_4	Na	K	Ca	Mg	NH_4	NO_3	B	F	Br	Li
1	42°34'94"	10°52'53"	41	6.20	144	21686	2866	11700	418	1141	1150	0.61	4.7	64.00	1.51	63	0.19
2	42°34'69"	10°52'79"	40	5.36	145	21640	3145	12620	415	1251	1131	0.55	16	66.00	1.23	65	0.21
Bagni Osa	42°33'07"	11°10'34"	30	6.77	535	6873	3125	3885	142	1250	499	9.30	0.21	39.00	3.1	24	0.39
Roselle	42°48'32"	11°08'36"	38	6.83	92	32	1490	35	10	621	12	1.00	0.07	1.10	0.44	0	0.04
seawater				8.15	135	18952	2648	10468	348	411	1331	0.11		4.60	1.3	65	0.17

sample 1	CO_2	N_2	Ar	CH_4	O_2	Ne	He	$\delta^{13}C\text{-}CO_2$*
mmol/L	9.202	0.911	0.022	0.0014	0.082	0.00001	0.0001	
% by vol	90.051	8.920	0.212	0.0135	0.803	0.00011	0.0010	
Bagni Osa	91.213	7.439	0.278	0.0761	0.162	0.00016	0.0000	
Roselle	83.029	14.299	0.370	0.0001	2.301	0.00019	0.0000	-2.3

Table 1: Water and gas composition of the thermal discharges at the islets of Formiche di Grosseto. Concentration of dissolved solutes are in mg/l. Concentrations of the gas compounds are in mmol/l (first row) and % by vol. (second row). Chemical composition of seawater and water (in mg/l) and gas (in % by vol.) samples from Bagni Osa and Roselle thermal springs are also reported. * The δ^{13}C-CO_2 value is from [1].

thick Mesozoic limestones of the Tuscan Series with intercalated anhydrite layers (Burano Formation). A significant contribution from an hydrothermal system may also explain the composition of the Formiche di Grosseto dissolved gas sample, showing relatively high CO_2 concentrations (up to 90 % by vol.), similar to those measured at the inland springs (Table 1). The C-CO_2 isotopic signature (- 2.3 ‰ V-PDB) of Bagni Osa spring [1] suggests a deep origin for the CO_2 of the thermal emissions discharging in this area.

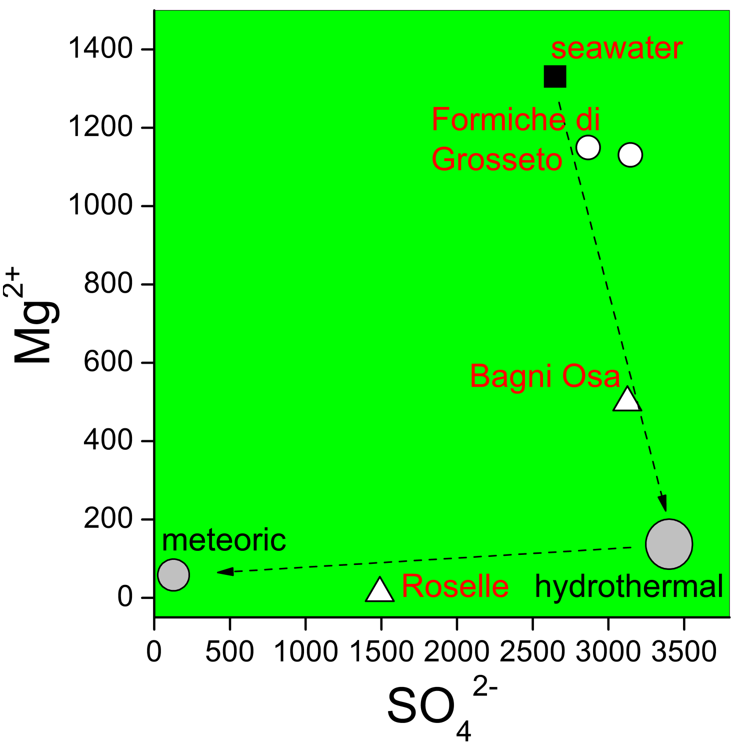

Figure 2: Mg vs. SO_4 binary diagram for the Formiche di Grosseto submarine fluid discharges. Hydrothermal and meteoric end-members are also reported, as well as the composition of seawater and Bagni Osa and Roselle springs.

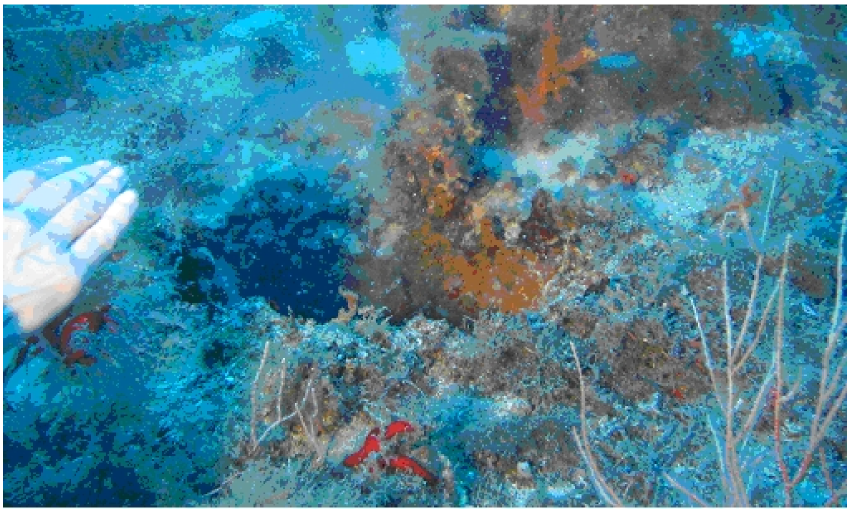

Figure 3: Submarine thermal emission at Formiche di Grosseto (Tuscany, Italy)

3 Conclusions

It is worthy of noting that the spatial distribution of the thermal springs of Tuscany is generally governed by regional tectonics and corresponds to the boundaries of the carbonate formation outcrops, which represent the main aquifer [1].

According to these considerations, the occurrence of CO_2-rich submarine thermal discharges at Formiche di Grosseto may conveniently be related to the regional anti-Apennine tectonic lineament passing through Torre Cannelle, which runs subparallel to the Follonica-Rimini line (Figure 1). Its presence was already suggested on the basis of offshore geophysical investigations carried out by mono and multichannel seismic reflection profiles [7, 8].

Figure 4: Formiche di Grosseto (Tuscany, Italy) main reef.

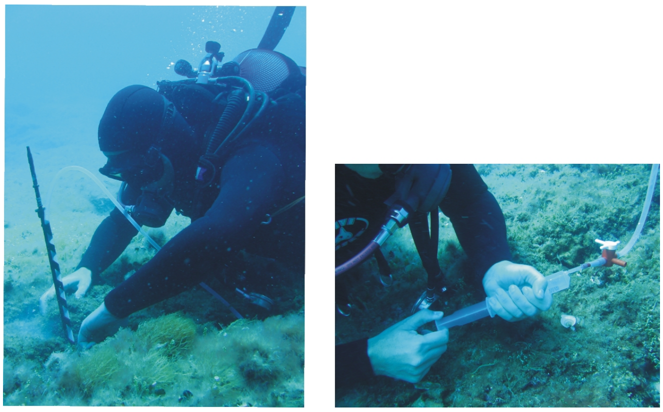

Figure 5: Water and dissolved gas sampling from submarine fluid discharge.

References

[1] A. Minissale, G. Magro, G. Martinelli, O. Vaselli, and F. Tassi. A fluid geochemical transect in the Northern Apennines (central-northern Italy): fluid genesis and migration and tectonic implications. *Tectonophysics*, (319):199–222, 2000.

[2] G. Motteran and G. Ventura and. Aspetti geologici, morfologici e ambientali dello Scoglio d'Africa (arcipelago toscano). *nota preliminare Atti Soc. Tosc. Sci. Nat.*, (Mem. A):51–60, 2005.

[3] R. Signorini. Note illustrative della Carta Geologica d'Italia, Foglio 135 Scala 1:100.000. *Carta Geologica d'Italia*, foglio 135(Orbetello), 1967.

[4] V. Pascucci, S. Merlini, and I.P. Martini. Seismic Stratigraphy of the Miocene-Pleistocene Sedimentary Basins of the Northern Tyrrhenian Sea and Western Tuscany (Italy). *Basin Research*, (11):337–356, 1999.

[5] W. F. Giggenbach. Geothermal solute equilibria. Derivation of Na-K-Mg-Ca geoindicators. *Geochim. Cosmochim*, Acta(52):2749–2765, 1988.

[6] L.B. Bischoff and W.E. Seyfried. Hydrothermal chemistry of seawater from 25 °C to 350 °C. *Am. J. Sci.*, (278):838–860, 1978.

[7] R. Bartole, L.Torelli, G. Mattei, D. Peis, and G. Brancolini. Assetto stratigrafico-strutturale del Tirreno settentrionale: stato dell'arte. *Pialli G., Barchi M. & Menichetti M. (Eds.), Studi Preliminari all'Acquisizione Dati del Profilo CROP 03 Punta Ala-Gabicce. Studi Geologici Camerti Volume speciale*, (1991/1):115–140, 1991.

[8] G. Cornamusini, A. Lazzarotto, S. Merlini, and V. Pascucci. Eocene-Miocene evolution of the north Tyrrhenian Sea. *Boll. Soc. Geol. It.*, Vol. Spec.(1):769–787, 2002.

The Evolution of the Coastline in Some Archaeological Sites in North-West Sardinia

D. Carboni[1,3], S. Ginesu[2,3]
1, Department of Theory and Research of Cultural Systems, University of Sassari, Italy
2, Department of Botanics, Ecology and Geology, University of Sassari, Italy
3, Institute for Biometeorology, CNR, Sassari, Italy
carbonid@uniss.it

Abstract

This report examines the connection between the archaeological sites and the sea level modifications which have taken place over the past 8,000 years in the area of the Porto Conte gulf. Here, the archaeological finds testify to the modifications of the coastline during the Neolithic, the Nuragic and the Roman ages. From our survey in the districts of the Roman villa of S.Imbenia, the nuragic complex of S. Imbenia, the nuragic village of Palmavera and the cave of Grotta Verde, it emerges that the sea level changed considerably in the time span referring to the monuments considered by the present study. In the reconstruction of past land uses by the local population, the localization of the mentioned archaeological sites takes into account the way in which the current geomorphology and landscapes have changed. The remarkable modification of the sea level, from the Neolithic, induces to suppose the coastline changed from the line of -15/-18m to the present bathymetric situation, and the Grotta Verde cave attest the existence of a coastline that used to be situated considerably offshore as opposed to its present position. The coastline during the Nuragic period was situated at the opposite end of the promontory, near Torre Nuova, in the west promontory. The littoral belt stretched for about 3 km from this point to the promontory of Capo Caccia, near Torre Tramariglio. The study of monuments located along this coastline requires an adequate geo-morphological reconstruction of the local natural environment.

1 An overview of the area

In recent decades, researches on past and current modifications of the coastline testify to the crucial role of archaeological sites in the reconstruction of sea level movements and of the phases of sea progradation and withdrawal. What follows is the result of our interest and enquiries into coastal erosion, starting from the work of Roland Paskoff, who has traced the modifications of the Tunisian coastline over the past 2,000 years [1]. In recent years, the Sardinian coast has also been studied so as to identify areas in which the presence of important archaeological sites and remains can help corroborate our knowledge of (pre)historic coastline variations [2]. Special attention has been given to the gulf of Porto Conte, an area rich in archaeological sites and recent deposits where it is possible to investigate both the geomorphologic evolution and the land use of the local territory [3].

Figure 1: Location of the studied area.

The gulf of Porto Conte (Figure 1) is a deep ria formed as a consequence of climate changes during the postglacial Age when the sea level raised in the deep surrounding karstic valley (today the entire area is underwater). The progradation of the sea was so rapid that both the epigeic and the hypogeic karst morphologies of the Mesozoic limestone of the area are still visible in the rocky seafloor surfacing among the sands and the banks of Posidonia Oceanica. Along the cliff of Capo Caccia and promontory of Punta Giglio, numerous caves of different depths are now underwater as a consequence of the progressive raising of the sea level. Some of these caves show evidence of modification and erosion on their surfaces and on the deposits of karst crusts due to the variations of the sea level and to its prolonged presence in the area [3].

2 The Roman villa of Sant'Imbenia (Porto Conte - Alghero)

The dislocation of Roman villas over the territory testifies to the Roman colonization of the area. The extra-urban villa was the organizational heart of the landed estate: it was there, in fact, that prestigious produce including olive trees and vineyards was cultivated and then shipped to the provinces in the mainland. In the villas, secondary economic activities were also carried out such as, for instance, the manufacturing of pottery and fish-farming

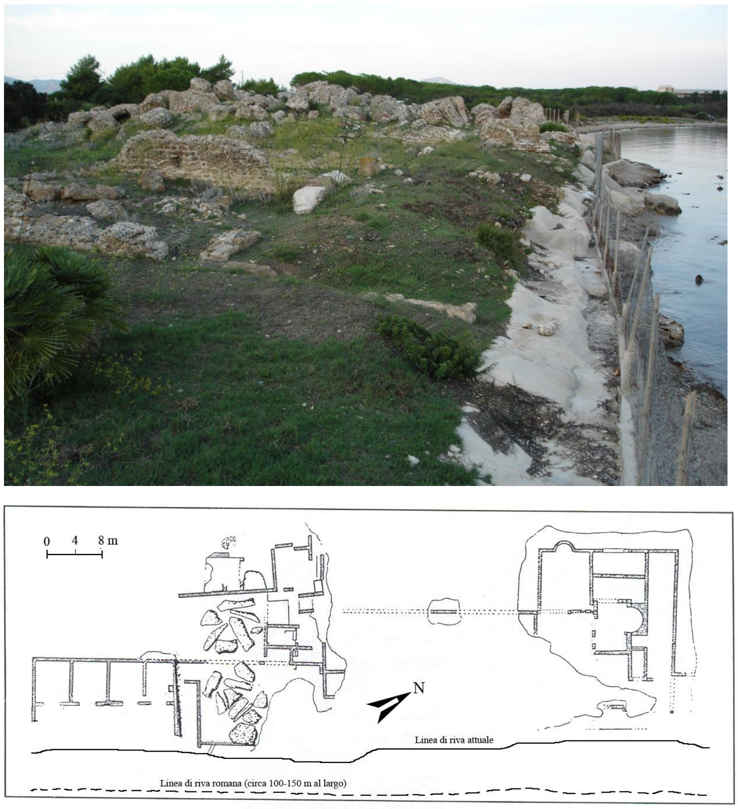

Figure 2: The Roman villa of Sant'Imbenia and its plant.

in seaside villas [4, 5, 6].

Near Sant'Imbenia, in an area overlooking the wide surrounding land of the Porto Conte (Alghero) gulf, the remains of a roman stone-built edifice (over 90 metres long) have been found (Figure 2).

The Sant'Imbenia complex attests the presence of an extended marine villa in one of the large landed estates which administered the agriculture of the wide midland area in the gulf of Porto Conte. Its coastal location had certainly been chosen so as to facilitate the sorting out of wheat and to guarantee its quick delivery to markets in the mainland. The quiet gulf of Porto Conte was a safe harbour: evidence of existing piers, in fact, can be found in its seafloor. The presence of small blocks of refined stone, situated perpendicularly to the shore and surfacing opposite the southern complex suggests that the area may have hosted a minor harbour. Recent studies further confirm that this rocky portion of the coast may have been used for fish-farming.

The Sant'Imbenia building has a rectangular plan with its longest sides extending in the direction of the coastline. It consists of two separate blocks: the first is situated

Figure 3: The Sant'Imbenia nuragic tower and its village.

in the south-western area, while the second is about 30 metres north of the first block. The south-western block has two dwellings: one overviews the beach, and is connected to the underwater parts of the building; the other is situated inland and at its back. The function of each room is yet to be ascertained though it may be suggested that some of them formed part of the living area of the villa.

The first block connects to the second (situated north of the first) through a rectilinear wall. Buildings such as this tend to have a rectangular plan, and are usually divided into different rooms. Most floors show mosaics, some of which display white plaster decorations. Such architectural and ornamental features suggest that this was a prestigious building with an important role [6]. It has also been suggested that the second block may have hosted a thermal unit, and that this connected directly to the living area of the villa. As to the chronology of the entire complex, in the absence of alternative data, we confirm Maetzke's thesis, according to which Sant'Imbenia dates back to the I century AD [7].

The southern part of the villa is currently exposed to marine erosion. The external courtyard is already underwater while there is a risk that the architectural frame may collapse. The coastline has evidently been eroded beyond the site of the villa, which was originally built far from the shore. The weak inclination of the beach has contributed to the vast transgression of seawater in the Sant'Imbenia place so that some remains of the Roman edifice are now at 1.20 metres under the present sea level.

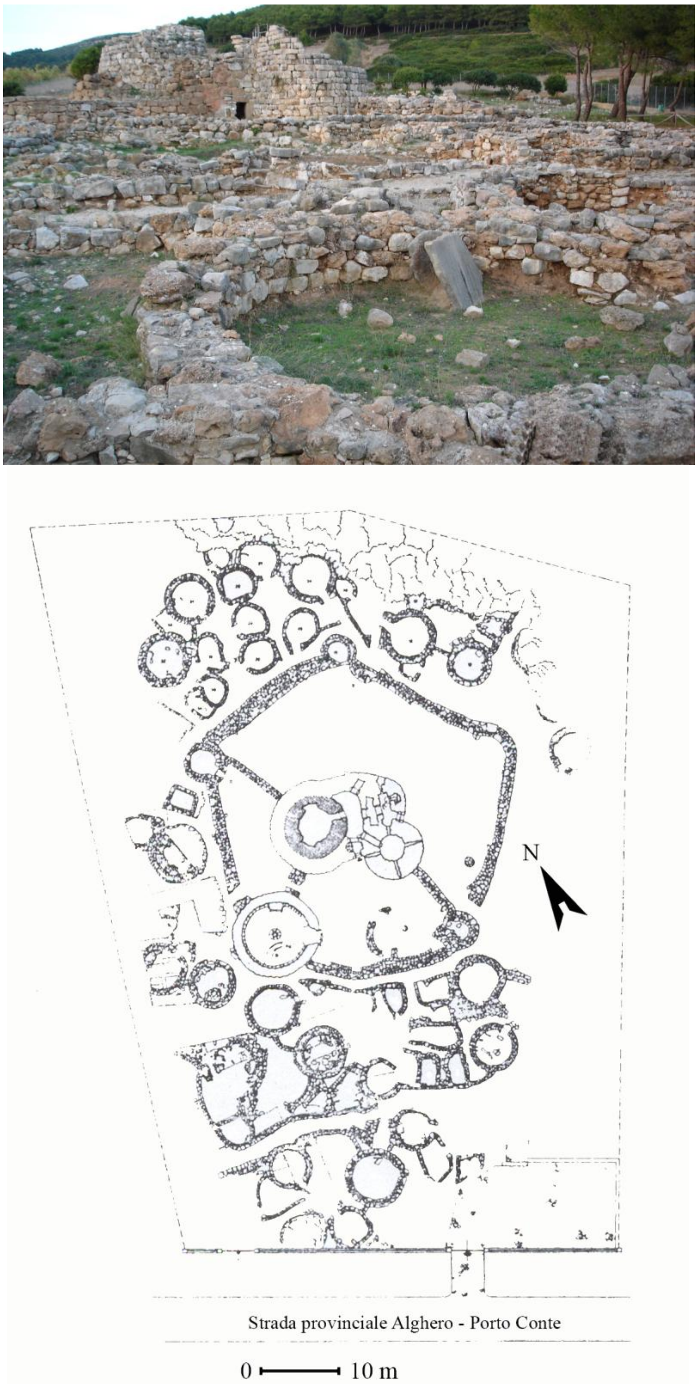

Figure 4: The nuragic village of Palmavera and its plant.

3 The nuragic complex of S. Imbenia (Alghero)

Numerous and recent archaeological finds demonstrate that between the IX and the VIII centuries BC significant exchange and trading activities took place between the inhabitants of the nuragic complex of Sant'Imbenia (Figure 3) and foreign peoples such as the Phoenicians, and probably the Greeks too [8].

The nuraghe, a dry-walled settlement structure with one central tower and two minor ones facing south-east, represents the nucleus around which a village would be erected at different stages and according to different plants. The primitive settlement dates back to the Middle Bronze Age, and it consisted of circular huts. Towards the end of the Bronze Age and the beginning of the Iron Age, new huts were built alongside the existing ones. These are called 'ad isolati' (organized in quarters) because they feature various lodgings separated by narrow streets and paved squares as if they were blocks belonging to different quarters. The village also has four wells [9, 8]. Its peripheral areas are characterised by soil of high agricultural quality, recently drained by the morphological process of reduction of a pond close by, which had dominated the area since c.a. 4000 BC [3]. This data testifies to the existence of a shoreline 3-400 m distant from the nuragic remains in relation to the the muddy deposit examined, which pertains to a humid environment. During the II century BC, the setting of the new nuragic complex was determined positively by the pedogenesis of remains in the old pond.

The sea nearby and its resources played, no doubt, a significant role in the predominantly agricultural economy of the complex. Recent studies have focused on this particular aspect with special attention to the possible existence of anchoring sites in the gulf.

4 The Palmavera Nuraghe and its village (Alghero)

The nuragic complex of Palmavera (Figure 4) is situated less than 2 km from the sea, at a height of 65 metres on Mount Palmavera along a natural path which goes from the gulf of Alghero to the gulf of Porto Conte. The nuraghe has a central tower with an annexed enclosure wall. The wall has an irregular elliptical structure with a tower, an internal courtyard and a corridor with niches, and served as a fortification of the nuraghe itself. The main structure is surrounded by a sea-wall with four fortified towers around which there lay, originally, the numerous villagers' huts. The main entrance faces south-west and it features an architrave leading in along a corridor and then out into a small courtyard. From this open-air space both the central and the secondary towers can be accessed. The upper part of the nuraghe originally featured a terrace with glacises [10].

The village, which presumably used to stretch southward beyond the current path and in the direction of the sea, comprises about forty huts, some of which are yet to be explored, and which are scattered along the pentagonal perimeter. Most of these huts are circular; some are rectangular and were probably built in replacement of the existing circular structures. The majority of them are made with limestone blocks but there are a few instances of larger edifices built with thicker walls. Among the latter, it is worth mentioning hut no. 2, the so-called 'Capanna delle riunioni', which was used for public meetings (it has a diameter of 12 metres long). Both the architectural and cultural elements observed in the village district suggest that there may have been three development phases between the XIII century BC and the end of the VIII century BC. It would seem that the village was abandoned in c.a. VII century BC [8, 10].

Evidence shows that the economy of the nuragic complex was based mainly on agriculture, which was practised especially in a fertile area near Maristella. The villagers combined agriculture with pastoral farming, a common activity in the proximity of the nuraghe as attested by the presence of uncultivated land characterized by soils known as 'Terre Rosse'. The finding of a fishhook in the area also confirms that the indigenous people carried out additional economic activities related to the sea despite the distance of the complex from the coast. The location of the nuraghe may have facilitated an economy based on the exploitation of the sea. It was undoubtedly selected for its strategic position, located between a plain in Terra Rossa (a fertile grazing area) and the near plain of Maristella, where the presence of completely different rocks made it particularly good for agricultural use. The exploitation of the sea, which was at the time, a lot more distant (about 150-200 metres in the Porto Conte Bay) largely contributed to a subsidiary type of economy.

5 The Grotta Verde (Alghero)

The Grotta Verde (Green Cave) is situated along the Cretaceous/Upper Mesozoic karst system in the promontory of Capo Caccia which close the gulf of Porto Conte and protects it from the north-west winds. The name 'Grotta Verde' is linked to the green mosses found on the 20 m high limestone columns of its entrance, which leads into a deep cavern like a wide sinkhole. The place is also known by the names of 'Grotta dell'Altare' and 'Grotta di S.Erasmo due to the finding of a Palaeo-Christian altar which may have been erected inside (Figure 5). This wide cave presents an entrance with an inclination of about 45°; it comprises an aerial cavern, a subterraneous passage like a tunnel, a submerged area, and a number of additional rooms. The aerial cavern stretches westward to a little salty lake (surrounded by stones with drawings on them), and onto a tunnel with four niches. The tunnel leads onto the submarine hall, a wide area 36 metres deep and rich with concretions. This hall is submerged in salty water for its most part with the exception of its upper part where water from the karst system is found. The remaining rooms are all interconnecting and under water, and they are yet to be explored. Archaeological evidence shows that the aerial cavern was used as a temporary dwelling place or settlement; it dates back to the Middle Neolithic and Recent Neolithic Ages. During the Palaeo-Christian Age this was used as a religious site. Ceramics found in the submarine hall and in the subterraneous passage testify to the daily use of pottery, probably deployed to carry water or for religious functions. The finding of human bones in the niches long the passage would also attest the presence of burial sites from a later age. The use of both areas may date back to a period between the Ancient and the Recent Neolithic Ages [11].

It should be noted that the sea level at

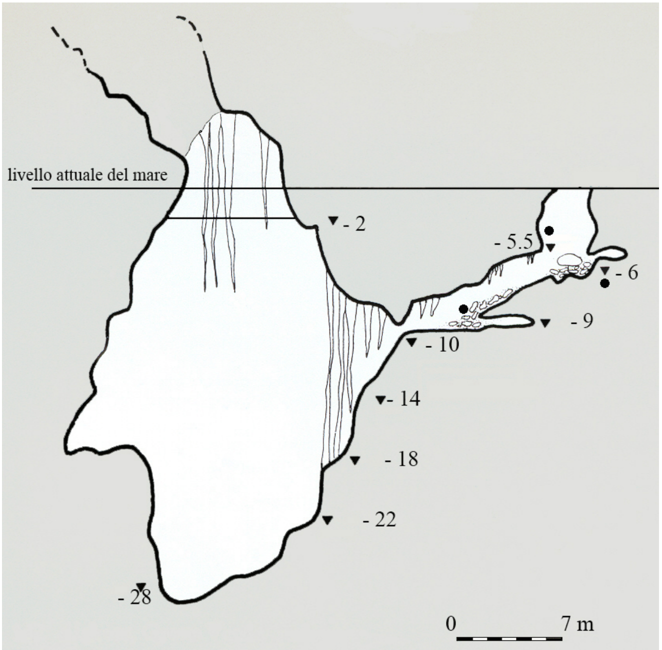

Figure 5: The section of the submarine part of the Grotta Verde cave.

the time was significantly lower than at present, and this allowed easy access to the inner part of the cave. Thus, given its current status, it is interesting to investigate the original entrance of this cave, which today is distinctively dark and difficult to access. Recent and ongoing studies carried out in cooperation with the Area Marina Protetta di Capo Caccia-Isola Piana (the local organization for the protection of the marine area) can relate the collapse of various caves to episodes of palaeo-seismicity which affected the region. This activity occurred during the post-Neolithic Age, and had an evident impact on the surrounding karst formations.

6 Conclusions

Thanks to recent studies and to the reconstruction of the old shortline on the basis of archaeological findings and their interpretation, numerous and precious information on the historic modifications of the said shoreline in areas across Sardinia have been acquired [2, 12]. These studies have attained useful information on the status of ther shoreline at a less recent stag, as well as focusing on the modifications of the sea in certain areas at certain times.

Based on the considerations above, it may be inferred that the sea level has changed significantly at different stages over the past 8,000 years (Holocene) (Figure 6). Both the evident sea modifications which have occurred from the Neolithic Age on, and additional information about the Sar-

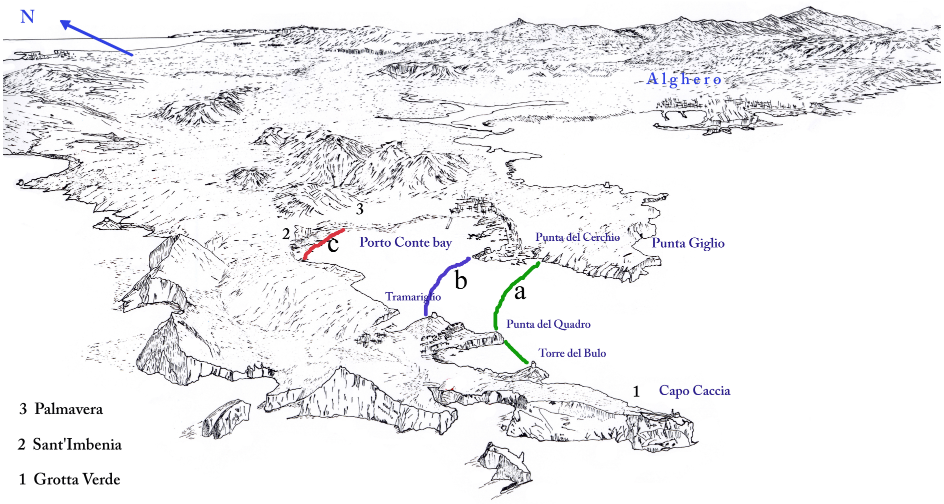

Figure 6: Panoramic picture of the Porto Conte gulf. The (a) line is the Neolithic beach line. The (b) line the Nuragic and the (c) one is the Roman coastline.

dinian coastline [2] suggest that the shoreline has retracted from 15-18 metres in depth. This is further confirmed by the research carried out into coastal erosion in the Sant'Imbenia area (Figure 2) and by the radiometric data in the nearby nuragic complex (Figure 3) [3].

The localization of the Grotta Verde on the edge of the promontory of Capo Caccia (Figure 5) confirms that the shoreline originally stretched further offshore. The bathymetric data demonstrate that the 50 m isobath was originally situated about 1 km away from the cliff of Punta Giglio, while the Grotta Verde is at about 300 metres from the cliff of Capo Caccia. This would prove the existence of a karst valley off the coast. The submarine morphologies and submerged caves in the area [13] further confirm the existence of a shoreline stretching externally which was situated where the present isobath between 15÷18 meters is situated, and which closed the inlet from the promontory of Punta del Quadro to Punta del Cerchio, on the opposite hand of the gulf. The continental deposits, mostly fossils, outcrop along the coast in the inner parts of this promontory, and this supports our theses above.

The planimetric reconstruction of the coastline during the Nuragic period, however, would be located in the furthest promontory of the Porto Conte gulf, near the Torre Nuova (the 'New Tower') in the western side. The littoral belt beginning at this point stretched for about 3 km to the promontory of Capo Caccia at the opposite end of the gulf and near the Tower of Tramariglio. The analysis of geomorphologic maps and the reconstruction surveys based on bathymetric data demonstrate that there was no hydrological network in the inner part of the bay [3]. This would also confirm the existence of a wide inland pond until the pre-nuragic period.

The supposed shoreline of the Nuragic period suggests that human settlements were then present in a portion of the coast situated more internally than at present, yet the people living in the area used to practice both coastal fishing and navigation (Figures 3, 4). It should be added that the pond was presumably a safe enough area for landing and for the harbourage of boats. As evidenced from the archaeological excavations in the area [11], the Neolithic Age coastline underwent a significant modification, closed the entire bay of Dragunara and thus formed a small pond between the Torre del Bulo cape and the Punta del Quadro. During the Nuragic period this coastline appeared to be withdrawn in the inner portion of the land where it preserved a smaller pond (Figure 6). Given the average sea retraction after the Post-Ice Age, the regression of the shoreline in the bay of Porto Conte was slightly over 1.5mm per annum, according to the Upper Pleistocene data in the inner part of the same territory [14]. This means that c.a. 12 km^2 between arable land and fisheries went lost at the time.

This data is further confirmed by the erosion of the Roman site in the Sant'Imbenia area, whereby the shoreline has lost hundreds of metres over the past 2,000 years (c.a. 1 cm each year).

In the reconstruction of past land uses, it is fundamental that the archaeological sites here considered take into account environment modifications by geo-morphological processes that have defined a new landscape and new morphologies.

It emerges that findings from the archaeological excavations confirm the existence of dominant economies in the area under scrutiny. Nevertheless, the geormorphologic reconstruction of the physical environment can help address the gap between hypothesis and reality. More specifically, the reconstruction of the old landscape becomes necessary where one considers pre-Roman times and the climatic changes which affected significantly the coastline at different times. To conclude, the archaeological monument suggests a possible date, yet this is not enoght to help reconstruct the morphological environment to which it belonged.

7 Note

For this work, the bibliographical research and the introduction are the joint effort of D. Carboni and S. Ginesu. D. Carboni has worked on the part dedicated to the Roman villa of Sant'Imbenia and the nuragic complex of Palmavera while S. Ginesu has written on the nuragic complex of Sant'Imbenia and the Grotta Verde.

References

[1] R. Paskoff and P. Sanlaville. Les côtes del la Tunisie. Variations du niveau marin depuis le Tyrrhénien. *Maison de l'Orient, Lyon*, 1991.

[2] S. Ginesu. Modificazioni della linea di costa in Sardegna a partire dai dati archeologici, in "Il contributo della geomorfologia e della Geografia fisica alla ricerca archeologica (a cura di S. Ginesu e S. Sias)". pages 18–24, 2003.

[3] P.R. Federici, S. Ginesu, and S. Sias. Lineamenti geomorfologici ed evoluzione

recente del paesaggio nella Nurra occidentale (Sardegna N.W.). La fascia costiera di Porto Conte – Porto Ferro, in "Protezione dell'ambiente e gestione delle risorse naturali (a cura di M. Gutierrez)". *Q. Ist. Studi Pol.-Giuridici*, pages 95–136, 1999.

[4] G. Nieddu and C. Cossu. Ville e terme nel contesto rurale della Sardegna romana, in" Atti del XII Conv. L'Africa Romana". *Edes, Sassari*, pages 611–656, 1998.

[5] G. Nieddu. Le ville, in "Storia della Sardegna antica (a cura di A. Mastino)". *Il Maestrale*, 2:180–183, 2005.

[6] A. Teatini. Elementi per uno studio della villa romana in Sardegna. Il complesso edilizio di Porto Conte. *Almanacco Gallurese*, pages 25–33, 1994.

[7] G. Maetzke. Scavi e Scoperte nelle Province di Sassari e Nuoro 1959-1961. Porto Conte (Alghero). *Studi Sardi*, 17:657–658, 1961.

[8] G. Caputa. I Nuraghi della Nurra. *Imago Media Ed.*, 2000.

[9] S. Bafico. Alghero (Sassari). Località Santa Imbenia. Villaggio nuragico. *Bollettino di Archeologia*, Bollettino di Archeologia:97–100, 1991.

[10] A. Moravetti. Alghero Loc. Palmavera, in "I Sardi. La Sardegna dal Paleolitico all'età Romana (a cura di E. Anati)". *Jaka Book, Milano*, pages 275–276, 1999.

[11] G. Tanda. Alghero Grotta Verde, in "I Sardi. La Sardegna dal Paleolitico all'età Romana (a cura di E. Anati)". *Jaka Book, Milano*, pages 273–275, 1999.

[12] F. Antonioli and G. Leoni. Siti archeologici sommersi e loro utilizzazioni quali indicatori per lo studio delle variazioni del livello del mare. *Il Quaternario*, 2(1):53–66, 1998.

[13] L.A. Chessa, L. Vitale, and M. Scardi. Descrizione dell'ambiente sommerso con censimento e studio delle grotte sottomarine, in "Protezione dell'ambiente e gestione delle risorse naturali (a cura di M. Gutierrez)". *Q. Ist. Studi Pol.-Giuridici*, pages 167–197, 1999.

[14] R.T. Melis and S. Sias. Il deposito pleistocenico di San Michele (Ploaghe, Sardegna settentrionale) ed i suoi rapporti con l'evoluzione morfologica del Logudoro. *Geogr. Fis. Dinam. Quat.*, 19:63–69, 1996.

Historical Change and Trend Evolution Assessment of Coastline between Salerno and Agropoli Towns, Sele Plain (Southern Italy)

B. D'Argenio[1], I. Alberico[2], V. Amato[4], P.P.C. Aucelli[3], G. Di Paola[4], G. Pappone[3], L. Giordano[1]
1, Institute for Coastal Marine Environment, CNR, Napoli, Italy
2, Interdepartmental Center for Environmental Resarch, University of Napoli "Federico II", Napoli, Italy
3, Department of Environmental Sciences, University of Napoli "Parthenope", Italy
4, Department of Science and Technology for the Environment and Territory, University of Molise, Pesche (IS), Italy
b.dargenio@iamc.cnr.it

Abstract

In the Mediterranean, the coastal population was estimated at 146 million in 1990 and the urban coastal population alone is expected to rise to 176 million by 2025, with 350 million of tourists per year. In these zones, to forecast the shoreline location and its changes through time, is fundamental to coastal scientists, engineers and decision-makers planning a reduction of the territorial vulnerability at both long and short term. The prediction of coastal evolution is complex because it is related to both the analysed spatial and temporal scales over which coastal changes occur, and to the interdependence between different components of the coastal system. Despite these difficulties, this prediction is necessary to identify the areas that could be more severely hit by erosion over decades to centuries.

The main aim of this paper is to define the shoreline variability of Sele Plain (Southern Italy) from Salerno to Agropoli towns in the last 140 years. To this purpose 170 transects, spaced every 200 m across nine shoreline tracts, were analysed in order to measure the variations between two successive shorelines, and the linear regression trend over 140 years. This analysis showed that in Sele Plain the highest rates of erosion, generally localized around the river mouths (Picentino river, mean value: -0.4 m$\cdot$y^{-1}; Sele river, mean value: -1.3 m$\cdot$y^{-1}), decreased in the last 20 years.

1 Introduction

In the Mediterranean area, the coastal population was estimated to be 146 million in 1990 and the urban coastal population alone is projected to rise to 176 million by 2025, with in additional 350 million of tourists per year [1]. In these zones, the location of the shoreline and its changes through time are fundamental to coastal scientists, engineers and decisional-makers to plan the reduction of the territorial vulnerability at both long and short term. This is the aim of the present work, for the coastal area of Sele Plain (Campania Region, Southern Italy), which represents a

territory that could be subjected to the effects of global climatic change.
The Sele Plain is about 400 km^2 wide, and has a triangular shape, limited seaward by a sandy coast, lying between the Salerno and Agropoli towns, and closed landwards by the Apennine chain (Figure 1).
In this area, the shoreline was in a progradational phase, with a mean value of about 0.3-0.4 $m \cdot y^{-1}$ from 1200 to 1809, in fact, the coastguard towers built in this period at short distance from the shoreline, are located at about 200 m from the sea at present [2, 3]. During that progradational phase, a coastal dune system (Sterpina dunes) grew. From 1809 to 1908 a strong progradation of littoral zone occurred over the whole coastal area, and it reached its maximum extension in the right side of the Sele mouth, while only the Tusciano mouth was interested by erosion [3]. From 1908-1954 the progradational phase was predominant in the areas located at both right and left side of Sele mouth, with the exception of the Sele mouth, whose right lobe was withdrawn of about 25 m. Since 1954, the coastal area of Sele plain was characterized by erosional phase [3, 4, 5].
In the present paper are reported for the first time the results of shoreline evolution of the coastline extended from Salerno to Agropoli towns over a period of 140 years. Photographs and maps, from 1870 to 2004 and beach surveys of 2009 were used as row data sources to image the shorelines at different time, to define the accretion-erosion zones, and the coastal trends. At this aim the ArcGis rel. 8.3 software and its extension Digital Shoreline Analysis System [6] were used to implement a Sele shoreline geodatabase, in order to calculate the shoreline change rates by using 170 transects, spaced at 200 m intervals and perpendicular to the nine shorelines drawn by historical maps and aerial photos.
Today, this analysis is considered a fundamental tool for coastal environment managers in relation to the current sea-level rise [7, 8] and its possible acceleration in the Mediterranean area during the last 20th years [9, 10, 11, 12].

2 Geological and geomorphological setting

The Sele Plain derives from the aggradation of a Plio-Quaternary depression located along the western margin of the southern Apennine Chain, known as Salerno Gulf-Sele Plain graben (Figure 2) [13, 14, 15]. It is about 400 km^2 wide and shows a triangular shape delimited seawards by a straight sandy coast stretching between the towns of Salerno and Agropoli, and landwards by the Lattari and Picentini carbonatic massifs toward North and North-West; as well as by Alburni and Soprano-Sottano carbonatic massifs, and Cilento mountains toward the South-East..
The boundaries of the plain are defined by NW-SE and NE-SW trending faults, which were active during Early and Middle Pleistocene [16, 17].
The easternmost portion of this structural embayment is characterized by hills formed by very thick clastic wedge, known as "Eboli Conglomerates" of Early and Middle Pleistocene age [18]. The southernmost portion of the plain is characterized by the presence of thick successions of travertine deposits known as Travertini di Paestum [19, 20] (Figure 2). Seawards and laterally to the travertines, there is a strip of coastal plain formed during the Last Interglacial (Tyrrhenian stage, OIS 5, [21, 22, 23] characterized by beach-

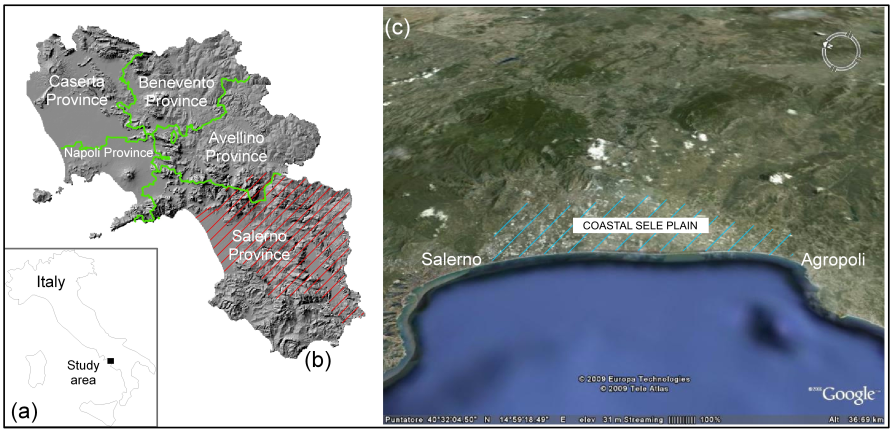

Figure 1: Location map of Sele River Basin at large (a) and small (b) scale. The green lines indicate the Provincial boundaries in the Campania Region, the red line encircles the Sele basin, while the location of the Sele coastal plain is shown in the overview (c).

dune ridges interfingered with lagoonal and fluvio-palustrine deposits (Figure 2). Only the youngest and most external of the ridges has still a clear morphological evidence (Gromola- S. Cecilia-Arenosola-Aversana ridges). A younger coastal sector occurs between the Tyrrhenian sandy-coastal ridge and the present shoreline and it represents the evolution of a barrier-lagoon system, shifted alternatively landward and seaward during the Holocene. It includes a composite sandy ridge system, elevated 1-5 metres a.s.l., which is partly exposed to the present coast and that disappears inland under a muddy depression, rising about 1 m a.s.l. (Figure 2).

3 Methods and data

Rate of shoreline changes between the Picentino mouth and Agropoli Town has been traced in detail, using a series of aerial photos, maps published in different years, and a differential GPS topographic survey (Table 1), to reconstruct and quantify historical shoreline evolution over a period of 140 years [24, 25, 26, 27, 28, 29, 30, 31, 32, 33, 34, 35].

We are aware that a wide range of potential error sources affect the accuracy of the assessed shoreline changes: suitability of sources materials, errors in positioning, distortion of the photographs due to reliefs displacements, residuals in georeferencing, seasonal shoreline variation, and accuracy in identifying and digitizing the land-water interface [36, 37, 38, 31, 33].

To reduce these errors, the aerial photographs were corrected to eliminate radial distortion, reliefs distortion, tilt and pitch of aircraft, and scale variations, caused by changes in altitude along the flight lines [36, 25, 38, 39]. At this aim, the software Erdas rel. 9.1 was used to compute interior and exterior orientation of aerial photos. The interior orientation was de-

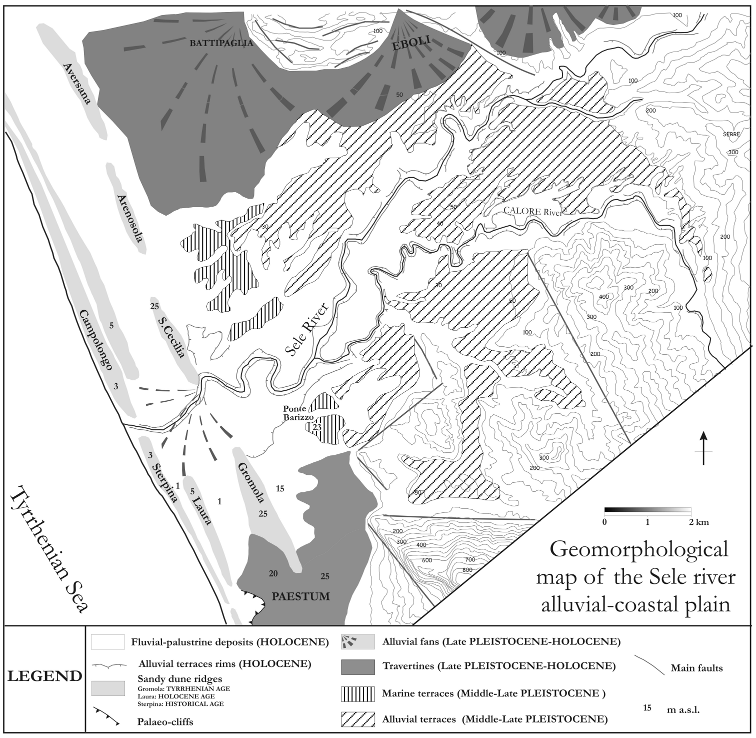

Figure 2: Geomorphological map of the Sele River coastal plain.

fined by using the image position of four fiducial marks (mean error=0.02 mm) and the focal length parameter. The problem related to the unknown parameters, necessary to define the exterior orientation, was solved by using the block adjustment photogrammetric technique. To this purpose, about 25 Ground Control Points (GCPs), located in unequivocal places [37], obtained from the geo-referenced technical map of Campania Region of 1998, and 15 tie points were used for each aerial photography stereo pairs. Taking into account the smooth topography of the studied area, a polynomial transformation was applied in the registration process [40] and the error related to the orthorectification was controlled through the root mean square error (RMSE), that is equal to $\pm$ 3m. The historical maps were georeferenced using a variable number of GCPs, selected through the comparison of each historical map to the georeferenced technical map of Campania Region of 1998 at scale 1:5.000. The errors associated to this procedure are showed by RMSE value; the highest RMSE are linked to the map with larger scale (Table 1).

Another factor that affects the precision and accuracy of aerial photogrammetric and historical map measurements is the correct location of the shoreline position. Different descriptions of shorelines may be found in the scientific literature, Camfield and Morang [41], defined the shore-

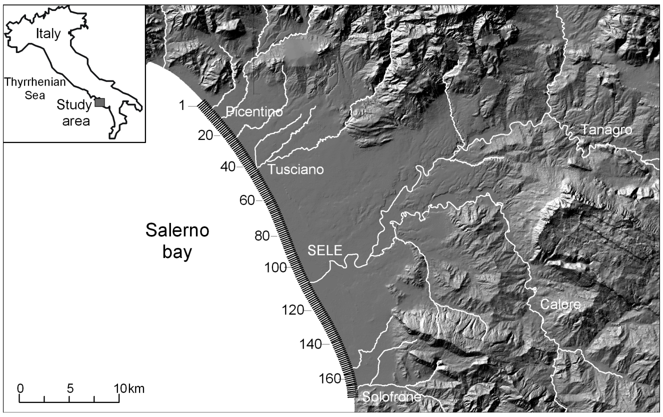

Figure 3: Plot of transects used to assess the shoreline variation from Picentino and Solofrone mouths. The Digital Elevation Model, with a cell of 20 m side, was defined starting from Technical Maps of Regione Campania of 1998, at scale 1:5.000.

Date	Data source	Scale	RMSE (m)	Date	Data source	Scale	RMSE (m)
1870	IGM Topographic Map	1:50.000	20	1984	Aerial-photo	1:26.000	3
1908	IGM Topographic Map	1:50.000	10	1998	Campania Region Technical Map	1:5.000	2
1944	Aerial-photo	1:18.000	3	2004	Ortho-photo	1:5.000	2
1954	Aerial-photo	1:39.000	3	2009	Field survey	GPS survey	0.3
1975	CASMEZ Topographic Map	1:5000	2				

Table 1: Data sources used to calculate the shoreline variations in Sele plain.

line as the intersection of the still water plane at a particular sea level datum with the shoreface, the zero-elevation line on maps. Langfelder et al. [42] considered the shoreline position as the high-water line, because its position on the upper fore shore represents the landward limit of the influence of average waves and water level. In this work, the shoreline position is defined as “the water line at the time of the photo” of the microtidal environment of the region [35]. Moreover, because it was not possible to reconstruct tidal conditions at the moment of the photo, it was assumed that the daily water line position is subject to a maximum uncertainty of about ± 1.6 m, taking into account the daily mean sea level change of about $\pm$ 20 cm (http://www.idromare.it/analisidati.php) and the intertidal slope of the studied beaches of about 12% in 2008. In addition, aerial photographs were taken in different periods of the year, thus seasonal fluctuations must be also considered [43, 44] equal to 3.2 m, corresponding to the maximum variability of the sea level during winter season (http://www.idromare.it/analisidati.php). The shoreline in 2009, surveyed by using a differential GPS R6 Trimble, was defined by interpolating the points surveyed with a spatial resolution of 50 m and characterized

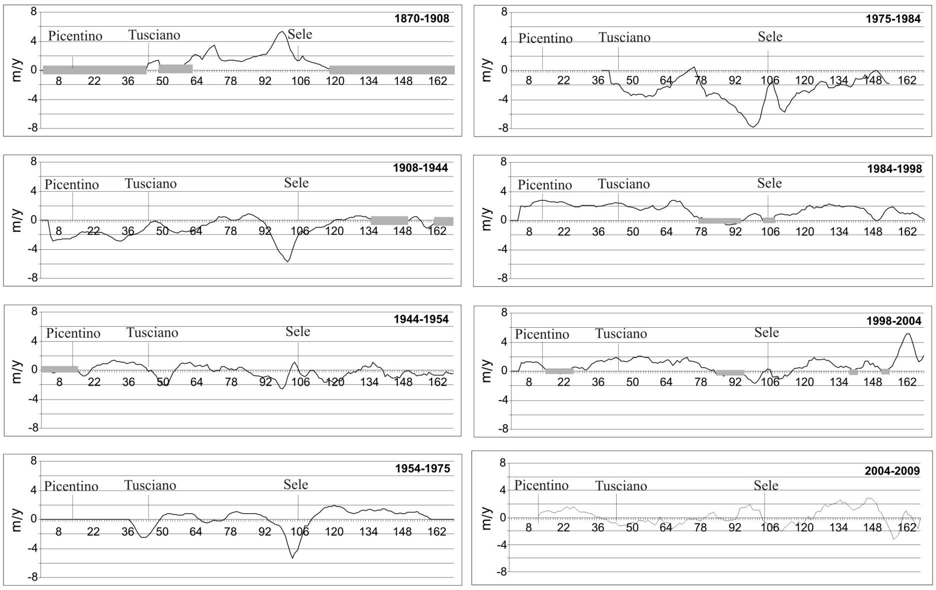

Figure 4: Shoreline variations in different years along the 170 transects showed in Figure 3. The gray polygon masks areas with shoreline variations smaller than the mapping error.

by the lowest root mean square error of all the other shorelines (Table 1). The different dynamic conditions characterizing the actual emerged beach were also outlined by using the morphological and granulometric analysis of beach profiles and the sand samples, respectively. At this aim during the survey in 2009, 11 topographic profiles along transects perpendicular to the coast line were measured and 4 samples of sediment along each transect were collected. Taking everything into account, the whole shoreline mapping errors in this study range from ±20 m to ± 0.5 m (Table 1) Shoreline change rates were calculated using the Digital Shoreline Analysis System [6], an extension of ArcGis software (ESRI, Redlands, California). DSAS aims at creating regularly spaced perpendicular transects to be used as measurement locations across multiple shorelines. Following this methodology, 200 m interval transects were created across nine shorelines (Figure 3) and surface variations were measured between two successive coastlines, at each transect [37, 45, 46, 47]. After that, all shoreline features were merged within a single line on the attribute table, enabling to append together the multiple shoreline files into a single shapefile. Historical rates of shoreline changes were then calculated at each transect, using linear regression [31].

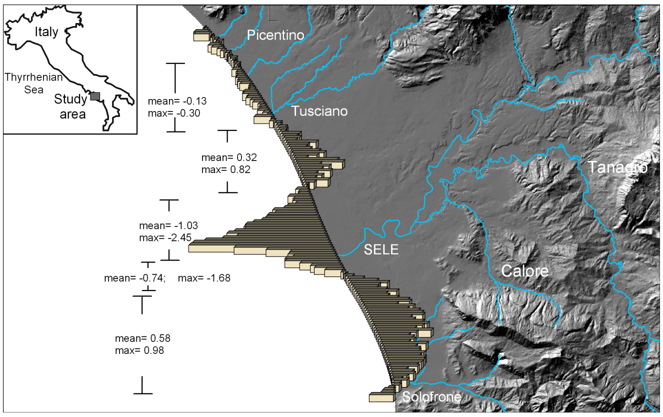

Figure 5: Shoreline trend from 1870 to 2009 calculated for the 170 transects (bar graph in yellow) showed in figure 3. For each homogenous area a mean and maximum values of variation (m·y^{-1}) are shown.

4 Shoreline change during the last 140 years

The shoreline variation occurred during each investigated time interval from 1870 to 2009 and the shoreline trend over all the investigated periods were recognized along the DSAS transects, by using the statistics reported in the attribute table of Sele shoreline geodatabase. The variation between the position of two shorelines each other successive in time shown in Figure 4, was calculated by dividing the shorelines movement along each of the 170 transects (Figure 3), by the time elapsed between them. In this figures is also evident the reduction of shoreline variation rate from the 1870-1984 to the 1984-2009 time intervals. These types of comparison are very important to understand step by step the shoreline behavior. Nevertheless, either its movement trend or its cyclicity are neglected in this type of analysis. Aiming at this, by using the weighted linear regression, available in DSAS framework, the shoreline trend was calculated, for each one of the 170 transects, over all the investigated period and in two time windows too (1870-1984 and 1984-2009). The trend analysis related to 1870-2009 period highlighted that the highest rates of coastal erosion occurred mostly around the river mouth, and that different retreat values characterized the right and the left side of Sele mouth zones, respectively characterized by maximum erosion values of -2.45 m·y^{-1} and -1.68 m·y^{-1} (Figure 5). The trend analysis from 1870 to 1984 is similar to the previous one, with the only exception regarding the mean and the maximum values of changes rate (Table 2a), while the trend analysis from 1984 to 2009 showed that only the Sele mouth zone is in erosion (Table 2b).

5 Results and Conclusion

The comparison of historical maps and aerial photographs of Sele Plain, allowed

Transect number	Mean value (m)	Max value (m)	Zone
1-57	-1.08	-1.87	Picentino-Tusciano
58-62	0.23	0.51	
63-71	-0.24	-0.49	
72-83	0.21	0.51	
84-114	-1.50	-4.81	Sele mouth
115-157	0.34	0.91	
157-170	-0.44	-0.78	Solofrone mouth

(a)

Transect number	Mean value (m)	Max value (m)	Zone
1-75	1.3	2.54	
76-114	-0.26	-0.58	Sele mouth
115-170	1.19	2.11	

(b)

Table 2: Mean and maximum values of shoreline variations from 1870 to 1984 (a) and from 1984 to 2009 (b).

to detect, beaches in erosion alternating with stable or prograding ones. The erosion zones are located at the river mouths, while the intermediate ones are in accretion or stable. The rate of erosion reached the highest value (about -8 m·y^{-1} at Sele mouth) between the years '70s and '80s of the last century, and decreased of about 2 m·y^{-1} in the subsequent years. This analysis suggests that the shoreline changes along the beaches of the Sele river basin might be mainly associated to a reduction of coarse grained sediment outflow from Sele river. Direct measurements of river sediment discharge are absent however, a recent study [48] combining numerical models and core stratigraphy, seems to support this hypothesis. In fact, the authors through a study on the sand movement outside the surf zone of Sele river during storm events, recognized in a very shallow water core sediment (at 14 meter water depth, located at 2.6 km southwest the Sele river mouth) a strong change in grain size sediments. In particular, at 1840 AD, corresponding to the end part of Little Ice Age (LIA) event, the studied core records a strong decrease in sandy layers and upwards at about 1930AD pelite deposition strongly prevails, confirming the reduced bed load yield of Sele river to the littoral cell after the construction of Sele dam in 1934 AD. This datum was also recorded in a deepest core (at 103 meter depth) at north of Sele river, where radioneuclids ages combined with information from benthic foraminifera, confirm the strong control on the continental shelf ecosystem from the construction of Sele dam [49]. The retreat of shoreline, mainly occurred at Sele mouth, was also due to the interaction between two longshore currents having opposite directions, that generate a cross-shore current directed seawards with a direction 220 N. This current coupled with oscillatory motion generates a nested current in the bottom boundary layer, that remove sand from littoral cells and release it on the inner shelf during major sea storms [50, 48].

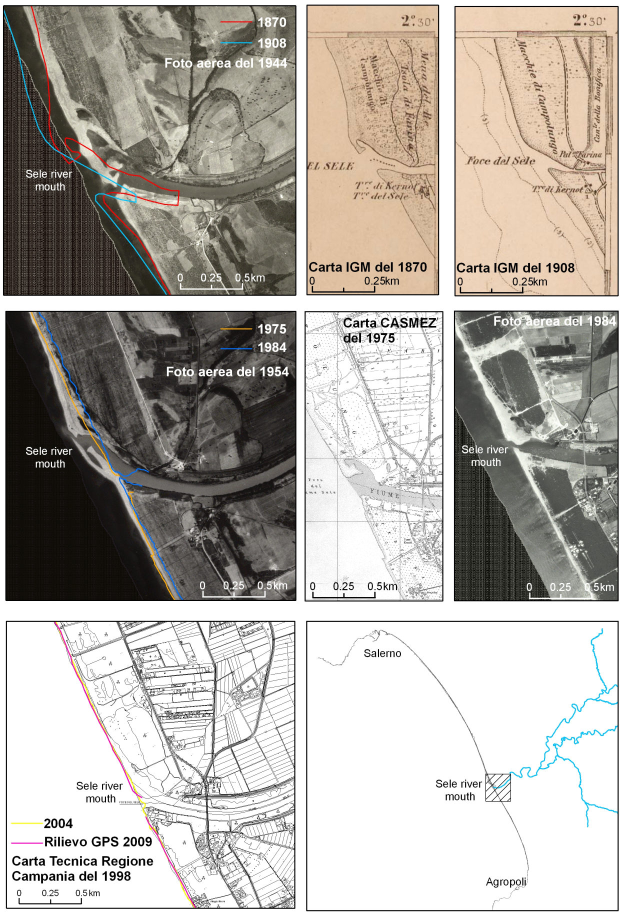

Figure 6: Three temporal steps of shoreline migrations over the last 150 years along the coastal sector of Sele mouth. The data source used to digitize the shorelines of this sector of study area were reported.

References

[1] D. Hinrichsen. Coastal Waters of the World. *Trends, Threats, and Strategies*, page 275, 1998.

[2] T. De Pippo, E. Cocco, M.A. De Magistris, M.T. Efaicchio, I. Giulivo, F. Tarallo, and A. Valente. Evoluzione e dinamica litoranea delle spiagge della Piana del Sele (Campania, Italia). *Pact.,*, 25(15):271–277, 1989.

[3] E. Cocco and M.A. De Magistris. Evoluzione storica e recente del litorale di Paestum (Golfo di Salerno). *Memorie della Società Geologica Italiana*, 41:697–702., 1988.

[4] E. Cocco and S. Iuliano. L'erosione del litorale in sinistra foce Sele (Golfo di Salerno): dinamica evolutiva e proposta di intervento a difesa e tutela della spiaggia e della pineta litoranea di Paestum. *Il Quaternario*, 12(2):125–140, 1999.

[5] G. D'Acunzi, T. De Pippo, A. Donadio, F. Peduto, U. Santoro, F. Sessa, F. Terlizzi, and M.D. Turturiello. Studio dell'evoluzione della linea di costa della piana del Sele (Campania) mediante l'uso della cartografia numerica. *Studi Costieri*, 14:55–67, 2008.

[6] E.R. Thieler, E.A. Himmelstoss, J.L. Zichichi, and T.L. Miller. Digital shoreline analysis system (DSAS) version 3.0. An ArcGIS© extension for calculating shoreline change. 1404, 2005.

[7] V. Gornitz, S. Lebedeff, and J. Hansen. Global Sea level in the Past Century. *Science*, 215:1611–1614., 1982.

[8] IPCC. Fourth Assessment Report: Climate Change 2007. *Working Group I Report The Physical Science Basis, http://www.ipcc.ch/ipccreports/ar4-wg1.htm*, 2007.

[9] F.M. Calafat and D. Gomis. Reconstruction of Mediterranean sea level fields for the period 1945-2000. *Global and Planetary Change*, 66(3-4):225–234, 2009.

[10] M. Klein and M. Lichter. Statistical analysis of recent Mediterranean Sea-level data. *Geomorphology*, 107:3–9., 2009.

[11] S. Mangiarotti. Coastal sea level trends from TOPEX-Poseidon satellite altimetry and tide gauge data in the Mediterranean Sea during the 1990s. *Geophys. J. Int*, 170:132–144, 2007.

[12] M. Marcos and M. Tsimplis. Coastal sea level trends in Southern Europe. *Geophys. J. Int*, 175:70–82, 2008.

[13] F. Ippolito, F. Ortolani, and M. Russo. Struttura marginale tirrenica dell'Appennino Campano: reinterpretazione di dati di antiche ricerche di idrocarburi. *Mem. Soc. Geol. It*, 12, 1973.

[14] R. Bartole, C. Savelli, M. Tramontana, and F. Wezel. Structural and sedimentary features in the Tyrrhenian margin of Campania, Southern Italy. *Marine Geology*, 55:163–180, 1984.

[15] D. Barra, G. Calderoni, A. Cinque, P. De Vita, C. Rosskopf, and E. Russo Ermolli. New data on the evolution of the Sele River coastal plain (Southern Italy) during the Holocene. *Il Quaternario*, 11:287 – 299, 1996.

[16] L. Brancaccio, A. Cinque, G. D'angelo, F. Russo, N. Santangelo, and I. Sgrosso. Evoluzione tettonica e geomorfologica della Piana del Sele (Campania, Appennino meridionale). *Geogr. Fis. e Dinam. Quat.,*, 10:47 – 55, 1987.

[17] L. Brancaccio, A. Cinque, P. Romano, C. Rosskopf, F. Russo, N. Santangelo, and A. Santo. Geomorphology and neotectonic evolution of a sector of the Tyrrhenian flank of the southern Apennines (Region of Naples, Italy). *Zeit. Geomorph. N.F., Berlin*, 82:47 – 58, 1991.

[18] A. Cinque, F. Guida, F. Russo, and N. Santangelo. Dati cronologici e stratigrafici su alcuni depositi continentali della Piana del Sele (Campania): i "Conglomerati di Eboli". *Geogr. Fis. e Dinam. Quatern.,*, 11:39 – 44, 1988.

[19] C. Violante and B. D'Argenio. I travertini all'origine e nel declino dell'antica città di Poseidonia-Paestum (2500-1000 anni prima del presente). pages 841–848., 2000.

[20] V. Amato, G. Avagliano, A. Cinque, M. Cipriani, G. Di Paola, A. Pontrandolfo, M. C. Rosskopf, and A. Santoriello. Geomorphology and geoarchaeology of the Paestum area: modification of the physical environment in historical times. *Mediterranee*, 112:129–135, 2009.

[21] L. Brancaccio, A. Cinque, G. Belluomini, M. Branca, and L. Delitala. Isoleucine epimerization dating and tectonic significance of upper Pleistocene sea level features of the Sele Plain (Southern Italy). *Zeit. Geomorph. N.F., Suppl. Bd.,*, 62:159 – 166, 1986.

[22] L. Brancaccio, A. Cinque, F. Russo, N. Santangelo, L. Allegri, M. Alessio, S. Improta G. Belluomini, M. Branca, and L. Delitala. Nuovi dati cronologici sui depositi marini della piana del sele e della costa settentrionale del Cilento (Campania). *Atti 74° Congresso Società Geologica Italiana*, pages 55 – 62, 1988.

[23] D. Barra, G. Calderoni, M. Cipriani, J. De La Geniere, L. Fiorillo, G. Greco, M. Mariotti Lippi, M. Mori Secci, T. Pescatore, B. Russo, M.R. Senatore, G. Tocco Sciarelli, and J. Thorez. Depositional history and palaeogeographic reconstruction of Sele coastal plain during Magna Grecia settlement of Hera Argiva (Southern Italy). *Geologica Romana*, 35:151–166, 1998.

[24] D. Stafford. An Aerial Photogrammetric Technique for Beach Erosion Surveys in North Carolina. Fort Belvoir, Virginia. 1971.

[25] R. Dolan, B. Hayden, P. May, and R. Suzette. The reliability of shoreline change measurements from aerial photographs. *Shore and Beach*, 48:22–29, 2007.

[26] R. Dolan, M.S. Fester, and S.J. Holme. Temporal analysis of shoreline recession and accretion. *Journal of Coastal Research*, 7(3):723–744, 1991.

[27] S. Leatherman. Shoreline mapping: a comparison of techniques. *Shore and Beach*, 51:28–33, 1983.

[28] J.A. Jimenez, A. Sanchez-Arcilla, J. Bou, and M.A. Ortiz. Analysing short-term shoreline changes along the Ebro Delta (Spain) using aerial photographs. *Journal of Coastal Research,*, 13(4):1256–1266., 1997.

[29] M.J. Pajak and S. Leatherman. The high water line as shoreline indicator. *Journal Coastal Research,*, 18(2):329–337, 2002.

[30] J.C. Gibeaut, R. Waldinger, T. Hepner, T.A. Tremblay, W.A. White, and L. Xu. Changes in Bay Shoreline Position, West Bay System, Texas. *Report of the Texas Coastal Coordination Council*, 02-225R, 2003.

[31] R.A. Morton, T. Miller, and L. Moore. Historical Shoreline Changes Along the US Gulf of Mexico: A Summary of Recent Shoreline Comparisons and Analyses. *Journal of Coastal Research*, 21(4):704–709., 2005.

[32] C.J. Hapke, D. Reid, B.M. Richmond, P. Ruggiero, and J. List. National assessment of shoreline change part 3: Historical shoreline change and associated coastal land loss along sandy shorelines of the California coast. *US Geological Survey*, 1219:79, 2006.

[33] C. Romagnoli, F. Mancini, and R. Brunelli. Historical Shoreline Changes at an Active Island Volcano: Stromboli, Italy. *Journal of Coastal Research*, 22(4):739–749, 2006.

[34] M.E. Dickson, M.J. Walkden, and J.W. Hal. Systemic impacts of climate change on an eroding coastal region over the twenty-first century. *Climatic Change*, 84(2):141–166, 2007.

[35] J.A.M. del Pozo and G. Anfuso. Spatial Approach to Medium-term Coastal Evolution in South Sicily (Italy): Implications for Coastal Erosion Management. *Journal of Coastal Research*, 24(1):33–42, 2008.

[36] M. Crowell, S.P. Letherman, and M.K. Buckley. Historical shoreline change: Error analysis and mapping accuracy. *Journal of Coastal Research*, 7(3):839–852, 1991.

[37] E.R. Thieler and W.W. Danforth. Historical shoreline mapping (II): application of the Digital Shoreline Mapping and Analysis Systems (DSMS/DSAS) to shoreline change mapping in Puerto Rico. *Journal of Coastal Research*, 10:600–620, 1994.

[38] L. Moore. Shoreline mapping techniques. *Journal Coastal Research*, 16(1):111–124., 2000.

[39] E.H. Boak and I.L. Turner. Shoreline definition and detection: A review. *Journal of Coastal Research*, 21(4):688–703, 2005.

[40] E. Chuvieco. Fundamentos de Teledeteccio´n Espacial. *Madrid, Spain: Ediciones Rialp*, page 567, 2000.

[41] F.E. Camfield and A. Morang. Defining and interpreting shoreline change. *Ocean & Coastal Management*, 3:129–151, 1996.

[42] L.J. Langfelder, D.B. Stafford, and M. Amein. Coastal erosion in North Carolina. *Journal of Waterways and Harbors Division*, 962:531–545., 1970.

[43] M. Crowell, S.P. Letherman, and M.K. Buckley. Erosion rate analysis: Long term versus short term data. *Shore and Beach*, 61(1):13–20., 1993.

[44] R.A Morton. Analysis of sequential shoreline changes. *Coastal Research and Department of Geology, Florida State Università*, page 43–48, 1978.

[45] C. Houser, C. Hapke, and S. Hamilton. Controls on coastal dune morphology, shoreline erosion and barrier island response to extreme storms. *Geomorphology*, 100:223–240, 2008.

[46] J. Leyland and S.E. Darbya. An empirical–conceptual gully evolution model for channeled sea cliffs. *Geomorphology*, 102(3-4):419–434., 2008.

[47] K.A. Addo, M. Walkden, and J.P. Mills. Detection, measurement and prediction of shoreline recession in Accra, Ghana. *ISPRS Journal of Photogrammetry & Remote Sensing*, 63:543–558, 2008.

[48] V. Ferrante, F. Budillon, M. Iorio, C. Lubritto, M. Monaco, E. Pugliese Carratelli, S.D. Russo, and D. Vicinanza. Tracing possible offshore sand movement during extreme sea storm events: an example from the Salerno Bay (Southern Tyrrhenian Sea) by comparing field data with numerical model results. *Rassegna delle attività di ricerca scientifica e tecnologica del CNR nell'ambito del mare e delle sue risorse*, 2011.

[49] M. Vallefuoco, F. Lirer, L. Ferraro, M. Sprovieri, et al. Evidences of natural environmental changes and human impact reflected by Foraminifera in the southern Tyrrhenian Sea for the last 520 years 2010. *Rassegna delle attività di ricerca scientifica e tecnologica del CNR nell'ambito del mare e delle sue risorse*, 2011.

[50] F. Budillon, D. Vicinanza, V. Ferrante, and M. Iorio. Sediment transport and deposition during extreme sea storm events at the Salerno Bay (Tyrrhenian Sea): comparison of field data with numerical model results. *Nat. Hazards Earth Syst. Sci.,*, 6:839–852, 2006.

Remote Sensing Technologies as a Contribution for Ecological Assessment of Transitional Waters: the Case Studies of the Lagoons of Venice, Goro and Orbetello

F. Braga[1], L. Alberotanza[1], R.M. Cavalli[2], S. Pascucci[3], F. Santini[3]
1, Institute of Marine Sciences, CNR, Venezia, Italy
2, Institute for Atmospheric Pollution, CNR, Roma, Italy
3, Institute of Methodologies for Environmental Analysis, CNR, Potenza, Italy
federica.braga@ismar.cnr.it

Abstract

Satellite and airborne hyperspectral remote sensing can provide an important contribution for assessing and monitoring the ecological status of transitional waters. The paper describe examples of hyperspectral Earth Observation applications such as priority habitat mapping (seagrass and macroalgae), the assessment of chl-a, suspended matter and dissolved organic matter concentration in the water column. Such applications have been carried out on areas with different level of complexity, connected to hydrodynamics and environmental conditions homogeneity. The works were performed on the lagoons of Venice, Goro and Orbetello. For these case studies, the common approach is to develop and improve a semiautomated mapping from hyperspectral airborne or satellite image datasets in association with field-survey and hydro-optical data in order to assess and monitor the quality status of such transitional environments, also considering the requirements of Water Framework Directive. The adopted techniques range from empirical algorithm for CDOM/chl-a retrieval, to classification techniques for macroalgae and submerged vegetation identification with spectral libraries and to complex physically based model. Furthermore, the study of the three case study provide an input to evaluate the contribution of commonly available EO facilities and the expected potential improvements provided by the next generation of hyperspectral sensors (EnMAP and PRISMA) of German and Italian Space Agencies.

1 Introduction

Remote sensing technology is a valuable tool for obtaining information on the ecological assessment and processes taking place in transitional waters. A major advantage of remote sensing observations over traditional measurements of environment monitoring is the provision of both spatial and temporal data. With the present and the expected advanced hyperspectral sensors, a large amount of water quality information could be observed on a regular basis [1]. The role of remote sensing technology in the coastal and transitional areas is therefore under scrutiny, given its potential capacity for systematic observations at scales ranging from local to global and for the provision of data archives extending back over several decades [2]. Transitional waters are bodies of surface water, like lagoons and estuaries that are partly saline in character as a result of their proximity to coastal waters, but which are substantially influenced by freshwater flows for the vicinity to river mouths. Under the EU Water Framework Directive (WFD 2000/60/EC), their good status is determined by both ecological and chemical assessment. Remote sensing data can be used synergistically with in situ traditional sources of information [3]. The utility of remotely-sensed data in supporting the ecological state assessment and the implementation of the WFD is largely determined by the definitions and requirements for the monitoring plans of transitional water status. Technically, remote sensing data can be used to monitor visible changes in the water surface. In particular, they can be used to estimate water quality variables such as chlorophyll-a (chl-a), total suspended matter (TSM), turbidity, Secchi disk depth, coloured dissolved organic matter (CDOM) and surface water temperature. Moreover, remote sensing data are a valuable support in the detection and classification of macrophyte associations (macroalgae and seagrasses), which represent an integrated index for the quality status assessment of Mediterranean transitional environments [4]. Many works have showed the accuracy of commonly available airborne and satellite hyperspectral image data sets for mapping water quality parameters and seagrass species composition and distribution [5, 6, 7, 8]. The present paper describes how the high spectral resolution remote sensing technologies can contribute to retrieve quantitative information on lagoon areas according with the specifications requested by national authorities for monitoring and analysis purposes.

2 Case studies

2.1 The Lagoons of Orbetello

The lagoons of Orbetello (Figure 1), located along the southern coast of Tuscany, consist of two shallow coastal reservoirs with a combined surface of approximately 27 km^2, an average depth of 1 m and is connected to the Tyrrhenian sea through one port at each end of the western lagoon and one at the south end of the eastern lagoon [9]. They are of great ecological interest for their peculiar characteristics, among the brackish wetlands still preserved in Italy. The whole area is relatively small but it shows complex aspects, both in its morphology and in its environmental dynamic processes. Anthropogenic influence on this region has induced a further decrease in the stability of this environment. Anoxic crises have been observed with increasing frequency over the past years due to eutrophication [10]. The main problem in the Orbetello lagoon is the control of the submerged vegetation, both in biomass and inventory, given the problematical coexistence between macroalgae and macrophytes. While macroalgae may cause dystrophic crises, macrophytes oxygenate and stabilise the sediment and thus control the nutrient flux into the water [11]. According to Bucci et al. [12], the more abundant submerged vegetation species are *Chaetomorpha sp., Gracilaria sp., Ulva sp.* and *Cladophora sp.* which are taxa typical of eutrophic and hypertrophic waters, while the distribution of *Ruppia sp.* and *Cymodocea sp.* has decreased in the last 20 years [13].

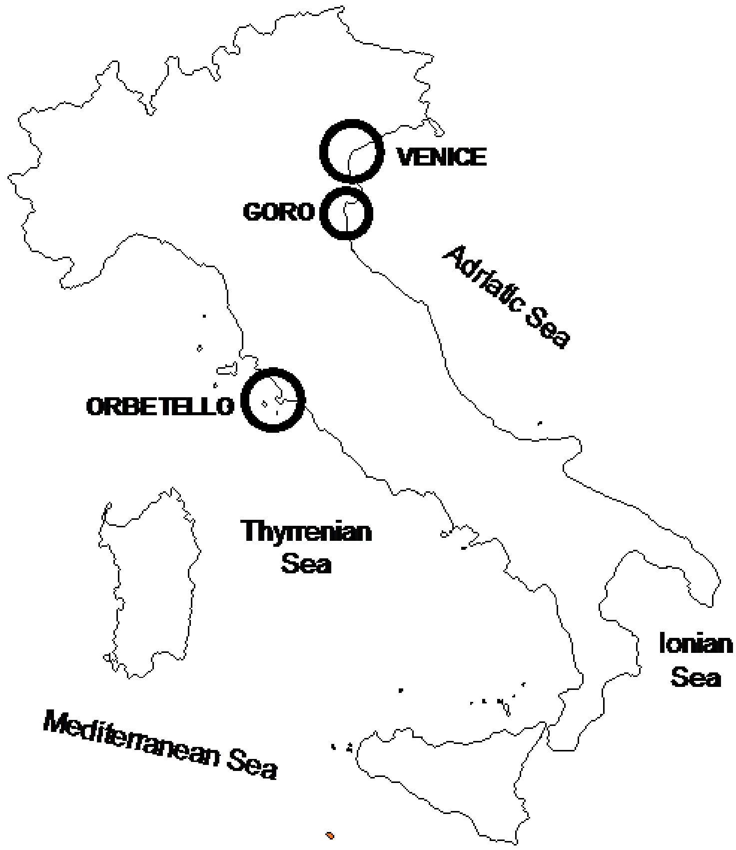

Figure 1: Location of case-study sites.

2.2 The Lagoon of Venice

The Lagoon of Venice is the largest shallow coastal lagoon in the Mediterranean region (area: 550 km^2; extension: 50 km along the coast; width: 15 km) and is located in the northern Adriatic Sea along the north-eastern coast of Italy (Figure 1). The lagoon is a complex combination of intertidal marshes, intertidal mudflats, submerged mudflats and navigation channels. Only 5% of the lagoon has a depth greater than 5 m, and 75% is less than 2 m, the average depth being 1.2 m. Water exchange between the lagoon and the Northern Adriatic Sea is through the Lido, Malamocco and Chioggia inlets. The Adriatic tides, which locally reach mean ranges of 35 cm during neap tides and about 100 cm during spring tides, govern water exchange inside the lagoon. The Venice lagoon can be considered a very interesting case of study. In a relatively small region, waters with different optical transparency coexist. A high variability in bottom depth and substrate, and the occurrence of hydrodynamic phenomena with short life times and small spatial scales like currents, wave and tides can greatly affect the optical appearance of examined areas. The water quality depends moreover on meteorological and seasonal effects and is influenced by anthropogenic presence [14]. There are mesotrophic or hyperdystrophic areas which can be scarcely or highly contaminated. In addition, the environment exhibits areas with hyperaline, mesoaline or hypoaline conditions, and also areas affected by river outfalls, urban sewage, industrial effluents, harbour activities, clamharvesting and areas intensively drained by seawaters. The subtidal areas of the lagoon are partially vegetated by phytoplankton, macroalgae and seagrasses (such as *Zostera marina*, *Z. noltii* and *Cymodocea nodosa*) forming pure and mixed populations [15], each prevailing on the other according to the different ecological conditions [16]. Considering seagrasses as an important bio-indicator of coastal and transitional waters ecological state, their extention and abundance have been monitored also through remote sensed data.

2.3 The "Sacca" of Goro

Sacca di Goro is a shallow lagoon located in the southern area of the Po river delta (Figure 1). Its surface is about 26 km^2 and its average depth about 1.2-1.5 m. According to the Ramsar Convention in 1971, the Goro Lagoon was classified as a wetland of international importance. It became a natural reserve in 1982 and, since 1988, it has been included in the Regional Park of the Po Delta [17]. The lagoon has four freshwater inlets (Po di Goro and Po di Volano rivers and Bianco and Giralda channels) and is separated from the Adriatic Sea by a narrow sandy barrier with two mouths regulating saltwater exchanges. Goro lagoon is directly influenced by tide regime, the flow and organic load of tributaries, and rain patterns. As for many eutrophic coastal environments, nutrient loads have led in the Sacca di Goro to the disappearance of rooted macrophytes and the appearance of opportunistic floating macroalgae. Since the late 1980s, the introduction of the exotic clam species *Tapes philippinarum* has locally enhanced the mollusk fishery, which still has not recovered since the great economic turndown of the late 1970s and the resultant market collapse. Today clam fishery covers an area of 10 km^2 and is concentrated in the south-central part of the lagoon. Average income from shellfish production is ca. 50 million euros, distributed among a 1000 local people, who depend directly or indirectly on the fishery [18]. This lagoon is one of the most important aquaculture systems in Italy but in the last decade the anthropogenic eutrophication processes and anoxic crises were intensified: the frequency of eutrophication and anoxic phenomena led to negative economic consequences. The fishery crisis gave rise to a new intervention policy aimed at improving the hydraulic exchanges between the lagoon and the adjacent river and sea in order to enhance lagoon circulation. Frequent mapping of water quality is required and the contribute of remote sensing has been important.

3 Materials

The strength of the hyperspectral remote sensing lies in the simultaneous use of spatial and spectral information for integrated analysis, and on the possibility to compare calibrated image data with field spectral measurements [19, 20]. In order to operate a complete study following the integration of airborne and ground-based data required by the GEOSS (Global Earth Observation System of Systems) 10-Year Implementation Plan: "Improving the management and protection of terrestrial, coastal, and marine ecosystems" [21], the surveys have been carried out acquiring hyperspectral measurements in situ and remotely. The hyperspectral data have been acquired by the airborne MIVIS sensor and by the Hyperion hyperspectral imaging spectrometer hosted on EO-1 satellite platform. The MIVIS is a whiskbroom scanner composed of 4 spectrometers covering the spectral domain from 420 to 12700 nm (visible, near-IR, mid-IR and thermal-IR spectral regions) by 102 channels. The scanner geometry is characterized by a Field of View of 90°. During the campaign, the altitude of the aircraft overpasses was chosen site by site, depending on which parameter was detected. The Hyperion is a pushbroom imaging instrument, which provides high quality calibrated data that can support evaluation of hyperspectral technology for Earth observing missions. It is a high resolution hyperspectral imager capable of resolving 220 spectral bands (from 400 to 2500 nm, 10 nm spectral resolution) with a 30 meter spatial resolution. The instrument provides detailed spectral mapping across all 220 channels with high radiometric accuracy. The ground-based acquisition was performed by means of a field portable multi-spectral radiometer PR-650 (Photo Research ®) operating between 380 and 780 nm with 4 nm resolution. The procedure for target spectral signatures measurement is based on the acquisition of the upwelling and downwelling radiance according to the SeaWifS Protocol [22]. Nine Multispectral Infrared and Visibile Imaging Spectrometer (MIVIS) surveys were made in the lagoons of Orbetello from 1994 to 1997 with the aim of evaluating the seasonal variation of dominant algal species, in order to assess the engineering works planned to improve hydrodynamic exchange and to prevent anoxic crises. A series of in situ spectral radiance measurements were collected during the MIVIS over flight on 23 July 1996. Algal species spectra were collected from a small boat with PR-650. A MIVIS aerial survey was executed at 9:36 GMT on 26 July 2001 at an altitude of 4000 m a.s.l. corresponding to a pixel size of 8 m over the Venice Lagoon The aerial strip covered the areas with benthic macroalgae located in the Northern and Central Basins of the lagoon and a wide part of the area with seagrasses located in the Southern Basin of the lagoon. Conditions were ebbing tide with a sea mean level of 4 cm at Punta della Salute. Consequently water thickness, above the submersed vegetation was estimated at about 50 cm in the Southern Basin. At Sacca of Goro, from June to October 2005, a series of in situ measurements were carried out monthly to perform a spectral characterization of the area at spatial (horizontal and vertical) and temporal (daily and seasonal) scales. Information on spectral behaviour of the bottom substrate, apparent and inherent optical properties and active optical component concentrations (chlorophyll, dissolved organic matter, and suspended matter) along the water column were collected with specific instruments. These dataset are necessary for the parametrization of a radiative transfer model in order to obtain water quality maps from hyperspectral satellite images.

				In situ measurement		
	Sensor	Spatial resolution (m)	Target	Spectral signatures	Optical properties of water column	Algorithm
Orbetello	MIVIS	4 m	Submerged vegetation	X	-	SAM
Venice	MIVIS	8 m	Submerged vegetation	X	-	SSAP
Goro	HYPERION	30 m	Chl-a, CDOM, TSM	X	X	SAMBUCA

Table 1: Summary of the materials and methods used in the case-studies.

4 Methods

The adopted techniques ranged from classification algorithm for algae and submerged vegetation identification with spectral libraries, to complex physically based model that consider analytical formulations of radiative transfer equations and the application of numerical simulations (Hydrolight software). An ad hoc methodology was developed for each case-study that took into consideration the environmental variability, either spatial (depth, clarity, kind of substrate, turbidity, distribution and abundance of macrophites, etc.), or temporal (daily in correlation with tide, connected to mean seasonal features of the basin, phase of vegetation growth, etc.). This implied intensive experimental field activities to collect radiometric measurements for environmental characterization, algorithm calibration and validation and for the construction of spectral and bio-optical libraries. Thus, in the described three case-studies, the procedures could be divided in two phases. The first phase concerned the removing of atmospheric scattering effects [24, 25], of sun-glint and sky-glint on water surface and of water column influence for submersed vegetation mapping. The second phase is the real classification. For the classification of the submerged vegetation, the procedure used was applied as follows:

- Selection of the spectral bands sub-sets from the full hyperspectral data set.
- Extraction of the water body mask image from the 1500-1550 nm bands.
- Selection of the reference spectra of submerged vegetation also taking into accounts the spectral signatures collected both in situ and from the remotely-sensed imagery. The training areas were selected from sea truth data collected during in situ survey campaign and from periodic surveys in the lagoon performed by the local authorities. The training areas were used to to determine the spatial distribution of the pure and mixture submersed vegetation population.
- Choice and application of the most suitable algorithm for submerged vegetation mapping, as a function of environmental characteristics, spatial and temporal variability and methodologies improvements.

On the Orbetello lagoons data, the Spectral Angle Mapper (SAM) was the supervised

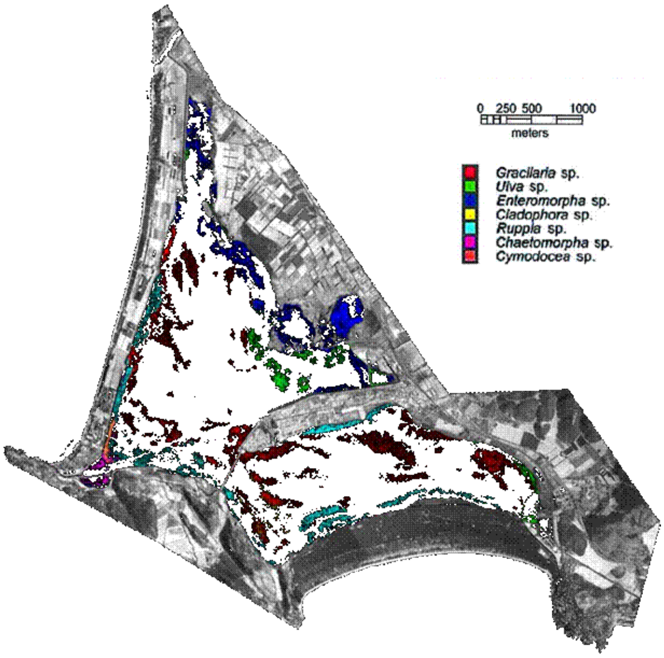

Figure 2: Map of submerged vegetation recognised using the adopted procedure applied to MIVIS data of 23 July 1996 (modified from [23]).

classification technique adopted. SAM is an automated method that permits rapid mapping of spectral similarity of image spectra to field spectra [26, 20]. The algorithm determines the similarity between two spectra by calculating the spectral angle between them, treating them as vectors in a space with dimensionality equal to the number of the spectral bands used [20]. This technique is relatively insensitive to illumination and albedo effects, because the angle between two vectors is invariant with respect to the length of the vectors [27]. The algorithm applied to the data of Venice lagoon is based on a particular implementation of the Subpixel Spectral Analytical Process (SSAP) method [28, 29]. SSAP method assumes that the spectrum of a single pixel is composed of a fraction of the material of interest (e.g., submersed vegetation species) while the remainder of the observed spectra contains background materials (i.e. other minor vegetation species, mixture species, lagoon bottom). SSAP method detects the most abundant material of interest of the pixel under investigation by subtracting iteratively fractions of candidates background spectra. The background and fraction remainders that produce the residual spectrum closest to the spectrum of the material of interest are then identified. The output of this procedure is presented in the form of fraction planes (fraction maps) for each material of interest. In the computations as candidate backgrounds we considered the composite signatures extracted from the training areas using the described procedure for all com-

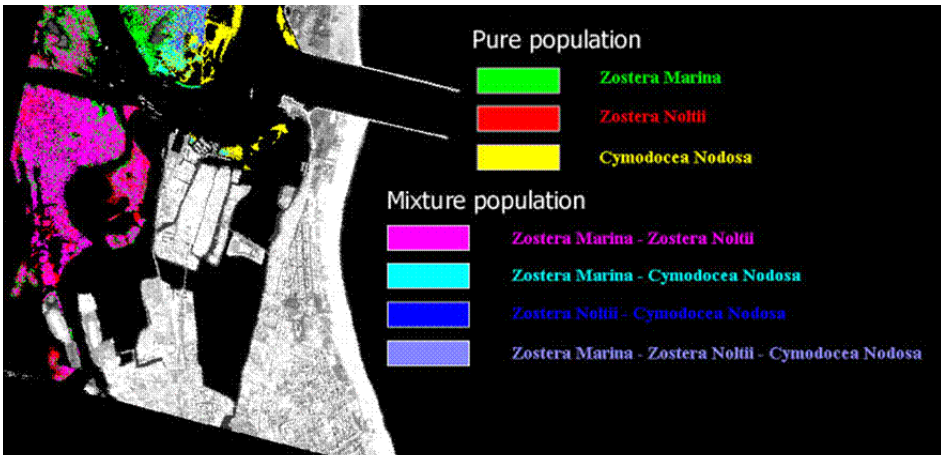

Figure 3: Seagrasses SSAP classification results for the Chioggia city areas (modified from [15]).

binations of the species under investigation plus a spectral signature of lagoon bottom without submersed vegetation for a total of 31 combinations. In order to improve the application of SSAP method for frequent monitoring, a detailed and specific spectral library was constructed of the three seagrass species and of the macroalgae of the Venice lagoon including, for each target, a collection of typical signatures as a function of season, geographic location, bottom cover, environmental conditions and phenological characteristics. For the characterization of the active optical parameters in the water of Sacca di Goro, a physics-based approach, based on radiative transfer theory in the water body, was adopted. The advantages of this choice with respect to empirical methods include: the application of only one algorithm to a temporal series of images, the capability of testing the ability of different sensors for a particular applications and a reduction of the amount of laboratory and in situ measurements to be made. The Semi-Analytical Model for Bathymetry, Unmixing, and Concentration Assessment (SAMBUCA) developed by the Environmental Remote Sensing Group, CSIRO-Land and Water of Canberra (Australia) [30], was adopted for the study. By inverting this model, it was possible to assess, pixel by pixel, chlorophyll concentrations, dissolved organic matter and non-algal particle concentrations, and to determine the bottom substrate composition and depth. The in situ measurements on spectral behaviour of the bottom substrate, apparent and inherent optical properties and active optical component concentrations (chlorophyll, dissolved organic matter, and suspended matter) along the water column was used to parameterize the SAMBUCA model and to validate the water quality products obtained by inverting two Hyperion images acquired on 14 and 30 August 2005 during two tidal cycles (Table 1).

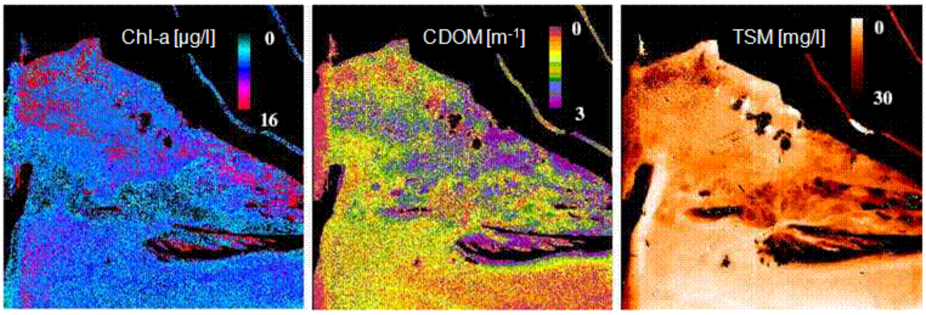

Figure 4: Maps of chlorophyll-a, Coloured Dissolved Organic Matter and Total Suspended Sediment concentrations, derived from Hyperion of 14 August 2005.

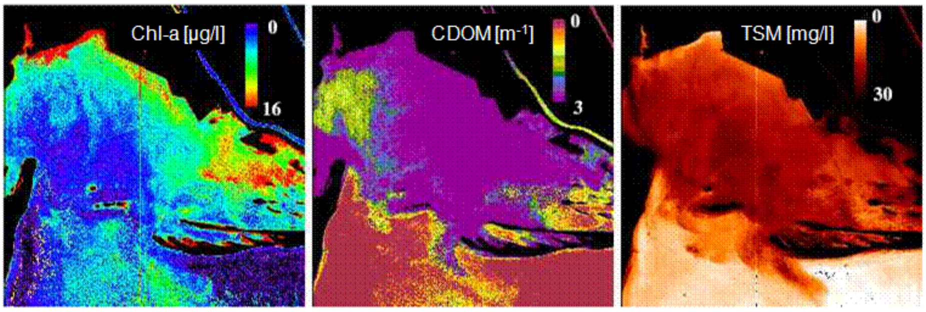

Figure 5: Maps of chlorophyll-a, Coloured Dissolved Organic Matter and Total Suspended Sediment concentrations, derived from Hyperion of 30 August 2005.

5 Results

5.1 The Lagoons of Orbetello

The results of the classification are shown in Figure 2. This map was in agreement with the partition of the lagoon into several ecotones depending on the gradients of salinity, water temperature and nutrient concentration as depicted by TEI [31] and on submerged vegetation abundance and dominance, as described by Lenzi [13] and by Bombelli and Lenzi [32]. The submerged vegetation species identified are *Gracilaria sp., Ulva sp., Enteromorpha sp., Cladophora sp., Chaetomorpha sp., Ruppia sp. and Cymodocea sp.*. The particular environmental characteristics of the lagoons made the comparison of the in situ collected upwelling radiance and MIVIS possible and significant. In fact, the weak tidal excursion and the flat and shallow morphology of the bottom associated with a poor hydrodynamic circulation give fair water transparency conditions and an almost constant water column height [23].

5.2 The Lagoon of Venice

For benthic macro-algae (*Ulva rigida, Gracilaria confervoides, Chaetomorpha aerea*) and seagrasses (*Zostera marina, Z. noltii and Cymodocea nodosa*), the maps of pure and mixture species distribution were produced separately (Figure 3). For species a fraction map was produced representing the material of interest in terms of percentage. The maps produced present a good agreement with the sea truth data [33] used for validation. This particular implementation of the SSAP method has represented a useful approach to solve the complex problem of submersed vegetation species spectra classification for the Venice lagoon, considering the number of variables associated to the depth and the scattering process occurring in the water column and the mixing of vegetation species and substrate contribution within a pixel [34].

5.3 The "Sacca" of Goro

The Figures 4 and 5 represent the maps of chlorophyll, CDOM and TSM concentrations obtained from the inversion of SAMBUCA model (implemented for the Sacca of Goro) to the Hyperion images acquired on 14 and 30 August 2005. The differences among the concentration maps derived from the two Hyperion images are connected to tidal cycle and meteorological conditions: in the image collected on 30-Aug-2005, the high turbidity in the whole lagoon is related to wind speed which caused sediment resuspension in shallow water. On 14-Aug-2005, the water clarity was relatively good, even because of flood tide. In situ measurements were used for the model calibration as no contemporary in situ samples, during image acquisition were available. Nevertheless the obtained concentrations of Chl, CDOM and TSM fall into the range of measured values therefore, this testifies how the model and the inversion procedure is suitable to describe the physical processes occurring in the water column of the Goro lagoon.

6 Conclusions

The selected case-studies results are encouraging in suggesting the usefulness of airborne and satellite hyperspectral techniques for the monitoring of transitional waters. For each site it was necessary to develop ad hoc methodologies for environmental parameters mapping, because there are different optical complexity levels connected to spatial and temporal variability of environmental conditions and hydrodynamics. Advancement in semi-automatic recognition procedures or implementation of radiative transfer model could lead imaging spectrometry to be used as a standard procedure for ecological management and monitoring. The efforts aim at improving these techniques and at making them routinely applicable to the next generation of hyperspectral sensors (EnMAP and PRISMA) of German and Italian Space Agencies, expected in 2012. Such satellite missions will provide high quality hyperspectral image data on a timely and frequent basis. One of the main objective is to investigate a wide range of ecosystem parameters, also in coastal zones and inland waters. According to the EU Water Framework Directive, specified biological, hydromorphological and physico-chemical parameters of water bodies have to be monitored on a regular basis. The high spectral resolution of EnMAP and PRISMA in the visible and near-infrared (VNIR) region will allow the assessment of the proposed optically visible parameters including chlorophyll-a content for determination of the phytoplankton-biomass, suspended matter and dissolved organic carbon concentration, algae composition and blooms, emersed and submersed macrophytes.

References

[1] Y. Zhang, J. Pulliainen, S. Koponen, and M. Hallikainen. Application of an empirical neural network to surface water quality estimation in the Gulf of Finland using combined optical data and microwave data. *Remote Sensing of Environmental*, 81(2-3):327–336, 2002.

[2] A. Rosenqvist, A. Milne, R. Lucas, M. Imhoff, and C. Dobson. A review of remote sensing technology in support of the Kyoto Protocol. *Environmental Science & Policy*, 6(5):441–455, 2003.

[3] Q. Chen, Y. Zhang, A. Ekroos, and M. Hallikainen. The role of remote sensing technology in the EU water framework directive (WFD). *Environmental Science & Policy*, 7:267–276, 2004.

[4] A. Sfriso, C. Facca, and P.F. Ghetti. Validation of the Macrophyte Quality Index (MaQI) set up to assess the ecological status of Italian marine transitional environments. *Hydrobiologia*, 617:117–141, 2009.

[5] A. Dekker, V.E. Brando, and J. Anstee. Retrospective seagrass change detection in a shallow coastal tidal Australian Lake. *Remote Sensing of Environment*, 97:415–433, 2005.

[6] A. Dekker, V.E. Brando, J. Anstee, S.K. Fyfe, T. Malthus, and E. Karpouzli. Remote sensing of seagrass systems: Use of spaceborne and airborne systems. In: Larkum A., Orth R., Duarte C. (eds.) Seagrasses: Biology, Ecology and Conservation. page 347−359, 2006.

[7] S. Phinn, C. Roelfsema, A. Dekker, V.E. Brando, and J. Anstee. Mapping seagrass species, cover and biomass in shallow waters: An assessment of satellite multi-spectral and airborne hyper-spectral imaging systems in Moreton Bay (Australia). *Remote Sensing of Environment*, 112:3413–3425, 2008.

[8] F. Santini, L. Alberotanza, R.M. Cavalli, and S. Pignatti. A two-step optimization procedure for assessing water constituent concentrations by hyperspectral remote sensing techniques: An application to the highly turbid Venice lagoon waters. *Remote Sensing of Environment, in press*, 114:887–898, 2010.

[9] I. Pratesi and A. Canu. Italy's coastal heritage. *Coastline*, 2:3–6, 1993.

[10] M. Lenzi and M. Mattei. Results of a four-year management of the lagoon ecosystem of Orbetello through algal biomass harvesting. *Biologi Italiani*, 2:7–12, 1998.

[11] E. Giusti and S. Marsili-Libelli. Modelling the interactions between nutrients and the submersed vegetation in the Orbetello Lagoon. *Ecological Modelling*, 184:141–161, 2005.

[12] M. Bucci, E. Ghiara, V. Gorelli, R. Gragnani, G. Izzi, J.G. Morgana, and L. Naviglio. Ecological conditions in the Orbetello Lagoon and suggest actions for its restoration. In Marine Coastal Eutrophication, edited by R. A. Vollenweider, R. Marchetti and R. Viviani, (Amsterdam: Elsevier), . pages 1179–1188, 1992.

[13] M. Lenzi. Experiences for the management of Orbetello lagoon: eutrophication and fishing. *In Marine Coastal Eutrophication*, pages 1189– 1198, 1992.

[14] S. Salviato, J. Barbaro, F. Braga, and L. Alberotanza. Analisi spettrale delle fanerogame marine in laguna di Venezia. *Rivista Italiana di Telerilevamento*, 33/34:91–107, 2005.

[15] A. Sfriso and P.F. Ghetti. Seasonal variation in biomass, morphometric parameters and production of seagrasses in the lagoon of Venice. *Aquatic Botany*, 61:207–223, 1998.

[16] A. Sfriso and C. Facca. Distribution and production of macrophytes in the lagoon of Venice comparison of actual and past abundance. *Hydrobiologia*, 577:71–85, 2007.

[17] U. Simeoni, G. Fontolan, U. Tessari, and C. Corbau. Domains of spit evolution in the Goro area, Po Delta, Italy. *Geomorphology*, 86:332–348, 2007.

[18] F. Cellina, G.A. De Leo, A.E. Rizzoli, P. Viaroli, and M. Bartoli. Economic modelling as a tool to support macroalgal bloom management: a case study (Sacca di Goro, Po river delta). *Oceanologica Acta*, 26:139–147, 2003.

[19] A.F.H. Goetz. Principles of narrow band spectrometry in the visible and IR: instruments and data analysis. *In Imaging spectrometry : fundamentals and prospective applications*, pages 21–32, 1992.

[20] F.A. Kruse, A.B. Lefkoff, J.W. Boardman, K.B. Heidebrecht, et al. The Spectral Image Processing System (SIPS) - interactive visualization and analysis of imaging spectrometer data. *Remote Sensing of Environment*, 44:145–163, 1993.

[21] GEOSS. 10-Year Plan Reference Document. 2005.

[22] G.S. Fargion and J.L. Mueller. Ocean Optics Protocols for Satellite Ocean Color Sensor Validation, Revision 2. *NASA Tech. Memo.*, pages 1–184, 2000.

[23] L. Alberotanza, V. E. Brando, G. Ravagnan, and A. Zandonella. Hyperspectral aerial images. A valuable tool for submerged vegetation recognition in the Orbetello Lagoons, Italy. *International Journal Of Remote Sensing*, 20(3):523–533, 1999.

[24] P.S. Chavez. An improved dark-object subtraction technique for atmospheric correction of multispectral data. *Remote Sensing of Environment*, 24:459–479, 1988.

[25] J.P. Gastellu-Etchegorry and G. Stancalie. Correction of atmospheric effects for the high resolution airborne spectrometric data. *In Proceedings of the First International Airborne Remote Sensing Conference and Exhibition, Strasbourg, France*, 1:121–130, 1994.

[26] R.H Yuhas, A.F.H. Goetz, and J.W. Boardmann. Discrimination among semiarid landscape endmembers using the Spectral Angle Mapper (SAM) algorithm. *In Summaries of the Third Annual JPL Airborne Geoscience Workshop*, pages 147–149, 1992.

[27] F.A. Kruse and L.L. Richardson V.G. Ambrosia. Techniques developed for geologic analysis of hyperspectral data applied to near-shore hyperspectral ocean data. *In Proceedings of the Fourth International Conference on Remote Sensing for Marine and Coastal Environments, Orlando, Florida*, 1:233–246, 1997.

[28] R.L. Huguenin. Subpixel analysis process improves accuracy of multispectral classification. *Earth Observation Magazine*, 3(7):37–40, 1994.

[29] M.A. Karaska, R.L. Huguenin, D. Van Blaricom, and B. Savitsky. Subpixel classification of cypress and tupelo trees in TM imagery. *In Techical Papers of the American Society for Photogrammetry and Remote Sensing*, pages 856–865, 1995.

[30] V.E. Brando and A.G. Dekker. Satellite hyperspectral remote sensing for estimating estuarine and coastal water quality. *IEEE Transactions on Geoscience and Remote Sensing*, 41(6):1378–1387, 2003.

[31] TEI Ingegneria dell'Ambiente Spa. Intervento globale di risanamento delle lagune di Orbetello dal fenomeno di eutrofizzazione del corpo idrico. Rapporto finale. 1989.

[32] V. Bombelli and M. Lenzi. Evoluzione del sistema laguno-costiero di Orbetello, rapporto tra eutrofizzazione, struttura dei popolamenti e produttività. *Biologia Marina Mediterranea*, 2:31–36, 1995.

[33] A. Rismondo, D. Curiel, F. Scarton, D. Mion, and G. Caniglia. A new seagrass map of the Venice lagoon. *Proc. VI International Conference of the Mediterranen Coastal Environment MEDCOAST*, 2:843–852, 2003.

[34] L. Alberotanza, R.M. Cavalli, S. Pignatti, and A. Zandonella. Classification of submersed aquatic vegetation of the Venice lagoon using MIVIS airborne data. *Annals Of Geophysics*, 49(1):271–276, 2006.

Earth Observation Facilities for Supporting the Coastal Management

R.M. Cavalli[1], L. Alberotanza[2], C. Bassani[1], F. Braga[2], L. Fusilli[1], S. Pignatti[3], F. Santini[3]
1, Institute for Atmospheric Pollution, CNR, Roma, Italy
2, Institute of Marine Sciences, CNR, Venezia, Italy
3, Institute of Methodologies for Environmental Analysis, CNR, Potenza, Italy
cavalli@lara.rm.cnr.it

Abstract

Coastal zones represent the centre of very complex natural system in which interactions between land, sea and air occur. Moreover, coastal zones are the most densely populated areas and therefore are very sensitive to the human activities. The complex components and processes that take place in the coastal areas require the definition of a system for environmental protection and risk management. An operational system needs to be designed taking into account the following four action phases to: i) increase territory and process understanding, ii) offer a useful environmental control, iii) support actions for an effective forecast and iv) provide a rapid and operational support during extreme events and disasters. In recent years, remote sensing products have achieved thematic accuracy, spatial and temporal resolutions meeting user requirements in the coastal zone. Research activities outline the improvements in the methodologies for providing valuable products for coastal applications such as coastal erosion assessment, water pollution detection, fluvial plumes characterization, etc. At present, research activities are based on an integrated approach considering available space segment, in situ data and models outputs. This paper presents activities related to the use of remote sensing data for developing new applications which can better contribute to the integrated coastal areas management and the risk monitoring.

1 Introduction

Coastal zone refers to a broad geographic area in which terrestrial and marine factors are mixed to produce unique landforms and ecological systems. Estuaries, lagoons, river mouths and human activities directly influence the coastal ecosystems. Continuous physical interaction between terrestrial, marine and atmospheric elements makes the coastal zone an area of intense dynamic processes. Apart from the natural causes, anthropogenic activities also play an important role in coastal environment changes. Various landforms, shoreline configuration, ecology and environmental conditions of this zone are constantly changing as a result of natural and anthropogenic activities. Water quality and coastal habitats are rapidly being impacted by pressure of urbanization, industrialization and recreation. Coastal areas and coastal waters are biologically and ecologically important and also have great economic potential. So there is an inevitable need to monitor and manage the coastal zones regularly, properly and optimally. In the recent decades, a helpful contribution has been obtained by the Remote Sensing data, which can significantly enhance the information available from traditional data sources, providing synoptic views of large portions of Earth with a relatively high revisiting frequency and therefore early detection of anomalies and degradation of the ecological status. The users devoted to support the environmental protection and the risk management need a set of products or a "system" organized in four action phases to:

(i) Better understand all aspects and peculiarities of the ecosystem and its processes to increase knowledge of temporal evolution of the latter;
(ii) Control and monitoring of the temporal processes;
(iii) Forecast the possible extreme events or disasters;
(iv) Control, monitoring the extreme events or disasters.

In the last years, Earth Observation by remote sensing has better met user requirements needs to support all phases of the environmental protection and the risk management. In order to ensure comprehensive and sustained Earth Observations, a coordination of the efforts, articulated in the GEOSS 10-Year Implementation Plan [1], Global Earth Observation System of Systems (GEOSS) was built to add value to existing Earth observation systems, filling critical gaps and supporting their interoperability. In particular, the working plan underlines the "Use of Satellites for Risk Management for Reducing loss of life and property from natural and human-induced disasters". The four action phases need products with specific characteristics in term of thematic and geometric accuracy, spatial and temporal resolutions. These specific user required characteristics cannot be the same for each phase. The actual remote constellation doesn't cover all range of the user required characteristics. The integration of remotely-sensed and in situ data and the combination of the forecast models better meets the user required characteristics of the products. In this paper, the authors present some research projects where they have investigated capability of remote sensing to meet the user required characteristics of the products (spatial and temporal resolutions, operational and quantitative requirements) in the coastal zone. All activities were performed to answer the customer requirements to support the environmental protection and the risk management. Following are the projects developed according to the GEOSS recommendations and classified on the basis four action phases:

- Hypad.com project was carried out to improve the knowledge of the Albanian and Montenegrin coastal areas and was supported by the Italian Ministry of the Environment (phase i);
- Northern Adriatic Coasts Asset project (supported by the Water Basin Authority) was carried out to understand the morphological evolution of shoreline and its vulnerability to erosion processes and to monitor fluvial plumes into Northern Adriatic Sea (phases i-ii). In the framework of the cooperation between the Italian Foreign Affair Ministry (through the University of Rome) and the Kenyan Authorities, the project on the Kenyan part of the Lake Victoria was carried out to identify the conditions for the occurrence of hazardous events such as abnormal macrophyte proliferation (phase iii) and to develop an up-to-date decision support

system devoted to an apprised territory, environment and resource management (phase iv).

2 Projects description

2.1 HYPAD.com project (i)

The HYPerspectral for ADriatic COastal Monitoring project was devoted to accomplish the requirements for understanding the coastal environments (i). The CNR (National Research Council) through the mediation of Italian Ministry for the Environment and Territory "Direzione Ambientale Ricerca e Sviluppo" cooperated with some Italian and foreign research agency for the success of the project. These agencies showed great interest in the project activities and willingness to constructively collaborate and propose suggestions. The Albanian - Montenegrin coastal environments have been selected as study areas in accordance to the local Institutions requests (Figure 1). The project focused on improving the knowledge of the Albanian and Montenegrin coastal areas by integrating different high resolution spatial and spectral remote sensing technologies. The HYPAD.COM project took place in a strategic moment, when the Earth Observation (EO) had become an essential component of the global effort to deal with global challenges. The purpose of the HYPAD.COM was to promote capacity building in EO, on existing initiatives and sector-specific needs, like GEOSS planned, in order to achieve comprehensive, coordinated and sustained in situ and airborne observations of the coastal area. The HYPAD.COM activity programme meets the need for timely and quality local scientific information as a basis for decision making, and enhances delivery of benefits to society especially in the following areas, recognized in the GEOSS 10-Year Implementation Plan: "Improving the management and protection of terrestrial, coastal, and marine ecosystems" [1]. In the framework of the HYPAD.COM, the integration of the EO hyperspectral data (airborne and ground-based) was performed to improve the quality of the information available from EO data as well as to characterize the Albanian and Montenegrin coastal areas and the surrounding lands. For the purposes of the HYPAD.COM project, the following scientific objectives, for the coastal area, were faced:

a. the characterization of the coastal water;
b. the detection of the coastal fresh water;
c. the characterization of submerged aquatic vegetation;
d. the characterization of vegetation and land use/cover in the coastal area.

On the basis of the scientific objectives and proposes defined in the project, several actions were taken:

1. three oceanographic cruises were carried out, in synergy with the Adricosmstar project [2] to spectrally characterize the constituents of the coastal waters along the Albanian and Montenegrin shorelines. About 90 water column stations were characterized [3];
2. fifty-three airborne hyperspectral MIVIS surveys were deployed on part of the Montenegrin and Albanian coasts and on the Buna/Bojana river;
3. spectral signatures of the main submerged vegetation species were collected on Montenegro coastal area in order to map the submerged vegetation extension (e.g. *Posidonia oceanica*) and to analyze the resulting impact of urbanization of the coastline. About 40 sites were characterized [3];

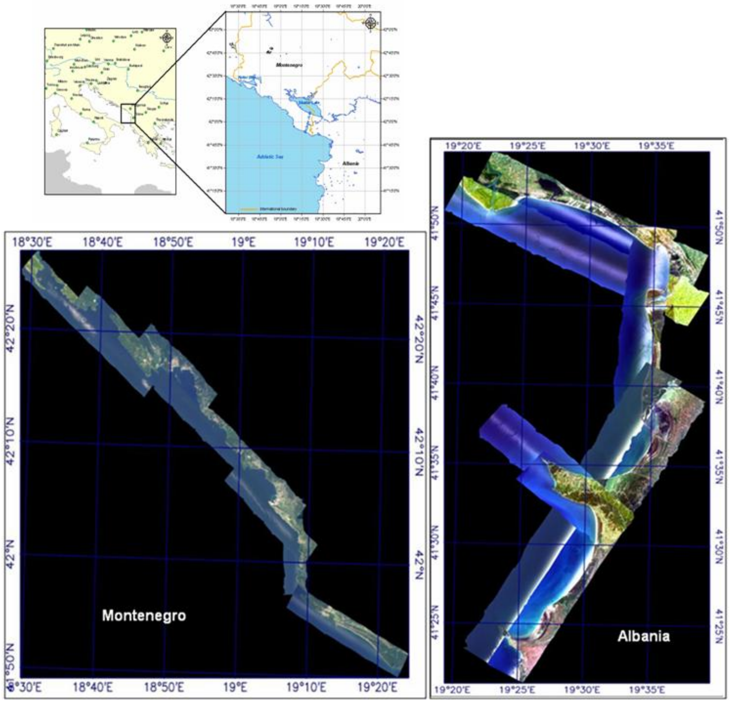

Figure 1: Study area and mosaic of the Multispectral Imaging Visible Infrared Scanner images.

4. CAL/VAL campaigns were organized in order to collect a spectral library of the main land cover units and of the more significant material.

The Members of the Joint Committee agreed that the project was very important in the definition of the monitoring activities and of the major environmental problems affecting the area [4], also considering the involvement of the Albanian Institutions (MoEFWA Institute of Energy, Water and Environment Institute of Albanologi Studies).

2.2 The northern Adriatic coast asset (i-ii)

A considerable amount of the North Adriatic coast is currently eroding despite the development of a wide range of measures to protect shorelines from eroding and flooding. The understanding of past and present natural and man-induced processes, which influence the coastal evolution of the North Western Adriatic Sea, is of prime interest for a proper management and preservation of these areas. Therefore it was necessary to process models, methodologies and information for devel-

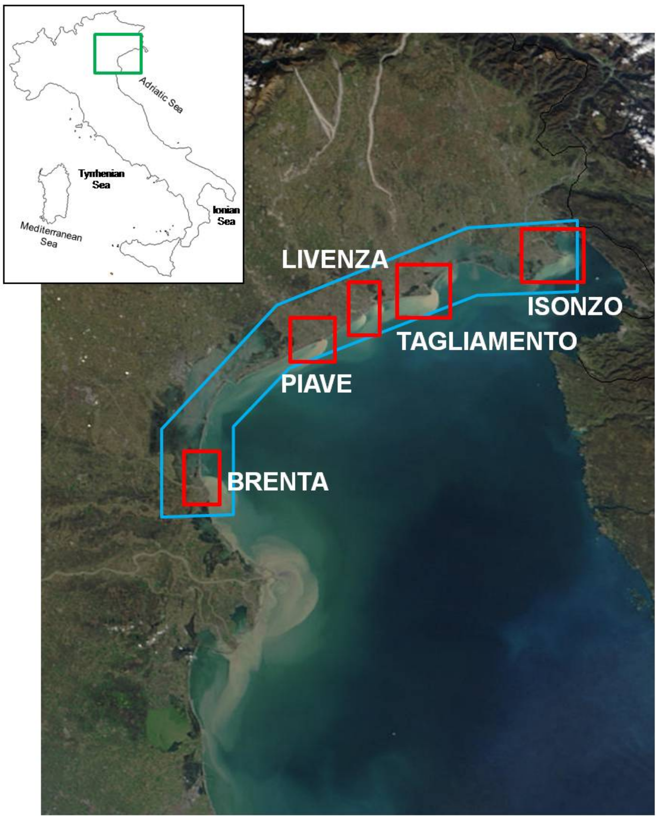

Figure 2: Location of interested coastal area and river mouths.

oping a management and monitoring plan (Water Framework Directive CE 2000/60), which supports and directs the near-term coastal interventions. This motivated initiating a specific research program concerning these issues started in 2003 by a cooperation among CNR-ISMAR, the Autorità di Bacino dei fiumi dell'Alto Adriatico (Water Basin Authority) and APAT, Servizio Laguna di Venezia (Italian Environment Protection and Technical Services Agency). In the last decades, intense exploitation of river resources, such as water and channel-bed materials and anthropic land use interventions, has caused a radical change in the morphology of the drainage basins and in the characteristics of the river regime [5]. The consequence of these changes is a dramatic reduction of the sediment load from the rivers and an increasing vulnerability to erosional processes of their terminal reaches and adjacent shores. A considerable effort was dedicated to the understanding and the reconstruction of the historical evolution of the coastline and to the investigation of the main forces driving the main variations in the longshore sediment transport and in the morphology of the wetlands and the nearby littoral. This knowledge is important in order to plan interventions for the hydraulic protection and to find adequate solutions to coastal erosion problems. To address these critical topics, the present remote sensing technologies have been successfully used.

2.2.1 Investigation on the morphological evolution of shoreline(i)

The most evident appearance of littoral changes is shoreline advancing and receding. These morphological variations are the result of natural processes, climatic conditions, such as eustatism, subsidence, meteo-marine climate, sediment load, aeolian action and anthropic interventions (protective structures, dunes destruction, beach renourishment, etc.). All these factors contribute to morphological changes of coastline between Brenta and Tagliamento river mouth in different way. Such modifications themselves make a diverse impact in function of coastal vulnerability and human activities or use of territory. In the littoral beyond the competence of Water Basin Authority, a study was carried out for comparing the shorelines extracted from historical maps, National cartography (IGM), Regional Technical Charts (CTR), aerial photos and Very High Resolution (VHR) satellite images (QuickBird and IKONOS) of the last 40 years (Figure 2). The VHR sensors, which acquired multispectral and panchromatic images with a resolution of about 2 m and 0.5 m respectively, have proved to be compatible with the spatial scale of phenomena that we have been observing on the coastline [6]. So monitoring coastal erosion through satellite data is a concrete and useful possibility, able to compete with the aerial photogrammetry, also considering that efficient methodologies for semi-automatic shorelines extraction can be developed exploiting multispectral bands. Moreover VHR images were used for the identification and discrimination of the emerged protective works, build on the littorals. At first, we have updated the littoral situation (shoreline, parallel and transversal protective structures, river jetties) with VHR images of 2004 and we have analyzed coastline morphological changes. Subsequently, we have examined closely the morphological evolution of the river mouths of Piave, Brenta and Tagliamento Rivers, because they are mainly exposed to erosion and deposition actions. The causes of these changes are due to river solid and liquid loads and meteo marine climate, subsidence, human interventions longshore and on hydrographic basins [7]. The study has been made using also bibliographic and cartographic materials and topographic and bathymetric profiles. Figure 3 shows the morphological evolution of river mouth and shoreline of Brenta, Piave and Tagliamento, in the last 40 years. To understand what is the influence of human interventions on morphological evolution, a database of protected works, realized along the beaches, was developed.

2.2.2 Mapping of fluvial plumes into Northern Adriatic Sea (ii)

In the framework of "the Adriatic coast asset" project, another application of remote sensing technologies was carried out: it regarded the characterization of river plumes and the analysis of their geometry for the extraction of information about sediment transport, useful to the calibration of coastal circulation models. The most important Italian rivers (Po, Adige, Brenta, Piave, Tagliamento, and Isonzo) flow into the Northern Adriatic Sea generating a fundamental supply of freshwater with its suspended material which generally tends to disperse depositing prevalent sandy material along the coastal areas. The distribution of suspended sediment concentration is a key issue for analyzing the deposition and erosion of the coasts and estuaries and for evaluating the material fluxes from river to sea and then along the shore. We applied semi-automatic algorithms to Landsat (TM and ETM+) and ASTER satellite images in order to obtain spatially distributed information for estimating and mapping the concentrations of Total Suspended Matter (TSM) and the Sea Surface Temperature (SST) of the rivers plumes. From the maps of TSM, SST and external borders of plumes it was possible to extract information for calibrating hydrodynamic and transport numerical models [8, 9]. The multitemporal maps of external borders of plumes have been superimposed and correlated to tide and wind conditions. From these maps, we could extract indications on preferential direction of the river fluxes along the coast [10].

2.3 Project on the Kenyan part of the Lake Victoria (iii-iv)

This project is presented as an example to show how satellite based observation can help to prevent (iii) and monitoring (iv) the possible special events or disasters. The study area (Victoria Lake) (Figure 4), even though it does not represent a marine coastal area, was included in the paper since the environmental perturbations affecting the lake are similar to those affecting the Mediterranean Sea coastal areas. In particular the analysed phenomena is related to the anomalous proliferation of algae and macro-algae, a phenomenon that can often occur in coastal areas at our latitudes. In particular this project refers to the abnormal growing of the aquatic weed Eicchornia crassipes (water hyacinth, Figure 5), that began to appear in the lake during 1989-90 and and is still present nowadays. The processing of remotely sensed data (ETM+/Landsat, TERRA/ASTER and ENVISAT/MERIS) were used to delevelop thematic maps suitable to support the risk analysis and management strategy for the Lake Victoria. In particular the authors obtained: a) the distribution of water hyacinth and associated macrophytes; b) the estimation of parameters related to water quality and composition, like concentrations of chlorophyll a (Chl a) coloured dissolved organic matter (CDOM) and total suspended solid (TSS) [11]. Therefore, whenever correlation between these quantities can be established, it can help determining the main causes of the fast growing of floating weeds that have infested the area over the last few years [12, 13].

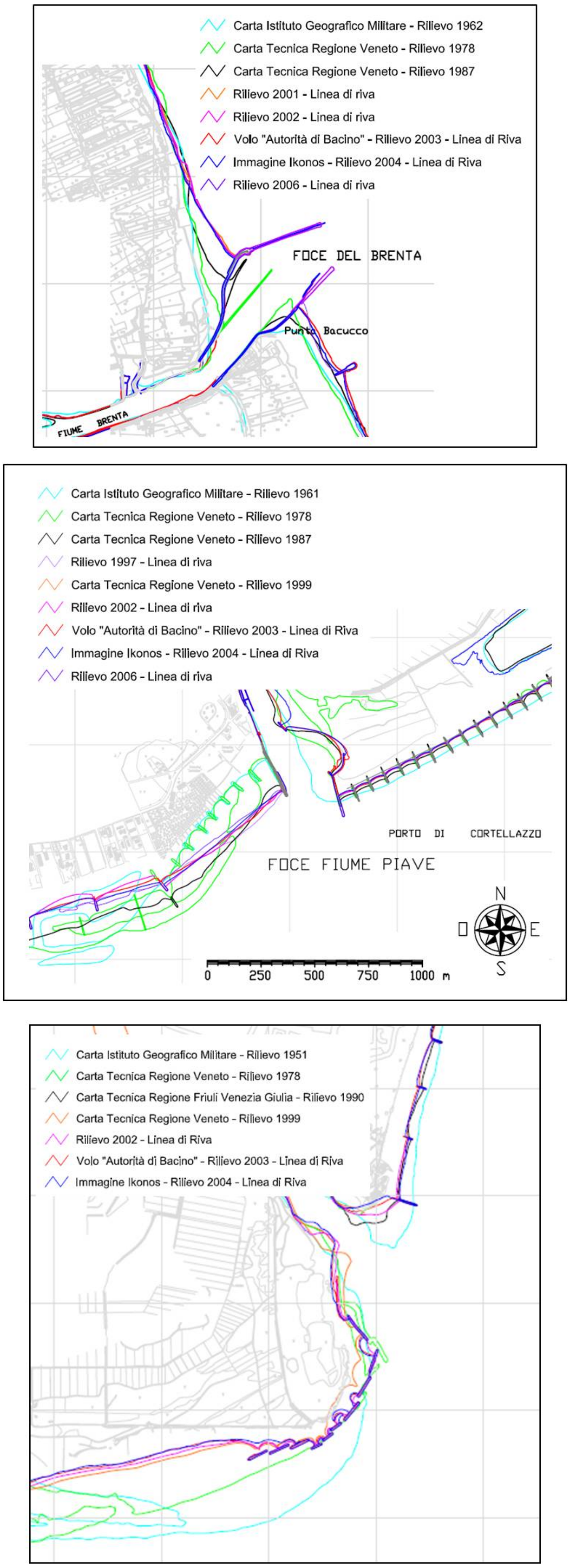

Figure 3: Changes of mouth of the Brenta, Piave and Tagliamento rivers.

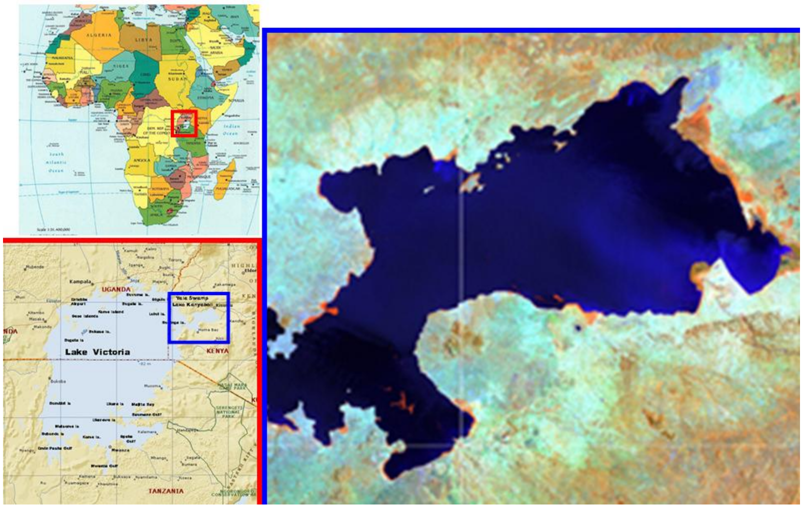

Figure 4: Location of study area.

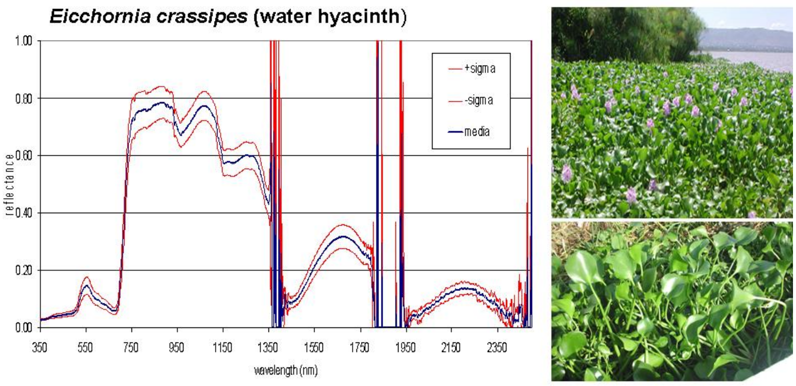

Figure 5: Eicchornia crassipes (water hyacinth) spectrum and pictures.

3 Future applications and conclusions

The experiences acquired during the described projects in the investigations of the capability of remote sensing to meet the user requirements in the four action phases reported above, allowed to perform the CIRCE (Controllo Integrato del Rischio CostiEro) project. CIRCE is one of the two Preliminary Projects devoted to coastal risk management and coastal monitoring presented to the Italian Space Agency (ASI). This project will support the user in all four phases of the environmental protection and risk management in the coastal areas. The final product will be a system that supports the user decision in case of disaster. This Preliminary Project is an eligible candidate to become a Pilot Project. The identified final users are the Civil Protection Department, the ISPRA Institute and other potential interested users. The Pilot Project purpose is to integrate new functionalities, based on earth observation data, in the decision support system of the users. Such pilot project must respond to clear user needs and must demonstrate service provision as a real operational test case [14]. It appears therefore that the recent advance in supplying high resolution EO data, both at spatial and spectral scale, allows to foresee how in the next future remote sensing will be a powerful tool for developing user products that can fully meet the technical requirements for operational needs.

References

[1] GEOSS. 10-Year Plan Reference Document. 2005.

[2] P. Oddo, N. Pinardi, and M. Zavatarelli. A numerical study of the interannual variability of the Adriatic Sea (2000-2002). *Science of the Total Environment*, 353:39–56, 2005.

[3] G.S. Fargion and J.L. Mueller. Ocean Optics Protocols for Satellite Ocean Color Sensor Validation: Revision 2. *NASA Tech. Memo.*, 2003.

[4] C. Bassani, C. Cattaneo, R.M. Cavalli, L. Fusilli, et al. The hyperspectral for adriatic coastal monitoring (hypad.com) project. *In: proceedings of ISRSE 33rd International Symposium on Remote Sensing of Environment. Sustaining the Millenium Development Goals*, 2009.

[5] A. Bondesan and M. Zunica. Modificazioni di foce ed erosioni di spiaggia in relazione al trasporto solido: il caso del Piave. *In: Atti del Convegno "Una Politica per la gestione e la tutela delle acque del Piave"*, 1993.

[6] N. Iandelli and E. Pranzini. Waterline extraction from Ikonos images for the scope of beach erosion monitoring. *Beach erosion monitoring*, 2008.

[7] F. Braga, L. Alberotanza, A. Cucco, M. Ferla, A. Rusconi, et al. Morphology of the Veneto coast, Northern Adriatic Sea, Italy. *Geo-Eco-Marina*, 9/10:77–81, 2005.

[8] M. Mestres, J.P. Sierra, A. Sanchez-Arcilla, J.G. del Rio, et al. Modelling of the Ebro River plume. Validation with field observations. *Scientia marina*, 67(4):379–391, 2003.

[9] S. Kaya, D.Z. Seker, S. Kabdasli, N. Musaoglu, et al. Monitoring Turbid Fresh Water Plume Characteristics by Means of Remotely Sensed Data. *Journal of Hydrological Processes*, 20(1):2429–2440, 2006.

[10] L. Alberotanza, F. Braga, and A. Zandonella. Estrazione dei bordi esterni dei pennacchi costieri dei fiumi dell'Alto Adriatico da immagini ETM+ ed ASTER. *In: Atti dell'13a Conferenza nazionale ASITA, Bari*, pages 71–76, 2009.

[11] F. Santini, L. Alberotanza, R.M. Cavalli, and S. Pignatti. A two-step optimization procedure for assessing water constituent concentrations by hyperspectral remote sensing techniques: An application to the highly turbid Venice lagoon waters. *Remote Sensing of Environment*, 2010.

[12] R.M. Cavalli, G. Laneve, L. Fusilli, S. Pignatti, and F. Santini. Remote Sensing water observation for supporting lake Victoria weed management. *Journal of Environmental Management*, 90:2199–2211, 2009.

[13] F. Santini, R.M. Cavalli, A. Palombo, and S. Pignatti. Optical model for the water characterization of the highly turbid water of the Winam Gulf (Victoria Lake). *Proceedings of SPIE*, 6743, 2007.

[14] C. Ananasso. Italian space agency pilot projects to support disaster management and eviromental monitoring. *In proceedings of "Tecnologie Geomatiche per il monitoraggio dell'ambiente"*, page 3, 2009.

Monitoring of Faecal Seawater Pollution by Advanced Methods and Technologies

G. Caruso[1], R. Zaccone[1], L.S. Monticelli[1], G. Zappalà[1], R. Caruso[2], E. Crisafi[1]
1, Institute for Coastal Marine Environment, CNR, Messina, Italy
2, University Hospital of Messina "G. Martino", Messina, Italy
gabriella.caruso@iamc.cnr.it

Abstract

Monitoring the microbiological quality of coastal seawaters through the detection of bacterial indicators of faecal pollution is recognised as a mandatory step to prevent hygienic-sanitary risks related to the recreational use of aquatic environments. The long analysis and response times of the methods conventionally accepted to determine the bacterial indicators make them inadequate to the early warning of environmental pollution episodes. New analytical methods, characterised by rapidity and specificity, are needed to protect both human and environmental health.

This paper aims at reviewing the main analytical protocols that since 1990 have been developed and applied to coastal marine monitoring in the framework of several research programmes performed at the Thalassographic Institute of Messina, now a section of the Institute for Coastal Marine Environment (IAMC). Particularly, studies focused on the fluorescent antibody method and beta-glucuronidase assay using the MUG test (based on the fluorogenic compound 4-methylumbelliferone-beta-D-glucuronide), which are able to detect, through quick and specific reactions, target bacterial species such as *Escherichia coli, Salmonella* spp., *Enterococcus faecium*. Both these methods offer a suitable tool to assess the pollution levels of coastal areas, allowing us to determine also the various physiological states in which bacterial pathogens persist in aquatic environments.

1 Introduction

1.1 Coastal microbial pollution

Coastal environments are recognised to be among the areas most vulnerable to the impact of anthropic activities, which affect both human and environmental health. The main problems are associated to the disposal of waste waters without adequate treatment; sewage outfall causes severe limitations of water use for recreation, aquaculture, fishing, etc. Moreover, exposure to seawaters of poor microbiological quality has been related to the occurrence of multiple diseases which have major public health and socio-economic impacts [1], making rapid and reliable routine monitoring of the microbiological water quality of utmost importance [2]. Seawater control relies on the set up of monitoring networks able to collect real time data on parameters characterizing environmental quality; bacteria or their metabolic activities represent effective indicators in microbiological monitoring. Traditionally, microbiological seawater controls for faecal pollution rely on the search for specific bacterial indicators. In fact, due to the variety of pathogens (bacteria, viruses and protozoa) that may be present in waters, their global detection cannot find application in routine analysis. Current guidelines for the assessment of water quality prescribe the quantification of microorganisms that are proposed as indicators of the health status of aquatic environments [3]. Normally, faecal bacteria by themselves are not necessarily pathogens, but simply they give early indication about the potential health hazard related to the occurrence of enteric pathogens [2]; thus, they act as early warning sentinels of the presence of potential pollution sources. Nevertheless, the use of classical bacterial indicators of water quality has been questioned [4]. Recent trends in environmental monitoring for public health preservation have highlighted the need of a deep revision of the indicators (i.e. total and faecal coliforms) until now used in seawater quality assessment [4, 5]. For the detection of faecal or sewage pollution, the scientific community in the framework of the bathing waters European Directive [EEC Directive COM (2002) 581] has suggested *Escherichia coli* or intestinal enterococci as the most appropriate indicators, as they are strictly related to the occurrence of enteric pathogens. Another important issue in microbiological monitoring studies, concerns the validity of the analytical methods currently used to detect and enumerate these microorganisms in seawater. Culture based assays also suffer from long analysis and response times, low accuracy, and a lack of sensitivity to detect environmental pathogens [6]. In the light of the limitations of culture approaches for water pollution monitoring, new rapid methods for microbiological analysis have been proposed and are often welcomed to get a more precise and accurate judgement on water quality [6]. To be practical, these new methods should be specific and sensitive, and provide reproducible results within the same working day or in short times [7].

In the context of environmental monitoring, the possibility to detect the viability status of pathogenic bacteria, acquires a special additional value. In fact, a number of studies have highlighted the failure of culture-based methods to recover stressed or injured bacteria. Also microscopic counts do not provide any indication on the cell viability and on the different physiological states in which bacterial cells may persist in the aquatic environment. It has widely been recognised that in natural waters enteric bacteria may enter into a viable but non-culturable (VNBC) state as a survival strategy [8]. In this state, they may retain their pathogenic potential.

Since 1990, the Institute for Coastal Marine Environment, formerly Thalassographic Institute of Messina, has gained expertise in the monitoring of marine pollution by new rapid methods and equipments, that addressed, among other parameters, also the determination of faecal indicators. Advances in this field have been achieved in the framework of the following research Projects: Italian National Research Council- Strategical Project "Marine pollution Monitoring in the South of Italy"(1989-1994); "Advanced Monitoring Systems" (SAM - Cluster 10, 2001-2004), funded by the Italian Ministry for University and Scientific Research; ARPA-Sicily "Studies aiming at the set up of a monitoring system for the first characterisation of the surface water bodies in the Sicilian region" (2005-2006). Particularly, efforts were devoted to the development of rapid analytical methods for the evaluation of faecal pollution, and to the set up of advanced technologies for coastal monitoring.

This note aims at reviewing the rapid methodologies developed, optimised and applied at our Institute to coastal marine monitoring. Three analytical protocols were chosen for the experimentation: the fluorescent antibody (FA) method, the FA method combined with the viability staining, and the assay of the enzyme beta-glucuronidase (MUG assay), which were specifically designed and compared with the standard methods for the detection and enumeration of *Escherichia coli* and *Enterococcus faecium* as indicators of the hygienic sanitary quality. Some of the results obtained by the application to "in situ" monitoring of these new rapid methods are reported.

2 Materials and mathods

2.1 Developed analytical methods

The Fluorescent antibody (FA) method - The FA method is a microscopical method which relies on the antigen-antibody complex produced by the labelling of *E. coli* cells with immune sera specific for the target bacteria. Similarly to other immunological methods, FA method is based on the antigenic structure of the cells, which is specifically recognized by antibodies. These latter can be conjugated with fluorescent organic probes ("fluorochromes"), such as rhodamine B or fluorescein isothyocianate (FITC); this binding makes the visualisation of the antigen-antibody complex possible using an epifluorescence microscope. After excitation with light of a wavelength appropriate to the specific fluorochrome, the cells labelled by FA become visible as green (FITC) or red (Rhodamine) fluorescent cells.

There are two different FA procedures. In the direct procedure, the immune sera containing the specific antibody directly labelled with the fluorochrome recognise the target antigen, producing the fluorescent antigen-antibody complex. In the indirect procedure, the labelling of target cells with specific immune sera is followed by the labelling with the secondary antibody (goat anti rabbit IgG conjugated to FITC).

For the search of *E. coli* as a faecal pollution indicator, an indirect FA protocol was applied [9, 10, 5, 7, 11]. A mix of *E. coli* agglutinating sera specific for the enteropathogenic serotypes (Murex Biotech, pool 2+3+4, diluted 1:40 in phosphate buffered saline, PBS) has been used. This reagent recognises a total of 14 *E. coli* enteropathogenic serotypes. The goat anti-rabbit IgG- whole serum (Sigma), diluted 1:80 in PBS, was used as the secondary antibody. Some strains of Enterobacteria (*Escherichia, Shigella, Salmonella*), both of clinical and environmental origin, were used for the specificity assay, in order to verify the analytical protocol was specific towards *E. coli* only.

For *Salmonella* spp., the anti-Salmonella polyvalent I sera (Behring), conjugated with FITC, were used as the specific immune sera, after a 1:80 dilution in PBS. The specificity of this reagent was preliminarly assayed against other enterobacterial strains (*Salmonella, Shigella, Citrobacter, Yersinia, Enterobacter and Proteus* spp. [12]. Moreover, FA method was successfully applied for the detection of *Enterococcus faecium* in coastal transitional waters. The analytical protocol of direct FA was based on the use of immune sera conjugated with FITC (Omnitope *Enterococ-*

cus spp. purchased from ViroStat, diluited 1:50 in PBS). The specificity assay was performed with other enterococcal strains (*Enterococcus faecalis, E. casseliflavus, E. avium*) isolated from the same studied environment [13].

Combined FA- viability staining protocol - A further development of the FA method was the combination of the analytical procedure with the labelling with viable stains such as the fluorochromes 5-cyano-2,3-ditolyl tetrazolium chloride (CTC) and propidium iodide (PI), respectively known as markers of active respiring cells and of membrane-damaged cells. Actively respiring cells are able to reduce CTC, which is not fluorescent, into CTC-formazan, which precipitates as red fluorescing granules inside the cells. PI, which penetrates the cell membranes of damaged cells only, has an emission peak in the red-orange spectrum (617-623 nm). After the staining protocols, it is possible to distinguish the actively respiring or dead cells, fluorescing in red due to CTC or PI labelling, within the total FA-labelled bacterial population, fluorescing in green due to FITC labelling, simply by switching from blue to green light filters [14, 11].

Beta-glucuronidase assay using the MUG fluorogenic substrate - The beta-glucuronidase (MUG) assay is a biochemical method based on the determination of the enzyme beta-glucuronidase, specific of *E. coli* and some strains of *Shigella*, an enterobacterium closely related to *E. coli*. This enzymes catalyzes the hydrolysis of beta-D-glucopyranosiduronic derivatives into D-glucuronic acid. The fluorogenic compound 4-methylumbelliferyl-beta-D-glucuronide (MUG) is cleaved by beta-glucuronidase in 4-methylumbelliferone (MUF), which is fluorescent. This method provides a measure of the potential metabolic activity of *E. coli* and therefore allows to detect faecal pollution in fresh as well as in marine waters [15, 16]. An enzyme assay using MUG as the substrate was developed for seawaters by Caruso et al. [17].

2.2 *"In situ"* application of FA and MUG methods

Detection of *E. coli* - A survey of Messina shoreline was performed during 2001-2004, as a part of the SAM Project, with the aim of assessing the bacteriological quality of bathing waters. A total of 101 seawater samples were collected from heavily or weakly-polluted sites and analysed using FA and MUG methods.

Starting from October 2002, a seasonal study was also carried out; surface waters (n=91) were collected from 8 coastal sites and examined by FA-CTC, FA-PI and MUG methods.

Detection of *E. faecium* - During 2005-2006, some transitional Sicilian areas, belonging to Cape Peloro and Vendicari ecosystems, were sampled, in order to monitor the abundance of enterococci in these shallow environments [13].

2.3 Collection and treatment of the samples

For FA counts, 100 ml water samples were fixed with filtered formalin (2% final concentration) and then stored at +4°C until analysis. According to FA method, samples were filtered through a Nuclepore black membrane (0.22 µm pore size), followed by incubation for 30 min at room temperature with the specific immune sera according to the target bacterial species to be detected. After rinsing with PBS,

the filter was mounted on a slide (in the case of the direct procedure) or incubated for 30 min at room temperature with the secondary antibody. The filter was then mounted on slide with FA mounting fluid (Difco) and observed with an epifluorescence Axioplan 2 microscope (Carl Zeiss Inc.), equipped with specific filters (blue light: BP 490, LP 510, FT 520 for FITC, green light: BP 510-560, LP 590, FT 580 for CTC and PI). Microscope counts were reported as the number of cells per ml.
For the MUG assay, seawater samples were concentrated 10 times by filtration through a 0.45 µm pore size Nuclepore membrane and re-suspended in sterile physiological solution. Ten millilitres subvolumes of each concentrated sample were added with increasing amounts of the fluorogenic substrate 4-methylumbelliferil-beta-D-glucuronide (MUG), according to Caruso et al. [17]. The fluorescence intensity was measured at time 0, immediately after the addition of the substrate, and after 3 hours of incubation at 44°C, using a Turner TD-700 fluorimeter at 365 and 440 nm (excitation and emission wavelengths, respectively). The fluorescence increase was converted into nanomoles of MUF released per hour and per 100 ml of sample. In parallel with FA and MUG methods, plate counts were performed: faecal coliforms (FC) were counted on m-FC agar incubated at 44.5°C for 24 hours, while enterococci were counted on Slanetz-Bartley (Oxoid) plates incubated at 35°C for 48 hours. Suspected enterococci were confirmed on Bile Aesculin Agar (Difco).

3 Results

3.1 Detection of *E. coli*

FA-labelled *E. coli* appeared as green fluorescing, rod shaped cells. FA counts were comprised between 5.04×10^3 and 4.50×10^5 cells/100ml, MUG activity values ranged from 0.00004 to 726.88 nmol/100 ml/h, while FC counts ranged from 1.0×10^1 to 4.0×10^4 CFU/100ml. As an example, cell counts and enzyme values obtained during April-May 2004 are reported in Figure 1. FA counts followed a behaviour similar to that of FC counts, although microscopic counts were, on average, 1-2 orders of magnitude higher than culture counts (3.18×10^4 cells and 2.36×10^3 CFU/100 ml respectively). This result confirmed that the standard method underestimated the bacterial concentration.
Comparing heavily contaminated samples, such as those collected during spring 2004, to low contaminated ones, such as those collected during 2003, at low pollution levels (n=57), FC and FA values were more significantly related (R2= 0.1401) than FC and MUG (R2= 0.1291). This could be due to the high presence of injured or damaged bacteria in oligotrophic waters. Conversely, for heavily contaminated samples (n=34), a better relationship between FC and MUG (R2=0.6161) was found, compared to that observed between FC and FA (R2= 0.5607). This could depend on the high organic matter available in highly polluted waters, which supported a higher proportion of metabolically active cells. Therefore, FA method is a method suitable for the bacteriological analysis of all the samples regardless of their pollution levels, whereas MUG assay should be used for heavily polluted samples.

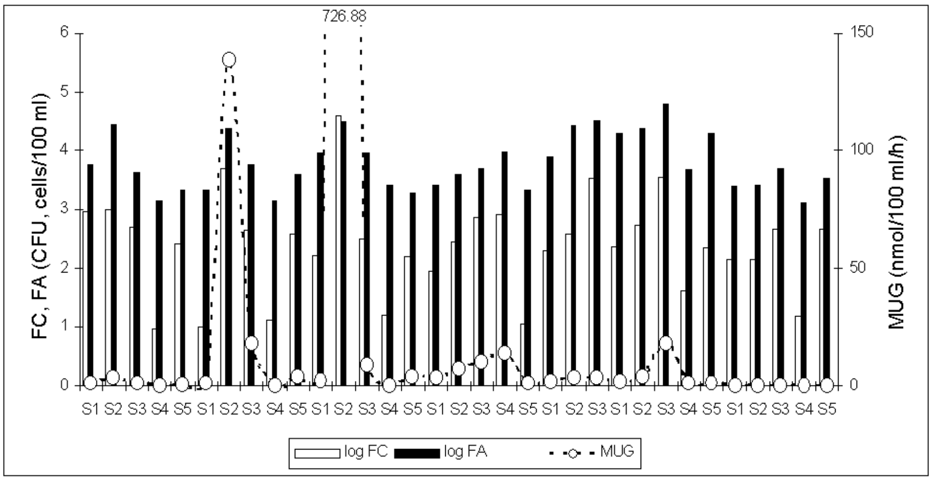

Figure 1: Cell counts (FA, FC) and MUG activity values found in Messina shoreline during April-May 2004

3.2 Assessment of bacterial viability: a seasonal study

Combined FA and viability staining protocols showed the occurrence of different physiological states of *E. coli*, depending on the different seasons. While total FA counts did not change significantly, MUG rates revealed active metabolising cells in autumn and spring. In summer, a low percentage (0.22% of the total) of culturable (FC) cells occurred, while the concentration of dead (PI+) cells increased (18.69% of the total), probably due to solar irradiance. In autumn, the percentage of CTC+ cells increased (49.58% of the total), unlike that of membrane damaged PI+ cells (3.79% of the total only). In winter, the high number of culturable cells (54.45% of the total) suggested continental runoff was an important source of pathogens or organic matter supporting bacterial survival. A high percentage of cells (26.08% of the total), however, became membrane damaged (PI+), or overcame adverse environmental conditions with a decrease of their metabolism and active respiration, as suggested by low MUG activity rates and CTC+ cells (19.47% of the total), respectively. In spring, temperature increased favouring the recovery of metabolic functions, as suggested by the increase of CTC+ cells (85.85% of the total) and MUG rates.

3.3 Detection of *E. faecium*

The distribution of *E. faecium* detected by FA followed similar trends to that of enterococci determined by plate method, although microscopical counts were 1-2 orders of magnitude higher than plate counts (range: 4.20×10^3-5.49×10^4 cells/100ml versus 1×10^1-9.9×10^3 CFU/100ml). Student's t value ($t=1.09 \times 10^{-4}$, $P<0.05$) confirmed the lack of statistical differences between the two methods.

4 Conclusions

Results of our studies show that real-time information on the hygienic-sanitary quality of seawater can be achieved through rapid analytical protocols which detect bacteria or their metabolic activites as effective bioindicators of marine pollution. The obtained data proved the suitability of FA and MUG methods for the detection of target bacterial pathogens, as alternative approaches to culture counts. Both methods can be applied for early warning of faecal pollution episodes, making results available in fast response times (less than 4 h) and with reduced costs. Coupling new rapid methods with advanced monitoring systems, such as automatic programmable multi-samplers installed on monitoring platforms [18], the early identification of critical zones affected by heavy sewage pollution is possible, allowing to quickly set up restoration measures. The combination of both new technological and methodological approaches can be considered the challenge strategy for easy control and safeguarding coastal marine environments in next years. Therefore, it is to be hoped that research in this field is continued in the future, since further developments and updates will provide end-users with suitable tools for achieving near real-time data on environmental status.

References

[1] M. Pommepuy, D. Hervio-Heath, M. Gourmelon, M.P. Caprais, et al. Emerging pathogens in coastal areas. *CIESM Workshop Monographs,Novel contaminants and pathogens in coastal waters*, 26:79–85, 2004.

[2] N. Ashbolt, W.O.K. Grabow, and M. Snozzi. Indicators of microbial water quality. *Water Quality: Guidelines, Standards and Health*, pages 289–316, 2001.

[3] WHO (World Health Organization). Bathing water quality and human health: fecal pollution. Outcome of an Expert Consultation. pages 1–158, 2001.

[4] S.C. Edberg, E.W. Rice, R.J. Karlin, and M.J. Allen. *Escherichia coli*: the best biological drinking water indicator for public health protection. *J. Appl. Microbiol.*, Suppl.88:106S–116S, 2000.

[5] G. Caruso, E. Crisafi, and M. Mancuso. Development of an enzyme assay for rapid assessment of *Escherichia coli* in seawaters. *J. Appl. Microbiol.*, 93(4):548–556, 2002.

[6] D.P. Sartory and J. Watkins. Conventional culture for water quality assessment: is there a future? *J. Appl. Microbiol.*, Suppl.85:225S–233S, 1999.

[7] G. Caruso, R. Denaro, M. Genovese, L. Giuliano, M. Mancuso, and M.M. Yakimov. New methodological strategies for detecting bacterial indicators. *Chem. Ecol.*, 20(3):167–181, 2004.

[8] Y. Rozen and S. Belkin. Survival of enteric bacteria in seawater. *FEMS Microbiol. Rev.*, 25:513–519, 2001.

[9] R. Zaccone, E. Crisafi, and G. Caruso. Evaluation of fecal pollution in coastal Italian waters by immunofluorescence. *Aquat. Microb. Ecol.*, 9(1):79–85, 1995.

[10] G. Caruso, R. Zaccone, and E. Crisafi. Use of the indirect immunofluorescence method for detection and enumeration of *Escherichia coli* in seawater samples. *Lett. Appl. Microbiol*, 31(4):274–278, 2000.

[11] G. Caruso, F. De Pasquale, M. Mancuso, D. Zampino, and E. Crisafi. Fluorescent antibody-viability staining and enzyme methods as rapid tools for monitoring *Escherichia coli* viability in coastal marine waters. *J. Immunoassay Immunochem.*, 27(1):1–13, 2006.

[12] T.L. Maugeri, R. Zaccone, G. Caruso, E. Crisafi, and C. Gugliandolo. Examen de la qualitè de l'eau de mer par immunofluorescence. *Rapp. Comm. Int. Mer Médit. (CIESM)*, 33:199, 1992.

[13] G. Caruso, L.S. Monticelli, R. Caruso, and A. Bergamasco. Development of a fluorescent antibody method for the detection and enumeration of *Enterococcus faecium* and its potential for coastal aquatic environment monitoring. *Mar. Poll. Bull.*, 56(2):318–324, 2008.

[14] G. Caruso, M. Mancuso, and E. Crisafi. Combined fluorescent antibody assay and viability staining for the assessment of the physiological states of *Escherichia coli* in seawaters. *J. Appl. Microbiol.*, 95(2):225–233, 2003.

[15] I. George, M. Petit, and P. Servais. Use of enzymatic methods for rapid enumeration of coliforms in freshwaters. *J. Appl. Microbiol.*, 88(3):404–413, 2000.

[16] P. Lebaron, A. Henry, A.S. Lepeuple, G. Pena, and P. Servais. An operational method for the real-time monitoring of *Escherichia coli* numbers in bathing waters. *Mar. Poll. Bull.*, 50(6):652–659, 2005.

[17] G. Caruso, E. Crisafi, and M. Mancuso. Immunofluorescence detection of *Escherichia coli* in seawaters: a comparison of different commercial antisera. *J. Immunoassay Immunochem.*, 23(4):479–496, 2002.

[18] G. Zappalà, G. Caruso, and E. Crisafi. Coastal pollution monitoring by an automatic multisampler coupled with a fluorescent antibody assay. *Coastal Environment V, Proceedings*, pages 125–133, 2004.

A Comparison Study of Six Mediterranean Lagoons with Numerical Modelling

G. Umgiesser[1], C. Ferrarin[2], A. Cucco[2], F. De Pascalis[1], M. Ghezzo[1], D. Bellafiore[1], M. Bajo[1], A.P. Ruzafa[3]
1, Institute of Marine Sciences, CNR, Venezia, Italy
2, Institute for Coastal Marine Environment, CNR, Oristano, Italy
3, Department of Ecology and Hydrology, Faculty of Biology, University of Murcia, Spain
georg.umgiesser@ve.ismar.cnr.it

Abstract

A numerical model (SHYFEM) has been applied to 6 Mediterranean lagoons and a comparison study between the lagoons has been carried out. The lagoons are the Venice lagoon and the Marano-Grado lagoon in the Northern Adriatic Sea, the Taranto basin in the Ionian Sea, the Cabras lagoon in Sardinia, the Mar Menor in Spain and the Nador lagoon in Morocco. These environments range from a leaky type of lagoons to a choked type and give a representative picture of the lagoons situated around the Mediterranean basin. This study has been mainly focused on hydrodynamics, exchange rates and residence time description. Wind and tidal stirring, which are the main forcings, normally prevent the lagoons from developing stratification, which justifies the application of the 2D version of the model. The exchange rate depends mainly on the inlet configuration, but also on the wind regimes in the case of multi-inlet lagoons. Residence time, which is mostly determined by the exchange rate, is a powerful concept that allows lagoons to be characterized with a time scale. In the case of the studied lagoons the residence time ranged from some days in the Marano-Grado lagoon to up to one year in the case of the Mar Menor. The analysis of the residence time frequency distribution allows identifying sub-basin and seasonal variations in the renewal time. The numerical study proved to be a powerful tool for the inter-comparison of the lagoons.

1 Introduction

Lagoons are highly productive areas that are situated in the transitional areas at the land-ocean boundary. They are important to mankind because many industrial, commercial and recreational activities are concentrated in these regions. The need to manage this part of the coastal zone makes it of paramount interest to understand processes occurring in these water bodies. In recent years these areas have become important because they provide the key to understand the general dynamics of the seas they are connected with. Their existence and their influence on the coastal zones have become a fundamental study topic in many disciplines. Comparisons between lagoons have been frequently proposed in literature. However, an extensive comparison study carried out with numerical modeling has never been applied. This is partly due to the complexity to set up, calibrate, validate and run a model for more lagoons. It is also a problem of methodology, because using results from applications of different models could bias the outputs. This is similar to the use of data collected with different sampling strategies and elaboration.

When trying to classify lagoons various parameters have been proposed, such as morphological parameters (area, volume, number of inlets), physical parameters (salinity, temperature) and various time scales such as flushing time and residence time. The last parameter deals with the openness of lagoons, and its exchange capabilities with the open sea. It is therefore an important parameter also for other processes, such as ecological evolution and pollution dispersion.

In this work a comparative study is proposed that uses the numerical model SHYFEM [1] applied to six Mediterranean lagoons. The applied model is therefore the same for all lagoons, assuring uniformity in the model results. The model has previously been applied and calibrated to all lagoons. This means that the model application deals with real data and that the results have already been verified.

In this work a classification of the lagoons is carried out using computed parameters such as fluxes, tidal prism and residence time. Using the distribution of the residence time inside the basins has also allowed to distinguish between different water bodies inside the same lagoon. This approach is important if lagoons cannot be considered homogeneous enough to be treated as a single entity. In this case numerical studies are needed as the ones presented here.

2 Description of Sites

In this work six Mediterranean lagoons have been studied. In the following an overview of the study sites is given and their characteristics are presented. Please see Figure 1 for reference.

Venice Lagoon: The Venice lagoon is located in the northwest Adriatic Sea (45° 12' N) and is the largest Mediterranean lagoon (surface 500 $km^{2,}$ vertical north-south length 50 km, mean horizontal width 15 km, Figure 1). Around 415 km^2 are subject to tidal excursion, the other areas are diked to create fish farms with water exchanges limited and regulated artificially [2]. Three inlets connect the lagoon with the open sea (Lido, Malamocco and Chioggia, from north to south with mean depth 14, 17 and 8 m respectively). The bathymetry is characterized by the presence of navigable channels, tidal flats and shoals. The latter ones can either be wet or dry depending on tidal level. Only 5 % of the lagoon area has a depth greater than 5 m and 75 % is shallower than 2 m. The mean depth is 1.5 m, but there are areas deeper than 30 m [3].

The Venice Lagoon is microtidal with mean tidal range from 50 cm during neap tide to 100 cm during spring tide. The mean water volume of the lagoon is around $632 \cdot 10^6$ m^3 and the exchange of water through the inlet in each tidal cycle is about a third of the total volume of the lagoon [4]. The tidal exchange of seawater and the freshwater input from river runoff define the brackish characteristics and the presence of seasonal spatial gradients in the distribution of the abiotic and biotic variables.

Marano-Grado Lagoon: The lagoon of Marano-Grado, in the northeaster part of the Adriatic Sea (Italy), is delimited by the

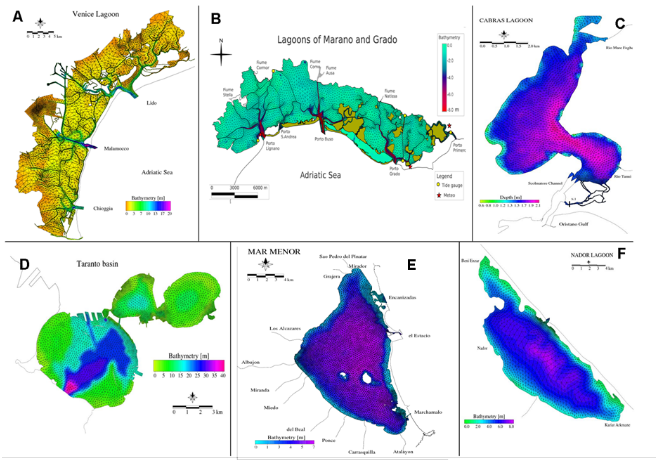

Figure 1: Grid and bathymetry of the six studied Mediterranean Lagoons, a) Venice Lagoon, b) Marano-Grado Lagoon, c) Cabras Lagoon, d) Taranto Sea, e) Mar Menor and f) Nador Lagoon.

rivers Isonzo and Tagliamento, and it is separated from the sea by a long shore bar composed by isles and more or less persistent sand banks (Figure 1). The area stretches out for about 16,000 ha, with a length of nearly 32 km and an average width of 5 km. Most of the lagoon is covered by tidal flats and salt marshes and some areas are constantly submerged (tidal channels and subtidal zones).

The lagoon system of Marano-Grado has been always formally divided in two major sub-basins: the lagoon of Marano and the lagoon of Grado. The Marano lagoon is a semi enclosed tidal basin, limited by the Tagliamento River delta westward. It is shallow, with a few areas above the sea level and several channels, receiving freshwaters from the adjacent rivers. Conversely, the Grado lagoon is shallower, has a series of morphological islands and marshes, and receives freshwater from a single tributary, the Natissa River [5]. The overall amount of average freshwater discharge was estimated to be 70-80 m^3/s, [6]. The lagoon basin is characterized by semi-diurnal tidal fluxes (65 and 105 cm mean and spring tidal range, respectively).

Taranto Sea: The Taranto Sea represents a coastal marine ecosystem that has been gradually modified by mankind. It is situated in the Ionian Sea in southern Italy and it is composed of two parts: the Mar Grande and the Mar Piccolo (see Figure 1). The Mar Grande covers an area of 35 km^2 with a maximum depth of about 42 m and an average depth of about 12 m. It connects with the Ionian Sea through two openings. The first one is about 1 km wide and is situated in the southern part of the basin, between S. Paolo Island and Capo S. Vito. The second one is about 100 m wide, located in the northwestern part of the Mar Grande near Punta Rondinella.

The Mar Piccolo of Taranto has a total surface area of 20.72 km^2 structured in two shelves, the 'First Seno' and the 'Second Seno'. The maximum depth is about 15 m for the First Seno and about 10 m for the Second Seno. The average depth of the two subsystems is about 5 m [7]. The Mar Piccolo is connected to the Mar Grande by two narrow channels, along the island of the old town of Taranto, the Navigabile channel and the Porta di Napoli channel. The Mar Piccolo is characterized by the presence of about 30 submarine fresh water springs, locally called 'Citri'.

Cabras Lagoon: The Cabras lagoon is a shallow water body (mean depth 1.7 m) located on the west coast of Sardinia, western Mediterranean Sea (39° 57' N, 8 29' E), and is one of the largest brackish water basins in the Mediterranean region with a surface of 20 km^2. The lagoon of Cabras extends normal to the shoreline and is connected to the Oristano gulf by means of a net of small creeks flowing into the main open channel, the Scolmatore channel. The northern part of the lagoon is connected to a small river, the Rio Tanui, which represents the major source of freshwater. A smaller river, the Rio Mare Foghe, enters in the southern lagoon sub-basin.

River discharge is rather limited due to a low rainfall regime in the region. The lagoon salinity may drop to 10 psu during rainfall periods and rise up to 30 psu, especially in summer. The tidal amplitude is $\pm$20 cm. As such water exchange between the lagoon and the coastal systems is very limited.

From the hydrological standpoint, the lagoon can be subdivided into 2 sub-basins, a northern one and a southern one. The lagoon, due to its morphology, responds rapidly to changes in forcing and is therefore characterized by wide temporal and spatial fluctuations in environmental variables.

Mar Menor: The Mar Menor is a choked and hyper-saline coastal lagoon, with a surface area of 136 km^2 located in SE Spain, a semi-arid region of the SW Mediterranean coastline (37° 42' N / 00° 47' W). The lagoon has a mean depth of 4.4 m and maximum of about 7 m. Water temperature shows a regular seasonal cycle with a maximum reached in August (30 °C) and a minimum in February (11.2 °C). Salinity shows heterogeneous spatial and temporal distribution depending on season, rainfall, runoff and Mediterranean influence through the main inlets, with a minimum of 38.1 and a maximum of 51 psu [8]. In general, hydrographic conditions permit to differentiate three different sub-basins [8]. The mean annual rainfall is less than 300 mm$\cdot$yr^{-1} and potential evapo-transpiration is close to 900 mm$\cdot$yr^{-1} [9, 8]. The hydrologic balance shows an annual deficit of above 600 mm/yr. Climatic and hydrologic features coupled to the geomorphology of the lagoon make it behave like a concentration basin.

Nador Lagoon: The Nador lagoon is situated in the Mediterranean coast of Morocco, at about 35° N. The lagoon basin has a volume of about 5.4$\cdot$10^8 m^3 and a surface of about 110 km^2. The lagoon has an oval shape, quite regular, and a single inlet. The length of the major axis of the lagoon is about 23 km, while for the minor axis is $\sim$7 km. The width of the inlet is about 130 m. The average depth of the lagoon is 4.8 m, with a maximum depth of 8 m. Small water discharges from some channels exist, but they are not important for the dynamics of the lagoon. The rainfall is of about 300 mm$\cdot$yr^{-1} and the prevalent wind come from W-NW and E, which is about the direction of the major axis of the lagoon.

Along the coast of the lagoon the city of Nador and other smaller settlements are present. The main human activities are iron and steel industry and the Beni Ansar harbor. These activities and the presence of the human settlements cause considerable water pollution.

3 Methods

3.1 Model Description

The hydrodynamic model SHYFEM here applied has been developed at ISMAR-CNR (Institute of Marine Science - National Research Council) [1]. It has already been applied successfully to several coastal environments [10, 11, 12, 13, 14, 15, 16, 17].

The finite element method permits to reproduce complex morphologies and bathymetries. The model resolves the shallow water equations in their formulations with water levels and transports.

The bottom friction is computed introducing the Strickler formulation, so that the friction coefficient is not a constant but varies with the water depth.

At the open boundaries the water levels are prescribed in accordance with the Dirichlet condition, while at the closed boundaries only the normal velocity is set to zero and the tangential velocity is a free parameter.

The model uses a semi-implicit algorithm for integration in time, which combines the advantages of the explicit and the implicit scheme. The terms treated semi-implicitly are the divergence term in the continuity equation and the Coriolis term and the barotropic pressure gradient term in the momentum equation. The bottom friction term in the momentum equation is treated fully implicitly, whereas all other terms are treated explicitly. It is unconditionally stable with respect to the gravity waves, the bottom friction and the Coriolis terms and allows the transport variables to be solved explicitly without solving a linear system. Compared to a fully implicit solution of the shallow water equations solving a linear system for the water levels, it reduces the dimensions of the matrix to one third. The spatial discretization of the unknowns has been carried out with the finite element method, partially modified with respect to the classic formulation. This approach was necessary to avoid high numerical damping and mass conservation problems, due to the combination of the semi-implicit method with the finite element scheme (Galerkin method). With respect to the original formulation, here the water level and the velocities (transports) are described by using form functions of different orders, being the standard linear form function for the water level, but stepwise constant form function for the transports. This will result in a grid that resembles a staggered grid often used in finite difference discretization. A more detailed description of the model equations and of the discretization method is given in [1].

3.2 The transport time scales

The water transport time scale has been used as fundamental parameter for the understanding of the ecological dynamics in lagoon environments [18]. In this work, assuming that advection and diffusion can be reasonably considered the main physical processes that influence the cleaning capacity of a lagoon ecosystem water compartment, two parameters are used to compute the water transport time, the Water Residence Time (WRT) and the Flushing Time (FT). The former parameter has been already been computed for the Venice Lagoon [13, 19] and the computed water res-

idence time agrees well with the apparent age of water calculated using the ratio of 224Ra and 228Ra ([20], in press). An exhaustive description of these transport time scales is given in [19].
In this study the Eulerian water residence time, WRT, has been defined as the time required for each element of the lagoon area to replace most of the mass of a conservative tracer, originally released inside the basin, with new water. More precisely, it is the time it takes for the concentration to reach 1/e of its initial value (e-folding time scale).
To compute the spreading and the fate of the tracer, a solute transport model has been used. The model solves the advection and diffusion equation.
The flushing time (FT) is the theoretical time necessary to replace the complete volume of the lagoon V with new water coming from the sea and from the rivers. If the in-going water flux is Q then the flushing time can be computed as FT = V / Q. The fluxes Q can be approximately computed through the tidal prism method. Please note that the flushing time becomes equal to the residence time in case the basin can be assumed well mixed.

3.3 Model Setup

A common model setup has been chosen for the simulations in the six Mediterranean Lagoons. The model runs in a 2D mode, with the non-linear advective terms and Smagorinski viscosity in the momentum equations. The temperature and salinity advection is computed. Heat fluxes are not computed while water fluxes between air and sea consist in the prescribed precipitation value minus the evaporation value computed by the SHYFEM model. Only for the Nador Lagoon both heat and water fluxes are neglected. The applied forcings for each simulation are wind, tides and freshwater river runoff. Forcings, initial and boundary conditions are imposed using measured values (wind, sea surface height, temperature and salinity), where available (Venice Lagoon, Marano-Grado Lagoon), and extracting time series from models, if missing (Nador Lagoon). For river runoff values, where daily data were not available, regression techniques from precipitation data (Cabras Lagoon) or runoff coefficients for each river, knowing the total basin freshwater input (Mar Menor), have been used. For Nador Lagoon no river discharges are considered, since they give negligible contribution to the dynamics of the system.

4 Results and Discussion

For each lagoon more than one simulation has been run for the year chosen in this study. Typical residence times computed for most of the studied lagoons are fractions of one year and this gave a possibility to repeat computations of residence times during the year. It also gives a possibility to compute the temporal variation and a statistical average of the residence time. In the case of Mar Menor only one replica has been computed, being the residence time longer than one year. Four repetitions have been performed for Taranto Sea, Cabras Lagoon and Nador Lagoon, six for Venice Lagoon and twelve for Marano-Grado Lagoon. In Table 1 values of basin area, flux at the inlets, tidal prism, water residence time (WRT) and flushing time (FT), for each lagoon, are provided. As is evident, values of FT are always much lower than WRT ones. As explained in section 3.2 FT and WRT values are equal only if the la-

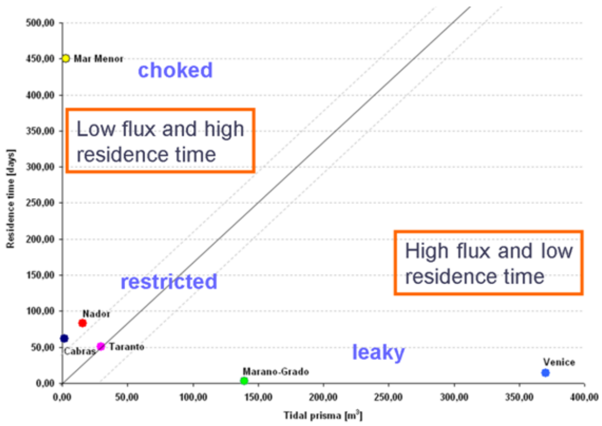

Figure 2: Classification of the six Mediterranean lagoons based on tidal prism and residence time values.

Lagoon	Area [km^2]	Flux [m^3/s]	Tidal Prism [$10^6\,m^3$]	WRT [days]	FT [days]
Venice	415.08	4288.19	370.50	14.6	1.7
Marano-Grado	131.62	1616.69	139.68	2.7	0.8
Taranto	56.77	342.25	29.57	50.7	22.7
Cabras	20.11	18.60	1.61	61.4	20.9
Mar Menor	136.06	30.28	2.61	450.0	229.0
Nador	110.92	179.85	15.54	83.0	34.5

Table 1: Table with basin areas, flux, tidal prism, residence time (WRT) and flushing time (FT) for the six studied lagoons.

goon is well mixed. Therefore, our results could be interpreted as an index of the different hydrodynamic behavior that characterizes the spatial heterogeneity inside the lagoons.
Following Kjerve [21], a classification of the studied lagoons on the basis of their average residence time and tidal prism has been carried out. The graph shown in Figure 2 identifies the Venice Lagoon and the Marano-Grado Lagoons as examples of leaky lagoons, the Taranto Sea, Cabras and Nador Lagoons as restricted lagoon, while the Mar Menor belongs to the choked type.
More than one value of residence times has been computed during the year, also to be able to provide a sort of seasonality, in the cases where WRT are fractions of the year. This kind of analysis, shown in Figure 3, has not been possible in the case of Mar Menor, where WRT is longer than one year. As can be seen from Figure 3, every lagoon shows longer residence times during the summer season, probably due to the main action of evaporation, with low precipitation and limited injections of freshwater from rivers, and a calmer situation of the wind regimes. A different behavior can

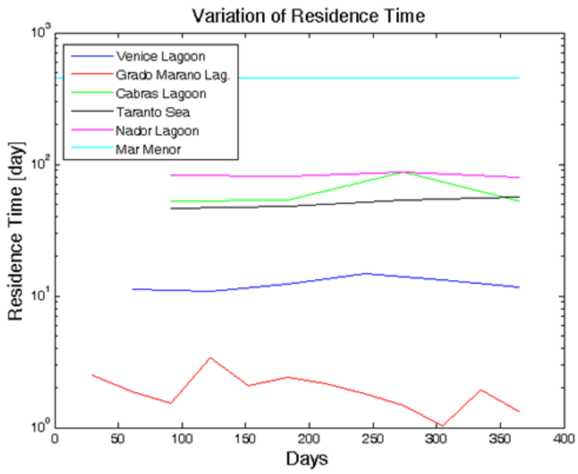

Figure 3: Water Residence Times for the six Mediterranean Lagoons, computed for each repetition during the simulated year.

be seen for Marano-Grado Lagoon where residence time is strongly dependent on local meteo-marine conditions. In fact, even a short storm can enhance the exchanges with the sea decreasing residence time over the whole lagoon. Variations are of the order of some days for Marano-Grado Lagoon, while bigger differences during the year are registered for the other lagoons (tens of days).

Finally graphs of the residence time frequency have been analyzed. This analysis consists in defining the percentage of the lagoon area characterized by a certain residence time. Four examples, Venice Lagoon, Taranto Sea, Mar Menor and Nador Lagoon, are shown in Figure 4.

For the Venice Lagoon a typical frequency curve for a tidal lagoon can be seen. It shows a uni-modal distribution with one maximum corresponding to a WRT of around 16 days, which is also close to the average WRT of 14.6 days of the lagoon (see Table 1 for reference).

Another uni-modal distribution can be seen for the Mar Menor. But now the maximum has been shifted to much higher values (450 days), with very low frequency values for low residence times. This might be due to an internal re-circulation cell that shows a spatially homogeneous high residence time, but that is very little participating in the exchange with the sea. The Mar Menor is a good example of a chocked lagoon.

The other two cases differ from the uni-modal curves seen before. The Taranto sea case shows a peculiar curve with three distinct peaks, corresponding to 60, 110 and 450 days. As is evident also from Figure 5, where residence time maps are shown, each of these values can be connected with one of the sub basins (Mar Grande, I Seno, II Seno). Finally for Nador Lagoon the major peak is around 100 days but some lower values identify secondary peaks that characterize the area around the inlet (Figure 5).

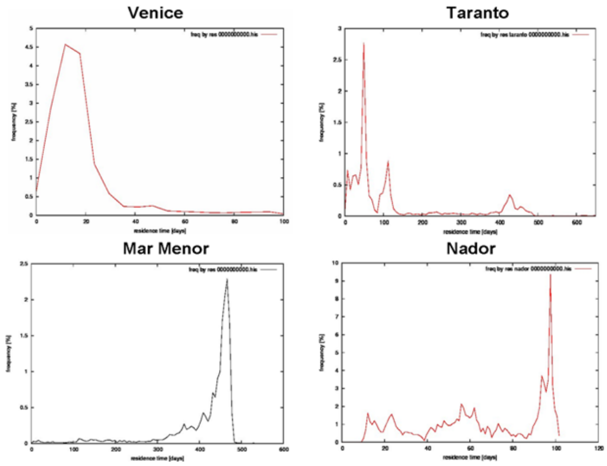

Figure 4: Residence time frequency graphs for Venice Lagoon, Taranto Sea, Mar Menor and Nador Lagoon.

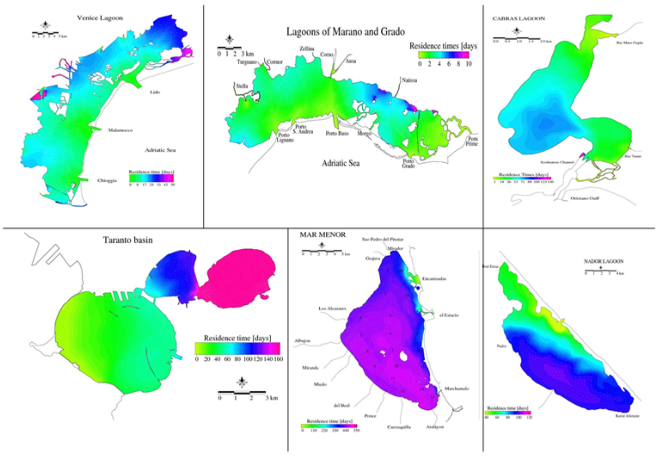

Figure 5: Residence time maps for the six Mediterranean lagoons.

5 Conclusions

A first attempt to use modeling as a suitable tool to classify and study the basic characteristics of a number of Mediterranean Lagoons has been presented. The studied parameters concern the hydrodynamics of lagoons, identifying residence time and interaction with the open sea they are connected with. Residence time and tidal prism have been used to classify six lagoons in leaky lagoons (Venice Lagoon, Marano-Grado Lagoon), restricted lagoons (Taranto Sea, Cabras and Nador) and choked lagoons (Mar Menor) and the analysis of residence time frequency and seasonal variation permitted to spatially and temporally characterize different water bodies inside each lagoon. In the next future a wider comparison will be performed, studying temperature and salinity fields and connecting the physical characteristics with other quantities (biological and ecological ones) to classify lagoons by means of numerical modeling.

6 Acknowledgments

The authors want to thank CMCC, VECTOR and ARPA-FVG for partial funding.

References

[1] G. Umgiesser, D. Melaku Canu, A. Cucco, and C. Solidoro. A finite element model for the Venice lagoon: Development, set up, calibration and validation. *Journal of Marine Systems*, 51:123–145, 2004.

[2] S. Guerzoni and D. Tagliapietra. *Atlante della Laguna - Venezia tra terra e mare*. Marsilio Editore, 2006.

[3] E. Molinaroli, S. Guerzoni, A. Sarretta, A. Cucco, and G. Umgiesser. Links between hydrology and sedimentology in the lagoon of Venice, Italy. *Journal of Marine Systems*, 68:303–317, 2007.

[4] M. Gačić, I. M. Mosquera, V. Kovacevic, A. Mazzoldi, V. Cardin, F. Arena, and F. Gelsi. Temporal variation of water flow between the Venetian lagoon and the open sea. *Journal of Marine Systems*, 51:33–47, 2004.

[5] R. Marocco. Sediment distribution and dispersal in northern Adriatic lagoons (Marano and Grado paralic system). *Geologia*, 57(12):77–89, 1995.

[6] M. Ret. Bilancio idrologico e circolazione idrica della laguna di Marano e Grado. Master's thesis, Faculty of Engineering, University of Udine, Italy, 2006.

[7] M. Pastore. *Mar Piccolo*. Nuova Editrice Apulia, Martina Franca, Taranto, 1993.

[8] A. Perez-Ruzafa, A. I. Fernandez, C. Marcos, J. Gilabert, J. I. Quispe, and J. A. Garcia-Charton. Spatial and temporal variations of hydrological conditions, nutrients and chlorophyll a in a Mediterranean coastal lagoon (Mar Menor, Spain). *Hydrobiologia*, 550:11–27, 2005.

[9] F. L. Bermudez, L. Ramirez, and P. M. de Agar. Analisis integral del medio natural en la planificacion territorial: el ejemplo del Mar Menor, 1981. (VII) Murcia 18, 11-20.

[10] I. Scroccaro, R. Matarrese, and G. Umgiesser. Application of a finite element model to the Taranto Sea. *Chemistry and Ecology*, 20 (Supplement 1):205–224, 2004.

[11] C. Ferrarin and G. Umgiesser. Hydrodynamic modeling of a coastal lagoon: the Cabras lagoon in Sardinia, Italy. *Ecological Modelling*, 188(2-4):340–357, 2005.

[12] G. Umgiesser, J. Chao, M. Bajo, I. Scroccaro, and A. Cucco. Residence time modelling in the Nador lagoon, Morocco. In F. Veloso Gomes, F. Taveira Pinto, L. das Neves, A. Sena, and O. Ferreira, editors, *Proceedings of the First International Conference on Coastal Conservation and Management in the Atlantic and Mediterranean (ICCCM'05)*, pages 389–397, 2005.

[13] A. Cucco and G. Umgiesser. Modeling the Venice lagoon residence time. *Ecological Modelling*, 193 (1-2):34–51, 2006.

[14] C. Ferrarin, A. Razinkovas, S. Gulbinskas, G. Umgiesser, and L. Bliudziue. Hydraulic regime based zonation scheme of the Curonian lagoon. *Hydrobiologia*, 611(1):133–146, 2008.

[15] D. Bellafiore, G. Umgiesser, and A. Cucco. Modeling the water exchange between the Venice lagoon and the Adriatic Sea. *Ocean Dynamics*, 58:397–413, 2008.

[16] C. Ferrarin, G. Umgiesser, I. Scroccaro, and G. Mattassi. Hydrodynamic modeling of the lagoons of Marano and Grado, Italy. In *Sedimentary Processes and Deposits within River-Sea Systems, Proceedings of Euro-EcoGeoCentre-Romania, Tusnad, Romania*, pages 13–19. Geo-Eco-Marina 15/2009, Bucaresti-Constanta, 2009.

[17] F. De Pascalis, A. Perez-Ruzafa, J. Gilabert, G. Umgiesser, and C. Marcos. Implementation of a numerical model in the Mar Menor coastal lagoon (Spain). *Hydrology*, 2010. (Submitted).

[18] W. Gong, J. Shen, and J. Jia. The impact of human activities on the flushing properties of a semi-enclosed lagoon: Xiaohai, Hainan, China. *Marine Environmental Research*, 65(1):62–76, 2008.

[19] A. Cucco, G. Umgiesser, C. Ferrarin, A. Perilli, D. Melaku Canu, and C. Solidoro. Eulerian and lagrangian transport time scales of a tidal active coastal basin. *Ecological Modelling*, 220:913–922, 2009.

[20] J. Rapaglia, C. Ferrarin, L. Zaggia, W. S. Moore, G. Umgiesser, E. Garcia-Solsona, J. Garcia-Orellana, and P. Masque. Investigation of residence time and groundwater flux in the Venice lagoon; comparing radium isotope and hydrodynamic model. *Journal of Environmental Radioactivity*, 2010. (In press, available online).

[21] B. Kjerve. Comparative oceanography of coastal lagoons. In D. A. Wolfe, editor, *Estuarine Variability*, pages 63–81. Academic Press, New York, 1986.

Numerical Modeling of Storm Surge Forecast for the Venice Lagoon

G. Umgiesser[1], M. Bajo[1], A. Cucco[2], L. Zampato[3]
1, Institute of Marine Sciences, CNR, Venezia, Italy
2, Institute for Coastal Marine Environment, CNR, Oristano, Italy
3, Tidal Forecasting and Early Warning Centre, Venezia, Italy
georg.umgiesser@ve.ismar.cnr.it

Abstract

An accurate sea level prediction for the Venice Lagoon is of great importance to the historical city maintenance. Here an operational forecasting system of the sea level for the Venice Lagoon, based on a finite element numerical model, is presented. The model solves the shallow water equations on two different finite element grids representing the whole Mediterranean Sea and the Venice Lagoon.
The system has been operational for 7 years and runs at the Centre for sea level forecasting and flood warnings of the Venice Municipality (ICPSM). The hydrodynamic model provides a five-day forecast for the Mediterranean Sea and it is focused on the prediction of the surge near Venice. It has been refined during this period through several improvements such as spatially variable wind enhancement coefficients and a post-processing procedure.
Results show that the system is capable of achieving forecasts comparable to the statistical models that are presently used by the Venice municipality as their flooding warning system. In particular, for forecasting periods of 24 hours and longer, the system out-performs the statistical models. For the application of the post processing routines, results near Venice are extracted and improved using neural networks. This method reduces by half the average error of the hydrodynamic model for the first day forecast (standard deviation of the differences of 4 cm) and maintains good performances also for longer forecasts.

1 Introduction

The city of Venice is subject to frequent inundations, called Acqua Alta, that flood the streets, often covering a considerable part of the city.
In 1968, the Venice municipality established a centre for sea level forecasting and flood warning (Istituzione Centro Previsioni e Segnalazioni Maree, ICPSM) that issues daily water level forecasts. Until some years ago, only statistical models ran at the ICPSM Centre. Though they obtain good results in short-range prediction (about 12 hours), for long-range forecasts they rapidly loose accuracy.
Recently also two hydrodynamic models became operational. The one described in this paper [1], and a model based on finite differences [2]. The final subjective prediction made by the technicians of the Centre is based on results of all the models, both statistical and dynamic, and on the last observations of sea level and of meteorologi-

cal parameters available.
The actual operational model here presented has a simple data assimilation routine based on an Artificial Neural Network (ANN). This procedure resulted to be very useful to improve the sea level forecast [3], as the results here exposed will show.
In section 2 the methods used are reported. The hydrodynamic model and the ANN are described. An explanation of the operational system and of the calibration process of the ANN are also provided. In section 3 results are exposed with a statistical analysis and with the exposition of a case study. At the end, in section 4, the conclusions are reported.

2 Methods

2.1 The hydrodynamic model

A hydrodynamic model based on a finite element discretization technique was used. The model is named SHYFEM (Shallow water HYdrodynamic Finite Element Model) and was developed at ISMAR-CNR in Venice [4, 5]. The code is freely distributed by the authors.
The model solves the shallow water equations. In this application, since we are interested only in the storm surge prediction, the 2-dimensional version was used and no baroclinic terms were considered.
The equations of the model include the Coriolis terms, a meteorological term due to the inverse barometer effect and the wind stress and the bottom friction. The wind stress is described through the Smith and Banke formulation [6]. The variables computed by the model are the surge level due to the meteorological forcing and the barotropic transport. Interactions with tides and waves are not considered.
A staggered finite element technique is used for the spatial integration, while, for the temporal integration, different schemes for each term are used. The water level gradients, the Coriolis terms and the divergence terms in the continuity equation use a semi-implicit scheme. The bottom stress has a fully implicit scheme. All the other terms use an explicit scheme.

2.2 Meteorological data

In order to predict the storm surge, the model is forced with wind and atmospheric pressure forecast fields. The meteorological fields are provided by the European Centre for Medium-Range Weather Forecasts (ECMWF).
ECMWF supplies mean sea level pressure and surface wind fields over the Mediterranean area, at synoptic hours 00, 06, 12, 18 UTC and with a spatial resolution of 0.5 degree both in latitude and longitude. The fields are interpolated spatially on each node of the finite element grid of the Mediterranean Sea and temporally for each time iteration.
Their overall quality is good but their resolution is low for the Adriatic Sea, where the complicated orography along the coasts can create structures that are not reproduced [7]. To overcome these difficulties several attempts to correct the wind fields in the Adriatic Sea were made [8, 9]. The operational model uses a spatial correction of the wind speed in function of the wind direction [10].

2.3 Set-up

A diagram showing all the phases of the operational system is reported in Figure 1. The hydrodynamic model runs on a computational grid of the Mediterranean Sea

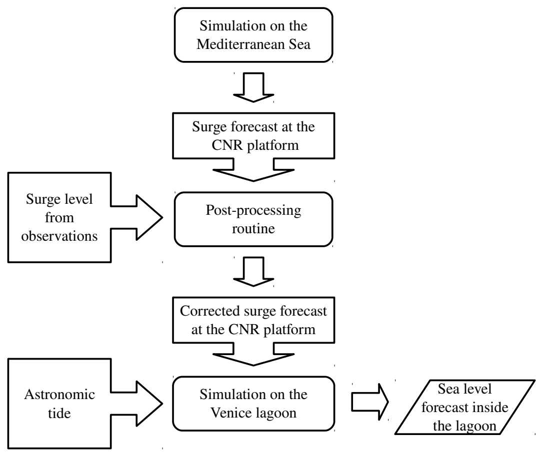

Figure 1: Diagram of the operational model. The hydrodynamic model is applied on two different grids. Between the two simulations the post-processing routine is applied to correct the results of the first simulation.

composed of 18,626 elements varying in size between 1.5 and 10 km in the Adriatic Sea and larger in the other parts (see Figure 2). The only open boundary is the Strait of Gibraltar, where the level is set to zero and fluxes are free. The surge level is extracted in a grid node near the Venice lagoon, 15 Km from the coast, in correspondence to the CNR oceanographic platform Acqua Alta. Then it is corrected applying a post-processing routine based on neural networks and a new time-series of surge level, composed by 120 forecast hours, is created. The new surge forecast is added to the astronomic tide and applied to the three inlets of the computational grid of the lagoon (see Figure 2), which represent the open boundaries of the grid. The simulation inside the lagoon provides the total sea level and currents. These are displayed through maps and time-series in the zones of interest (e.g., Punta Salute, Burano, Chioggia).

2.4 Post-processing by neural networks

2.4.1 The ANN

The ANN library used in this work is named Fast Artificial Neural Network (FANN). FANN is developed under LGPL (Lesser General Public License) by Steffen Nissen of the University of Copenhagen [11]. The library is written in C language and is freely downloadable from the web (http://leenissen.dk/fann). The network architecture is multilayer feedforward.

The FANN library allows to set many features of the neural network. The most important are the number of hidden layers, the number of neurons in each layer, the activation function, the learning rate and

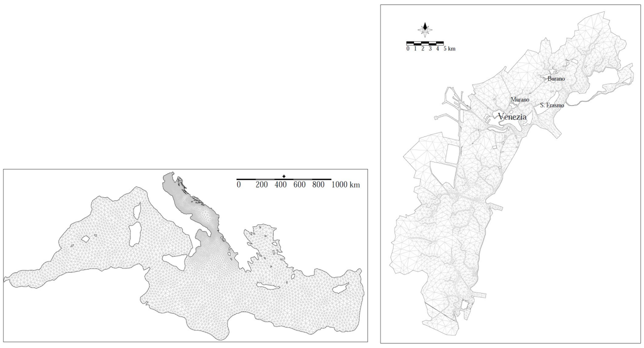

Figure 2: Computational grids of the Mediterranean Sea and of the Venice lagoon.

the training algorithm. In the present case a sigmoid activation function and a back-propagation training algorithm were used.

2.4.2 Implementation

The post-processing routine here described is a simple data assimilation technique to improve local model results at the CNR platform. Since the model forecast is 120-hours ahead, a different ANN is used for each forecast hour.
After each run of the model in the Mediterranean Sea, the hourly sea level observations recorded at the CNR platform are collected. Since the model runs the first hours of the day, the observations collected are the 24 values of the day before. The astronomic tide is subtracted and the residue is used as input for the neural network. Also the corresponding values computed by the model are collected, and the differences between these values and the residues coming from the observations are computed. The 24 differences are also used as input for the ANN.
The last three inputs to the network differs for each ANN depending on the forecast hour. They are the model values of the forecast hour, of one hour before and one hour after.
The ANNs were trained with a database of three years, from 2003 to 2005. Different network configurations were tested during the testing phase, with a database of 2006. The final ANNs have 51 input neurons, described before, 13 neurons in one hidden layer and 1 output neuron that provides the corrected surge level for the forecast hour represented by each ANN. Finally the ANNs were validated in a third phase, the validation phase, with the data of the year 2007.

3 Results

3.1 Statistical evaluation

For each forecast hour the differences between the surge computed by the model and the one coming from the observations were computed to evaluate the model performances. The same differences were computed also for the post-processed surge. The mean and standard deviation of the differences for the validation phase (2007) are reported in Table 1. Daily av-

eraged values are reported for the distributions relative to the model data (Mod) and the ones relative to the post-processed data (FANN). The last two columns of the table report also the correlation coefficients with the surge computed from the observations. The post-processed results show a good performance. The mean values are strongly reduced and now have values near to zero (see Table 1). For all the forecast days the mean values is lower than 4 cm.
For the post-processed data, the standard deviation of the differences (Std FANN) is considerably lower. The results of the model without post-processing (Mod) have an average standard deviation of 9.4 cm both during the first day of forecast and in the second one. The post-processed results, as it is possible to see in Table 1, the standard deviation has an average value of 4.7 cm for the first day of forecast. In the second day the standard deviation has a value of 6.2 cm. This represent a strong improvement with respect to the results of the hydrodynamic model. For longer forecast lags, more than 48 hours, the standard deviation has an average improvement of about 2 cm with respect to the model results without post-processing.
The correlation coefficients reported in the Table 1 are plotted in Figure 3. It is possible to see as the post-processing routine strongly changes the accuracy for short and medium forecasts. The correlation coefficient of the model (Mod) data have a constant trend in the first part of the forecast. On the contrary, the post-processed data (FANN) have a linear trend during the whole forecast period. However a good improvement is present also for the long forecast.

3.2 A case study

In Figure 4 the forecasts at 5, 3 and 1 day ahead of a flood event that happened in 2006 are presented. The observed total sea level (Obs), the one computed by the model (Mod) and the post-processed one (FANN), are represented. The event was not very strong, the sea level reached a maximum value of 103 cm at 10:00 CET at the CNR platform. However, the model strongly overestimated the event. In Figure 4, top panel, the 5-days forecast is shown. The model gives an estimation of the peak of almost 150 cm, more than 40 cm with respect to the observed one. The post-processed surge is much more accurate during all the forecast period and succeed in giving a good estimation of the peak. Looking at the 3-day and 1-day forecast, in the central and bottom plots, it is possible to see how the post-processed surge is better than the original one in each part of the curves and maintains a good estimation of the maximum peak. This is in general the most important information for the ICPSM Centre, since the population has to be alerted in case of floods of the City. This case study shows as the post-processing routine is able to avoid possible false alarms.

4 Conclusions

In this paper an operational hydrodynamic model for the surge forecast in Venice was presented. A post-processing method, based on the use of neural networks to improve the surge prediction, has been developed and validated. A mean standard deviation of the differences of 4.7 cm was obtained for the first forecast day and a value of 8.9 cm for the fifth day. The accuracy of the fifth day of forecast is now higher

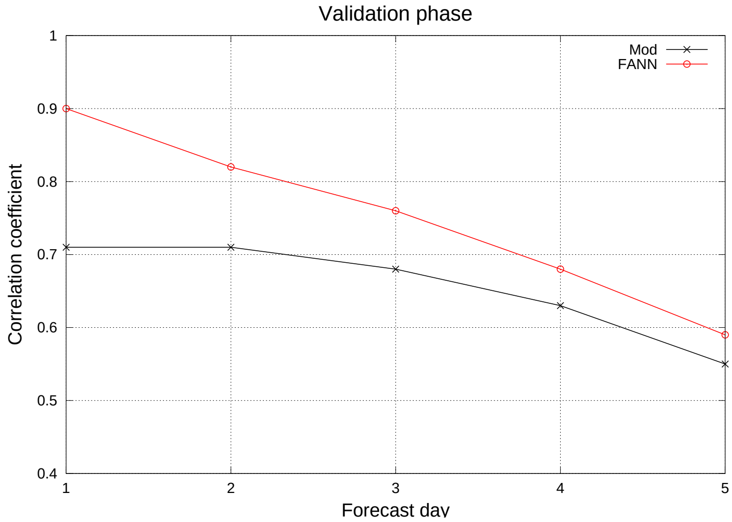

Figure 3: Correlation coefficients for each day of forecast relative to the model results (Mod) and to the post-processed data (FANN).

than the one of the first day of the model without the ANN correction that is of 9.4 cm (see Table 1). The method has obtained good results also in reducing the systematic errors of the model expressed by the mean values of the differences. The quality of the post-processed routine is demonstrated also by the correlation coefficients. Now the correlation coefficient of the first day forecast with the observations reaches a value of 0.9.
Though in this paper only non operational results are reported, the system is running for more than one year and the expectations seem confirmed.
Further improvements of the system can be obtained adding other inputs to the ANN, for example the residual level in other locations of the Adriatic Sea, atmospheric pressure gradients, and wind speed and direction.
Meteorological quantities both from observations and from forecasts can be used. A new training of the ANN with more data is also necessary.

5 Acknowledgements

This work was funded by the ICPSM Centre and partially supported by the projects CMCC and VECTOR. We especially thank Ing. Paolo Canestrelli for his advice. We thanks also Dr. Steffen Nissen, the creator of the FANN library and Dr. Aleardo Zuliani from ISMAR-CNR of Venice.

Forecast day	Std. Dev.		Mean		Corr. coeff.	
	Mod	FANN	Mod	FANN	Mod	FANN
1-day	0.094	0.047	0.023	0.002	0.71	0.90
2-day	0.094	0.062	0.023	0.004	0.71	0.82
3-day	0.095	0.071	0.018	0.003	0.68	0.76
4-day	0.105	0.080	0.016	0.002	0.63	0.68
5-day	0.115	0.089	0.012	0.000	0.55	0.59

Table 1: Standard deviations, means of the differences (in metres) and correlation coefficients for the model results (Mod) and the post-processed results (FANN). All the quantities are computed for the validation phase and are averaged over each forecast day.

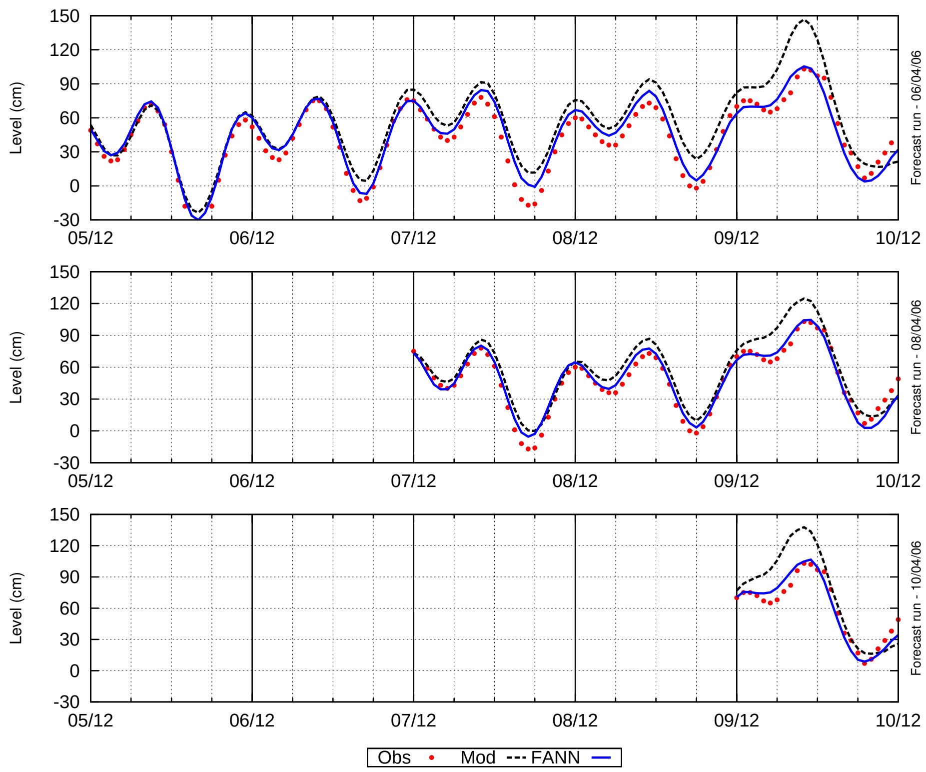

Figure 4: Forecasts at 5, 3 and 1 day ahead of a storm surge event happened on December 09, 2006. The observed total sea level (Obs), the one computed by the model (Mod) and the post-processed one (FANN), are represented.

References

[1] M. Bajo, L. Zampato, G. Umgiesser, A. Cucco, and P. Canestrelli. A finite element operational model for storm surge prediction in Venice. *Estuarine Coastal and Shelf Science*, 75(1-2):236–249, 2007.

[2] P. Lionello, A. Sanna, E. Elvini, and R. Mufato. A data assimilation procedure for operational prediction of the storm surge in the northern Adriatic Sea. *Continental Shelf Research*, 26(4):539–553, 2006.

[3] M. Bajo and G. Umgiesser. Storm surge forecast through a combination of dynamic and neural network models. *Ocean Modelling*, 33(1-2):1–9, 2009.

[4] G. Umgiesser and A. Bergamasco. A staggered grid finite element model of the Venice Lagoon. In J. Periaux, K. Morgan, E. Ofiate, and O.C. Zienkiewicz, editors, *Finite Element in Fluids*, pages 659–668. Pineridge Press, Swansea, 1993.

[5] G. Umgiesser; D. Melaku Canu; A. Cucco; C. Solidoro. A finite element model for the Venice Lagoon. Development, set up, calibration and validation. *Journal of Marine Systems*, 51:123–145, 2004.

[6] S.D. Smith and E.G. Banke. Variation of the sea surface drag coefficient with wind speed. *Quart. J. Roy. Meteorol. Soc.*, 101:665–673, 1975.

[7] L. Cavaleri and L. Bertotti. Accuracy of the modelled wind and wave fields in enclosed seas. *Tellus*, 56A(2):167–175, 2004.

[8] L. Cavaleri and L Bertotti. In search of the correct wind and wave fields in a minor basin. *Monthly Weather Review*, 125:1964–1975, 1997.

[9] P. Lionello, L. Zampato, P. Malguzzi, A. Tomasin, and A. Bergamasco. On the correct surface stress for the prediction of the wind wave field and the storm surge in the northern adriatic sea. *Il Nuovo Cimento*, 22(5):515–532, 1998.

[10] Luigi Cavaleri. Valutazione dell'accuratezza del vento sull'Adriatico prodotto dall'ecmwf. Report interno, ICPSM, 2007.

[11] S. Nissen. Implementation of a Fast Neural Network Library (FANN). Technical report, Department of Computer Science, University of Copenhagen (DIKU), Copenhagen, 2003.

The Use of a Test Battery in Marine Ecotoxicology: a Case Study

E. Prato, F. Biandolino
Institute for Coastal Marine Environment, CNR, Taranto, Italy
linda.prato@iamc.cnr.it

Abstract

Sediments are an ecologically important component of the aquatic environment and may play a key role in mediating the exchange of contaminants between particulate, dissolved and biological phases. For a comprehensive assessment of potential sediment toxicity, the use of a single species may not detect toxicant with a specific mode of action. Therefore it is advisable to carry out ecotoxicological tests on a base-set of taxa utilizing test species belonging to different trophic levels.
This paper describes the ecotoxicological evaluation of marine sediments from seven sites of Mar Piccolo estuary (Southern, Italy), four of them were located in the first inlet and three in the second inlet of Mar Piccolo estuary. Sediment samples from a site in Taranto Gulf were used as control sediment. *Dunaliella tertiolecta*, *Tigriopus fulvus*, *Mytilus galloprovincialis* and *Corophium insidiosum*, were employed to identify the quality of sediments. The integration of biological tests results showed that all sampling sites located in the first inlet of Mar Piccolo were identified as toxic, according to all tests, while the sites of second inlet were found not toxic. The results obtained in this study indicate that the use of a battery of biological tests have important implications for risk assessment in estuarine e coastal waters.

1 Introduction

A significant proportion of anthropogenic contaminants occurs in marine and estuarine costal system, particularly in areas heavily industrialized. In these areas the sediments, because of their high potential for accumulating contaminants, may serve as sinks and secondary sources for many persistent chemicals [1] constituting a significant environmental problem [2]. This represents a serious risk to benthic organism, since they may affect natural populations of aquatic organisms in different way. Sediments are ecologically important components providing habitat, feeding and spawning for many aquatic organisms, which play a significant role in maintaining the trophic status of any water body [3].
In the past, risk assessment for sediment has predominantly been determined by chemical analysis, but chemical information alone is often not satisfactory to provide an evaluation on the potential toxicity [4, 5]. Ecotoxicological assessment of water and sediment quality is a regulatory requirement of Italian legislation (D.Lgs.152/99) providing information complementary to chemical characterizations and ecological surveys. They are used to determine whether the concentration of contaminants in water or sediments is biologically available and likely to produce harmful biological effects. Ideally a

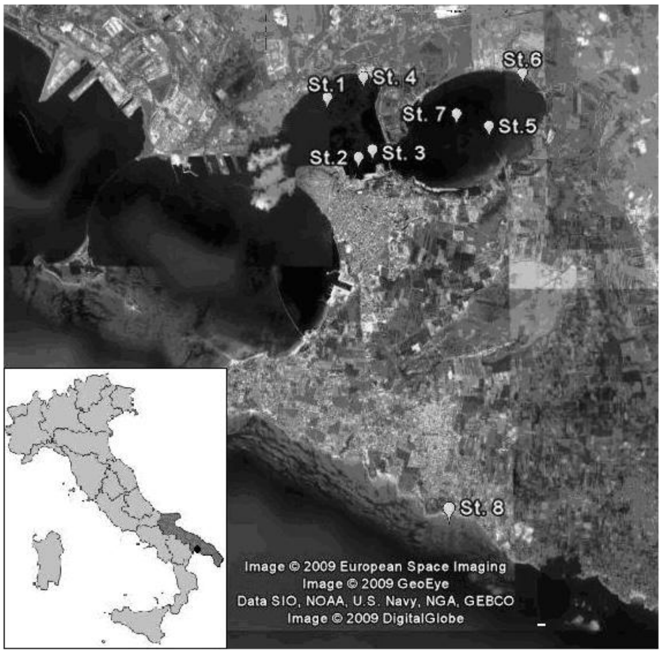

Figure 1: Sampling stations in the study area.

toxicity test should use a local species, to be relatively simple and capable of providing answers quickly, and to have sensitive endpoints that are easily interpreted and ecologically relevant.

Nowadays numerous researchers indicated the use of a battery bioassay, as a screening tool, in order to discriminate a wide spectrum of adverse environmental conditions, since a sensitive species to the all environmental contaminants does not universally exist, multi-species battery is strongly recommended [6, 7, 8]. The selection of appropriate test species is the most the critical step in developing a sediment bioassay strategy [9]. In this work, four different species representing different trophic levels were used to analyze the toxicity of sediments from Mar Piccolo in Taranto (Ionian Sea, southern Italy). The selected species are autochtonous of Mediterranean coastal waters: *Dunaliella tertiolecta*, *Tigriopus fulvus*, *Mytilus galloprovincialis* and *Corophium insidiosum*.

Dunaliella tertiolecta Butcher 1959 (Chlorophyceae) chosen for its high ecological relevance as primary producer, its a significant role for matter and energy transfer through the benthic food webs and for oxygen production. It has been frequently used as bioindicator in algal bioassays both in several studies and official method [10, 11].

Mytilus galloprovincialis Lamark, (Mollusca, Bivalvia) has a wide distribution in the Mediterranean sea and shows a high sensitivity in bioassays, as reported in several studies [12, 13].

Copepoda is the principal and essential link between the phytoplankton and higher trophic levels. The species *Tigriopus fulvus* Fisher, 1860 (Crustacea Harparticoida) is a meiobenthic species widely distributes in the Mediterranean they are exposed to sediment particles not only through direct contact, but also through ingestion [14]. Previous study indicate the suitability of this species in toxicity tests [15, 16].

Corophium insidiosum, is a tube-building species living in the brackish and estuarine water of the infralittoral zone, where it is widely distributed and available in a large number and it feeds both on sediment and suspended particulate matter. This species was selected for this study, because preliminary tests demonstrated their tolerance to non-contaminant variables (biotic and abiotic) and sensitivity to reference toxicants [17, 18]. The objective of this study was to develop a battery of bioassays for the ecotoxicological screening of sediments from the Mar Piccolo basin (Ionian sea, Southern Italy).

2 Materials and methods

2.1 Study area

Mar Piccolo is located in the Northern area of the Taranto town with a total surface area of 20.72 km^2 structured in two shelves, "First Inlet" and "Second Inlet", which have a maximum depth of 13 and 10 m, respectively. It is an inner sea with a restricted water circulation and it communicates with the Gulf of Taranto (Ionian Sea), through two channels.

Mar Piccolo basin is affected by urbanization, industry, agriculture, aquaculture and commercial fishing. The principal problems of environmental impact are due to14 sewage pipes from the Northern area in Taranto and nearby cities into the Mar Piccolo, the ship yard of the Italian navy with its dry docks (located in the First Inlet).

2.2 Sampling collection

Sediments were sampled in eight stations (Figure 1). Four of them were located in the first inlet of Mar Piccolo (stations 1, 2, 3 and 4) and three in the second inlet (5,6 and 7) and one in the Taranto Gulf (station 8) chosen as a control reference, since this area is far from anthropogenic sources of contaminants and for which a previous study indicated this one as a uncontaminated site, [18]. At each sampling site, sediment was collected, using a Van Veen grab, from three random samplings. These samples were then pooled and homogenized thoroughly in order to minimize site intra-variability and ensure that sediment was really representative of each site. The samples were stored at 4°C in a polyethylene bag. Sediment toxicity tests were started within 1 week of sample collection from the field. For the preparation of elutriates, synthetic seawater was added to sediments in the ratio 4:1 (volume/dry weight) and placed in a shaker bath for 24h at 4 °C. After stirring, the sediment/water mixture was allowed to settle for 1 h. The unsettled portion (due to the high pelite content) was centrifuged at 3500 rpm for 20 minutes at 4°C and filtered (0.45 µm). The resulting elutriate was used within 24 h for the bioassay. Porewater samples were obtained for each sediment by centrifugation of sediments at 13,000 rpm (N10,000 g) for 30 min at 4 °C in a Beckman Ultracentrifuge using polycarbonate bottles.

2.3 *Dunaliella tertiolecta*

Dunaliella tertiolecta was obtained from culture collection of microalgae of CNR

Species	*D. tertiolecta*	*T. fulvus*	*M. galloprovincialis*	*C. insidiosum*
Test type	Static	Static	Static	Static
Test duration	72h	96h	48h	96h
End- point (LC50)	growth inibition rate	mortality rate	abnormality rate	mortality rate
Validity criteria	Control growth rate >0.9/day	Mortality in control ≤10%	Mortality in control ≤20%	Mortality in control ≤15%
Reference Toxicant	K_2CrO_7	CuCl2	CuCl2	CuCl2
Concentrations (mg/L)	3.12-6.25-12.5-25-50	0,015-0,030-0.060-0.12-0.25-0.5	0.025-0.050-0.1-0.2-0.4	0.4-0.8-1.6.3.2-6.4
Bioassay	Elutriate	Elutriate	Pore-water	Whole Sediment
Bioassy duration	72h	96h	48h	10 days
Salinity ‰	32±1	38±2	36±2	36±2
Temperature	20±2	18±1	18±2	16±2
pH	8±0.5	8±0.3	8±0.5	8±0.5
Aeration	Absent	Absent	Absent	Present
Test chambers	Glass flask	Multiwell plates	Multiwell plates	Glass beakers
No organisms/test chambers	-	10	100	20
Stage of development	-	Nauplii (24-48h)	larvae	Juveniles

Table 1: Summary of toxicity test methods.

IAMC section of Taranto (Italy). Test was carried out according to Mecozzi et al. [19], with some modifications. The culture medium for algal growth was prepared according to the ISO protocol [20]. Nutrients without EDTA were added to ensure that the reduction in growth was not due to nutrient limitation. Artificial seawater was filtered on a 0.45 µm Millipore® membrane and used for toxicological tests of elutriate and for dilution of standard samples of reference toxicants.

As quality control test, reference tests with potassium dichromate, $K_2Cr_2O_7$, were performed to ensure validity of test method. Bioassays were conducted on sediment elutriate. For the preparation of elutriates synthetic seawater was added to sediments in the ratio 4 : 1 (volume/dry weight) and placed in a shaker bath for 24h at room temperature. Then the supernatant was collected by centrifugation at 3500 rpm for 20 minutes, filtered (0.45 µm) and used within 24 h for the bioassay. The samples were placed in sterilized glass flasks, in triplicate. An algal suspension sampled during the phase of exponential growth was prepared with an initial concentration 1 1.2×10^6 cells/mL measured. Then an aliquot of 0.5 mL was added to each sample by means of an analytical microsyringe. The glass flasks were placed in a thermostatic chamber (20 $\pm$ 2°C) and illuminated by a cool white light source in the 7000–8000 lux range for 72 h. The negative control consisted of three replicates of the culture medium, prepared without EDTA. The cell density of each replicate was measured after 72 using a Burker chamber. Average percentage inhibition of growth were calculated for each sample.

2.4 *Tigriopus fulvus*

Bioassays were carried out using nauplii originating from a synchronized culture (24-48h), of ovigerous females reared in a massive culture, according to Faraponova et al. [15]. A natural population of *T. fulvus* from northern coast of the Tyrrhenian Sea (Livorno, Italy) was used. The copepods were cultured in artificial sea water (Instant Ocean®) and maintained at 20$\pm$1 °C in 16/8 h light–darkness cycle, in 250 mL flasks, with weekly water renewal. A diet based on cells of Tetraselmis suecica and Tetramarin® were provided twice per week in all culture flasks. The tests were performed on elutriates sediment in multiwell testing plates. The experimental conditions are summarized in Table 1. For each sample and control three replicates were carried out. At the end of the tests (96h) the multiwell plate was placed under a microscope and the total number of died nauplii was counted for each replicate to determine the mortality rate. Established mortality criterion was absence of movement of the appendages within 10 seconds after slight disturbing with a pipette. Copper chloride ($CuCl_2$) was employed as a reference toxicant (positive control) to ensure the validity of test.

2.5 *Mytilus galloprovincialis*

Adults of *M. galloprovincialis* were sampled from natural populations of the Gulf of Taranto, at a site far from pollution point sources [21]. The embryotoxicity test was performed according to the method proposed by His et al.[22], on the basis of the standard protocol of US EPA [23]. Porewater was the test matrices used in this bioassay; sediments were centrifuged at 13,000 rpm (N10,000 g) for 30 min at 4°C in a Beckman Ultracentrifuge using polycarbonate bottles. Surnatant was collected avoiding the resuspension of particulate matter.

Adults of *M. galloprovincialis* were cleaned and immerged in unfiltered reference water at 18°C for 30 min before a thermal shock (28°C, 30 min). Specimens emitting gametes were placed in baths of filtered reference water. Eggs (1000 mL) were fertilized by injecting 10 mL of sperm. Fecundation was monitored under the microscope. Egg density was determined by counting four subsamples of known volume. Fertilized eggs, added to test solutions in order to obtain a density of 10–20 eggs/mL, were incubated for 48h at 18°C and fixed with buffered formalin. The abnormality rate is determined on the basis of a count of 100 larvae per well (three replicates per sample) distinguishing between normal larvae (D-shaped) and abnormalities (malformed larvae and prelarval stages). The acceptability of test results was based on negative control with a percentage of normal D-shaped larvae $\geq$80% [12]. The responses for each treatment (% of abnormalities) were corrected for effects in control tests by applying Abbott's formula [24], obtaining the percentage of effect. Copper chloride ($CuCl_2$) was employed as a reference toxicant (positive control).

2.6 *Corophium insidiosum*

Amphipods were collected from a clean site of the Gulf of Taranto, using a 0.5 mm sieve. In the laboratory the organisms were placed in aerated glass containers with their native sediment and were acclimated for 3-4 days, before the tests. The general design of toxicity tests was based on the standard guides for conducting acute sediment toxicity tests with marine–estuarine amphipods, with some modifications [25, 26]. Standard 10-day sediment toxicity tests were conducted on the sediment collected at each station.

Three replicates were prepared per treatment and twenty young-adults (2-4 mm) of amphipods were randomLy selected and introduced into a 1 L glass beaker containing approximately 2 cm of sediment and 750 mL of filtered seawater (0.45 μm). Summary of experimental conditions is shown in Table 1. During 10-day exposure, no food was added to the test chambers. At the end of the test, the contents of each replicate beakers were sieved and the survivors were counted. Missing organisms were considered dead and apparently dead individuals were considered living, if movement was exhibited after gentle stimulation. Copper chloride ($CuCl_2$) was employed as a reference toxicant (positive control).

2.7 Data analysis of biotest endpoints

Data from positive control tests were analysed by the Trimmed Spearman–Karber method [27] to determine LC50 and EC50, with their respective 95% confidence limits.

The difference between mortality/inhibition growth in the test sediment and control sediment was determined (ΔI%, Δm%). The bioassay was considered valid if the growth inhibition/mortality in the controls followed the validity criteria for each species reported in Table 1. The sediment was considered toxic, if significantly differed from control mortality (t test; $p<0.05$).

In order to integrate the results of the various biological tests, the criterion used is an elaboration of the toxicity scales of each test, using the following expression: $Y=0.374\ \Sigma\ Ti$ (Y=value of integrated toxicity; Ti=value of toxicity of the single test) [28]. Toxicity scale of these considered bioassays are reported in Table 2. The comprehensive toxicity evaluation was reported in Table 3.

Analysis of variance (one-way ANOVA) was performed to assess differences among stations and among species. If significant differences ($p<0.05$) occurred among sampling events, Fisher's least significant difference (LSD), was applied to identify the source of significant difference. The statistical analysis was made with the Statgraphics Plus 2.1.

3 Results

Dunaliella tertiolecta showed a mean EC50 value for the reference toxicant potassium dichromate of 10.40 (95% C.I.=15.41-7.02) mg/L, corresponded to the concentration that inhibited 50% of the microalgal growth (Table 4).

The toxicity analysis carried out with the sediment elutriate samples indicated that the sediments from the stations 5 and 6 did not determine toxicity effects on *D. tertiolecta* while all sediment elutriates from the first inlet of Mar Piccolo showed significant inhibitory effect on the growth of this species as evidenced by significant differences in the average cell density respect to the negative control (t-test; $p<0.001$). Multiple mean comparison evidenced a highest sensitivity of this microalga for sediments from station 3 and 4 (LSD; $p<0.001$) (Tables 5, 6).

As regard *Tigriopus fulvus* the sensitivity analysis revealed a 96 h LC50 value of 0.15 (95% C.I.= 0.24-0.08) $mg \cdot L^{-1}$ for the reference toxicant copper chloride (Table 4). These results are similar to the sensitivities reported by Faraponova et al. [15]. Toxicity analysis carried out with the elutriate of the sediment, presented significant differences in survival with respect to the control, but only in the samples from those located in the first inlet (ANOVA $p<0.001$) (Tables 5, 6).

Mytilus galloprovincialis reported a mean EC50 value for the reference copper chloride of 0.13 (0.14-0.09) $mg \cdot L^{-1}$, similar to that reported by Annicchiarico et al.[21] (Table 4). The negative controls presented an average 92.3% of normality. Toxicity data on porewaters for each bioassay used are reported in Table 5. The stations 1, 2, 3 and 4 presented significant differences with respect to negative control. There was no

D. tertiolecta		*T. fulvus*		*M. galloprovincialis*		*C. insidiosum*		Toxicity
Growth Inibition	*P-value*	Mortality difference	*P-value*	Abbott Correction (A)	*P-value*	Mortality difference	*P-value*	
0≤ΔI≤ 8	≥ 0.05	Δm < 10	≥ 0.05	0 <A ≤ 8	≥ 0.05	Δm < 10	≥ 0.05	Absent (0)
8<ΔI≤16	< 0.05	Δm ≤ 10	< 0.05	0 <A ≤ 8	< 0.05	Δm ≤ 10	< 0.05	Low (1)
	≥ 0.05	Δm ≥10	≥ 0.05	A>8	≥ 0.05	Δm ≥10	≥ 0.05	
16<ΔI≤32	< 0.05	10 <Δm≤ 20	< 0.05	8 <A ≤ 24	< 0.05	10 <Δm≤ 20	< 0.05	Medium (2)
32<ΔI≤64	< 0.05	20 <Δm≤ 40	< 0.05	24 <A ≤ 56	< 0.05	20 <Δm≤ 40	< 0.05	High (3)
ΔI>64	< 0.05	Δm >40	< 0.05	A>56	< 0.05	Δm >40	< 0.05	Very High (4)

Table 2: Toxicity scale

Y value	Toxicity
0	Absent (0)
0<Y≤1	Low (1)
1<Y≤2	Medium (2)
2<Y≤3	High (3)
3<Y<6	Very high (4)

Table 3: Values of Y and toxicity evaluation

significant difference in the larvae abnormality between the stations located in the second inlet and the negative sediment control (Tables 5, 6).

The sensitivity of *C. insidiosum* to copper in aqueous phase showed a 96-LC50 value of 1.15 (0.71-1.39) mg/L (Table 4). This results is lower than other Corophidae species used in sediment toxicity assessment. LC50 of *Corophium volutator* ranged from 1.85 to 5.30 mg Cd/l [29]; *C. orientale* showed a LC50 value ranging from 2.91 to 4.28 mg Cd/L [30, 31]. The mean survival in negative control was 96.7% confirming holding parameters and handling techniques were acceptable for the 10-day duration.

In the whole sediment direct contact test, samples from the first inlet, showed a generally higher toxic effect than those the stations located in the second inlet (Table 5).

The results obtained in all bioassays were integrated following the approach described by Ennas et al. [28]. The results of the biological tests evidence the same global toxicity evaluation using all biological tests (Table 7). The sites of the second inlet showed no evidence of toxicity. Although the sediment from the station 7 was recorded toxic for *D. tertiolecta* but the final judge deriving by the results integration classifies this sediment as medium toxic. The sites located in the first inlet (1, 2 3 and 4) showed a significant higher level of toxicity than those located in the second inlet (ANOVA $p<0.001$). This is confirmed by hierachical clustering analysis (HCA) (Figure 2).

4 Discussion

The bioavailable contaminant fraction affecting organisms can only be determined

Test species	LC50 (mgL^{-1})	Confidence Limits
D. tertiolecta	10.40	15.41-7.02
T. fulvus	00:15	0.24-0.08
M. galloprovincialis	00:13	0.14-0.09
C. insidiosum	1.15	0.71-1.39

Table 4: Test results of *D. tertiolecta*, *T. fulvus*, *M. galloprovincialis* and *C. insidiosum* to sediment samples exposure

	D. tertiolecta			***T. fulvus***			***M. galloprovincialis***			***C. insidiosum***		
Stations	Growth Inibition	ΔI%	*P-value*	Mortality (%)	Δm%	*P-value*	Abnormality %	ΔA%	*P-value*	Mortality (%)	Δm%	*P-value*
1	23.3	22.3	<0.001	20	13.3	<0.001	32.3	24.6	<0.001	18.3	15	<0.001
2	32.3	31.3	<0.001	20	13.3	<0.001	27	19.3	<0.001	28.3	25	<0.001
3	39	38	<0.001	23.3	16.6	<0.001	29	21.3	<0.001	35	31.7	<0.001
4	39	38	<0.001	13.3	6.6	<0.001	22.6	14.9	<0.001	28.3	25	<0.001
5	2.4	1.4	>0.05	3.33	-3.4	<0.002	14	6.3	<0.05	6.7	3.4	<0.05
6	7	6	>0.05	0	-6.7	<0.001	8.3	0.6	>0.05	13.3	10	<0.001
7	34	33	<0.001	13	6.3	<0.001	13.6	5.9	<0.05	3.3	0	>0.05

Table 5: t-test statistical analysis of each test species used in bioassays.

by using toxicity bioassays [32], which have been shown to be promising tools for assessing the quality of contaminated sediments. The ecotoxicological evaluation of the sediments carried out using different species established an approach for determining a site's environmental risk. The main point of the test battery was to include living organisms at two or more trophic levels to determine the potential effects based on different endpoints and sediment matrices.

The test battery used in this study allows us to evaluate overall sensitivity and applicability of the selected species, for the preliminary ecotoxicological screening of sediment from Mar Piccolo.

Phytoplankton is an energy source critical to most aquatic ecosystems. Changes in their density and composition can affect the chemical and biological quality of the habitat [33]. Furthermore, algae have been shown to be more sensitive to toxicants than fish or invertebrates [34]. The values of cell density were subjected to considerable variation according to the different sampling sites and the exposure period, as confirmed by the results obtained in this study. Of the four species used, *D. tertiolecta* was the most significant sensitive species followed by *M. galloprovincialis*. Indeed, the station 7 showed a high toxicity for *D. tertiolecta*, in respect to that observed with the other species.

Ecotoxicological responses of *T. fulvus* were not as pronounced as those of *D. ter-*

	F Ratio	*p-value*	LSD
D. tertiolecta	284.94	***	Control=St.5=St.6<St.1<St.2<St.7<St.3=St.4
T. fulvus	71.67	***	6=5<Control<7=4<1=2<3
M. galloprovincialis	83.95	***	Control=6 <7<5<4<2<3<1
C. insidiosum	151.55	***	Control=7<5<6<1<4=2<3
Integration toxicity results	6.65	***	Control=6=5=7<1=4=2=3

Table 6: Results of one-way ANOVA test. Level of signifance: ***$p<0.001$; LSD test: $p<0.05$

Stations	***D. tertiolecta***	***T. fulvus***	***M. galloprovincialis***	***C. insidiosum***	**Integrated toxicity**
1	2	2	3	2	4
2	2	2	2	3	4
3	3	2	2	3	4
4	3	1	2	3	4
5	0	0	1	0	1
6	0	0	0	1	1
7	3	1	0	0	2

Table 7: Data of single acute toxicity test and integrated toxicity battery of sediment examined.

tiolecta, *M. galloprovincialis* and *C. insidiosum*. This underlines that each test has its own specific sensitivity and, thus, may predict the potential hazards associated with contaminated sediment, thus undue emphasis should not be placed on any single result [35, 9].

Toxicity tests on embryos of bivalves, even if these organisms are not naturally exposed to porewater, are generally accepted and utilised, since larval stages are a good instrument for detecting otherwise not measurable sub-lethal effects [36, 37, 38].

For the embryotoxicity test, all samples evidencing medium or high acute toxicity come from site located in the first inlet, thereby confirming the choice of this biological model as a sensitive tool for evaluating the biological quality of contaminated sediments. The porewaters which do not show acute toxicity are from site located in the second Inlet.

The accumulation of pollutants is maximum in the upper few centimeters of the sediment, which is important for a number of biological processes [39]. *C. insidiosum* is therefore an ideal species for toxic sediment assessment because it comes into contact with the compounds through both physical contact and ingestion of sediment material. Furthermore, Prato and Biandolino [18] have also demonstrated that this species fulfills most criteria required for suitable sediment toxicity tests. In this study *C. insidiosum* did not tolerate sediments from stations 1, 2, 3 and 4 for which mortality was very high, compared with control sediment.

Some considerations can be made about the comparison among the species used in toxicity tests. Since the microalgae and

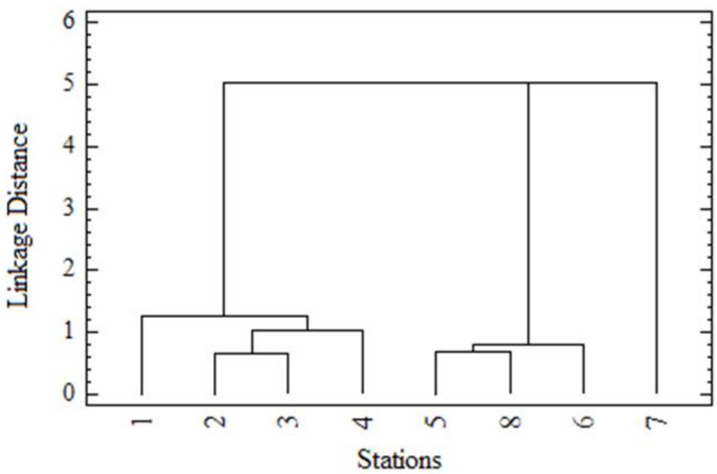

Figure 2: Hierachical clustering dendrogram of the seven stations from Mar Piccolo estuary based on the results of the toxicity integration.

embryos are known to be more sensitive species in toxicity test than the other test species used, we expected some sample to show toxicity only with these species.

This is true for a samples from the station 7 for which high toxicity was clearly evidenced only for *D. tertiolecta*.

Every species reacted differently to the samples tested: there were, indeed, significant differences in the ecotoxicological response among all species employed towards all samples, except for those collected in the station 5, for which no significant differences were observed between *D. tertiolecta* and *T. fulvus* sensitivities, and for the station 7 between *T. fulvus* and *M. galloprovincialis* (LSD; $p<0.05$). From the results integration, the sites located in first inlet of Mar Piccolo showed a very high level of toxicity. As studied by [40, 21, 9], the metal concentration in these sites showed a wide range of Hg, Pb, Cu and Ni levels, depending on the anthropogenic impact, and they were highest in sediments from the first inlet. The determination of toxicity, even if qualitative, allows us to emphasize that all these bioassays can discriminate the toxicity of sediments from sites with different pollution levels.

The variation in results among species and sediment phases found in this study highlights the need for the employment of a multi-trophic battery of biotests with a multi-phase, multi-exposure-time approach to sediment assessment.

References

[1] R. Bettinetti, C. Giarei, and A. Provini. Chemical Analysis and Sediment Toxicity Bioassays to Assess the Contamination of the River Lambro (Northern Italy). *Arch. Environm. Contam. Toxicol.*, 45:72–78, 2003.

[2] C. Magalhaes, J. Coasta, C. Teixeira, and A.A. Bordalo. Impact of trace metals on denitrification in estuarine sediments of the Douro River estuary, Portugal. *Mar. Chem.*, 107:332–341, 2007.

[3] M. Singh, A.A. Ansari, G. Muller, and I.B. Singh. Heavy metals in freshly deposited sediments of Gomti river (a tributary of the Ganga river): Effects of human activities. *Environ. Geol.*, 29(3-4):246–252, 1997.

[4] P.M. Chapman, R.C. Swartz, B. Roddie, H.L. Phelps, P. van den Hurk, and R. Butler. An international comparison of sediment toxicity tests in the North Sea. *Mer. Ecol.Prog. Ser.*, 91:253–264, 1992.

[5] M. Davoren, N.S. Illeabhain, J. Ohalloran, M.G.J. Hartl, D. Sheehan, N.M. Obrien, F.N.A.M. Van Pelt, and C. Mothersill. A test battery approach for the ecotoxicological evaluation of estuarine sediments. *Ecotoxicology*, 14:741–755, 2005.

[6] B.J. Dutka, T. Tuominen, L. Churchland, and K.K. Kwan. Fraser river sediments and waters evaluated by the battery of the screening tests and techniques. *Hydrobiologia*, 188/189:301–305, 1989.

[7] Oslo and Paris Commission (OSPARCOM). Guidelines for the management of dredged material. page 32, 1999.

[8] M. Nendza. Inventory of marine biotest methods for the evaluation of dredged material and sediments. *Chemosphere*, 48:865–883, 2002.

[9] M. Narracci, R.A. Cavallo, M.I. Acquaviva, E. Prato, and F. Biandolino. A test battery approach for ecotoxicological characterization of Mar Piccolo sediments in Taranto (Ionian Sea, Sothern Italy). *Environmental Monitoring Assessment*, 148:307–314, 2009.

[10] US Environmental Protection Agency. Quality criteria for water, Office of water and hazardous materials. US EPA, Washington DC. 1974.

[11] APHA/AWWA/WEF. Standard Methods for the Examination of Water and Wastewater, 20th ed. 1999.

[12] E. His, R. Beiras, and M. Seaman. The assessment of aquatic contamination: bioassays with bivalve larvae. *Adv. Mar. Biol.*, 37:1–178, 1999.

[13] A. Volpi Ghirardini, C. Losso, A. Arizzi Novelli, A. Baugrave, E. His, and P.F. Ghetti. *Mytilus galloprovincialis* as bioindicator in embryotoxicity testing to evaluate sediment quality in the lagoon of Venice (Italy). *Chem. Ecol.*, 21(6):455–463, 2005.

[14] A. Carli and M.A. Fiori. Sviluppo larvale de1 *Tigriopus fulvus* Fischer. *Atti IX Congr. S.I.B.M., Lacco Ameno d'Ischia 19-22/5/77*, pages 181–190, 1977.

[15] O. Faraponova, D. De Pascale, F. Onorati, and M.G. Finora. *Tigriopus fulvus* (Copepoda, Harparticoida) as a target species in biological assays. *Meiof. Mar.*, 14:91–95, 2005.

[16] L. Pane, E. Giacco, and G.L. Mariottini. Uso di *Tigriopus fulvus* (Copepoda: Harpacticoida) nella valutazione del rischio ecotossicologico in ambiente marino. *Biol. Mar. Medit.*, 14:186–188, 2007.

[17] E. Prato and F. Biandolino. *Gammarus aequicauda* (Crustacea: Amphipoda): a potential species test in marine sediment toxicity assessment. *Aqu. Ecosyst. Health Manag.*, 8(4):475–482, 2005.

[18] E. Prato and F. Biandolino. Mono*Corophium insidiosum* (Crustacea, Amphipoda) as a candidate species in sediment toxicity testing. *Bull. Environ. Cont. Toxicol.*, 77(1):1–9, 2006.

[19] M. Mecozzi, F. Onorati, F. Oteri, and A. Sarni. Characterisation of a bioassay using the marine alga *Dunaliella tertiolecta* associated with spectroscopic (visible and infrared) detection. *Int. J. Environ. Poll.*, 32(1):104–120, 2008.

[20] ISO. Water Quality Marine Algal Growth Inhibition Test with *Skeletonema Costatum* and *Phaeodactylum tricornutum*, Revision of first edition (ISO/DIS 10253:1995). 2004.

[21] C. Annicchiarico, F. Biandolino, N. Cardellicchio, A. Di Leo, S. Giandomenico, and E. Prato. Predicting toxicity in marine sediments in Taranto Gulf (Ionian Sea, Southern Italy) using sediment quality guidelines and a battery of bioassay. *Ecotoxicology*, 16:239–246, 2007.

[22] E. His, R.N.L. Seaman, and R. Beiras. A simplified bivalve larval bioassay method for seawater quality assessment. *Water Research*, 31:351–355, 1997.

[23] US EPA. Short-term methods for estimating the chronic toxicity of effluents and receiving waters to west coast marine and estuarine organisms. EPA/600/R-95/136, Cincinnati, Ohio, USA. 1995.

[24] ASTM. Standard Guide for Conducting Static Acute Toxicity Tests Starting with Embryos of Four Species of Saltwater Bivalve Molluscs. PA: Philadelphia E 724–98. 21. 2004.

[25] ASTM. Standard guide for conducting 10-d static sediment toxicity tests with marine and estuarine amphipods. In Annual Book of ASTM Standards, Water and Environmental Technology 11.04, E1367-92. ASTM, Philadelphia. 1993.

[26] SETAC-Europe. Guidance document on sediment toxicity assessment for freshwater and marine environments. 1993.

[27] M.A. Hamilton, R.C. Russo, and R.V.Thurston. Trimmed Spearman- Karber method for estimating median lethal concentrations in toxicity bioassays. *Environ. Sci. Technol.*, 11:714–719, 1977.

[28] C. Ennas, C. Mugnai, L. Kozinkova, N. Bigongiari, and D. Pellegrini. Application of a bioassay battery for toxicity assessment of harbour sediments contaminated by heavy metals. *Atti Associazione Italiana Oceanologia e Limnologia*, 15:53–62, 2002.

[29] S. Ciarelli. Guideline for conducting 10-day static sediment toxicity tests using marine or estuarine amphipods. Report from the Tidal Water Division, Middelburg, The Netherlands. Report RIKZ. 94.031. 1994.

[30] F. Onorati, D. Pellegrini, and A. Ausili. Valutazione della tossicità naturale nel saggio Microtox® in fase solida: La normalizzazione pelitica. *Acqua e Aria*, 6:83–91, 1999.

[31] F. Onorati, N. Bigongiari, D. Pellegrini, and S. Giuliani. The suitability of *Corophium orientale* (Crustacea, Amphipoda) in harbour sediment toxicity bioassessment. *Aquatic Ecosys. Health Manag.*, 2:465–473, 1999.

[32] R. Beiras. Comparison of methods to obtain a liquid phase in marine sediment toxicity bioassays with *Paracentrotus lividus* sea urchin embryos. *Arch. Environm. Contam. Toxicol.*, 42:23–28, 2002.

[33] F.E. Round. The ecology of algae. *Cambridge University Press*, page 653 pp., 1981.

[34] W.E. Miller, J.C. Greene, and T.C. Shirocyama. The Selenastrum capricornum, Prinz. Algal assay bottle test. Experimental design, application and data interpretration protocol.US EPA 600/9-78-018. pages 1–126, 1978.

[35] G.C. Castillo, I.C. Vila, and E. Neild. Ecotoxicity assessment of metals and waste water using multitrophic assays. *Environm. Toxicol.*, 15:370–375, 2000.

[36] R. Robert and E. His. Combined effects of salinity and cadmium chloride upon embryos and larvae of the Japanese oyster, *Crassostrea gigas*. *Mar. Environ. Res.*, 15:303–312, 1985.

[37] R. Beiras and E. His. Effects of dissolved mercury on embryogenesis, survival and growth of *Mytilus galloprovincialis* mussel larvae. *Mar. Ecol. Prog. Ser.*, 126:185–189, 1995.

[38] C. Losso, A. Arizzi Novelli, M. Picone, P.F. Ghetti, and A. Volpi Ghirardini. Pore-water as a matrix in toxicity bioassays with sea urchins and bivalves: Evaluation of applicability to the Venice lagoon (Italy). *Environ. Int.*, 35:118–126, 2009.

[39] S.A. Levin and S.F. Kimball. New perspectives in ecotoxicology. *Environ. Manag.*, 8:375–442, 1985.

[40] E. Prato, A. Di Leo, F. Biandolino, and N. Cardellicchio. Sediment toxicity tests using two species ofmarine amphipods: *Gammarus aequicauda* and *Corophium insidiosum*. *Bull. Environ. Cont. Toxicol.*, 76(1):1–9, 2006.

A Multidisciplinary Approach to the Study of Contaminated Coastal and Fresh Water Sediments

L.G. Bellucci, S. Giuliani, S. Romano, C. Mugnai, S. Albertazzi, M. Frignani
Institute of Marine Sciences, CNR, Bologna, Italy
luca.bellucci@ismar.cnr.it

Abstract

Industrial activities and urban settlements, discharging without control, were responsible for the contamination of coastal environments. To face this situation, decision makers and stakeholders need sound scientific information on the quality of endangered areas, chronologies of the inputs and present trends. This information can be achieved through the study of sediment records. However, sampling sites and techniques should be carefully chosen to obtain unbiased data. Our methodological approach can include: 1) bathymetry and high resolution seismic, to select sampling sites that have likely preserved a good chronology; 2) collection of undisturbed sediment cores; 3) X-radiography to reveal on sediment structures; 4) multiple-core correlation through whole-core magnetic susceptibility; 5) high resolution subsampling with exclusion of material probably affected by smearing; 6) accurate sample handling, storage and preparation. Contaminant concentrations are interpreted in the context of the information about sample characteristics: 1) porosity and dry bulk density; 2) mineralogy; 3) grain size; 4) organic matter content and composition (OC, ON, C/N ratio, δ^{13}C and δ^{15}N). 100-year time scale chronologies are usually obtained through activity-depth profiles of radiotracers such as ^{210}Pb and ^{137}Cs. Examples of important results are provided from our studies of Italian, Mexican, Moroccan and Vietnamese sites.

1 Introduction

The sources of contaminants to the coastal zone are many, but urban settlements, ports and factories are responsible for the highest pressure and only wastewater regulations permit to limit their negative influence. In order to cope with the environmental problems relative to endangered areas, decision makers and stakeholders need sound scientific information on contaminant levels and distributions. Furthermore, assessing the chronology of inputs and clarifying present trends is especially important when responsibilities have to be established (e.g., when different managements have been in charge of a plant) and to understand if the environment is presently recovering or not. In this context, accreting aquatic sediments can be extremely important in that they behave as natural archives through the retention of significant information about environmental conditions at the time of particle deposition and strata formation. However, sampling sites and techniques should be carefully chosen to avoid that expensive, high-quality analyses are preceded by inaccurate sample collection and preparation.

Therefore, this paper aims at describing a good practice to obtain the most useful information from the study of sediments in polluted areas. The most significant results from studies both in Italy and in developing countries will be presented to exemplify the theoretical concepts.

2 Working strategies

Based on our experience, we suggest an operative scheme of activities that span from the collection of available information present in scientific literature and administrative archives, to pre-sampling surveys and, finally, to sample treatment and analysis. The basic requirement entails the minimization of all efforts (both human and economic) while still getting the required results. Therefore, we will discuss hereafter each different activity, following a conceptual framework that should ensure the achievement of correct and useful scientific information.

We applied the complete procedure especially to the study of some Italian "areas of national interest", such as the ports of Augusta and Porto Torres and the Maggiore Lake.

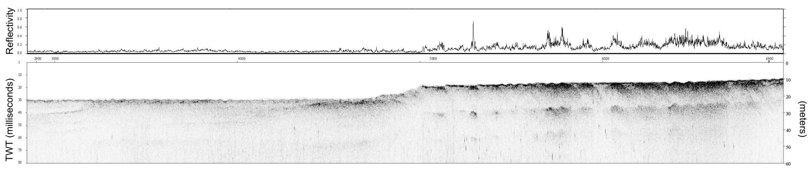

Figure 1: SBP-CHIRP profile from the Augusta Port (SR, Italy) with reflectivity data (on the top). Vertical scales of the SBP profile are in meters (rigth) and milliseconds (left).

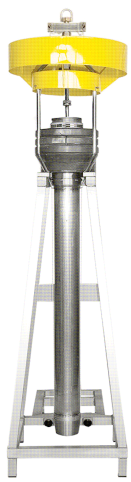

Figure 2: Picture of the SW-104 corer.

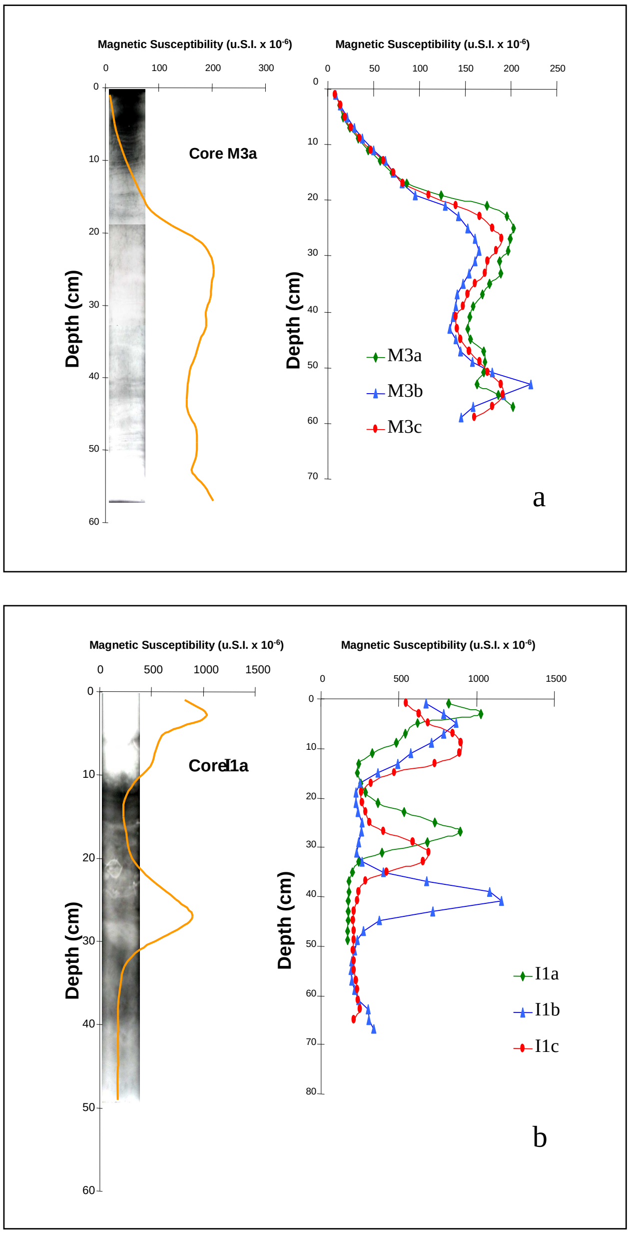

Figure 3: X radiographs for core M3 (a) and I1 (b) from the Venice Lagoon (Italy). The magnetic susceptibility profiles of three replicates are also shown.

3 System definition and sediment core collection

The collection of available information should always be the first step. It is fundamental to gather all the relevant papers published about the characteristics of the study area, its contamination and also the documents concerning the history of industrial productions, waste management and public works.

A second step may follow, that consists in performing bathymetry and high resolution seismic, to obtain an overall picture of the basin characteristics and sediment distribution. This is especially important for the selection of sampling sites that have likely preserved a high degree of information. At ISMAR-CNR, the Sub Bottom Profiler CHIRP (SBP-CHIRP) technology is used, a system able to generate calibrated frequency-modulated acoustic signals that permit very high resolution even if with limited penetration. It is also able to reveal areas where sediment accumulation is more regular and to distinguish where bottom morphology is affected by phenomena such as slumping, mass accumulation, presence of gas, etc. Furthermore, any change in the sediment reflection coefficient is due to grain size variations, making it possible to recognize silt/clay sediments (more suitable for chronology and contamination studies) from sandy bottoms. Figure 1 shows an example of a SBP-CHIRP profile obtained in the Augusta Port (Italy).

Having acquired a fair knowledge of the bottom in the study area, the number of sampling sites should be chosen in accordance to the research purposes: higher for a general site characterization (often provided by surficial sediments) to check sources, distribution and level of pollution; and lower for more specific issues (e.g. for the definition of sediment and mass accumulation rates, dates, chronologies, fluxes and trends). This approach should prevent the production of biased results, often resulting from the analysis of many samples to an insufficiently high vertical resolution (e.g., this is what happens when following the rules set by the Italian legislation relative to site characterisation procedures).

Once sampling sites have been selected, one or more sediment cores need to be collected for each site, using a device able to preserve the sediment water interface. This is particularly important for those studies that deal with historic reconstructions of events and recent changes in the dynamics of the environment. Figure 2 shows a Sea-Water 104 (SW-104) corer, endowed by ISMAR-CNR, that is able to collected short (1-1.2 m) cores with an undisturbed water-sediment interface and the overlying bottom water. The system was originally designed to provide undisturbed phases for the study of sediment-water exchange of nutrients and pollutants but it then revealed to be perfect also for studies on sediment sequences. Soon after collection, the cores should be X-radiographed and then scanned for whole-core magnetic susceptibility, in order to get some preliminary information about sediment structures and sedimentary mechanisms. As an example, Figure 3 shows the X-radiographs of two sediment cores (M3 and I1) from the Venice lagoon, together with the magnetic susceptibility profiles of three replicates taken from each sites. In one case the three samples are fairly similar (core M3, Figure 3a) whereas the cores from the other site show significant differences (core I1, Figure 3b). Multiple-core correlations based on depth profiles of common features (e.g., sediment porosity, magnetic suscepti-

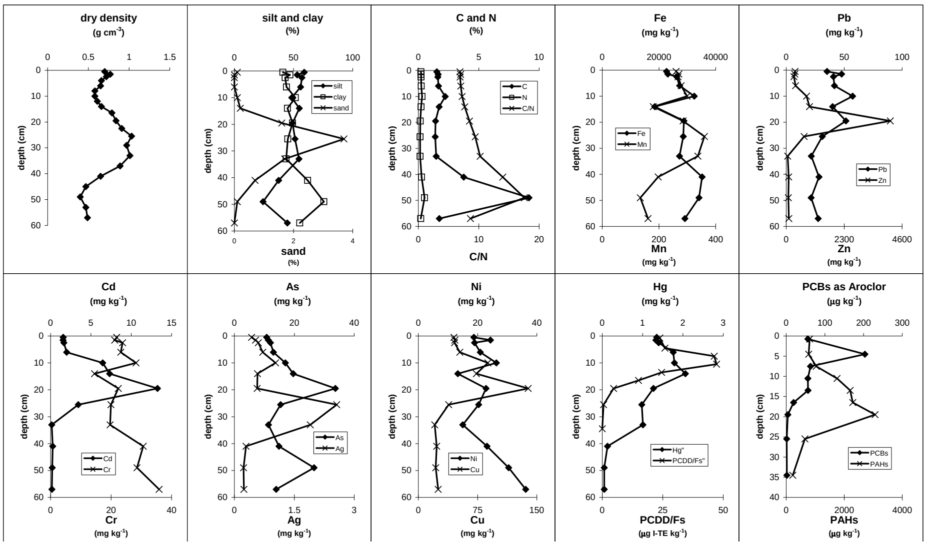

Figure 4: Depth distributions of bulk dry density, grain size composition (% of sand, silt and clay), organic matter content (% of C and N, and C/N), Fe, Mn, selected heavy metals (Pb, Zn, Cd, Cr, As, Ag, Ni, Cu and Hg,), PCDD/Fs, PCBs and PAHs in core E (Venice Lagoon, Italy).

bility, grain size composition) are also useful to compare accumulation rates and decide which core presents the most complete and readable record.

4 Subsampling, sample storage and handling

We generally use a high resolution subsampling: 0.5-4 cm thick slices, with smaller thicknesses close to the sediment-water interface. This permits to obtain detailed information about the most recent times, where variations might be very significant. Usually, the core is kept vertical until the sediment is extruded from the plastic tube. Slices are cut at pre-determined intervals and the part that has been in contact with the walls of the sampler is removed, thus eliminating the effects of smearing. This latter can severely bias the analytical results, in particular when it transfers very polluted surficial or subsurficial sediment to the deeper layers. In most cases, it is not necessary to analyse all sediment sections to get a good level of information. However, some more samples can be analysed if the profile obtained from the first determinations appears incomplete. It is easy to demonstrate that a low resolution subsampling can completely change the information provided by a profile, and this effect is higher with low sediment accumulation rates [1].

After extrusion and removal of the outer part, subsamples can be divided and put in special vessels according to the planned analyses (i.e., plastic for metals and glass for organic chemicals). Silanised glass jars are sometimes used. All samples must then be stored at a proper temperature (from –18 to 4°C). Before the analysis, sediments are generally lyophilised or dried at relatively low temperature (maximum 60°C).

5 Analysis of sediment parameters

It is important to understand whether the areal and vertical (along the sediment column) distributions of a contaminant are driven by distance from the source, transport mechanisms and changes of input fluxes or by variations of sediment characteristics. These latter are often linked to hydrodynamics and sources of the sedimentary material that, in turn, may be influenced by anthropogenic activities. Therefore, contaminant concentrations, both in surficial sediments and downcore, have to be interpreted in the context of the information about sample characteristics: 1) porosity and dry bulk density; 2) mineralogy; 3) grain size and 4) organic matter content and composition (OC, ON, C/N, δ^{13}C and δ^{15}N). In addition, the depth profiles of Fe and Mn provide information on the role of redox processes in accumulating trace metals at certain levels in cores. Figure 4 shows the depth distribution of the most important physical and compositional parameters in a sediment core of the Venice Lagoon. In this case the profile is clearly driven by contaminant inputs from the source rather than by sediment composition and diagenesis.

6 Chronologies

100-year time scale chronologies are usually obtained through activity-depth profiles of radiotracers such as ^{210}Pb and ^{137}Cs in cores not significantly affected by physical mixing and/or bioturbation. The assessment of sediment accumulation rates (cm y^{-1}) and mass accumulation rates (g $\mathrm{cm}^{-2}\mathrm{y}^{-1}$) allows not only the dating of environmental changes and contaminating events, but also the calculation of fluxes of both sedimentary materials and contaminants.

^{210}Pb dating method is based on the depth distribution of the fraction in excess with respect to the sediment natural background ($^{210}\mathrm{Pb}_{ex}$). This is the fraction of the radiotracer that is supplied from the aquatic environment and decays as a function of time, and depth. Differently, the supported ^{210}Pb is produced within the sediment by decay of the naturally present ^{226}Ra. The activity of $^{210}\mathrm{Pb}_{ex}$ at any depth is a function of both particle and tracer inputs, and time elapsed since burial. Simple (no mixing or bioturbation) or more complex models (variable sedimentation patterns, disturbing mechanisms) can be used to obtain sediment accumulation rates and dates. If processes such as physical mixing and bioturbation are not accounted for, the rates obtained are overestimated and can be considered upper limits.

Usually, also ^{137}Cs activity is determined because its depth distribution in cores can be used as independent check of the reliability of ^{210}Pb chronology. The peak caused by the Chernobyl accident (1986) is a useful time marker in Europe, and permits to calculate average rates after the year of deposition. In addition, the peak due to bomb testing should identify the level deposited in 1963, but its position could be biased by ^{137}Cs diffusion in interstitial waters. Even less reliable is the base of the profile, which should correspond to 1954. Discussion of the dating procedures

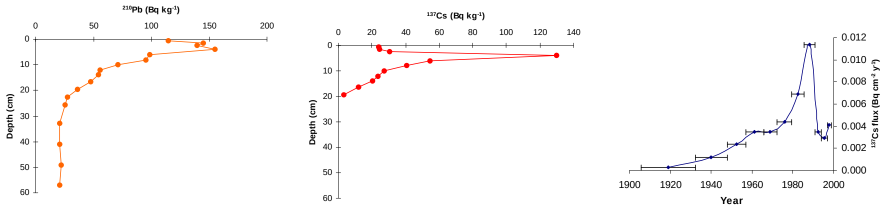

Figure 5: Radionuclides in core M3 (Venice Lagoon, Ialy). Left: depth profile of ^{210}Pb. Center: depth profile of ^{137}Cs. Right: ^{137}Cs fluxes associated to dates obtained from ^{210}Pb measurements.

and related problems can be found in Sorgente et al. [2], Frignani et al. [3] and references therein. An example is shown in Figure 5 for the salt marsh core M3 of the Venice Lagoon, where dates obtained from $^{210}Pb_{ex}$ depth profile are associated to fluxes of ^{137}Cs [4].

7 Contaminants and statistic analysis of data

The pattern of contaminant concentrations and fluxes is by itself important to recognize past and present trends and to understand if the environment is recovering or not. Obviously, the information can be much improved when dates are associated to sediment levels and fluxes can be calculated. In the case of organic contaminants, such as dioxins and furans (PCCD/Fs), polychlorinated biphenyl (PCBs), polycyclic aromatic hydrocarbons (PAHs) and other classes of compounds of environmental interest, the information can be completed by providing the congener or homologue profiles and, therefore, insight into the composition and probable source of the mixture.
An example is shown in Figure 6, with the discussion of the depth distributions of PCDD/Fs in sediment cores E1 from the Venice Lagoon [5]. The analysis of PCDD/Fs was carried out using established GC-MS methods (EPA 1613/94/revision b) for the determination of 17 congeners 2,3,7,8 substituted. Details of the analytical procedure were provided by Bellucci et al. [6]. TEQs, which sum the seventeen 2,3,7,8-substituted congeners on the basis of their toxic equivalence to 2,3,7,8-TCDD (tetrachlorinated dibenzo-*p*-dioxin), were calculated from PCDD/F concentrations using the international toxic equivalent factors (I-TEFs) [7]. Profiles of PCDD/Fs, in the form of histograms, were obtained by summing the 2,3,7,8 substituted homologues with the same grade of chlorination and recalculating the relative contributions of the various groups as % with respect to the total.
Contamination began in the early ‘1920s after the construction of the 1st Industrial Area, peaked in the late ‘1930s and then started increasing again in the late 1940s. The situation improved after 1980, when dredging operation in the North Industrial Canal ceased. Bellucci et al. [6] and Frignani et al. [5] showed that high PCDD/F concentrations and inventories can still be found in sediments of the canals of the Porto Marghera industrial area, and there

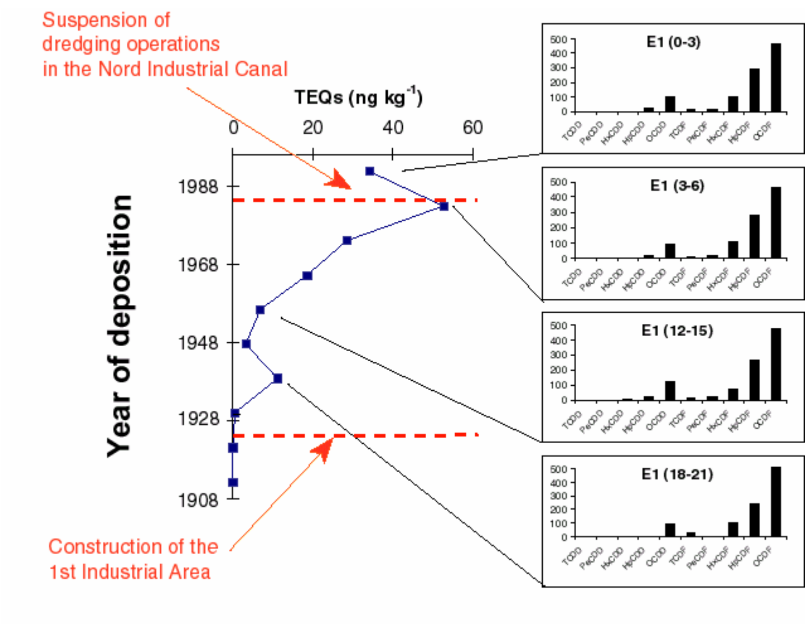

Figure 6: Concentration-depth profile of PCDD/Fs (as ng TEQs g^{-1}) in core E1 (Venice Lagoon, Italy). Homologue profiles at selected depths are also shown.

is the possibility for this polluted material to be resuspended and partially transferred to lagoon sediments as a result of anthropogenic activities, such as dredging and passage of large ships.

About PCDD/F composition and sources, from the work of Bellucci et al. [6] and Frignani et al. [5] we know that tThree different PCDD/F homologue profiles can be found in the lagoon, accounting for as much different sources [6, 5]: 1) octachlorinated dibenzo-*p*-dioxin from combustion; 2) almost only octachlorinated dibenzofuran from the production of vinyl chloride (CVM) and 3) dibenzofurans in fixed proportions, characteristic of activities carried out in the past within the 1st Industrial Area. This latter situation characterises all analysed levels in core E1, thus suggesting the contamination from a prevailing source all over the time. This contamination appears to be typical of sediments from the 1st Industrial area.

An example of historical reconstruction of PCB delivery that is worth mentioning, even if not relative to the coastal zone, has been provided by Piazza et al. [8] and is shown in Figure 7a. The core, was taken as representative of a small lake, Espejo de los Lirios, located in the northern part of the Mexico City Metropolitan Zone. A ^{210}Pb-derived chronology, was used to reconstruct the historical PCB fluxes to the site during ~84 years (1911-95). The highest input fluxes occurred in 1977, after a significant increase since the late 1940s. This trend is clearly the consequence of the expansive growth of the area with the on-

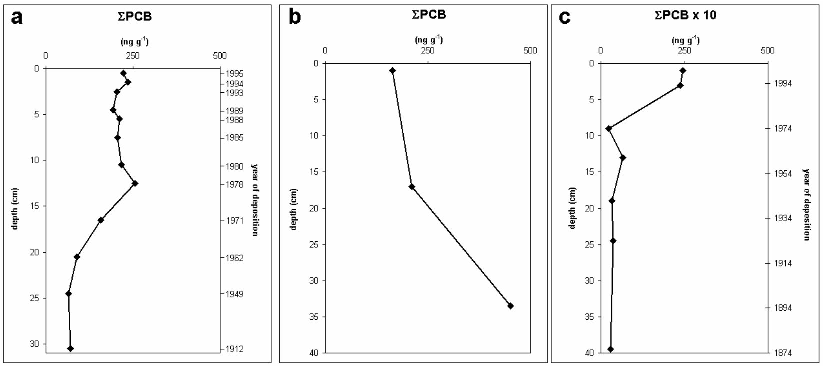

Figure 7: Examples of PCB distributions: a) depth and temporal profiles in the Espejo de Los Lirios lake, Mexico City (Mexico); b) depth profiles in the Port of Tangier (Morocco); c) depth and temporal profile in core 10c from the Tam Giang-Cau Hai Lagoon (Central Vietnam).

set of industrial activities starting from the early 1970s. A phase of decrease, after the ban of the PCB use in open systems, ended in 1989, and in 1995, at the time of sampling, the trend was toward a new increase to the highest levels. This may be due to the atmospheric transport since presently the most important sources of PCBs to the atmosphere are the contaminated materials in landfills. The contamination levels found in the sediments are relatively high, reaching values above the threshold effect level (TEL) guidelines and, in two cases, close to the probable effect level (PEL) which means that some adverse effects on the fauna may have occurred all over the time interval represented by the core. The same authors shoved that, among the Mexican aquatic environments they studied, the maxima are just to be found in Mexico City lakes [9].

Figure 7b shows also the PCB depth profile in a sediment core from the port of Tangier [10]. As for many other ports, concentrations are relatively high even in absence of industrial settlements in the mainland. Actually, ports are usually contaminated by PCBs that were extensively present in ships because of their multiple many uses (hydraulic fluids, electric cables, etc.). The core was not dated because of the unsuitable distribution of ^{210}Pb and the very low levels of ^{137}Cs, and PCB concentration depth profile is not detailed enough to provide a complete insight on temporal changes. However, the trend roughly shows a significant decrease in surficial layers with respect to downcore sediments, where PCBs largely exceed international guidelines and may constitute a hazard for biota in case of resuspension following the deep dredging of the port sediments. A third example (Figure 7c) refers to a core (10c) taken from the northern part of the Tam Giang-Cau Hai (TG-CH) Lagoon, the largest in South East Asia and located in Central Vietnam [11]. In this case the chronology had to rely only on $^{210}Pb_{ex}$, due to the lack of the ^{137}Cs signal. However, especially for the TG-CH

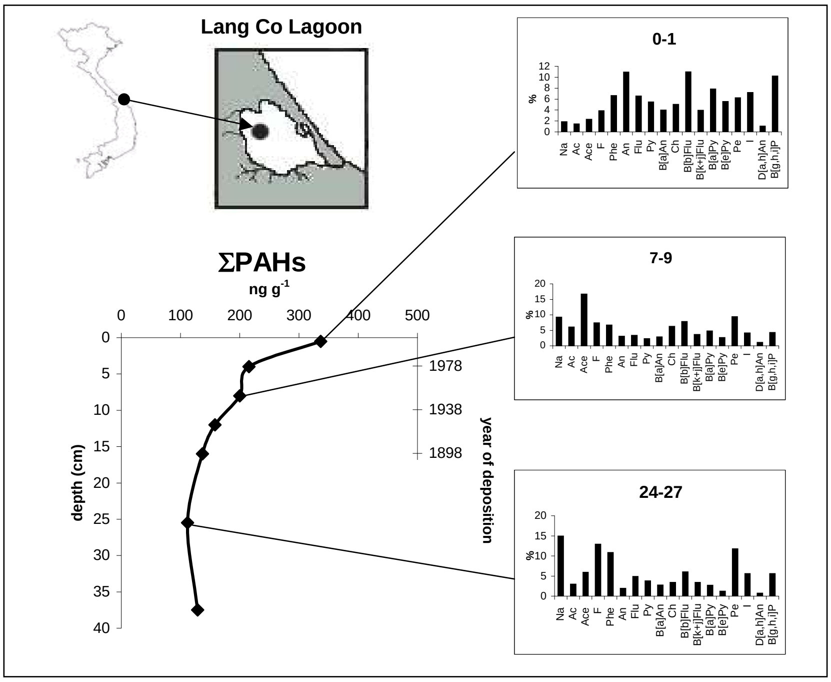

Figure 8: PAH concentration profile vs depth and year of deposition in the Lang Co Lagoon (Central Vietnam). Congener profiles at selected depths are also shown.

Lagoon, the application of the most common conceptual models to the calculation of rates and dates [12] is not straightforward, since ^{210}Pb concentration changed over time, mainly due to variations of sediment accumulation. In practice, it can be hypothesised that most of the model assumptions, which refer to the inputs of particles and/or radiotracer onto the sediment, are not met. We were then forced to assume that the depth where ^{210}Pb reaches the background value corresponds to 100 years, providing a mean sediment accumulation rate of 0.31 cm y^{-1}, as a first approximation. PCB distribution and dating was discussed by Frignani et al. [11]. It is noteworthy that, contrary to the patterns found in many polluted environments all over the world, at the time of sampling (2002) PCB were still increasing at this site.

Another example is that provided by Giuliani et al. [13] about the PAH distributions in sediment cores from nine coastal lagoons of Central Vietnam. Sediment accumulation rates, calculated as described above, were in the range 0.10-0.28 cm y^{-1}. These values are rather low and are probably the results of strong hydrodynamic processes and an efficient exchanges with the sea. Figure 8shows the depth profile of the sum of eighteen PAH congeners, 16 of which were are the priority pollutants recommended by US EPA, with their relative importance at selected depths in a core from the Lang Co Lagoon. Contaminant distribution is also plotted against estimated years of deposition. In this case contamination, though relatively low, is still increasing. The sediment accumulation rates for the Central Vietnam minor lagoons, calculated as above, were in the range 0.10 to 0.28 cm y^{-1}. These values are rather low and are probably the results of strong hydrodynamic processes and an efficient exchange with the sea.

Throughout the years many different guidelines have been published and the threshold effect level (TEL), below which we can assume any effect to rarely occur to biota [5], appears the most restrictive one. Its value (870 ng g^{-1}) is always higher than the sum of congeners and the individual PAHs present very few values (generally relative to low weight congeners, Acenaphtene in particular) higher than their respective TELs [13]. Both Cluster Analysis and principal Component Analysis (PCA) can be usefully applied to find similarities among groups of samples. We used often statistical tools (e.g., Figure 9a) to compare PCB homologue compositions with the original Aroclor technical mixtures [9]. Giuliani et al. [13] performed a simple cluster analysis, based on the Euclidean distance calculated over percent amounts of each measured congener, in order to highlight the similarities among the different PAH assemblages found in sediments of Vietnamese lagoons. The result is shown in Figure 9b and account for a great dissimilarity between the three consecutive levels from 14 to 28 cm depth in core 02 (TG-CH Lagoon) and all the others. Interestingly, these levels provide a considerable subsurface concentration peak, their LMW/HMW ratios are the lowest for the entire data set (0.14, 0.25 and 0.12 for levels 14–16, 20–23 and 26–28, respectively) [13], and they seem contemporary to the Indochinese War period (1950–1975, Figure 9b). What follows, then, is that between 1950 and 1975, a strong PAH input, mainly composed by combustion generated congeners, reached the northern sector of the TG-CH Lagoon, probably vehicled by the O Lau River, the closest to the 17th parallel and the DMZ (DeMilitarised Zone). The origin of such PAH assemblage might be explained by forest fires that were artificially set in the area to facilitate military operations. No such great differences are observed among the other lagoons and in the southern sector of the TG-CH Lagoon.

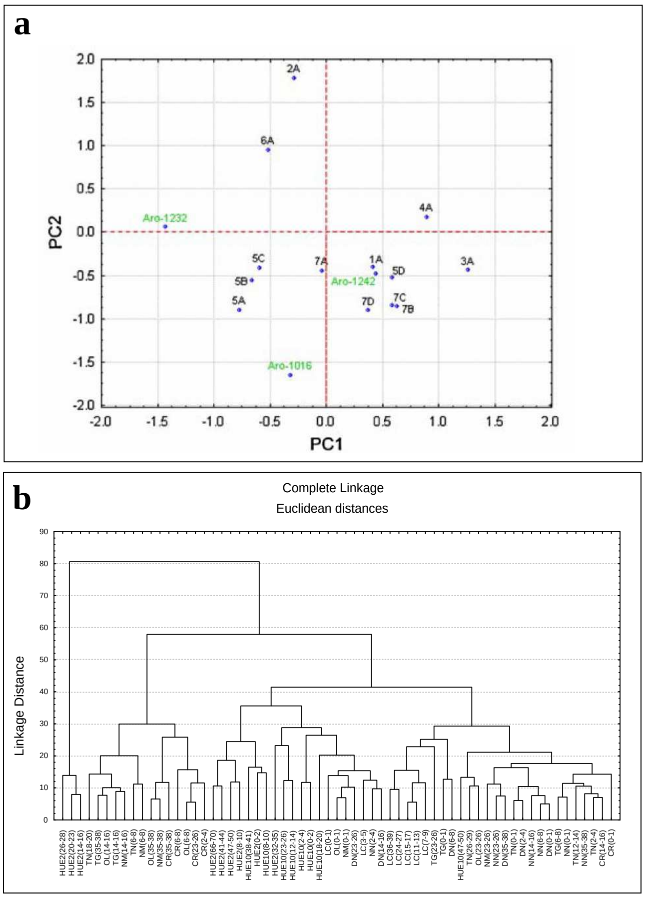

Figure 9: Examples of statistical applications to environmental parameters: a) Principal Component Analysis of PCB homologue compositions in mexican sediments and Aroclor mixtures; b) Cluster Analysis of PAH assemblages in sediments of Vietnamese lagoons.

8 Conclusions and perspectives

The analysis, with sufficient resolution, of carefully sampled and subsampled sediment cores permits to trace the history of contamination in the study area and, at the same time, to obtain crucial information about the processes that characterise the aquatic system and their evolution. Whenever possible, the integration of several different information (in order to choose the best sampling sites) guarantees the best and most reliable results.
However, the approach here described should be integrated in a more complete framework, able to model the behaviour of contaminants in terms of input-output, speciation, transport, distribution, bioaccumulation, biomagnification and toxicity, as described by Mugnai et al. (this volume).

9 Acknowledgements

This paper discusses results obtained in the framework of different research projects funded by EniChem SpA, the Ministry of Public Works, through the Magistrato alle Acque di Venezia and the Consorzio Venezia Nuova, and co-funded by CNR and/or the Ministry of Foreign Affairs (MAE).
This is contribution No. 1727 from the Istituto di Scienze Marine, U.O.S. di Bologna.

References

[1] M. Frignani, L.G. Bellucci, and S. Giuliani. Detailed reconstruction of contaminating events through the study of coastal marine sediments. *Proceedings of the BOSICON Meeting (Rome, 14-15 February 2006)*, 2006.

[2] D. Sorgente, M. Frignani, L. Langone, and M. Ravaioli. Chronology of marine sediments - Interpretation of activity-depth profiles of ^{210}Pb and other radioactive tracers, part 1. *IGM-CNR Technical Report n. 54*, 1999.

[3] M. Frignani, D. Sorgente, L. Langone, S. Albertazzi, and M. Ravaioli. Behaviour of Chernobyl radiocesium in sediments of the Adriatic sea off the Po River delta and the Emilia-Romagna coast. *Journal of Environmental Radioactivity*, 71:299–312, 2004.

[4] L.G. Bellucci, M. Frignani, J.K. Cochran, S. Albertazzi, L. Zaggia, G. Cecconi, and H. Hopkins. ^{210}Pb and ^{137}Cs as chronometers for salt marsh accretion in the Venice Lagoon - links to flooding frequency and climate change. *Journal of Environmental Radioactivity*, 97:85–102, 2007.

[5] M. Frignani, L.G. Bellucci, C. Carraro, and M. Favotto. Accumulation of polychlorinated dibenzo-*p*-dioxins and dibenzofurans in sediments of the Venice Lagoon and the industrial area of Porto Marghera. *Marine Pollution Bulletin*, 42:544–553, 2001.

[6] L.G. Bellucci, M. Frignani, S. Raccanelli, and C. Carraro. Polychlorinated dibenzo-*p*-dioxins and dibenzofurans in surficial sediments of the Venice Lagoon (Italy). *Marine Pollution Bulletin*, 40:65–76, 2000.

[7] U.S. Environmental Protection Agency. Interim procedures for estimating risk associated with exposures to mixtures of chlorinated dibenzo-*p*-dioxins and dibenzofurans (CDDs and CDFs) and 1989 upgrade. *Risk Assessment Forum, Washington D.C EPA/625/3-89/016*, 1989.

[8] R. Piazza, A.C. Ruiz-Fernández, M. Frignani, M. Vecchiato, L.G. Bellucci, A. Gambaro, L.H. Pérez-Bernal, and F. Páez-Osuna. Historical PCB fluxes in the Mexico City Metropolitan Zone as evidenced by a sedimentary record from the Espejo de los Lirios lake. *Chemosphere 75, 1252-1258*, 75a:1252–1258, 2009a.

[9] R. Piazza, A.C. Ruiz Fernàndez, M. Frignani, R. Zangrando, L.G. Bellucci, I. Moret, and F. Paez Osuna. PCBs and PAHs in surficial sediments from aquatic environments of Mexico City and the coastal states of Sonora, Sinaloa, Oaxaca and Veracruz (Mexico). *Environmental Geology*, 54:1537–1545, 2008.

[10] R. Piazza, B. El Moumni, L.G. Bellucci, M. Frignani, M. Vecchiato, S. Giuliani, S. Romano, R. Zangrando, and A. Gambaro. Polychlorinated biphenyls in sediments of selected coastal environments in northern Morocco. *Marine Pollution Bulletin*, 58:424–455, 2009b.

[11] M. Frignani, R. Piazza, L.G. Bellucci, N.H. Cu, R. Zangrando, S. Albertazzi, I. Moret, S. Romano, and A. Gambaro. Polychlorinated biphenyls in sediments of the Tam Gan-Cau Hai Lagoon, Central Vietnam. *Chemosphere*, 67:1786–1793, 2007.

[12] J.A. Robbins. Geochemical and geophysical application of radioactive lead. *The Biogeochemistry of Lead in the Environment*, 1978.

[13] S. Giuliani, M. Sprovieri, M. Frignani, N.H. Cu, C. Mugnai, L.G. Bellucci, S. Albertazzi, S. Romano, M.L. Feo, E. Marsella, and D.H. Nhon. Presence and origin of polycyclic aromatic hydrocarbon in sediments of nine coastal lagoons in central Vietnam. *Marine Pollution Bulletin*, 56:1504–1512, 2008.

Present Relative Sea Level Rise in the Northern Adriatic Coastal Area

L. Carbognin[1], P. Teatini[1], L. Tosi[1], T. Strozzi[2], A. Tomasin[1]
1, Institute of Marine Sciences, CNR, Venezia, Italy
2, GAMMA Remote Sensing Research and Consulting AG, Gümligen, Switzerland
luigi.tosi@ismar.cnr.it

Abstract

Relative sea level rise (RSLR), that has been occurred along the entire coastal areas of the Northern Adriatic Sea, includes land subsidence, both natural and man-induced, and eustacy. Their combined effect has produced relative ground settlements ranging from centimetres to meters. RSLR represents one of the geologic hazards threatening the low-lying coast. Recent progresses made in understanding these two processes are presented. Synthetic Aperture Radar (SAR) interferometry has significantly improved the knowledge of actual land subsidence. In particular, comprehensive maps of the vertical displacements occurred over the period 1992-2009 in the region between Venice and Ravenna reveal a significant spatial variability, ranging from a slight 1 to 2 mm$\cdot$yr^{-1} uplift, to a serious subsidence of more than 15 mm$\cdot$yr^{-1}. The availability of tide gauge data in Trieste, Venice, and Ravenna allows accurate assessment and meaningful observations on sea level change. The period 1896-2006 is characterized by an average rise of 1.2$\pm$0.1 mm$\cdot$yr^{-1}. The analyses here performed show that a time series at least 50 yr long must be used to obtain statistically significant results and reliable trend, due to the 7-8 year pseudo-cyclicity, recorded at many Mediterranean coastal stations. In Venice and Ravenna the influence of land subsidence on the RSLR amounts to 57% and 85%, respectively. This percentage has been estimated in 95% at the Po Delta.

1 Introduction

The Northern Adriatic (NA) Sea is characterized by a shallow water depth and a subsiding sedimentary basin underlies its western side (Figure 1). The Italian coastland is characterized by low-lying environments such as deltas, lagoons, wetlands, and farmlands subjected to a marked anthropogenic impact and at great hydrogeological risk. The relative sea level rise (RSLR), i.e. the interaction between land subsidence and eustacy, has been responsible for significant changes in coastal morphology over millennia, and is still today one of the major environmental hazards. The NA coastland developed after the last glacial maximum during the Holocene transgression and from about 5,000 yr BP, over highstand times, the coastline began to prograde seaward due to the sediment supply from major rivers, and delta and lagoon systems developed. During the last millennium, the NA coastland has been even more affected by anthropogenic impacts. The formation of the modern deltaic system of Po River dates back to about 500 yr BP. In general the whole coast reached the

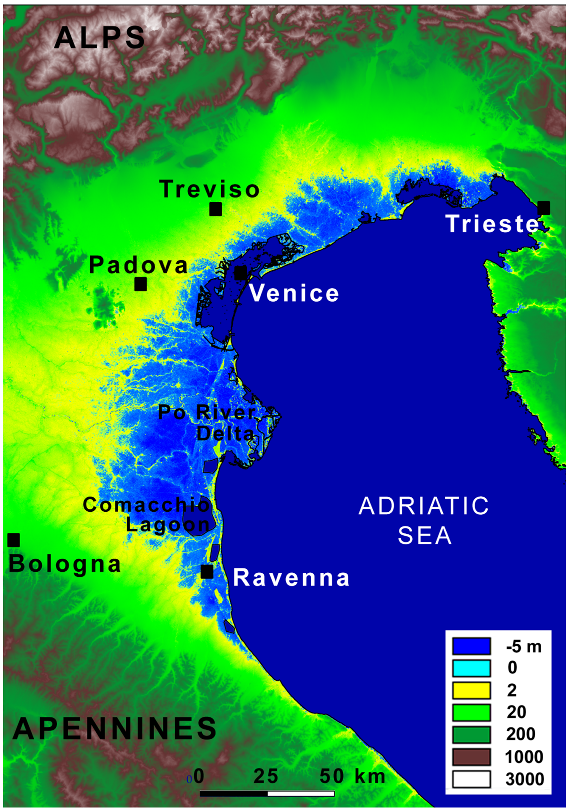

Figure 1: DEM of the NA region with the location of the most important cities. The coastland lying below the m.s.l. is highlighted by the blu-scale colour.

present setting only a couple of centuries ago under the strong influence of human interventions [5, 6].

Man-induced land subsidence has greatly affected the NA coastland over the 20th century, and especially after World War II, when overexploitation of subsurface fluids was responsible for a general lowering of the coastal plain and a significant coastline retreat [7, 8]. After the 1960s-1970s, when the relationships between land settlement and fluid withdrawal clearly emerged, the drastic reduction of the pumping rates produced a significant decrease of the subsidence rates. However, land subsidence is a process that is still affecting the study area. Rise of the sea level during the 20th century and at present is a well documented process worldwide that is linked to climate changes, mainly ice melting and the consequent variation in the mass and volume of the oceans. The relatively modest warming recorded throughout the last century has however induced global rises of sea level that have approached 1.2-2.0 mm$\cdot$yr^{-1} [9]. In this respect, it is important to point out that the comparison between long tide-gauge records around

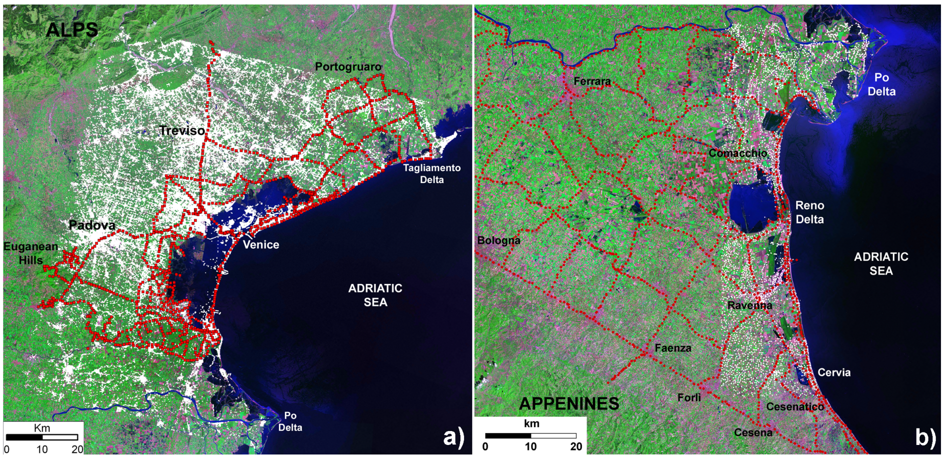

Figure 2: Land subsidence monitoring networks in the a) Venetian, and b) Emilia-Romagna costal plains. White dots represent the position of the persistent scatterers detected by PSI on ERS-1/2 acquisitions and the red dots are the location of the levelling benchmarks. The information are provided after [1] and [2] for the Venice region and after [3] and [4] in Emila-Romagna.

the world shows an eustatic rate in the NA Sea, along with the whole Mediterranean Sea, significantly lower (by approximately 35%) than the global mean value. This is likely due to Northern Atlantic Oscillation (NAO)-induced changes in atmospheric pressure, temperatures, and salinity variation, on account also of the specific features of this almost closed sea (e.g., [10]).

In this work we investigate the present RSLR by using Synthetic Aperture Radar (SAR)-based interferometry and long and nearly continuous tide gauge records that allow to separate the two components, i.e. vertical land movements and eustacy, respectively.

2 Data and methods

Levelling surveys, though not made on a regular basis, have been periodically carried out in the NA coastland since the end of the 19th century. Significant enlargement of the levelling networks has been carried over the last 20 yr in the areas characterized by the stronger land sinking. Global Positioning System (GPS) has been used to monitor vertical movements mostly from the 1990s when GPS measurements reached a millimetre-level accuracy.

Differential and Continuous Global Positioning System (DGPS and CGPS) surveys have then been extensively used to complement the ground-based surveys.

Furthermore, land subsidence monitoring has been significantly improved over the last couple of decades by space-borne earth observation techniques based on SAR interferometry. The measurements were ini-

tially carried out by the DInSAR approach [11] and more recently by Persistent Scatterer Interferometry (PSI) [12].
Recently, SAR-based interferometry has been widely adopted in the NA coastland. Two classes of PSI process i.e., the Permanent Scatterers (PS) (e.g., [13]) and the Interferometric Point Target Analysis (IPTA) (e.g., [14]), have significantly improved the knowledge of the land movements for the areas North and South of the Po River, respectively. Levelling and GPS measurements have been processed with the main purpose of calibrating the SAR surveys (Figure 2).
Here we present the PSI results obtained with the following satellite images:

- ERS-1/2 satellites: available scenes are acquired on a 100×100 km^2 area with a 35-day frequency. The images have been processed to map the movements occurred in the whole coastland from 1992 to 2002 [13, 15, 3, 1, 16, 17, 4];
- ENVISAT satellite: available scenes are acquired on a 100×100 km^2 area with a 35-day frequency. The images have been analyzed to monitor the recent coastland displacements from the northern portion of the Po River delta to the Tagliamento River between 2003 and 2007 [16] ;
- TerraSAR-X satellite: available scenes are acquired on a 30×60 km^2 area with a 11-day frequency. The images acquired from March 2008 to February 2009 have been used to measure the present ground movements along the littoral strips of the Venice Lagoon [18].

Concerning the sea level observation, we analyze the tide gauge measurements from the Trieste, Venice, and Ravenna stations. The available records span the period between 1896 and 2006 (Regione Emilia Romagna, 1996, [19]).

3 Relative sea level rise

RLSL is due to the superposition of natural land subsidence, anthropogenic land subsidence, and eustacy. The separation of each contribution is a difficult task and an accurate computation at a regional/local scale is possible for the last century over which data are available from regular instrumental records. In fact, from the beginning of 1900 spirit levelling and, presently GPS and SAR have been used to survey land elevation. Moreover, starting from the end of 1800 tide-gauge has been adopted to monitor sea level height.

3.1 Land subsidence: an overview

Vertical displacements in the NA coastal areas are caused by both natural and anthropogenic factors. Their understanding is essential to estimate land loss or gain and, consequently, predict the relative sea level changes. Natural and anthropogenic components act on different timescales (millions to thousands years and hundreds to tens years, respectively), reflecting the geological history and the human development of the territory. The role played by the long-term natural causes, i.e. tectonics and glacio-isostasy, is negligible in modern times, while natural compaction of recent alluvial fine-grained deposits has assumed a major importance. As a general statement, a certain correlation exists between the thickness of the Quaternary formations and the amount of natural subsidence, so that the sinking rate exhibits a non-uniform space distribution [20]. Natural land subsidence occurred and continues to occur unevenly at different rates. In particular it has been estimated in the range of 0.5-1.0 mm$\cdot$yr^{-1} in the Venetian territory

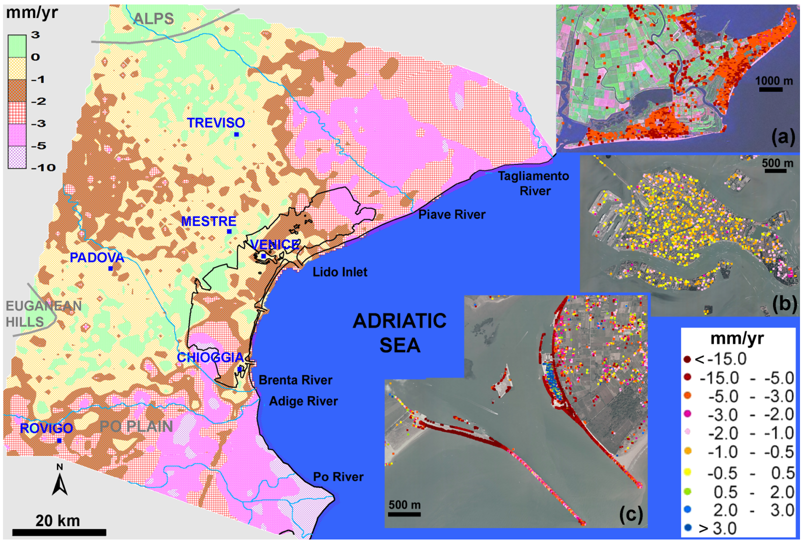

Figure 3: Map of the average displacement rates (mm·yr^{-1}) in the Venice region over the decade 1992-2002 (after [8, 1] and [31]). Negative values mean subsidence and positive uplift. The insets detail the displacements at: a) the Tagliamento river mouth from 2003 to 2007, b) the city of Venice from 1992 to 2000, and c) the Lido inlet from March 2008 to February 2009, obtained by IPTA on ENVISAT, ERS-1/2 and TerraSAR-X scenes, respectively.

(e.g., [21, 22]), about 2.0-2.5 mm·yr^{-1} in the Ravenna area (e.g., [23, 8]), and twice as much in the Po River delta (e.g., [24, 25]). Anthropogenic subsidence due to subsurface fluid withdrawal become a key problem for the land stability over the 20th century, and especially after World War II, when the civil, industrial, agricultural, and tourist development required huge amounts of water and an increasing energy supply. Different fluids were withdrawn along the study coastland: groundwater in the Venice area, gas-bearing water in the Po Delta, and both freshwater from confined aquifers and gas from deep reservoirs in the Ravenna region. Levelling surveys have shown that the cumulative subsidence has reached values of some centimetres in the Venice area [26], 2-3 m in the Po River delta [27, 28, 29], and as much as 1.5 m southward along the Romagna coastland (e.g., [3, 30]). The largest settlement rates of 17 mm·yr^{-1}, 300 mm·yr^{-1}, 110 mm·yr^{-1} were recorded at Venice-Marghera, Po Delta, and Ravenna industrial zone, over the periods 1968-1969, 1950-1957, and 1972-1973, respectively. From the early 1960s, in the Po delta area, and 1970s in the another places, countermeasures have been taken and anthropogenic subsidence strongly reduced or stopped.

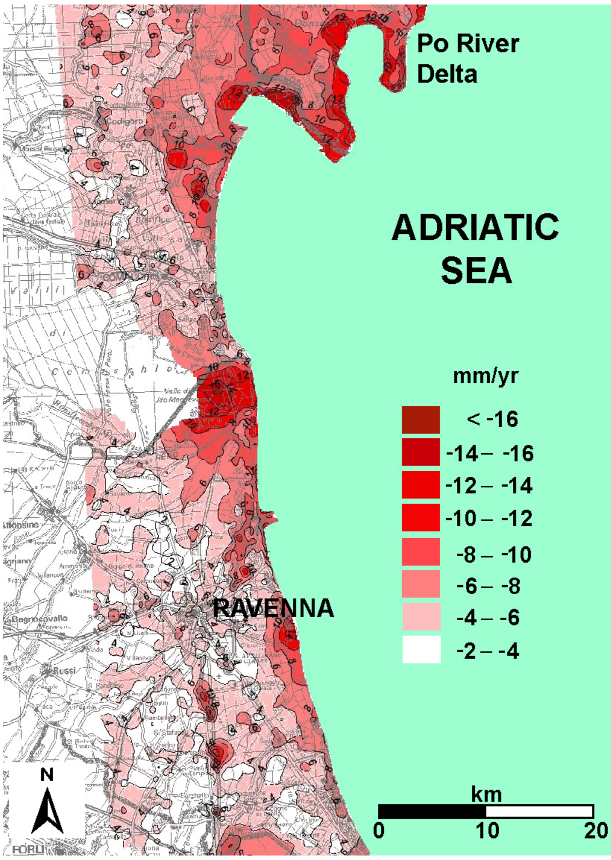

Figure 4: Map of the displacement rates ($mm{\cdot}yr^{-1}$) in the Emilia Romagna coastland obtained by PS analysis over the 1992-2000 period using ERS-1/2 images (after [17, 4]).

3.2 Land subsidence: recent quantification

The SAR-based techniques have allowed to map the land subsidence, which is currently affecting the Northern Adriatic coastland, with high accuracy and spatial detail. The result exhibits a resolution never obtained before.

An innovative Subsidence Integrated Monitoring System (SIMS), which efficiently merges the different displacement measurements obtained by levelling, GPS, and SAR-based interferometry, has been designed to accurately and reliably keep land movements under control in the Venice coastland from the Po River to the South to the Tagliamento River northward [1]. Using the ERS-1/2 images acquired between 1992 and 2002, the SIMS provides a comprehensive map of the ground vertical displacements in the Venice region (Figure 3), and shows that, as observed in other coastlands, their movement rates

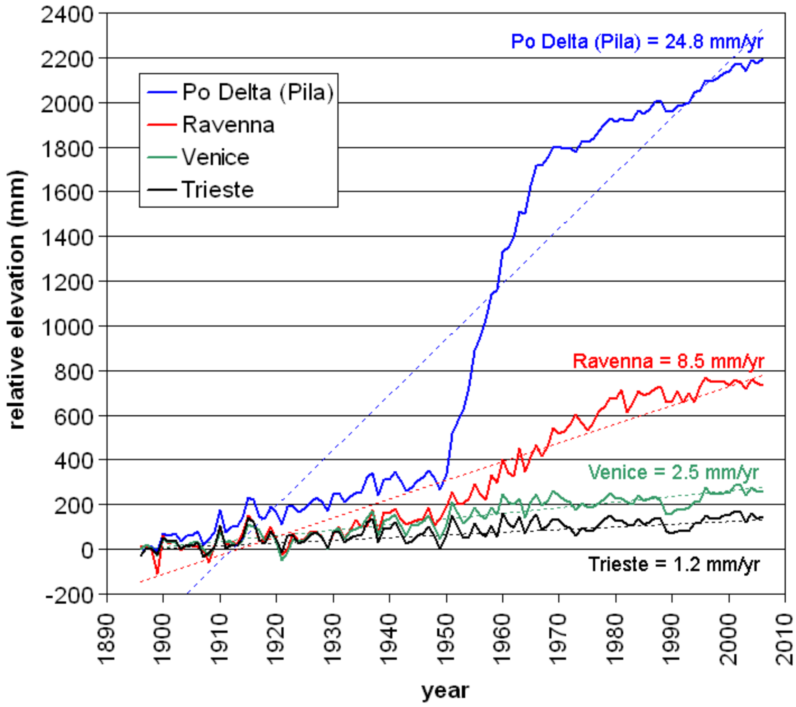

Figure 5: Mean sea level at Trieste, Venice, and Ravenna from 1896 to 2006. The linear regressions of the yearly values are represented together with the average eustatic rate. Ravenna records have been updated after Regione Emilia Romagna (1996). Venice and Trieste records after [32]. The Po Delta time series has been reconstructed as described in the text.

are highly variable. General land stability has been detected in the central part of the study area, including the major cities of Venice, Padova, and Treviso, with scattered local bowls of subsidence of up to 2 to 3 mm·yr^{-1}. Conversely, land settlement has appeared as a widespread phenomenon in the northern and southern coastlands and at the lagoon extremities, with rates of up to 5 and 15 mm·yr^{-1}, respectively. Uplift rates ranging from 0.5 to 1.5 mm·yr^{-1} have been measured in two different large areas located north of Treviso and south of Padova, respectively, whereas higher values are restricted to the eastern sector of the Euganean Hills. The highest sinking rates are recorded in the Po Delta (see also Figure 4). Here the movement rates show a significant spatial variability, with the maximum values of up to 15 mm·yr^{-1} measured at the delta tips.

IPTA allows also to study with very high resolution the movements occurring at local scale. A detail of the displacements at the mouth of the Tagliamento River obtained by ENVISAT scenes for the 2003-2007 period is reported in Figure 3a.

The area, where the Bibione and Lignano

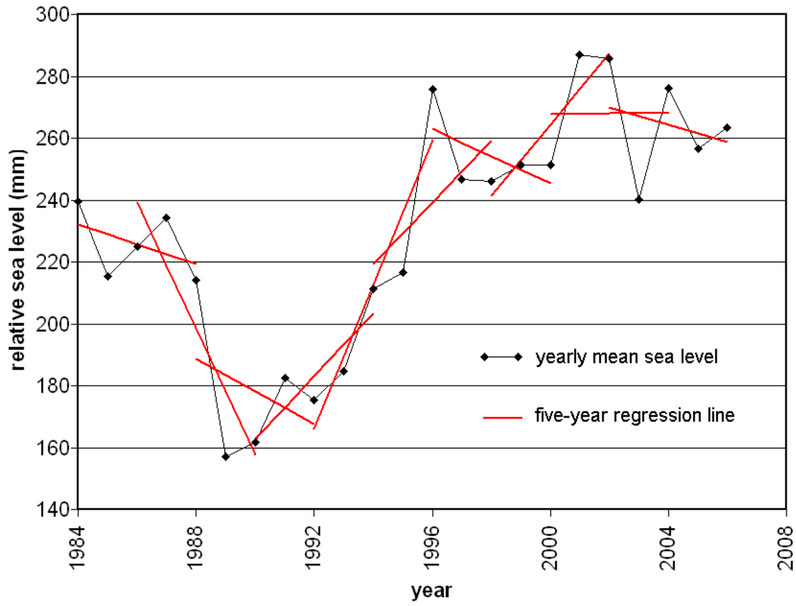

Figure 6: The yearly values of mean sea levels at Venice in the last 25 yr show a significant oscillating behaviour and contradictory tendencies.

tourist towns are located, is subsiding at a rates from 3 to 7 mm·yr^{-1}. Figure 3b shows the ground vertical movements of the Venice historical center obtained by ERS-1/2 scenes from 1992 to 2002. The city has been stable over the past decade, with the displacement rates generally smaller than 1 mm·yr^{-1} [16]. Only the eastern and, subordinately, western and northern tips of the urban area, which coincide with the city sectors built up after 1500 and where soil consolidation process may still be continuing [15], have subsided at a rate on the order of 1-2 mm/year. We used TerraSAR-X with the aim to reveal the impact of the mobile barrier works, the well known Modulo Sperimentale Elettromeccanico (Mo.S.E.), on Venice coastland stability [18]. An example of the displacements detected in 2008 at the Lido inlet is reported in Figure 3c. Consolidation related to these ongoing works is causing local settlement rates of up to 50 mm·yr^{-1}. Note that the central part of the craft harbor under construction is uniformly rising by almost 10 mm·yr^{-1} due the load of the surrounding structures and of the hydraulic overpressure acting on the lock bottom located at about 10 m below the mean sea level which is currently drained.

Investigations by the PS method have allowed to extend south of the Po Delta the mapping of the land displacements to the Ravenna area, [13, 17, 4]. Figure 4 shows the subsidence rates averaged over the 1992-2002 period. Although SAR-based measurements show that at present the mainland, e.g. the area surrounding Ravenna, appears to be substantially stable, subsidence still continues over a few

kilometre wide coastal strip at a rate of about 10 mm·yr^{-1}, lesser than in the past decades, but significantly larger than the natural settlement rate. Two local portions of the littoral belt are sinking at a higher rate (up to 15 mm·yr^{-1}), probably due to gas removal from deep reservoirs located below the coastline.
It is worth reminding that researches recently performed have shown that some portions of the reclaimed farmland bounding the Venice, Po Delta and Comacchio lagoons are sinking up to 20-30 mm·yr^{-1} because of either peat soil oxidation, occurring in response of drainage for agricultural purposes, and salinisation of clayey sediments (e.g., [33, 34, 35]).

3.3 Eustacy

An analysis of the mean sea level records at the Adriatic stations of Trieste, Venice, and Ravenna over the period from 1896 to 2006 shows results that vary noticeably between the different areas. Although presenting short-cycle fluctuations, the historical tide-gauge data at Trieste, a city known to be stable, are characterized by a unique linear trend for the whole period, with a mean eustatic rise of 1.2 mm·yr^{-1} [32]. Contrasting, the average rising rate for the mean sea level at Venice and Ravenna is equal to 2.5 mm·yr^{-1} and 8.5 mm·yr^{-1}, respectively. The differences are due to the subsidence component of the RSLR that has affected Venice and Ravenna producing an apparent higher sea level rise (Figure 5). Unfortunately any long tide gauge series exists at the Po River delta. Nevertheless, we have performed a simulation trying to reconstruct the likely behaviour of a tide gauge located in the Po Delta by adding the SLR recorded at Trieste and the vertical land movement measured in the deltaic area, in particular at the Pila site. The subsidence time series has been derived from the available literature: from 1896 to 1950 after [25], from 1950 to 1957 after [24], from 1958 to 1967 after [27], from 1968 to 1974 after [28], and between 1975 to 2006 after [29] and [31]. The reconstructed behaviour of the Po Delta tide-gauge is shown in Figure 5.
Analyses of the Mean Sea Level (m.s.l.) clearly show that the use of short periods to derive a tendency of eustatic rise yields contradictory findings and suggests that a great caution must be taken in a “trend analysis”. It should be stressed that to identify a meaningful “sea level trend” it is necessary to use homogeneous and long time records. A time series at least 50 yr long must be used [32], as also suggested by [36]. For example, m.s.l. analysis at Venice shows a steady decrease (-0.8 mm·yr^{-1}) between 1971 and 1993, followed by a serious rise (5.5 mm·yr^{-1}) from 1994 to 2000, and a new lowering phase (-2.6 mm·yr^{-1}) between 2001 and 2006. As a peculiar example of the observed up-and-down behaviour, the annual m.s.l. data at Venice over the last 25 yr is reported in Figure 6 along with a few five-year regression lines. The highly oscillating behaviour clearly shows that this short period is not significant for a trend computation.

4 Environmental remarks

RSLR has been and currently appears to be the main process for the increased vulnerability of the NA coastal areas. Although nowadays the subsidence induced by subsurface fluid removal does not represent a major problem being generally under control, it has led to an irreversible loss in elevation with respect to sea level with a consequent increase of environmental hazard. The serious amount of the occurred RSLR has harmed urban zones, industrial areas, beaches, and the surrounding vast marshland reclamations which become even more prone to be submerged. A variation in the relationship between the land and the sea has occurred along the entire coast, with notable changes in geomorphologic and ecological features including coastal erosion and regression concurrently with the deepening of the sea bottom slope near the shoreline (e.g., [37]), increased flooding and coastal inundations, and damage to coastal infrastructure. In the Po Delta the morpho-ecological setting of the territory was completely altered. Changes occurred in the hydrographic net with the inversion of the original discharge direction thus requiring restoration works. A noteworthy saltwater intrusion in shallow aquifers and surficial waters has occurred along the coast (e.g., [35]). Some areas have become brackish swamps with severe consequences on the ecological system. Soil contamination by saltwater has produced detrimental consequences on the agricultural and fishing activities, which are normally located in transitional zones.

In the Venetian area, the RSLR of modest figure with respect to other areas (about 250 mm from the beginning of 1900 until today) has become of crucial importance for Venice emerging today only 900 mm above the NA [38]. Presently, relative sea level rise has increased the flood frequency by more than seven times with severe damages to the valuable urban heritage, enhanced erosion processes within the lagoon, and worsened the precariousness of the coastal strip, and ever more frequent restorative interventions are carried out.

One can say that the entire NA low coast is already experiencing the effects of the expected variation in climatic conditions, associated with the risk of a global rise in sea level. Even if land subsidence is generally no longer a major threat, further few centimetres of relative rising of the sea could be a serious peril for the survival of these coastal zones. During the 21st century, sea level is expected to rise considerably faster that in the20th, but because of uncertainties in the climate forecasting, it is not clear how rapidly this will occur. In particular, uncontroversial projections for the Adriatic Sea, that assumes very peculiar and different characteristics due to its shape and low depth, are still not available.

Reasonable forecasts of possible RSLR during this century are of paramount importance for the survival of the NA coastland and the development of effective mitigation strategies. For example, concerning the operational efficiency of Mo.S.E. at the Venice lagoon inlets, [32] propose plausible local scenarios of RLSR over the next century at Venice considering the regional subsidence history, the recorded sea level trend, along with the IPCC A1B mid-range. The results show that RSLR projections by 2100 give a large range from 170 to 530 mm, i.e. between a moderate nuisance to an unsustainable aggression. In fact the flooding events requiring the inlet closure could increase to 20 or even 250 times per year with respect to the present annual frequency of 4 times.

5 Conclusive discussion

SAR-based interferometry has opened new perspectives for studying ground surface dynamics, allowing for high resolution investigation on large areas. PSI has been applied on the NA coastland between Ravenna and the Tagliamento River over the last two decades. Once calibrated and validated by levelling and GPS measurements, this remotely-sensed technique has provided very interesting results both at "regional" and "local" (few km^2) scales. Recent (1992-2002) and present (2003-2009) maps of land vertical movements highlight a significant spatial variability with displacement rates ranging from a slight (1-2 $mm \cdot yr^{-1}$) uplift to a serious coastal subsidence of more than 15 $mm \cdot yr^{-1}$. These considerations hold for the entire NA coast. In general, differential consolidation of the Pleistocene and Holocene deposits and tectonics, and subsurface fluid withdrawals, land reclamation, and locally farmland conversion into urban areas, superimpose to produce the observed displacements.

A very detailed analysis performed over the Venetian region distinguishes the displacement components on the basis of the depth of their occurrence [40]. Deep causes, acting at a depth generally greater than 400-600 m below m.s.l., refer to downward movements of the pre-Quaternary basement and land uplift (up to 2 $mm \cdot yr^{-1}$) most likely related to neotectonic activity connected with the Alpine thrust belts and fault systems. Medium causes, acting at a depth between about 400 m and 50 m below m.s.l., are of both natural and anthropogenic origin. The former refers to the Medium-Late Pleistocene deposits that exhibit a larger cumulative thickness of clayey compressible layers at the lagoon extremities with respect to the central lagoon area where stiffer sandy formations prevail. Land subsidence due to aquifer exploitation mainly occurs in the north-eastern sector of the coastland where thousands of active wells are located. In a 10-15 km wide coastal strip the thickness, texture, and sedimentation environment of the Holocene deposits [41, 42, 43] play a significant role in controlling shallow causes of land subsidence. Other factors that contribute in increasing land sinking at a lesser areal extent are the salinization of clay deposits due to saltwater intrusion, and the biochemical oxidation of outcropping peat soils (e.g., [33, 34]). The load of buildings and structures after the conversion of farmland into urbanized areas causes superficial compaction of very local sites.

The counterpart to the land movements, as stated above, is the evolution of the m.s.l. In the study area, an heritage of secular tide-gauge data is available at Venice, Trieste, and Ravenna. Their comparison, also including the series reconstructed for the Po Delta area, is precious. Since Trieste is located on a stable area, the rate of 1.2 $mm \cdot yr^{-1}$ is attributable to the eustatic rise only [32]. This value agrees with the eustatic rise measured at other stations in the Mediterranean Sea [44]. Moreover, considering the shape of the Adriatic Sea and the location of the tide gauges, it is plausible to assume as true the trend in Trieste, and apparent those of the other places (see Figure 5). In fact in Venice, Po Delta, and Ravenna the influence of land subsidence on the relative sea/ground elevation changes results equal to 57%, 95%, and 85%, respectively (Figure 7).

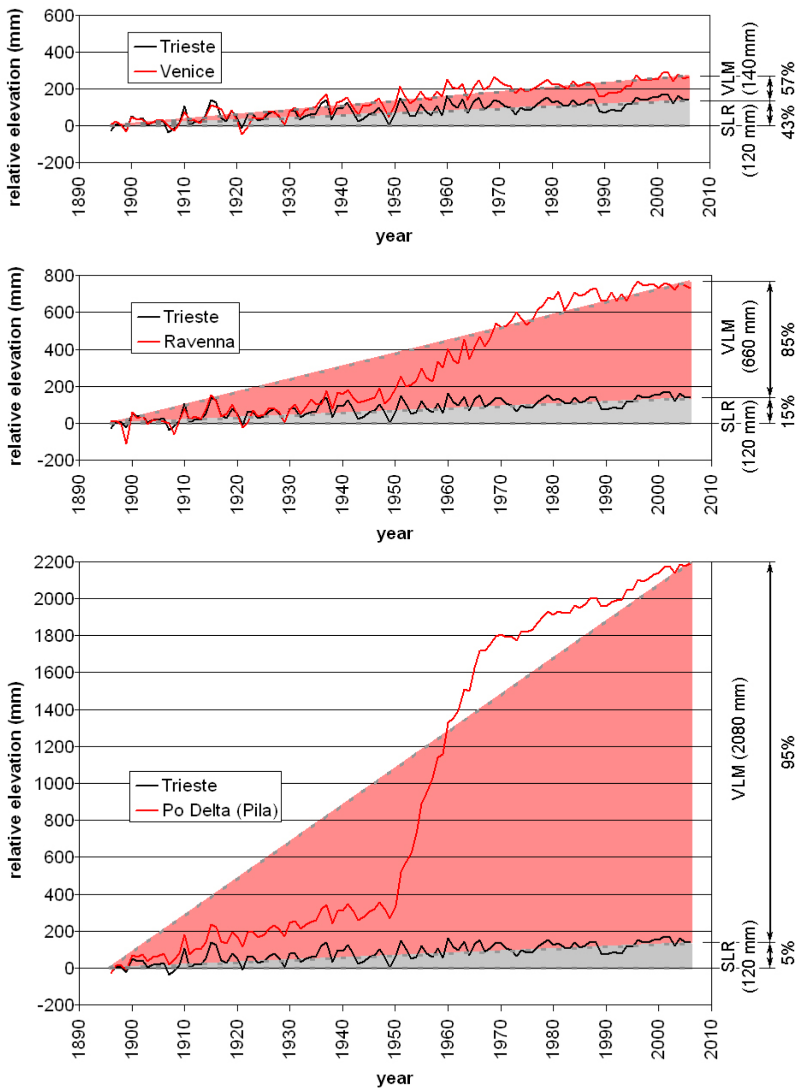

Figure 7: Yearly average sea level at Venice, Po Delta, and Ravenna compared with that of Trieste over the period between 1896 and 2006. At Venice, Po Delta, and Ravenna the contribution of land subsidence (VLM) to the overall RSLR is separated from the contribution due to the eustatic sea level rise (SLR) using the tide gauge records at Trieste (updated after [39]).

References

[1] P. Teatini, L. Tosi, T. Strozzi, L. Carbognin, U. Wegmuller, and F. Rizzetto. Mapping regional land displacements in the venice coastland by an integrated monitoring system. *Remote Sens. Environ.*, 98:403–413, 2005b.

[2] L. Tosi, P. Teatini, L. Carbognin, and J. Frankenfield. A new project to monitor land subsidence in the northern venice coastland (italy). *Enviorn. Geol.*, 52(5):889–898, 2007.

[3] F. Bonsignore and M. Carati. Subsidenza in emilia-romagna: la rete di controllo in internet. *ARPA-ER Rivista*, 3:32–33, 2003.

[4] M. Preti. Subsidenza: un problema storico per la costa emiliano-romagnola lontano dalla soluzione. *ARPA-ER Rivista*, Supplemento and 11(1):16–18, 2008.

[5] L. Carbognin and F. Marabini. Evolutional trend of the po river delta (adriatic sea, italy). In *28th Int. Geol. Congress*, volume I, pages 229–238, Washington D.C., 1989. AGU.

[6] M. Stefani and S. Vincenzi. The interplay of eustacy, climate and human activity in the late quaternary depositional evolution and sedimentary architecture of the po delta system. *Mar. Geol.*, 222-223:18–48, 2005.

[7] L. Carbognin and L. Tosi. Interaction between climate changes, eustacy and land subsidence in the north adriatic region and italy. *Mar. Ecol.*, 23(1):38–50, 2002.

[8] P. Teatini, M. Ferronato, G. Gambolati, W. Bertoni, and M. Gonella. A century of land subsidence in ravenna, italy. *Environ. Geol.*, 47(6):831–846, 2005.

[9] S.J. Holgate. On the decadal rates of sea level change during the twentieth century. *Geophys. Res. Lett.*, 34(L01602):doi:10.1029/2006GL028492, 2007.

[10] M. N. Tsimplis and M. Rixen. Sea level in the mediterranean sea: The contribution of temperature and salinity changes. *Geophys. Res. Lett.*, 29(2136):doi:10.1029/2002GL015870, 2002.

[11] A.K. Gabriel, R.M. Goldstein, and H. Zebker. Mapping small elevation changes over large areas: differential radar interferometry. *J. Geophys. Res.*, 94:9183–9191, 1989.

[12] S. Usai and R. Klees. Sar interferometry on a very long time scale: A study of the interferometric characteristics of man-made features. *IEEE Trans. Geosci. Remote Sens.*, 37(4):2118–2123, 1999.

[13] A. Ferretti, C. Prati, and F. Rocca. Permanent scatterers in sar interferometry. *IEEE Trans.Geosci. Remote Sens.*, 39(1):8–20, 2001.

[14] C. Werner, U. Wegmuller, T. Strozzi, and A. Wiesmann. Interferometric point target analysis for deformation mapping. In *IGARSS 2003, International Geoscience and Remote Sensing Symposium*, volume VII, pages 4362–4364. IEEE, 2003. CD-ROM.

[15] L. Tosi, L. Carbognin, P. Teatini, T. Strozzi, and U. Wegmuller. Evidences of the present relative land stability of venice, italy, from land, sea, and space observations. *Geophys. Res. Lett.*, 29(12):doi:10.1029/2001GL013211., 2002.

[16] P. Teatini, T. Strozzi, L. Tosi, U. Wegmuller, C. Werner, and L. Carbognin. Assessing short- and long-time displacements in the venice coastland by synthetic aperture radar interferometric point target analysis. *J. Geophys. Res.*, 112(F01012):doi:10.1029/2006JF000656, 2007.

[17] F. Bonsignore. Subsidenza: il monitoraggio in emilia-romagna. *ARPA-ER Rivista*, Supplemento and 11(1):12–13, 2008.

[18] T. Strozzi, P. Teatini, and L. Tosi. Terrasar-x reveals the impact of the mobile barrier works on the venice coastal stability. *Remote Sens. Environ.*, 114:2682–2688, 2009.

[19] Regione Emilia-Romagna IDROSER SpA. Progetto di piano per la difesa dal mare e la riqualificazione ambientale del litorale della regione emilia-romagna. relazione generale, 1996.

[20] A. Brambati, L. Carbognin, T. Quaia, P. Teatini, and L. Tosi. The lagoon of venice: geological setting, evolution and land subsidence. *Episodes*, 26(3):264–268, 2003.

[21] G. Bortolami, L. Carbognin, and P. Gatto. The natural subsidence in the lagoon of venice, italy. In A.I. Johnson et al., editor, *Land Subsidence*, pages 777–785. IAHS Publ. No.151, 1984.

[22] V.D. Kent, D. Rio, F. Massari, G. Kukla, and L. Lanci. Emergence of venice during the pleistocene. *Quat. Sci. Rev.*, 21:1719–1727, 2002.

[23] L. Carbognin, P. Gatto, and G. Mozzi. Case history no.9.15: Ravenna, italy. In J.F. Poland, editor, *Guidebook to Studies of Land Subsidence Due to Ground-Water Withdrawal*, pages 291–305, Paris, 1984. UNESCO.

[24] A. Puppo. L'affondamento del delta padano: primi lineamenti di una cinematica del fenomeno. *Metano and Petrolio e Nuove Energie*, XI(10):567–575, 1957.

[25] G. Salvioni. I movimenti del suolo nell'italia centro-settentionale. dati prteliminari dedotti dalla comparazione di livellazioni. *Boll. Geodesia e Scienze Affini*, XVI(3):325–363, 1957.

[26] L. Carbognin, P. Gatto, and G. Mozzi. Case history no.9.3: Venice, italy. In J.F. Poland, editor, *Guidebook to Studies of Land Subsidence Due to Ground-Water Withdrawal*, pages 161–174, Paris, 1984. UNESCO.

[27] M. Caputo, L. Pieri, and M. Unguendoli. Geometric investigation of the subsidence in the po delta. *Boll. Geof. Teor. Appl.*, 47:187–207, 1970.

[28] M. Bondesan and U. Simeoni. Dinamica e analisi morfologica statistica dei litorali del delta del po e alle foci dell'adige e del brenta. *Mem. di Sc. Geol.*, XXXVI:1–48, 1983.

[29] L. Carbognin, J. Frankenfield Zanin, and F. Marabini. River delta region and italy. an overview of environmental evolution and land subsidence, 2000. La Garagola Publ., Italy, 42 pp.

[30] P. Teatini, M. Ferronato, G. Gambolati, and M. Gonella. Groundwater pumping and land subsidence in the emilia-romagna coastland, italy: Modeling the past occurrence and the future trend. *Water Resour. Res.*, 42(W01406):doi:10.1029/2005WR004242, 2006.

[31] L. Tosi, P. Teatini, T. Strozzi, L. Carbognin, G. Brancolini, and F. Rizzetto. Ground surface dynamics in the northern adriatic coastland over the last two decades. *Rendiconti Lincei-Scienze Fisiche e Naturali*, 21(Suppl. 1):115–129, 2010.

[32] L. Carbognin, P. Teatini, A. Tomasin, and L. Tosi. Global change and relative sea level rise at venice: What impact in term of flooding. *Clim. Dyn.*, 35(6):1055–1063, 2010.

[33] G. Gambolati, M. Putti, P. Teatini, M. Camporese, S. Ferraris, G. Gasparetto-Stori, V. Nicoletti, F. Rizzetto, S. Silvestri, and L. Tosi. Peatland oxidation enhances subsidence in the venice watershed. *EOS Trans. AGU*, 23(86):217–220, 2005.

[34] L. Carbognin, G. Gambolati, M. Putti, F. Rizzetto, P. Teatini, and L. Tosi. Soil contamination and land subsidence raise concern in the venice watershed, italy. In C. A. Brebbia et al., editor, *Management of Natural Resources, Sustainable Development and Ecological Hazards*, pages 691–700. WIT Press., 2006.

[35] M. Antonellini, P. Mollema, B. Giambastiani, K. Bishop, L. Caruso, A. Minchio, L. Pellegrini, M. Sabia, E. Ulazzi, and G. Gabbianelli. Salt water intrusion in the coastal aquifer of the southern po plain and italy. *Hydrogeol. J.*, 16(8):1541–1556, 2008.

[36] IPCC Intergovernmental Panel on Climate Change. Climate change 2007: Synthesis report, 2007. Geneva, 52 pp.

[37] L. Carbognin, P. Gatto, and F. Marabini. Correlation between shoreline variations and subsidence in the po river delta, italy. In A.I. Johnson et al., editor, *Land Subsidence*, pages 367–372. IAHS Publ. No.151, 1984c.

[38] L. Carbognin, P. Teatini, and L. Tosi. Eustasy and land subsidence in the venice lagoon at the beginning of the new millennium. *J. Mar. Syst.*, 51(1-4):345–353, 2004.

[39] L. Carbognin, P. Teatini, and L. Tosi. The impact of relative sea level rise on the northern adriatic coast. In C. A. Brebbia et al., editor, *Management of Natural Resources, Sustainable Development and Ecological Hazards II*, pages 137–148. WIT Press., 2009.

[40] L. Tosi, P. Teatini, L. Carbognin, and G. Brancolini. Using high resolution data to reveal depth dependent mechanisms that drive land subsidence: The venice coast. *Tectonophysics*, 474(1-2):271–284, 2009.

[41] L. Tosi, F. Rizzetto, M. Bonardi, S. Donnici, R. Serandrei Barbero, and F. Toffoletto. Note illustrative della carta geologica d'italia alla scala 1:50.000, foglio 128 ”venezia”, 2007. APAT, Dip.Difesa del Suolo and Servizio Geologico d'Italia, System Cart, Roma, 164 pp., 2 maps.

[42] L. Tosi, F. Rizzetto, M. Bonardi, S. Donnici, R. Serandrei Barbero, and F. Toffoletto. Note illustrative della carta geologica d'italia alla scala 1:50.000, foglio 148-149 ”chioggia-malamocco”, 2007. APAT, Dip.Difesa del Suolo and Servizio Geologico d'Italia, System Cart, Roma, 164 pp., 2 maps.

[43] L. Tosi, F. Rizzetto, M. Zecchin, G. Brancolini, and L. Baradello. Morphostratigraphic framework of the venice lagoon (italy) by very shallow water vhrs surveys: Evidence of radical changes triggered by human-induced river diversion. *Geophys. Res. Lett.*, 36(L09406):doi:10.1029/2008GL037136, 2009.

[44] M. Marcos and M. N. Tsimplis. Forcing of coastal sea level rise patterns in the north atlantic and the mediterranean sea. *Geophys. Res. Lett.*, 34(L18604):doi:10.1029/2007GL03064, 2007.

Application of Biomarkers in Marine Organisms to Assess the Conditions of Estuarine and Coastal Areas in the Adriatic Sea

L. Da Ros, V. Moschino, N. Nesto
Institute of Marine Sciences, CNR, Venezia, Italy
luisa.daros@ismar.cnr.it

Abstract

Benthic organisms are commonly used as suitable indicators in the environmental quality assessment of coastal-marine ecosystems. To this end, two different methodologies are normally approached, namely: 1) evaluating contaminant body burdens; 2) quantifying biological responses to pollutants throughout biological markers (biomarkers). Biomarkers, contributing to elucidate the health status of the selected species, may also supply indirect evidence of the health status of their living environment. The main objective of this study was to show the deleterious effects caused by contaminants and other environmental stressors at various levels of biological organization, from whole organism –where relevant physiological and behavioural effects were evidenced, to tissues and sub-cellular compartments – where biochemical and histochemical changes were recorded. In particular, the results of different sets of individual biomarkers tested in mussels, polychaetes and fish native to various coastal areas of the Adriatic sea, namely the lagoon of Venice, the gulf of Trieste and the Boka Kotorska Bay, were helpful in elucidating the ecotoxicological conditions of these environments. The results of the various biomarkers, tested in both native and transplanted organisms, provided helpful information on the impact of certain classes of contaminants and of natural stressors, suggesting the use of biological effect data as pragmatic screening tools for programming further close examinations in routine monitoring programs.

1 Introduction

Coastal pollution monitoring programs cannot be solely founded on chemical analyses of environmental samples, since this approach is inadequate to inform us about the actual biological effects of contaminants, their bioavailability and toxicity, and does not take into consideration the further emerging impacts due to contaminant mixtures. Alternatively, the effectiveness of the ecological approach, which offers quite standard tools such as the biodiversity indices to reach more comprehensive information of the "environmental health", could be limited by the large time gap between detecting the pollutants and observing the consequent ecological effects. To overcome somehow these complications, it has been proposed and developed in this context the concept of early warning bio-indicators which is at the basis of the large amount of biomarker laboratory studies and field applications in the last twenty years. This approach is borrowed from human medicine and the use of biomarkers as a measure of exposure to and effects of pollutants and other stressors has been increasingly adopted in coastal monitoring as useful tool for direct measurements of the quality status of life conditions. In fact, pollutants may have sub-lethal effects at different levels of their biological organization (cells, organs, individuals, community) and the biomarker approach includes a variety of measures of specific biochemical, cellular and physiological responses to contaminant exposure [1].

Fish and mussels exhibit different rates of biotransformation and/or bioaccumulation with respect to xenobiotics [2] and are widely used as specific indicators of different environmental compartments in relation to their habitat and food web position. They have been used for about thirty years in the monitoring of marine environments and currently adopted for monitoring both short and mid/long- term biological effects of accidental oil spills, as the one caused by the Prestige wretch [3, 4]. Moreover, recent studies indicated also the suitability of polychaetes to be used as bioindicators of oil pollution in the sediments [5, 6].

At present, the current Italian laws for the coastal pollution control, addressed by the Water Framework Directive (EC 2000/609), take into account for the first time the assessment of both chemical and ecological status of coastal waters. Although biological effects on indicator organisms are at the moment not included as a tool for such evaluation, biomarkers may be helpful in defining environmental health status. It is now well-known that assessment of the well-being of various indicator species through the application of a suite of biomarkers leads to a better comprehension of the fate and effects of the main pollutants affecting their habitats.

In this study, we evaluated the health of mussels, fish and polychaetes native to three diverse coastal areas of the Adriatic Sea (Figure 1), differently affected by anthropogenic inputs, by determining suites of biomarkers encompassing organism and sub-organism responses at biochemical and cellular levels. These were chosen on the basis of their responsiveness, to include the best field-validated markers for the three selected taxa, considering their physiological role in terms of reactions to both general and specific stressors.

Lastly, taking into account the different ecological features of the three study areas, one of the two field methods at present accessible for biomonitoring marine coastal environments was applied in each environment: either the passive approach - biomonitoring native species, or the active method -translocation of specimens from a reference area to the sites to be monitored [7].

2 Materials and Methods

2.1 Sampling sites and specimen collection

2.1.1 Lagoon of Venice (Italy)

The Lagoon of Venice is a shallow transitional environment, located along the North Adriatic coastline, with a total surface of about 550 km^2. This aquatic ecosystem has suffered considerable anthropogenic impact, due to industry, agriculture, and urban activities. Specimens originated from native populations of *Mytilus galloprovincialis*, *Perinereis rullieri* and *Zosterisessor ophiocephalus* were collected in July 2005 in two differently impacted sites located inside the central part of the Lagoon: S. Giuliano, an area

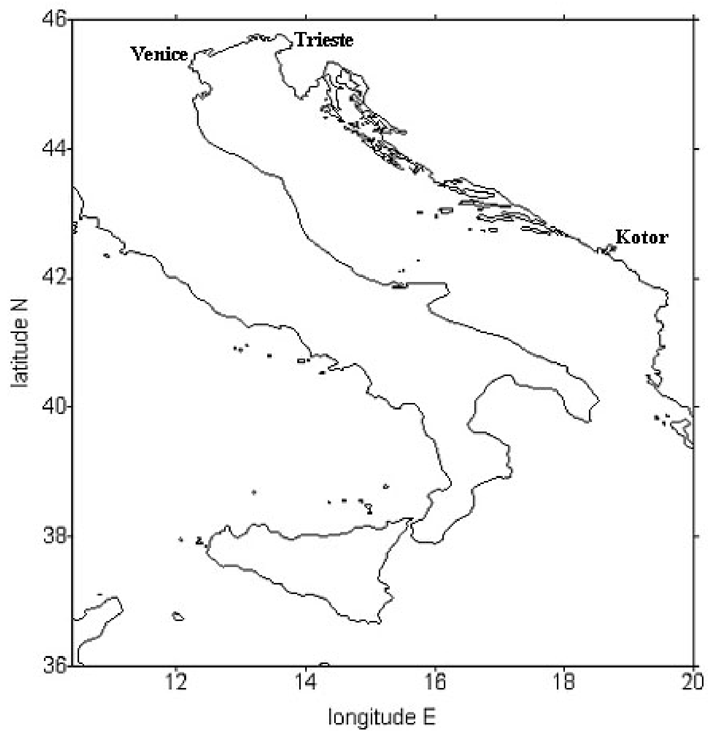

Figure 1: Localization of the study coastal areas in the Adriatic sea

close to the inner border where the mainland industrial site of Porto Marghera is located, and Sacca Sessola, placed towards the outer lagoon and deeply affected by boat traffic and clam fishing. Metallothioneins (MT), malondialdehyde (MDA), lysosomal membrane stability (LMS) and lipofuscins (LF) were determined in mussels, *M. galloprovincialis*, MT and MDA in polychaetes, *P. rullieri*; MT, MDA and ethoxyresorufin-D-deethylase activity (EROD) in fish, *Z. ophiocephalus*.

2.1.2 Boka Kotorska Bay (Montenegro)

The Boka Kotorska Bay is a complex coastal system consisting of various wide and deep inlets and bays located along the south-eastern border of the Adriatic Sea, encompassing part of the Montenegrin coast. Specimens originated from resident populations of *M. galloprovincialis* were collected in June 2008 in two areas known to be differently impacted, each one located in one of the two inner bays of the system, i.e. a reference site facing the village of Perast, in the Bay of Kotor, and

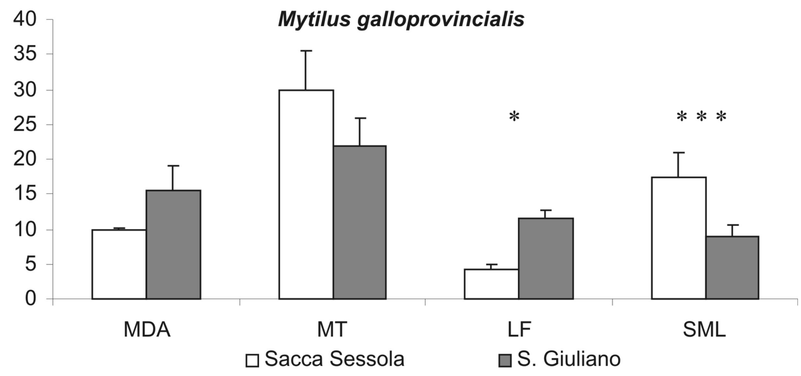

Figure 2: Variations of malondialdehyde, metallothioneins, lipofuscins and lysosomal membrane stability (as labilization time), in *M. galloprovincialis* from two sites of the Lagoon of Venice. MDA: nmol·g^{-1} ww, mean±s.e, n=3; MT: nmol (GSH)·g^{-1} ww, mean±s.e, n=3; LF: (μm^3 · μm^{-3}) x100, mean±s.e, n=10; LMS: minutes, mean±s.e, n=10. Statistical analysis: Kruskal-Wallis: * $p<0.05$; *** $p<0.001$.

Site	Species	Biomonitoring approach	Biomarkers
Lagoon of Venice	*M. galloprovincialis*	Passive	MDA – MT – LF - LMS
	P. rullieri	Passive	MDA – MT
	Z. ophiocephalus	Passive	MDA – MT - EROD
Boka Kotorska Bay	*M. galloprovincialis*	Passive	LMS - LF
Gulf of Trieste	*M. galloprovincialis*	Active	LMS - LF

Table 1: Species, type of monitoring and biomarkers used in the various monitored sites (MDA: malondialdehyde; MT: metallothioneins; LF: lipofuscins; LMS: lysosomal membrane stability; EROD: ethoxyresorufin-D-deethylase).

a more impacted area in front of the old naval dockyard of Tivat, in the Bay of Tivat. Samples were processed for LMS and LF analyses.

2.1.3 Gulf of Trieste (Italy)

The Gulf of Trieste is the northernmost section of the Adriatic Sea, with a surface area of about 600 km^2. It is characterized by an overall shallowness, 10% of the average bottom depth being less than 10 m, and reaching the maximum depth around 23 m in the southern part. The biological effects due to anthropogenic impacts were evaluated in *M. galloprovincialis* applying the active biomonitoring approach. Mussels were collected in May 2009 from a clean marine farming area as a reference (sample T0), then sub-sampled and arranged in similar experimental bags. The bags were translocated to the impacted site within the port area of Trieste (sample M) and relocated within the farm area for a period of 12 weeks (sample T1). At the end of the

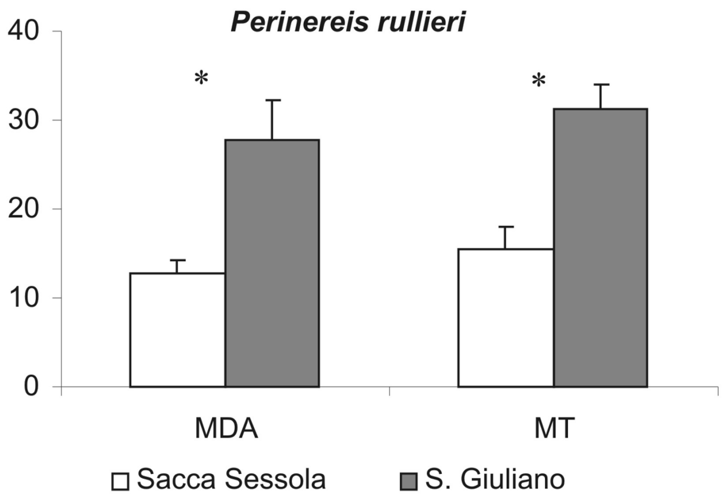

Figure 3: Variations of malondialdehyde and metallothioneins in *P. rullieri* from two sites of the Lagoon of Venice. MDA: nmol·g^{-1} ww, mean±s.e, n=3; MT: nmol (GSH)·g^{-1} ww, mean±s.e, n=3. Statistical analysis: Kruskal-Wallis: * $p<0.05$.

period, mussels were sampled from the two sites, and processed for LMS and LF analyses.

2.2 Biomarker analyses

The content of MDA and MT were determined sprettrophotometrically in pooled digestive glands of mussels, in pooled body flesh of polychaetes and in pooled livers of fish according to the methods of Gèrard-Monnier et al. [8] and Viarengo et al. [9], respectively. EROD activity was measured fluorometrically in the individual liver tissue of 10 fish, according to the method described by Burke & Mayer [10]. LMS was determined in mussels either histochemically or citochemically. The first method measures the labilisation time in digestive cell lysosomes. To this end, 10 mussel digestive glands were cryopreserved, processed, cut at 10μm, and the resulting slides were treated according to the reaction for N-acetyl-β-hexosaminidase as a lysosomal marker enzyme [11]. The second method measures the labilization time in haemocytes lysosomes *in vivo*, according to the neutral red retention assay [12]. LF content was determined histochemically in 10 mussel digestive glands by the Schmorl's reaction [13]. A stereological procedure was then applied to quantify the extent of lipofuscin staining on an automated image analysis system according to Lowe et al. [14]. Statistical comparisons between sites were performed according to the non-parametric Kruskal-Wallis test.

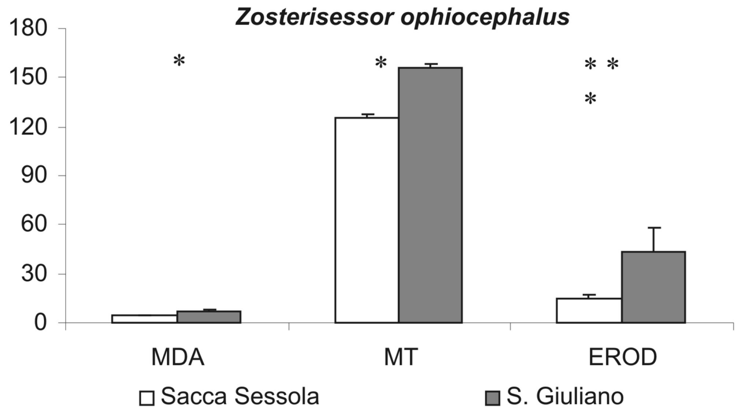

Figure 4: Variations of malondialdehyde, metallothioneins and ethoxyresorufin-D-deethylase in *Z. ophiocephalus* from two sites of the Lagoon of Venice. MDA: nmol$\cdot$g^{-1} ww, mean$\pm$s.e, n=3; MT: nmol (GSH)$\cdot$g^{-1} ww, mean$\pm$s.e, n=3; EROD – pmol$\cdot \mathrm{min}-1 \cdot \mathrm{mg}^{-1}$ prot, mean$\pm$s.e, n=3. Statistical analysis: Kruskal-Wallis: * $p<0.05$; *** $p<0.001$.

3 Results and Discussion

In this study we applied different biomarkers in the three study coastal areas to assess the health status of estuarine organisms which may be considered good indicators of their surroundings, in relation to their specific feeding habits. *M. galloprovincialis* is a filter-feeder bivalve mollusc used worldwide as a quality indicator of the water column; conversely, the ragworm *P. rullieri*, which is mainly a deposit-feeder and the grass goby *Z. ophiocephalus*, a bottom-dwelling predator, are considered possible indicators of the sediment quality. The suites of biomarker deployed in the various organisms for the monitoring of the three study areas are shown in Table 1.

In the Lagoon of Venice we examined the three species living in two differently impacted sites. As for MDA and MT levels in *M. galloprovincialis*, no significant differences were detected between the two study areas of S. Giuliano and Sacca Sessola (Figure 2). In contrast, polychaetes and fish living at S. Giuliano revealed a significantly higher induction of both biomarkers (Figures 3 and 4). MDA is a metabolite indicating generic oxidative stress caused by excess of membrane lipid peroxidation and it may react with DNA to form adducts; MT are low-molecular-weight, cysteine-rich proteins playing an important role in metal detoxification mechanisms, acting as chelating agents for intracellular excesses of non-essential metals (such as Cd, Hg or Ag) and controlling the homeostasis of essential metals (Zn and Cu); they also protect organisms against ionizing and oxidative stress. The induction of MDA and MT in two of the three examined species, highlighting the most stressful condition affect-

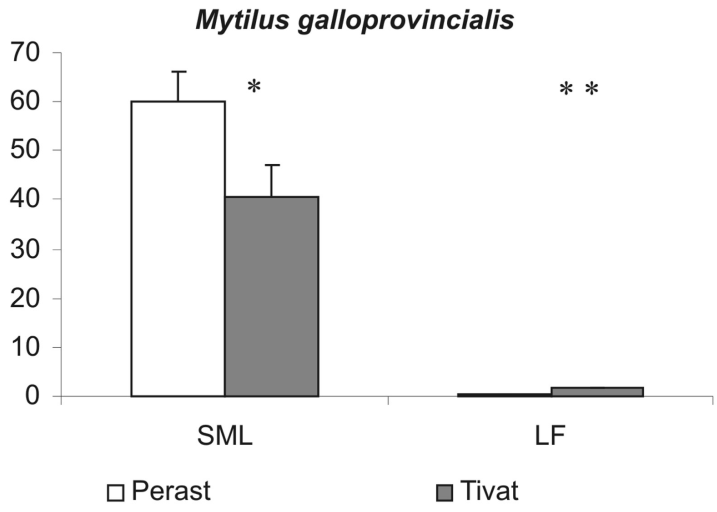

Figure 5: Variations of lysosomal membrane stability (as neutral red retention time), and lipofuscins in *M. galloprovincialis* from two sites of the Boca Kotorska Bay. LMS: minutes, mean±s.e, n=10; LF: ($\mu m^3 \cdot \mu m^{-3}$) x100, mean±s.e, n=10. Statistical analysis: Kruskal-Wallis: * $p<0.05$; ** $p<0.01$.

ing organisms originated from S. Giuliano, could be suggestive of the higher contamination levels previously recorded at this site in the sediments. Further negative environmental effects on the fish living at S. Giuliano were confirmed also by their highest EROD activity. Effectively, this enzyme is considered as the most sensitive catalytic probe for determining the induction of the cytochrome P450 system in fish by micro-organic pollutants, particularly PCBs. The lysosomal parameters evaluated in mussels exhibited more relevant differences between the two monitored sites than the biochemical responses, revealing the best performances in organisms from Sacca Sessola, which exhibited significantly longer labilization times as well as lower lipofuscin contents in digestive cell lysosomes (Figure 2). Lysosomal membrane alterations and lysosomal content changes are widely used as cellular biomarkers especially in bivalve molluscs and are reliable indices of early adverse effects following organism exposure to extreme variations of various environmental parameters, and to pollutants. In particular, lipofuscins are cellular catabolic pigments which, in the digestive cells of molluscs, increase with the organism's age but also with exposure to pollutants; they may sequester metal ions, which may be stored in the residual bodies, thus contributing to metal detoxification. Lysosomal membrane stability, basically evaluated as variation in membrane permeability, is the parameter most diffusely used for describing lysosomal responses to a wide range of pol-

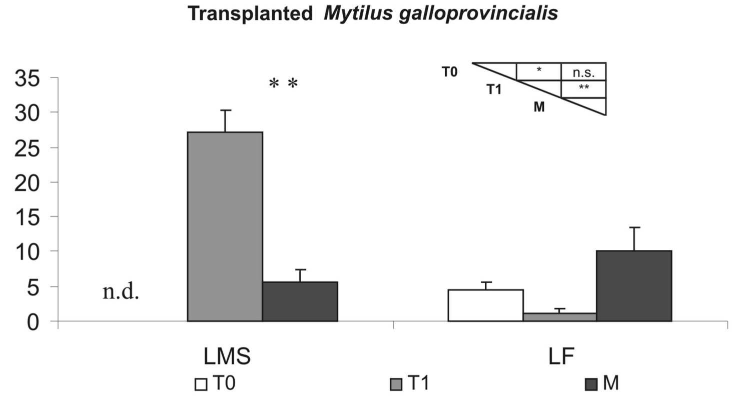

Figure 6: Variations of lysosomal membrane stability (as labilization time) and lipofuscins in *M. galloprovincialis* transplanted in the Gulf of Trieste. LMS: minutes, mean±s.e, n=10; LF: ($\mu m^3 \cdot \mu m^{-3}$)x100, mean±s.e, n=10. Statistical analysis: Kruskal-Wallis: * $p<0.05$; ** $p<0.01$.

lutants, and it is considered a very reliable biomarker of general stress. Labilization times measured in mussels from both study sites were typical of moderately polluted areas [15], not different from values found at other lagoon sites similarly impacted [16].

In the Boka Kotorska Bay, mussels were collected from natural populations living at two sites known to be differently impacted by human activities. Both lysosomal membrane stability and lipofuscin content were evaluated in the two samples (Figure 5). The values recorded for the two lysosomal biomarkers highlighted the worst condition of mussels collected in the most contaminated area, located in front of the old naval dockyard of Tivat, where lower values of neutral red retention times in haemocyte lysosomes and significantly higher rate of accumulation of lipofuscins were evidenced.

The active biomonitoring approach, transferring organisms from a clean reference site to the sites to be monitored, was adopted in the case of the port area of Trieste. It is well known that this is a method to enhance the discrimination potential of the biomarker responses among sites, mainly because by the use of organisms similar for age and origin we may acquire more reliable biological responses, throughout the reduction of both genetic heterogeneity and compensatory adaptative mechanisms (already observed in native populations living in chronically contaminated areas). After the transplantation period, significant differences in the labilization times were detected comparing the sample relocated within the farm to mussels translocated at the port site. Also lipofuscins were more highly accumulated in this last sample, revealing the general worsening of mussel health conditions during the exposure period at the impacted site in the port of Trieste (Figure 6).

In conclusion, both general stress and specific biomarkers applied in the three study areas have been suitable to provide useful information about the biological effects quite likely attributable to different environmental stress, at coastal sites differently affected by anthropogenic inputs. In particular, higher responsiveness has been revealed through biochemical biomarkers evaluated in polychaetes and fish, and through lysosomal alterations evaluated in mussels. Lastly, both active and passive biomonitoring approaches were suitable methods to highlight the gradient of stress experienced by the organisms, albeit the information provided by the transplanted mussels seemed more complete and complementary.

4 Acknowledgements

This study was partially founded by CORILA, 2004-2007 Research Program and by EU COWAMA-Coastal Water Management, 2007-2008. We are grateful to a number of colleagues for assisting us and/or providing facilities in field sampling, particularly to V. Macic (Institute of Biology, Kotor), and P. Del Negro and C. De Vettor (OGS, Trieste).

References

[1] B.L. Bayne, D.A. Brown, K. Burns, D.R. Dixon, A. Ivanovici, D.R. Livingstone, D.M. Lowe, M.N. Moore, A.R.D. Stebbing, and J. Widdows. The effects of stress and pollution on marine animals. 1985.

[2] C. Porte and J. Albaiges. Bioaccumulation patterns of hydrocarbons and polychlorinated-biphenyls in bivalves, crustaceans, and fishes. *Archives of Environmental Contamination and Toxicology*, 26:273–281, 1994.

[3] A. Cravo, B. Lopes, A. Serafim, R. Company, L. Barreira, T. Gomes, and M.J. Bebianno. A multibiomarker approach in *Mytilus galloprovincialis* to assess environmental quality. *Journal of environmental monitoring*, 11(9):1673–1686, 2009.

[4] C. Martinez-Gomez, B. Fernandez, J. Valdes, J.A. Campillo, J. Benedico, F. Sanchez, and A.D. Vethaak. Evaluation of three-year monitoring with biomarkers in fish following the Prestige oil spill (N Spain). *Chemosphere*, 74(5):613–620, 2009.

[5] P. Scaps. A review of the biology, ecology and potential use of the common ragworm *Hediste diversicolor* (O.F. Muller) (Annelida: Polychaeta). *Hydrobiologia*, 470:203–218, 2002.

[6] C. Morales-Caselles, C. Lewis, I. Riba, T.A. DelValls, and T. Galloway. A multibiomarker approach using the polychaete *Arenicola marina* to assess oil-contaminated sediments. *Environmental Science and Pollution Research*, 16(6):618–629, 2009.

[7] W.C. de Kock and K.J.M. Kramer. Active biomonitoring (ABM) by translocation of bivalve molluscs. page 51–84, 1994.

[8] D. Gerard-Monnier, I. Erdelmeier, K. Regnard, N. Moze-Henry, J.C. Yadan, and J. Chaudiere. Reactions of 1-methyl-2-phenylindole with malondialdehyde and 4-hydroxyalkenals. Analytical applications to a colorimetric assay of lipid peroxidation. *Chemical Research in Toxicology*, 11:1176–1183, 1998.

[9] A. Viarengo, E. Ponzano, F. Pondero, and R. Fabbri. A simple spectrophotometric method for metallothionein evaluation in marine organisms: an application to Mediterranean and Antartic molluscs. *Marine Environmental Research*, 44:69–84, 1997.

[10] M.D. Burke and R.T. Mayer. Ethoxyresorufine: direct fluorimetric assay of a microsomal O-dealkylation which is preferentially inducible by 3-methylcholanthrene. *Drug Metabolism and Disposition*, 2:583 – 588, 1974.

[11] M.N. Moore. Cytochemical responses of the lysosomal system and NAPDH-ferrihemoprotein reductase in molluscan digestive cells to environmental and experimental exposure to xenobiotics. *Marine Ecology Progress Series*, 46:81–89, 1988.

[12] D.M. Lowe and R.K. Pipe. Contaminant induced lysosomal membrane damage in marine mussel digestive cells: an in vitro study. *Aquatic Toxicology*, 30:357–365, 1994.

[13] A.G.E. Pearse. Histochemistry, Theoretical and Applied. 1972.

[14] D.M. Lowe, M.N. Moore, and K.R. Clarke. Effects of oil on digestive cells in mussels: quantitative alterations in cellular and lysosomal structure. *Aquatic Toxicology*, 1:213–226, 1981.

[15] UNEPMAP (United Nations Environment Programme Mediterranean Action Plan). Manual of biomarkers recommended for the Med. Pol. – Biomonitoring Programme – Ramoge. pages 1–39, 1999.

[16] L. Da Ros and N. Nesto. Cellular alterations in *Mytilus galloprovincialis* (Lmk) and *Tapes philippinarum* (Adams & Reeve, 1850) as biomarkers of environmental stress: field studies in the Lagoon of Venice (Italy). *Environment International*, 31:1078– 1088, 2005.

Short-Medium Term Assessments of Coastal Erosion and Marine Inundation Effects on Natural and Anthropic Environments (Apulia, Southern Italy)

M. Delle Rose[1], L. Beccarisi[2], T. Elia[3]
1, Research Institute for Geo-Hydrological Protection, CNR, Bari, Italy
2, Department of Biological and Environmental Sciences and Technologies, University of Salento, Lecce, Italy
3, Santa Teresa s.p.a., Brindisi, Italy
marco.dellerose@cnr.it

Abstract

Coastal erosion and inundation are global problems. Three processes are considered, over time scales consistent with natural hazard analysis: sea level rise, changes in storm climate, human interference. Such global causes are differently evaluated by scientific communities. This report discusses the effects on environment and human activities over a time span consistent with territorial planning and resource governance. The study area is an example of Mediterranean low-lying coastal landscape. The research was conducted by dealing with some issues related to the coastline retreat (evaluation of past coastline changes, hazards assessment and prediction of coastal changes). All beaches of the study areas have undergone erosion process during the second half of the 20^{th} century. The associated coastline retreat ranges from nearly zero values to about 20 ($\pm$ 5) m. In the short term, an increase in frequency of extreme storm events may result in intense coastal erosion, severe shoreline retreat and significant coastal flooding. This involves changes on coastal ecosystems with notable consequences also from the standpoint of environmental conservation. In the mid term, the sea level rising can cause severe damages at urban and industrial areas.

1 Introduction

Coasts are dynamic systems, undergoing adjustments of form and processes at different time and space scales in response to geomorphologic and oceanographic factors [1]. From a human point of view, coastal erosion and marine inundation are global problems. Three processes are usually considered, over time scales consistent with natural hazard analysis: Sea Level Rise (SLR), changes in storm climate, human interference. These worldwide causes are differently evaluated by the scientific communities. As an example, the prediction of the 21^{st} century Global Sea Level (GSL) spans from neglectable values to few meters above the present level (cf. e.g. [2, 3]). The large uncertainty about the magnitude and impact of these processes implies a poor understanding of the effects on both the environments and the human activities located along the coast areas.

Since the first half of the 20^{th} century,

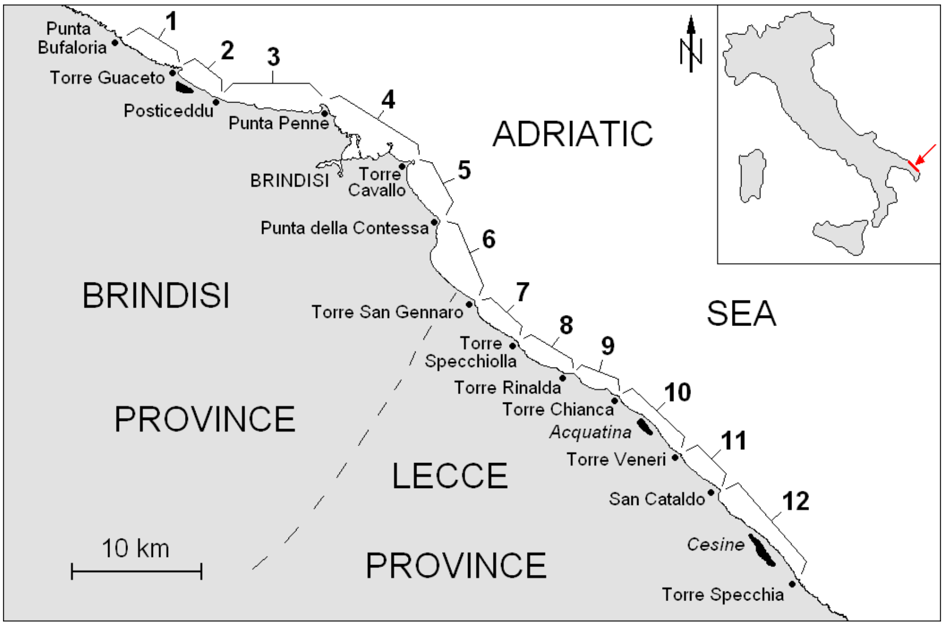

Figure 1: Sketch-map of the study area. Second-order physiographic units are numbered (see text, Figure 2).

a number of studies on the Italian coast evolution has been carried out by different research groups, sometime coordinated by the Consiglio Nazionale delle Ricerche (CNR-National Research Council). In the last decades the CNR promoted a series of interventions that provided the theoretical basis for the protection of the coasts. Finally, at the end of the '90s, the CNR published the Atlas of the Italian Beaches [4] that represented an innovative product addressed to experts of public and local authorities, planners, sea work designers, all users of the coastal zones and the scientific community.

Erosion of sandy beaches involves a redistribution of sand among the emerged and submerged coastal environments, which occurs mainly (but not only) during storms. The grains, which are re-suspended and transported by the waves and carried along shore and offshore, partially return to the beach after storms by the long-period swell waves during normal meteorological and oceanographic conditions. Exchanges between sandy beaches and dunes are fundamental to keep a morphological-depositional equilibrium in the medium term. Regarding the inundations, as sea level rises, the high water line migrates more and more landwars as the average slope of the coastal area decreases. Nevertheless, morpho-sedimentological processes, such as the dismantling of dune ridges, may cause the flooding of costal areas. So, where the slope is very gentle and the dunes are highly vulnerable, the impact from the sea level rising and coastal erosion can be severe. Many coastal areas of the world, both natural and anthropized,

unit	Morpho-sedimentological characteristics	
1	discontinuous low carbonate cliff	inlets like pocket-beach; dunes
2	continuous sandy shoreface	borders of dunes and submerged bars
3	silty clayey sand coastline	narrow beach at the foot of cliff
4	gently sloping carbonate ramp	pervasive defence constructions
5	silty clayey sand coastline	narrow beach at the foot of cliff
6	silty clayey sand coastline	narrow beach at the foot of cliff
7	gently sloping carbonate ramp	discontinuous dunes
8	gently sloping carbonate ramp	discontinuous dunes; coastal dolines
9	gently sloping carbonate ramp	outfall of a spring alimented streams
10	gently sloping carbonate ramp	water basins along the coast; dunes
11	gently sloping carbonate ramp	discontinuous dunes; coastal dolines
12	gently sloping carbonate ramp	large back-dune swamps

Figure 2: Main features of the second-order physiographic units.

are presently interested by these processes and the most vulnerable sites are subject to drastic morphological and sedimentological changes even in the short term. This report dealing with the effects on environment and human activities of both coastal erosion and inundation assessed over time span ranging from a few years to about a century. This interval was chosen according to the time needed for the territorial planning and resource governance. The study area is the south-western Adriatic coast (Apulia, south Italy) which represents a significant example of Mediterranean type low-lying coastal landscape with different kinds of human activities and some important areas of environmental interest.

2 Study area

According to the Atlas of the Italian Beaches [4], on the about 300 km of beaches and low rocky coasts (with sand or gravel at their foot) of the Apulia, only 1 km (0.3%) showed evidence of progradation, whereas nearly the 30% was resulted in erosion and the 70% was stable. Nevertheless, a GIS application study by the Agenzia per la Protezione dell'Ambiente e per i Servizi Tecnici (APAT, Environment Protection and Technical service Agency) has produced substantially different conclusions [5, 6] stating that the Apulia beaches in accretion (22.6%) are even more represented than the beaches in retreat (21.4%).

The coastal segment here considered is comprised between Punta Bufaloria and Torre Specchia and is about 70 km long. It can be subdivided into two main morpho-sedimentological types (first order physiographic units) such as, namely, from north-west to south-east: "terraced coast" and "rectilinear coast" (respectively named by Ferretti et al. [7] as "coste terrazzate" and "coste di litorale diritto"). The limit between the above mentioned types is located about at Torre San Gennaro, where the administrative boundary of the Brindisi and Lecce provinces also occurs (Figure 1). The longshore sand transport along

the study coastal segment mainly develops from NW to SE, according to the dominant wind direction.
The "terraced coast" is mainly constituted by a silty clayey sand succession which forms a cliffed coastline elevated up to 10 m above the sea level. Landslides frequently occur along the terraced coast and supply narrow and discontinuous beaches but without determining significant aggradation [8]. The "rectilinear coast" is characterized by a series of low-lying headlands made up of calcarenite. Headlands delimit concave-seaward sandy shores which are extended some hundred of meters on average. Locally the headlands form the basis of sandbars which, in turn, border back-dune swamps. The adjacent coastal plains are extensively characterized by karst subsidence phenomena [9, 10, 11]. Differently from other Italian coasts of the Adriatic (supplied by sediments eroded from the land mass), the beaches of the study area are mainly supplied by biogenic sediments consisting of exoskeleton and bone fragments of dead sea creatures, produced in shallow marine water. The average grain-size of the biodetritic component of the sand becomes coarser and coarser from NW to SE [8].
The coastal area analysed in this study is interesting from the standpoint of nature conservation. The 35% of its length falls within the perimeters of several terrestrial protected areas, such as Wetlands of International Importance (Natura 2000 areas) state and regional reserves.
Discontinuous dune systems occur along the study coast. They are interested by enhanced "degradation" phenomena (in sensu lato) regarding both the morpho-sedimentological characteristics and the environmental aspects [6]. In a few cases the consolidations of dune has been attempted by planting vegetation in order to stabilize the dune sand at Torre Guaceto, Acquatina and Cesine (Figure 1). In the study area, the beach erosion has triggered a significant socio-politic problem since the early '90s. In spite of the several project of coastal defense based on beach replenishment that have been realized, or only planned, presently the administrative authorities are unable to solve the problem. As an example, a project of nourishment of the San Cataldo beach (Figure 1) by using sand of sand dredged from north of Brindisi offshore, was dropped owing to both administrative arguments and environment impacts. Conflict between different local interests have played the main role in abandonment of the project.

3 Methods

The research was conducted by considering different issues related to the shoreline retreat, such as: evaluation of the coastline changes of the past; field mapping, inside the main morpho-sedimentological types of coast, of second order physiographic units; evaluation of the hazards by means of morphological and sedimentological observations; analyses of vegetational communities changes.
Maps of the Istituto Geografico Militare (IGM), aerial photographs and orthophotos covering the second half of the 20th century, and the digitalized Carta Tecnica Regionale (CTR, Regional Technical Map, 2008) were utilized to detect the past shoreline changes. All these data were georeferenced in a GIS-environment. The difficulty in matching of the aerial photographs on the IGM topographic maps that constitute very different kinds of landscape representations, was overcome by select-

ing and georeferencing a series of "stable" points or features (e.g. historical buildings, roads). Such procedure allowed us to obtain an accurate matching of maps and photographs within each physiographic unit and thus evaluate the shoreline changes through time. The main headlands define the borders of the physiographic units. The interferences on the longshore sediments transport caused by headlands was in situ observed. Such field oriented research was based on the identification of discrete coastal segments characterized by individual sediment budgets. Both morphological features (e.g. topography and geometry of the costal landscapes, coastline, notch) and sedimentological ones (textural features and sedimentary structures) of each second order unit were considered to quantify the natural components of coastal erosion and inundation hazards according to the sensitivity concept [12, 13].

To get an interdisciplinary view of the studied processes, an integration with botanical approach (cf. [14]) was conducted according to two different scales: a) interpretation of a set of six aerial photographs between 1943 and 2002 addressed to the analysis of the evolution and spatial characteristics of the existing plant cover (landscape scale); b) a sampling directed to structural analysis in the field of present plant communities (community scale). Finally, a prediction of the future position of shoreline was attempted. The collected data were used to improve the traditional Brunn's mathematical approach, considering the role of sediment availability as a control on morphological evolution [15, 16].

4 Main results

The performed field work allows to subdivide the main morpho-sedimentological types of coast (chapter Study area) into twelve second-order physiographic units (Figure 1). Their main morpho-sedimentological characteristics are illustrated in Figure 2.

Each second order unit presents unique conditions. As an example, unit 1 is characterized by low-relief carbonate cliffs which are interrupted by a series of pocket beach-like inlets. The erosion of these sandy shores, which had occurred after the '40s, had been partially attenuated by sediment supply coming from the dismantling of the adjacent dunes caused by both wind and sea-wave actions.

The dunes west of Torre Guaceto (Figure 1), up to 10 m high, are colonized by a xerophilous vegetation. They may be regarded as a representative example of the dune systems that occur along the entire coast studied. On the basis of the photointerpretation of an area of 28 hectares it has been observed that the eastern and western parts of such dune system show different characteristics and evolution. There is evidence that prior to the '50s the scrub was still consistent and unfragmented across the dunes. During the '60s and '70s there has been a strong depletion of shrubs in the western part of the site, mostly involving the the fore-dune and back-dune areas. The latter area was destined to a camping site and recreative activities. Furthermore, from those years on, a network of trails has developed also within the eastern part of dune system (increasing of human interference). The current series of plant communities, starting from the shoreline devoid of vegetation (Figure 3) is: 1) communities with nitrophilous annuals, such as *Salsola*

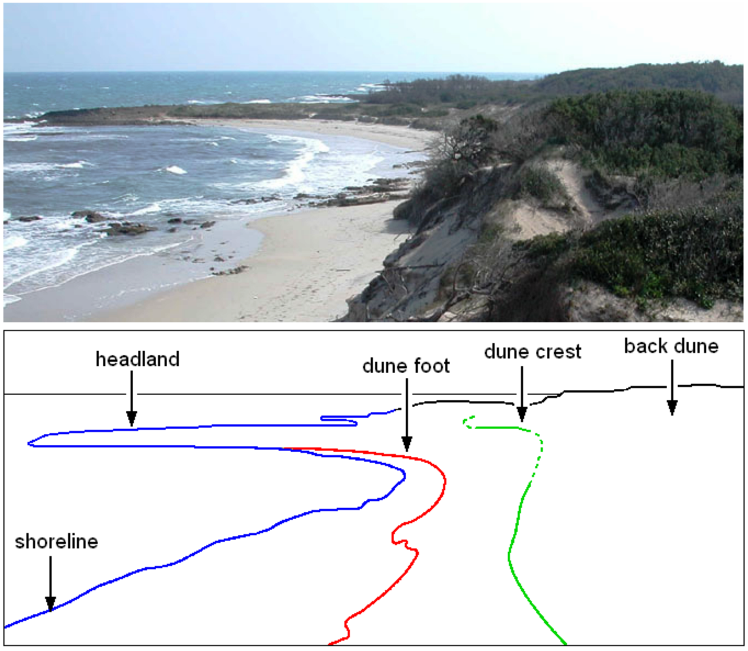

Figure 3: NW of Torre Guaceto: the died shrub specimens and the extreme reduction of herbaceous communities are clear signs of the ongoing erosion.

kali and *Cakile maritima*, on the shoreface; 2) communities with herbaceous perennial *Sporobolus pungens* at the foot of the dune; 3) communities with herbaceous perennial *Ammophila arenaria* on the slopes of fore dune; 4) communities with shrub junipers (*Juniperus oxycedrus* subsp. *macrocarpa* and *J. turbinata*) that extends inland (dune crest and back dune) and is gradually replaced by a oak forest.

This series corresponds to a general model (cf. [17]); however, here the width of the belts is different, depending on the side of the dune, suggesting that the two sides have different histories and different dynamic substratum features. In the western part *Ammophila arenaria* colonizes the top of the dunes and shrubs is very backward inland, whereas in the eastern shrubs are located on the summit and *Ammophila* has to struggle to remain on the steep slopes. The resulting pattern suggests an ongoing erosion. In both cases, nitrophilous annuals communities are very restricted and the beach is mostly devoid of vegetation, due to the wave action and the anthropogenic frequentation. A *Crucianellia maritima* community, typical of consolidated dunes (so-called “gray dunes”), is documented in the past for this area [18], but is no longer observable today.

Differently from unit 1, unit 2 presents a continuous sandy shoreline, which is bordered landward by dunes and is protected seaward by submerged sand bars. Such peculiar situation seems to have assured

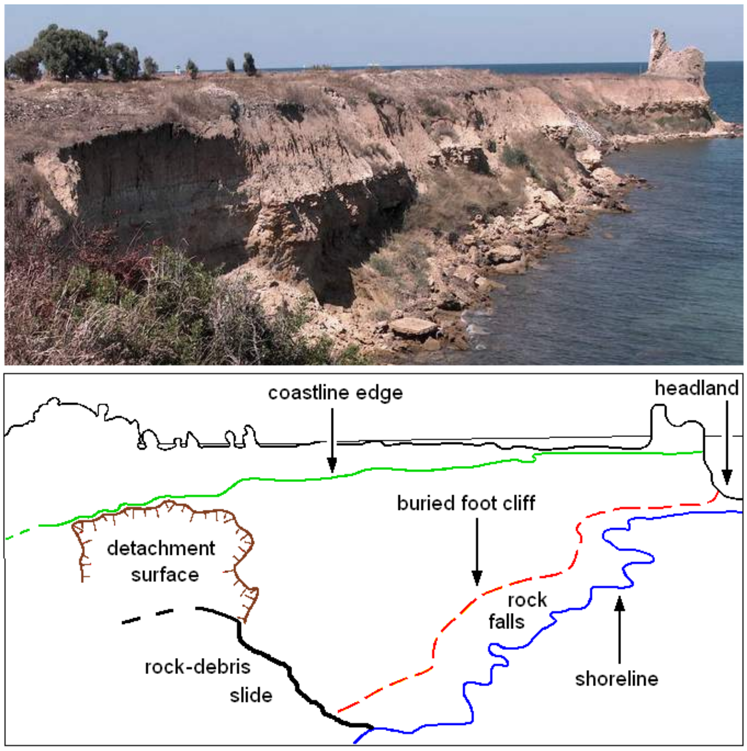

Figure 4: SE of Punta della Contessa: high sensitivity coast. Note the “natural seawalls” of rock fall accumulation.

the relative stability of the shoreline, as it can be deducted by the photointerpretation analyses.

Units 3, 5 and 6 are characterized by silty clayey sand coastlines, which are discontinuously bordered by narrow sandy beaches at their foot. They are locally protected by the marine erosion by means of groynes and seawalls. Quite different is the stretch of coast of unit 4, which is formed by low-relief cemented sand-bar deposits. It results stable and largely protected by a number of effective coastal defence constructions. Moreover, inside unit 4, a few substantially unchanged pocket-beaches are located. The shorelines of units 3, 5 and 6, even if they apparently stable during the last two decades, they are quite unstable owing to the frequent occurrence of landslides along the cliffs. The rock debris and sediments involved into landslides temporarily provides a sediment input source. As a consequence, single stretches of shoreline may result in a net progradation if its evolution is evaluated over a short time span (5÷10 years).

At Punta della Contessa, as an example, the headland, which is elevated about 5 meters above sea level and divides the physiographic unit 5 and 6 (Figure 1), rock falls and rock slides detached from a calcarenite layer lying on the silty clayey sand

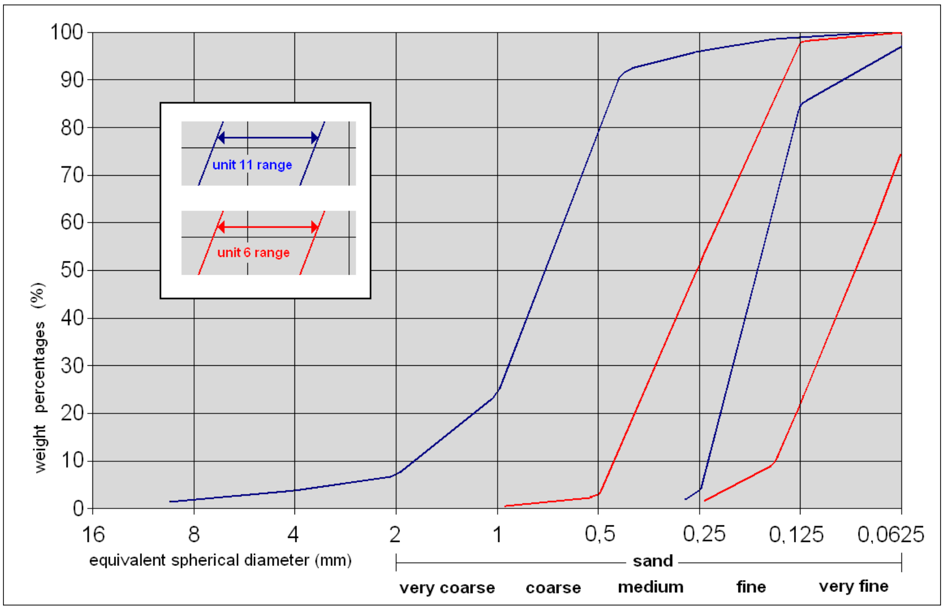

Figure 5: Grain size cumulative distributions.

succession, may provide ephemaral protection to the foreshore, and result into partial seaward shift of the shoreline. On the other hand, extreme marine storms rapidly destroy this ephemeral coastal impingements and cause an intense erosion of the notches at the base of cliffs. These observations suggest a very intense coastal dynamics characterized by rapid changes in the morphology of the beach system (Figure 4). In spite of the hardness of the calcarenitic top layers, the erodibility of the soft silty clayey sand, at the base of Punta della Contessa cliff, results in a relatively rapid retreats of the coastline (in the order of 1÷5 (± 2) m /100 years). To be mentioned is also the evidence of substantial absence of sediment exchange between units 5 and 6. In fact, the fine-grained materials which are produced by the erosion of Punta della Contessa cliff, are transported and distributed offshore by sea-waves.

Units 7 to 12 are formed by a number of concave-seaward sandy beaches, bounded by few elevated headlands. They are characterized by a sub-surficial gently sloping calcarenite substratum and can be considered lithologically homogeneous at the scale of the present study. The hydrogeological conditions, i.e. the presence of a costal calcarenite aquifer, and the peculiar topography of hundreds of meters wide costal plains, which are elevated no more than few meters above the sea level, had favoured the development of a diffuse karsism in the area just below the topographic surface. This, in turn, had determined the occurrence of collapse dolines. Where coalescent dolines widely characterise the landscape, such as at Acquatina and Cesine sites (Figure 1), waste wet and

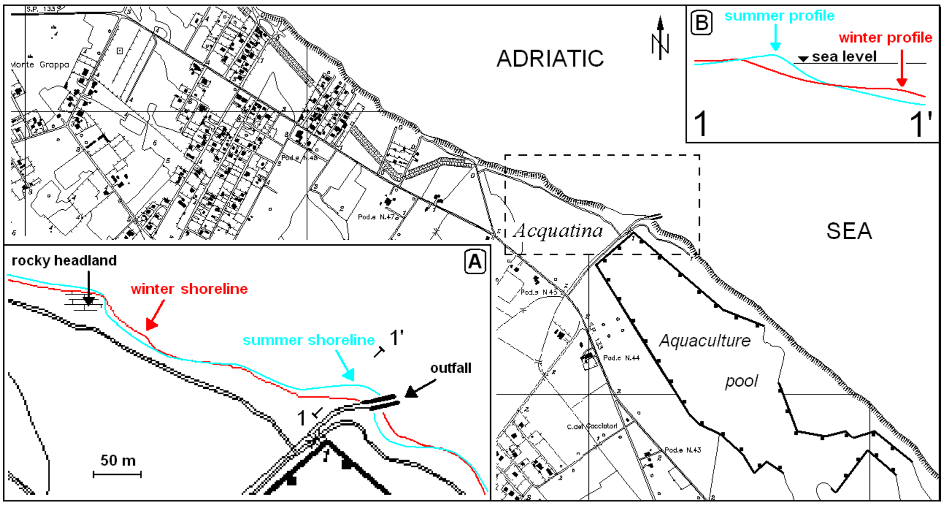

Figure 6: Acquatina seasonal evolution (topography from Lecce Province Technical Map). A: shoreline shift; B: profile change, for section 1-1' see insert A.

inland pools occur.

A preliminar grain size analysis of sediments sampled from units 6 and 11 was conducted. The samples collected, even though not statistically significant (cf. [8]), suggest the occurrence of two distinct but partially overlapping grain size ranges (Figure 5). The samples of unit 6 are represented by very fine and fine sands, while those of unit 11 primarily fall between the medium and the coarse sand. The composition of these sediments gradually varies from mixed terrigenous-biogenic sand (unit 6) to mainly biogenic sand (unit 11). The trends of textural characters of these sediments are seemingly consistent with the above mentioned morphological features and sedimentary processes.

The physiographic units belonging to the "rectilinear coast" (see study area chapter), show different conditions of sensitivity. As a general rule, the ability of changing in response to "external" forcing (namely the increasing frequency of large marine storm events) is evident where complete dune-beach-offshore sandy deposits cover a rocky substratum. As an example, a high sensitivity must be assigned to the beach adjacent the "aquaculture and fisheries research centre" of Acquatina (physiographic unit 10, see Figure 1). Such body of brackish water, resulting from extensive karst subsidence phenomena, has been modified as a consequence of the reclamation and aquaculture practice. As observed a few years of field observations (2005-2009), the beach was constantly changing shape and shifting position in response to winds, waves and human interferences (dynamic equilibrium). As a result of periodic changes in the seasonal stormy activity, during summer the Acquatina beach was wider, higher and coarser than in the winter, probably because this is the period when significant sand volumes are tem-

unit	Beach erosion hazard	Coastline retreat tendency	Inundation hazard
1	High	Low	High
2	Middle	Middle	Middle
3	High	High	Low
4	Middle	Low	Middle
5	High	High	Low
6	High	High	Low
7	High	Low	Middle
8	High	Low	High
9	High	Low	Middle
10	High	Low	High
11	Middle	Low	Middle
12	High	Low	High

Figure 7: Erosion hazard, inundation hazard and coastline retreat tendency evaluation.

porarily transported nearshore to form submerged coastal bars (Figure 6). During the main annual storms period, a part of the feet of dunes is deeply eroded. Following such a period (which may occur from the late winter to the early summer), part of the nearshore sand is transported back to the shoreline to form the onshore beach. The finest sand fraction may successively be asported by wind action and moved toward the dunes. Moreover, always with annual periodicity, at Acquatina beach an intense alternate longshore transport occurs. As a consequence, during summer the south-eastern part of the beach displays enhanced seaward growth; while the opposite side of the beach displays enhanced seaward progradation during the winter. Such sand transport may result in an alternate shoreline shift that exceeds 30 m, measured along an artificial outfall protection, over a period of six months (Figure 6 cf. also [8]).
Along the coastal segment here considered, several seasonal ponds may be found in the back-dune area. The largest of them are located at Torre Guaceto, Punta della Contessa, San Cataldo and Cesine. These ponds display variuos degrees of seasonal variability of water level and the anthropic and biological features. For example, the three ponds located at Punta della Contessa, formerly used for salt production, tend to dry up completely in summer. All others are affected by severe fluctuations in water level but only rarely dry up. The occurrence of these wet areas represent a habitat variable that affects the distribution of different specialized biological communities that spend only part of their lives under water, like: salt meadows, halophilous scrubs and Mediterranean temporary ponds [19].
This research allow to associate to each second order physiographic unit, a qualitative evaluation (low, middle, high) for both the marine erosion and inundation hazards (Figure 7).
The sensitivity of each coastline to erosion and retreat over a decadal time span are also showed (Figure 7, third column).
In a general scenario of relatively high values of hazard (Figure 7, column 2), some units appear relatively less vulnerable to marine erosion. Peculiar morpho-

sedimentological conditions (namely a nearly stable dune system and a series of submerged bars) suggest unit 2 is characterized by an hazard level lower than the values of the contiguous units 1 and 3. The middle hazard level of the unit 4 is the consequence, instead, of both intrinsic erosion resistance of the carbonate substratum and the widespread occurrence of defence constructions, which reduces the vulnerability to erosion of the pocket-beaches. As to the unit 11, its middle level of erosion hazard was assigned on the basis of a relative historical stability, which was evaluated by means of the photointerpretation. Such peculiar property probably come from the morphological features of a relatively shallow foreshore, as well as the presence of a consolidate *Posidonia oceanica* grassland. About units 3, 5 and 6, it has to be noted that the high values of the erosion hazard of the beaches are counterbalanced by a high tendency of the coastlines to retreat. By contrast, for the same units, only the existence of coastlines elevated up to 10 m above sea level, although easily erodible, ensures low values of inundation hazard (Figure 7, column 4). The higher value of inundation hazard is assigned to the units 1, 8, 10 and 12. As a matter of fact, it can be argued that a number sites pertaining to such units, show processes of incipient dismantling of dunes caused by storms. Moreover, a number of dune systems are more or less degraded, like at Torre Guaceto (south-east end of the unit 1 and north-west end of unit 2, Figure 1). Finally, other places such as the protected area of Cesine wetland (see Figure 1 for location) display dunes that are nearly all dismantled.

As a whole, the general pattern of morphologies generated by the wind erosion may be partially attributed to human interferences. Presently, the vegetations don't play a significant role in the stabilization and growth of the dunes. As a consequence, dunes no more constitute a defence during storms, but they are rather progressively dismantled by the marine erosion which causes an overall negative sediment budget, and net shoreline retreat through time.

5 Discussion and conclusions

Although the coastal erosion and marine inundation effects on natural and anthropic environments may be effectively analysed at local scale, the policy practice regarding both the territorial planning and the resource governance follows principles of worldwide interest. As a matter of fact, the assessment of the effects of the future shoreline retreats is a planetary societal priority ([20, 21] cum bibliography) especially tacking into account the predicted increasing of both the global Sea Level Rise (SLR) [15, 3] and the extreme storm events [22]. With the pragmatic exception of the short term evaluations, also other mechanisms that can determine the shifts of shores must be consider. They are: variations of the sediments supplies, topographic surface movements due to earth crust processes (tectonic, isostatic), human-induced processes (e.g. subsidence caused by exploitation of aquifer). In a general agreement, the worldwide gently sloping lower coasts are the most vulnerable areas affected by both erosion and inundation hazards. The shoreline response involves complex physical reorganization of sedimentary materials rather than simple flooding. To predict the future retreat of local shore-

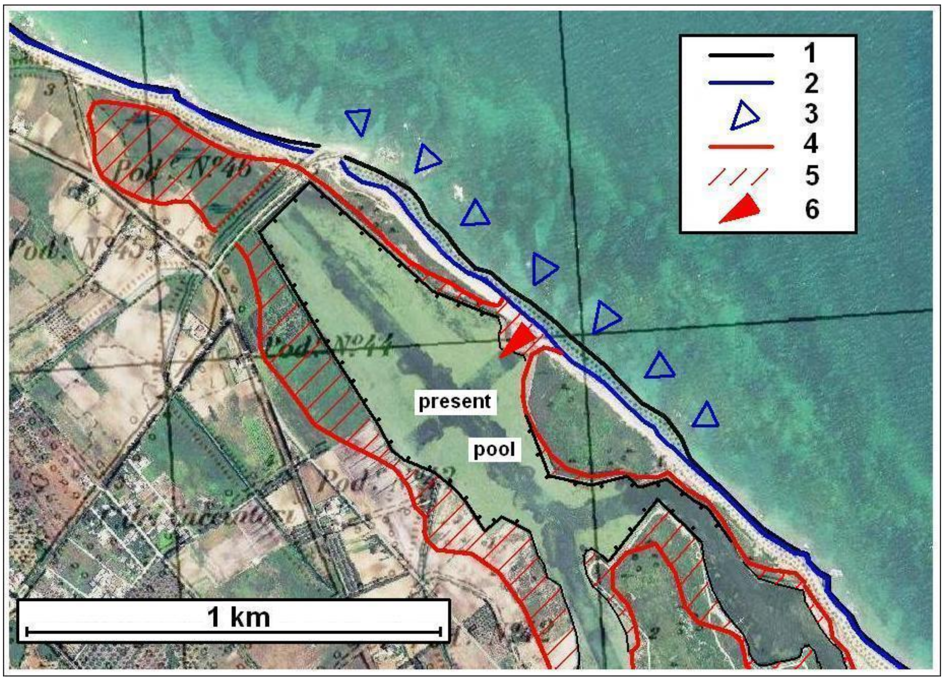

Figure 8: Shoreline changes at Acquatina (primal images from National Cartographic Portal). 1: 1948 shoreline; 2: present shoreline; 3: retreat since the '40s; 4: predicted shoreline; 5: flooded area; 6: dune dismantling.

lines, researchers and operators usually use temporal-extrapolation of assessments of past shoreline changes or mathematical models [23, 24].

About the evaluation of past changes in the morphology of the study coast, on the available maps and photos, it must be noted that some intrinsic problems exist (i.e. deformations of the real surface on the 2D images, differences of the methodology and quality of maps and photos, subjectivity of the identification of the shorelines on the photos, difficulties to put each shoreline deducible from the images, into summer-winter morpho-sedimentological evolution, etc.). Although faced with a critical approach (see chapter 3) the applied method implies errors of the same order of the appreciable shoreline retreats. Nevertheless, based on the GIS elaboration of maps, aerial photographs and orthophotos it can be concluded that during at least the second half of the 20^{th} century, all beaches of the study areas were undergoing erosion. The associated shoreline retreated was ranging from virtually zero to about 20 ($\pm$ 5) m.

An example of past shoreline changes evaluation is showed in Figure 8. It represents the Acquatina area which belongs in the physiographic unit 10 (cf. Figure 1). In dark is drawn the shoreline according to the IGM 1:25.000 map (1948 edition series) whereas in blue is plotted the shorelines

of the 2008 Regional Technical Map. The largest retreat (blue triangles) had affected the central segment of the coast, which coincides with the dune systems bordering the adjacent pond (the Aquaculture pool of Figure 6). South-east and north-west of this coastal sector, only minor modifications of the shoreline are recorded.
High degrees of retreats were encountered also within discrete segments of physiographic units 1, 7 and 12. As a whole, the surface of beaches lost can be estimated in about 20 ($\pm$ 10) % of the original surface (i.e. compared to the '50s). Regardless the real amount of shoreline retreat, such changes cannot be explained exclusively as the result of the backward shift of the shoreface along the same beach profile. Longshore sediment transport, migration of submerged coastal bars, dunes-beaches sediments exchanges, dismantling of dune systems and other sedimentological processes must be taken into account to explain the observed modifications.
Rocky outcrops and morphological features must have had an important role in determining the evolution of sandy beaches. In fact, simple mathematical models that do not take into account morphological and sedimentological features of the study sites are likely inadequate to describe the observed coastal dynamics [15]. More comprehensive models, considering the morpho-sedimentological features of the coasts and especially the role of the sediment availability as a control on the evolution, are hence needed to better predict future shoreline shifts (cf. [16]). As an example of an improving of Brunn method, the Figure 8 can be considered. In the case of a lack of coastal defece actions, the combination of the dismantling of the dunes (red triangle) and a sea level rise of about 0.5 m, will entail a retreat of the shoreline from the present-day position (from blue to red line in Figure 8), which is larger than a coastal modification simply due to topography. A consequence of this model would be the transformation of the pool (see Figure 8), presently used aquaculture and fishing research, into a lagoon, and the related social and economic impacts.
Other implications of this forecast are the evolution of ephemeral ponds into permanent lagoons, with dramatic consequences in terms of distribution of specialized biological communities, management strategies of protected areas and, more generally, exploitation of the natural resources.
In any case, regarding coastal erosion and marine flooding effects on environment and human settlements, different considerations need to be discussed respectively for the short term and the medium term coastal evolution. In the short term, an increase of storm extreme events frequency may cause an intense coastal erosion, severe shoreline retreat and dramatic coastal flooding. This would involve changes on coastal ecosystems with notable consequences also in terms of of environmental conservation. In the middle term, the sea level rising can cause severe damage in the urban and industrial settlements of Brindisi. Clearly also small villages that become highly populated during the summer period, such as Torre Chianca and San Cataldo (Figure 1), may suffer severe problems especially concerning the local viability and the sewer conducts [11, 8].
This research showed that the dune vegetation alone can not prevent from erosion. Most of the interventions of consolidation of the dune using planting of live vegetation did not lead to expected results. These interventions usually suffered from insufficient planning of monitoring strategies in the short to medium term. These miscon-

ceptions have hampered so far the development of appropriate strategies for the conservation of the coast, and have caused the loss of economic resources, and/or damage.

Finally, the results discussed in this paper substantially confirm the shorelines tendency of the South East Apulia illustrated in the Atlas of the Italian Beaches [4], which still represents an updated tool addressed to experts of authorities, planners, sea work designers, all users of the coastal zones and shoreline researchers. Further research will be needed in order to obtain a more advanced understanding of the morphological, sedimentological and ecological issues related to the coastal zone management. Particularly, more detailed field works will permit a better assessments of the effects of both erosion and inundation on environment and human activities, which are fundamental aspects in the territorial planning and resource governance.

6 Acknowledgments

We thank the referee for comments and suggestions that have led to substantial improvements of the paper.

References

[1] P.J. Cowell, M.J.F. Stive, A.W. Niedoroda, D.J.P. Swift, et al. A conceptual approach to aggregated modelling of low-order coastal change. *Journal of Coastal Research*, 19:812–827, 2003.

[2] N.A. Mörner. Estimating future sea level changes from past records. *Global and Planetary Change*, 40:49–54, 2004.

[3] J.A. Church and N.J. White. A 20th century acceleration in global sea-level rise. *Geophysical Research Letters*, 33:L01602, 2006.

[4] CNR. Atlante delle Spiagge Italiane (108 maps). 1999.

[5] APAT. Sistema informativo geografico costiero. Studi per la caratterizzazione della costa (in press). 2006.

[6] Regione Puglia. Piano Regionale delle Coste. 2009.

[7] O. Ferretti, I. Delbono, S. Furia, and M. Barsanti. Elementi di gestione costiera. Tipi morfo-sedimentologici dei litorali italiani. page 43, 2003.

[8] M. Delle Rose and T. Elia. Aspetti geologici della conservazione delle spiagge del Salento. *Geologi e Territorio*, 1/2:3–19, 2008.

[9] M. Delle Rose and A. Federico. Karstic phenomena and environmental hazard in Salento Coastal plains. *Proceedings IX° IAEG Congress*, pages 1297–1305, 2002.

[10] M. Delle Rose and M. Parise. Karst subsidence in south-central Apulia, southern Italy. *International Journal of Speleology*, 30B:181–199, 2002.

[11] M. Delle Rose. Studi per la previsione delle dinamiche evolutive della costa adriatica ad est di Lecce. *Geologi e Territorio*, 3/4:181–191, 2007.

[12] D. Brunsden. A critical assessment of the sensitivity concept in geomorphology. *Catena*, 42:99–123, 2001.

[13] J.D. Hansom. Coastal sensitivity to environmental change: a view from the beach. *Catena*, 42:291–305, 2001.

[14] L. Beccarisi, P. Ernandes, and V. Zuccarello. Zona costiera del Salento: cambiamenti degli habitat prioritari, d'interesse comunitario e d'interesse regionale negli ultimi 50 anni. Il tratto di costa ionica di Porto Cesareo come caso di studio. *Fitosociologia*, 44:139–155, 2007.

[15] O.H. Pilkey and J.A.G. Cooper. Society and Sea Level Rise. *Science*, 303:1781–1782, 2004.

[16] R.J. Nicholls and M.J.F. Stive. Society and sea level rise requires modelling. *Science, E-Letter responses to: Pilkey and Cooper (2004)*, (issn):0036–8075, 2004.

[17] E. Biondi. Diversità fitocenotica degli ambienti costieri italiani. In: M. Don, G. Sburlino, V. Zuccarello (eds.). Aspetti ecologici e naturalistici dei sistemi lagunari e costieri. pages 39–105, 1999.

[18] F. Macchia and F. Vita. Vegetazione del litorale adriatico della Puglia centro-meridionale. *Atti III Simposio Nazionale sulla Conservazione della Natura*, II, 1973.

[19] European Commission DG Environment. Interpretation Manual of European Union Habitats. EUR 27. 2007.

[20] J.A.G. Cooper and J. McKenna. Social justice in coastal erosion management: the temporal and spatial dimensions. *Geoforum*, 39:294–306, 2008.

[21] G.S. Dwarakish, S.A. Vinay, U. Natesan, T. Asano, et al. Coastal vulnerability assessment of the future sea level rise in Udupi coastal zone of Karnataka state, west coast of India. *Ocean and Coastal Management*, 52:467–478, 2009.

[22] H.A. Viles and A.S. Goudie. Interannual, decadal and multidecadal scale climatic variability and geomorphology. *Earth-Science Reviews*, 61:105–131, 2003.

[23] P. Bruun. Sea-level rise as a cause of shore erosion. *Journal Waterways and Harbour Division*, 88:117–133, 1962.

[24] E.R. Thieler, O.H. Pilkey, R.S. Young, D.M. Bush, and F. Chai. The Use of Mathematical Models to Predict Beach Behavior for U.S. Coastal Engineering: A Critical Review. *Journal of Coastal Research*, 16:48–70, 2000.

Heavy Metal in the Sediment of the Shallow Water Areas Surrounding Venice (Italy)

M. Botter[1], D. Cassin[1], A. Pesce[1], M. Scattolin[1], R. Zonta[1]
1, Institute of Marine Sciences, CNR, Venezia, Italy
2, Comune di Venezia, Venezia, Italy
m.botter@ve.ismar.cnr.it

Abstract

The sediment of the shallow water areas surrounding Venice was investigated in order to assess the heavy metal contamination and to evidence possible contributions from the city canal network. The latter receives particulate matter and pollutants from the urban sewage system and different point and non-point sources, and a fraction of this load is transferred to the lagoon by tidal currents. Contaminants can therefore accumulate in the sediment of the nearby mudflats, which are characterized by a slack hydrodynamics. Thirty centimetres-long cores were collected in 2003 and 2004 from 69 sampling sites; a further sampling of 26 cores was done in 2008. Cores were sliced into 10 cm layers and analyzed for grain-size distribution and heavy metal concentration. A moderate pollution level was observed, with concentration of the main contaminants ranging between 6% (Cd) and 29% (Hg) of the mean value measured in the canal network. A clear fingerprint due to the city is observed for Hg, which values exceed the NOAA-ERM guideline (0,71 mg·kg^{-1} d.w.) in 75% of samples.

1 Introduction

Urban sources are one of the main factors in the overall budget of man induced pollutants, leading to potentially poisoning of air, water and soil. When the waste produced by domestic activities and transport is flushed into an urban stream or waterbody, the quality of the receiving water and underlying sediment are affected as well. In this framework, the efficiency of the facilities for pollution control is of a great importance; frequently, waste is not properly disposed and pollutants directly dump into waterways, impairing the quality of water up to making it unsuitable for aquatic organisms to live in.

Concerning heavy metals, domestic wastewater effluents are among the major sources for the aquatic ecosystems at a worldwide scale [1]. Coastal sediments near large urban areas are typically contaminated by heavy metals, which can largely accumulate with respect to their natural background level. Metals behave as conservative pollutants, and many of them are characterised by a high toxicity for living organisms. Humans, being located at the top of the trophic chain, are especially sensitive to these contaminants due to bioaccumulation.

The city of Venice is a peculiar case of urban settlement, which is located in the middle of a transitional shallow water la-

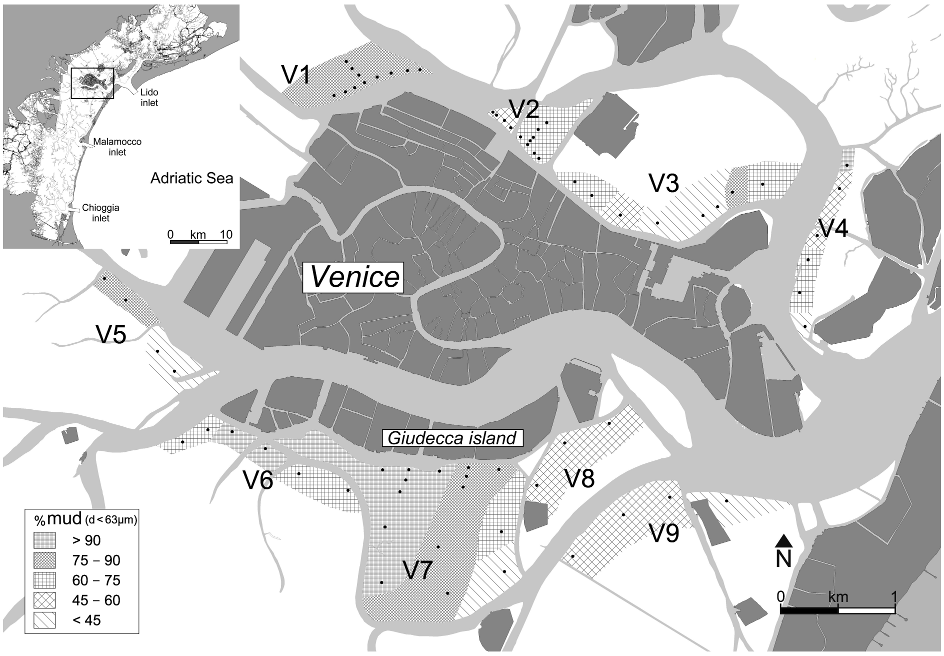

Figure 1: Location of sampling sites (dots) and distribution of the mud content in the surface sediment layer (0-10 cm) of the mudflats surrounding Venice. The Venice Lagoon is showed in the insert.

goon (mean depth = ca. 1 m) where many of the pollution problems typically affecting a coastal environment can be observed (Figure 1, insert).

Despite the drainage basin [2] and the industrial area of Porto Marghera [3] may be regarded as the main sources of pollution to the lagoon, the city of Venice represents a potential relevant source of nutrients, heavy metals and organic micropollutants for the surrounding shallow water areas of the lagoon.

2 Aim of the study

The city of Venice (60000 inhabitants plus 75000 daily tourists and commuters) is crossed by a 40 km long canal network, which receives inputs of particulate matter and pollutants from the urban sewage system, as well as from other point and non-point sources, such as atmospheric deposition and urban runoff, building erosion and corrosion of metal structures, boat traffic [4]. The low current velocity characterising the canal network and the flocculation/precipitation processes occurring when domestic freshwater enters the canal salt water, promote the settling of particles (see, for example: [5]), resulting in the accumulation of a strong reduced, organic rich, fine grained, and highly polluted sediment on the canal bed. Concerning metals, Cu, Pb, Zn, and Hg are particularly enriched in the sediment deposit [4]. Periodic dredging operations are necessary to allow navigation and to assure adequate hygienic conditions. Even though the canal network has a high capability in retaining particles and associated contaminants, a fraction of the total load is transferred to the lagoon by tidal currents [6]. The export is enhanced by particle resuspension due to the boat traffic in the canal network. Contaminants originated from the urban system can therefore accumulate in the sediment of the neighbouring shallow water areas (mudflats), which are characterised by quite low hydrodynamics. The quantification of the pollutant loads produced by the city, retained by canals sediment, and exported towards the lagoon is an important issue. Aim of the study here described was the assessment of the heavy metal contamination of sediment in the mudflats surrounding the city, in order to evidence possible contributions of urban origin.

3 Experimental

Thirty centimetres-long sediment cores were collected in 2003 and 2004 from 69 sampling sites, distributed in the mudflats neighbouring Venice (Figure 1). A further sediment characterisation survey was made in 2008, collecting 26 new cores. Since the mudflats have not a proper name, they are labelled with letter "V" followed by a number (from 1 to 9). Most sampling sites were located few tens of meters away from the edge of the channels surrounding the city; the sampling was also extended to the inner sector of three mudflats (V1, V2 and V7) to acquire information about spatial variability of pollutant concentration with the distance from canals. Collected cores were sliced into 10 cm layers and analyzed for grain-size distribution, As and metal (Cd, Cr, Cu, Fe, Hg, Mn, Ni, Pb, Zn) concentrations.

Grain-size distribution in the diameter range d <700 μm was measured, by means of a laser beam analyser (Microtrac mod. X-100, Leeds and Northrup, USA), in sediments of the upper layer (0 - 10 cm).

For the As and heavy metals (excepting Hg) concentration analysis, a sample aliquot was digested in hot HNO_3 [7], and the leachate was analyzed by atomic absorption spectrophotometry (Perkin Elmer, Analyst 100 USA) or inductively coupled plasma atomic emission spectrometry (ICP-AES) (Optima 2100DV, Perkin Elmer, USA) [8].

For mercury, a refluxing hot digestion with a H2SO4 - HNO_3 mixture was performed and the analytical determination was made by cold vapour AAS technique [9].

4 Results and discussion

Sediment displays a high variability in the grain-size characteristics. A positive gradient of the mud (diameter d < 63 μm) content is observed towards the West (Figure 1). The coarsest grain-size characterises sediments of mudflats V8 and V9 (the fraction with d > 16 μm amounting for about 85% of the total), whereas sediments characterised by a high content of mud (from 81 up to 93%, in the mean) are found in V1, in the western sector of V5, in the central sector of V6, and in both the north-western and central parts of V7.

The grain-size distribution in the investigated sediments is the results of a sedimentation pattern determined by the tidal water circulation and the suspended particles transport and settling [10]. The slack hydrodynamic characterising the mudflats compared to the canals surrounding the

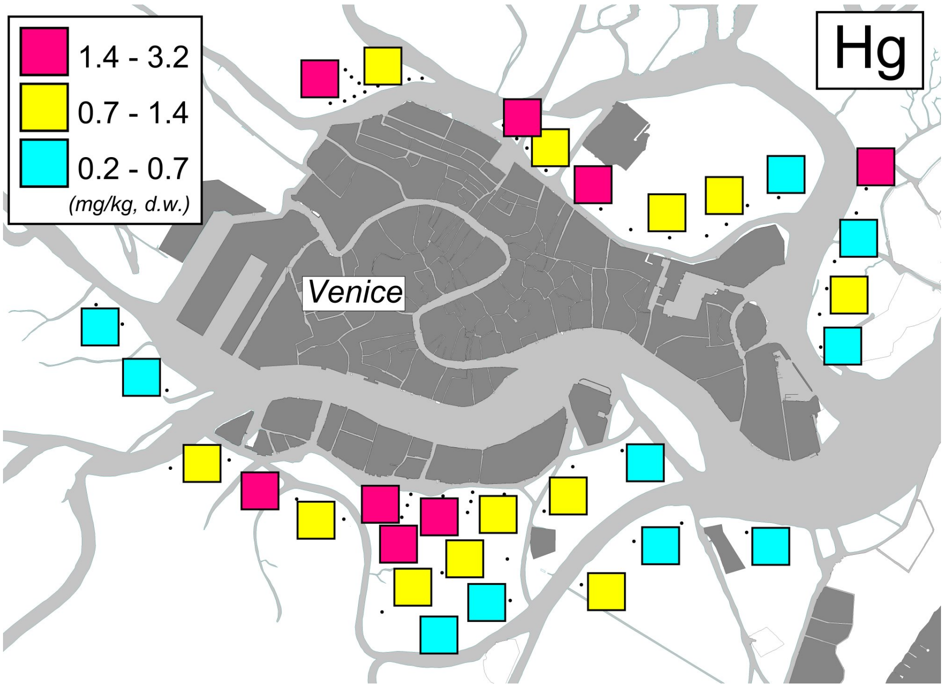

Figure 2: Distribution of Hg concentration in the surface sediment layer (0-10 cm) of the mudflats surrounding the city of Venice.

city, favours the deposition of the fine grained particles. The hydrodynamic regime in the canals is driven by tidal forcing, and as a consequence of phase lags and level gradients occurring at the city boundary [11]. In particular, during the flood tide, when the flow is predominantly from SE to NW, mudflat V1 is interested by a flow of water coming from the northern canals of the Venice urban network. Likewise, the central sector of V6 and the north-western sector of V7 are interested by a flow of water coming from the Giudecca island, which is part of the historical centre of Venice. These waters are generally characterised by a high particle content, because of the urban wastewaters discharge occurred in the previous phase of minimum tide. Moreover, in the daytime the low water level condition in the canal network enhances the effect of particle resuspension from the canals bottom due to boat traffic.
The spatial distribution of metals concentration mainly reflects the finer particles content, resulting in a different degree of contamination of the sediment in the surveyed mudflats. The greater variability of concentrations concerns Cd (from 0,1 to 6,9 mg$\cdot$kg^{-1} d.w.), Cu (5 - 144), Pb (4 - 126), and Zn (27 - 327). The highest concentrations are found in mudflats V1 and V7, as a consequence of the water circulation patterns previously described, which determine a flow of pollutants directly from the urban canal network to these areas.
Concerning the heavy metal concentration

		As	Cd	Cr	Cu	Fe	Hg	Mn	Ni	Pb	Zn
mean	layer 0-10 cm	6,9	0,71	10	28	11083	1,06	239	7	23	99
	layer 10-20 cm	8,0	0,57	13	29	13821	1,10	275	8	27	90
	layer 20-30 cm	8,2	0,40	15	28	15713	1,09	305	9	29	74
	Venice canals network	16,6	6,60	31	245	n.a.	3,70	n.a.	36	222	889

Table 1: Heavy metal mean concentrations (mg·kg^{-1}, dry weight) in the investigated mudflats and in the Venice canal network (n.a. = not available).

trends along the sediment vertical profile, As, Cr, Fe, Mn, Ni, and Pb mean concentration decreases toward the surface sediment in all the investigated mudflats (Table 1). This decrease is more relevant in mudflats V2, V8 and V9. In particular, Cr, Fe and Pb concentrations in the deeper layer (20-30 cm) of the mudflat V8 are about twofold the concentrations observed in the upper one (0-10 cm).

With respect to the previous species, Cd and Zn concentrations show an opposite trend with the depth, in particular in the cores collected in mudflats V1, V2, V5, V6 and V7. In the latter the ratio between Cd and Zn mean concentration in the upper and in the deeper layers is equal to 3.5 and 1.9, respectively. Copper and Hg do not show significant differences with the depth.

In order to compare contamination levels observed in the mudflats and in the city of Venice, mean heavy metal concentrations in the canal network are reported in the last row of Table 1. These data were determined by analysing sediment cores (mean length = 40 cm, σ = 7 cm) collected form 775 sites uniformly distributed in the 40 km of the canal network [4]. The comparison allows to investigate eventual contributions from the canals system to the surrounding mudflats. On the average, Cd, Cu, Pb and Zn concentration in the mudflats is low (about 10%) when compared to the value measured in the canal network. Arsenic, Cr, and Ni concentrations are low both in the mudflats and in the canal network. The more evident fingerprint due to the city is observed for Hg (Figure 2), particularly in the mudflats V1, V2, V3, and V7. High concentrations of Hg (up to 46 mg·kg^{-1}) were found in the Venice inner canals sediment due to point sources. Mercury in the urban environment is released principally by dental amalgam, pharmaceuticals and pesticides, as well as light-bulbs, thermometers, batteries, combustion of fossil fuels and medical wastes [12, 13, 14].

Sediments of the Venice canal network were classified in the years from 1994 to 2000, on the basis of their contamination level, prior to a comprehensive dredging intervention. At the beginning of '90s, in fact, a layer of polluted sediment up to 1 m thick accumulated in the network, and a classification was needed in order to identify appropriate disposal sites. Three classification limits were established in 1993 by a specific protocol of the Italian Ministry of the Environment, which discrimi-

		As	Cd	Cr	Cu	Hg	Ni	Pb	Zn
% samples	class A	100	87	100	86	13	100	94	96
	class B	0	13	0	12	87	0	6	4
	class C	0	0	0	3	0	0	0	0
% samples	< ERL	59	91	100	80	0	100	96	88
	ERL - ERM	41	9	0	20	25	0	4	12
	> ERM	0	0	0	0	75	0	0	0

Table 2: Percentage distribution of sediment samples from the mudflats with respect to the classification classes established by the Italian Ministry for the Environment (first 3 rows) and NOAA sediment quality guidelines (last 3 rows).

nate four classes corresponding to increasingly strict constraints for the disposal. Non-polluted sediment (class "A") can be used for restoration of the lagoon morphology (salt marsh reconstruction, reclamation works); moderately polluted sediment (class "B") can also be used for restoration but only when ensuring a permanent confinement against the release of contaminants in the lagoon, polluted sediment (class "C") can only be used for reclamation of elevated areas that are never in contact with the lagoon water or subjected to erosion or dispersion by infiltration; finally, highly polluted sediment (class ">C") must be disposed in controlled landfills outside the lagoon.

Even if it was addressed to the urban canal network, this classification was frequently used in the last 15 years as a basis to characterise the sediment contamination of the Venice Lagoon. The percentage distribution of sediment samples collected in the mudflats with respect to the above classification classes is shown in Table 2. At each site the mean value analysed in the three sampling layers was considered. Only in 2 sites (in the mudflats V1 and V7) the sediment is classified as polluted (class "C"), and this is due to the Cu concentration. However, the metal concentration values (60,4 and 68,5 $mg \cdot kg^{-1}$ d.w., respectively) are very close to the B limit for copper (50 $mg \cdot kg^{-1}$ d.w.). Most sites fall in the B class due to the Hg concentration level. Without considering mercury, sediments would fall in the non-polluted class in 60 of the 69 sites (87%).

Table 2 also shows the percentage distribution of the collected samples with respect to the three concentration ranges discriminated by the NOAA Sediment Quality Guidelines (SQGs): effect range-low (ERL) and effect range-median (ERM). The ERL and ERM represent the concentrations below which adverse effects are expected to occur rarely and frequently, respectively (Long, 1998). They were established by using simultaneous observation of sediment contamination and sediment toxicity or benthic impacts reported for estuaries and marine bays throughout the North America. Chromium and Ni are always below ERL values, while Cd, Cu, Pb and Zn exceed it at few sites. Arsenic concentrations are higher than ERL in the mudflats V1 and V7. Mercury concentration is always higher than the ERL value (0,15 $mg \cdot kg^{-1}$ d.w.), and it is higher than the ERM value (0,71 $mg \cdot kg^{-1}$ d.w.) in 75 % of samples, which implies a high likelihood of causing adverse effects on sediment associated biota.

In conclusion, the investigation points out a presence of Hg in the sediment of the mudflats surrounding Venice, which is enhanced by the load originated in the urban canal network and implies an ecotoxicological risk for the environment.

References

[1] J.O. Nriagu and J.M. Pacyna. Quantitative assessment of worldwide contamination of air, water and soils by trace metal. *Nature*, 333:134–139, 1988.

[2] F. Collavini, C. Bettiol, L. Zaggia, and R. Zonta. Pollutant loads from the drainage basin to the Venice Lagoon (Italy). *Environment International*, 31:939–947, 2005.

[3] R. Zonta, M. Botter, D. Cassin, R. Pini, M. Scattolin, and L. Zaggia. Sediment chemical contamination of a shallow water area close to the industrial zone of Porto Marghera (Venice Lagoon, Italy). *Marine Pollution Bulletin*, 55:529–542, 2007.

[4] R. Zonta, L. Zaggia, F. Collarini, F. Costa, and M. Scattolin. Sediment contamination assessment of the Venice canal network (Italy). pages 603–615, 2005.

[5] H. Paucot and R. Wollast. Transport and transformation of trace metals in Scheldt estuary. *Marine Chemistry*, 58:229–244, 1997.

[6] R. Zonta, A. Zuliani, E. Coraci, C. D'Este, and A. Pesce. Fluxes of particulate, metals and nutrients in a test canal of Venice (Italy). *Proc. 41st International Conference ECSA, Venice, Italy, 15 -20 October*, page 106, 2006.

[7] USEPA (Environment Protection Agency of United State of America). Method 3050B, Acid digestion of sediments, sludges and soils. 1996.

[8] USEPA (Environment Protection Agency of United State of America). Method 200.7, Determination of Metals and Trace Elements in water and Wastes by Inductively Coupled Plasma-Atomic Emission Spectrometry. 1994.

[9] USEPA (Environment Protection Agency of United State of America). Method 245.1, Mercury (Manual Cold Vapour Technique). 1974.

[10] C. Ferrarin, A. Cucco, G. Umgiesser, D. Bellafiore, and C.L. Amos. Modelling fluxes of water and sediment between Venice Lagoon and the sea. *Continental Shelf Research*, 30:904–914, 2010.

[11] E. Coraci, G. Umgiesser, and R. Zonta. Hydrodynamic and sediment transport modelling in the canals of Venice (Italy). *Estuarine, Coastal and Shelf Science*, 75:250–260, 2007.

[12] US Department of Health and Human Services. Toxicological profile for mercury. page 676, 1999.

[13] L. Sorme, B. Bergback, and U. Lohm. Century perspective of heavy metal in urban areas. A case study in Stockholm. *Water, Air and Soil Pollution: Focus*, 1:197–211, 2001.

[14] J. Sviden and A. Jonsson. Urban metabolism of mercury turnover, emissions and stock in Stockholm 1795-1995. *Water, Air and Soil Pollution: Focus*, 1:179–196, 2001.

Management Plan for the Beach-Cast Seagrass in Calabria

N. Cantasano
Institute for Agricultural and Forest Systems in the Mediterranean, CNR, Rende (Cs), Italy
n.cantasano@isafom.cs.cnr.it

Abstract

The wracks of *Posidonia oceanica* leaves and the "banquette" formation on the sandy beaches of Calabria are one of the most important defence against the erosion processes. The management of the beach-cast sea-grass in Italy has been, generally, realized through the mechanical removal and the transport in dumping of the beach-cast material. This system, apparently simple and fast, produces, instead, a net loss of sediments from the sandy beaches and, therefore, a deficit in the sedimentary budget of coastline leading the coastal system to possible shore erosions. The ideal solution is to keep these vegetable deposits on spot so to warrant a positive sedimentary budget, the protection of coastline and the tourist value of the regional beaches to improve tourism in the seaside resorts with bathing vocation.

1 Introduction

The Mediterranean endemic sea-grass *Posidonia oceanica* (Linnaeus) Delile, forms extensive beds, named "prairies", in the infra-littoral bottom of the basin, according to favourable environmental conditions. A long time ago, the prairies of *Posidonia oceanica* surrounded a large part of the Mediterranean seashore forming an almost continuous belt along the coasts of the basin. Nowadays, we attend to a widespread regression and/or to the complete disappearance of these natural barriers along the Mediterranean coasts. Healthy meadows have been replaced, in the damaged areas, with deserts of dead "mattes" or have been colonized again by algal populations of *Caulerpa prolifera* (Forsskål) J.V. Lamouroux or by the other common Mediterranean sea-grass *Cymodocea nodosa* (Ucria) Ascherson. In these last decades, this trend has been reported in many areas of the Italian coasts where the 72% of the prairies have deteriorated, as shown by the partial data, related to five regions, produced by the "National Program of characterization and development of *Posidonia ocenica*" started up on 1989 by Ministero dell'Ambiente e della Tutela del Territorio e del Mare [1].

The problem of the reduction of Mediterranean meadows takes place also in Calabria and, in particular, along the calabrian Tyrrhenian coasts where the 62% of the prairies is in regression [2]. The phenological data and, in detail, the trend of the density shoots of these prairies point out the bad conditions of the Mediterranean meadows as reported in literature [3, 4, 5, 6]. The widespread deterioration of the coastal environments, in the Mediterranean basin, implies a global vision of the problem. The critical state of the Italian coasts has became in these last years a serious problem along our coastal boundary where the 42% is in erosion [7]. These negative conditions are particularly severe in the calabrian coastal boundary where the 43% of the beaches are in erosion [8]. The particular position of this region, surrounded by the Tyrrhenian and the Ionian seas, for a coastal boundary of 725 km, as 1/5 of the national coastal perimeter, suggests the solution of some problems linked to the protection and the improvement of its coastal line, transition area between the terrestrial and the marine environments. So, the coastal defence must become the main appointment for the national and the regional authorities.

The dynamic environmental balance of sandy beaches comes from two different processes: from one side, the transport of solid materials through the sedimentary supply of rivers flowing into the sea; from the other side, the losses of sands and littoral pebbles due to hydrodynamic forces. In ideal conditions of a stable balance these processes are equal and the beach keeps stable its profile. In real conditions, instead, it takes place advancing or, more frequently, erosion of the coastline. The coastal advancing happens if the value of the supplies exceeds the losses while in the opposite case, much more common, we can observe the erosion processes. The sedimentary budget of sandy beaches is made by three basic elements: the shoreface, the shoreline and the coastal dune amongst which take place exchanges so to grant the littoral sedimentary equilibrium and the right working of coastal system. The sedimentary loop between the underwater and the terrestrial shore begins at the end of the vegetative period when leaves senesce and detach off the rhizomes [9]. This leaf loss can reach values of 10-20 tons of vegetable fragments for hectare of meadow [10] of which 5% is exported outside, 70% remains in the "intermattes" of the meadow and 25% is washed by wave action on adjacent shorelines, forming deposits known as "banquettes" [11]. Indeed, during their life, the plants lose a lot of leaves that are carried by hydrodynamic pressure onto the beach on clumps and are accumulated on sandy beaches where form very conspicuous wedge-shaped deposits up to 2 m height [10]. The "banquettes" play, also, a leading role trapping high amounts of sediment inside the overlapping layers of the deposits. The leaf piles and their sediment store carry out an important functional and structural task by attenuating wave and stream energy and limiting coastal erosion.

2 The coastal trophic system

The meadows of *Posidonia oceanica* play a basic function in the sensitive biological balance of the Mediterranean Sea even though they cover only the 0,2% of its floor for a surface area of about 20.000 square miles. The prairie, climax community on mobile substrates in the infralittoral bottom of the basin [12], produces a big amount of organic substances that my reach a high primary production as 20 $g{\cdot}C{\cdot}m^{-2} \cdot d^{-1}$ in the summer season. A large part of this energy and material inputs come into the trophic loop through the detritus chain formed by the dead leaves of the plants that settle inside the channels and in the "intermattes" of the meadow. A lot of studies, indeed, indicate the central role played in the overall structure of the food web by the leaf detritus [13]. The 50%

of this amount of organic substances produced by the meadow is consumed inside it, the 30% is exported towards the open sea and the remaining 20% is carried by hydrodynamic pressure towards the line-coast [14]. The ecosystems of *Posidonia oceanica* (PP) play, therefore, an important role for the primary productivity of the coastal system where they carry out a central task in the handling of energy and materials between coastal, pelagic and terrestrial systems (Figure 1).

3 Functions, dynamics and structures of "banquettes"

The "banquettes" are a potential nutrient sinks for the coastal trophic net and, consequently, for its whole productivity. The organic material in these leaf deposits consisted of about 95% by *Posidonia oceanica* brown leaf blades and of about 5% by rhizomes and seaweeds [15]. Leaf litter biomass in the banquettes ranges from 18 to 500 kg dry wt m-1 of shoreline [16]. This big amount of organic supply sinks temporarily in the banquettes where is partially consumed by terrestrial detritus feeders, such as amphipods, isopods, coleoptera and diptera, and partly constitutes an important and temporary C, N and P sink for *Posidonia oceanica* meadows. Therefore, the sea-grass wrack is an intermediate and important product in the life cycle of the plant that should end into the sea. These wedge-shaped accumulations all along the Mediterranean coasts are, indeed, the final result of a dynamic process of formation/accretion/destruction arranged in the following temporal sequence:

A) Formation
   - October: First equinoctial storms and beginning of wave action - detach of leaf blades – suspension of dead leaves of *Posidonia oceanica* and their transport towards underwater shore.
   - November: Transport of dead leaves of *Posidonia oceanica* from underwater shore to terrestrial one.

B) Accretion
   - December: Accumulation and deposit of *Posidonia oceanica* leaf litter on the shoreline.
   - January: Severe winter storms and increasing of wave action $>$ vertical and horizontal increases of "banquettes" – hydrodynamic reduction.

C) Erosion
   - February: Beginning of erosion at the base of "banquette".
   - March: Increase of erosion and formation of a step at the base of the "banquette" – reduction in height of the deposit.

D) Collapse
   - March: Breaking in blocks and collapse into the sea of the "banquette".

The "banquettes" are solid and elastic structures and provide a very remarkable level of compactness because, during their formation, the air spaces amongst the leaves are eliminated and the hydraulic conductivity of the structure is reduced [16]. These conditions allow the "banquette" to offer a considerable resistance against wave action so to oppose coastal erosion (Figure 2).

The wedge-shaped deposits of *Posidonia oceanica* leaf litter, that pile up on the sandy beaches of the Mediterranean basin, are a temporary sink of organic matter made up of detached leaves of the plants but include, also, inorganic materials as sands and water. The amount of sediments in the "banquettes" depends on their grain

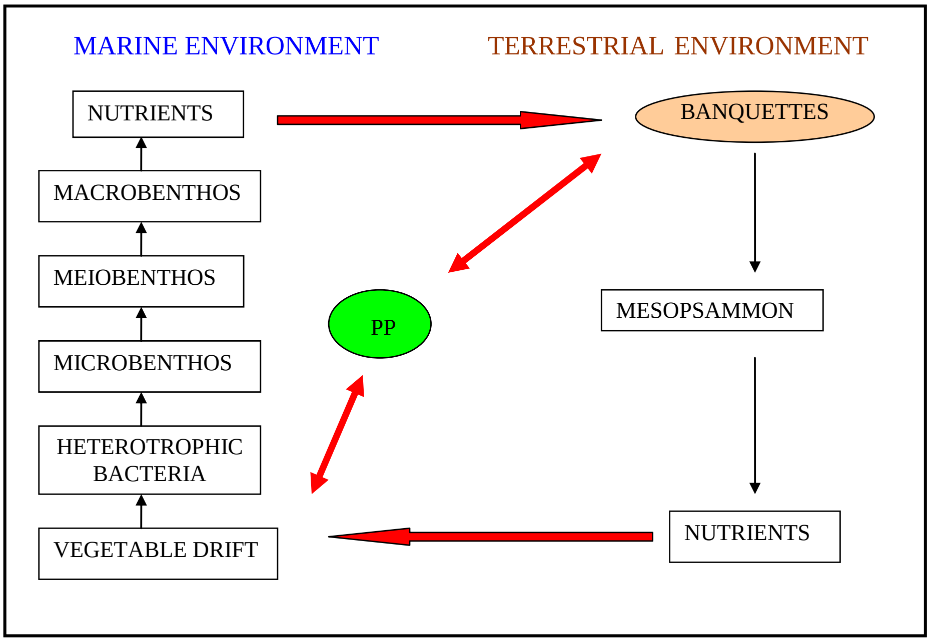

Figure 1: Conceptual scheme of trophic and energy transfers between terrestrial and marine environments.

size. The quantity of sand trapped in the "banquettes" is very high in the beaches of coarse – grained while it decreases in those of medium and thin – grained. The results of Arena Project, carried out along the Sardinian coasts, prove that the removal of 100 m^3 of "banquettes" from beaches of coarse texture causes a loss of sediment of 11,2 tons like a loss of 11,2 kg from the beach [17]. These conditions produce a negative beach sediment budget and, consequently, possible shore erosions following storm events. Therefore, it is necessary to value the percent in weight and in volume of the organic and inorganic fractions contained in these deposits so to establish the physic function of "banquettes" in the coastal dynamics. The first results of this method, held by the Environmental Department of Livorno Province [18], prove that the sandy fraction of the deposits is very high, ranging from 37% (percent in volume) to 56% (percent in weight) and, consequently, these wedge – shaped deposits of *Posidonia oceanica* leaf litter can be considered basic for the hydrodynamic equilibrium of littorals.

4 Problems and solutions

The cleaning operations of the beaches and the whole removal of these beach – cast litter produce a subtraction of sediments from the beaches and may lead to possible shore erosions. These conditions produce, also, the deterioration of coastline and the loss of dune vegetation. The de-

Figure 2: The "banquette" of Punta Santa Litterata (Cs).

sertification of sandy beaches gives raise, long-term, to substantial changes in beach morphology. From a biological point of view, the "banquettes" are an important and potential sink of biogenic elements for the sea-grass ecosystems [16]. These vegetable biomasses accumulate, indeed, a large amount of organic carbon valuable from 18 to 500 kg of dry wt m-1 of shoreline [19]. The complete removal of the "banquettes" causes a nutrient depletion for the trophic chain of coastal ecosystem and, in particular, a permanent loss of C, N and P. The N and P losses are respectively 5,4% and 1,2% of the annual requirement of the plant [20, 9, 21].

The removal operations, made by coastal municipalities, using heavy machinery such as bulldozers and excavators, are carried out to keep the tourist value of sandy beaches. The following loss of sediments from the shoreline impacts upon the littoral stability and may support erosive processes on the beaches exposed to high hydrodynamic pressure. Therefore, it's reasonable to avoid this kind of procedure or to carry out late actions of displacement in the months of May or June, at the beginning of steady anti-cyclonical conditions, to minimize the impacts of removal. It's necessary, in these circumstances, to avoid the mechanical handing of the deposits while it's right to work manually so to avoid the direct removal of sandy materials.

The solution to the problem should be to leave these vegetable deposits to their natural process of maturation keeping the "banquettes" on the spot or to stock them on the ground in the highly tourist areas and to move them inside the coastal dune or in retired belts close to the shoring events within the point of maximum wave expansion. It is necessary, in this instance, to proceed by hand so to avoid health risks. This kind of operations may contribute to the protection of the coastline against erosion processes and to the stability of substrates behind the fore-dunes allowing, at last, a real saving of financial resources. These suggestions have been recently ratified by a ministerial memorandum of Ministero Ambiente dated 17 March 2006 (DPN/VD/2006/08123) concerning the management of beach-cast litter found in coastal areas. This provision states three alternative solutions: the removing and dumping of beach-cast litter, the moving of the deposits or the maintenance on spot of the "banquettes". The first solution is to avoid because it produces a great loss of sediments from the sandy beaches and a deficit in the sedimentary budget of coastal system leading the shoreline to possible erosions. The second one is suggested only in case of problems with the touristic development of some seaside resorts with bathing vocation. In this particular situation, the removal operations must be carefully executed with late actions of displacement, avoiding the use of heavy machineries. The third one is the ideal solution to the problem and in this event the coastal municipalities have to inform the public opinion and, particularly, the tourists through posters and placards to improve the presence of *Posidonia oceanica* meadows in those areas as pattern of ecological shore like the "biobeaches" of French coasts [22]. In this sense the joined presence of meadows and "banquettes" could become the main factor of wildness of the coastal area. The final result will be a steady and tourist attending of the beaches.

5 The new outlooks: the G.I.P.O.S. project

The project, held by C.N.R. – I.S.A.Fo.M. Rende Research Unit (Prot. n. 131 AXIII/I), aims to evaluate the beaching processes of these conspicuous wedge-shaped accumulations all along the coasts of "Riviera dei Cedri" Marine Regional Park. This is the first trial, in Calabria, to tackle the problem of a correct management of leaf litter on the grounds of previous scientific researches carried out in some Italian regions as Lazio, Tuscany and Sardinia. The research line, named G.I.P.O.S., aims to share into the knowledge of the process of banquette storing along the regional sandy beaches and to study their structures so to evaluate their physical and biological functions in the erosive process, still going on the calabrian Tyrrhenian coasts.

The "Riviera dei Cedri" Marine Regional Park (Figure 3) is an area of high environmental value and is marked out by the presence of four Sites of Community Interest (S.I.C.) in the sea-beds of Isola di Dino, Capo Scalea, Isola di Cirella and Diamante where are located some of the most important regional prairies of *Posidonia oceanica*. The coastline of the Park, between the marine villages of Praia a Mare (CS) and Acquappesa (CS), spreads over 55 kilometres. The eleven coastal municipalities of this area have been interested in the implementation of the project through the compilations of a set of questions concerning the reports of *Posidonia oceanica* beaching in the period 1998 – 2007.

The scientific program consists of three stages. The first step aims to identify the coastal areas where have been reported events of beaching of *Posidonia oceanica*

Figure 3: Map of "Riviera dei Cedri" Marine Regional Park.

in the decade 1998-2007 and the related managements methods realized by coastal municipalities of the Park. The second step regards the study of the chemical and structural pattern of "banquettes" in order to evaluate its functional role in the sedimentary budget of coastline. In the third step, at last, are sieved the different methods of moving these massive deposits of leaf litter of *Posidonia oceanica* and are suggested the best solutions for a correct management of the beach-cast sea-grass.

Recently, the wracks of dead sea-grass have been collected and transformed into compost in the Mediterranean coastal countries for agricultural purposes. The use of compost as soil enrichment enhances plant growth and increases crop productivity. The addition of seaweeds into the compost can increase pore volumes, aggregate stability, cationic exchange capacity, microbial mass and biological activity of the soil for horticultural species and for the farming.

Nowadays in our country have been tested some technologies for the use of vegetable biomasses in composting as biological fertilizer [23, 24], but also as covering dumping grounds, as agricultural drainage and as mulching of the soils to remove weeds. The problem arises from our national laws that forbids the use of *Posidonia oceanica* as composting matrix for agricultural purposes (D.Lgs.217/2006). In this lawgiving national contest the Italian Composting Pool has sent to U.E. an application for the review of this ministerial decree. Therefore, after the passage of the new law, it will be allowed to compost the marine vegetable wastes as long as they don't exceed the 20% of total weight compost [25]. So, it will be possible to obtain a mixture of Mediterranean sea-grass with shredded municipal yard and landscape green wastes after a composting period of 150 days and several rinsing to eliminate all chlorides and heavy metal compounds. The composting material will be rich in carbon, phosphorus and nitrogen and will improve the physical conditions and the microbial biomass of soil so to stimulate plant growth and increase crop productivity.

6 Conclusions

The vegetable biomasses known as "banquettes" are an excellent indicator of the quality of marine coastal environment for the presence of extensive *Posidonia oceanica* meadows on the marine sea-beds. Therefore, the presence of these massive supra-littoral deposits of leaf litter along the coastal areas of the "Riviera dei Cedri" Marine Regional Park is a clear sign of a sea in a good environmental health. The wedge-shaped deposits, placed on some stretches of the protected coastline, perform an important mechanical and biological rule in the trophic and sedimentary budget of coastal system. Therefore, these deposits cannot be considered a simple waste material but, instead, a natural resource for the sensitive balance of coastal ecosystems. The actual technologies and the current management practices about "banquettes" must change from the simple beach wrack removal to their maintenance on spot providing a protection to the foreshore and reducing erosion processes. At last, it is necessary to revalue the ecological function of *Posidonia oceanica* "banquettes", natural elements of some calabrian coasts, that could become the "bio-beaches" of the coastal regional boundary so to improve the tourism in the seaside resorts with bathing vocation.

References

[1] Si.Di.Mar. Ministero dell'Ambiente e della Tutela del Territorio e del Mare. Programma Nazionale di individuazione e valorizzazione della Posidonia oceanica.htpp://www.sidimar.tutelamare.it/praterie_ posidonia.jsp. 2008.

[2] N. Cantasano. Il nostro mare, la flora. *Dossier del W.W.F. Calabria, Vibo Valentia. http:/www.wwf.it/UserFiles/File/AltriSitiWWF/Calabria/documenti*, 2008.

[3] H. Augier and C.F. Boudoresque. Vegetation marine de l'ile de Port Cross. La baie

de Port-Man et le problem de la regression de l'herbier de posidonies. *Bull. Mus. Hist .Nat., Marseille*, 30:145–166, 1970.

[4] J.M. Astier. Regression de l'herbier de Posidonie en rade des Vignettes a Toulon. *Ann. Soc. Sci. Nat. Toulon Var. Ann.Soc.Sci.Nat.Archeol. Toulon*, 24:97–103, 1972.

[5] A. Meinesz and R. Laurent. Cartographie et état de la limite inferieure de l'herbier de Posidonia oceanica dans les Alpes-Maritimes (France). *Bot. Mar.*, 21:513–526, 1978.

[6] J.M. Pérès. La regression des herbiers a Posidonia oceanica. International workshop on Posidonia oceanica beds. *Boudouresque C.F., Jeudy de Grissac A., Olivier J. eds,. Gis Posidonie*, 1:445–454, 1984.

[7] Consiglio Nazionale delle Ricerche C.N.R. Atlante spiagge. Progetto Strategico N. 6. *Collana Multimediale Progetti Strategici. Progetto Mezzogiorno. Roma*, 1999.

[8] Gruppo Nazionale per la Ricerca sull'Ambiente Costiero. Le spiagge della Calabria. Studi Costieri. 10:33–38, 2006.

[9] M.A. Mateo and J. Romero. Detritus dynamics in the seagrass Posidonia oceanica: elements for an ecosystem carbon and nutrient budget. *Mar. Ecol. Prog. Ser.*, 151:43–53, 1997.

[10] J.R. Medina, J. Tintoré, and C.M. Duarte. Las praderas de Posidonia oceanica y la regeneración de playas. Rev. De Obras Públicas. *Bot. Mar.*, 409(3):31–43, 2001.

[11] C.F. Boudouresque and A. Meinesz. Découvert de l'herbier de Posidonie. *Cah. Parc. Nation. Port-Cross, Fr.*, 4:1–79, 1982.

[12] E. Ghirardelli. La vita nelle acque. *Utet, Torino*, pages 392–402, 1981.

[13] V. Zupo. The use of feeding indices for the study of food webs: an application to a Posidonia oceanica ecosystem. *Coenoses*, 8(2):85–95, 1993.

[14] N. Cantasano. La Posidonia, polmone verde del Mediterraneo. *Dossier del W.W.F. Italia, Stampa Poligrafica, Amantea (Cs.)*, pages 10–11, 2001.

[15] N. Cantasano. La gestione di Posidonia oceanica spiaggiata in Italia. *Biologi Italiani XXXIX*, pages 65–70, 2009.

[16] M.A. Mateo, J.L. Sánchez-Lizaso, and J. Romero. Posidonia oceanica "banquettes": a preliminary assessment of the relevance for meadow carbon and nutrients budget. Estuarine, Coastal and Shelf Science, 56: 85-90. 2003.

[17] G. De Falco, S. Simeone, and M. Baroli. La rimozione della Posidonia dalle spiagge: conseguenze sulla stabilità dei litorali. *Fondazione IMC, Oristano*, pages 1–14, 2006.

[18] Provincia di Livorno. Linee guida "Gestione integrata della Posidonia oceanica". *Provincia di Livorno. Assessorato alla difesa suolo e coste*, pages 1–32, 2006.

[19] C.M. Duarte. How can beaches be managed with respect to seagrass litter? *In Borum J., Duarte C.M., Krause-Jensen D., Greve T.M. (Eds), "European seagrasses: an introduction to monitoring and management". EU project Monitoring and Managing of European seagrasses (M&MS). Evk3-CT-2000-00044: 83-84.*, 2004.

[20] J. Romero, G. Pergent, C. Pergent-Martini, M.A. Mateo, and C. Regnier. The detritic compartment in a Posidonia oceanica meadow: litter features, decomposition rates and mineral stocks. *Mar. Ecol. PSZN*, 13(1):69–83, 1992.

[21] E. Gacia, C.M. Duarte, and J.J. Middelburg. Carbon and nutrient deposition in a Mediterranean seagrass (Posidonia oceanica) meadow. *Limnol. Oceanogr.*, 47(1):23–32, 2002.

[22] C.F. Boudouresque, G. Bernard, P. Bonhomme, et al. Préservation et conservation des herbiers á Posidonia oceanica. *RAMOGE publ.*, pages 1–202, 2006.

[23] F. Seri, L. De Gara, S. Caretto, L. Leo, and P. Santamaria. Influence on an increased NaCl concentration on yield and quality of cherry tomato grown in Posidonia oceanica (L.) Delile. *J. Sci. Food Agric.*, 84:1885–1890, 2004.

[24] Consiglio Nazionale delle Ricerche C.N.R. – I.S.P.A. La Posidonia spiaggiata è una risorsa per le colture. *Il Floricoltore n. 9*, Settembre 2008.

[25] M. Centemero. Fertilizzanti. IV Forum Interregionale sul compostaggio. *C.I.C. Consorzio Italiano Compostatori. Torino,*, 5 marzo 2008.

Evaluation of Heavy Metal Contents in Benthic Foraminifera to Record Effects of Anthropogenic Impact on Coastal Marine Areas

P. Rumolo[1], D. Salvagio Manta[1], M. Sprovieri[1], R. Coccioni[2], L. Ferraro[1], L. Giordano[1], E. Marsella[1]
1, Institute for Coastal Marine Environment, CNR, Napoli, Italy
2, DISTEVA, PU (affiliazione non presente, segnalare)
paola.rumolo@iamc.cnr.it

Abstract

A systematic investigation on the concentrations of a selected number of trace elements (Cd, Co, Cu, Li, Ni, Pb, V and Zn) in carbonate shells of the benthic foraminifera *Ammonia tepida* collected from surface sediments of the highly polluted harbour of Naples was carried out. Cleaning procedures, combined with Scanning Electron Microscopy investigation (SEM) provided accurate quantification, by ICP-MS technique, of the elements in the carbonate lattice. Then, values of biogenic carbonate/seawater distribution coefficients reported in the literature were used to calculate the ranges of variability of total dissolved trace elements in the studied marine environment. High concentrations of Zn, Cd, and Cu calculated in seawater (two/three order of magnitude higher than those reported for uncontaminated Mediterranean seawaters) testify the intense effects of anthropogenic impact on the harbour mainly related to the industrial and commercial activities carried out in the neighboring area. These results emphasize the high potential of measurements of trace elements in the biogenic carbonates of benthic organisms as suitable "tool" for investigation of anthropogenic impact on seawater and reliable proxy of potentially bio-available forms (as free ions and/or more labile organic complexes) of seawater dissolved metals.

1 Introduction

An important achievement of the past two decades in the field of carbonate geochemistry is the experimental evidence that foraminifera faithfully record the changes of the environmental conditions in which they live (e.g., [1, 2, 3, 4]). In particular, calcareous foraminifera incorporate into their tests accessory cations, for example divalent metal ions (Me), proportionally to their concentration in surrounding seawater (e.g., [5, 6]), this means that when the Me/Ca ratio in seawater increases, the Me/Ca ratio in the $CaCO_3$ foraminifera shell also increases (e.g.,[3, 4, 7, 8]. In general, divalent cations with an ionic radius close to Ca ($\sim$1.0 Å) have a partition coefficient (DMe) close to 1, where

$$D_{Me} = \frac{Me/Ca_{carbonate}}{Me/Ca_{seawater}}.$$

For example, Cd has an ionic radius of 0.95 Å [9] and is incorporated in benthic foraminifera with a DCd$\sim$2 [10, 11, 12], while Cu has an ionic radius of 0.73 Å and a partition coefficient of $\sim$0.2 [13]. In view of the above, trace element concentrations in carbonate shells of foraminifera have proved to be useful in reconstructing general dynamics in ancient oceans (e.g., [14, 15, 6, 16, 17, 18, 7, 19, 20, 21, 22]). Surprisingly, only very few ongoing researches are dedicated to the investigation of metal contents in foraminifera shells as reliable tracers of contamination in seawater and thus as proxies of anthopogenic impact on the marine environment (e.g., [23, 24, 25, 26]. Metals occur naturally in the environment, often as trace constituents in rocks, soils, waters, plants and animals. However, their concentration generally increases, reaching levels of potential toxicity for the ecosystems in marine coastal areas, which are typically affected by major commercial and tourist activities and too often become natural collection basins of industrial, agricultural, domestic waste [27]. Metal bioavailability in the marine environment depends on their chemical forms [28], therefore, a simple estimate of the total concentration of heavy metals is generally not sufficient to provide reliable information on the potential of their negative effects on the ecosystem [29]. Although some forms of organic metal complexes were reported to be available for organic and intra-cellular activities, free metal ions appear the most "bioavailable" dissolved chemical species and consequentially the most dangerous for marine ecosystem [30]. The analytical techniques available for reliable investigation of the speciation of heavy metals in seawater (e.g., anodic stripping voltammetry (ASV) and differential pulse anodic stripping voltammetry (DPASV) are extremely time consuming and expensive. Thus, in the last few years the scientific community has focused on new alternative tools for the determination of trace metals in labile form in seawater. The short life cycle of benthic foraminifera and their immediate response to the contamination of the surrounding environment, unequivocally confirmed by clearly verified in several studies in terms of changing assemblage, distribution and morphology (e.g., [31, 32, 33, 34], makes this group of organisms a particularly suitable indicator of early warning signs of possible anthropogenic pollution of the marine environment [35]. Once the values of the carbonate/seawater metal distribution coefficients are known, appropriate investigations of the chemistry of the carbonate shells of benthic foraminifera may represent an excellent and reliable method to monitor short-term changes in the chemistry and bioavailability of toxic elements in seawater. Research in this field is in its first stages and requires huge efforts for the acquisition of new experimental data, the development of reliable bio-mineralization models and calculation of appropriate distribution coefficients in order to verify the validity and suitability of such an approach.

This study aims to provide a high-quality dataset of trace element concentrations in the carbonate of the benthic foraminifera species *A. tepida* collected from the surface sediments of the highly contaminated coastal area: the harbour of Naples, one of the largest and most important commercial and tourist port of the Mediterranean, located in the south-eastern Tyrrhenian Sea margin (Gulf of Naples) (Figure 1). Application of appropriate cleaning and analytical techniques to measure concentration of elements, with verified toxic effects, in substitution to Ca^{+2} in the biogenic carbonate lattice along Rwith a wide spectrum

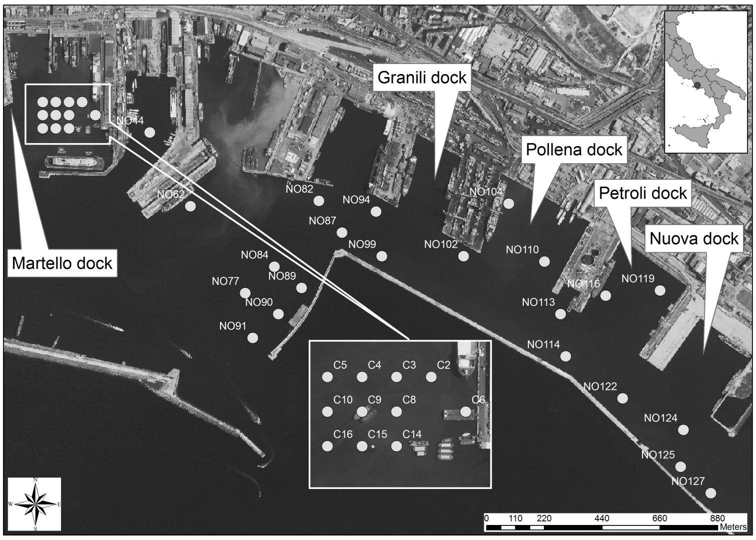

Figure 1: Location map of the studied samples (circles).

of chemico-physical information on the studied environment previously published by [36, 34, 37], provide an intriguing opportunity to verify the reliability of the carbonate chemistry of benthic foraminifera as tracers of heavy metal contamination of seawater.

2 Materials and methods

2.1 Sampling and trace elements analysis

Foraminifera were picked from superficial sediments (0-2 cm) collected from the harbour of Naples, in November 2004 (Figure 1). Because several sediments did not show a suitable number of specimens, a total of only 33 foraminifera samples was obtained, each of these containing an average of 20-25 individuals of *Ammonia tepida* not broken or reworked. All of samples were cleaned following procedures modified from Lea and Boyle [38] before chemical analysis performed by ICP-MS for Cd, Co, Cu, Mn, Ni, Pb, and Zn contents and by ICP-AES for Ca determinations. Details on collection and analytical methods (cleaning approach and ICP-MS and ICP-AES measurements) are reported in [39].

2.2 Diagenesis effects and suitability of cleaning procedures

When using trace elements in marine calcite as proxy for seawater composition, one has to assume that their content has not been modified by diagenetic processes. Although there are no irrefutable methods demonstrating that samples have not been altered, several lines of evidence suggest that diagenetic modification in the studied samples can be neglected relative to the analytical error associated to each measure. On the basis of intensive scanning elec-

Sample	Mn/Ca	Co/Ca	Ni/Ca	Cu/Ca	Zn/Ca	Cd/Ca	Pb/Ca
	µmol/mol	µmol/mol	µmol/mol	µmol/mol	µmol/mol	µmol/mol	µmol/mol
NO44	<dl	99,0	32,8	636,6	3000,9	14,6	320,3
NO62	**897,4**	222,3	2740,3	<dl	5778,6	23,0	210,2
NO77	166,1	39,7	465,6	3298,5	10900,0	8,6	71,9
NO82	210,1	877,1	10020,0	5300,0	20233,8	84,9	816,3
NO84	**3688,0**	68,2	1317,7	1673,6	97240,3	31,5	216,3
NO87	272,7	10,2	84,4	26,4	237,9	0,5	23,3
NO89	**2701,0**	32,3	399,8	248,1	2742,1	5,2	75,2
NO90	**706,2**	62,1	11791,8	5903,8	19424,7	34,6	329,0
NO91	95,7	<dl	137,6	<dl	364,3	1,1	28,2
NO94	101,7	48,8	197,6	<dl	2055,8	8,0	79,5
NO99	388,7	18,1	260,5	154,5	461,9	5,1	52,1
NO102	184,2	19,8	286,3	<dl	578,3	1,2	15,1
NO104	<dl	<dl	<dl	<dl	<dl	<dl	<dl
NO110	172,9	3,7	35,0	<dl	97,5	0,1	5,6
NO113	331,8	96,6	799,3	1864,1	2665,8	15,7	139,5
NO114	270,2	46,9	326,7	3869,7	8837,4	5,7	68,7
NO116	481,8	17,7	51,5	2211,6	1765,2	1,0	28,9
NO119	172,9	<dl	219,6	<dl	1556,9	<dl	35,7
NO122	247,0	7,8	43,8	26,8	154,9	0,5	12,4
NO124	127,9	93,0	968,3	205,1	1681,6	<dl	183,0
NO125	220,2	<dl	1147,0	<dl	2066,5	10,5	59,7
NO127	12,6	<dl	53,0	258,1	289,8	0,8	4,2
MMC2	103,4	6,6	31,1	<dl	168,9	0,5	10,1
MMC3	178,8	11,5	9,2	1,8	219,0	1,0	15,3
MMC4	163,1	34,6	2,5	<dl	751,7	4,0	41,0
MM C5	264,8	2,6	21,4	0,9	46,0	<dl	5,2
MM C6	46,0	70,7	<dl	2080,0	7089,3	9,3	95,8
MM C8	<dl	161,5	<dl	60,6	3902,2	22,1	198,5
MM C9	217,8	1,6	<dl	16,6	<dl	<dl	9,3
MM C10	231,5	<dl	38,0	<dl	417,0	<dl	4,4
MM C14	**2479,0**	<dl	<dl	<dl	<dl	<dl	57,5
MM C15	228,1	<dl	102,7	35,2	8,5	<dl	15,8
MM C16	0,1	<dl	<dl	<dl	<dl	<dl	<dl
Median		27,2	102,7	205,1	751,7	4,6	32,3
Mean		83,4	666,7	1179,2	2782,1	9,8	90,0
Standard deviation		191,7	2063,52	1649,7	4623,1	18,7	166,0
Non-outlier range		0.2-161.5	2.5-465.6	0.9-636.6	8.5-3902.2	0.1-101	4.2-198.5
I-III Quartile		7.8-101	38-286.3	60.6-636.6	168.9-2665.8	1.0-101	12.4-95.8

Table 1: Me/Ca ratio values measured in *A. tepida* shells.

tron microscope observations, performed on a total of 5 samples selected at random, all the picked foraminifera tests appeared substantially free of calcite overgrowths and re-crystallizations. In general, $(Mn/Ca)_{carb}$ ratios measured on the samples (Table 1) are in the range of variability of living foraminifera and/or specimens collected in sedimentary traps (e.g., [40, 8, 41, 22]). This again suggests a negligible influence of calcite overgrowths on the carbonate shells and the efficiency of the adopted cleaning procedures to limit the effects of trace element incorporation into Fe-Mn hydroxideoxide coatings. Samples with Mn/Ca ratios above 500 μmol$\cdot \mathrm{mol}^{-1}$ (highlighted in Table 1) were considered irremediably contaminated [42] and relative Me/Ca results were eliminated from the dataset. In brief, although we are not able to definitively exclude a potential contribution of diagenesis on the studied samples, several lines of evidence seem to bar a predominant control of secondary sedimentary processes on the trace element chemistry of the studied carbonate shells.

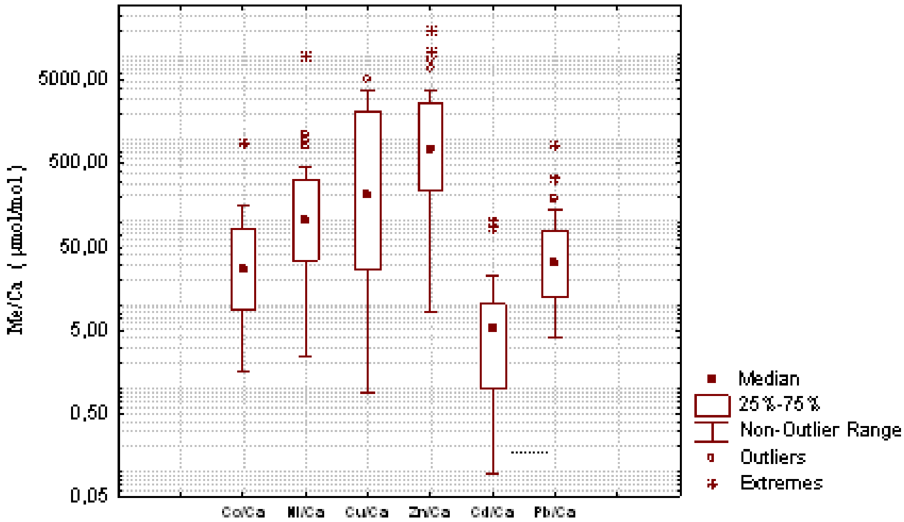

Figure 2: Basic statistics of the measured in the carbonate shells of *A. tepida*.

3 Results

Results of chemical analysis are reported as Me/Ca ratios in Table 1, while related basic statistics are synthetically presented in the Box-Wiskers plots of Figure 2. The largest "non-outlier ranges" of variability (about 3 orders of magnitude) were recorded for Zn/Ca (8.5–3902.2 μmol·mol^{-1}), Cu/Ca (0.9 - 636.6 μmol·mol^{-1}), and Cd/Ca (0.1–101 μmol·mol^{-1}) (Table 1, Figure 2). Median values measured for these Me/Ca ratios are 1–3 orders of magnitude greater than those measured in benthic foraminifera collected from unpolluted areas reported by other authors [43, 44] (Figure 2).

On the other hand, Pb/Ca (4.2–198.5 μmol·mol^{-1}), Co/Ca (0.2–161.5 μmol·mol^{-1}) and Ni/Ca (2.5–465.6 μmol·mol^{-1}) ratios showed a lower variability in concentration (Table 1, Figure 2). The correlation matrix calculated for non-outlier values shows statistically significant ($p < 0.05$) high correlation coefficients ($r > 0,65$) for Co/Ca, Cd/Ca, Pb/Ca and Zn/Ca while non-statistically significant correlation was calculated between metal/calcium ratios in the benthic foraminifera and trace element concentrations, pH, Eh, TOC, and grain size measured on the surface sediments of the same sampling points collected in the Naples harbour [39].

4 Discussion

The trace element concentrations measured in the carbonate shells of *A. tepida* collected from the surface sediments of the harbour of Naples offer a unprecedented opportunity to indirectly estimate the labile fraction (more bioavailable forms: free hydrated ions and/or labile bound complexes)

	Co/Ca	Cd/Ca	Pb/Ca	Zn/Ca	Ni/Ca	Cu/Ca
Co/Ca	1,00	**0,82**	**0,94**	**0,66**	**0,53**	0,11
Cd/Ca		1,00	**0,75**	**0,73**	**0,51**	-0,03
Pb/Ca			1,00	**0,75**	0,13	0,07
Zn/Ca				1,00	0,42	**0,48**
Ni/Ca					1,00	-0,10
Cu/Ca						1,00

Table 2: Correlation matrix calculated on non-outlier dataset. Marked correlation are significant at $p < 0.05$.

of total dissolved metals present in the seawater of a highly polluted marine coastal environment. By using the distribution coefficients values (DMe) reported for benthic foraminifera in the literature (DCu = 0.25 and DCd = 2.15 from [13]; DZn = 9 from [44]) we calculated the concentrations of the same total of dissolved elements in seawater using the equation:

$$Me_{seawater} = \frac{(Me/Ca)_{foram}}{D_{Me}} * Ca_{seawater}$$

where: $Me_{seawater}$ = concentration of total dissolved elements in seawater; Me/Ca_{foram} = element/Calcium ratio measured in the foraminifera shell; D_{Me} = calcite/seawater distribution coefficient; $Ca_{seawater}$ = Calcium concentration in seawater. Final estimates were carried out considering: i) a constant value of 10.4 mmol·l^{-1} for the highly conservative dissolved concentration of calcium in seawater [45]; ii) constant distribution coefficients for the trace elements in *A. tepida* over the detected wide range of metal concentrations and iii) substantially non-species dependent metal incorporation processes in benthic foraminifera shells.

Calculated values for non-outlier data of Cd, Cu and Zn (see [39] for the original dataset and Table 2 for basic statistic data) were generally 2- 4 orders of magnitude higher than those reported for unpolluted Mediterranean natural seawaters (e.g., [46, 47, 48, 49]). These data were then compared with data relative to polluted areas and results were as follows: i) Zn concentration in seawater of the Naples harbour is comparable to that reported from other polluted harbours of the Mediterranean area [50]; ii) Cd and Cu mean concentration values were 1- 2 and 1- 4 orders of magnitude higher than those reported from other anthropized areas (e.g., [23, 51]. This suggests a significant impact of anthropogenic activities, particularly related to the industrial and commercial sectors, currently present in the coastal area in front of the studied basin and in agreement with results reported for the same environment, from geochemical bulk sediment investigations, by Sprovieri et al. [37].

Cu, Cd, and Zn generally show high affinity for organic ligands. Their large bioavailability, indirectly calculated for the bottom waters of the Naples harbour using distribution coefficients, may be due to strong antropogenic input of these metals into seawater environment. In particular, when total dissolved concentration exceeds the content of the organic ligands present in solution speciation shifts towards forma-

tion of free ions and/or weak bound complexes in seawater [52].
The limited number and non-homogeneous spatial distribution of the studied samples did not allow us to statistically show a reliable distribution pattern for calculated Cu, Cd, and Zn concentrations in seawater. However, the evident high variability in metal concentration recorded in the studied environment can be reasonably associated to point-sources related to shipyard, industrial activities and urban wastewaters. In particular, washout of antifouling paints used for maintenance and re-generation of a huge number of vessels present in the harbour of Naples, as well as the intense tyre and line abrasion processes in rail and tramways present in the adjacent city centre of Naples may also be responsible for impulsive and delimited metal inputs to the seawater.
Verified absence of any statistically significant correlation among trace elements measured in foraminifera shells and in the superficial bottom sediments (see [37] for the original dataset), confirms the substantial lack of a direct control of the polluted sediments on the chemistry of biogenic carbonates, due to disoxic conditions present at the seawater-sediment interface [37].
Application of a conceptual box model to the coupled sediment-seawater system we tried to quantitatively calculate the potential effects of trace metals release from sediments to the seawater in oxide conditions. This exercise should provide a unreal (due to evident reducing conditions measured to the bottom of the studied system) end-member for release of heavy metals to the bottom seawaters from sediments. Assuming a thickness of about 2 cm of sediment involved in the potential release of trace metals to a $\sim$10 cm of overlying water column, and combining the total metal concentrations reported by Sprovieri et al. [37] for harbour sediments with sequential extraction data about more metal labile fraction reported by [36], was possible to calculate the amount of trace elements transferred from the sediments to the column water. Estimated values were about 1 to 2 order of magnitude higher than those deriving from our carbonate analysis, highlighting the important "trapping effect" played by the reduced sediments in the harbour of Naples. Of course, this does not exclude those events of sudden supply of oxygen at the bottom of the basin, induced by the high dynamicity of the harbour, that could induce rapid and short-term releases of heavy metals from sediments to the seawater.

5 Conclusions

In view of our findings the following conclusions can be drawn: 1) measurements of heavy elements on "cleaned" carbonates of the benthic foraminifera *A. tepida* from the sediments of the Naples harbour indicate high concentration values of the same metals (Cd, Cu, Zn) in dissolved phase, from 2 to 100 times higher than those measured in unpolluted Mediterranean seawaters; 2) a highly reduced sedimentary environment (with generally very low Eh values) and application of a conceptual box model exclude a significant release of heavy elements from the sediments to the seawater; 3) calculated total dissolved metal concentrations in seawater using available carbonate/water partition coefficients, were considered as semi-quantitative estimates (reasonably overestimated by using distribution coefficients relative to the total dissolved metal concentration) of free ion and/or labile forms of metals in seawater offering an unprecedented test of the reliability and usefulness of the carbonate chemistry of benthic foraminifera as monitors of potential bio-availability and toxicity of heavy metals in seawater.

Finally, for those elements for which distribution coefficients values are not available in the literature (in this study Co, Ni and Pb), we offer first order measurements and semi-quantitative information useful to plan investigations on theoretical distribution coefficients in the carbonate lattice and collection of simultaneous seawater and carbonate concentrations in highly contaminated and natural marine environments. This should provide new insights on the potential of these elements in the carbonate structure of biogenic calcite, for suitable and reliable monitoring of seawater contamination.

References

[1] J. Erez and B. Luz. Experimental paleotemperature equation for planktonic foraminifera. *Geochim. Cosmochim. Acta*, 47:1025–1031, 1983.

[2] M.L. Delaney, A.W. Bé, and E.A. Boyle. Li, Sr, Mg and Na in foraminiferal calcite shells from laboratory culture, sediment traps, and sediment cores. *Geochim. Cosmochim. Acta*, 49:1327–1341, 1985.

[3] D.W. Lea and H.J. Spero. Assessing the reliability of paleochemical tracers: Barium uptake in the shells of planktonic foraminifera. *Paleoceanography*, 9:445–452, 1994.

[4] A.D. Russell, S.R. Emerson, B.K. Nelson, J. Erez, and D. Lea. Uranium in foraminiferal calcite as a recorder of seawater uranium concentrations. *Geochim. Cosmochim. Acta*, 58(2):671–681, 1994.

[5] E.A. Boyle and L.D. Keigwin. Comparison of Atlantic and Pacific paleochemical records for the last 215000 years: changes in deep ocean circulation and chemical inventories. *Earth Planet Sci. Lett.*, 76:135–150, 1985/86.

[6] D.W. Lea and E.A. Boyle. Barium content of benthic foraminifera controlled by bottom water composition. *Nature*, 338:751–753, 1989.

[7] D.W. Hastings, S. Emerson, and A. Mix. Vanadium in foraminiferal calcite as a tracer for changes in the areal extent of reducing sediments. *Paleoceanogr.*, 11:665–678, 1996.

[8] D.W. Lea, T.A. Mashiotta, and H.J. Spero. Controls on Magnesium and Strontium Uptake in Planktonic Foraminifera Determined by Live Culturing. *Geochim. Cosmochim. Acta*, 63:2369–2379, 1999.

[9] R.D. Shannon. Revised effective ionic radii and systematic studies of interatomic distances in halides and chalcogenides. *Acta Crystallogr.*, 32:751–767, 1976.

[10] E.A. Boyle. Cadmium, zinc, copper and barium in foraminifera tests. *Earth Planet Sc Lett*, 53:11–35, 1981.

[11] G.T. Havach, A. Chandler, and Wilson-Finelli Shaw T.J. Experimental determination of trace element partition coefficients in cultured benthic foraminifera. *Geochim. Cosmochim. Acta*, 65:1277–1283, 2001.

[12] N. Maréchal-Abram, J.P. Debenay, H. Kitazato, and H. Wada. Cadmium partition coefficients of cultured benthic foraminifera Ammonia beccarii. *Geochem. J.*, 38:271– 283, 2004.

[13] L.J. de Nooijer, G.J. Reichart, A. Duenas-bohorquez, M. Wolthers, S.R. Ernst, P.R.D. Mason, and G.J. Van Der Zwaan. Copper incorporation in foraminiferal calcite: Results from culturing experiments. *Biogeosciences*, 4:961–991, 2007.

[14] K. Hester and E.A. Boyle. Water chemistry control of cadmium content in recent benthic foraminifera. *Nature*, 298:260–262, 1982.

[15] E.A. Boyle. Cadmium and δ13C paleochemical ocean distributions during the stage 2 glacial maximum. *Ann. Rev. Earth Planet Sci.*, 20:245–287, 1992.

[16] E.A. Boyle. Limits on Benthic Foraminiferal Chemical Analyses as Precise Measures of Environmental Properties. . *J. Foram. Res.*, 25:4–13, 1995.

[17] D. Nürnberg, J. Bijma, and C. Hemleben. Erratum to "Assessing the reliability of magnesium in foraminiferal calcite as a proxy for water mass temperatures". *Geochim. Cosmochim. Acta*, 60:803–814, 1996.

[18] Y. Rosenthal, E.A. Boyle, and N. Slowey. Temperature control on the incorporation of magnesium, strontium, fluorine, and cadmium into benthic foraminiferal shells from Little Bahama Bank: Prospects for thermocline paleoceanography. *Geochim. Cosmochim. Acta*, 61:3633–3643, 1997.

[19] H. Elderfield and G. Gansen. Past temperature and δ18O of surface ocean waters inferred from foraminiferal Mg/Ca ratios. *Nature*, 405:442–445, 2000.

[20] Y. Rosenthal and G.P. Lohmann. Accurate estimation of sea surface temperatures using dissolution-corrected calibration for Mg/Ca paleothermometry. *Paleoceanography*, 17:161–166, 2002.

[21] Y. Lear, C.H.and Rosenthal and N. Slowey. Benthic foraminiferal Mg/Ca-paleothermometry: A revised core-top calibration. *Geochim. Cosmochim. Acta*, 66:3375–3387, 2002.

[22] P. Anand, H. Elderfield, and M. Conte. Calibration of Mg/Ca thermometry in planktonic foraminifera from a sediment trap time series. *Paleoceanography*, 18(2):28–31, 2003.

[23] A. van Geen and S.N. Luoma. A record of estuarine water contamination from the Cd content of foraminiferal tests in San Francisco Bay, California. *Mar. Chem.*, 64:57–69, 1999.

[24] H. Elderfield, C.J. Bertram, and J. Erez. A biomineralization model for the incorporation of trace elements into foraminiferal calcium carbonate. *Earth Planet Sc. Lett.*, 142:409–423, 1996.

[25] F.M.M. Morel and J.G. Hering. Principles and Applications of Aquatic Chemistry. *A. Wiley-Interscience Publication, New York*, 1993.

[26] D. Munsel, U. Kramar, D. Dissard, G. Nehrke, Z. Berner, J. Bijma, G.J. Reichart, and T. Neumann. Heavy metal uptake in foraminiferal calcite: results of multi-element culture experiments. *Biogeosciences Discuss.*, 7:953–977, 2010.

[27] B. Elberling, K.L. Knudsen, P.H. Kristensen, and G. Asmund. Applying foraminiferal stratigraphy as a biomarker for heavy metal contamination and mining impact in a fiord in West Greenland. *Environ. Res.*, 55:235–256, 2003.

[28] I. Riba, E. Garcia-Luque, J. Blasco, and T.A. Del Valls. Bioavailability of heavy metals bound to estuarine sediments as a function of pH and salinity values. *Chem Spec Bioavailab*, 15:101–114, 2003.

[29] W. Ahlf and U. Forstner. Managing contaminated sediments. *J. Soil Sediment*, 1:1–7, 2001.

[30] M.J. Kennish. Ecology of Estuaries: Anthropogenic Effects. CRC Press Inc, Boca Raton 1992, FL, USA. 1992.

[31] V. Yanko, A. Arnold, and W. Parker. Effect of marine pollution on benthic foraminifera. In: Modern Foraminifera. Kluwer Academic Publishers, Dordrecht. page 217–235, 1999.

[32] R. Coccioni. Benthic foraminifera as bioindicators of heavy metal pollution: A case study from the Goro Lagoon (Italy). *In Environmental Micropaleontology. Kluwer Academic/Plenum Publishers, New York*, pages 71–103, 2000.

[33] D.B. Scott, F.S. Medioli, and C.T. Schafer. Monitoring of Coastal Environments Using Foraminifera and Thecamoebian Indicators. Cambridge University Press. page 176, 2001.

[34] L. Ferraro, M. Sprovieri, I. Alberico, F. Lirer, L. Prevedello, and E. Marsella. Benthic foraminifera and heavy metals distribution: A case study from the Naples Harbour (Tyrrhenian Sea, Southern Italy). *Environ. Pollut.*, 142:274–287, 2006.

[35] K.J.M. Kramer and J. Botterweg. Aquatic biological early warning system: an overview. In Jeffrey DW, Mudden, B. and editors. Bioindicators and Environmental Management. London: Accademic Press. pages 95–126, 1991.

[36] P. Adamo, M. Arienzo, M. Imperato, G. Naimo D, Nardi, and D. Stanzione. Distribution and partition of heavy metals in surface and sub-surface sediments of Naples city port. *Chemosphere*, 61:800–809, 2005.

[37] M. Sprovieri, M.L. Feo, L. Prevedello, D. Salvagio, S. Sammartino, S. Tamburrino, and E. Marsella. Heavy metals, polycyclic aromatic hydrocarbons and polychlorinated biphenyls in surface sediments of the Naples harbour (southern Italy). . *Chemosphere*, 67:998–1009, 2007.

[38] D.W. Lea and E.A. Boyle. Barium determination in foraminifera and corals by isotope dilution plasma mass spectrometry. *Chem. Geol.*, 103:73–84, 1993.

[39] P. Rumolo, D. Salvagio Manta, M. Sprovieri, R. Coccioni, L. Ferraro, and E. Marsella. Heavy metals in benthic foraminifera from the highly polluted sediments of the Naples harbour (Southern Tyrrhenian Sea, Italy). *Science of the Total Environment*, 407:5795–5802, 2009.

[40] T.A. Mashiotta, D.W. Lea, and H.J. Spero. Glacial- Interglacial changes in Subantartic sea surface temperature and d18O water using foraminiferal Mg. *Earth Planet Sc. Lett.*, 170:417–432, 1999.

[41] D.W. Lea, D.K. Pak, and H.J. Spero. Climate impact of late Quaternary equatorial Pacific sea surface temperature variations. *Science*, 289:1719–1724, 2000.

[42] P.A. Martin and D.W. Lea. A simple evaluation of cleaning procedures on fossil benthic foraminiferal Mg/Ca and Sr/Ca. *Geochem Geophys Geosyst*, 23:8401, 2002.

[43] D.W. Lea. Trace elements in foraminiferal calcite. In: Modern Foraminifera. Kluwer Academic Publishers: Great Britain. pages 259–257, 1999.

[44] T.M. Marchitto, W.B. Curry, and D.W. Oppo. Zinc concentrations in benthic foraminifera reflect sweater chemistry. *Paleoceanography*, 15:299–306, 2000.

[45] A.M. Shiller and J.M. Gieskes. Processes affecting the oceanic distribution of dissolved calcium and alkalinity. *J. Geophys. Res.*, 85:2719–2728, 1980.

[46] N.H. Morley and J.D. Burton. Dissolved trace metals in the northwestern Mediterranean Sea: spatial and temporal variations. *Water Pollution Research Report*, 28:279–92, 1991.

[47] N.H. Morley, J.D. Burton, Tankere S.P.C., and J.M. Martin. Distribution and behaviour of some dissolved trace metals in the western Mediterranean Sea. *Deep-Sea Res.*, 2:675–691, 1997.

[48] UNEP. Assessment of the state of pollution of the Mediterranean Sea by zinc, copper and their compounds. *MAP Technical Report Series*, 105, 1996.

[49] UNEP. Technical annexes to the report on the state of the marine environment. *UNEP Regional Seas Reports and Studies*, 114(1), 1990.

[50] M. Vega. Ecotoxicology and other issues for the Mediterranean Sea. *ERA*, 2002.

[51] R. Beiras, N. Fernández, J. Bellas, V. Besada, A. González-Quijano, and T. Nunes. Integrative assessment of marine pollution in Galician estuaries using sediment chemistry, mussel bioaccumulation, and embryo–larval toxicity bioassays. *Chemosphere*, 52:1209–1224, 2003.

[52] I.B. Velasquez, G.S. Jacinto, and F.S. Valera. The speciation of dissolved copper, cadmium and zinc in Manila Bay, Philippines. *Mar. Pollut. Bull.*, 45:210–217, 2002.

C Fluxes and the Role of Microbes in Marine Ecosystems: the Activity of the Water Research Institute (IRSA-CNR)

A. Puddu, S. Amalfitano, S. Capri, S. Fazi, L. Patrolecco, M. Pettine, A. Zoppini
Water Research Institute, CNR, Montelibretti (RM), Italy
puddu@irsa.cnr.it

Abstract

The Water Research Institute (IRSA) has expertise in different fields including water resource management, water treatment and water quality, the latter regarding aquatic ecosystem functioning and response to anthropogenic impacts.
Since the 90's IRSA researchers have been investigating microbial communities and C cycling in marine ecosystems, the main activities aimed to describe the origin, the distribution and the fate of organic matter in coastal ecosystems affected by allochtonous inputs. The phenomenon of mucilage occurrence has been also investigated describing the mineralization processes mediated by microbial communities and the bioavailability of algal excreta involved in the formation of aggregates.
Recently, IRSA has been involved in research studies dealing with climate change. In this framework, the role of the IRSA Microbial Ecology group is to contribute to the understanding of CO_2 flux in the seawater column mediated by biological processes.

1 The rationale of the research activity

1.1 Seawater: CO_2 sink or source

Factors controlling organic matter production and consumption processes affect the biogeochemical cycling of carbon in the oceans and the efficiency of the "biological pumping" of carbon out of the euphotic zone [1].
Conceptual models of atmospheric C cycle often consider the aquatic ecosystems as a sink for CO_2 due to its fixation by primary producers. Nevertheless the net flux of CO_2 between the atmosphere and the ocean is mostly controlled by the balance among three key processes: C uptake by phytoplankton photosynthesis, C mineralization back to CO_2 (community respiration) and the C export toward the ocean depths.
Phytoplankton is responsible for roughly half of the CO_2 fixation on Earth [2] and at least 50% of fixed C is channeled through the microbial food web in the dissolved phase [3]. Heterotrophic bacteria in pelagic ecosystems mediate a significant conversion of Dissolved Organic Carbon (DOC) into Particulate Organic Carbon (POC) which is then transferred to the food web. The bacterial efficiency in the use of the DOC pool is of critical importance in cycling organic C and in the regen-

eration of inorganic nutrients. Only a small fraction of this organic matter is buried in marine sediments, being the bulk of the produced organic matter re-mineralized through respiration [4]. As a consequence, the oceans can act as net source or sink of carbon depending on the production or decomposition of organic matter due to biological activities. Recent findings emphasize that coastal and marginal seas contribute to the global carbon budget significantly more than what expected from their surface area enhancing the ocean storage of anthropogenic CO_2 [5].
Moreover, several recent comparative studies have suggested that respiration may systematically exceed production in large areas of the oceans [6, 7, 8] as well in estuaries [9]. On the contrary, results from Williams and Bowers [10] showed that the open ocean is in metabolic balance. These conflicting conclusions mainly derive from the inadequacy of the data sets and data analysis.

1.2 Dissolved organic matter as source of energy for the microbial food web

The Dissolved Organic Matter (DOM) in the oceans is one of the largest reservoir of organic carbon at the Earth surface. This carbon pool behaves as a dynamic component in the interaction between geosphere, hydrosphere, and biosphere and as such has the potential to influence the global carbon cycle and climatic changes [11].
A large portion of the DOM pool consists of refractory compounds. The identification of these compounds and the understanding of processes which control their presence are still open questions since less than 30% of organic matter has been characterized at a molecular level ([12] and references therein).
In the recent years, studies on sources, distribution and fate of DOM, involving its strong interrelationships with biological activities, have received a prioritary attention [13].
The major source of DOM in marine ecosystem is the in-situ phytoplanktonic production while terrestrial sources contribute for about 10% to total seawater DOM on global scale [14].
The dissolved carbon fluxes in the ocean follow the sequence: DOM, bacteria, protozoa, metazoa. The importance of bacteria and protozoa, first argued by Pomeroy in 1974, has been stressed by the introduction of the microbial food loop theory [15] according to which bacteria are exploited by protozoa that are in turn exploited by ciliates. The grazing activity is accompanied by excretion of substances which are in turn used by the bacteria, so that the system operates in a semi-closed circuit.
Carbon flowing through bacterial compartment is highly variable both quantitatively and qualitatively, depending on the capacity of the resident bacterial assemblage to uptake the specific DOM. It may range from 0 to $>$100% of the local primary production [16]. The microbial food web predominates in stratified waters where the exudates from phototrophic picoplankton are not dispersed and can therefore be used by heterotrophic bacteria.
The availability of DOM to heterotrophic bacteria likely depends on the qualitative characteristics of the organic substrate (i.e. biochemical composition and molecular size), but it is also strongly influenced by the availability of inorganic nutrients. Therefore, in carbon rich marine areas, improving the qualitative and quantitative characterization of the DOM pool

is a priority step for a better understanding of the microbial food-web and the evaluation of modes of organic carbon transfer among the dissolved, colloidal and particulate pools.

According to a number of studies and modeling exercises, the microbial food web constitutes a sink for biogenic carbon since most of the autotrophic production would be processed under these conditions by microorganisms. As a consequence, biogenic carbon tends to be oxidized (respired) within the microbial loop in the euphotic layer rather than being exported in the form of metabolic energy to higher-order consumers, or in the form of particle fall-out to deep waters. Recently, Williams [17], reporting some results from the Plymouth Marine Laboratory (C. Turley), has stressed the importance of the microbial food web in reducing fish production in the eastern Mediterranean, where bacteria process 85% of the phytoplankton production.

1.3 Aggregation phenomena and its impact on C-flux

Marine aggregates represent a buildup of suspended organic and inorganic material entrapped in a polymeric network inside which microorganisms, both auto- and heretotrophic, may live and actively reproduce. Aggregates have recently received much attention because of their importance in the export of organic matter to the ocean interior. Aggregates with sizes from 0.5 mm to a few cm are defined as "marine snow", and may occur in all the marine environments. Particles greater than a few micron are transported to bacterial cells by collision in turbulent shear. Aggregation not only brings larger colloids into regimes dominated by turbulent shear, it also brings them into close contact with bacterial cells [18] that need only to expend energy for exoenzyme production to gain access to these substrates. Biological activities inside the flock can influence the enlargement, the buoyancy and the aging of aggregates.

A new class of gel-like mucilaginous particles, called TEP (transparent exopolymer particles), was discovered to be abundant in the ocean and their importance as major factors triggering aggregation phenomena and marine snow formation in the case of diatoms was demonstrated [19].

Azam and collaborators, based on their observations of a preferential regeneration of N and P relative to C in the marine aggregates, proposed a central role of bacteria living in the aggregates in the accumulation of DOC [20]. The extremely high alkaline phosphatase activity measured in the aggregates would cause very rapid P turnover able to support a prolonged high level of primary production. The preferential N and P regeneration relative to C causes an increasing in the C/N and C/P ratios in aged aggregates where slow-to-degrade polysaccharides tends to be enriched.

Chin et al. [21] proved that marine polymer gels can assemble from free DOM polimers, and that their formation mechanism, physical characteristics and mineralization can be understood in term of polymer gel theory. The principles and methods of polymer gel physic thus have the potential to provide profound new insights into processes controlling the exchange between the DOM and POM pools and the cycling of marine organic carbon.

Direct observations of the evolution over time and space of marine aggregates showed high variability in concentrations and sizes. Ruiz [22] explained the short time scale (hours) dynamics in aggregate concentration as due to dial variation in turbulence, while the effects of phytoplankton populations and grazers on the aggregates composition may be noted on a longer time scale.

2 IRSA research activity and major results achieved

Following the experience gained in previous years on coastal eutrophication, in the period 1990-1992 a research program on microalgae activity and trophic status was conducted in the central Adriatic Sea in collaboration with the ISMAR of Ancona [23].

Nutrients and microplankton standing crop over a 2-year period and primary production rates over a 1-year period were measured at three stations located 1.5, 6 and 15 nautical miles (NM) from the coast, about 100 NM south of the Po river mouth. Both nutrients and standing crop showed a concentration gradient from West to East with marked changes of average values from 6 to 15 NM off the coast. Nutrients and standing crop appeared to be positively correlated and both showed an inverse dependence on salinity which was mainly influenced by freshwater inputs from the major Italian river, the Po river. Primary production rates (PP) showed values of about 260 and 210 $\mathrm{g{\cdot}C \cdot m^{-2} \cdot year^{-1}}$ at the 1.5 and 6 NM stations respectively, indicating the presence of a narrow coastal belt characterized by productivity levels significantly higher than those previously reported for other Adriatic areas affected by the Po. The offshore station (15 NM) showed an average annual production of about 120 $\mathrm{g{\cdot}C \cdot m^{-2} \cdot year^{-1}}$ which lies in the range reported for lagoons and coastal waters in the Po delta area. The photosynthetic efficiency (PP/Chlorophyll a) was similar at the 1.5 and 6 NM stations but significantly lower at the 15 NM station. This difference reflected either different nutrient levels in inshore and offshore stations or different structures in phytoplankton community: diatoms and phytoflagellates prevailed at 1.5 and 15 NM, respectively. Photosynthetic efficiency increased with increasing concentration of nutrients. The relation was linear as a function of total dissolved phosphorus, and hyperbolic as a function of total dissolved nitrogen. This different dependence suggested a surplus of nitrogen with respect to phosphorus for photosynthetic processes, which is consistent with the assumption of phosphorus as limiting element for the northern Adriatic.

In the Adriatic Sea the first evaluation of in-situ bacterial production was carried out by IRSA in the framework of the national research program PRISMA1, which was funded by the Italian Government (MURST) to inquire into environmental problems in the Adriatic Sea. The seasonal and spatial distribution of bacterial production and biomass along a salinity gradient was investigated in the area surrounding the Po river mouth during the first phase of the project. Experimental activities were carried out along with IAMC (Istituto per l'Ambiente Marino Costiero) and Istituto Zooprofilattico Umbria e Marche and related results were published by Puddu et al. [24]. Bacterial C production as ^3H-thymidine incorporation, bacterial abundance as DAPI direct count, autotrophic biomass as chlorophyll *a* and total biomass as ATP, from three areas in the Northern Adriatic Sea, were analyzed. The three sites, differently influenced by riverine discharges, were sampled seasonally over two

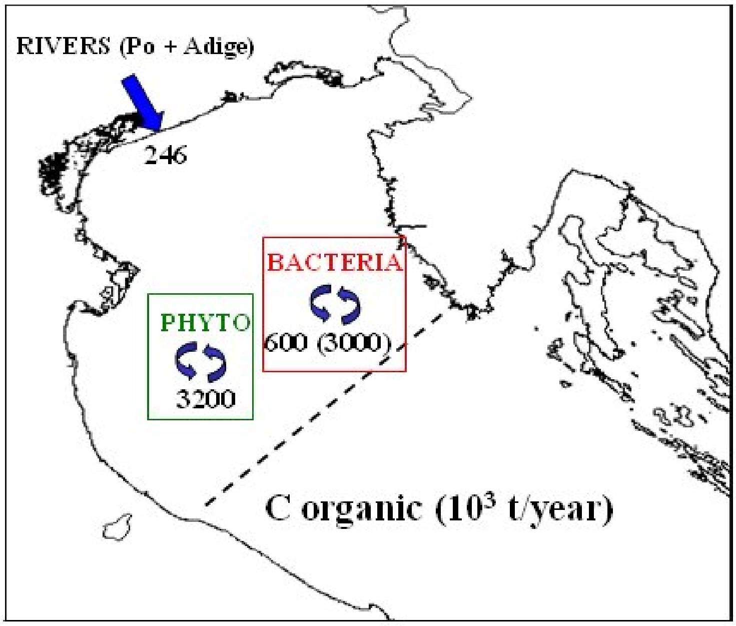

Figure 1: Estimate of C fixed by phytoplankton and incorporated by bacteria in the Northern Adriatic (PRISMA1 project). In bracket the bacterial C demand.

days, in four surveys from April 1995 to January 1996. BCP, strongly correlated with primary production, was extremely high near the coast in low-salinity, high-nutrient waters. Such high values of BCP reflected an increase in phytoplankton production that was stimulated by the inputs of riverine nutrients. In the warm months bacterial activity was higher than in cold months. While bacteria abundance did not appear to be related to the salinity gradient, bacterial production (from 0.6 to 372 pM ^{3}H-thymidine h^{-1} incorporated, corresponding to 0.01-8.2 μg $Cl^{-1}h^{-1}$) and the related generation times (from 0.2 to 35 days) showed a high range of values from estuaries to the ocean. The resulting role of the bacterial community in the carbon cycle appeared to be very consistent, processing amounts of carbon which were estimated as high as 80% and 260% of those synthesized by autotrophs in summer and winter, respectively.

The results obtained from the PRISMA1 project, allowed a tentative estimation of C cycling through the microplanktonic compartment in the Northern Adriatic Sea (Figure 1).

Bacterial utilization of different size classes of DOC and demand for inorganic nutrients in the Northern Adriatic Sea was investigated by Zoppini et al. [25]. The aims were to highlight factors controlling the carbon cycling and triggering mechanisms favouring the persistence and colloidal aggregation of DOM in this area. DOC classes were separated using a cascade ultrafiltration system (1 and 10 kDa

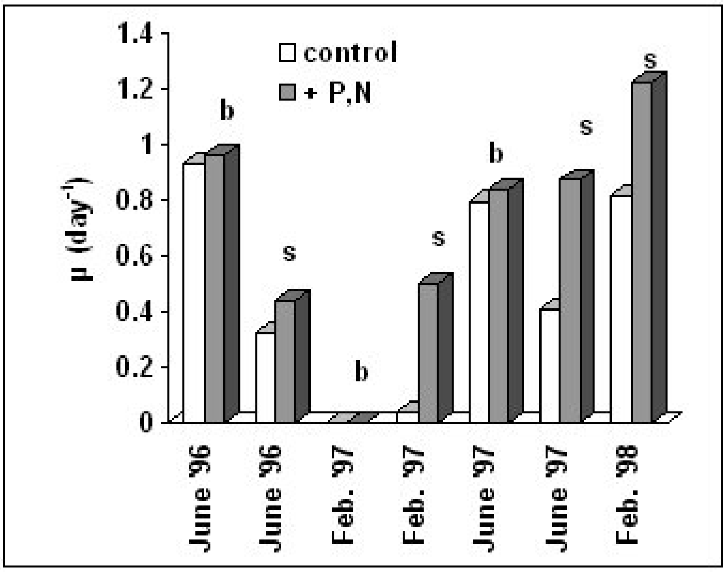

Figure 2: Bacterial growth rates on surface (s) and bottom (b) sea water samples untreated (control) or amended with inorganic P and N (+P,N) - PRISMA2 project.

molecular weight cutoff). In all the experiments the lowest bacterial growth efficiency and DOC utilization rates were observed in samples containing the high molecular weight fraction (1-10 kDa). The latter molecular fraction seemed to cycle slower when compared to the very high (>10 kDa) and low molecular weight fractions (<1 kDa). Nutrient addition (P+N) to bacterial cultures increased DOC utilization rates suggesting a nutritional limitation. The Authors suggested that a prioritary attention should be devoted to the high molecular weight fraction of DOC that showed the lowest bioavailability and gave the highest contribution to the overall DOC pool in this area. These findings highlighted the necessity of further studies to individuate the factors limiting bacterial C uptake and improve the knowledge on the chemical composition of the various DOC size fractions.

Accordingly, the dynamics of DOM in the Northern Adriatic Sea waters and mucilaginous aggregates were intensively investigated during the second phase of the PRISMA project, named PRISMA2 ([26] and [27]). In the framework of this project, the relationships between organic matter composition and heterotrophic activity were investigated. The sampling included four surveys (June 1996, February 1997, June 1997 and February 1998). Samples were collected in two frontal regions, one in the north under the direct influence of the Po River and the other in the south, close to the border-line between the northern and the middle Adriatic.

The overall set of data ranged from 53 to 281 μM for DOC, 44 to 98 μM for

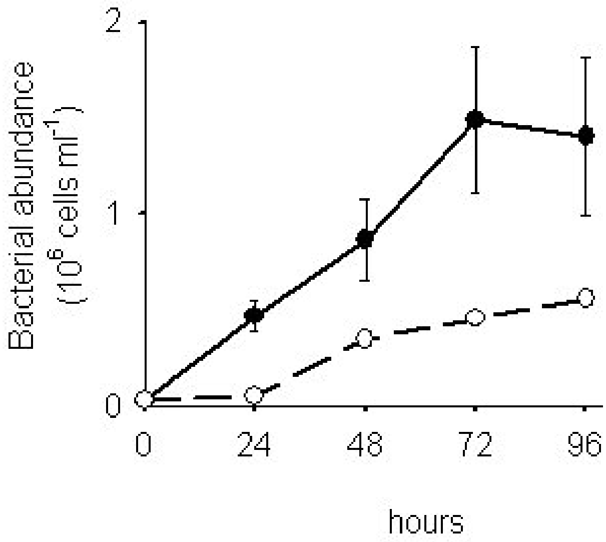

Figure 3: Bacterial growth in exudates from *C. closterium* cultured in P-balanced (•) and P-depleted (○) conditions (MAT project).

colloidal organic carbon (COC), 6 to 72 μM for total dissolved carbohydrates (TDCHO-C), 0.1 to 2.4 μM for free amino acids (DFAA-C), 1.2 to 9.4 μM for total dissolved amino acids (TDAA-C) and 0.01 to 7.1 μg C $l^{-1}h^{-1}$ for BCP. COC and TDCHO data showed tight relationships with DOC values, which were in turn negatively dependent on salinity. DOC showed increases of 76$\pm$10 μM in surface waters with respect to the background value. Seasonal changes were dependent on the riverine discharge curve and related to the trophic dynamics. The most marked increases were observed in June 1996 and, based on average values, amounted to 104 and 62 μM DOC in the north and south frontal regions, respectively; in the following June 1997, the corresponding increases were 47 and 20 μM. COC concentrations gave a high contribution to DOC and showed a large fraction of the high molecular weight compounds. Contrary to the increases in DOC and COC concentrations, which were stronger in 1996 than 1997, mucous macroaggregates showed a much stronger occurrence in June 1997 compared to the June 1996 survey. Considering that the aggregation of colloids is one of the main processes leading to the formation of macroaggregates, the different behaviour of DOC seasonal changes and mucilage occurrences in the two years may suggest that the qualitative characteristics of the DOC and COC pools are probably more important than their quantitative concentrations in controlling the partitioning between dissolved and aggregate matter.

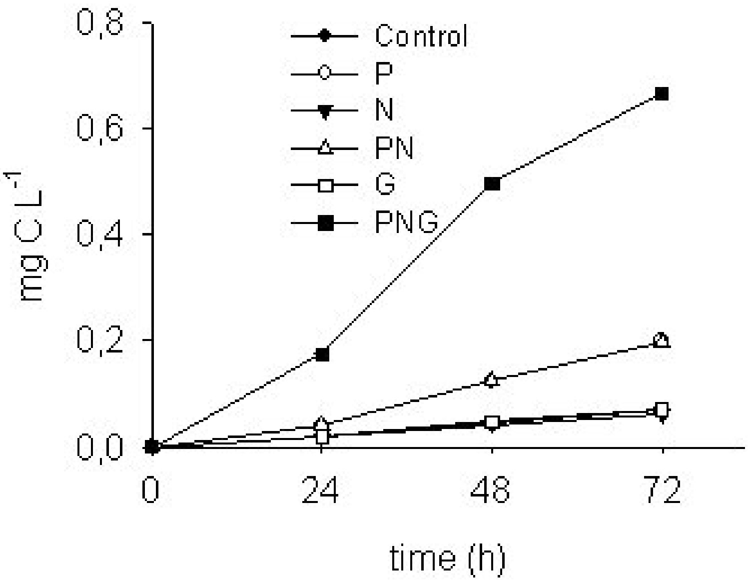

Figure 4: Cumulative bacterial production after enrichments of seawater from macroflocs (P=phosphorus; N=nitrogen; G=glucose) – MAT project.

Bacterial production rates showed a large variability during the study period, which reflected concentration gradients of inorganic and organic nutrients and different nutrient limitations. Bioassays carried out on samples collected in different seasons and at various salinities suggested an apparent strong limitation of the bacterial activity by phosphorous.

Further results were reported by Pettine et al. [28], concerning specifically dissolved and colloidal organic carbon, free amino acids, total dissolved carbohydrates and heterotrophic activity. Main factors controlling organic matter degradation were also studied by laboratory tests. Dissolved organic matter showed seasonal accumulation, which was markedly different from year to year, and large contributions by colloidal and saccharide components. Heterotrophic activities were found to play an important role in the carbon cycle and laboratory runs highlighted that limitations caused by the aging of organic matter, other than phosphorus deficiency, affected degradation rates (Figure 2).

In the frame of MAT Project (2001-2003), funded by the Italian Ministry of the Environment, IRSA research activity contributed to investigate the mucilage phenomenon occurring in those years in both the Adriatic and the Tyrrhenian seas. This

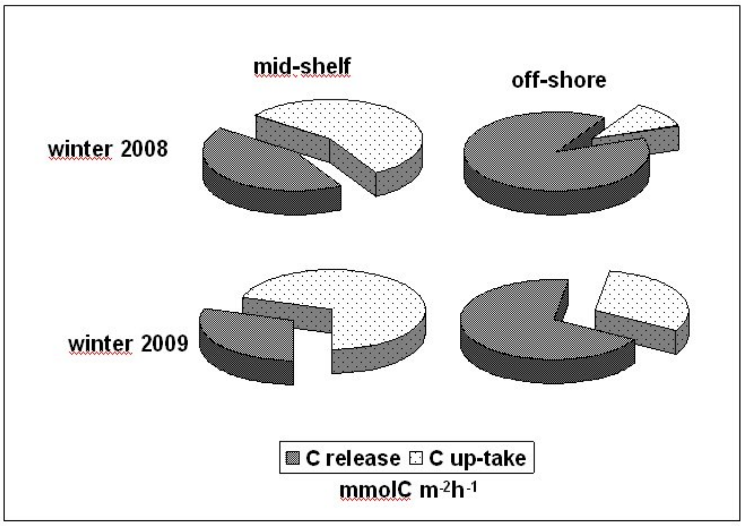

Figure 5: Comparison of depth-integrated C up-take, by primary productivity, and C release, by community respiration, in two consecutive winter seasons in the mid-shelf and in the off-shore station in the Cilician basin (SESAME project).

challenge was faced conducting a two fold laboratory activity to understand the role of P limitation either on the bacterial uptake of photosynthetic extracellular products or on the bacterial degradation of different types of mucilaginous aggregates sampled in the Adriatic Sea.
Laboratory experiments on bioavailability of algal excreta were conducted utilizing the diatom species *Cylindrotheca closterium* grown in P-balanced and P-depleted media [29]. Excreted organic carbon produced during the exponential growth phase was inoculated by a grazer-free marine bacterial community. The growth and the structure of the bacterioplankton community were monitored in short term cultures (Figure 3). Estimates of bacterial abundance, production and mineralization rates were performed every 24 hours for four days. Fluorescent in-situ hybridization (FISH) and cytometric (apparent DNA content) techniques were applied to investigate the community structure.
Bacterial carbon demand and specific growth rates were significantly lower in the excreta from P-depleted algae (30% and 24% reduction, respectively).
The origin of the excreta appeared also to affect the taxonomic composition of the bacterioplankton assemblage, mainly reducing the development of gamma-proteobacteria.
By extrapolating these results to the natural environment, we might expect that under P-limited conditions some phytoplankton species release DOM with refractory properties, slowing down the bacterial uptake. The presence in the water column of long lived organic compounds, released from P-starved algal cells, could represent an additional factor affecting the DOM cycle

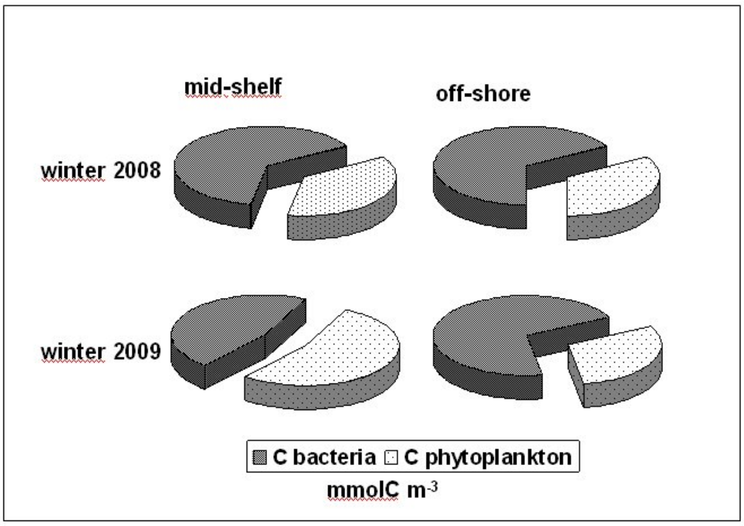

Figure 6: Comparison of phytoplankton and bacterial biomass, expressed as C content, in two consecutive winter seasons in the mid-shelf and in the off-shore station in the Cilician basin (SESAME project).

in the Northern Adriatic Sea where high N:P ratios have been observed all over the year.

Results on bacterial degradation of mucilaginous aggregates collected during two summer events (2001-2002) in the Adriatic Sea within the above MAT project have been reported in Zoppini et al. [30]. The objective was to describe the microbial metabolism on the aggregates, especially regarding hydrolyzing activities, focusing on the age and composition of flocs. Mucilaginous aggregates that were collected in the Northern Adriatic Sea had a variety of specific configurations, from creamy layers to stringers and macroflocs. This study confirmed that macroflocs represent the first macroscopic form of mucus material that under appropriate conditions develop in stringers and clouds.

In the native aggregates, the proteins and the organic phosphorous were actively hydrolyzed as aminopeptidase and alkaline phosphatase activities represented up to 87 and 25% of total activity respectively. Polysaccharides were less hydrolyzed and the highest activities were observed for beta-glucosidase (5% of the total). This hydrolyzing pattern tends to a progressive accumulation of long persistent polysaccharides.

During short term incubations nutrient addition (P, N and Glucose) differently stimulated bacterial growth in the seawater from aggregates: P played the main role in stimulating bacterial production from 3 to 6 folds higher than in the control, whereas a secondary C-limitation was observed only for bacteria growing on seawater from macroflocs (Figure 4).

The scarce DOC bioavailability was confirmed by the lower DOC removal (13%

macroflocs, 36% stringers). The total amount of carbon incorporated by bacteria living on aggregates was similar (0.58 mg C L^{-1}) both in the control and under P enrichments showing a more balanced condition with respect to the seawater. Hence the well-known P limitation in the Northern Adriatic Sea appeared to affect only dissolved organic carbon uptake without influencing the uptake of aggregated organic matter.

Organic matter limitation was observed only on stringers on which total C incorporated raised to 0.96 mg C L^{-1} after PNG addition. Macroflocs release of refractory compounds led to DOC accumulation (73 μM DOC) contributing to inflate the pool of refractory DOC in the surrounding waters. Several evidences, including different monosaccharide composition of stringers and macroflocs (glucose 15 and 56 % on stringers and macroflocs, respectively), brought to the conclusion that stringers were in an older stage in comparison with macroflocs. Community composition described by fluorescence in situ hybridization did not show significant differences between free-living and attached bacteria but it was modified by the different enrichment conditions: Cytophaga-Flavobacteria prevailed after inorganic nutrients enrichments while organics advantaged gamma-Proteobacteria.

In conclusion, the mucilage environment seemed to constitute a kind of "self-sustaining" system where bacteria feed on internal sources (i.e. living or dead organisms entrapped in the matrix). Actually the mucilage matrix itself represents an exhausted source of food for bacteria (see C-limitation in the aged aggregates), and tends to persist in the environment at least over a time scale of several weeks.

Research activities on CO_2 fluxes have been developed in the framework of the European Integrated Project SESAME (Southern European Seas: Assessing and Modelling Ecosystem changes, FP6 2006-2010) and, at national level, by a "curiosity driven" project funded by CNR.

Experimental activities in both the above projects have the aim to describe and quantify the carbon uptake and release by water column processes.

In SESAME the study area was the Cilician basin, in the Eastern Mediterranean, considered one of the most oligotrophic regions in the world in terms of both primary productivity and autotrophic biomass. This oligotrophic character is related to the eastward increase in P limitation in the Mediterranean Sea.

The specific aim was to enhance the understanding of mechanisms for cycling, export and sequestration of C at sub-basin scale, with respect to biological processes involved in C fixation and mineralization. Information on C cycling are not available for the Cilician basin and are limited for the Adriatic Sea. Data provided by IRSA activities within SESAME along with those obtained by SESAME Partners in other Mediterranean areas, will contribute to define the behavior of different regions of the Mediterranean as CO_2 sink or source.

The field activity within the SESAME project concluded in February 2009. Results obtained on C-fluxes mediated by microbial communities (Figure 5) show a prevalence of mineralization processes in the off-shore station.

A further interesting result derived from the comparison of heterotrophic and autothrophic microplanktonic biomasses (Figure 6) showing that in this oligotrophic system microbial biomass was mainly dominated by bacteria.

The CNR funded project is still ongoing, in collaboration between IRSA and ISMAR (Venezia), and field activities on board of n/o Dalla Porta concluded on November 2009. The study area is the central Adriatic Sea, characterized by strong trophic gradients from the coast to the central basin due to the variable effect of inland waters.

Results will allow to estimate sink and source of CO_2 due to biological processes in relation to the physico-chemical water masses characteristics and the planktonic chain structure. Information obtained in both the above projects will implement the knowledge on CO_2 circulation at global scale.

References

[1] U. Riebesell, K.G. Schulz, R.G.J. Bellerby, M. Botros, , et al. Enhanced biological carbon consumption in a high CO_2 ocean. *Nature*, 450:545–548, 2007.

[2] M.J. Berhenfeld and P.G. Falkowski. Photosynthetic rates derived from satellite-based chlorophyll concentration. *Limnology Oceanography*, 42(1):1–20, 1997.

[3] H.W. Ducklow and C.A. Carlson. Oceanic bacterial production, in "Advances in Microbial Ecology". 12:113–181, 1992.

[4] H.W. Ducklow. Ocean biogeochemical fluxes: New production and export of organic matter from the upper ocean. *Rev. Geophys. Suppl.*, pages 1271–1276, 1995.

[5] H. Thomas, Y. Bozec, K. Elkalay, and J.W. De Baar. Enhanced open ocean storage of CO2 from shelf sea pumping. *Science*, 304:1005–1008, 2004.

[6] P.A. Del Giorgio, J.J. Cole, and A. Cimbleris. Respiration rates in bacteria exceed phytoplankton production in unproductive aquatic systems. *Nature*, 385:148–151, 1997.

[7] C.M. Duarte and S. Agusti. The CO_2 balance of unproductive aquatic ecosystems. Science. *Science*, 281:234–236, 1998.

[8] C.M. Duarte, S. Agusti, J. Aristegui, N. Gonzales, and R. Anadon. Evidence for a heterotrophic subtropical northeast Atlantic. *Limnology Oceanography*, 46(2):425–428, 2001.

[9] K. Preen and D.L. Kirchman. Microbial respiration and production in the Delaware Estuary. *Aquatic Microbial Ecology*, 37:109–119, 2004.

[10] P.J. le B. Williams and D.G. Bowers. Regional carbon imbalance in the oceans. *Science*, 284:1735b, 1999.

[11] J. Farrington. Overview and key recommendations. Marine organic geochemistry workshop. *Marine Chemistry*, (39):5–9, 1992.

[12] S.P. Seitzinger, H. Hartnett, R. Lauck, M. Mazurek, et al. Molecular-level chemical characterization and bioavailability of dissolved organic matter in stream water using electrospray-ionization mass spectrometry. *Limnology Oceanography*, 50:1–32, 2005.

[13] A. Puddu, A. Zoppini, and M. Pettine. Dissolved organic matter and microbial food web interactions in the marine environment: the case of the Adriatic Sea. *International Journal of Environment and Pollution*, 13(1-6):473–494, 2000.

[14] K.J. Meyers-Schultz and J.I. Hedges. Molecular evidence for a terrestrial component of organic matter dissolved in seawater. *Nature*, 321:61–63, 1986.

[15] F. Azam, T. Fenchel, J.G. Field, J.S. Gray, et al. The ecological role of water-column microbes in the sea. *Marine Ecology Progress Series*, 10:257–263, 1983.

[16] L.R. Pomeroy, W.J. Wiebe, D. Deibel, R.J. Thompson, et al. Bacterial responses to temperature and substrate concentration during the Newfouland spring bloom. *Marine Ecology Progress Series*, 75:143–159, 1991.

[17] N. Williams. The Mediterranean Beckons to Europe's oceanographers. *Science*, 279:483–484, 1998.

[18] P.E. Kepkay and B.D. Johnson. Coagulation on bubbles allows the microbial respiration of oceanic dissolved organic carbon. *Nature*, 385:63–65, 1989.

[19] A.L. Alldredge, U. Passow, and B. Logan. The existence, abundance, and significance of large transparent exopolymer particles in the oceans. *Deep Sea Research*, 40:1131–1140, 1993.

[20] D.C. Smith, M. Simon, A.L. Alldredge, and F. Azam. Intense hydrolitic enzyme activity on marine aggregates and implications for rapid particle dissolution. *Nature*, 359:139–142, 1992.

[21] W.C. Chin, M.V. Orellana, and P. Verdugo. Spontaneous assembly of marine dissolved organic matter into polymer gels. *Nature*, 391:568–572, 1998.

[22] J. Ruiz. What generates daily cycles of marine snow? *Deep-Sea Research*, 44(7):1105–1126, 1997.

[23] A. Zoppini, M. Pettine, C. Totti, A. Puddu, et al. Nutrients, standing crop and primary production in western coastal waters of the Adriatic sea. *Estuarine Coastal and Shelf Science*, 41:493–513, 1995.

[24] A. Puddu, R. La Ferla, A. Allegra, C. Bacci, et al. Seasonal and spatial distribution of bacterial production and biomass along a salinity gradient (Northern Adriatic Sea). *Hydrobiologia*, 363:271–282, 1998.

[25] A. Zoppini, C. Bacci, S. Fazi, M. Pettine, and V. Tandoi. Bacterial utilization of different DOC size classes and demand for inorganic nutrients in the northern Adriatic sea. *Fresenius Environmental Bulletin*, 7:42–50, 1998.

[26] M. Pettine, L. Patrolecco, M. Manganelli, S. Capri, and M.G. Farrace. Seasonal variations of dissolved organic matter in the Northern Adriatic Sea. *Marine Chemistry*, 64:153–169, 1999.

[27] M. Pettine, S. Capri, M. Manganelli, L. Patrolecco, et al. The dynamics of DOM in the northern Adriatic sea. *Estuarine and Coastal Shelf Science*, 52:471–489, 2001.

[28] M. Pettine, S. Capri, M.G. Farrace, M. Manganelli, et al. Variability of dissolved organic matter in northern Adriatic coastal waters. *Chemistry and Ecology*, 18:13–25, 2002.

[29] A. Puddu, A. Zoppini, S. Fazi, M. Rosati, et al. Bacterial uptake of DOM released from P-limited phytoplankton. *FEMS Microbiology Ecology*, 46:257–268, 2003.

[30] A. Zoppini, A. Puddu, S. Fazi, M. Rosati, and P. Sist. Extracellular enzyme activity and dynamics of bacterial community in mucilaginous aggregates of the northern Adriatic Sea. *Science of the Total Environment*, 353:270–286, 2005.

The Application of a Mathematical Model to the Coastal Evolution at the Archaeological Site of Egnathia (Apulia, Southern Italy)

R. Pagliarulo[1], G.M. Gentile[2]
1, Research Institute for Geo-Hydrological Protection, CNR, Bari, Italy
2, Department of Civil and Environmental Engineering, Polytechnic of Bari, Italy
r.pagliarulo@ba.irpi.cnr.it

Abstract

This paper describes an original numerical model based on the energy flux applied by the wave motion to the coastline where the archaeological site of Egnathia (Apulian Adriatic coast) is located. The remnants of the ancient port are actually submerged. The program "Perfect Storm" uses the flux energy applied by the wind-induced wave actions to the shorelines. Sea storms occurred in the range 1951-2000 have been considered. The program allows to define, in consecutive steps, the model of energy obtained by each breaker wave to the shoreline The correlation among the model results, the geological set up, the amount of sediments moved by wave actions and currents, particularly during storms, and the chronological data of the archaeological structures allow the reconstruction of the morphological evolution of the area facing the ancient site. The amount of sediment transported is related to the climate conditions. The erosional and depositional phases have greatly controlled the geomorphological changes of the coastline and, as a consequence, also the town-planning choices during the life of the ancient town.

1 Introduction

The archaeological sites where ancient ruins are present both submerged, such as the case examined in this paper, and emerged like docks and harbours, are special markers. They provide a more precise chronological correlation with the events and play a remarkable role in understanding the coastal morphodynamics and sea level changes [1]. These structures can be considered real archaeo- geodetic benchmarks giving a basic contribution to the researches on eustatic changes and, indirectly, on palaeoclimatology [2]. During glacial and interglacial periods, sea level has changed due to astronomic, climatic and biological causes. In coastal morphodynamic the climatic changes have a main role also in the balance between sea and land; that is the destructive and constructive processes caused by sea actions. Battering waves tear apart coastal rocks, grind them down with their abrasive tools of gravel and sand, and, with longshore currents, carry the sediments away. Also streams provide sediments, so landforms along shorelines take shape by tearing down as well as by building up. These phenomena derive from wind-induced waves and currents. Wave motion transfers the wind energy from one place to another. It depends on weather and for the long- term on climate. The vicissitudes of the harbour of Egnathia have been influenced in the course of its history by the amount of sediments drifted longshore, (Figure 1). Starting from this consideration the present research describes the program "Perfect Storm", based on the energy flux applied by wave motion to the shoreline [3, 4]. The model has been applied to the shore facing the archaeological site aiming at reconstructing the coastal morphological evolution and correlating the past climatic phases to the different sea level stands. The amount of sediments drifted by wave motions and longshore currents, particularly during the storms occurred in the years 1951-2000 has been calculated [5].

2 The Numerical Model

The coastal morphological evolution of Egnathia has been reconstructed applying an original numerical model (by Gentile) that takes into account the wave motion energies occurred longshore. The program "Perfect Storm" uses the flux energy applied by the wind–induced wave actions to the shorelines. Sea storms (2786) occurred in the range 1951-2000 have been considered [6]. The program allows to define, in consecutive steps, the model of energy obtained by each breaker wave to the shoreline and considers the equations proposed by the Coastal Engineering Research Center [7] based on Svedrup-Munk- Bretschneider (SMB) method included in the Shore Protection Manual. In the case of study the input data of the program are:

- Anaemometric observations (Bari-Palese Air Force stations) for the years 1951-2000. It can be assumed as a basic statement that the kinetic energy of wind is the source of wave motion that have a main role in order to destructing and/or constructing the shore landscape. The wind inducing waves transfers its energy to the land [8].
- The ortho-photos of the coastline. Analytically, the program schematizes the coast as straight stretches. The first definition has concerned 6 km of the coast, schematized in 152 stretches. After, a detailed study (72 stretches) has focused the coastal section (1, 5 km) where the ancient submerged structures are located (Figure 2).

The data processing with "Perfect Storm" can be divided into two phases, each of them provides different steps as following:

a) The selection of the anaemometric data, blowing within the traverse area, with a minimum threshold value (10 Knots) able to induce wind storms and sea currents moving sediments toward the Egnathia coast. The traverse area identified has the vertex corresponding to the old harbour and included in the two directions from North 310° to North 110°;
b) The creation of a data base with all the storms recorded, 2786 in the range of years 1951-2000.

The characteristics of the significant wave have been calculated for each storm using the three equations (SMB method) and correlating each storm with the direction and wind speed and fetch lenght:

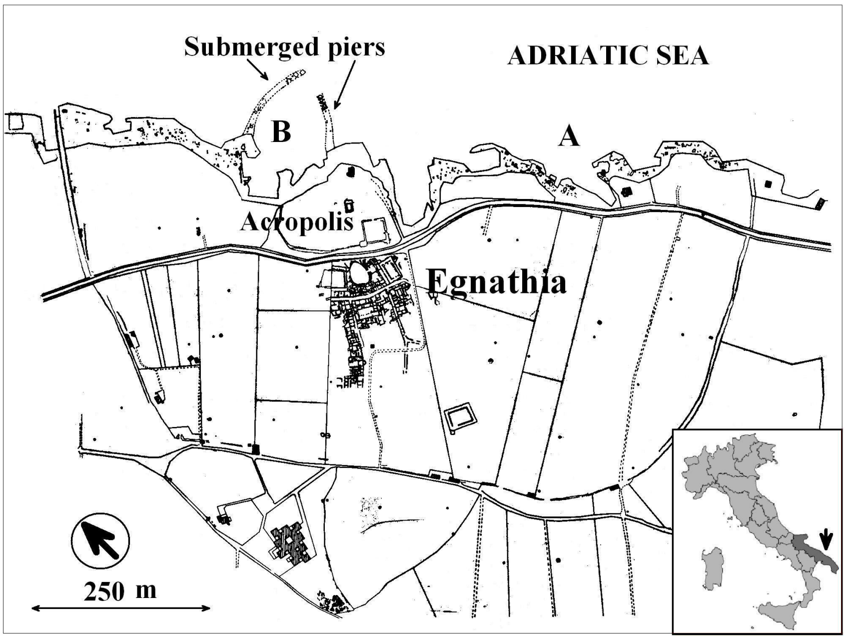

Figure 1: Map of the area: A) Location of the more ancient harbour; B) The Roman harbour with the submerged piers.

$$
\begin{aligned}
\frac{gH}{U^2} &= 0.283 \tanh \left[0.0125 \left(\frac{gF}{U^2} \right)^{0.42} \right] \\
\frac{gT}{2\pi U} &= 1.20 \tanh \left[0.077 \left(\frac{gF}{U^2} \right)^{0.25} \right] \\
\frac{gt}{U} &= K \exp \left\{ \left[A \left(ln \frac{gF}{U^2} \right) - B \ln \left(\frac{gF}{U^2} \right) + C \right]^{1/2} + D \ln \left(\frac{gF}{U^2} \right) \right\}, \quad (1)
\end{aligned}
$$

where: g = 9.81 m·s^{-2} (gravitational acceleration); U = wind speed [knot]; H = wave height [m]; T = period [sec]; t = duration of event [hour]; F = fetch length [nautical miles]; A, B, C, D = constants; exp = exponential; tanh = hyperbolic tangent. These equations allow to define:

- H$^{1/3}$ = significant wave height;
- T = period;
- The duration of the event either in transient and/or steady state.

The SMB method, although in some way dated, is used here in order to introduce a systematic error in defining the significant wave height at a period T. This error is adjusted when the fluxes of any storm are

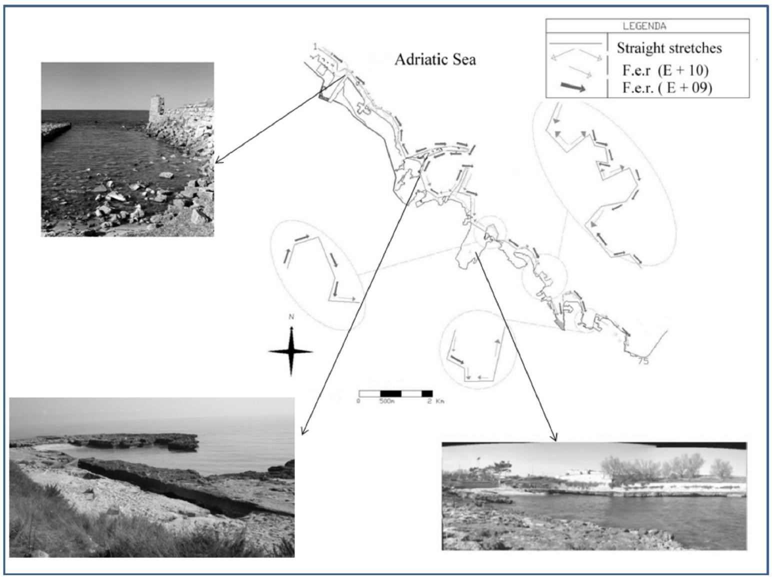

Figure 2: F.e.r. obtained in processing the detailed study of Perfect Storm.

added.

In the second phase the program estimates the energy flux that each of the 2786 storms considered has applied to the 152 stretches of the coast schematized and to the 72 ones in the detailed study.

Assuming that in a rough sea, the water particles included between two vertical lines, at a distance of 1 meter, perpendicular to two progressive wave crests have energy Eo that can be expressed by means the following equation:

$$\mathrm{E}_0 L_0 = \frac{1}{8}\rho g H_0^2 L_0. \tag{2}$$

For a wave length unit or, better, the energy owned by a 1 m^2 of rough sea the equation becomes:

$$\mathrm{E}_0 = \frac{1}{8}\rho g H_0^2, \tag{3}$$

where ρ is the water density and g is the gravitational acceleration.

As a consequence, the energy flux per unit of crest wave length or, in other words, the quantity of energy transmitted by the wave beyond a unit length plane perpendicular to the ahead direction is:

$$p = ECg = \frac{1}{8}\rho g H^2 C_g, \tag{4}$$

where Cg = group wave speed. As a front wave approaching the shore describes different angles of incidence α, the energy flux is given by:

$$p_{ls} = \frac{1}{16}\rho g H_b^2 C sen 2\alpha_b. \tag{5}$$

Therefore, the resultant of energy fluxes (flussi di energia risultante - f. e. r.) has been calculated. F.e.r. is the amount of energy, on a certain period, required by sediments, such as pebbles, sands and silts to move longshore. F.e.r. measured in Joule$\cdot$yr^{-1}r for a meter of shore is directly

proportional to the wave height and function of the angle incident to the stretch of the coast considered.
According to the last formulas the same storm may yield different f.e.r., depending on the angle α. This angle is described between the direction of the approaching front wave and each of the straight stretches of the coast. F.e. r. is the algebraic sum of the energy flux of all single storm, so it is a quantity characterized by a negative/positive sign, direction and it is measured in Joule$\cdot$yr^{-1}r for meter of shore. Finally the amount of f.e.r. means the chance, the velocity and the direction required by sediments to be moved and drifted by currents and wave longshore.

3 The archaeological site and the harbour

The ancient town of Egnathia is mentioned by authors such as Strabone, Orazio and Plinio il Vecchio. The town had a great importance as a commercial center for its location and the presence of the harbour. The earliest human presence in the area dates back to the Bronze Age (XV century BC). Later on, in the VIII century BC the town was inhabited by Messapi becoming an urban settlement with the realization of public buildings. The Early Imperial period saw the construction of port facilities around the inlet just to the North of the acropolis; the inlet was enlarged and better protected through the construction of two artificial piers. In the IX century AD the harbour, became unfit for use. The astronomer Tolomeo reported that the function of this harbour, was, above all, as halting, intermediate and refuge place. Di Ceglie [9, 10] remarks that the coastline presents five natural anchorage points. The deeper and wider inlet, at South-East, could be the more ancient harbour, without defensive structures and in line with the anchorage for the boats of a little village as Egnathia was in that period [11]. Schmiedt [12] pointed out the largest inlets where the banks seem straightened and traces of man made indentations typicals of some Greek harbours are still visible. During the Hellenistic and Roman phases due to the enlargement of the town, the ancient location became inadequate, therefore an external port, to the North of the acropolis, was realized. The submerged structures belong to the ancient Roman port [13] (Figure 3).

4 Geological and geomorphological outlines

The archaeological site of Egnathia lies at the eastern end of a plain, extending for some kilometers and separated from the Murge Plateau by a NW-SE fault system. The local geological set-up is characterized by Pleistocenic calcarenites, and variably cemented sandy- clayey calcarenites and calcilutites related to the Tufi delle Murge Formation, transgressive on the Cretaceous basement made up by the limestones known as Calcari di Bari Formation. The calcarenitic sequence is poorly stratified with fossils such as Ostrea sp. and Pecten sp. and shows high permeability due to fractures and karst. A mesostructural study of the calcarenitic outcrops show different joint systems. The karstic landforms are more evident along these [14]. Sea water intrusion occurs along the whole shoreline and the brackish waters caused by mixing with the fresh groundwater seem to be more aggressive relating

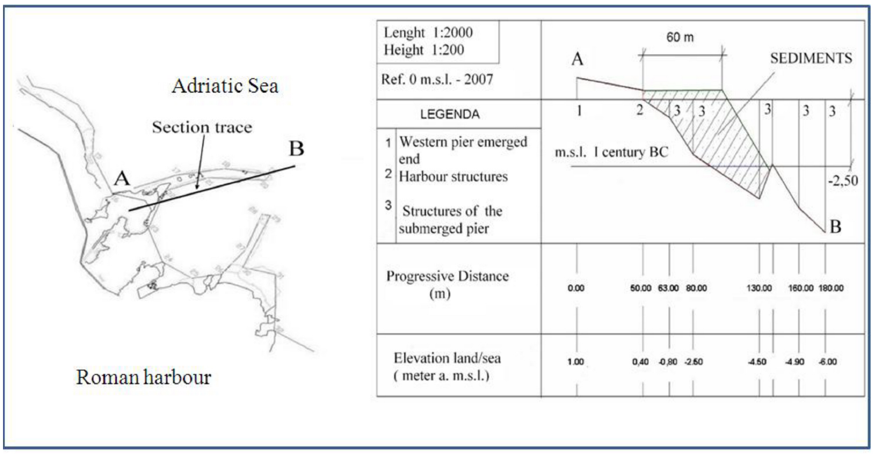

Figure 3: Map and section of the harbour area.

to the karst processes [15]. The human activity increased this action. The coastal calcarenites have been quarried and used as building stones. The man- made cuts have been further worked out by the wave motion so that, sometimes, it is not possible to recognize the original coastal trend. The morphology is characterized by a sequence of sub-horizontal surfaces gently sloping toward the sea and making up a series of marine terraces parallel to the coastline. These surfaces are related to marine abrasion occurred since the Middle Pleistocene and are caused by the superimposition of regional uplift and the eustatic sea level changes. Along the coastline also several series, from poor to well cemented dunes, can be identified. The coast is cut by bays, with locally pocket beaches, and inlets, corresponding to the mouth of short valleys. They are poorly defined, straight valleys, generally parallel one to each other and perpendicular to the coastline, locally called "lame", sometimes deeply incised in the Pleistocenic calcarenites. They correspond to a relict drainage network and are related to sapping processes [16]. During the past rainy seasons these valleys (similar to creeks) conveyed abundant sediments coming from the Murge Plateau toward the sea. The valley bottoms are generally flat and locally covered by alluvial deposits and coarse sands and pebbles. A poorly defined wave cut platform and a discontinuous notch are shaped by sea.

5 Sea level changes and climatic phases

According to Auriemma et al. [13] the submerged structures of the harbour in Opus reticulatum are referable to Roman Age and indicate that the sea level during the I century BC was about – 2,5 m below the present one. This value fits also the depth of the bottoms of Messapic tombs, actually below the sea level. A recent study [15], reconstructing the piezometric surface during IV- II century BC by correlating the bot-

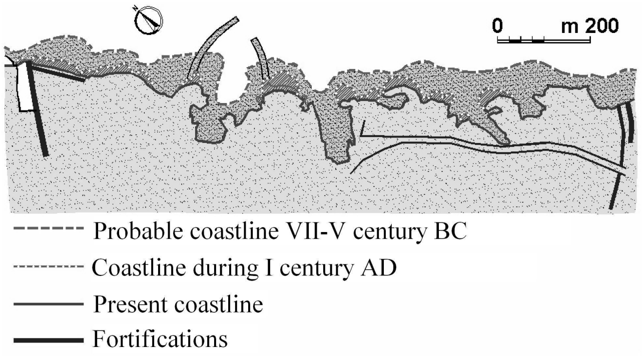

Figure 4: Coastline evolution during the history of Egnathia (after [17]; modified).

toms of wells and cisterns in the archaeological park, allows to assume sea level stands consistent with the uplift rate. On the basis of field observations and biological indicators the uplift pattern of the Eastern Apulian foreland [18] is characterized by a mild uplift (0,08-1,1 mm$\cdot$yr^{-1}) although Lambeck et al. [19] consider the Egnathia area in slow downlift, (Figure 4).
The impact of climatic changes is remarkable not only on sea level, but also on the ecosystems and on the rain trend. Since the Last Glacial Maximun (LGM) about 22 $\pm$ 2 ka cal BP, when the average air temperature was about 4,5° C lower that today, the temperature has been increasing until 8 $\pm$ 1 ka cal BP at Holocene Climatic Optimum (HCO) with an average air temperature of about 2°C higher than today [20, 21].

6 Discussion and conclusion

The main result obtained by the model is the definition of f. e. r. This quantity represents the energy required by waves to move sediment particles back and forth. Coarser grains move by rolling, sliding and jumping, while finer ones are suspended in the water. As breaking waves approach the shore at a low angle, water piles up at first and then is forced to flow parallel to shore as a long shore current.
At present day, the total energy applied by the wave motion to the shoreline has a southward direction as well as the drifting of sediments. The detailed study allows to define that sediments moved during strong sea storms would tend to fill up the inlets along the coastline and to form small and pocket beaches. Considering the present climatic conditions, warm and dry, with poor solid materials conveyed from inland to the coastline, an erosive phase can be recognized and only a few small and relict beaches are present within the little bays facing the archaeological site.
After correlating the results of “Perfect storms” to the climatic conditions existing in the period 1951-2000 we can extend the discussion to different past climatic stages and reconstruct the geomorphological evolution of this coastline and the role of sediments in the history of the harbour.
The vicissitudes of the harbour of Egnathia

have been influenced by the amount of sediments drifted longshore and the sea level stands. The first millennium BC was characterized by a cold and humid climate. Likely, the amount of sediments transported by the "lame" was remarkable as well as the heavy rainfall. The coastal landscape was characterized by flat calcarenites alternating with pebbly-sandy beaches. The sea level was lower and the distance between the old town and the sea was wider than the present. This reconstruction explains the presence of the Messapian necropolis actually below the sea level. The oldest harbour located in the southern inlet could be abandoned due to the filling up with sediments just during this period. On the other hand, this inlet corresponds to the mouth of a "lama" although the urbanization and the human activities does not allow to recognize all the traces on field. During the Roman Age the piers of the new port were founded on a thick layer of pebbles and coarse sediments. Starting from the first century AD the climatic condition changed with less rainfall as well as the contribution of sediments. The coastal erosional processes prevailed with the disappearance of the beaches. The repeated and continuous changes in the amount of sediments reaching the coastline from inland and then moved by currents and waves have shaped the shoreline. The structures of the Roman harbour are visible thanks to the erosional present phase and so well preserved as for the coverage of sediments in the marine deposition during the Little Ice Age.

References

[1] C. Cherubini, G.M. Gentile, and R. Pagliarulo. I sedimenti nella evoluzione storica del tratto costiero prospiciente il sito archeologico di Egnazia. *Geologi e Territorio. Periodico di Scienze della Terra*, 3/4:193–200, 2008.

[2] F. Antonioli and G. Leoni. Siti Archeologici sommersi e loro utilizzazione quali indicatori per lo studio delle variazioni recenti del livello mare. *Il Quaternario*, 11(1):53–66, 1998.

[3] G.M. Gentile and C.I. Giasi. Costruzione di una spiaggia con sterili di cava. Una metodologia di intervento ambientale ecocompatibile. *GEAM (Geoingegneria ambientale e Mineraria) anno XXXVIII*, 2-3, 2001.

[4] G.M. Gentile and S. Selicato. Pianificazione e gestione dei sistemi costieri marini. Ipotesi di naturalizzazione e recupero di coste urbane in Puglia. Atti "International Conference Landscapes of Water; History, Innovation and Sustainaible Design", Monopoli. 2002.

[5] G.M. Gentile and M. Mastrorilli. Determinazione del rapporto fra materiale dissolto ed energia del moto ondoso incidente su una falesia in materiali sabbiosi-argillosi: possibilità di determinazione diretta dell'arretramento del ciglio della falesia. *Ingegneria Ambientale*, 9, 1997.

[6] M. Dodd, A.M. Stoker, R. Garnier, G. Vittori, F. De Los Santos, M. Brocchini, L. Soldini, and M.A. Losada. Use of numerical models to study land-based sedimentation and subsequent nearshore morphological evolution. *Coastal Engineering*, 55:601–621, 2008.

[7] CERC. Shore Protection Manual. *US Army Coastal Engineering Research Center*, 1984.

[8] M. Bottema and G. Van Vledder. Effective fetch and non linear four-wave interactions during wave growth in slanting fetch conditions. *Coastal Engineering*, 55:261–275, 2008.

[9] S. Di Ceglie. Il Porto di Egnazia. 1972.

[10] S. Di Ceglie. Gnathia Forma della città delineata mediante la prospezione archeologica. Lab. Centro Aerofotografico. *Università di Bari Ed.*, 1981.

[11] A. Guerricchio, M. Guerricchio, and A. Maruca. Sul presunto antico porto romano di Egnazia (Br). *Centro Editoriale Librario Università degli studi della Calabria*, 1997.

[12] G. Schmiedt. Atlante Geografico delle Sedi Umane in Italia. Firenze. 1970.

[13] A. Auriemma, G. Mastronuzzi, and P. Sansò. Middle to Late Holocene relative sea level changes recorded on the coast of Apulia (Italy). *Geomorphologie: relief, processus, environment*, 1:19–34, 2004.

[14] M. Delle Rose, R. Pagliarulo, and M. Parise. Some insight for the evolution of the Adriatic coastline, as inferred from research at the archaeological site of Gnathia (Apulia, Southern Italy). *GI2S Coast, Research Publication*, (1):69–72, 2002.

[15] M. Millella, C. Pignatelli, M. Donnaloia, and P. Mastronuzzi. Sea level during $4^{th} - 2^{nd}$ century B.P. in Egnazia (Italy) from archaeological and hydrogeological data. *Il Quaternario*, 19(2):251–258, 2007.

[16] G. Mastronuzzi and P. Sansò. Pleistocene sea-level changes, sapping processes and development of valley networks in the Apulia region (southern Italy). *Geomorphology*, 46:19–34, 2002.

[17] A. Donvito. Egnazia - Dalle origini alla riscoperta archeologica. *Schena Editore*, page 176, 1988.

[18] L. Ferranti, F. Antonioli, B. Mauz, A. Amorosi, G. Dai Pra, G. Mastronuzzi, et al. Markers of the last interglacial sea level high stand along the coast of Italy: Tectonic implications. *Quaternary International*, 145:30–54, 2006.

[19] K. Lambeck, F. Antonioli, A. Purcell, and S. Silenzi. Sea-level change along the italian coast for the past 10,000 yr. *Quaternary Science Reviews*, 23:1567–1598, 2004.

[20] F. Antonioli, G.B. Vai, and L. Cantelli. Litho-palaeoenvironmental maps of Italy during the last two climatic extremes. Explanatory notes edited by Antonioli and Vai, 32^{nd} IGC Publication, Florence. pages 1–80, 2004.

[21] S. Silenzi, S. Devoti, M. Gabellini, E. Magaletti, M.F. Nisi, M. Pisapia, F. Angelelli, F. Antonioli, and A. Zarattini. Le variazioni del clima nel Quaternario. *Geo-Archeologia*, 1:15–50, 2004.

Towards Assessing the Adriatic Sea Coastal Vulnerability to Regional Climate Change Scenarios: Preliminary Results

S. Carniel[1], M. Sclavo[1], A. Bergamasco[1], A. Marcomini[2], S. Torresan[3]
1, Institute of Marine Sciences, CNR, Venezia, Italy
2, Department of Environmental Sciences, University "Ca' Foscari", Venezia, Italy
3, Euro-Mediterranean Centre for Climate Change, Impacts on Soil and Coast Division
c/o Consorzio Venezia Ricerche, Venezia, Italy
sandro.carniel@ismar.cnr.it

Abstract

Preliminary results from numerical climate simulations of the Adriatic sea at high resolution (1/25°), performed during two time-slice integrations, are presented for the period 1960-90 and the 21^{st} century (2070-2100), according to the "A1b" scenario defined by IPCC.
This aims at addressing the feasibility of downscaling procedure in a regional basin, resolving features that are generally still not included when using global models and gaining useful indications on climate-change induced impacts on the wave climate and ocean circulation.
For this purpose, a fully coupled version of the ROMS-SWAN model has been implemented, using interpolated meteorological forcings from the SINTA Project (SImulations of climate chaNge in the mediTerranean Area, a joint scientific cooperation of CMCC-INGV-Univ. of Belgrade).
Within the Impacts on Soil and Water Division (ISC) of the CMCC, the numerical downscaling approach is integrated in a GIS-based Decision Support System (DSS) aimed at the integrated analysis of climate change impacts and risks on coastal zones at the regional, aimed at guiding decision-makers in the definition of adaptation strategies.
Despite further experiments are needed to reach definitive results, the outcomes indicate the feasibility of the numerical downscaling approach; nevertheless, they also highlight uncertainties intrinsic to this approach that may be leading, at least at the present state of the art, to results of difficult interpretation.

1 Introduction

Within the framework of activities of the FISR funded Project "VECTOR", namely the WP1 tasks "CLICOST, Coastal climatology and circulation in the Adriatic Sea", several numerical studies have been performed to assess the climate-change related effects and modifications on the wave climate and circulation in the Adriatic region. Here we present preliminary results from numerical climate simulations of the Adriatic sea at high resolution (1/25°), performed during two time-slice integrations: the periods covering years between 1960-

90 and 2070-2100, the later reflecting "A1b" scenario as defined by IPCC. The aim of the activity was that of addressing the feasibility of a numerical downscaling procedure from global models to regional scale, resolving features that are generally not included in the former and gaining therefore useful indications on climate-change induced impacts on the wave climate and ocean circulation at a regional scale.

For this purpose, a fully coupled version of the ROMS-SWAN model has been implemented, forced by interpolated meteorological fields as resulting from the SINTA Project (SImulations of climate chaNge in the mediTerranean Area, a joint scientific cooperation of CMCC-INGV-University of Belgrade). SINTA is a dynamic downscaling experiment of the global climate model SINTEX-G (maintained by CMCC-INGV Italy, this global model is constituted by ECHAM4 model in the atmosphere and OPA model in the ocean, and provides output at 1° resolution every 6 hours). The SINTA project adopted a Regional Coupled Model (RCM) named EBU-POM, maintained by the Univ. of Belgrade, Serbia, and constituted by the Eta Belgrade University for the atmosphere and the POM for the ocean. This RCM runs at 1/5° with 6 hour resolution, using initial and boundary conditions from the global model. EBU-POM downscaling experiments were initialized with database MODB in 1960 and using SINTEX-G fields in 2071.

Additional information about SINTA can be found in Gualdi et al. [1].

The fields resulting from SINTA were then adequately interpolated on the new high resolution grid and used to force the full Adriatic sea basin for the years 1960-90 and 2070-2100. Analysis of the results focused on ocean currents, temperature, salinity, density fields, as well as significant wave height, wave periods, directions and energy, and on the combined wave-currents bottom stress.

Within the Euro-Mediterranean Centre for Climate Change (CMCC, www.cmcc.it) the numerical simulations performed to study climate change impacts on wave climate and ocean circulation in the Northern Adriatic Sea region are included in a risk-based Decision Support System (DSS) aimed at the integrated assessment of climate change impacts on coastal zones at the regional scale. The DSS will guide decision-makers in the identification of relevant climate change hazards on coastal systems (e.g. erosion, inundation, extreme storm surges and water quality variations) and in the assessment of the related impacts and risks, in order to guide the definition of adaptation strategies. As discussed in the following paragraph, the use of high resolution hydrodynamic models forced by Global Climate Models (GCMs) and Regional Climate Models (RCMs) gives the opportunity to construct climate change hazard scenarios and provide science advancements for the delivery of climate change information to stakeholder and decision-makers.

2 Discussion

A careful assessment on how climate-change induced variations in the winds and heat fluxes may impact the wave climate and the ocean circulation at regional scale in the Adriatic region is still missing in the international literature.

To our knowledge, a tentative has been produced by Pasaric and Orlic [2], limited though to the anlaysis of available meteo-

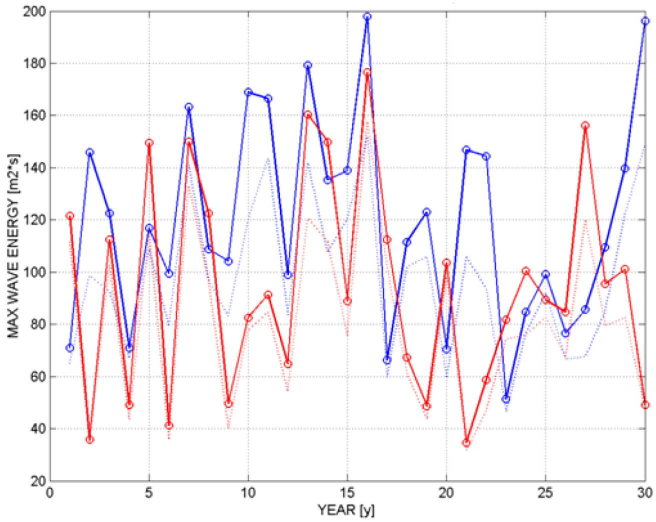

Figure 1: Yearly maximum wave energy comparison between 21^{st} century case (red line) and the 20^{th} century one (blue line).

rological fields at a coarse resolution.
In the novelty approach presented in this paper, though, SINTA bora winds feeding the high-resolution implementation in the Adriatic sea seem to be underestimated, a fact that may play a crucial role in driving the overall circulation and dense water formation in the basin.
The significant wave height fields resulting in the Adriatic basin show a decreasing trend in the 21^{st} century w.r.t. those of the 20^{th} century, a tendency confirmed for the wave energy incident to the coast and for the bottom stress due to currents-waves interactions. In Figure 1 the yearly maximum wave energy comparison between 21^{st} century case (red line) and the 20^{th} century one (blue line) is shown for a region including the Venice littoral. In this region, the expected extreme wave with a return period of 100 years is indeed moving back from about 5.5 m to 5.1 m.
Nevertheless, the seasonal and spatial variation of wave energy can show different features; for instance, Figure 2, presenting the percentage variation of averaged wave energy between 21^{st} and 20^{th} century, highlight a relative increase in wave energy impacting the coast in the Trieste gulf. These results, as far as the data until 1999, are well integrated by those presented by Martucci et al. [3]. First 3D current analysis of the difference in the surface mean circulation between the two centuries evidences the formation of a recirculation area in the northern Adriatic gyre, as well as a decrease in the intensity along the western coast (the WAC, Western Adriatic Current), at least until the Gargano promontory. Associated to this, there is evidence of a generalized increase in the surface temperature in the whole basin, while

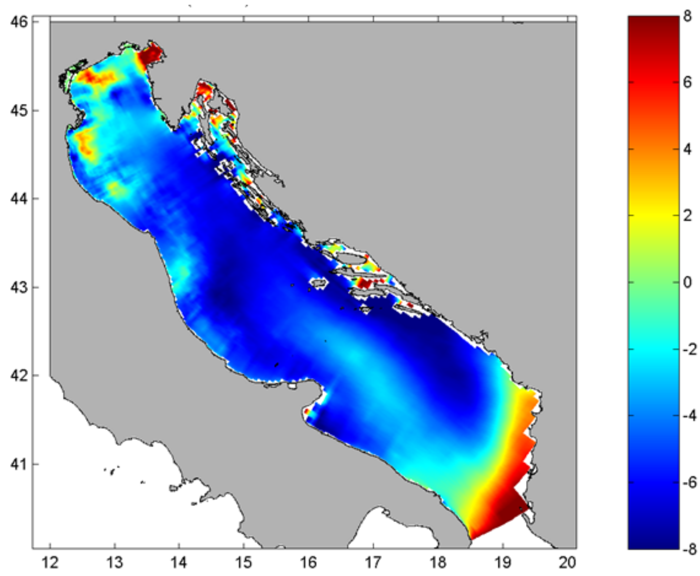

Figure 2: Percentage variation of averaged wave energy between 21^{st} and 20^{th} century.

in the bottom regions this seems to be valid only for the northern Adriatic sub-basin.

Focusing on the northern Adriatic basin (northern than 44.0 ° N), the heat fluxes seem to increase in the 21^{st} century, becoming slightly positive, even though different type of boundary conditions (e.g. river flows) should be tested for this hypothesis. This may play a crucial role in triggering the formation of dense water masses that, originated in this region of the Adriatic basin, are subsequently deepening and sinking flowing southward. Within the northern Adriatic sub-basin the mean temperature increases of about 1.5-2.0 °C in the 21^{st} century w.r.t. the 20^{th} century; interestingly, the sea surface temperature seems to increase of about 1-1.5°C, therefore suggesting that the heat adjustment within the water column is probably once again entering and regulating the highly non linear interplay between these water masses and the different ones intruding from south, the real engine of the Adriatic circulation.

Last, Figure 3 presents the difference of averaged bottom stresses (due to the combined effect of currents and waves) between the 21^{st} and 20^{th} century in the Northern Adriatic basin log10 (N $m^{-2)}$. From the figure it is visible that there is a tendency showing a decrease in the stress along the western coast of the basin, thus suggesting that the intensity of the WAC related current may be weakening during the next century w.r.t the current status.

Within the risk-based DSS developed to study climate change impacts on coastal zones at the regional scale, numerical results and maps obtained for the North Adriatic Sea basin (including the analysis of ocean currents, temperature, salinity, wave

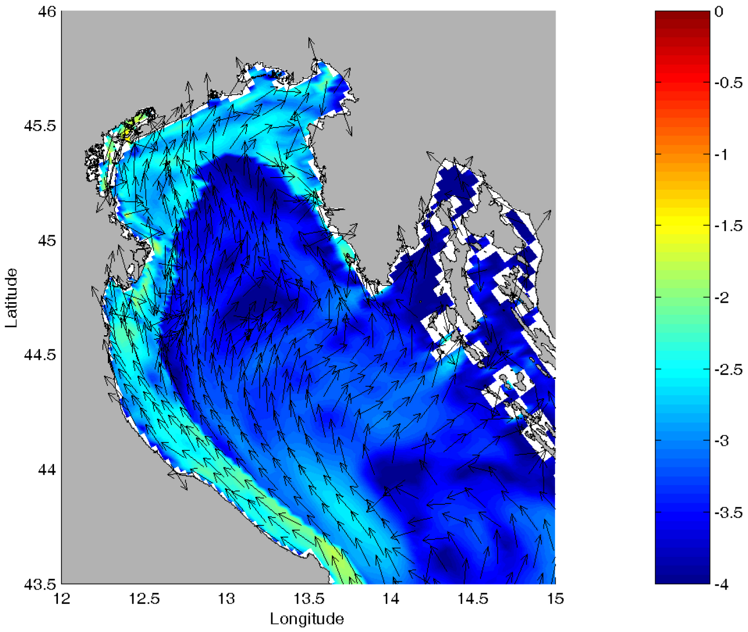

Figure 3: Difference between the average 21^{st} and 20^{th} century bottom stresses (N m^{-2}) due to current and waves. Units are shown in $\log_{10}$.

periods, heights, directions, energy and bottom stress) are used to construct climate change hazard maps representing the exposure to climatic changes against which a system operates.

The conceptual framework of the DSS is composed of 3 main phases: the Scenarios Construction phase which is aimed at the definition of future climate scenarios for the examined case study area at the regional scale, the Integrated impact and risk assessment phase which is aimed at the prioritization of impacts, targets and affected areas at the regional scale, and finally the Risk and impact management phase which is devoted to support adaptation strategies for the reduction of the risks and impacts in the coastal zone, according to Integrated Coastal Zone Management (ICZM) principles. Within the aforementioned framework, the main output of the second phase is the development of GIS-based risk maps obtained through the integration of hazard maps (i.e. maps resulting from the analysis of outputs provided by high resolution numerical models) and vulnerability maps (i.e. maps representing the spatial distribution of environmental and socio-economic vulnerability factors).

3 Conclusions

The numerical downscaling seems to be a feasible approach from global climate models to regional ones, even tough intrinsic uncertainties may be leading to results of difficult interpretation.

Despite further experiments are needed to reach definitive results, the outcomes indicate the feasibility of the numerical downscaling approach from global climate models to RCM ones. At the same time, they also highlight uncertainties intrinsic to this approach that may be leading, at least at the present state of the art, to results of difficult interpretation and that should be drawn with precaution.

For instance, since bottom sediments mobilization is linked mostly to episodic highly energetic events, their dynamics would surely benefit from higher resolution forcings w.r.t. the currently available ones.

The numerical downscaling approach developed to study climate change impacts on coastal dynamics at the regional scale is also an innovative way to bridge the gap between the coarse information of climate scenarios provided by GCMs and RCMs and the detailed information necessary to investigate climate change impacts and risks at the regional/local level. However, precaution is still needed to identify and evaluate the main sources of uncertainty and to transfer information to stakeholders and decision-makers, improving adaptation and ICZM processes.

4 Acknowledgments

We kindly acknowledge V. Djudjevic (Univ. of Belgrade and SEEVCCC, Serbia) and S. Gualdi (CMCC Bologna, Italy) for having made available the SINTA data. This work has been supported by the "VECTOR"-FISR Project and the EU-funded Project "EQUIMAR". The collaboration with CMCC and Consorzio Venezia Ricerche is also acknowledged.

References

[1] S. Gualdi, B. Rajkovic, V. Djurdjevic, S. Castellari, E. Scoccimarro, A. Navarra, and M. Dacic. SINTA - SImulations of climate chaNge in the mediTerranean Area - Final scientific report. *Earth-prints T.R. (see http://www.earth-prints.org/)*, page 70, 2008.

[2] M. Pasaric and M. Orlic. Meteorological forcing of the Adriatic - present vs. projected climate conditions. *Geofizika*, 21:69–87, 2004.

[3] G. Martucci, S. Carniel, J. Chiggiato, M. Sclavo, P. Lionello, and M. B. Galati. Statistical trend analysis and extreme distribution of significant wave height from 1958 to 1999 – an application to the Italian Seas. *Ocean Science*, 6(6):525–538, 2010.

Short Term Coastal Process Modeling: an Integrated Approach to the Wave-Current Problem

S. Carniel[1], M. Sclavo[1], A. Bergamasco[1], A. Ricchi[2]
1, Institute of Marine Sciences, CNR, Venezia, Italy
2, Department of Science and Technology, University of Napoli “Parthenope”, Italy
sandro.carniel@ismar.cnr.it

Abstract

Hydrodynamic numerical models able to correctly simulate nearshore processes are essential for a variety of applications, ranging from beach protection to search and rescue activities and support to engineering operations. Within this context, the capability of correctly accounting for processes such as wetting-drying, wave-currents interactions, turbulent mixing, sediment resuspension and transport are very desirable both for research and practical applications. In the last decade there has been a considerable advance in the direction of the “integrated models”, both thanks to improvements in the theoretical background and to recent advances in the computer performances that allowed higher-resolution, long-term integrations and ensemble runs. The growing availability of long time-series and large forcing outputs from meteorological and sea-state numerical models are now allowing to employ complex, integrated numerical tools to model coastal dynamical processes, to support decision makers in the field of coastal erosion and vulnerability.

1 Introduciton

The issue of reproducing nearshore processes at a high fidelity level is a theme of paramount importance for many reasons. Surface velocities, turbulent mixing, energy redistribution in shallow regions are heavily impacting the environment by means of reshaping morphology and coast lines, influence engineering operations and affect critical themes such as Search and Rescue (SAR). From this perspective, it is mandatory for state of the art numerical models not only to be able to reproduce the 3D fields of circulation under wind and tidal forcings, but also to account for bidirectional interactions between waves and currents and to consider cases of wetting and drying of the domain. This paper describes the main features of a numerical model suitable for simulating the above mentioned nearshore aspects, and the implementation of a common test case. In the following we provide a few background information about the model, methods for two way coupling to a wave model, and some results from the specific implementation carried out.

2 Numerical models adopted

2.1 Hydrodynamic models

The Regional Oceanographic Modeling System (ROMS, www.myroms.org) is a numerical coastal ocean circulation model

developed by a community of scientists, interacting through internet and periodic meetings. ROMS is a three dimensional, free surface, terrain following numerical model that solves finite-difference approximations of the Reynolds averaged Navier Stokes (RANS) equations using the hydrostatic and Boussinesq assumptions with a split explicit time stepping algorithm.
The horizontal dimension is discretized by means of an Arakawa C grid. In the vertical coordinate, the model uses a stretched S coordinate system, similar to sigma coordinates with additional flexibility since the layers need not be a fixed percentage of the water column. Vertical resolution can be adjusted to allow increased resolution near the surface and bottom boundaries.
The grid can be either rectilinear, with constant or varying grid spacings, or curvilinear to allow focusing of the mesh to specific areas, for example to accommodate land sea boundaries.
ROMS adopts a flexible structure that allows choices for many of the model components, including options for advection schemes (second order, third order, fourth order, and positive definite), turbulence submodels, and boundary conditions. It includes bottom and surface boundary layer submodels, air sea fluxes, surface drifters, a sediment transport module, a biogeochemical one and a fully developed adjoint model for computing model inverses and data assimilation.
The density field is determined from an equation of state that accounts for temperature, salinity, and suspended sediment concentrations. Eddy diffusivities are calculated using, among the others, the K profile parameterization, Mellor and Yamada level 2.5 (MY2.5) method or the generic length scale (GLS) method as implemented by Warner et al. [1], that also includes the option for surface fluxes of turbulence kinetic energy due to wave breaking.
ROMS includes radiation stress terms to the momentum equations based on Mellor approach, where a vertical coordinate transformation and phase averaging are used to derive interacting current and surface gravity wave equations, yielding equations with mean (wave phase averaged) velocities in a Lagrangian reference frame, related to the Eulerian one by the Stokes velocities (subtracted from Lagrangian velocities to maintain a consistent Eulerian reference frame for the entire model dynamics). Another relevant feature when describing nearshore processes is the wetting and drying capability, based on an algorithm that detects cells with water depths less than a user specified value, and prevents outward flux of water from those cells, a process called cell flux blocking. Flux of water onto cells is always permitted. Model inputs and output files are written using the NetCDF data architecture, while the code is written in modular Fortran90 and runs in serial mode or on multiple processors using either shared or distributed memory architectures (OpenMP or MPI).

2.2 Wave Model

The modification of the momentum equations to include the effects of surface waves requires information on basic wave properties such as wave energy, propagation direction, and wavelength. Other algorithms, such as the bottom boundary modules and turbulence submodels may also require wave information such as wave period, bottom orbital velocity, and wave energy dissipation rate. These quantities are obtained from a wave-model, e.g. SWAN, a wave averaged model that solves

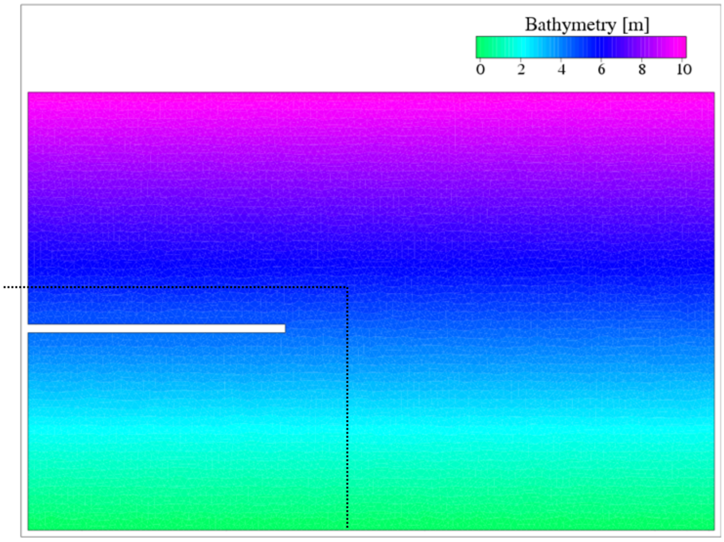

Figure 1: Bathymetry and model domain of the BREAKWATER test case. Incident wave height (wave height of 2.0 m, period of 8.0 seconds) is entering the domain from the northern boundary. The dashed region is the one presented in the following Figures.

transport equations for wave action density (energy density divided by relative frequency) accounting for shoaling and refraction. Source and sink terms are represented by wind wave generation, wave breaking, bottom dissipation, and nonlinear wave interactions. SWAN can also account for diffraction, partial transmission, and reflection. The selected wave model can be run separately and the output used to force the hydrodynamic and sediment routines (one way coupling with ROMS). Alternatively, the wave model can be run concurrently with the circulation model via a two way coupling, whereby currents influence the wave field and waves affect the circulation.

ROMS and the coupled wave model (e.g. SWAN) can use the same computational grid, which may be Cartesian or curvilinear. The same minimum depth can be specified in both codes to exclude common points during wave and hydrodynamic computations.

3 Model coupling techniques

In the following we will select SWAN as the wave model. The coupling ROMS-SWAN is performed by using the Model

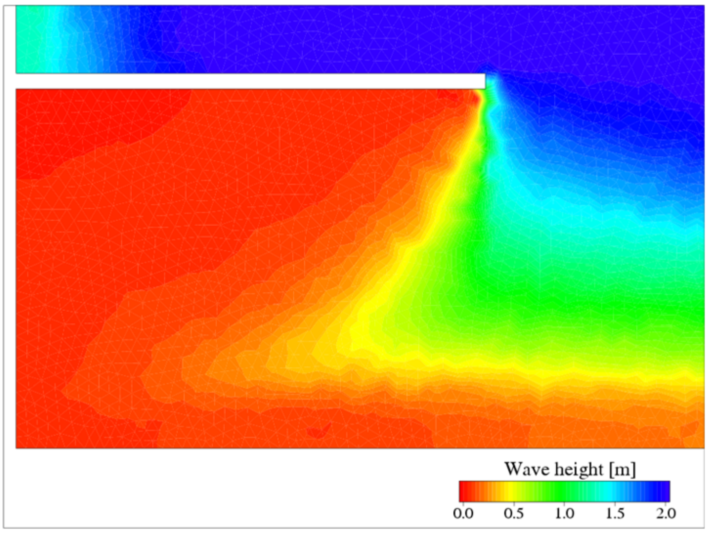

Figure 2: Significant wave height (m) distribution after 24 hours of simulation, as resulting from the coupled system ROMS-SWAN in the BREAKWATER test case.

Coupling Toolkit, an open source software library for constructing a coupled model system from individual component models, each of them retaining its own grid and running on its own set of processors. The MCT has protocols for decomposition and allocation of model grids among different processors, transfer of data fields between the different models, and interpolation algorithms for the data fields that are transferred.

At a given synchronization time, SWAN send to ROMS arrays of wave height, wavelength, average wave periods at the surface and near the bottom, wave propagation direction, near bottom orbital velocity, and wave energy dissipation rate. On the other hand, the hydrodynamic model provides to the wave ones arrays of water depth, sea surface elevation and current velocity.

4 The "BREAKWATER" test case

In this section we provide an example of dynamic coupling for wave-current interactions in a test case [2]. The test is inspired on an example proposed by Nicholson et al. [3], where it was, however, run only using one-way coupled wave hydrodynamic models. It consists of a test basin of rectangular shape with wall boundaries,

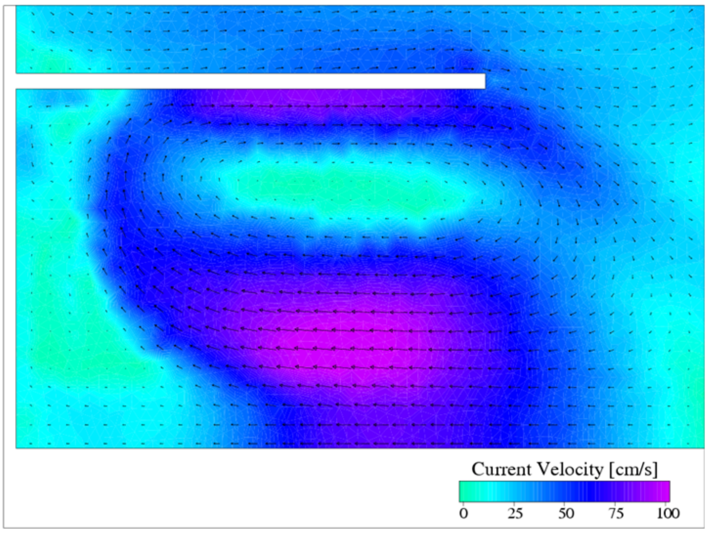

Figure 3: Integrated velocities (cm·s^{-1}) as resulting from the coupled ROMS-SWAN system in the BREAKWATER test case.

having dimensions of 800 m by 500 m. A breakwater, 300 m length, is located on the western side at 220 m from the SW edge. The domain and the associated bathymetry are presented in Figure 1. Forcings is represented by a southerly directed waves having a peak period of 8.0 s and wave height of 2.0 m. In this paper we focus on the integrated circulation arising from the wave currents bidirectional interaction, without bathymetry modification induced by sediment transport dynamics. No wind forcing is insisting on the basin. The model is employed in its 3D configuration.

Figure 2 presents the significant wave height field (m) at the end of the first day of simulation as resulting from ROMS-SWAN integration, again in the dashed portion of the model domain (see Figure 1).

The vertically integrated velocities (cm per second) as resulting after 24 hours of integration in a portion of the total model domain are shown in Figure 3. An anticyclonic gyre has formed past the breakwater, which acted as a protection to the incoming wave from north. Velocities are up to 100 cm per second, and the gyre location seems to be in relatively good agreement with results from [3]. The intensity and location of the gyre seem to be very sensitive to the choice of the bottom friction value.

5 Conclusions

We presented a coupled wave-current oceanographic circulation model suitable for applications in rivers, lakes, estuaries, coastal environments, and the coastal ocean. Among the rest (fully non linear, 3D, wind and tidal driven), it incorporates nearshore radiation stress terms and wetting and drying, extremely useful when accounting for surfzone (nearshore) processes.
The results presented demonstrate, at least qualitatively, a good level of agreement with previous studies, in addition to more desiderable aspects such as modern computational techniques and a sophisticated sediment transport module that will be discussed in another paper of the volume.

6 Acknowledgements

Follow up activities of this work are partially supported by the PRIN-2008 Project 2008YNPNT9_005 and the FIRB Project #RBFR08D825 (Project DECALOGO).

References

[1] J.C. Warner, C.R. Sherwood, R.P. Signell, C.K. Harris, and H.G. Arango. Development of a three-dimensional, regional, coupled wave, current, and sediment-transport model. *Computer and Geoscience*, 34(10):1284–1306, 2008.

[2] L. Cavaleri, S. Carniel, C. Ferrarin, M. Sclavo, and G. Umgiesser. Analysis and intercomparison of two coupled circulation-wave model systems. XXXII IAHR Conference 2007, 2-6 July, Venice (ISBN 88-8940-506-6). II:442, 2007.

[3] J. Nicholson, I. Broker, J.A. Roelvink, D. Price, J.M. Tanguy, and L. Moreno. Intecomparison of coastal area morphodynamic model. *Coastal Engineering*, 21:97–123, 1997.

Predicting Sediment Transport at Coastal Structures: an Integrated Model Approach

S. Carniel[1], M. Sclavo[1], A. Boldrin[1], L. Da Ros[1], M. Tondello[2], T. Minuzzo[1]
1, Institute of Marine Sciences, CNR, Venezia, Italy
2, HydroSoil s.r.l., Padova, Italy
sandro.carniel@ismar.cnr.it

Abstract

The open-source 3-D hydrodynamic Regional Ocean Modeling System includes nearshore processes and wave-current interactions (e.g. via a two-way coupling with SWAN model), the effects of wave breaking, a state-of-the-art description of sediment resuspension and transport as well as a wetting and drying algorithm. The resulting integrated model is capable to predict coastal circulation of water and sediments dynamics in coastal and estuarine regions, and from the shelf through the surfzone, helping assessing scouring in the proximity of coastal structures. Here we describe the model components and demonstrate the applicability of the model to simulate circulation and sediment morphodynamics around a groin. Results qualitatively agree with generally observed patterns, providing a quantitative tool to estimate the impact of coastal structures on sediment transport and water turbidity, which may turn out to be of particular interest also in proximity of aquaculture and mollusc culture activities.

1 Introduction

The issue of reproducing nearshore processes at a high-fidelity level is of paramount importance for engineering operations. Nearshore velocities, turbulent mixing, energy redistribution in shallow regions are heavily impacting the coastal environment by reshaping morphology and coast lines.
It is nowadays feasible to use complex, coupled integrated models in order to assess these issues, provided the most relevant scientific features are dynamically taken into considerations.
An application of such a model to a very shallow area in presence of a groin is presented, focusing on the relevance of a dynamical two-way coupling between waves and currents on the local sediment dynamics.
Local scour is indeed one of the most likely reasons for groin collapse, since the steepening of the slope can be the origin of the armored layer elements rolling down or slope instability. It should also be remarked that local scour holes are a serious concern for recreational activities in seaside resorts as in their surroundings a not negligible number of deaths by drowning are reported.
Results highlight how it is possible to predict nearshore processes of coastal circulation and sediment transport using integrated numerical models.

2 The numerical models adopted

The Regional Ocean Modeling System (ROMS, www.myroms.org) is a free-source, state of the art numerical model that allows to simulate the 3D circulation fields under wind, wave and tidal forcings, accounting for bi-directional interactions between waves and currents and considers wetting and drying of the domain. It also solves the transport equations for multiple classes of suspended and bed load sediments, multiple bed layers, and tracks bottom stratigraphy and bed morphology [1, 2].

ROMS is a three dimensional free surface model that solves finite difference approximations of the Reynolds averaged Navier Stokes equations using the hydrostatic and Boussinesq assumptions. It uses a horizontal curvilinear Arakawa C grid and vertical stretched terrain following coordinates. ROMS provides a flexible structure that allows several choices for many of the model components, including several options for advection schemes (second order, third order, fourth order, and positive definite) and boundary conditions. It includes bottom and surface boundary layer submodels, air sea fluxes, Additionally the density field is determined from an equation of state that accounts for temperature, salinity, and suspended sediment concentrations.

Eddy viscosities and eddy diffusivities are calculated using one of the several options implemented for turbulence closure models, among which the generic length-scale (GLS) method that also includes the option for surface fluxes of turbulent kinetic energy due to wave breaking.

ROMS has also been modified to include physical processes that are important in nearshore regions by adding depth dependent radiation stress terms in the three dimensional momentum equations and depth independent terms to the two dimensional momentum equations.

The modification of the momentum equations to include the effects of surface waves requires information on the basic wave properties such as wave energy, direction, and wave length. Other processes such as the bottom boundary modules and turbulence closures may additionally require wave periods, bottom orbital velocities, and wave energy dissipation. These wave quantities are obtained from the coupling with a wave model such as the Simulating WAves Nearshore (SWAN) one.

SWAN is a wave averaged model that solves transport equations for wave action density (energy density divided by relative frequency), accounting for shoaling and refraction, source and sink terms representing effects of wind wave generation, wave breaking, bottom dissipation, and nonlinear wave wave interactions. It also can account for diffraction, partial transmission, and reflection. SWAN can be run separately and the output used to force the hydrodynamic and sediment routines (one way coupling) or, as performed in the study presented here, run concurrently with the circulation model (two ways coupling) whereby currents influence the wave field and waves affect the circulation.

3 Sediment transport and morphology modules

ROMS can handle an unlimited number of user-defined size classes of non cohesive sediments. Each class has attributes of grain diameter, density, settling velocity,

critical shear stress for erosion, and erodibility constant. The sediment bed is represented by three-dimensional arrays that contain a fixed number of layers beneath each horizontal model cell.
Each cell of each layer in the bed is initialized with a layer thickness and a variable number of sediment classes each containing a grain size, porosity and density. The bed framework also includes two dimensional arrays that describe the evolving surficial properties of the seabed, including bulk properties of the surface layer (active layer thickness, mean grain diameter, mean density, mean settling velocity, mean critical stress for erosion) and descriptions of the sub-grid scale morphology (ripple height and wavelength). These properties are used to estimate bed roughness in the BBL formulations and feed into the bottom stress calculations. The bottom stresses are then used by the sediment routines to determine resuspension and transport, providing a feedback from the sediment dynamics to the hydrodynamics.
During computation the bed layers are modified to account for erosion and deposition via the computation of an active layer thickness. Each sediment class can be transported by suspended load and/or bedload. Sediment suspended in the water column is transported by solving the advection and diffusion equation with the addition of source and sink term for vertical settling and erosion. Suspended-load mass is exchanged vertically between the water column and the top bed layer; in this case, the mass of each sediment class available for transport is limited to the mass available in the active layer.
Bed load mass is exchanged horizontally between the top layers of the bed. ROMS implements two methods for computing bedload transport: a) the Meyer and Peter Mueller formulation for unidirectional flow and b) the formulae of Soulsby and Damgaard, that accounts for combined effects of currents and waves [3].
Suspended sediment that is deposited or bed-load that is transported into a computational cell is added to the top bed layer. During suspended load transport, if sediment continues to deposit in the top layer so that it becomes thicker than a user defined threshold, a new layer is provided to begin accumulation of the depositing mass. To keep the total number of vertical bed layers constant, the bottom 2 layers are then combined to conserve sediment mass. After erosion and deposition is applied, the active layer thickness is recalculated and bed layers adjusted to accommodate it.
The bed model accounts for changes in sea floor elevation resulting from convergence or divergence in sediment fluxes, being completely mass conserving.
A morphological scale factor can be activated to provide an increased rate of morphological change as would be useful for simulating trends over time periods longer than typical simulations.

4 Bottom stress calculations

Reynolds stresses, production and dissipation of turbulent kinetic energy, and gradients in velocity and suspended sediment concentrations vary over short vertical distances near the bed, so they are difficult to resolve with the vertical grids used in regional scale models. ROMS implements sub-models to parameterize some of these subgrid scale processes in the bottom boundary layer (BBL).
Treatment of the BBL is important for the

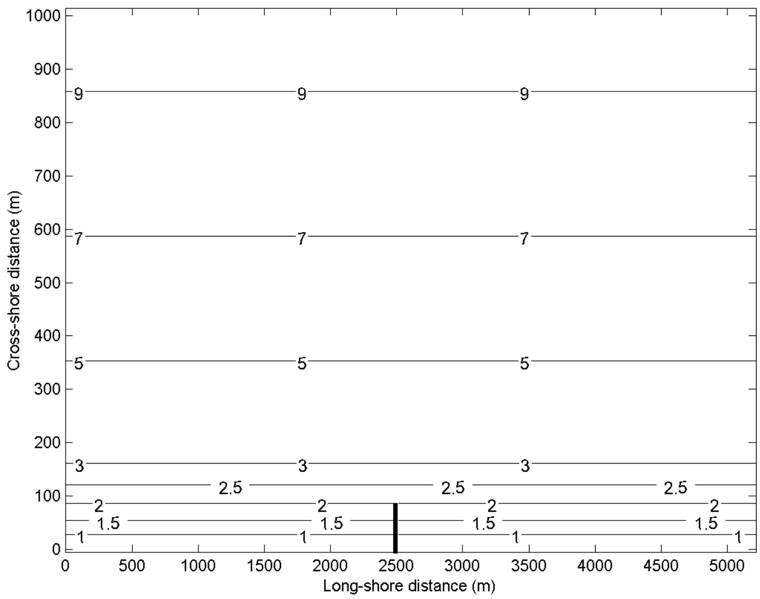

Figure 1: Domain bathymetry (meters).

circulation model solution because it determines the stress exerted on the flow by the bottom, which enters the governing equations as a boundary conditions for momentum in the x and y directions. Determination of the BBL is even more important for the sediment-transport formulations because bottom stress affects the transport rate for bedload and the resuspension rate for suspended sediment.
ROMS implements both simple drag coefficient expressions for representing BBL processes (such as linear bottom friction, quadratic bottom friction, or a logarithmic profile) and more complex formulations that represent the interactions of wave and currents over a bed and couple them with calculations of bottom roughness.
In short, the more advanced BBL routines calculate current and wave boundary layer bottom stresses under the combined influence of wave, currents, and mobile sediments. These stresses directly influence flow near the bottom and act as agents for sediment resuspension and bed load transport.

5 Model coupling strategy

ROMS is coupled to SWAN via the Model Coupling Toolkit, MCT, an open source software library and set of Fortran90 modules for constructing coupled models from individual component models, each having its own grid and running on its own processor(s).
Data is exchanged between the wave and

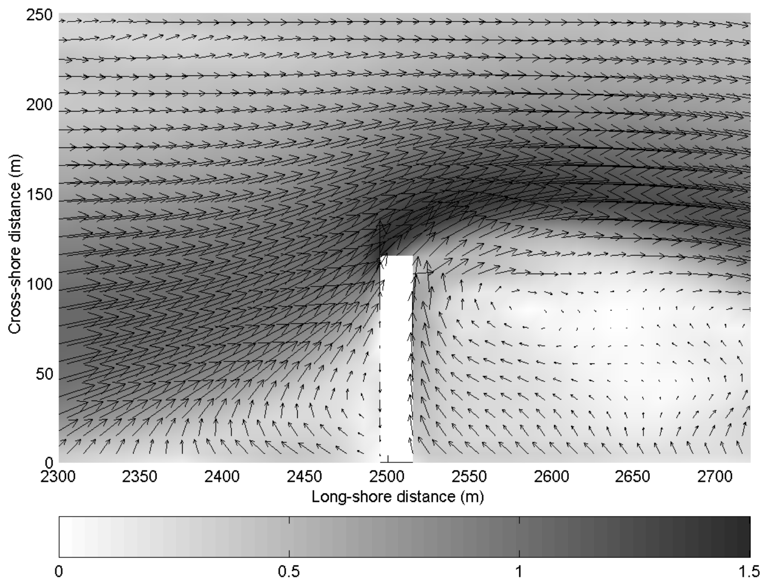

Figure 2: Surface currents around the groin ($m \cdot s^{-1}$) after 24 hours of integration. Every second point of the grid is shown.

the circulation model at user defined synchronization intervals, the frequency of data exchange depending on the model application and the temporal and spatial variability of the wave and currents fields.

The wave model sends to ROMS arrays of wave height, wave length, wave periods for the water surface and near bed, wave direction, near bottom orbital velocity, and wave energy dissipation rate; ROMS provides water depth, sea-surface elevation, and current velocities to the adopted wave model.

6 Sediment transport in proximity of a groin

The capabilities of the ROMS model have been tested on a shallow water case, in presence of a single groin. The domain is presented in Figure 1, and consists of a rectangular basin with wall boundaries, having dimensions of 5200 m by 1000 m, following a Dean profile consistent with the uniform sediment grain size (0.200 mm), having A=0.0992.

Three-dimensional circulation is schematized via a 10 layer water column, the thickness of each layer depending upon the local depth.

An impermeable groin (20 m wide) is extending 120 meters, until approximately to

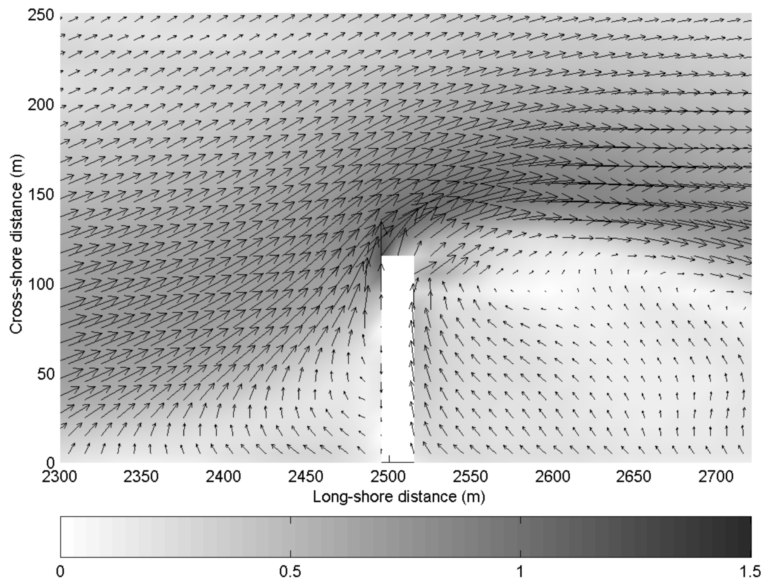

Figure 3: Bottom currents around the groin (m·s^{-1}) after 24 hours of integration. Every second point of the grid is shown.

a depth of 2.3 m, seaward of the shoreline to trap littoral drift and prevent updrift erosion. It is located in the middle of the domain, about 2500 m from the boundaries. Forcings is represented by a wave, having a peak period of 7.0 s and a significant wave height of 1.5 m, with an offshore mean direction from 330° N. Wave spectrum is a JONSWAP type, peak factor 1.8 directional spreading is 18.

A constant wind of 13.0 m per second, coming from 330° N is also superimposed on the basin.

The bed is initialized with 5 layers, each of them having a thickness of 0.1 m, and the sediment has no porosity. Critical stress for bottom resuspension is 0.17 N/m, settling velocity is 20.0 mm/s.

The hydrodynamical and wave models are integrated, respectively, using a time step of 3 and 360 seconds, the wave and ocean coupling interval is 360 seconds. The results are extracted after the forcings has been kept constant for 24 hours. Since at this stage the activity is aiming at qualitatively reproducing a typical behaviour, no attempt to calibrate the model was carried out, and results are intended to be semi-quantitative.

Results description will focus on the integrated circulation arising from the wave and currents bidirectional interaction, including resulting bathymetry modification induced by sediment transport dynamics.

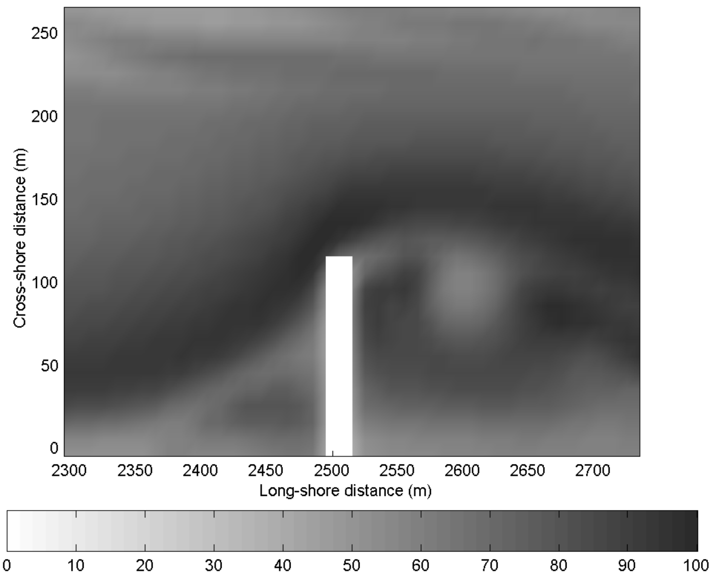

Figure 4: Suspended sediment concentration in the water column (non-dimensional units).

Figure 5: Example of suspended sediment (turbidity) around a groin located in the Adriatic sea.

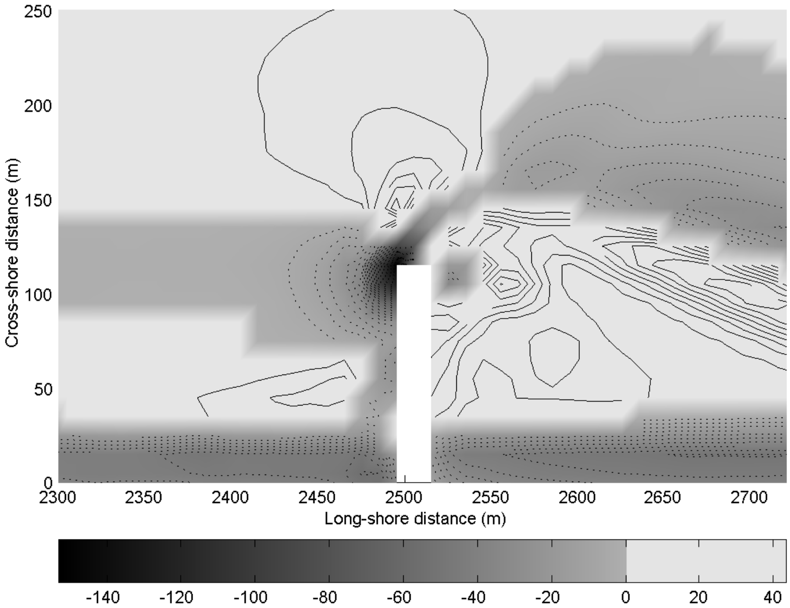

Figure 6: Seabed erosion/deposition (dotted/continuous lines) around the groin (mm) after 24 hours of simulation.

7 Results and discussion

Local scour is one of the most likely cause of failure of coastal protection structures. The capability of the new generation of three dimensional coupled hydrodynamic plus wave plus sediment models to simulate seabed modifications such as local scour, allows the prediction of scour patterns and, if properly calibrated, the estimation of maximum scour depth.

The numerical results of simulations in terms of surface and bottom currents (Figures 2 and 3) and resulting suspended sediment concentration (Figure 4) show a good agreement with what is generally observed in the surrounding of groins.

Figure 5 presents a picture of the suspended sediment distribution around a groin. The shape of the plume seems to be qualitatively depicted by the numerical model, also in consideration of the fact that the real/simulated coastal structures differ, that the shoreline initial conditions are not equal and that in our numerical test the meteorological forcing was reflecting a storm from a constant direction.

Figure 6 presents the seabed erosion or accumulation regions as modeled by ROMS around the groin. Again, the scour around the coastal structure seems to be in good qualitative agreement with real examples, such as the bathymetric survey carried out using MultiBeam technique and presented

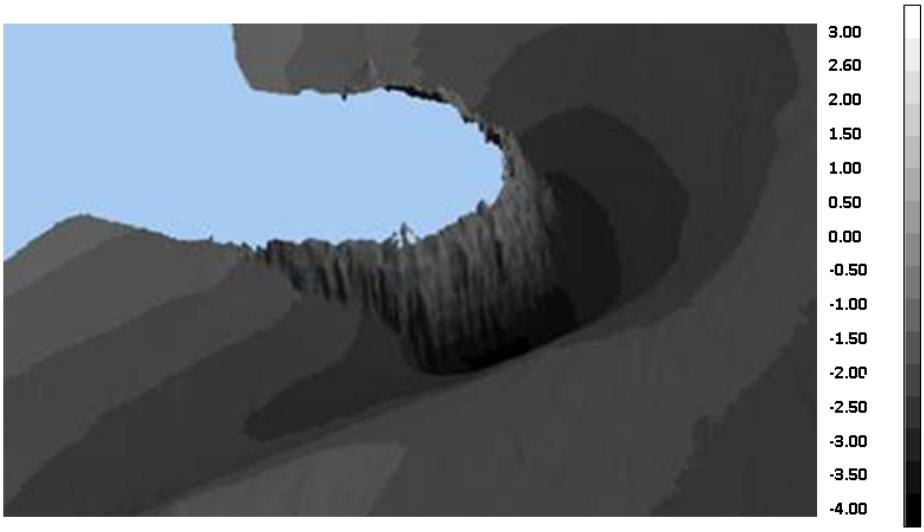

Figure 7: Typical scour pattern around a groin (meters).

in Figure 7.

As a conclusion, it is now possible to start using such integrated numerical models to optimise structure layout in order to reduce scour phenomena or, at least, to design structure that will withstand the effect of the expected scour.

Moreover, these models can provide a quantitative tool to estimate the impact of coastal structures on sediment transport and water turbidity, which may turn out to be of particular interest also in proximity of aquaculture and mollusc culture activities.

8 Acknowledgements

Follow up activities of this work are partially supported by the PRIN-2008 Project 2008YNPNT9_005 and the FIRB Project #RBFR08D825 (Project DECALOGO).

References

[1] J.C. Warner, C.R. Sherwood, R.P. Signell, C.K. Harris, and H.G. Arango. Development of a three-dimensional, regional, coupled wave, current, and sediment-transport model. *Computer and Geoscience*, 34(10):1284, 2008.

[2] C.R. Sherwood, S. Carniel, L. Cavaleri, J. Chiggiato, H. Das, J. Doyle, et al. Sediment dynamics in the Adriatic Sea investigated with coupled models. *Oceanography*, 17(4):58, 2004.

[3] R.L. Soulsby and J.S. Damgaard. Bedload sediment transport in coastal waters. *Coastal Engineering*, 52(8):673, 2005.